IAEA-CN-199
Paris, France, 4-7 March 2013
Paper CN-199-127

Status of ASTRID nuclear island pre-conceptual design

Manuel SAEZ[1], Jean-Charles ROBIN[1], Bernard RIOU[2], Alexandre VILLEDIEU[2], Dominique DEPREST[3], Gérard PRELE[3]
[1]: CEA Cadarache, DEN/DER/CPA, 13108 Saint-Paul lez Durance Cedex, France
[2]: AREVA NP, 10 rue Juliette Récamier 69456 Lyon Cedex 06, France
[3]: EDF SEPTEN, 12-14 avenue Dutrievoz, F-69628 Villeurbanne Cedex, France
Contact author: Manuel SAEZ, +33442253465, manuel.saez@cea.fr

Abstract. Being part of the answer to the French Act of the 28th of June 2006 about nuclear materials and waste management, the ASTRID (Advanced Sodium Technological Reactor for Industrial Demonstration) Project has the objective to demonstrate, from 2020s, at the industrial scale progress on identified domains of Sodium-cooled Fast Reactor (safety, operability, economy) and to perform transmutation demonstrations. CEA (French Commission for Atomic Energy and Alternative Energy) is the leader of the ASTRID project, with support of industrial partnerships to cover main engineering design works.
The pre-conceptual design is the first important milestone, with preliminary investment cost evaluation. In this phase, innovation and technological breakthroughs are favoured, while maintaining risk at an acceptable level. The pre-conceptual design, started in 2010, will be delivered by the end of 2012, and will consider some open options.
This paper presents a status of the ASTRID nuclear island pre-conceptual design. The most promising options are highlighted as well as the less risky and back-up options. Each option is evaluated in terms of economy, safety, In Service Inspection and Repair (ISIR), operability, robustness, and project risk.
Items addressed in the paper include Above Core Structure, Intermediate Heat Exchanger, primary and secondary pumps, Decay Heat Removal systems, core catcher. Also included are the options for Steam Generators or sodium-gas heat exchanger, as well as global architecture in connexion with the selection of Power Conversion System.

1. Introduction

Sodium-cooled Fast Reactors (SFR) is one of the Generation IV reactor concepts. It has been selected to secure the nuclear fuel resources and to manage radioactive waste.
A June 2006 French law on sustainable management of radioactive materials and wastes requests that, concerning transmutation of long-lived radioactive elements, studies and investigations shall be conducted, in order to provide by 2012 an assessment of the industrial prospects of those systems. Fast Reactor strategy was confirmed in May 2008 at Ministry level and in September 2010 an agreement was published between CEA and French Government in order to conduct design studies of ASTRID prototype and associated R&D facilities [1].
Input data for ASTRID pre-conceptual design are a sodium-cooled pool reactor of 1500 MWth generating about 600 MWe. ASTRID lifetime target is 60 years. Two Power Conversion Systems (PCS) are studied in parallel until the end of pre-conceptual design phase: Rankine steam cycle or Brayton gas based energy conversion cycle. ASTRID design is guided by the following major objectives compared to previous SFRs: improved safety, simplification of structures, improved ISIR, improved manufacturing conditions for cost reduction and increased quality, reduction of risks related to sodium fires and Sodium-Water Reaction (SWR), and improved robustness against hazards.
The first phase of the Preliminary Design Project, the pre-conceptual design phase, was conducted from mid-2010 till the end of 2012. Innovation and technological breakthroughs have been favoured, while maintaining risk at an acceptable level. However, the pre-conceptual design delivered by the end of 2012 still includes some open options. On completion of this phase it has been possible to obtain, for the important deadline set by the June 2006 law, the first investment cost estimation. During the pre-conceptual design phase, interactions were initiated with the Safety Authorities on safety objectives and

orientations. The conceptual design will be delivered by the end of 2014. During the conceptual design phase, the ASTRID design choices will be finalized and the Safety Option File will be submitted. Then from 2014 onwards, the basic design phase will start. ASTRID demonstration prototype is to be commissioned in the 2020 decade [2].
A first paper has presented the ASTRID nuclear island pre-conceptual design status at the end of 2011 [3]. This paper presents the foreseen status of the nuclear island at the end of the pre-conceptual design phase, with reservations as the paper is written while some final decisions regarding pre-conceptual design are still to be consolidated by the end of 2012.
The nuclear island scope includes the primary (figure 1) and secondary circuits and their components (intermediate heat exchanger, pump, Steam Generator, sodium-gas heat exchanger), the components handling systems, the fuel handling systems, safety related elements (core catcher, Decay Heat Removal), the vault, sodium auxiliary systems, and gas auxiliary systems.

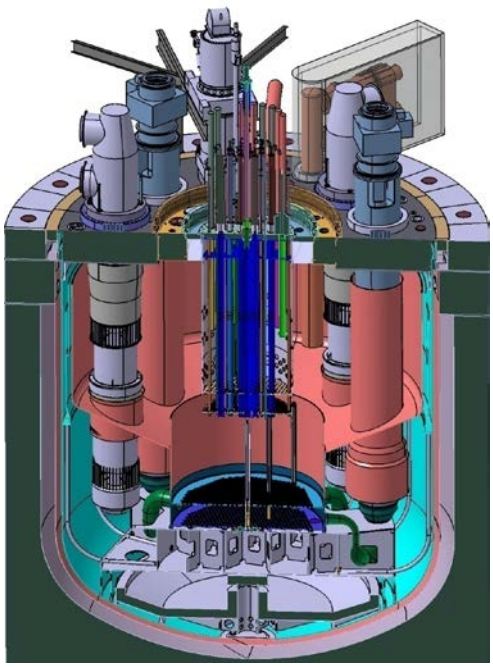

FIG.1. Primary circuit architecture
ASTRID Project Business Confidential Information, CEA and AREVA NP property designs

2. Core

ASTRID core design is mainly guided by safety objectives. The first one is prevention of the core meltdown accident, at first through natural favourable behaviour of the core and of the reactor, and with addition of passive complementary systems if natural behaviour is not sufficient for some transient cases. The second one is the mitigation of the severe accident to guarantee that core melting accidents do not lead to significant mechanical energy release. Core design objectives are the following:

- Natural favourable behaviour for transients of Unprotected Loss Of Flow (ULOF) and Unprotected Loss Of Heat Sink (ULOHS), target criteria: no sodium boiling for an ULOF.
- Sodium void effect minimized (target criteria: negative sodium void effect).
- Natural favourable behaviour for a complete control rod withdrawal, with no detection (target criteria: no fuel pellet melting).
- Performances (target criteria: cycle length about 480 EFPD, high fuel burn-up: 100 GWd/t, and a zero or positive breeding gain).

A first version of the CFV (French acronym for Low Sodium Void Effect) core called CFV V1 demonstrated the pre-feasibility of this concept [4]. CFV core, compared to previous SFR core like SUPERPHENIX or EFR in France, or to homogeneous standard SFR core, exhibit improvements in terms of performance and natural behaviour.
Feedback coefficients are optimized (in particular sodium void coefficient) to allow better natural behaviour in case of unprotected loss of flow transients: no sodium boiling with enough margins (short term behaviour), and temperature of neutronic shutdown reduced (long term behaviour) compared to SUPERPHENIX core.
These characteristics allow the possibility to eliminate energetic severe accident scenarios for the CFV core in case of ULOF.
The overall negative sodium void coefficient provides margin in case of global core boiling or sodium draining. This new specificity compared with standard core (void coefficient>$5) can be extrapolated to large industrial core.
The low core pressure drop is also favourable in case of rapid loss of flow transient or in case of natural convection flow.
The weak loss of reactivity of the core during irradiation cycle is also favourable in case of the Control Rod Withdrawal accident.
Analysis of severe accident conditions is under progress. On-going definition of an updated version of CFV core should lead to improve their natural favourable behaviour, with the objectives to increase the sodium boiling margin and robust demonstration of no fuel melting in case of Control Rod Withdrawal accident.

3. Reactor

3.1. Core support structure

The core support structure aims to support the core and to position the assemblies in order to ensure the reactivity control and rods fall in normal and accidental conditions. It also drives sodium coolant toward the core in normal and accidental conditions.
Additionally, ASTRID core structure design aims to improve ISIR, and the associated constraints to severe mitigation strategy accident such as corium course toward the core catcher.
Several options have been investigated. The selected design option is made up of a strongback supported by a skirt welded onto the main vessel at the bottom. Core support is designed with redundant load path at periphery (see figure 2). It is to be noted that for ASTRID, cold plenum is extended to primary vessel bottom.

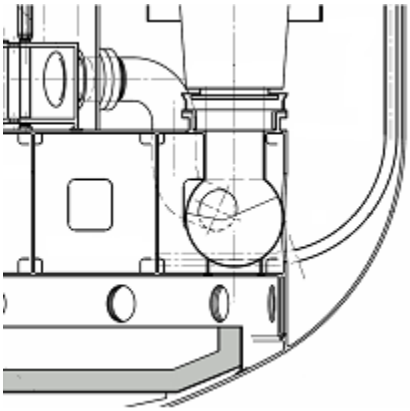

FIG.2. ASTRID core support structure design

3.2. Inner vessel

The inner vessel separates the hot pool, where are located the core subassemblies and the IHX (intermediate heat exchanger) inlets, from the cold pool where are located the IHX outlets and the primary pumps inlets.
Several internal vessel architectures were examined: single conical redan, cylindrical inner vessel outside IHX and primary pump components circle, cylindrical inner vessel located within IHX and primary pump components, and stratified redan inner vessel [5]. Pool-type reactor with conical redan is chosen, a solution extrapolated from previous reactors and the EFR project, with expected improvement related to ISIR, especially with regard to accessibility. Other solutions were discarded because considered as insufficiently mature (stratified redan) or offering poor ratio "technological challenge versus potential benefits".
The redan bottom is directly welded on the peripheral shell of the diagrid.
Mechanical seals are integrated for the IHX hot/cold pool leak tightness in order to limit any risk of gas entrainment into the core in comparison with a gas bell.

3.3. Main vessel

The main vessel is fabricated in austenitic steel (316L(N)). The main vessel cooling system is achieved using a derived cold flow from the diagrid lower plate through pipes routing to the main vessel cylindrical part. An immersed weir limits the risk of gas entrainment and ensures creep and fatigue resistance of the main vessel over 60 years. Automatic welding for 316L(N) is foreseen for vessels and inner components.

3.4. Safety vessel

Safety vessel is an envelope around the main vessel, with two main functions: contribute to confinement, and prevent core uncovering in case of sodium leakage outside the main vessel. Because of the latter function, the gap between the two vessels should be limited, so that the sodium free surface drop in the main vessel is limited in case of leakage. However, the gap between the main vessel and safety vessel should be large enough to accommodate a wheeled ISI vehicle for inter-vessel inspection and to avoid main and safety vessels contact in case of Core Disruptive Accident. The gap width may also be impacted by the choice of technology for Decay Heat Removal (DHR) through vessel.
Two options are kept open in the pre-conceptual design, associated to the different concepts of core catcher: suspended vessel (with core catcher in the main vessel or outside the safety vessel), or supported vessel (with core catcher between the main vessel and safety vessel). The gap between the two vessels would be filled with nitrogen. The safety vessel may be fabricated using another grade than main vessel to avoid common mode failure.

3.5. Above Core Structure

The main functions of the Above Core Structure (ACS) are to support the control rod drive mechanisms and core instrumentation, and to control the primary sodium flow distribution into the hot pool to achieve the required thermal-hydraulic conditions and quality of the sodium free surface. The ACS supports the Direct Lift Charge Machine that allows for core centre fuel sub-assemblies handling.. The main sub-assemblies of the ACS are as follows: the outer shell, the baffle plate, the grid plate, the shroud tubes, instrument guide tubes, the thermocouples and the multiple layer insulation.
The ACS extends over one row of radial steel reflector.
Various designs have been considered, for ACS, such as conical or cylindrical body. Studies resulted in the choice of cylindrical ACS, as this design allows for the integration of full core instrumentation (thermocouples, failed fuel location sampling, fission chambers…).

The adequate alignment between ACS and the core sub-assemblies must be maintained, except during the refuelling, to allow the entry of absorber rods in both normal and incidental/accidental situation. Distortion must therefore be minimized.
One of the most important problems to be solved for the ACS design is to get a structure rigid enough to resist the core sodium outlet flow without vibration and displacement and the seismic loadings, but flexible enough to accommodate thermal differential stresses due to core coolant emerging flow temperature variations and gradients.
Another important challenge is the lifetime of this component. While it is initially foreseen for 60 years operation, its lower part may incur important irradiation damage, and the possibility of replacement of this component is now considered.

3.6. Roof and rotating plugs

The roof slab ensures several functions. The first function is to ensure the containment of the primary circuit in the same way as the main vessel and the rotating plugs. The second function is the support of the components, the rotating plugs and the ACS. The third function is the radiological protection of the personnel in normal operation and during maintenance periods.
Metallic roof is cooled, without water, down to 120°C at the lower surface, to avoid sodium aerosols deposition. Roof has enhanced resistance to CDA (Core Disruptive Accident).
Rotating plugs are pieces made of thick plate steel, making a consistent closure design regarding core accident.

3.7. Core catcher

Despite design studies for ASTRID in order to prevent the risk of core melting, this accident is taken into account with the implementation of a core catcher.
The main core catcher function is to collect and manage the corium (melted core and metallic structure) after the Core Disruptive Accident, contributing to the three main safety requirements: confinement (collection of the whole corium, preventing any uncontrolled scattering of corium solid fragments or liquid phase), control of reactivity (maintaining of sub-criticality of fissile material), and efficient and long term post-accidental DHR.
The core catcher design includes the tray to collect the corium, plus one or more material layer(s) to protect the component and/or to maintain corium subcriticality.
Mechanical structure shall resist to the highest energetic accident considered (CDA) and to external aggressions (earthquake, plane crash…). Lifetime of 60 years, plus post-accident management period is integrated in design studies. All materials shall be compatible with its environment in normal and accidental conditions (sodium, gas, corium). Component shall not interfere with normal operation of the reactor.
At this stage of the studies, several core catcher implementation options are considered.
The first concept proposed is an internal core catcher (inside the main vessel). Main vessel is protected, and the system benefit from Decay Heat Removal systems implemented in the vessel. Nevertheless, the core catcher is kept in sodium environment for the whole lifetime of the reactor due to its location below core support structure, raising difficulties associated to material selection, accessibility for inspection and repair…
The second concept investigated is an inter-vessel core catcher, located between the main vessel and the safety vessel. Safety vessel is protected, without drawback associated to long time residence in sodium. Nevertheless, the concept needs a dedicated cooling system, which may interfere with inspection requirements (vessels, internals). It would also increase the inter-vessel gap width, with consequences on sodium level drop in case of main vessel leakage.

The third concept evaluated is an external core catcher, placed at the bottom of the reactor vault, below safety vessel. This concept eliminates drawbacks associated to long time residence in sodium, and presents an easier access for inspection of core catcher, and a limited interference with reactor operation or ISIR. Nevertheless, this implementation of the core catcher requires to establish safety function in the reactor vault (both main and safety vessel integrity are considered lost in case of core melting).

3.8. Intermediate Heat Exchanger

The IHX is the component where heat resulting from nuclear reactions is transferred from the primary sodium to the secondary sodium, hence being the gate toward the Power Conversion System. The IHX is a straight tube counter flow heat exchanger with primary sodium on the shell side of the tubes. It forms a leak tight barrier between primary and secondary sodium. The unit with embedded radiological protection is fitted with instrumentation.
Four units will be implemented, their weight being carried by the roof structure. They are designed to be inserted and removed vertically through the reactor roof penetration, with handling mode (vertical or horizontal) still to be confirmed. Each of the four IHXs is required to transfer 375 MW of heat from the primary sodium to the secondary circuit sodium. The IHX unit is connected physically and functionally to both the primary and secondary sodium circuits and as such is designed to meet the specified secondary circuit pressure (assumed value 55 bars, category 4) for the Steam Generator unit design based accident.
The IHXs are made from austenitic stainless steel, grade 316L(N).

3.9. Primary mechanical pump

Primary pumps aim at circulating sodium through the core to remove the thermal power produced into the core. The three primary pumps are incorporated into the reactor vessel and pump primary sodium from the cold pool plenum, at the outlet of the 4 IHXs, to the diagrid, where it is directed to the reactor core. The elements installed on the reactor roof also provide radiological protection. Each primary pump contains a cylindrical casing and vertical shaft machine, inserted into the primary circuit via a penetration of the reactor roof. The primary pump design includes the following main features: single flow impeller, top inlet entry flow to the impeller, subcritical drive-shaft. It's designed to operate with the first critical whirling speed having an adequate margin above the maximum operating speed and synchronous drive motor. As an alternative to oil bearing, the pump shaft could be supported at the top by magnetic thrust and radial bearing. A hydrostatic sodium bearing is located at the bottom (alternative: above) of the shaft above the impeller and is fed with high pressure sodium from the reception sphere. The bottom end is connected by pipes to the diagrid of the reactor, while the pumps suction side (inlet to the impeller) communicates directly with the reactor's cold pool via a suction skirt.

3.10. In-vessel Fuel Handling System

Fuel Handling System is reviewed to improve handling rates and its reliability; fuel loading and unloading will continue to be performed in sodium since this provides greater operating flexibility in normal and incident conditions. This system consists of two rotating plugs, a DLCM (Direct Lift Charge Machine), a FACM (Fixed Arm Charge Machine), the exchange or transfer positions (put down, take over positions in the core), and the load unload station in the reactor. Access to any core positions is achieved by rotation of rotating plugs, with help from the FACM for the outer handling zone. The DLCM is used for removal and insertion of core components belonging to the inner handling zone. The FACM is accommodated on the LRP (Large Rotating Plug). It is used for removal and insertion of core subassemblies belonging to the outer handling zone. Furthermore, it forms the link between the load unload station in the reactor and the direct lift charge machine using intermediate put down / take over positions at the inner core zone boundary.

Two solutions are identified for the subassembly fuel transfer from the primary vessel: using an inclined fuel transfer machine or a cask. Subassemblies are evacuated to sodium External-Vessel Storage Tank defined to cool the assemblies before their cleaning and unloading.

3.11. Decay Heat Removal

Decay Heat Removal is one out of the three main safety functions for nuclear reactors. Consequences of a failure of DHR function leads to an increase of sodium temperature, thus degradation of structures and may eventually reach sodium boiling point. However, SFR presents advantages when compared to other reactors: large margin before sodium boiling extended grace period due to large thermal inertia, and architecture favouring natural convection priming.
Goal of DHR systems is to ensure reactor cooling after shutdown in all conditions.
ASTRID design aims to the practical elimination of the long duration total failure of DHR systems. Demonstration of practical elimination is based on deterministic approach (multiple systems, redundant and separated) and on high reliability of the systems (probabilistic safety assessment).
Various DHR systems have been used or suggested in the past, which are summarized on figure 3.

- Sodium-air loop, using secondary circuit (connected circuit on secondary pipes, or dedicated heat exchanger integrated in Intermediate Heat Exchanger).
- Circulation of air along Steam Generators vessels.
- Dedicated circuit set outside of reactor vessel, using vessel wall as heat exchange surface.
- Dedicated sodium/air loop, with its own heat exchanger located in the primary circuit.

ASTRID current reference considers three independent systems:

- (1) Dedicated sodium-air loop, with its own heat exchanger located in the primary circuit, with natural convection flow (two in-vessel decay heat exchangers in the cold plenum).
- (2) Dedicated sodium-air loop, with its own heat exchanger located in the primary circuit, with forced convection flow (two in-vessel decay heat exchangers in the hot plenum); this system can operate under natural convection with lower performance
- (3) Dedicated circuit set outside of reactor primary vessel, using vessel wall as heat exchange surface. This system through the vessel is mainly intended to provide cooling in severe accident condition, with the objective to complement above Direct Reactor Cooling systems (1) and (2).

The following options are also under evaluation: integration of DHR heat exchangers in IHX for system (1) or (2), and use of alternative fluid (such as NaK or oil) to prevent coolant freezing in coolant/air heat exchanger.

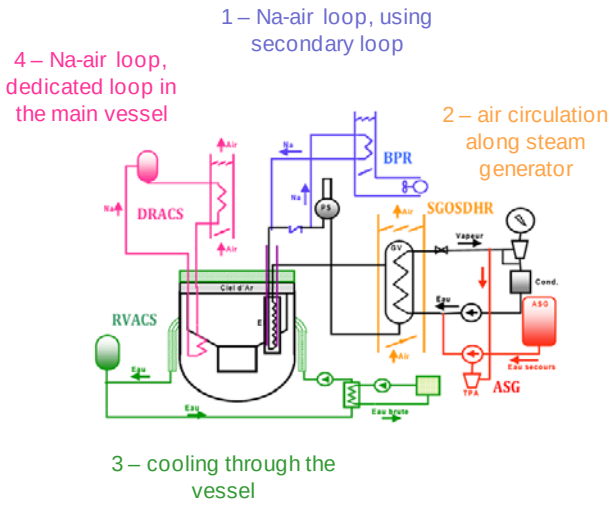

FIG.3. Decay Heat Removal systems

4. Secondary loop

4.1. General features

The four secondary loops route the secondary sodium from the IHX to Steam Generators or the sodium-gas heat exchanger according to PCS selection. These loops are running through tunnels in order to reduce sodium risk. Loop architecture depends on PCS type. In the reference loop layout, the secondary pump is an Electro Magnetic Pump. The function of expansion vessel is taken over by the cover gas filling Steam Generator headers. The efficiency and reliability of the systems designed to detect sodium leaks and fires will be improved. The possibility of installing double-envelope pipes, inerting rooms or using confinement measures to stifle fires is also considered.

4.2. Secondary Electro Magnetic Pump

As previously mentioned, the ASTRID pre-conceptual design phase kept open several sub-systems options. Innovative options and technical breakthroughs are favoured during this phase, while maintaining risk at an acceptable level. Among the open options, Electro Magnetic Pump (EMP) is considered for replacing mechanical pumps on secondary sodium loops. Both technologies are investigated and the decision to implement EMPs on ASTRID secondary loops should be taken before the end of the conceptual design phase (before end 2014). The main objective of future work is to design EMP for ASTRID secondary loops and to bring out technical elements to support the go/no go decision for the EMP implementation at the ASTRID start-up [6].

4.3. Steam Generator

One of the objectives for the ASTRID reactor is related to the elimination or better mastering of SWR [7].
As Rankine steam water cycle remains an option for the project, studies related to Steam Generators design aim to the elimination of large size SWR, or to be able to mitigate the consequences of such a reaction. This led to the selection of two main technologies presented below, both comprising a tube bundle enclosed in a vessel: classical design and inverted design (sodium flowing inside the tube bundle).
Modular Steam Generator concept is selected for ASTRID, as it intrinsically limit the mechanical consequences of a postulated large SWR, by limiting the sodium available in a single module for the reaction. It also brings flexibility for the expertise of failed modules after their removal.
Steam Generator technical solutions considered are presented below (see figure 4).
Two sub-families are considered to represent the “classical” design, where sodium flows in the vessel while water circulates inside the tube bundle. The first one is a helical Steam Generator made of Alloy 800. The hot sodium entering each Steam Generator module is collected in an inner distribution plenum, from which it flows down around the helical tubes. The sodium level within the distribution plenum is allowed to vary freely, in order to absorb pressure waves due to SWR. Moreover, a design adapted to a compact secondary loop with hot leg and cold leg connected at the bottom part of the Steam Generator is under investigation.
The second technology is characterized by straight tubes bundle, made of 9%Cr. The development of a straight tubes design Steam Generator was launched based on preliminary economic estimations showing that the straight tubes design was cheaper than the helical one, and expected easier manufacturing, in particular for an in line production. Major drawback of straight tubes concept appears to be faster wastage effect when compared to helical concept.
The second family, so called inverted design, offers sodium flowing inside the tube bundle, while water circulates in the vessel. This concept proves to be very preferable from the leakage viewpoint because the evaluation of the tube wall damage is slower and qualitatively different to the Steam Generator types where water flows inside the tubes. Major issues are the SWR consequences, design with external pressurized shell, and in service inspection.

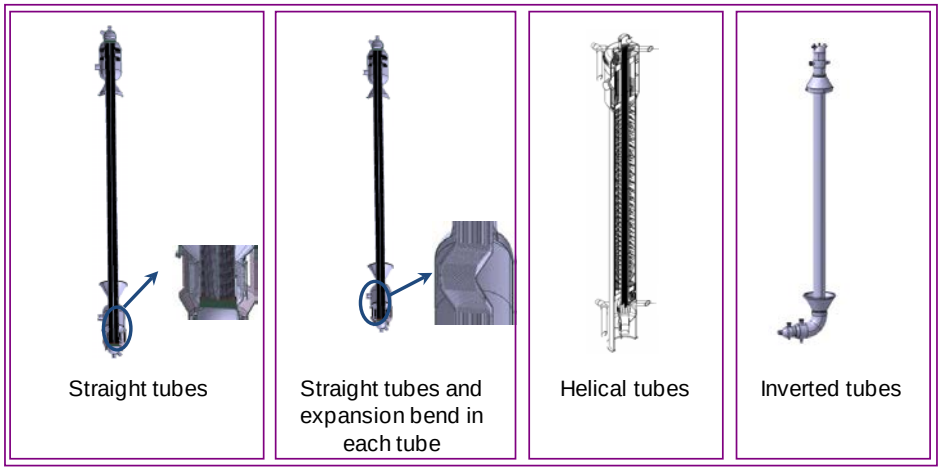

FIG.4. Steam Generator concepts

4.4. Sodium-gas heat exchanger

One solution to prevent SWR is the use of alternative coolant to water to feed the turbine. For ASTRID, the alternative open solution during conceptual design studies is the Brayton gas cycle. In this case, selected gas is nitrogen. One of the biggest challenges for this option is the development of the key component where heat is transferred from secondary sodium to gas: the sodium-gas heat exchanger.
Several technical solutions are considered for this component [8].
The first family, the "compact plates exchangers", are based on a bundle (or stack) of corrugated plates, where sodium and gas flows through channels, the bundle being placed in a pressure vessel. Plates Machined Heat Exchangers (PMHE) is retained, where the corrugations are made by machining (classical, chemical etching…). The diversity of feasible heat transfer patterns is very large: classical micro-channels of different cross-section area could be used, up to fins which could be machined in the plate. The most common PMHE is the one developed by HEATRIC Company, where the plates are assembled by uni-axial diffusion bonding.
The second family is based on shell and tubes heat exchanger design. The concept is a more robust back-up option, but leads to heavy components and large floor space requirements; feasibility and integration remain to be evaluated more in detail.
Beside the mechanical and thermal constraints for designing a compact heat exchanger, the design of the sodium-gas heat exchanger must incorporate constraints associated to the ease of inspection and the disassembly of the component during phases of maintenance, while keeping the component compactness.
The design of ASTRID is based on the French design and manufacturing code RCC-MRx, which do not include in its current release rules corresponding to this type of exchangers, thus code development is on-going in parallel to the design.

5. Conclusions

This paper presented a status of the pre-conceptual design of the ASTRID prototype. The most promising options are highlighted. The pre-conceptual design has been delivered by the end of 2012. The conceptual design will be delivered by the end of 2014.

NOMENCLATURE

ACS	Above Core Structure
ASTRID	Advanced Sodium Technological Reactor for Industrial Demonstration

CDA	Core Disruptive Accident
CFV	Cœur à Faible effet de Vide sodium (low void effect core)
DHR	Decay Heat Removal
DHX	Decay Heat Exchanger
DLCM	Direct lift charge machine
EFPD	Effective Full Power Days
EFR	European Fast Reactor
EMP	Electro Magnetic Pumps
FACM	Fixed Arm Charge Machine
IHX	Intermediate Heat eXchanger
ISI	In Service Inspection
ISIR	In Service Inspection and Repair
LRP	Large Rotating Plug
PCS	Power Conversion System
PMHE	Plates Machined Heat Exchangers
PP	Primary Pump
RCC-MRx	Règles de Conception et de Construction des Matériels Mécaniques des Installations Nucléaires – Réacteurs Rapides et Réacteurs Expérimentaux (in French) – Design and Construction Rules applicable to equipment of Fast Reactors and Experimental Reactors
SFR	Sodium-cooled Fast Reactor
SWR	Sodium-Water Reaction
ULOF	Unprotected Loss Of Flow
ULOHS	Unprotected Loss Of Heat Sink

REFERENCES

[1] F. Gauché; The French Prototype of 4th Generation Reactor: ASTRID; Annual meeting on nuclear technology, Berlin, May 17&18th; 2011.

[2] P. Le Coz *et al.*; Sodium-cooled Fast Reactors: the ASTRID plant project; Proceedings of ICAPP'11, Nice France, May 2-5, 2011; Paper 11249.

[3] M. Saez *et al.*; The pre-conceptual design of the nuclear island of ASTRID; Proceedings of ICAPP'12, Chicago United-States, June 24-28, 2012; Paper 12070.

[4] F. Varaine *et al.*; Pre-conceptual design study of ASTRID core; Proceedings of ICAPP'12, Chicago United-States, June 24-28, 2012; Paper 12173.

[5] E. Breuil *et al.*; Assessment of pool type Sodium Fast Reactor design options; Proceedings of ICAPP'11, Nice France, May 2-5, 2011; Paper 11151.

[6] G. Laffont *et al.*; Large capacity EMP design for application in ASTRID sodium cooled fast reactor; Proceedings of FR13, Paris France 4-7 March 2013; Paper CN-199-263.

[7] M. Saez *et al.*; Sodium-Water Reaction approach and mastering for ASTRID Steam Generator design; Proceedings of FR13, Paris France 4-7 March 2013; Paper CN-199-126.

[8] G. Laffont *et al.*; ASTRID Power Conversion System: assessment on steam and gas options; Proceedings of FR13, Paris France 4-7 March 2013; Paper CN-199-262.

Gas Cooled Fast Reactors: recent advances and prospects

C. Poette[a], P. Guedeney[b], R. Stainsby[c], K. Mikityuk[d], S. Knol[e]

[a] CEA, DEN, DER, F-13108 Saint-Paul lez Durance, CADARACHE, France.

[b] CEA, DEN, DEC, F-13108 Saint-Paul lez Durance, CADARACHE, France.

[c] AMEC Knutsford UK

[d] PSI Villigen Switzerland

[e] NRG Petten Netherlands

Abstract. The paper presents the current status of the Gas cooled Fast Reactor system development which is shared within the Generation IV International Forum including Euratom through the 7th Framework Programme project GoFastR. The various areas considered will include suitable fuel compounds and high temperature resistant cladding materials options, core design optimisation, primary system boundary, energy conversion. The safety approach, mainly oriented on core cooling for the moment, will be recalled together with a discussion of the results obtained. Further potential improvements or simplification of the system safety, at the light of the Fukushima accident, including an indirect coupled cycle for the energy conversion and a self sustainable Decay Heat Removal loop will be mentioned. The main issues related to the necessary R&D programme accompanying the system development will be recalled (fuel and materials, helium coolant technology, components such as gas circulators, valves and heat exchangers, thermal barriers).

1. Introduction

The attractive GFR concept aims to combine the benefits of fast spectrum and high temperature (up to 850°C), using helium as the coolant.

The high coolant temperature allows targeting high energy conversion efficiency (43-48%) and opens the possibilities for new application of nuclear energy, such as process heat production for example for metallurgy, hydrogen or synthetic hydrocarbon fuel production. The GFR concept aims to serve these new applications in a sustainable manner for the long term. In addition, the potential merits of the helium coolant regarding safety, in-service inspection and repair, operability and dismantling are acknowledged in spite of the longer development time needed by this new reactor line:

- no threshold effect due to phase change, very limited void reactivity effects, providing a quasi-decoupling of the reactor physics from the state of the coolant, no chemical reaction,
- optical transparency, temperature measurement capabilities, inert and non toxic, not activated.

This concept is clearly innovative, as no demonstrator has ever been built, and challenging because of the relatively poor thermal properties of the coolant compared with liquid metals, used traditionally as fast reactor coolants. This technology combines the constraints of fast reactor systems, in particular high power densities and poorer cooling capacity of gases, in this case helium, which must be pressurised in normal operation to achieve sensible gas velocities in the core with reasonable gas pumping power. These constraints are at the basis of the two major issues of this reactor system:

- The design of a high temperature fuel element, able to retain integrity in case of a loss of forced cooling accident, to withstand high fast neutron fluxes, and offering good neutronic performance,
- The safety and the decay heat removal in case of loss of helium pressure.

The development roadmap includes parallel viability studies of:

- the target commercial electricity generating reactor (~ 2400 MWth) and its fuel,
- a moderate power demonstrator, ALLEGRO (< 100 MWth) without electricity generation as a necessary step towards an electricity generating prototype before series production of commercial reactors.

2. Fuel element

The GFR fuel element needs to answer to challenging specifications with high operating temperatures. In normal operation, the helium core outlet temperature is 850°C, with a clad temperature around 900 to 1100°C. The clad must remain leak-tight in accidental conditions up to 1600°C and the cooling of the fuel element must be possible up to 2000°C.

The CEA has developed a totally innovative fuel element concept, based on composite ceramic honeycomb plate silicon carbide structures. The honeycomb structure includes mixed carbide (U,Pu)C pellets (see Fig. 1). Such a plate concept is attractive, because it allows a close confinement of the fission product around each fuel pellet.

The choice of a carbide fuel appears necessary for several reasons:

- its high thermal conductivity allows acceptable maximum operating fuel temperatures,
- the high helium fraction in the core introduces a neutronic penalty (to obtain self sustaining cores without fertile blankets) which is partially compensated by the high carbide fuel density , also favourable to limit the in-core Plutonium inventory.

Refractory metallic cladding materials, such as niobium, molybdenum or tungsten were discarded as being too strong neutron absorbers. The silicon carbide ceramic appeared the best compromise and the reference cladding material choice. Nevertheless, technical plate fabrication difficulties appeared which could compromise the leak-tightness of the fuel element resulting in a shift of attention to concentrate on a more classical pin concept. (see Fig. 1 also). Recent advances on the concept are described in [1]. They include (see Fig. 2):

- a ceramic matrix composite cladding comprising a sandwich of SiC cladding and a thin internal metallic liner to ensure the leak tightness of the pin [8];
- a “buffer” , porous carbon structure placed between the pellet and the cladding allowing higher heat exchanges and moderate clad/pellet mechanical interaction [9].

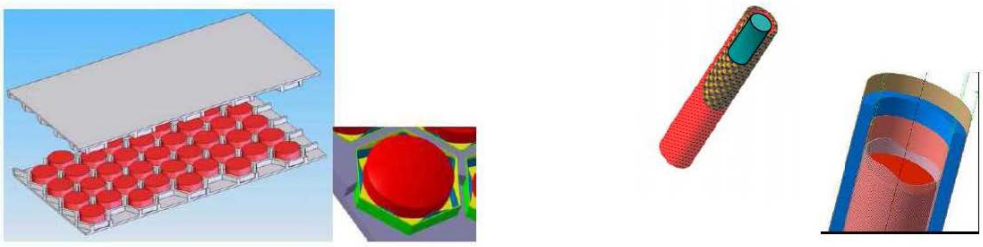

Fig. 1 : illustration of the two GFR fuel element concepts : honeycomb plate on the left and pin on the right

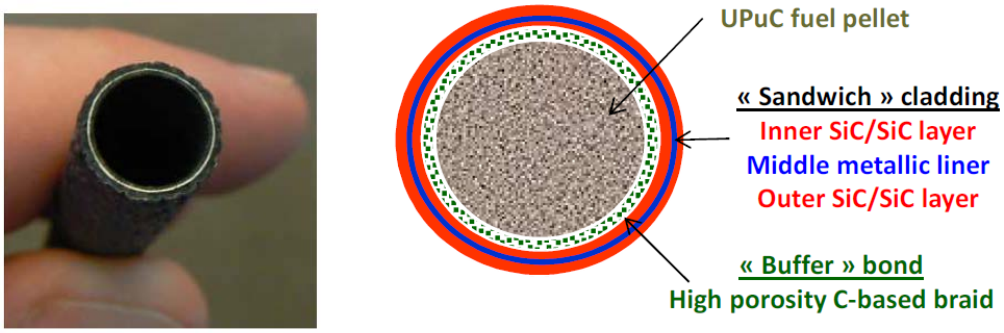

Fig. 2: sandwich cladding and buffer bond

Modelling efforts between different codes showed discrepancies due to uncertainties in the experimental data. To extend the lifetime of fuel elements, analytical irradiations on (U, Pu)C would provide useful data on swelling, fission gas release and restructuring. For a full qualification eventually an irradiation in representative conditions would be required.

3. Core design optimization

The concept of closed sub-assemblies (hexagonal tube similar to SFR concepts) constituting independent channels with independent gas feeding is the reference for the core design. The hexagonal geometry of the tube ensures optimal core stability and its mechanical equilibrium.

Considerations of transport, handling and fabrication lead to limit the pin length to about 1.50m. So, the total fissile length is made of two half pins to form the fissile column as it is shown in Fig. 3. This arrangement allows obtaining a fissile length in the range of 1 to 2 meters (1.65 m in the case of the reference core).

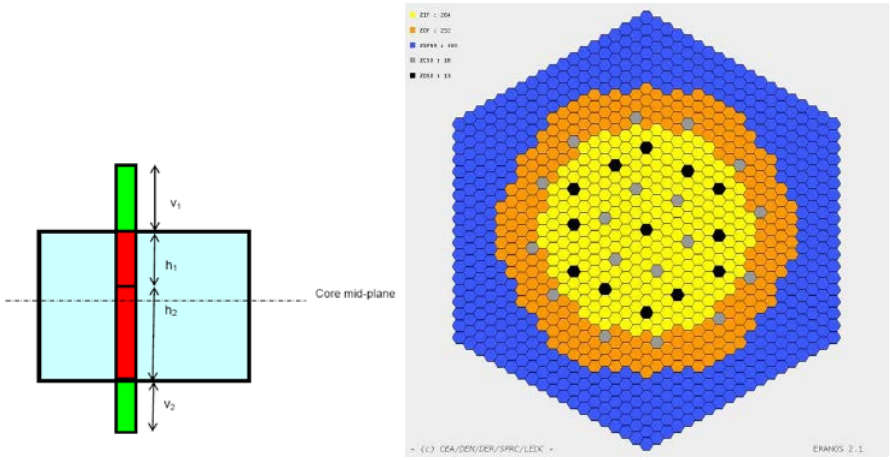

Fig. 3 : scheme of the principle of two half pins and core loading map ; h1, v1, h2, v2 are the fissile and fission gas expansion lengths of the upper and lower pins respectively

Usually, the core design of Generation IV reactors is essentially iterative. Because of the complexity of such a multi-physics system, several iterations between neutronics, thermal-hydraulics and thermo-mechanics are required before converging towards a concept with satisfactory features. Moreover, safety aspects are usually addressed in a very simplified manner (maximum temperature, core pressure drop, etc …) during the core pre-design phase, with most safety analyses being performed after the core pre-design phase, resulting in a few more iterations. Therefore, strong incentives push to improve the core features such as increasing the economy (higher burnup), decreasing the in-core and fuel cycle plutonium inventory, while improving the inherent core safety features (less constraints on DHR means, better natural behaviour,..). A tool, called FARM, belonging to the family of the meta-models, was developed at CEA in the frame of a PhD [2] [3] which consists in coupling directly the different analysis domains, using simplified models (analytical or interpolation of reference calculations), in order to optimize both core performances and safety characteristics. This tool was applied to the GFR cores and Fig. 4 illustrates an example of result of this optimization process (in terms of key performance and safety estimators) for the recent advanced fuel element concept (“Mathieu” core) compared to the reference (with metallic liner on cladding inner surface and without buffer).

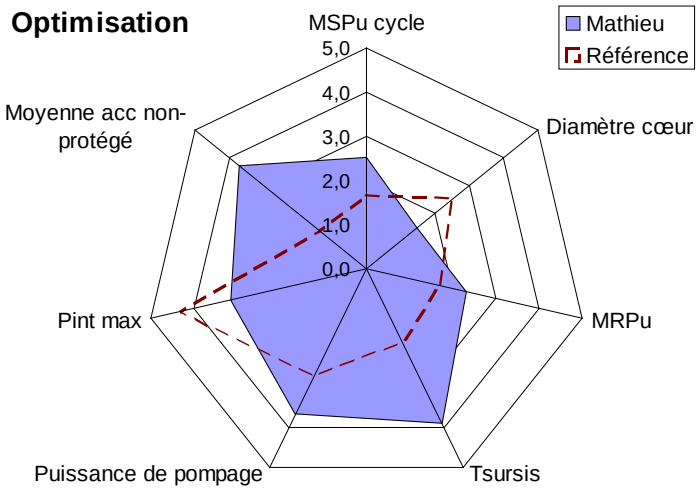

Fig. 4: Illustration of core performance parameters and safety indicators for the “Mathieu” core vs the reference core

(key: MSPu cycle = plutonium inventory per GWe in the equilibrium cycle, Diamètre Coeur = core diameter [inverse relative value in fact → smaller diameter is better], MRPu= reprocessed plutonium mass per GWe x year, Tsursis = Fuel grace time: time delay before cladding degradation, in adiabatic conditions with a decay heat power law, for a homogeneous pin temperature, Puissance de pompage = pumping power in LOCA conditions, Pint max = internal pin maximum nominal pressure, Moyenne acc non-protégé = mean value of the 3 Asymptotic fuel temperatures for slow ULOHS, USTOP and ULOF.)

It can be seen that most parameters of "Mathieu" are improved and especially the safety parameters. The core performances are also improved despite a slight increase of the core diameter. Such a core could become a new GFR reference if the buffer technology viability is confirmed.

4. System design

The indirect combined cycle was selected as the reference power conversion system. As shown on Fig. 5 , the system is arranged around three main primary loops of 800 MWth each, with a share in three secondary circuits (mixture He/N_2, 3 steam generators) and with only one tertiary loop (one steam turbine). The share of electric power delivered by the secondary/tertiary circuits is optimised from the thermodynamic efficiency point of view: it is respectively 23/77%.

The primary circuit is pressurized at 70 bar. This pressure value results mainly from the feedback experience of existing High Temperature Reactors: this is a trade-off between high pressures reducing the circulator power requirement and the limitations of pressure vessel strength in nominal conditions and also considering the impact of energy release in a depressurisation accident. This choice appears reasonable but was never optimized from the GFR point of view.

The secondary pressure remains close to the primary pressure to minimize the mechanical stresses on the intermediate heat exchanger (IHX) in normal operation being about 5 bar lower than the primary pressure. This choice remains open. The present configuration allows a quick detection of an IHX leak.

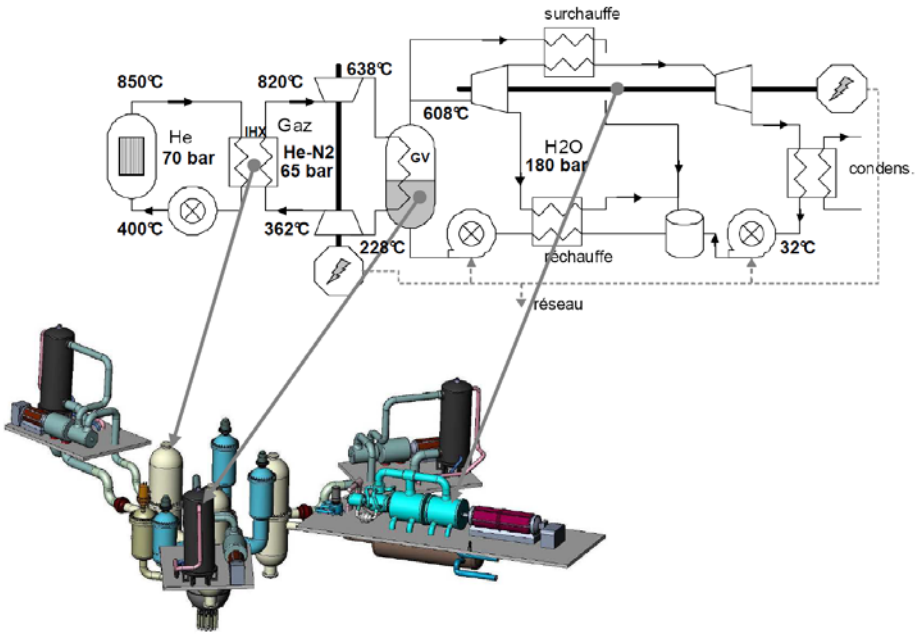

Fig. 5 : reference indirect combined cycle for GFR 2400 MWth

5. Safety aspects

The decay heat removal (DHR) systems and their operation rely on the initial design status [4] and evolutions proposed in further studies [5]. Generally speaking, the DHR function is ensured by:

- The circulation of helium gas contained in the primary circuit ;
- Depending of the situation encountered, the connected circuits are:
  a) Normal circuits, operated in forced (pony motor on the primary side) or natural circulation (on the secondary side); basically, heat is transferred to the steam/water circuit and rejected to the normal heat sink ; in case of problem with the steam/water circuit or heat sink, secondary circuits can be reconfigured to bypass the steam generator and the turbomachine and reject heat to the atmosphere using air cooler(Fig. 6 left side). Aero-refrigerants as well as steam generator water feed-pumps need electrical energy supply but only the air cooler is powered by the emergency supply (safety classified components supplied by battery and/or Diesel generator).
  b) Dedicated DHR loops connected to the primary circuit operating in forced or natural circulation (Fig. 6 right side). These loops are put into operation after isolation of the main loops, e.g., a primary circuit reconfiguration by valves actuation. Secondary coolant is pressurized liquid water and heat is rejected via natural circulation in a water pool disposed in the reactor building (hereafter DHR pool); each loop permits 24h of autonomous cooling considering the thermal inertia of the DHR pool. The DHR pool itself is cooled by active means.

A guard vessel (close containment) envelopes the primary circuit to ganerate a backup pressure of 5-10 bar in case of a breach in the primary circuit (LOCA). During a LOCA, nitrogen can be injected from passive accumulators directly in the primary circuit in order to enhance natural circulation in case of loss of active means. Nevertheless, the operation of the natural circulation DHR under nitrogen injection will require experimental qualification to be confirmed or more defined as a DHR means.

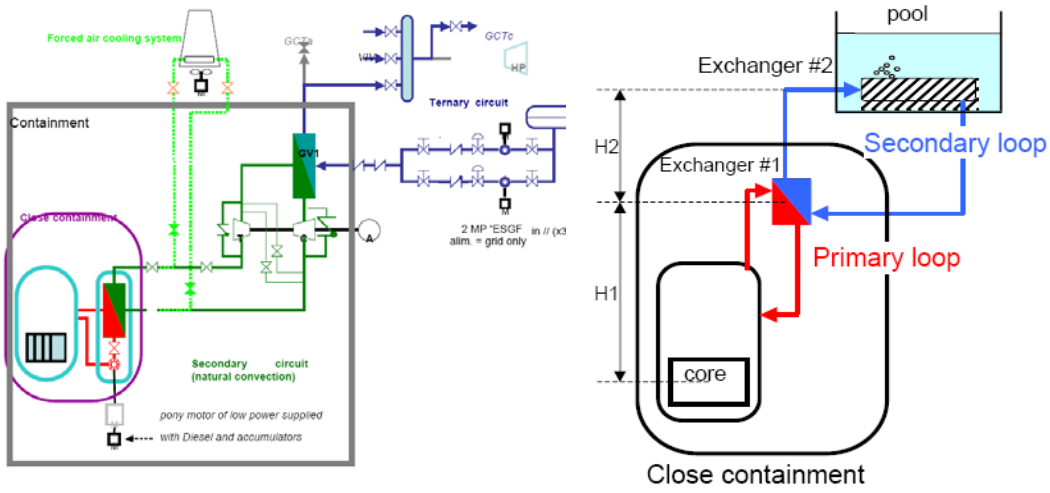

Fig. 6: DHR using the main circuits (left) and dedicated DHR loops (right)

In detail, there are a total of 4 dedicated DHR loops for diversity and redundancy. Each DHR loop is able to realize the function alone and is equipped with one circulator operating at variable speed (not represented on Fig. 6) so it can accommodate the various pressure conditions and configurations (number of circulator being in operation). Two of them (HP loops) cover the situations of primary pressure ranging from high to medium values (70-4 bar) and can be operated also in natural circulation depending on gas pressure ; the two others (LP loops) cover the situations of primary pressure ranging from medium to low values (4-2 bar) ; this low pressure range corresponds to a postulated situation with a break on the primary system cumulated with a break on the guard vessel (2 bar is the minimum

pressure when the primary gas inventory is released in the reactor building). Active cooling is required to meet the design criteria on the fuel element and the reactor structure in LOCA situations combined with the close containment failure. Fig. 7 illustrates the global integration of the primary system and DHR loops in the close containment.

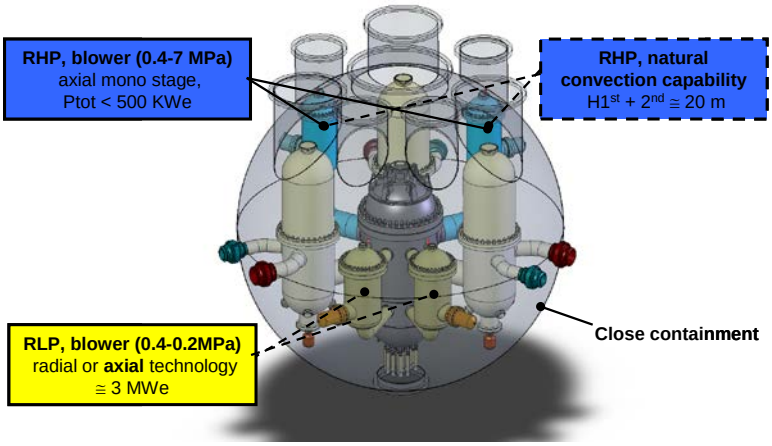

Fig. 7 : Integration of primary system and DHR loops in the close containment

Provisional conclusions based on CEA work, to be confirmed by the ongoing work shared in the FP7 GoFastR project, have confirmed the **encouraging potential of the reactor system** (about 50 Initiating Events considered, covering a wide range of representative GFR full power operating conditions, corresponding to about thirty characteristic accidental situations with potential aggravating failures).

Nevertheless, the operation of the DHR loops requires the primary circuit to be reconfiguerd by the actuation of valves. Valve actuation needs limited energy to be supplied by batteries, the latter are considered to be available even if there is no main power on site. Additionally, a failsafe configuration of flow path is a possibility but the feasibility of the associated components, i.e, valves with passive actuation has not yet been investigated.

The hypothetical situation of a loss of energy supply combined with the total failure of primary circuit reconfiguration cannot be totally excluded. The “system” composed of the primary coolant, the fuel and core materials has a poor thermal inertia. The temperature increase just limited by its thermal inertia would lead to a core degradation accident in a few minutes.

Further improvement of the GFR robustness is recommended and complementary design improvements emerged from the reflection, which are presented below.

6. Design Improvements

1 - Coupled-cycle

The objective is to cool the core for a long time period on a passive mode before reconfiguring the primary circuit and actuation of the DHR loops, **especially in the case of a primary system depressurisation.** This positive attribute is obtained with the “coupled-cycle” [6], a design option in which the primary circulator is connected to the same shaft as the secondary turbo machine(see Fig. 8) Some CATHARE2 calculations gave promising results, i.e., the feasibility of autonomous cooling during 24 hours in the case of a Large Break LOCA seems to be achievable, which improves significantly the grace time in which to switch from the main loop to the DHR loops. Such a concept could also be less demanding with regard to the requirement to have a guard vessel.

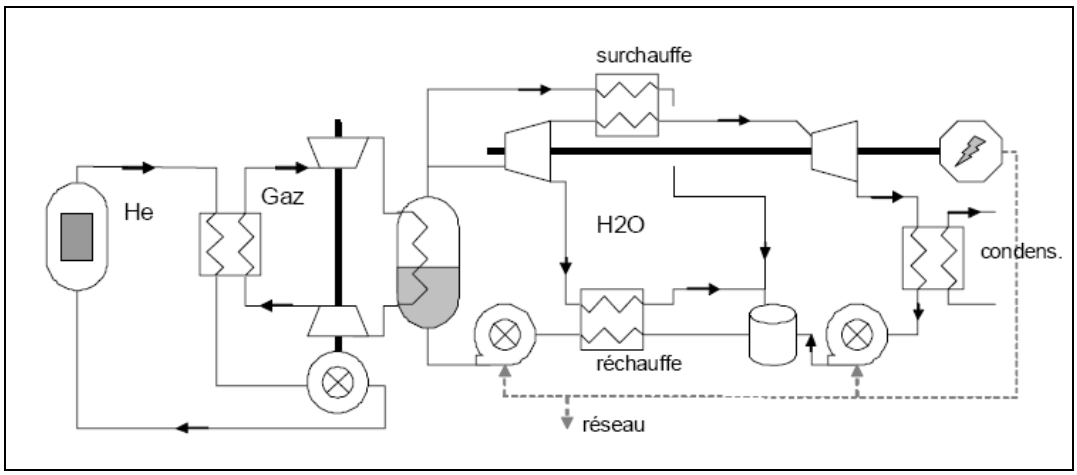

Fig.8: Principle scheme of the indirect coupled cycle: the primary circulator is mechanically coupled to the secondary circuit turbo-machine

2 - Autonomous DHR system

Exploratory studies have been performed to investigate the feasibility and performance of an autonomous DHR system designed to be operated at low pressure conditions and connected to the primary system similarly as the aforementioned DHR loops [7]. The particular feature of this system is that the primary gas circulation is ensured by a small turbo machine driven by the residual heat of the core (see Fig. 9). This quasi-passive system would complement the natural circulation in low pressure conditions.

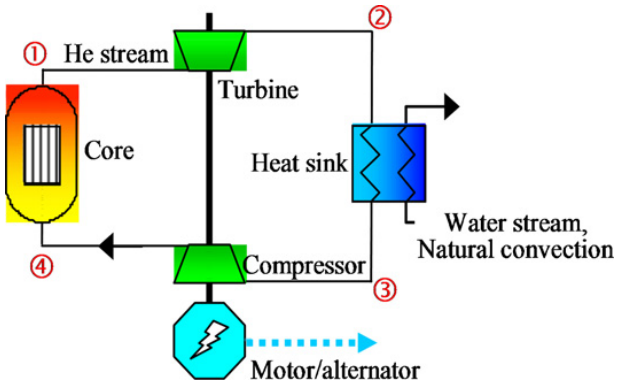

Fig. 9: Principle scheme of the autonomous DHR loop

7. R&D program

The main R&D issues related to the GFR system development were identified from the FP7 GoFastR and ADRIANA projects. The work performed was a unique opportunity for specialists (from CEA, NRG, KIT, ENEA, UJV and IRSN) of gas cooled reactors to meet and have a common reflexion on the specific technology needs for GFR and the ALLEGRO prototype. A network of contact persons in the various organizations having skills and facilities in the area of helium technology and related materials was established.

In addition to the qualification of the calculation tools, the following items appeared particularly important:

Fuel and materials:

This is a **key viability point** for the GFR system. It is necessary to develop at first a clad which answers to the core specifications in terms of length, diameter, surface roughness, apparent ductility, level of leak tightness (including the need of a metallic liner on the clad) , compatibility with polluted Helium, irradiation conditions. The needs include fabrication capacities and material characterization under normal and accidental conditions for fresh and irradiated fuel. The following points can be mentioned in particular:

- The use of a ceramic material implies to adapt a specific codes & standards approach, connected to appropriate tests and modelling,
- The SiC behavior in accidental situations must be fully characterized,
- Beyond the cladding, it is necessary to find solutions for the encapsulation of the pins, these studies being at a very early stage ,
- A program of irradiation of components and of qualification of fuel elements is, of course, also necessary.

The needs cover also helium coolant technology, including:

- The development of individual components or systems (fuel handling, thermal core instrumentation taking benefit of the helium transparency, compressors able to work in large pressure ranges, valves, check-valves, compact gas/gas heat exchangers, gas quality management, thermal barriers), for which existing Helium loops could be valued,
- The demonstration that these components and systems are able to work together especially for the safety demonstration. This requires large helium loops which need to be constructed at mid term.

8. Conclusion

The paper presents the current status of the Gas cooled Fast Reactor system development which is shared within the Generation IV International Forum including Euratom through the 7th Framework Programme project GoFastR. Provisional conclusions of the safety analysis have confirmed the **encouraging potential of the reactor system**. About 50 Initiating Events considered, covering a wide range of representative GFR full power operating conditions, corresponding to about thirty characteristic accidental situations with potential aggravating failures. Nevertheless, some situations require a rapid switch-over from the main loop to the DHR loops and, at the moment, the failure of this primary circuit reconfiguration cannot be totally excluded, partiuclarly considering the Fukushima accident initiators. Significant improvements of the design robustness are possible using the principle of primary circulator coupled to a secondary gas circuit turbo-machine. Even in case of primary circuit depressurization, the core cooling could be ensured for several hours, thus giving a large grace time to switch-over to the DHR loops at low decay heat power. The diversity and reliability of the DHR loops could also be improved using the principle of autonomous turbo-machine on one of them. This quasi-passive system would complement the natural circulation in the low pressure range.

The GFR development is connected to a R&D program on materials, calculations tools validation and specific helium technologies. The main items and potential facilities able to achieve this program were recalled. In particular, the **fuel material development** (high temperature resistant silicon carbide cladding) and the **qualification of safety relevant tools and components** appear as high priority needs.

ACKNOWLEDGEMENTS

The authors wish to thank EURATOM for their support to the 7th Framework Program GOFASTR project.

REFERENCES

[1] M. Zabiego et al., Overview of CEA's R&D on GFR fuel element design: from challenges to solutions, Proceedings of FR13 Conference, Paris, March 2013

[2] X. INGREMEAU et al., FARM: A new tool for optimizing the core performance and safety characteristics of Gas Cooled Fast Reactor cores, Proceedings of ICAPP'11, Nice, France, May 2-5, 2011. Paper 11053

[3] X. INGREMEAU, Méthodologie d'optimisation d'un cœur de réacteur à neutrons rapides, application à l'identification de solutions (combustible, cœur, système) permettant des performances accrues, thèse de doctorat de l'université Paris-sud 11, December 2011

[4] JY. MALO et al., Gas Cooled Fast Reactor 2400 MWth, status of the conceptual design studies and preliminary safety analysis, ICAPP'09, Tokyo, May 2009

[5] F. BERTRAND et al., Synthesis of the safety studies carried out on the GFR2400, Nuclear Engineering and Design, 253, pp 161-182, 2012

[6] N.TAUVERON et al., Preliminary design and study of the indirect coupled cycle: An innovative option for Gas Fast Reactor, Nuclear Engineering and Design, 247, pp. 76-87, 2012

[7] EPINEY et al., A standalone decay heat removal device for the Gas-cooled Fast Reactor for intermediate to atmospheric pressure condition, Original Research Article, Nuclear Engineering and Design, Volume 242, January 2012, Pages 267-284

[8] M. ZABIEGO, C. SAUDER, C. LORETTE, P. GUEDENEY, Tube multicouche amélioré en matériau composite à matrice céramique, gaine de combustible nucléaire en résultant et procédés de fabrication associés, Patent submitted 1 August 2011, in French

[9] « Joint d'Interface Solide à porosité ouverte pour crayon de combustible nucléaire et pourbarre de commande nucléaire », Brevet d'invention déposé le 16/06/2010 auprès de l'INPI, sous le N° 1054781, au bénéfice du CEA, in French

Recommendations for a demonstrator of Molten Salt Fast Reactor

E. Merle-Lucotte, D. Heuer, M. Allibert, M. Brovchenko, V. Ghetta, P. Rubiolo, A. Laureau

LPSC-IN2P3-CNRS / UJF / Grenoble INP, Grenoble, France

Abstract. There is currently a renewed interest in molten salt reactors, due to recent conceptual developments on fast neutron spectrum molten salt reactors (MSFRs) using fluoride salts. This concept, operated in the Thorium fuel cycle, may be started either with ^{233}U, enriched U and/or TRU elements as initial fissile load. It has been recognized as a long term alternative to solid fuelled fast neutron systems with a unique potential (such as large negative temperature and void coefficients, lower fissile inventory, no initial criticality reserve, simplified fuel cycle, wastes reduction…) and is thus one of the reference reactors of the Generation IV International Forum. This paper will focus on recommendations to define a demonstrator representing the key points of the reference MSFR power reactor (3000 MW_{th}, fuel salt volume of 18 m^3). The MSFR demonstrator is designed to assess the technological choices of this innovative system (fuel salt, structural materials, fuel heat exchangers…). It seems finally possible to slightly modify such a demonstrator which could then be a self-breeder modular reactor

1. Introduction and presentation of the MSFR concept

Molten Salt Reactor (MSR) technology was studied in the 1950's and 1960's in USA (Oak Ridge National Laboratory), including two demonstration reactors. These Molten Salt Reactors were initially designed as thermal-neutron-spectrum graphite-moderated reactors. Since 2004, the National Centre for Scientific Research (CNRS, Grenoble-France) has been focused R&D efforts on the development of a new fast-spectrum reactor based on the MSR concept. The reference MSFR (Molten Salt Fast Reactor) combines then the generic assets of fast neutron reactors (reduced neutron absorptions in the fission products, waste minimization) with those related to molten salt fluorides as fluid fuel and coolant (low pressure, high boiling temperature and optical transparency) [1][2][3][4]. As opposed to thermal molten salt reactors, the specificity of the MSFR is the absence of any solid moderator (usually graphite) in the core. This concept has been recognized as a long term alternative to solid fuelled fast neutron systems with a unique potential (large negative temperature and void coefficients, lower fissile inventory, no initial criticality reserve, simplified fuel cycle, wastes reduction…) and has thus been selected as one of the reference reactors of the Generation IV International Forum [5][6][7].

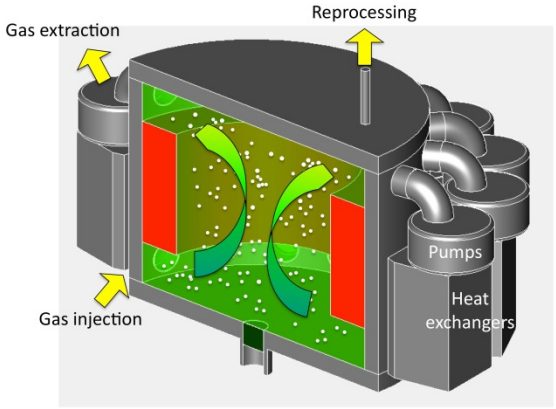

FIG. 1. Schematic conceptual MSFR design

The reference MSFR is a 3000 MWth reactor with a total fuel salt volume of 18 m^3, operated at a mean fuel temperature of 750°C. Figure 1 sketches the general component outlines for such a MSFR. The core consists of a circulating fluoride salt loaded with the fuel (note the absence of solid matter in core). The fuel salt composition currently being investigated is a binary fluoride salt with 77.5% of lithium fluoride enriched in ^7Li to 99.995 %; the other 22.5% are a mix of heavy nuclei fluorides. This proportion, set throughout the reactor evolution and corresponding to an eutectic point with a melting temperature of 565°C, leads to a fast neutron spectrum. This MSFR system thus combines the generic assets of fast neutron reactors (extended resource utilization, waste minimization) with those associated to a liquid-fuelled reactor. The characteristics of the MSFR are detailed in Table 1.

Table 1. Characteristics of the reference MSFR

Thermal power (MWth)	3000
Mean fuel salt temperature (°C)	750
Fuel salt temperature rise in the core (°C)	100
Fuel molten salt - Initial composition (mol%)	LiF-ThF_4-$^{233}UF_4$ or LiF-ThF_4-($^{enriched}U$+Pu+MA)F_3 with 77.5 % LiF
Fuel salt melting point (°C)	565
Fuel salt density (g/cm^3)	4.1
Fuel salt dilation coefficient (/°C) [8]	$8.82\ 10^{-4}$
Fertile blanket salt - Initial composition (mol%)	LiF-ThF_4 (77.5%-22.5%)
Breeding ratio (steady-state)	1.1
Total feedback coefficient (pcm/K)	-5
Core dimensions (m)	Radius: 1.1275 Height: 2.255
Fuel salt volume (m^3)	18 9 in the core 9 in the external circuits
Blanket salt volume (m^3)	7.3
Total fuel salt cycle in the fuel circuit	3.9 s

In the MSFR, the liquid fuel processing is performed during the reactor operation [9]. The on-site salt management of the MSFR combines a salt control unit, an online gaseous extraction system in the core (with gas injectors and bubble separators) and an offline lanthanide extraction component by pyrochemistry where a small stream (10 to 40 liters per day) of the molten salt is set aside to be processed for fission product removal and then returned to the reactor. This is fundamentally different from a solid fuel reactor where separate facilities produce the solid fuel and process the Spent Nuclear Fuel. Because of this design characteristic, the MSFR can operate with widely varying fuel compositions. Thanks to this fuel composition flexibility, the MSFR concept may use as its initial fissile load, ^{233}U or enriched natural uranium and/or also the transuranic (TRU) elements currently produced by PWRs in the world. The only natural fissile matter on earth is ^{235}U (0.72% of natural uranium), which can be used directly as enriched uranium in breeder reactors for their initial fissile load, or which can be loaded in fertile blankets in nuclear reactors to produce either ^{239}Pu by irradiating ^{238}U, or ^{233}U by irradiating ^{232}Th. To start a first fleet of MSFRs, we have thus investigated the following solutions [10]:

- Producing ^{233}U in the fertile blanket of other reactors (SFR…) or by irradiating ^{232}Th in an ADS for example, to start the MSFR directly with this ^{233}U as initial fissile matter. Once an initial park of the MSFRs based on the Th/^{233}U cycle is launched, ^{233}U will also be produced in MSFRs which are breeder reactors, allowing the deployment of such ^{233}U-started MSFRs in a second time period even if no ^{233}U is produced elsewhere.

- Using as initial fissile matter the plutonium produced in current PWRs or in future EPRs or, even better, the mix of transuranic elements (TRU) produced by these Generation 2-3 reactors. The calculations show that the initial Pu proportion of a TRU-started MSFR reaches the solubility limit given for a LiF-ThF_4 salt. A solution to limit the Pu initial proportion in the fuel salt consists in adding small amounts of ^{233}U or $^{enriched}U$ to reach criticality (see below).
- Starting the MSFR with enriched uranium as initial fissile matter, with an enrichment ratio lower than 20% due to proliferation resistance issues.
- A mix of the previous starting modes. For example, ^{233}U may be produced by using special devices containing Thorium and Pu-MOx (called "MOx-Th" thereafter) in current PWRs or in future EPRs.

Table 2. Initial heavy nuclei inventories per GWe of the different MSFR starting modes

Starting mode	^{233}U [kg]	TRU (Pu UOx) [kg]	^{enr}U + TRU [kg]	MOx-Th [kg]
Th 232	25 553	20 396	10 135	18 301
Pa 231				20
U 232				1
U 233	3 260			2 308
U 234				317
U 235			1 735	45
U 236				13
U 238			11 758	
Np 237		531	335	54
Pu 238		229	144	315
Pu 239		3 902	2 464	1 390
Pu 240		1 835	1 159	2 643
Pu 241		917	579	297
Pu 242		577	364	1 389
Am 241		291	184	1 423
Am 243		164	104	354
Cm 244		69	44	54
Cm 245		6	4	

In order to initiate the work and the discussions on possible ranges for the reactor parameters, basic drawings have been developed from the preliminary conceptual design. Figure 2 illustrates one of the possible geometrical configurations (height/diameter ratio = 1). In these preliminary designs, the core of the MSFR is a single compact cylinder (2.25m high x 2.25m diameter) where the nuclear reactions occur within the liquid fluoride salt acting both as fuel and as coolant. The return circulation of the salt (from the top to the bottom) is divided into 16 loops located around the core, each loop contaning a pump and a fuel heat exchanger (also labelled IHX for Intermediate Heat Exchanger). The total fuel salt volume ($18m^3$) is distributed 50% of it in core, 5% in auxiliary volumes (overflow tank, spaces…) and 45% in the bubble separators, the pumps and pipes, and the heat exchangers [11][12]. Since here the fuel salt also plays the role of the coolant, one of the main constraints on the design of the fuel circuit of the MSFR is the ability to evacuate the heat generated while restraining the fuel salt volume mobilized for that task. The time circulation of the fuel salt in the whole fuel salt circuit is of the order of a few seconds.

The neutronic reflectors, made of NiCrW-based alloy [13] in our calculations, constitute the lower and upper walls of the core. The lower reflector is connected to a draining system: in case of a planned

shut down or incident/accident leading to a temperature increase in the core, the fuel configuration may be changed passively by gravitational draining of the fuel salt in tanks located under the reactor where a passive cooling will be achieved.

The radial reflector includes a fertile blanket (50 cm thick - red area in Fig. 1 and 2) to increase the breeding ratio. This blanket is filled with a fertile salt of LiF-ThF_4 with initially 22.5mole % $^{232}ThF_4$. The blanket is surrounded by a 20cm thick layer of B_4C, which protects the external circuit from the remaining neutrons.

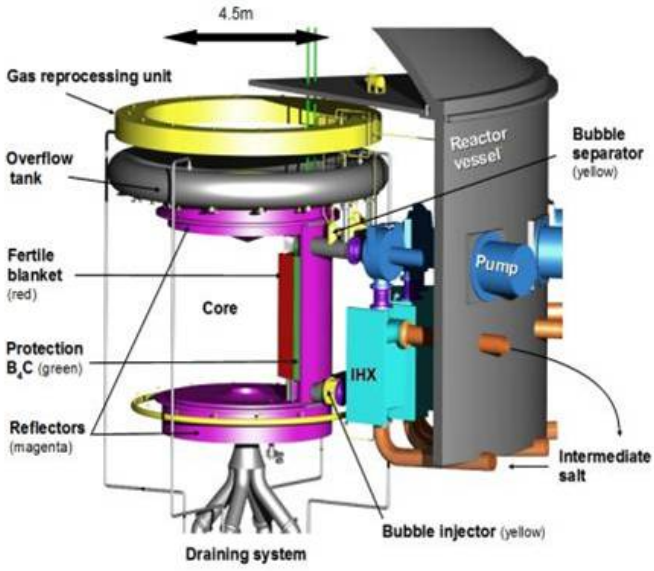

FIG. 2. Pre-design of the fuel salt circuit of the MSFR

2. Demonstration and Demonstrators of MSFR

2.1. What needs to be demonstrated

Given the nonconformity of the concept and the lack of current expertise, it is clearly not possible to move directly to a demonstration phase involving actinides. Prior to that, a variety of experimental setups have to be devised to validate insofar as possible the technological solutions, with non-radioactive or weakly radioactive materials, and demonstrate their viability to the safety authorities. The want of experts in the specific field of molten salts entails, in any case, a time lag due to the training of both the designers of the concept and the safety authority personnel.

In the frame of this R&D, the experimental setups can and should, in the initial phases of the demonstration, be limited in size and complexity so as to facilitate the necessary modifications that will be associated to the developments. Thus, at the early stages, the experiments may work with "simulant salts" and move to a fuel salt depleted in fissile elements (containing neither Pu nor ^{233}U/$^{enriched}U$) only when it will become really necessary for the assessments considered. The devices that are to be planned later must go as far as the quantification of the characteristics so as to allow the validation of the mathematical models which will be used to define precisely the details of a demonstrator that integrates all the previously tested functions. Finally, experimental studies will have to involve a salt with induced fissions to demonstrate the viability, strictly speaking, of the concept.The section 2.4 will focus on this final demonstrator called "power demonstrator".

2.2. Phases of the demonstration and conception of the demonstrator

The demonstration phases comprise 3 degrees corresponding to 3 radioprotection levels: non radioactive (simulant salt), radioactive (^{nat}LiF-ThF_4-$^{depleted}UF_4$-$^{depleted}UF_3$), and radioactive with

induced fissions. All technical innovations will have to be first tested with simulant salts and the move to radioactive systems should only prove that the innovations validated in non-radioactive devices are still valid. It is thus necessary to have access to equipments that have already demonstrated their operational aptitudes without the handicap of necessary radio-protection and with which the exploration of wide operational domains (temperature, flow speeds, gas and suspended particle loads, sizing and particular geometries) will have established our understanding and at least partly validated the mathematical models.

2.3. Demonstrator with a simulant salt - test benches

The most common simulant fluoride is the "FLiNaK" eutectic (LiF-NaF-KF). Mixtures such as LiF-NaF-ZrF_4 or NaF-KF-ZrF_4, however, can be used to improve the viscosity and density. These salts are liquid beyond 450°C and they are thermally quite stable. They are also representative of the intermediate circuit salt (if this option is retained). The mastering of the following issues, some of which are interdependent, needs to be demonstrated or quantified:

- The handling of large amounts of molten salts.
- The design of the pumps, how well they perform, their reliability, how they withstand wear.
- The validation of the hydrodynamic flow models.
- The development of the instrumentation.
- The validation of molten salt heat exchanger components.
- The separation and extraction of dissolved gases and suspended particles.
- The validation of the flushing system components.

The FFFER (Forced Fluoride Flow for Experimental Research) facility [14], which is currently being built, constitutes a preparatory step towards this endeavor. It will be operated between 500 and 700°C, with a LiF-NaF-KF salt. One of its objectives is to evaluate the efficiency of this bubbling process in a fluoride salt, by reproducing the gases extraction of the MSFR at a 1/10th scale in a simulant salt at high temperature.

2.3.1. Radioactive demonstrator without induced fissions

The aim of these demonstrators is to take into account the specifics of the salt with actinides, in relation to the flow dynamics and to the salt chemistry. Some of the items are:

- A small corrosion demonstrator subjected to heat gradients.
- A small chemical processing demonstrator.
- A large scale hydrodynamic demonstrator, including the heat exchangers.

2.3.2. Radioactive demonstrator with induced fissions

The purpose of this demonstrator is:

- To obtain approval from the safety authorities, i.e. to answer beforehand any issues they might raise.
- To demonstrate that the reactor can be controlled (start-up, power changes, shut-down).
- To manage shut-downs and flushing in the specific conditions of the thermally active liquid.
- To generate gaseous and condensed fission products (that cannot be realistically simulated) and extract them.
- To validate the heat evacuation system in realistic conditions
- To irradiate the system as a whole and not just samples.

These items do not all have to be addressed with a single machine, that would accumulate the difficulties and the associated costs. The first two can be achieved with a small, very low specific power reactor (infrastructure economy). The other items require much larger power for the production of fission products and the production of representative irradiation damages (displacements per atom, He production, transmutations), as detailed in the next section.

2.4. Power demonstrator of the Molten Salt Fast Reactor

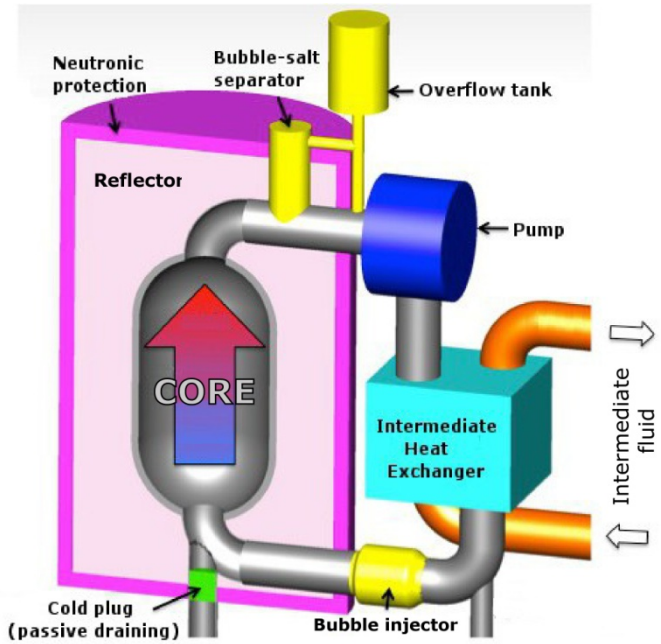

FIG. 3. Schematic view of the MSFR demonstrator with one of the 6 external loops

A 100MW_{th} or so demonstrator seems necessary to produce a sufficient amount of gaseous and metallic fission products to test the on-line gaseous fuel processing system. The salt volume involved (1.8 m^3) would be one tenth that of the reference reactor (18 m^3) with 60% of the salt in the core, to have a system representative of the reference MSFR in terms of heat exchangers (fluid velocity, thickness of the plates and gap between the plates - both on the side of the fuel salt and of the intermediate fluid), irradiation damages and neutronic behavior. It would be operated during only a few years. The batch reprocessing will thus not be mandatory but the system could provide, eventually, salt samples useful to test the off-line salt reprocessing (soluble fission product extraction). Since this demonstrator will be operated on a short period only, having a self-breeder system is not mandatory. Consequently, and to simplify the design, the fertile blanket will be replaced by a radial inert reflector identical to the axial reflectors, as illustrated in Figure 3. The return circulation of the salt (from the top to the bottom) is here divided into 6 loops located around the core, similar to the external loops of the reference MSFR.

Table 3. Characteristics of the MSFR power demonstrator

Thermal power (MWth)	100
Mean fuel salt temperature (°C)	725
Fuel salt temperature rise in the core (°C)	30
Fuel Molten salt initial composition (mol%)	LiF-ThF_4-$^{233}UF_4$ or LiF-ThF_4-(^{enriched}U+MOx-Th)F_3 with 77.5 % LiF
Fuel salt melting point (°C)	565
Fuel salt density (g/cm^3)	4.1
Core dimensions (m)	Radius: 0.556 Height: 1.112
Fuel Salt Volume (m^3)	1.8

	1.08 in the core 0.72 in the external circuits
Total fuel salt cycle in the fuel circuit	3.5 s

Ideally, having a ^{233}U initial load of about 650kg available will be the simpliest way to start such a demonstrator. Failing that, starting with transuranic elements only as initial fissile load seems not possible here: the plutonium solubility constraint becomes more pressing than for the reference MSFR, because a reduction of the size of the reactor leads to increasing the fissile proportion in the salt by about one third. Start-up with ^{enriched}U mixed with transuranic elements has been studied, as presented in Figure 4 where the configuration at the top of the right axis is equivalent to the configuration started with TRU elements only (and located largely above the Pu solubility line as already mentionned). The configurations located at abscissa 0 correspond to an initial fuel salt composition without Thorium but with enough TRU elements to reach criticality. The blue line labeled "no TRU" at the bottom left represents different simulations of the MSFR started with enriched Uranium only, while the purple line labeled "^{enr}U at 100%" represents the results for MSFR configurations with pure ^{235}U mixed with Thorium and the amount of TRU elements necessary to reach criticality. The other solid line curves (labeled 10% to 30%) show the maximum concentrations in valence-III elements obtained during the reactor operation as a function of the (Th/Th+U) initial ratio for Uranium enrichment ratios from 10% to 30%.

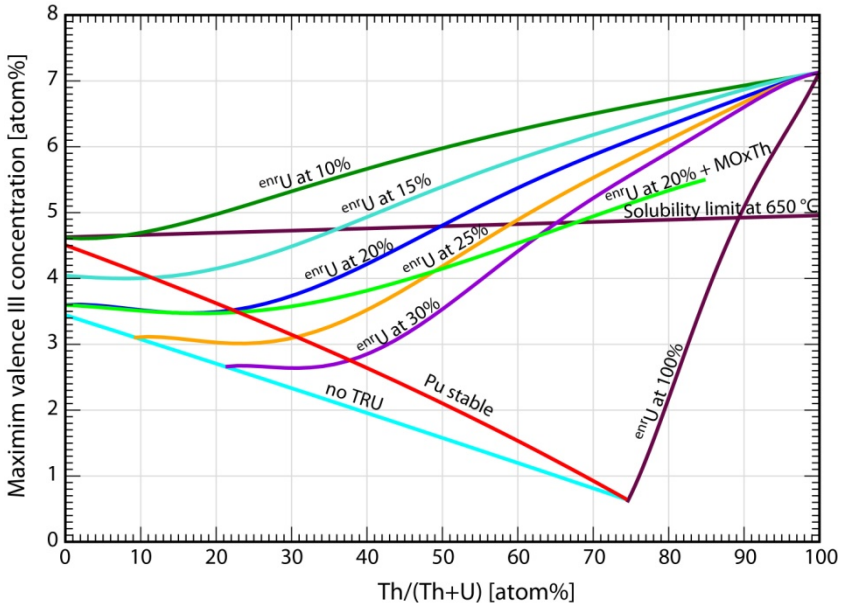

FIG. 4. Maximal concentration in valence-III elements in the initial fuel salt when starting with enriched Uranium and TRU elements, as a function of the Uranium enrichment and of the initial Th/(Th+U) ratio

In the area located on the left of the red line labeled "Pu stable", the maximal Pu concentration is reached after a few years of reactor operation, while it decreases during the entire reactor lifetime for the MSFR configurations located on the right of this line. For the configurations placed exactly on this line, the Pu concentration being stable during the first years of operation to then decrease and reach a Pu concentration equivalent to a ^{233}U-started MSFR at equilibrium. The more interesting configurations are thus placed on this line or on its right. Only the configurations located below the line "Solubility limit at 650°C" (650°C being the colder point of the salt in the fuel circuit) can be considered. Start-up with ^{enriched}U mixed with transuranic elements is then possible with enrichment between 15% and 20%.

Another option consists in mixing this enriched uranium with irradiated MOx-Th (contaning ^{233}U) that will have to be produced in today's reactors. One can see from this study (see light green curve

labelled "^{enr}U at 20% + MOx-Th" in Figure 4) that such a demonstrator may easily be started with an initial fissile salt composed of Uranium enriched at 20% mixed with MOx-Th with a ratio of Th/(Th+U) between 20 to 65%. The larger the amount of Thorium is in the initial fuel salt, the better the breeding ratio of such a reactor will be.

2.5. From the MSFR demonstrator to a modular reactor

At the present time, it seems possible to slightly modify such a demonstrator which could then be a self-breeder modular reactor thanks to the addition of fertile blankets and a slow chemical reprocessing of the fuel salt ($1/10^{th}$ of the reprocessing rate of the reference MSFR only). It should be combined with a system to extract the uranium from the fertile blankets in order to provide the fissile matter feed-in. It is interesting to note that such a reactor could be operated at a power of up to $300MW_{th}$. This would then be a "modular" reactor that could be exploited commercially.

Table 4. Breeding capacities of different configurations of modular MSFR operated during 30 years

	No radial blanket and H/R=2	**No radial blanket and H/R=2**	**Radial blanket and H/R=2**	**Radial blanket and H/R=2**	**Radial blanket and H/R=3**	**Radial blanket and H/R=3**
Power [MW_{th}]	100	200	100	200	100	200
Initial ^{233}U load [kg]	654	654	667	667	677	677
Fuel reprocessing of 1l/day						
Feeding in ^{233}U [kg/an]	11.38	23.38	1.72	4.70	-0.07	0.98
Breeding ratio	-29.83%	-30.64%	-4.52%	-6.16%	***0.18%***	-1.29%
Total ^{233}U needed [kg]	1013.87	1388.37	738.83	835.16	715.05	754.25
Breeding ratio with an additional axial fertile blanket			***1.81%***	***-0.04%***		
Fuel reprocessing of 4l/day						
Feeding in ^{233}U [kg/an]	11.20	22.58	1. 48	3.58	-0.38	-0.26
Breeding ratio	-29.37%	-29.59%	-3.88%	-4.69%	***1.00%***	***0.34%***
Total ^{233}U needed [kg]	1001.86	1353.13	722.50	794.21	709.74	723.03
Breeding ratio with an additional axial fertile blanket			***2.49%***	***1.54%***		

Four parameters have been considered for the evaluation of the breeding capacities of such a reactor, as detailed in Table 4: the produced power (100 and 200 MW_{th}), the ratio of the height/radius (H/R) of the core, the addition (columns labeled 'Radial blanket') or not (columns labeled 'No radial blanket') of a radial fertile blanket around the core, and the impact of the reprocessing rate of the fuel salt between 1 and 4 liters per day. The results written in bold italic in Table 4, whose breeding ratio is higher or equal to zero, represent the configurations suitable for a breeder reactor. It is to be noted that the trends deduced from the calculations are correct but that the numerical results reported here are impacted by uncertainties on the nuclear data (mainly on the capture over fission ratio of ^{233}U) leading to +/- 2 to 3% margins on the breeding ratios.

With a reprocessing rate of 1 liter of fuel salt per day, only the configuration producing 100 MW_{th} with a ratio H/R equal to three and including a radial fertile blanket corresponds to an iso-breeder reactor. With a reprocessing rate of 4 liters of fuel salt per day, the two configurations with an elongated core (H/R=3) are breeder.

The addition of an axial fertile blanket above the core on top of the radial fertile blanket has been checked to improve the breeding capacities of the modular reactor. As presented in Table 4, this solution leads to breeder configurations even for a core whose height/radius ratio equal to 2 (height=diameter). A molten salt modular reactor could be operated at a power of $300MW_{th}$ in a breeder mode only with such an axial blanket.

ACKNOWLEDGEMENTS

The authors wish to thank the PACEN (Programme sur l'Aval du Cycle et l'Energie Nucléaire) and NEEDS (Nucléaire : Energie, Environnement, Déchets, Société) programs of the French National Centre for Scientific Research (CNRS), the IN2P3 department of CNRS, and the European program EVOL (Evaluation and Viability of Liquid Fuel Fast Reactor System) of FP7 for their support. We are also very thankful to Elisabeth Huffer for her help during the translation of this paper.

REFERENCES

[1] MATHIEU L., HEUER D. et al, The Thorium Molten Salt Reactor: Moving on from the MSBR, Prog in Nucl En, 48, 664-679 (2006).

[2] FORSBERG C.W.et al, "Liquid Salt Applications and Molten Salt Reactors", Revue Générale du Nucléaire N° 4/2007, 63 (2007).

[3] MATHIEU L., HEUER D., MERLE-LUCOTTE E. et al., Possible Configurations for the Thorium Molten Salt Reactor and Advantages of the Fast Non-Moderated Version, Nucl. Sc. and Eng., 161, 78-89 (2009).

[4] MERLE-LUCOTTE E., HEUER D. et al, Optimizing the Burning Efficiency and the Deployment Capacities of the Molten Salt Fast Reactor, Contribution 9149, Global 2009 - The Nuclear Fuel Cycle: Sustainable Options & Industrial Perspectives, Paris, France (2009).

[5] US DOE Nuclear Energy Research Advisory Committee and the Generation IV International Forum, A Technology Roadmap for Generation IV Nuclear Energy Systems, GIF-002-00 (2002).

[6] RENAULT C. et al., The Molten Salt Reactor (MSR) in Generation IV: Overview and Perspectives, http://www.gen-4.org/GIF/About/documents/30-Session2-8-Renault.pdf, Proceedings of the GIF Symposium 2009, Paris, France (2009).

[7] BOUSSIER H. et al, The Molten Salt Reactor in Generation IV: Overview and Perspectives, Proceedings of the Generation4 International Forum Symposium, San Diego, USA (2012).

[8] IGNATIEV V., FEYNBERG O., MERZLYAKOV A. et al, Progress in Development of MOSART Concept with Th Support, Proceedings of ICAPP 2012, Paper 12394 Chicago, USA (2012).

[9] DELPECH S. MERLE-LUCOTTE E. et al, Reactor physics and reprocessing scheme for innovative molten salt reactor system, J. of Fluorine Chemistry, Volume 130, Issue 1, p. 11-17 (2009).

[10] MERLE-LUCOTTE E. HEUER D. et al, Launching the Thorium Fuel Cycle with the Molten Salt Fast Reactor, Contribution 11190, Actes de la conférence International

Congress on Advances in Nuclear Power Plants (ICAPP), Nice, France (2011).

[11] BROVCHENKO M. et al, Preliminary safety calculations to improve the design of Molten Salt Fast Reactor, PHYSOR 2012 Advances in Reactor Physics Linking Research, Industry, and Education, Knoxville, Tennessee, USA (2012).

[12] MERLE-LUCOTTE E., HEUER D. et al, Preliminary Design Assessment of the Molten Salt Fast Reactor, Contribution A0053, Proceedings of the European Nuclear Conference ENC2012, Manchester, UK (2012).

[13] DELPECH S. MERLE-LUCOTTE E. AUGE T. HEUER D., MSFR: Material issues and the effect of chemistry control, 2009 Generation4 International Forum Symposium, Paris, France (2009).

[14] GHETTA V. et al., Boucle en convection forcée pour l'étude du nettoyage en ligne de caloporteurs de type sel fondu, Contribution 0574, Proceedings of the Materiaux 2010 Conference, Nantes, France - In french (2010).

Calculation of Sodium Cooled Fast Reactor Concepts
Preliminary results of an OECD NEA benchmark calculation

Ádám Tóta, István Pataki, András Keresztúri

Centre for Energy Research, Hungarian Academy of Sciences
Budapest Hungary

Abstract. In this paper we present the results of our calculations of the OECD NEA benchmark on generation-IV advanced sodium-cooled fast reactor (SFR) concepts. The aim of this benchmark is to study the core design features, moreover the feedback and transient behaviour of four SFR concepts. At the present state, static global neutronic parameters, e.g. k_{eff}, effective delayed neutron fraction, Doppler constant, sodium void worth, control rod worth, power distribution; and burnup were calculated for both the beginning and the end of cycle. In the benchmark definition, the following core descriptions were specified: two large cores (3600 MW thermal power) with carbide and oxide fuel, and two medium cores (1000 MW thermal power) with metal and oxide fuel. The calculations were performed by using the ECCO module of the ERANOS code system at the subassembly level, and with the KIKO3DMG code at the core level. The former code produced the assembly homogenized cross sections applying 1968 group collision probability calculations; the latter one determined the core multiplication factor, the radial power distribution using a 3D nodal diffusion method in 9 energy groups. We examined the effects of increasing the energy groups to 17 in the core calculation. The reflector and shield assembly homogenization methodology was also tested: a "homogeneous region model" was compared with a "concentric cylindrical core" calculation. The breeding ratio was also determined for the beginning of cycle.

1. Introduction

We present the first results of an OECD NEA benchmark aiming at the calculations of four generation-IV advanced sodium cooled fast reactor conceptions [1]. The benchmark has been defined by the Working Party on Reactor and System, Expert Group on Reactor Physics and Advanced Nuclear Systems. In this paper, the preliminary calculations of a participating institute, the Centre for Energy Research (Hungarian Academy of Sciences) are presented. It includes the determination of the most important neutronic characteristics (e.g. effective multiplication factor, reactivity feedback coefficients), control rod worth and breeding ratio of the four core conceptions.

One of the final objectives of the core designs is the enhanced safety performance, especially for unprotected transients. The aim of the present benchmark activity is to perform a shared analysis of the feedback and transient behaviour of the cores. At the present state of the work, static results are obtained for some core neutronic and burnup parameters.

Two different core sizes were analyzed: large size cores with 3600 MW thermal (MWth) with carbide and oxide fuel, and medium size cores with 1000 MWth with metal and oxide fuel. The core definitions contain geometry and material data, no thermal-hydraulic modeling is necessary presently.

The calculations were performed using the ERANOS code package's ECCO module and the KIKO3DMG nodal multi-group diffusion code. The former code provided the subassembly multi-group cross sections for the latter one, which performed the core and burnup calculations.

2. Core concepts

The main characteristics of the four studied cores are given in Table 1. Two temperature values were specified, one for the fuel and the other one for the remaining (e.g. structure, absorbent, coolant)

regions. On the external boundaries of the cores, vacuum boundary condition was defined. Isotope concentrations were given for all materials in five axial layers. The fission products were replaced with molybdenum.

Table 1. Basic parameters of the SFR core concepts

Parameters	**Large oxide core**	**Large carbide core**	**Medium oxide core**	**Medium metal core**
		Nominal values		
Thermal power (MW thermal)	3600	3600	1000	1000
Average fuel temperature (°C)	1227	987	1027	534
Average structure temperature (°C)	470	470	432.5	432.5

2.1. Large size cores

The core descriptions have been provided by CEA for the two large-core 3600 MWth concepts; one with oxide and the other one with carbide fuel. The radial core layouts are presented in Fig. 1. The oxide core is designed to be self-breeding without a fertile blanket. As the burnup depends on the position in the core, two fuel compositions are defined: one for the inner core and the other for the outer core. The isotope densities are given for each subassembly and structure material at the beginning of equilibrium cycle (BEC). The fuel pins are placed into a hexagonal wrapper tube in a triangular arrangement. The outermost row of the assembly, next to the wrapper, consists of 10 and 13 fuel pins in the carbide and oxide core, respectively. The fuel pins contain MOX pellets surrounded with helical wire spacers and filled with helium. In the ECCO model, wire spacers are smeared into the cladding. The oxide fuel pins contain a central hole, filled with helium. The active part of the fuel pin - containing the pellets - is surrounded with an axial reflector and a gas plenum. The primary and secondary control rods are comprising natural and enriched ^{10}B boron carbide pins, filled with helium. The reflectors contain steel pellets.

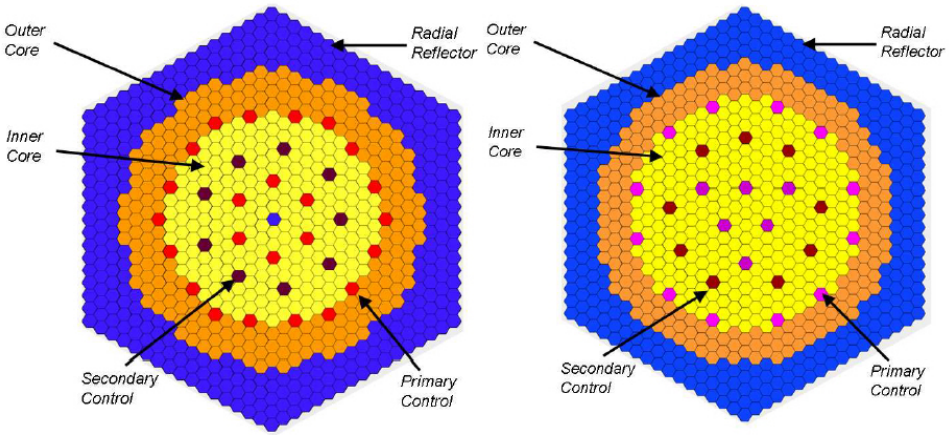

FIG. 1. Large oxide core (left) and large carbide core (right), radial layouts (from [1])

2.2. Medium size cores

The 1000 MWth metallic and oxide core definitions are based on the Advanced Burner Reactor (ABR) concepts [2], developed under the Global Nuclear Partnership program. Conventional or reasonably proven materials were utilized in the ABR core concepts so that the core stays within current fast reactor technology knowledge base. The ABR equilibrium cycle was determined by recycling all discharged transuranium (TRU) with an external makeup TRU feed recovered from LWR used nuclear fuel [1].

The fuel assemblies of the metallic and the oxide cores are classified into two and three groups, according to their isotope concentrations at BEC. Otherwise, the radial layouts of the two medium cores are the same (Fig 2.). The fuel assemblies of both medium cores contain an active section bounded on the bottom by the lower structure (homogeneous mixture of sodium and steel). At the top of the active section in the oxide core, there is a gas plenum filled with helium. In case of the metal core, the space between the active section and the upper gas plenum is filled with sodium. The fuel pins are placed into a hexagonal wrapper tube in a triangular arrangement - just as in case of the large cores. At the outermost row, next to the side of the wrapper, there are10 pins in both cores. The fuel pins contain MOX pellets and surrounded with helical wire spacers and filled with helium. In the ECCO model, wire spacers are smeared into the cladding.

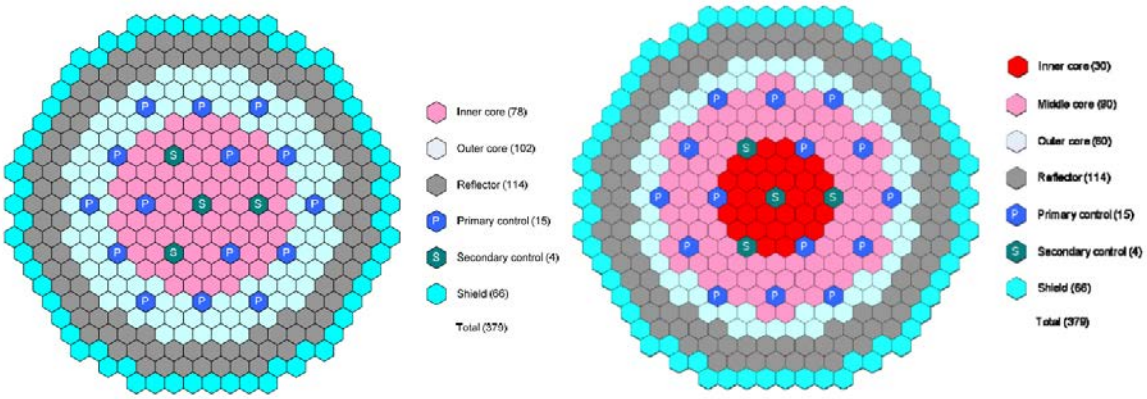

FIG. 2. Medium metal (left) and medium oxide (right) cores (from HIV)

3. Calculation methodology

Calculations were performed in two levels. In the first level the multi-group assembly cross sections were generated by using the ECCO module of the ERANOS code system, while the core calculations were performed by using the KIKO3DMG code for determining the power distribution and the effective multiplication factor (k_{eff}). The ERANOS is a neutronic calculation code system applicable for fast neutron reactors; it has been developed by the CEA (Commissariat á l'Energie Atomique). It includes the ECCO cell code; which is able to perform 1D and 2D transport calculations. The KIKO3DMG is a nodal 3D multi-group diffusion code.

For the burnup calculations, stationary operation at nominal power in one cycle was specified. We calculated the isotope concentrations of the end of cycle with KIKO3DMG using the flux belonging to the beginning of cycle. The obtained EEC concentrations were used as an input to the ECCO assembly calculation, and the resulted multi-group assembly cross sections were used in a further EEC core calculation.

In the following subsections, we present our calculation steps and we test some calculation options. It should be emphasized that no reference solution is available so far; hence at the present state no final conclusions can be drawn about the calculation options.

3.1. Assembly calculations with the ECCO module

The ECCO code is able to perform multi-step calculations, e.g. it is possible, that in the first step one determines the critical buckling (so that the k_{eff} is equal to one) in a broad energy group structure containing 33 energy group microscopic cross sections. In the second step, a fine-group (containing 1968 energy group microscopic cross sections for most of the isotopes) calculation accomplished using the previous buckling. It makes a flux-weighted spatial homogenization and an energy group

condensation possible for the desired group structure of the core calculation. The calculations were done for the 2D radial sections of the assemblies, called cells. All different axial sections of an assembly (e.g. gas plenum, axial reflector, active core) were modelled in separated cells.

In the present calculations, KIKO3DMG uses 9 energy groups; accordingly all ECCO output libraries are condensed to this energy structure.

Fuel assemblies are modelled in a pin-wise (heterogeneous) geometry, while for the non-fuel assemblies only a so called “homogeneous model” are implemented into the assembly cross section calculations. In case of the heterogeneous calculations, ECCO solves the problem with the collision probability method.

For the fuel cells, reflective boundary condition is assumed, which is equivalent to an infinite lattice approach. The medium cores are calculated by applying heterogeneous geometry option and using the fine (1968) energy group library. The large cores are first treated with heterogeneous geometry using the broad-group library, and just after the spatial homogenization the fine energy group structure is applied. All five axial fuel layers with different isotope concentrations are treated as different cells.

For any non-fuel cell – not containing any fissionable isotope - an external neutron source is necessary which is given as the output from the nearest fuel cell calculation. For the sake of simplicity, a volume-homogenized approach is to be performed for all non-fuel regions at the present state of the benchmark in spite that detailed geometrical descriptions are also provided for the control assemblies. Non-fuel cell calculations were done using the fine-group library.

3.2. Core calculations by using the KIKO3DMG

KIKO3DMG is a nodal code, the nodes are the assemblies subdivided by axial layers of the homogenized subassemblies or structure elements. The number of the axial layers are 11 (large cores) and 16 (medium cores). In the base calculations 9 energy groups are used.

KIKO3DMG is the advanced version of KIKO3D [3], which was originally developed to thermal-neutron light water reactor calculations. The basic theoretical assumptions of KIKO3DMG are as follows [4]:

- arbitrary number of energy groups;
- supported geometries: hexagonal, square, triangular, slab;
- nodal method: the nodes are the subassemblies subdivided by axial layers;
- the unknowns are the scalar flux integrals on the node interfaces;
- linear anisotropy of the angle dependent flux on the node boundaries assumed;
- nodal equations obtained from the condition that the scalar flux and net current integrals are continuous on the node interfaces;
- analytical solutions of the diffusion equation inside the nodes: exponential or/and trigonometric “wave functions” perpendicular to the node interfaces;
- generalized response matrices of the time dependent problem and time dependent nodal equations;
- IQS (Improved Quasi Static) factorization; shape function equations and point kinetic equations;
- the absorbers and the reflectors can be represented by pre-calculated albedo matrices (not used in this benchmark, everything is represented by cross sections);
- possibility of the up-scattering;
- optimized iterations for multi-thread processing;
- graphical output for radial distributions (e.g. flux, power, temperature);

— hexagonal geometry input can be cut into triangular pieces in an automated way, and the hexagonal output can be synthesized from the triangular results.

Since only stationary calculations are done in the benchmark so far, the time dependent feature of the code is not exploited. Up-scattering is not applied for this benchmark.

3.3. Comparison of 9 and 17 energy-group core calculations

As arbitrary number of energy groups is applicable in the KIKO3DMG, we decided to examine the effect of increasing the number of energy groups. Besides the 9 group base modeling, we calculated the medium oxide core with 17 groups. For that, only the final number of the energy group condenzation had to be modified in the ECCO input of the assembly calculation,

The compared quantities are the radial assembly power distributions averaged for each ring, moreover the k_{eff}. The k_{eff} was increased from 1.03178 to 1.03993 by changing the energy group number from 9 to 17; which is a 0.79% increase. The assembly averaged radial power distributions can be seen in Fig. 3. The power has increased in the middle and inner rings, while a relatively small decrease can be observed in the outer region.

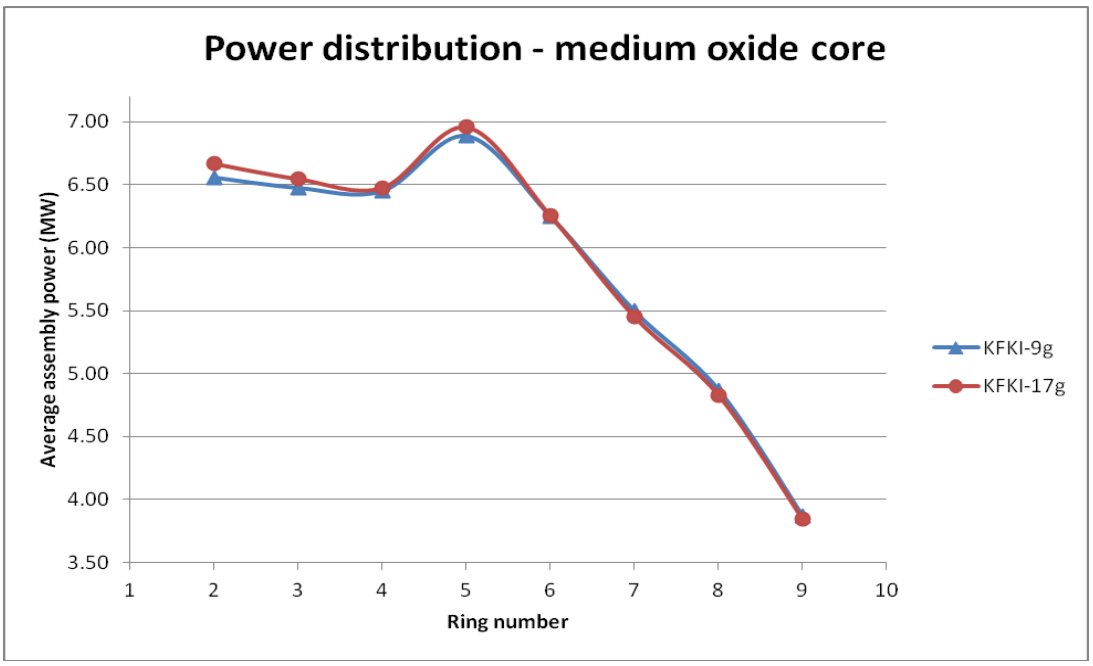

FIG. 3. Radial power distributions of the medium oxide core with 9 and 17 group calculations

3.4. Reflector and shield cylindrical calculation

The effect of neglecting the spectral impact of the neighbour cells on the group constants of the radial reflector and shield assemblies was analyzed. The radial flux distribution in the core varies significantly in the vicinity of the radial reflectors located in the outer part of the core. Accordingly, in ECCO the investigated reactor core was modelled as concentric cylinders, where the volume of the cylinders was equivalent to the volume of the represented assemblies. (The original calculation model was an infinite homogeneous region for the reflectors and shields). The multi-group cross sections for the reflector and shield assemblies created this way are used in the KIKO3DMG core calculation. The medium cores are more effected by the reflectors because of their size, therefore the medium metal core was chosen to be studied. The radial distribution of the averaged assembly power values depending on the ring number is shown in HIV-fig. The two curves represent the results of the infinite

homogeneous and the concentric cylindrical core model. The first ring contains only an absorber assembly and there are two reflector rings starting from the 10th ring position. Using the cylindrical core model, another, modified power distribution is obtained in comparison to the original one. The power values are decreased in the outer rings and increased in the inner rings. It means that the power distribution is more balanced in case of the cylindrical model. The k_{eff} of the core with original and cylindrical models are 1.03836 and 1.04206, respectively; the increase is 0.36%.

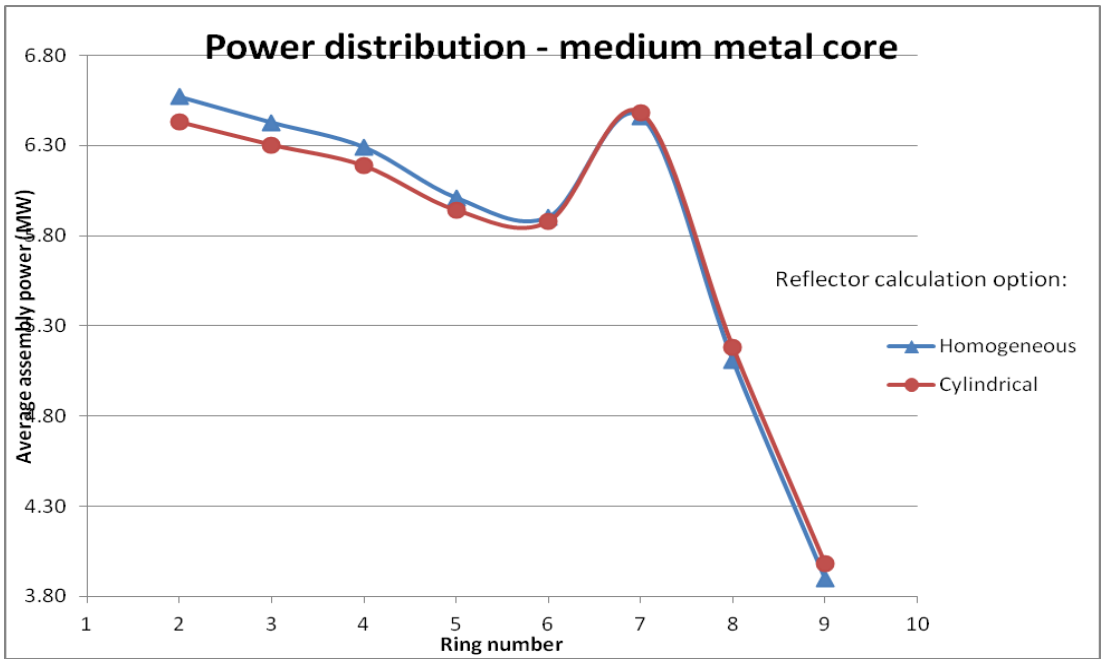

FIG. 4. Radial power distributions of the medium metal core using different reflector cross section calculation options

4. Results

The results presented here are calculated using the "original" methods described in Section 3, i.e. the non-fuel assembly cross sections are created with an infinite homogeneous region model, and the core calculation was done in 9 energy groups. The first requested results for the benchmark are the following:

- effective core multiplication factor (k_{eff})
- effective delayed neutron fraction (β_{eff})
- sodium void worth
- Doppler constant
- control rod worth
- isotope concentrations for EEC
- radial power distribution.

Calculations of these parameters are presented for both the BEC and EEC states. The following definitions are applied. The sodium void worth is the difference of the reactivity values corresponding to the voided and nominal states. In the voided state, the sodium concentration in the active core is changed to zero (exactly it is in the order of 10^{-15} atoms/cm^3 in ECCO). The Doppler constant is the difference of the reactivity values corresponding to the high-temperature and nominal states, divided

by *ln(2)*. In the high-temperature state, the average fuel temperature is the double of the nominal value in Kelvin. Note, that it is not normalized to a unity temperature change. The EEC is defined as the core state after one cycle irradiation time, corresponding to:

- 410 days with full nominal power rating for the large oxide core;
- 500 days with full nominal power rating for the large carbide core;
- 328.5 days with full nominal power rating for medium metallic and oxide fuel cores, which is equivalent to one-year cycle length with 90% capacity factor.

Control rod positions are not modified during the irradiation. The control rod worth was defined as the difference of the reactivity values corresponding to the fully withdrawn and inserted positions.

Besides the requested benchmark parameters, we determined a breeding ratio (BR), for which the following definition was used based on [5]

$$BR = \frac{\sum_m C_m}{\sum_m D_m},$$

where C_m is the production and D_m is the destruction reaction rate of the fuel isotope m. In the present calculation, the ^{239}Pu and ^{241}Pu isotopes are taken into account.

The calculated results for all of the core concepts are summarized in Table 2. The mass of uranium, plutonium and americium for each core are listed here instead of individual isotopes. The radial power distributions of the cores at the BEC and EEC states are shown in Fig. 5. and 6. The power values of the Figure are obtained averaging solely the fuelled regions.

Table 2. Main calculation results

		Large carbide core	**Large oxide core**	**Medium metallic core**	**Medium oxide core**
k_{eff} (all rods out)	BEC	1.00850	1.03128	1.03836	1.03178
	EEC	1.02576	1.03602	1.03339	1.03205
k_{eff} (all rods in - shutdown)	BEC	0.95458	0.96371	0.83130	0.81941
	EEC	0.96387	0.96518	0.82363	0.81793
Breeding ratio	BEC	1.15024	1.081747	0.79317	0.83938
β_{eff}	BEC	0.405%	0.393%	0.366%	0.357%
	EEC	0.393%	0.384%	0.367%	0.356%
Doppler constant ($)	BEC	-2.79	-2.42	-1.06	-2.31
	EEC	-2.77	-2.44	-1.09	-2.33
Sodium void worth ($)	BEC	5.73	5.19	5.06	4.87
	EEC	6.01	5.39	4.95	4.85
Outer control rod group worth ($)	BEC	0.28	0.24	1.35	1.25
	EEC	0.25	0.24	1.34	1.23
Inner control rod group worth ($)	BEC	0.39	0.38	3.80	3.67
	EEC	0.58	0.45	4.13	3.90
Uranium (kg)	BEC	66 343	63 322	10 251	11 045
	EEC	64 206	61 674	10 009	10 781
Plutonium (kg)	BEC	11 995	12 766	2 640	3 397
	EEC	12 206	12 848	2 562	3 337
Americium (kg)	BEC	205	247	154	211
	EEC	266	282	146	202

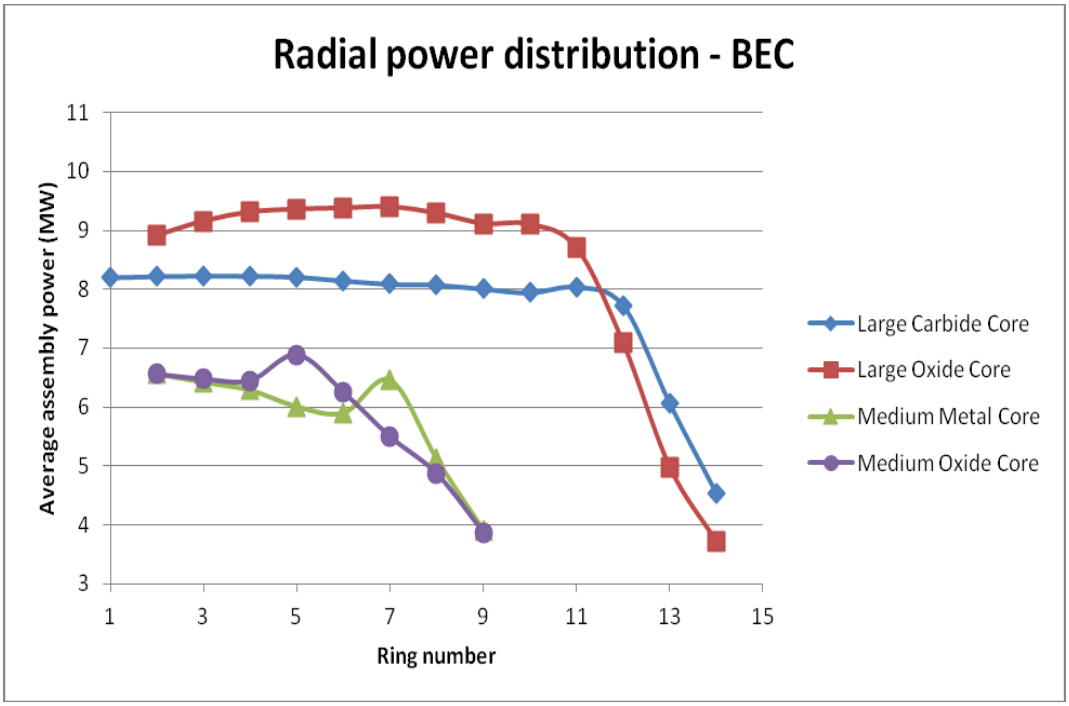

FIG. 5. Radial power distributions at the BEC state

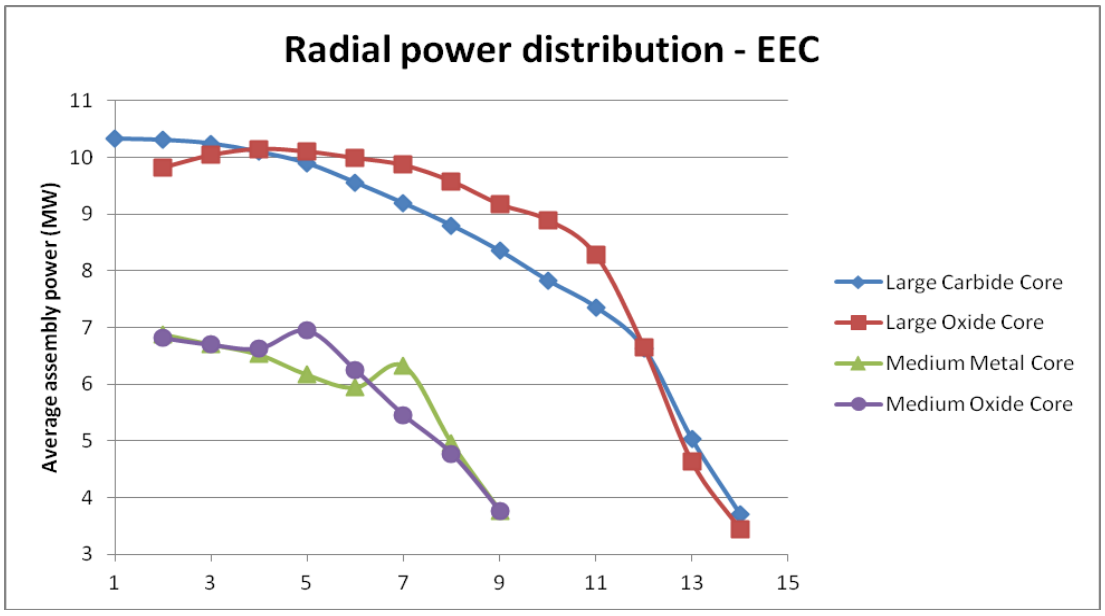

FIG. 6. Radial power distributions at the EEC state

4.1. Comparison of the four core concepts

We wish to emphasize that presently only stationary calculations were performed. A far as the evaluation of the concepts must take into account both the safety and the fuel cycle aspects, the breeding ratios were also compared. The breeding ratio and the k_{eff} values at the BEC and EEC states show, that the large cores (with BR > 1) are more advantageous regarding the sustainable fuel cycle than the medium ones (BR <1). Americium isotopes tend to increase significantly in the large cores,

while they are decreasing in the medium ones. Note that the breeding ratio is strongly dependent on the BEC fuel isotope concentration.

The sodium void worth is about 5 - 6 $ for each core for both cycle states. It is crucial to compensate this effect, which can be achieved with a large enough negative Doppler constant. The large cores have slightly higher absolute values, but they have also a little higher void worth. The medium metal core has significantly smaller Doppler effect – about half than the others. The medium oxide core has a slightly smaller Doppler effect than the large cores, nevertheless its void worth is also smaller.

The control rod worth values of the medium cores are significantly higher – about 1.3 $ in the outer and 4 $ in the inner core, - than in the large cores, namely they are between 0.25 - 0.6 $. High values can be problematic during an uncontrolled absorber withdrawal event; even worse if it couples with a low Doppler effect, as it is in case of the medium metal core.

5. Summary

Four advanced SFR core concepts were analyzed according to the first part of an OECD NEA benchmark. The ECCO (ERANOS) and the KIKO3DMG codes were used to calculate the basic neutronic parameters and feedback effects. The 9 and 17 group diffusion calculations of the medium oxide core were compared It was found that the k_{eff} increased less than 1% in the latter case. Two options were used to investigate the assembly cross section calculation methodology applied for the outer reflectors and shields, namely an infinite homogeneous region and a concentric cylindrical core model were applied. The difference in the k_{eff} is 0.36% for the medium metal core. The burnup calculations showed that the breeding ratio of the large cores are significantly higher (>1) than in case of the medium cores (<1). High positive values of the sodium void worth were obtained for all cores. The Doppler constants were negative for each core, but the smallest absolute value was found in case of the medium metal core. The radial power distributions in the inner zone for the two large cores are more balanced comparing them to the two medium cores, but they are decreasing more significantly next to the reflectors. The high control rod worth in the medium cores can cause safety problems during an uncontrolled absorber withdrawal transient.

ACKNOWLEDGEMENTS

We wish to thank the ANL and CEA for specifying the benchmark and permitting to present our preliminary results.

REFERENCES

[1] BLANCHET, D., et al., Sodium Fast Reactor Core Definitions (2011), http://www.oecd-nea.org/science/wprs/sfr-taskforce/
[2] KIM, T. K., et al., “Core Design Studies for a 1000MWth Advanced Burner Reactor”, Annals of Nuclear Energy 36 (2009) 331-336
[3] KERESZTÚRI, A., et al., “Development and validation of the three-dimensional dynamic code - KIKO3D”, Annals of Nuclear Energy 30 (2003) 93-120.
[4] PATAKI, I., KERESZTÚRI, A., “Calculation of the Second AER Kinetic Benchmark Problem by Using a New Nodal Method”, 22th AER Symposium, Pruhonice (2012)
[5] BELL, G.I., GLASSTONE, S., Nuclear Reaktor Theory, Van Nostrand Reinhold (1970)
[6] ALLEN, K., et al., “Benchmark of Avanced Burner Test Reactor model using MCNPX 2.6.0 and ERANOS 2.1”, Progress in Nuclear Energy 53 (2011) 633-644

THE TAPIRO AS A FAST RESEARCH REACTOR FOR GENERATION IV TECHNOLOGIES

Fabrizio Pisacane[a], Luca Ricci[b], Alfonso Santagata[a], Augusto Gandini[b], Tommaso Murgia[b], Luca Cretara[b], Vincenzo Peluso[c], Massimo Sepielli[a], Mario Carta[a], Valentina Fabrizio[b]

[a] ENEA CR Casaccia, Via Anguillarese, 301, 00123 Rome, Italy

[b] University of Roma "Sapienza", Corso Vittorio Emanuele II, 224, 00186 Rome, Italy

[c] ENEA CR Bologna, Via Martirii Montesole, 440129 Bologna, Italy

Abstract. TAPIRO is a 5kW fast neutron source operating at the ENEA CASACCIA Research Center since 1971 in Italy. The reactor, included in the Mediterranean Research Reactor Network (MRRN) promoted by IAEA for maximize the utilization and the collaborations of RRs in the Mediterranean region, is composed by a high-enriched core made of Uranium-Molybdenum alloy cooled by He and surrounded by a copper reflector and a large concrete biological shield. A large experimental cavity, labeled thermal column, is suitable for the installation of experimental assemblies for any research purpose. Aim of this paper is to describe the main feature of TAPIRO fast neutron research reactor and analyze, by deterministic (ERANOS) and probabilistic (MCNP) simulation codes, the feasibility of an experimental campaign of neutron propagation in lead, using the thermal column of the TAPIRO reactor. Measurements of neutron spectra or reaction rates evaluations, well correlated to integral parameters of the reference reactor, can be considered as a valuable basis for the design of next generation of LFR. In this concern, a key factor is the correlation coefficient between integral parameters (for example vacuum effect and reaction rates), evaluated in different cores, is a measure of the impact of the physical characteristics of the systems on the assessment of such integral quantities. The results obtained in this preliminary study are encouraging since they indicate a significant degree of correlation between the quantities considered in TAPIRO and in the reference system taken into account.

1. INTRODUCTION

In the seventies at ENEA/Casaccia there was an important commitment in relation to methods for exploiting the experimental data relevant to integral quantities measured in critical facilities, the so called 'a posteriori' information along with Bayes' terminology, with the objective of 'adjusting' neutron group cross section data, the 'a priori' information, adopting statistical inference methods. Such commitment stemmed on the possibility of rapidly calculating the sensitivity coefficients required making use of the Generalized Perturbation Theory (GPT) methodology, on development in the same period [1] [2]. Such differential data adjustment approach was also proposed in some cases for exploiting experimental data measured in shielding benchmarks [3]. As mentioned above, the adjustment methodology is based on statistical inference methods and have been first proposed by Linnik [4]. This methodology, adapted to the nuclear domain, is illustrated in [5] and [6]. In [5] the nuclear data do be adjusted were assumed to be in a multi-group form, which was considered an unavoidable (at that time) limitation. Its application for the definition of optimal multi-group cross section set libraries, as well as appropriately assessed covariance matrices based on integral experiments on experimental facilities, has been however pursued by different laboratories (see comments on this and equivalent methodologies in Ref. [7]). In particular, in the 70s and 80s at CEA it was decided to use integral experiments to assess multi-group cross-section uncertainties by using adjustment procedures. The library ERALIB1 [8] used with the ERANOS code system [9] is the result of this methodology. The interest in high-quality integral benchmark data is increasing as efforts to

quantify and reduce calculational uncertainties accelerate to meet the demands of next generation reactor and advanced fuel cycle concepts. The International Reactor Physics Experiment Evaluation Project (IRPhEP) and the International Criticality Safety Benchmark Evaluation Project (ICSBEP) continue to expand their efforts and broaden their scope to identify, evaluate, and provide integral benchmark data for method and data validation. Benchmark model specifications provided by these two projects are used heavily by the international reactor physics, nuclear data, and criticality safety communities [10]. To note that in the IRPhEP integral data base are included also experiments relevant to the TAPIRO reactor as described in Ref. [11]. The most meaningful activities performed at TAPIRO reactor and connected to the present work were performed in the early 70's for studying the propagation of neutrons along the axis of a large sodium tank inserted in place of the graphite column. It was a measurement campaign made in collaboration with CEA Cadarache within the fast reactor program and had a similar purpose, i.e., that of testing the ability of neutronic codes to reproduce the measured quantities [12]. This paper is focused on a preliminary analysis of a propagation expertiment correlation in a lead block placed in the thermal column of the TAPIRO reactor. In particular the above mentioned GPT methodology have been applied to study a potential correlation among integral quantities relevant to the TAPIRO and to a reference system. ELSY reactor has been selected as reference system. MCNPX [13] and ERANOS codes have been used for the analysis.

2. INTEGRAL DATA CORRELATION ANALYSIS

Consider that the experimental information available is contained in the measurements of integral quantities $Q_{A,\ell}$ (ℓ=1, 2, …, L) obtained from an experimental facility (system A). This information has to be transposed to a set of quantities $Q_{B,m}$ (m=1, 2, …, M) relevant to a reference system (system B). Let's define the (LxJ) and (MxJ) sensitivity matrices $\mathbf{S}_A$ and $\mathbf{S}_B$, with elements, respectively,

$$s_{A,\ell j} = \frac{p_{o,j}}{Q_{A,\ell}^{cal}} \frac{\partial Q_{A,\ell}}{\partial p_j} \tag{2.1}$$

$$s_{B,mj} = \frac{p_{o,j}}{Q_{B,\ell}^{cal}} \frac{\partial Q_{B,m}}{\partial p_j} \tag{2.2}$$

which can be calculated via GPT methods [1][2]. The transposition of the experimental information to the set of quantities $Q_{B,m}$ can be made using different statistical inference method, for instance the Lagrange's multipliers [14]. As a result we can obtain adjusted estimates of the quantities $Q_{B,m}$ or, in a more convenient form, estimates of the relative quantities

$$y_{B,m} = \frac{Q_{B,m} - Q_{B,m}^{cal}}{Q_{B,m}^{cal}} \tag{2.3}$$

where $Q_{B,m}^{cal}$ represents the same quantities calculated with the 'a priori' differential information. Vector $\tilde{\mathbf{y}}_B$ of the new estimates $\tilde{y}_{B,m}$, defined as

$$\tilde{y}_{B,m} = \frac{\tilde{Q}_{B,m} - Q_{B,m}^{cal}}{Q_{B,m}^{cal}}, \tag{2.4}$$

results [14]

$$\tilde{\mathbf{y}}_B = \mathbf{S}_B \mathbf{C}_p \mathbf{S}_A^T (\mathbf{C}_A + \mathbf{S}\mathbf{C}_p \mathbf{S}_A^T)^{-1} \mathbf{y}_A^{ex} \tag{2.5}$$

where $\mathbf{C}_A$ is the dispersion matrix of the integral experimental data, $\mathbf{C}_P$ is the cross-section dispersion matrix and where $\mathbf{y}_A^{ex}$ is a vector of elements

$$y_{A,\ell}^{ex} = \frac{Q_{A,\ell}^{ex} - Q_{A,\ell}^{cal}}{Q_{A,\ell}^{cal}} \tag{2.6}$$

Let us now consider the extreme case in which we wish to evaluate a single quantity Q_B relative to the reference system, on the basis of the information contained in a single measurement, $Q_{A,1}^{ex}$, more or less correlated with Q_B. By following the above procedure we obtain its relative correction estimate,

$$\frac{\tilde{y}_B}{\varepsilon_B} = r_{B,1}\frac{y_{A,1}^{ex}}{\varepsilon_{A,1}}\ , \tag{2.7}$$

where $r_{B,1}$ is the correlation coefficient

$$r_{B,1} = \frac{S_{A,1}^T D S_B}{\sqrt{(S_{A,1}^T D S_{A,1})(S_B^T D S_B)}} \tag{2.8}$$

while $\varepsilon_{A,1}$ and ε_B are the *a priori* errors associated with $Q_{A,1}^{cal}$ and Q_B^{cal}, respectively. From this equation we can clearly see how, as expected, the relative correction $\tilde{y}_B$ increases proportionally with the correlation coefficient $r_{B,1}$, with the *a priori* error ε_B and with the ratio $y_{A,1}^{ex}/\varepsilon_{A,1}$. To note that the value $r_{B,1}$ lies between 0 and 1. The closer it is to unity, the more the information inherent with the experiment in A is significant with respect to the integral quantity considered in the reference system. The correlation coefficient expressed by the Eq.(2.8) can be defined as 'relative' as there is assigned more weight to energy groups in which the cross sections are affected by larger relative errors. An 'absolute' correlation coefficient, that is, independent from nuclear data errors, could also be defined by the same expression (2.8) in which the dispersion matrix D is replaced by a unitary one. The correlation coefficients represent indeces of representativity of quantities measured in an experimental facility with respect to quantities of interest of a reference reactor. They may be used to reduce their uncertainties, along with equation (2.7) which gives the correction estimates based on the experimental ('a posteriori') data. This use implies adopting a full variance/covariance matrix, so to take into proper account the 'a priori' information relevant to the differential data errors. If a unitary dispersion matrix is used, which implies disregarding this information, the correlation coefficients represent only indeces of representativity. They may be considered 'pure' representativety indeces in the sense that only the sensitivity profiles enter in their definition.

3. TAPIRO EXPERIMENTAL FACILITY

TAPIRO (TAratura PIla Rapida a Potenza 0) is a fast neutron source reactor licensed in 1971 for a maximum thermal power of 5 kW. The project, entirely developed by ENEA's staff, was based on the general concept of AFSR (Argonne Fast Source Reactor - Idaho Falls). Since 1971, it has been used for fast reactor shielding experiments, biological effects of fast neutrons, electronic component neutron damage, etc. The reactor has a homogeneous HEU uranium-molybdenum alloy (98.5 % U, 1.5 % Mo in weight) cylindrical core with about 6 cm of radius and 11 cm of height. The core is divided in two parts: the upper one is fixed to the reactor structure whereas the lower one is movable and can be dropped in order to rapidly shut-down the system. For a thermal power greater of 50 W the core is cooled by mean of forced circulating of helium. The core is totally reflected by copper (cylindrical-shaped) of about 30 cm of thickness. The reflector is divided into two concentric blocks: a 10 cm thick inner block is contained inside the primary cooling system and a outer block about 20 cm thick. Finally, the reactor is surrounded by borate concrete shielding about 170 cm thick. The reactor is controlled by 5 control rods, made of copper, positioned in 5 cavities realized inside the inner reflector

where the control rods can be moved controlling the amount of reflector, and therefore the number of nuclear fissions inside the core. Furthermore, a rapidly shut down may be realized dropping the mobile core part. With regard to the irradiation facilities the reactor has 6 main experimental channels (4 horizontal and 2 vertical channels) and a large cavity, labeled thermal column (parallelepiped 110×110×160 cm^3). One mid-plane channel crosses the core allowing irradiations of small samples (≈ 1 cm) in an almost pure U-235 fission spectrum. In the thermal column a more energetic neutron spectrum is realized removing a 60° sector from the outer reflector. At the maximum thermal power, the total core integrated neutron source strength is of ≈ 3×10^{14} n/s that is equivalent to a total neutron flux of ≈ 4×10^{12} n/cm^2/s at the core centre and a total neutron flux of ≈ 1.5×10^{10} n/cm^2/s at the entrance of the thermal column. A vertical and horizontal section of the reactor are shown in figure 1.

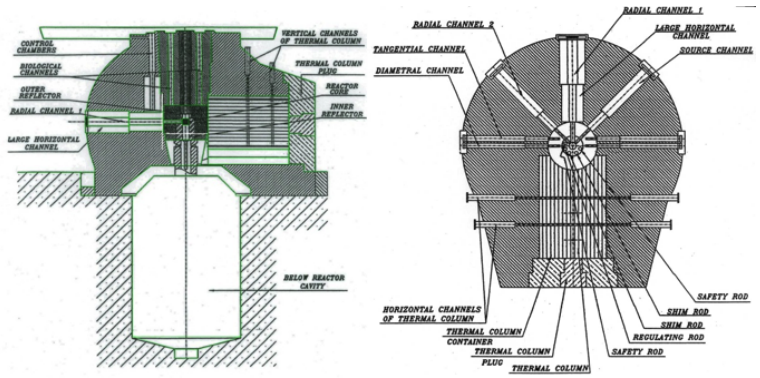

Figure 1. TAPIRO vertical section (left) and horizontal section (right)

4. ELSY "REFERENCE" REACTOR

The ELSY project (European Lead Fast Reactor) [15] has been developed from September 2006 to February 2010, in the frame of the Sixth Framework Programme of EURATOM. The ELSY reference design is a 600 MWe pool-type reactor cooled by pure lead. The ELSY project demonstrates the possibility of designing a competitive and safe fast critical reactor using simple engineered technical features fully compliant with the Generation IV goal of sustainability and minor actinide (MA) burning capability. Currently the project ELSY provides two possible geometric configurations: the first is with rectangular elements, and the second with hexagonal elements. Table 2 shows reference data on rectangular elements configuration on which is based the ERANOS model described in the next paragraph.

Table 1. ELSY main characteristics.

ELSY REFERENCE CONFIGURATION		UNIT
THERMAL POWER	1530	MW
NUMBER OF FUEL ASSEMBLIES	272	
CORE DIAMETER (D)	5,24	m
TOTAL HEIGHT (H)	3,63	m
ACTIVE HEIGHT	1,11	m
PINS PER FUEL ASSEMBLY (FA)	17x17- 5 pins (284)	
INNER/INTERMEDIATE/OUTER FAs NUMBER	132/72/68	
INNER/INTERMEDIATE/OUTER PU ENRICHMENT (VF)	13,4/15/18,5	%
AVERAGE LINEAR POWER	220	W/cm
COOLANT INLET TEMPERATURE	400	°C
COOLANT AVERAGE OUTLET TEMPERATURE	480	°C
CLAD MAXIMUM TEMPERATURE	540	°C

5. CALCULATIONS SPECIFICATIONS

The simulated experiment in TAPIRO, and the calculated integral data (reaction rate ratios) obtained, are relevant for measurements at different axial positions in an exponential column made of lead. The TAPIRO serves here as a neutron source reactor. The neutron source (only its energy distribution is of interest) at the side of the column facing the core has been calculated by the Monte Carlo code MCNP. The TAPIRO reactor is assumed of course at critical conditions. The integral quantities in the lead column, with a fixed neutron source at one side, calculated using the ERANOS code, may be then assumed as quantities to be measured in a typical exponential experiment. The value calculated in ELSY correspond to integral quantities at conditions assumed critical. The correlation coefficients are indeces of representativity of integral data measured in an experimental set-up (in TAPIRO) with respect to integral data relevant to a reference reactor (ELSY). Since the integral data considered here are strongly dependent on the neutron spectrum, comments on the calculated spectra profiles are introduced first in "RESULTS".

5.1. MCNPX TAPIRO model and source calculation

The investigation of the neutron propagation in a lead block inserted into the TAPIRO thermal column, concerning the correlation analysis with LFR ELSY “reference reactor”, requires GPT methods calculations [section 2]. ERANOS, differently from MCNPX, allows to perform these calculations. However it is quite difficult to realize an accurate ERANOS model of the TAPIRO experimental facility due to the presence of particular heterogeneities in the facility. To face this problem, in the present work it has been established to characterize the neutron source spectrum at the column entrance using a MCNPX TAPIRO model. Subsequently the estimated MCNPX neutron source has been coupled to a “semplified” TAPIRO lead column ERANOS model, as described in the next section. The MCNPX TAPIRO input model has been suitably modified (see Fig.2). Lead has been take into account inside the “thermal column”. Three different total flux detectors (F-4 track length tallies type) have been considered in correspondence of the middle-plane of the lead column. Radially, the detector positions have been considered at the entrance of the lead column in correspondence. The 60° copper outer reflector sector has been considered removed from the core and replaced by void (in order to try to reproduce a harder neutron spectrum closer to the ELSY one). To well estimate the “effective” neutron source entering the lead column, filtered by the lead back-scattering contributions, in the KCODE simulation has been set to 0 the neutron transport importance of the lead medium on the left side (green area of fig.2).

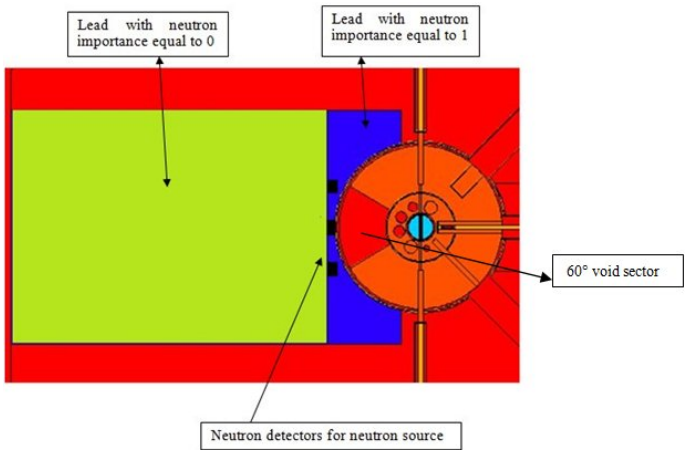

Figure 2. MCNPX TAPIRO model.

5.2. ERANOS TAPIRO lead column model with MCNPX source

Since ERANOS nuclear code is able to perform perturbation and sensitivity analysis only in 2D dimension, the TAPIRO lead column facility (TLF) has been modeled as an XY slab. The model,

shown in Fig.3, consists in the lead thermal column surrounded by concrete biological shield. Inside the first calculation mesh of the lead column has been inserted the neutron external source estimated by MCNPX. The neutron propagation has been performed in transport approximation by 2D ERANOS BISTRO module. The neutron flux spectrum has been analyzed in correspondence of 3 neutron detectors placed at three different positions (DET1 40 cm, DET2 80 cm, DET3 140 cm) along the central axis of the lead column, as shown in Fig. 3.

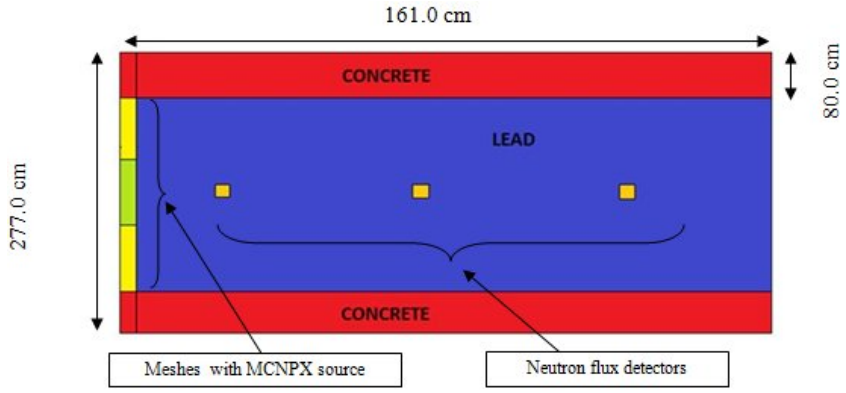

Figure 3. TAPIRO lead column X-Y model in ERANOS calulations.

5.3. ERANOS RZ model of "reference" ELSY reactor

The ELSY ERANOS calculation has been performed in R-Z cylindrical geometry, with a heterogeneous cell treatement of the rectangular fuel elements. The core layout model used for perturbation calculations is shown in Fig. 4. The core model take into account the presence of three different enrichment active zones (indicated such as Fuel_INN, Fuel_INT and Fuel_OUT), radially sorrounded by a control rod zone ('active zone' with B_4C enriched at 90% in B^{10}) and an external lead reflector (Pb_EXT in the figure).
The whole fuel zone is sorrounded axially by two upper and lower fertile UO_2 insulation zones and by two (even upper and lower) plenum zones with steel, lead and void volumes homogenized in one region.

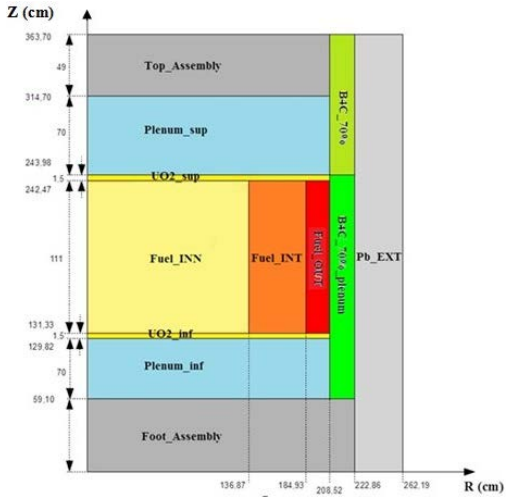

Figure 4. (R-Z) ERANOS ELSY model – axial section.

5.4. ERANOS GPT calculations

The analysis performed by ERANOS aimed to calculate the Correlation Coefficient (Eq. 2.8) between ELSY and TAPIRO systems for the following spectral indexes: F8/F5 and F7/F5. The F8/F5 and F7/F5 behaviour following a lead density variation of -10%, has been analyzed by GPT procedures of

BISTRO ERANOS modules [9]. All the calculations have been performed at 33 energy groups, P_0 transport approximation, using JEFF 3.1 as nuclear data library. GPT calculations have been carried out as follows:

(1) calculation of the importance function [1] relative to F8/F5 and F7/F5 spectral indexes for both TAPIRO and ELSY systems;
(2) calculation of the sensitivity coefficients for both systems and spectral indexes;
(3) calculation of the correlation coefficient using both the variance-covariance dispersion BOLNA matrix at 15 energy groups [16] and a unitary matrix at 33 energy groups, as mentioned in section 2.

The adjoint function has been calculated by placing the spectral index functionals in a 2x2 square mesh area around the following points:

- TAPIRO: X = 40.0 cm Y = 138.5 cm
- ELSY: R = 68.3 cm Z = 181.85 cm

6. RESULTS

Fig.5 shows the MCNPX neutron source estimation at the lead column entrance. It can be noticed that, in comparison with the quasi fission spectrum in the core, at the column entrance we have a neutron spectrum picked around 300-400 keV.

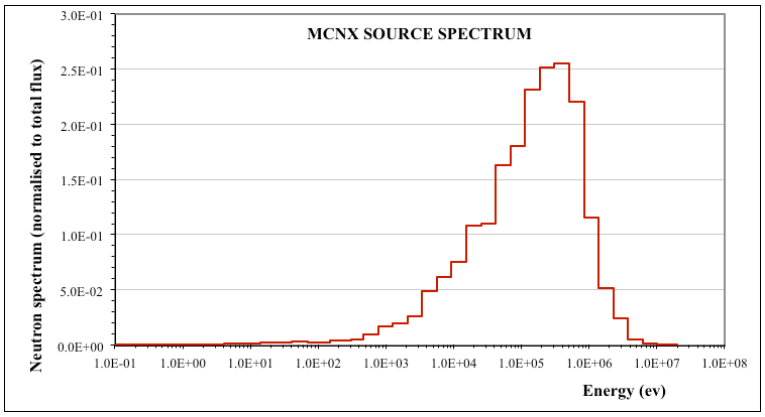

Figure 5. MCNPX source spectrum.

Fig.6 shows the ERANOS and MCNPX comparison relative to the neutron flux estimation of the first detector. It can be seen that there are some remarkable differences in the energy region below about 300 keV. Such differences can affect the results of the F7/F5 spectral index taking into account the threshold.

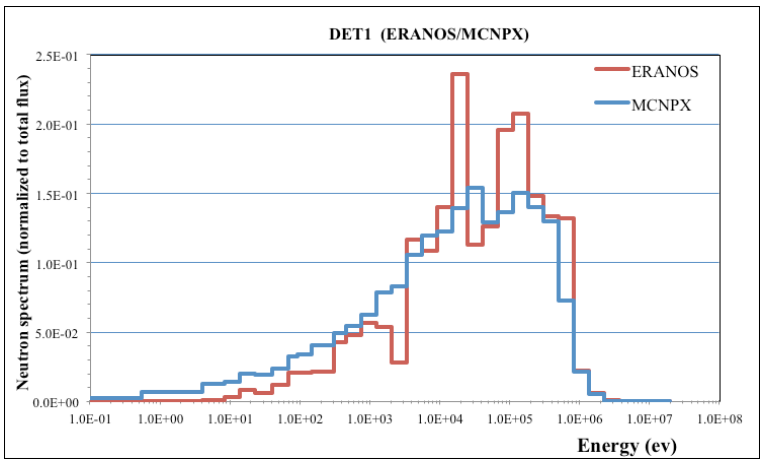

Figure 6. ERANOS/MCNPX spectra at detector 1 position (40 cm in lead).

Fig.7 shows the attenuation of the neutron flux through the central axis of the lead column.

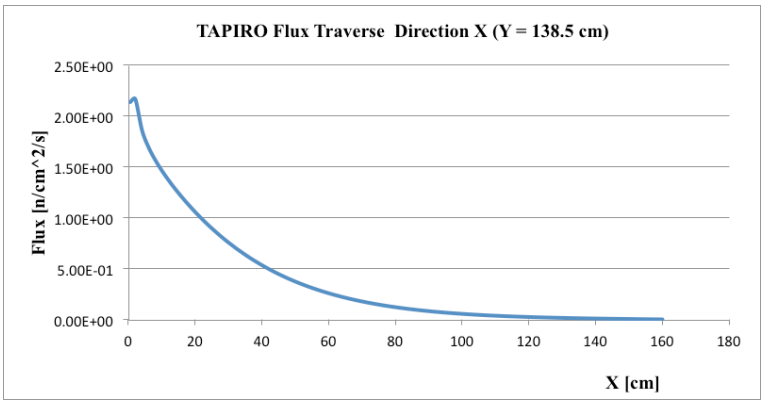

Figure 7. TAPIRO flux profile in X direction through the lead medium.

Fig. 8 shows the comparison between TAPIRO and ELSY in correspondence of the two systems locations where the spectral indexes correlation has been studied. It can been noticed that there are some remarkable differences between the two profiles, even if for energies above 1 MeV some analogies can be evinced concerning the relative behaviour of the two spectra.

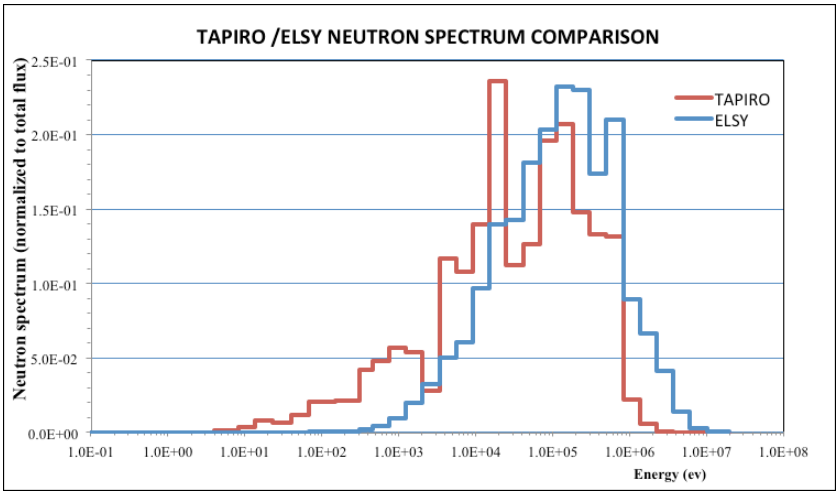

Figure 8. ERANOS/MCNPX spectra comparison.

The results show a good correlation between the integral quantities considered in the reactor facility TAPIRO and the reference system considered (ELSY), as shown in Table 2.
In Table 2 are shown the results concerning the correlation coefficients for the spectral indexes F8/F5 and F7/F5. The results partially reflect the spectral differences noticed between TAPIRO and ELSY in the preselected locations. Being such differences mainly detectable in the energy below 1 MeV, these can partially explaines the relative good correlation obtained for the F8/F5 spectral index respect to the F7/F5 one. Of course further investigations are needed in particular for different locations in TAPIRO lead column. (The meaning of the values in the column 'Unitary dispersion matrix' of Table 2 is given in Section 2)

Table 2. Correlation coefficients

Reaction rates in TAPIRO to be correlated with the 10% void effect in ELSY	**Variance-Covariance BOLNA dispersion matrix**	**Unitary dispersion matrix**
fiss_U238 / fiss_U235	0.775	0.623
fiss_Np237 / fiss_U235	0.509	0.564

7. CONCLUSIONS

This report has been focused on the sensitivity and correlation analysis performed by the ERANOS GPT procedure in relation to the “reference” LFR ELSY reactor and the TAPIRO lead column facility (TLF). The results obtained in this preliminary study indicate that a certain degree of correlation for the spectral index F8/F5, which has an high energy threshold, can be observed. To note that the correlation coefficients of the integral quantities (fission reaction ratios) relevant to the TAPIRO lead column facility with respect to the lead void effect in ELSY result larger than the value (0.38) obtained in a similar study [17] relevant to a 10% lead density reduction effect in both the GUINEVERE reactor facility [18] and ELSY. In a more recent study [19], the correlation coefficients were fission reaction ratios (F9/F5, F8/F5 and F7/F5) for both systems at unperturbed and perturbed (by lead density reduction) conditions. In this case the correlation coefficients exceed the 0.9 value.
Further different TLF configurations are envisaged in a next step of simulation analysis. The possibily of interposing a neutron spectrum filter material (e.g., iron, grafite, etc.) will be in particular investigated in view of obtaining an even better correlation between the integral quantities considered the two systems. In conclusion, these first results of the simulation study, appear to confirm the role of the TAPIRO reactor facility as a useful tool for the design of next generation of LFRs.

ACKNOWLEDGEMENTS

We wish to thank Dr.Giuseppe Palmiotti, of INL for his precious suggestions in the use of ERANOS, and Dr. Nunzio Burgio, of ENEA, for his advise in the use of MCNPX.

REFERENCES

[1] A. Gandini, “Generalized Perturbation Theory (GPT) Methods. A Heuristic Approach”, Advances Nucl.Sci.Techn., Vol 19, Plenum Press, 1987
[2] A. Gandini et al, “Analysis and Correlation of Integral Experiments in Fast Reactors with Nuclear Parameters”, Int. Conf. Physics Fast Reactors, London 1969.
[3] A.K. McCracken, NEA Specialist Meeting on SensitivityStudies and Shielding Benchmarks. Paris, 22 November 1977.
[4] Y.V. Linnik, "Method of Least Squares and Principles of the Theory of Observation", Pergamon Press, London, 1961 [transl. from Russian, original edition 1958].
[5] A. Gandini, "Nuclear Data and Integral Measurements Correlation for Fast Reactors. Part 1:

Statistical Formulation",CNEN Re. RT/FI(73)5 (1973).
[6] A. Gandini, M. Salvatores, “Nuclear data and Integral Measurements Correlation for Fast reactors. Part 3: The Consistent Method”, CNEN Rep. RT/FI(74)3 (1974).
[7] “Assessment of Existing Nuclear Data Adjustment Methodologies”, Document NEA/NSC/WPEC/DOC/(2010)429.
[8] E. Fort, et al., "Improved Performances of the Fast Reactor Calculation System ERANOS-ERALIB1", Annals of Nuclear Energy, vol. 30 (2003).
[9] G. Rimpault, et al., “The ERANOS Code and Data System for Fast Reactor Neutronic Analyses,” Proc. Physor 2002 Conference, Seoul (Korea), October 2002.
[10] J. Blair Briggs, Lori Scott, Enrico Sartori, Yolanda Rugama, “Integral Benchmarks available through the International Reactor Physics Experiment Evaluation Project and the International Criticality Safety Benchmark Evaluation Project”, Int. Conference on Reactor Physics, Nuclear Power: A Sustainable Resource, Casino-Kursaal Conf. Center, Interlaken, Switzerland, Sept. 14-19, 2008.
[11] NEA-1764 IRPhE-TAPIRO-ARCHIVE [see webpage: http://www.oecd-nea.org/tools/abstract/detail/nea-1764].
[12] D. Calamand, A. Desprets, H. Rancurel, R. Vienot, J.C. Estiot, J.P. Trapp, M.L. Bargellini, L. Bozzi, M. Martini, P. Moioli, D. Antonini, A. De Carli, V. Rado, "Results of Neutron Propagation in Steel Sodium Mixtures with Various Source Spectra on HARMONIE and TAPIRO", 5th International Conference on Shielding, Knoxville, USA, 18-22 April 1977.
[13] http://mcnpx.lanl.gov/opendocs/FeaturesList.pdf
[14] A. Gandini, "Uncertainty Analysis and Experimental Data Transposition Methods Based on Perturbation Theory" in Handbook of Uncertainty Analysis, Y. Ronen Ed., CRC Press, Boca Raton, Florida, 1988.
[15] V. Sobolev, E., H. Aït Abderrahim "Preliminary Fuel Pin, Hexagonal Assembly and Core design for ELSY-600", ANS/826/07-15 (SCK·CEN)
[16] M. Salvatores, G. Aliberti, G. Palmiotti, “Nuclear data needs for advanced reactor systems. A NEA nuclear science committee initiative”, in: ND 2007: International Conference on Nuclear Data for Science and Technology, Nice, April 23 2007.
[17] L. Cretara, Thesis. University of Rome “Sapienza”, 2012
[18] G. Bianchini, M. Carta, F. Pisacane, “Set-up of a Deterministic Model for the Analysis of the GUINEVERE Experience”, PHYSOR Malambu 2010 – Advances in Reactor Physics to Power the Nuclear Renaissance, Pittsburgh, May 9-14, 2010.
[19] M. Carta, A. Gandini, V. Fabrizio, V. Peluso, G. Bianchini. "Sensitivity analyses by Generalized Perturbation Theory (GPT) methods applied to GUINEVERE and MYRRHA lead fast reactors", This Conference.

Study of Thorium Utilization in a Large Scale Sodium Cooled Fast Reactor

Zhang Jian, Chen YiYu, Yu Hong, Hu Yun

China Institute of Atomic Energy

Abstract. The breeding performance of ^{232}Th in fast reactor is better than ^{238}U, since the capture cross section of ^{232}Th is slightly higher than ^{238}U under the fast neutron spectrum. There are much less fission neutrons in the blanket, so the proportion of neutron with energy above 6MeV (the threshold energy of (n,2n) reaction of ^{232}Th) is very small. Therefore, the ^{233}U produced in fast reactor blanket would have high purity. In this paper, an large scale fast reactor core was taken as the reference core for ^{232}Th utilization study. In the calculation results, the whole capability of ^{233}U production is about 443kg/(GWe•a) in the blanket; at the end of the first cycle (160EFPD), the ^{233}U production per unit mass of ^{232}Th is about 10.71g/(kgTh), and the weight fraction of ^{232}U in actinium is less than 0.019%. It is an attractive technology option to produce ^{233}U in the blanket.

1. Introduction

Unlike uranium, natural thorium does not have intrinsic fissile content and can't be burned directly as reactor fuel, but ^{232}Th is a kind of fertile nuclide which can be converted into ^{233}U by β decay after absorbing neutrons like ^{238}U, and the product nuclide ^{233}U is a fissile material with excellent nuclear properties to be used as driving fuel in a reactor core. So the most important aspect for utilization of Thorium is how to produce ^{233}U more efficiently with a reasonable technology.

In the process of ^{233}U conversion, along with irradiation of ^{232}Th, the main problem is production of ^{232}U, which will emit high energy γ radiation. It brings great difficulties in reprocessing of spent fuel and in manufacturing of new fuel. So it is an important consideration that how to reduce the ^{232}U content in the ^{233}U product.[1]

This paper mainly discusses the utilization of thorium in fast reactor, including the basic neutronics features of ^{232}Th and ^{233}U, and the estimation of breeding capability in the referenced large scale fast reactor core.

2. Neutronics property of Thorium in fast reactor

The process of nuclide conversion is actually a balance of neutron amount in the reactor system. In fast reactors, there are more excess neutrons, as a result of more neutron release per fission and less useless neutrons absorbed. So it is suitable to breed fertile material in fast reactor core.

Due to that the excess neutron is abundant in fast reactors, the core design usually contains some blankets fueled with fertile material to improve the breeding performance. In addition, ^{232}Th capture cross section in fast spectra is slightly higher than that of ^{238}U, which means that ^{232}Th is very suitable to be bred in the blanket of fast reactor.

At the same time, the fission neutron proportion is very small in the blanket, due to the very low fission rate. As shown in FIG.1, ^{232}U is mainly produced by ^{232}Th through the (n,2n) reaction, which is a threshold energy reaction with the threshold of 6MeV. So the fission neutron is the main causation of ^{232}U production, and we can get much purer ^{233}U product in the blanket.

It is an attractive scheme to load ThO_2 in fast reactor blanket to produce ^{233}U of high purity effectively.

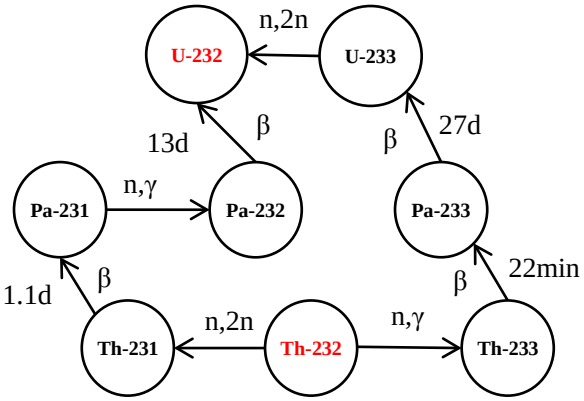

FIG. 1. The reaction chain from ^{232}Th to ^{232}U

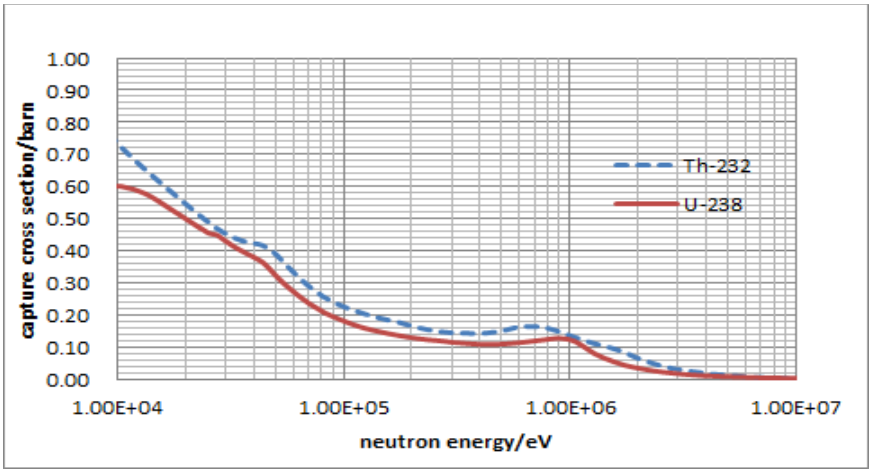

FIG. 2. Capture cross section of ^{232}Th and ^{238}U in fast neutron spectrum

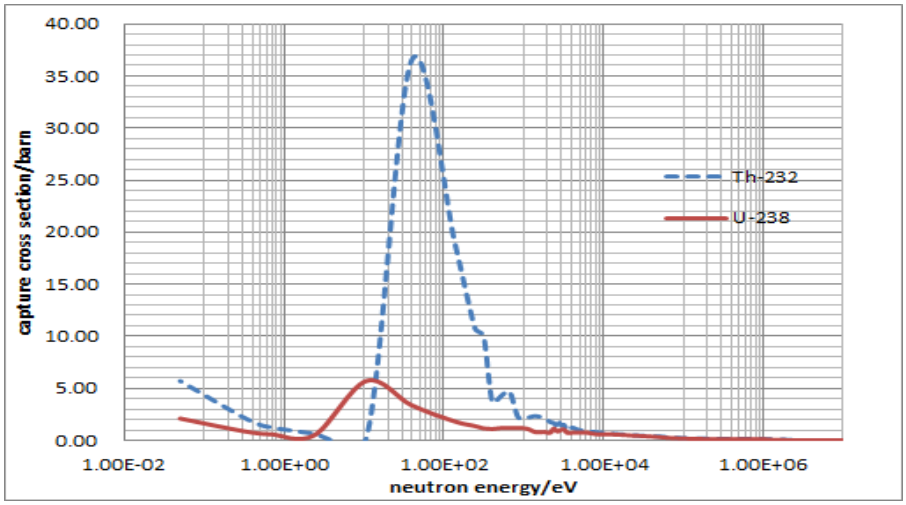

FIG. 3. Capture cross section of ^{232}Th and ^{238}U in the whole neutron spectrum

^{233}U is very suitable for thermal reactors,[2] so the most attractive technology scheme of utilization of Thorium resources is to breed pure ^{233}U in fast reactor and to burn ^{233}U in thermal reactor. This is a

kind of closed fuel cycle, which can give full play to the thorium fuel in fast reactor and the advantage of thermal reactors.

3. Calculation and analysis based on referenced core design

3.1. Information of calculation model and code

In this paper, the main calculation is based on an large scale fast reactor core design, which is a large scale breeding fast reactor with a pool-type sodium-cooled design. The electric power is 870MW with the thermal power 2100MW. And the core layout information is shown in FIG.4. Some design parameter of the referance core is shown in Table 1.

To study the production capacity of ^{233}U with ThO_2 in the referenced core, several schemes have been calculated and analyzed as following:

1) ThO_2 fertile assembly loaded in 4 different positions in the core.

2) ThO_2 fertile material loaded in the whole radial blanket.

3) ThO_2 fertile material loaded in the whole radial blanket and axial blanket.

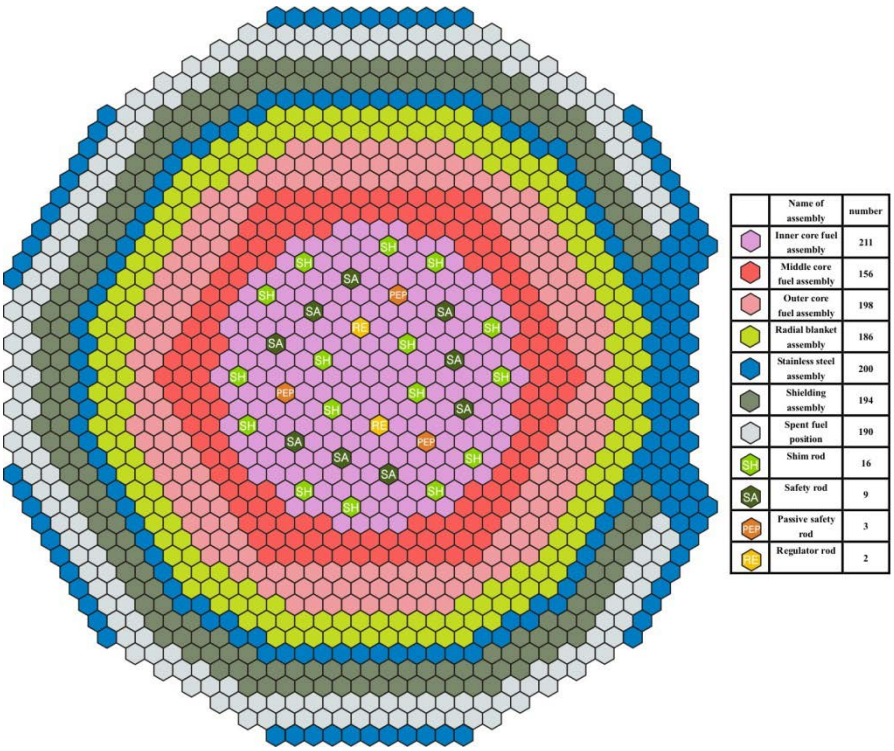

FIG. 4. Referenced core layout

This study use the ERANOS2.0 (European Reactor Analysis Optimized System) code to do calculations. This system can do the reactor physical calculations as diffusion, transport, burn-up, perturbation, fine irradiation and so on. Its nuclear data libraries are mainly derived from the JEF2.2 nuclear data evaluated files. It has already been used in CEFR checking calculation, and the calculation result is satisfactory.

Table 1. Neutron flux and proportion of high energy neutron

Parameters	Value
Power/MWt	2100
Core life/a	40
Coolant	Na
Design burnup(max)/GWd/tHM	100
Max linear power density/kW/m	49
Cycle length/EFPD	160
Fuel type	MOX
Fuel zone length/mm (uper fertile zone/active zone/lower fertile zone)	0/880/350

3.2. Breeding performance of ThO_2 assembly in different positions in referenced core

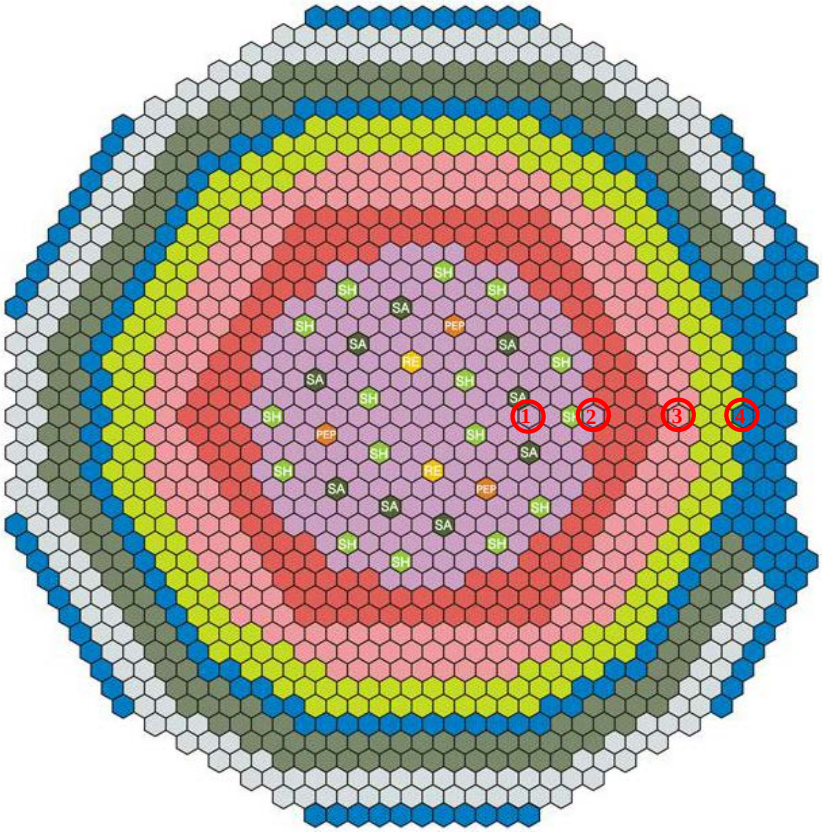

FIG. 5. 4 positions of ThO_2 assembly for irradiation

Table2. gives the average neutron flux density in ThO_2 region in the irradiation assembly, as well as the proportion of high energy neutron flux (>6MeV). In the core fuel zone, neutron flux continuously decrease from center to the fuel zone edge, but the neutron flux proportion of neutron energy higher than 6MeV is basically the same. In core radial blanket, neutron flux is significantly reduced, and at the same time the proportion of neutron flux with energy higher than 6MeV also significantly

decreases, for the reason that the proportion of fission neutron in blanket is very low. As shown in FIG.6, neutron spectrum in fuel zone is nearly the same, while it is obviously softer in the blanket.

Table 2. Neutron flux and proportion of high energy neutron

	Position1	Position2	Position3	Position4
neutron flux/n/(cm2•s)	3.91E+15	3.77E+15	2.41E+15	6.23E+14
proportion of high energy neutron flux(>6MeV)	0.24%	0.26%	0.25%	0.06%

* E+15 means $\times 10^{15}$

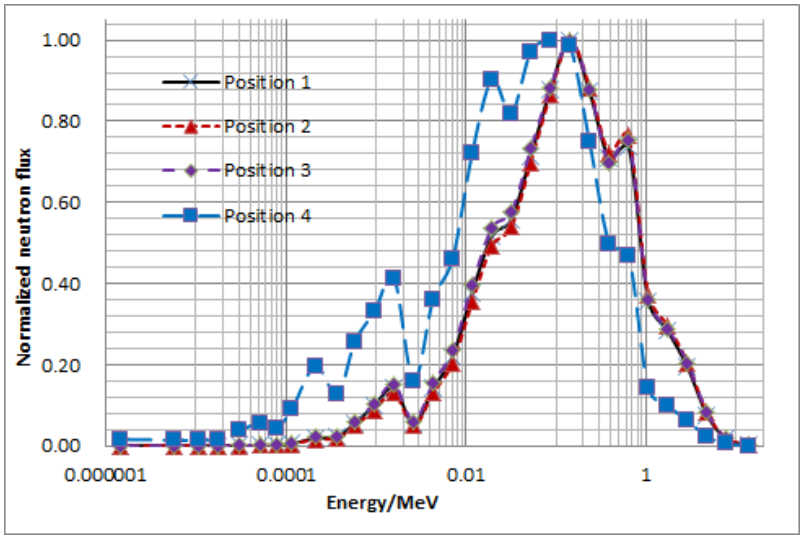

FIG. 6. Neutron spectrum in the irradiation assembly

In FIG.7, ^{233}U accumulation and ^{233}U production per unit mass of ^{232}Th are given. In the fuel zone, the conversion speed is much faster, for the neutron flux is higher. Along with burn-up accumulating, the production speed of ^{233}U in the irradiation assembly will decrease gradually. While in the blanket, ^{233}U mass accumulation is basically in a linear growth trend, due to low burn-up.

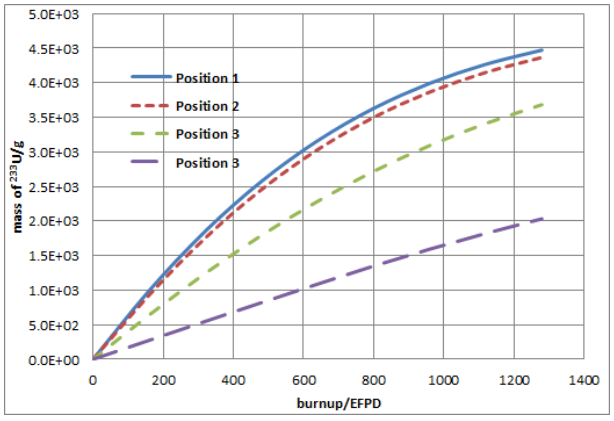

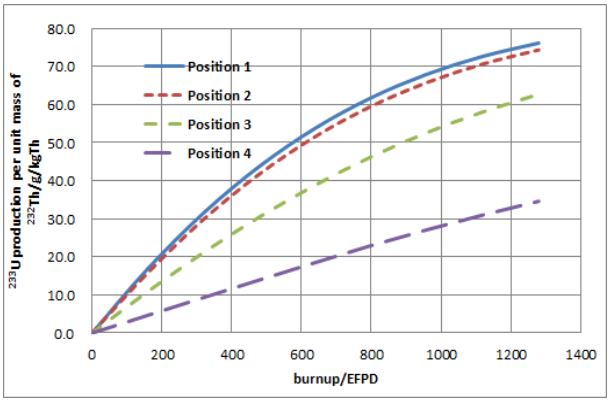

FIG. 7. ^{233}U mass and ^{233}U production per unit mass of ^{232}Th in the assembly

As shown in FIG 8., ^{232}U proportion in actinium is given. In the fuel zone, the ^{232}U proportion is higher, as the neutron spectrum is biased to higher energy, which leads to stronger radioactivity of spent fuel. At the same time, along with burn-up increase, the fission rate also rises as the ^{233}U content increased, which leads to a faster growing of ^{232}U accumulated. In the blanket, the mass percentage of ^{232}U in actinides is very low, which means it's easy to get pure ^{233}U production in the fast reactor blanket.

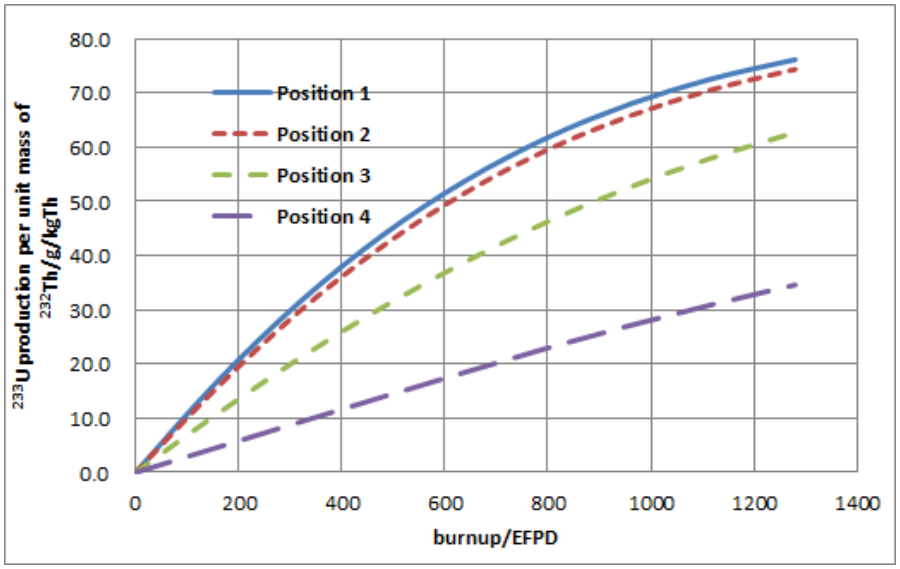

FIG. 8. ^{232}U proportion in actinium

3.3. Two ThO2 loading schemes in referenced core blanket

(1) Scheme 2, the most feasible scheme of ThO_2 loading in referenced core

In this scheme, the radial blanket is fully loaded with ThO_2 assemblies. In the first fuel cycle, the production capacity of ^{233}U is about 246kg/(GWe•a), and the ^{233}U production per unit mass of ^{232}Th is about 8.58g/(kgTh). At EOC of the first cycle, the ^{232}U mass percentage in uranium isotopes is 0.019%, and the ^{232}U mass percentage in actinium is about 0.0002%.

As the main parameters of core with the blanket loaded with ThO_2 assemblies are almost the same with standard referenced core design, this scheme to use ThO_2 fuel in the referenced core is more realistically feasible.

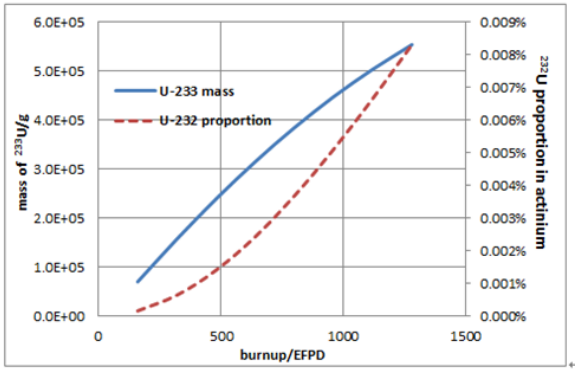

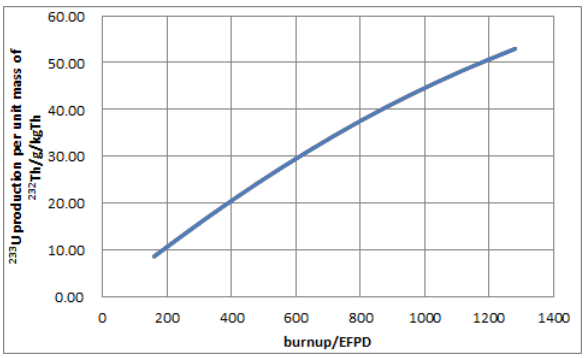

FIG. 9. ^{233}U mass, ^{232}U proportion and ^{233}U production per unit mass of ^{232}Th

(2) Scheme 3, the scheme of ThO_2 loading in referenced core with highest ^{233}U production

In this scheme, the radial blanket is fully loaded by ThO_2 assemblies, and the axis blanket is also filled with ThO_2. In the first fuel cycle, the largest production capability of ^{233}U in the referenced core is about 443kg/(GWe•a), and the ^{233}U production per unit mass of ^{232}Th is about 10.71g/(kgTh). At EOC of the first cycle, the ^{232}U mass percentage in uranium isotopes is 0.018%, and the ^{232}U mass percentage in actinium is about 0.0002%.

As shown in FIG.10, the trend of the accumulation of ^{233}U and ^{232}U is similar with scheme 1.

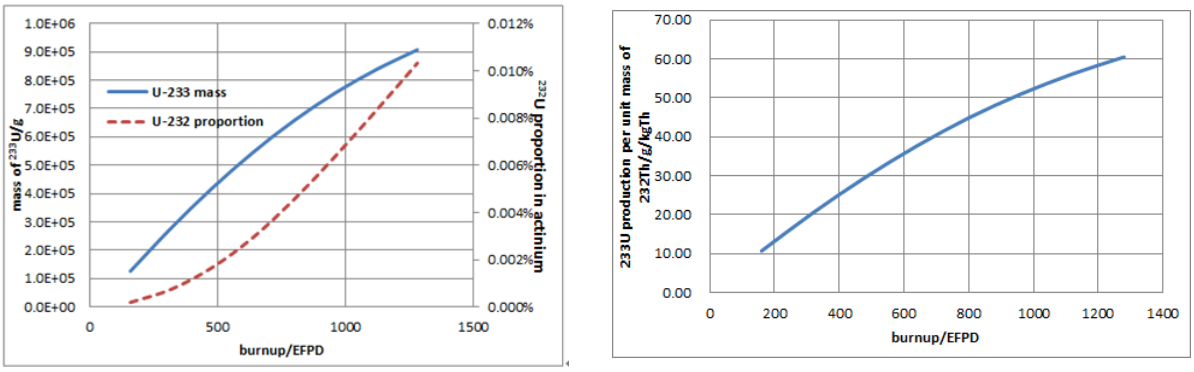

FIG. 10. ^{233}U mass, ^{232}U proportion and ^{233}U production per unit mass of ^{232}Th

4. Conclusion

According to the preliminary neutronics calculations and analyses, some conclusion can be made as the followings:

First of all, the relative high purity of produced ^{233}U is an important advantage in the utilization of thorium fuel in fast reactors. And the neutron balance of fast reactors and breeding performance of ^{232}Th are attractive solution for the utilization of thorium fuel.

Secondly, in the radial blanket of the referenced core, production capacity of ^{233}U using ThO_2 as fertile material is about 246kg/(GWe•a), and the mass percentage of ^{232}U in uranium isotopes is about 0.019%. This scheme will bring less impact on the reference core design and can be the easiest scheme realized in the future.

Finally, when using all blanket of the referenced core, production capacity of ^{233}U is about 443kg/(GWe•a), and the mass percentage of ^{232}U in uranium isotopes is about 0.018%. It is the largest production capacity of ^{233}U in the blanket of the referenced core using ThO_2 as fertile material.

ACKNOWLEDGEMENTS

The authors wish to acknowledge the support of this work by China Institute of Atomic Energy. And the work is partially supported by the CNNC, in the research project of ‘Breeding Performance Study of Large Sodium Cooled Fast Reactor’.

REFERENCES

[1] GU Zhongmao，the Study of Thorium Utilization in Nuclear Energy, technical report of CIAE，2006.

[2] IAEA. Thorium Fuel Cycle－Potential Benefits and Challenges.IAEA-TECDOC-1450. 2005.

Romanian Contribution to the Development of Lead Cooled Fast Reactors

I. Turcu, S. Valeca, M. Constantin

Institute for Nuclear Research, Pitesti, Romania

Abstract. In Romania the nuclear energy is considered an important component of energy mix and for a country sustainable development. Presently based on PHWR CANDU technology, the research and development activities, part of the national nuclear power programme, provide an increased effort towards generation 4, dedicated to support fast reactor lead technology. In the European framework (EU R&D Framework Programmes, European Sustainable Nuclear Industry Initiative) devoted to the development of GenerationIV technologies, Romania is contributing as a partner in EU R&D projects together with a large number of EU research organizations and in the ALFRED MoU, having ANSALDO Nucleare, ENEA and INR as initial members. ALFRED (Advanced Lead Fast Reactor European Demonstrator) project aims to build a 125MWe lead cooled fast reactor demonstrator, connected to the electrical network, with a target date for operation start-up in 2025. In February 2011 Romanian Government approved the option to host ALFRED demonstrator. Based on the access to European structural funds, existing nuclear experience and EU orientation to build the demonstrators in the new member states, Romania is an important option for siting process. An investigation of the existing national capabilities, identification of additional infrastructure and identification of the professional development needs in order to prepare the siting national support are presented in the paper. The main approaches and needed resources to meet expected requirements for ALFRED implementation are discussed as well.

1. Introduction

Today, nuclear energy represents about 16% of electricity production in the world and about 30% in the European Union. The sustainability of nuclear energy is strongly connected with free carbon emmissions, high efficiency of the technology, use of natural resources that aren't very used by other industies, high level of skills and embedded knowledge.

At the same time some difficulties appeared in the relation with the society due to fear of severe accidents and long term consequences of the radioactive waste disposal. Recently, the multi-units accident at Fukushima plant introduced a great public debate and a very emmotionally reaction occurred both for the public and a part of the policy-makers. A tsunami of panic hit some capitals causing strong and rapid decisions like immediate closure of NPPs or moreover a planning for the end of the nuclear power on their country. Such reactions were determined by the national context especially in the perspective of future elections and taking into consideration the position of green parties and ecologist organizations. Other countries reaffirmed the trust in nuclear power as a major option for the energy mix, but improved safety for new nuclear facilities is needed.

Beyond these reactions, the experts tried to emphasize the lessons give us by the accident. One of the most important is connected with the hypotheses of the safety analysis: coincidence of two unlikely phenomena is very unlikely and therefore negligible. Fukushima accident showed us once again that a very low probability event e.g. the coincidence earthquake – tsunami can not be neglected.

Some voices raised the ideea to simplify the complexity of nuclear systems. Many independent systems designed to provide a good redundancy during accidental situations can be replaced by the

design of a simple and robust system that works on principles that preclude the occurrence of such events leading to accidents. This would be the way the public could be more easily convinced about reliability and nuclear safety.

Another fact is connected with the economic efficiency. This parameter shouldn't be the most important for the selection of NPP location and for the plant size. After March 2011 it is questionable if in the future NPPs may be located on the coasts and have multiple units on the site. Maybe modular design should be a good solution from this point of view.

Another fact is bounded to the importance of the residual heat and of the water supplies for the long-term safe shutdown of nuclear reactors. The capacity of intervention (possibility to use water for intervention, availability of water, availability of roads, existing emergency resources etc.) is a crucial point for the mitigation of an accident.

Other important questions are related with the optimal plant life time, how we may maintain the access to the plant during such catastrophic phenomena and what are the correct approaches to mitigate a severe accident in such circumstances: dificult acess, high level of radiation, unpredictible consequences of the interventions.

Beyond of these important aspects raised by the international debate the efficiency of the use of the resources is more and more important since the uranium reserves are limited. The competitiveness of nuclear fission, together with the sensitive problem of the management of spent fuel and radioactive waste are the short and medium term key issues addressed by the Strategic Energy Technology Plan of the European Union (SET Plan) thorough 2020 objectives for nuclear energy. A new generation of reactors, so-called Generation IV, is expected to be in the commercial stage in 30-40 years. SNETP (Sustainable Nuclear Energy Technological Platform) has defined the strategy and priorities for European R&D aimed to build the Generation IV systems in order to meet energy needs and the requirements for security of supply, safety, sustainability, and economic competitiveness. Three fast reactor systems are in development according with SNTEP and ESNII (European Sustainable Nuclear Industry Initiative) vision: the Sodium Fast Reactors (SFR), Lead cooled Fast Reactors (LFR), and Gas cooled Fast Reactors (GCR), ref.[1], [2].

It is clear that nuclear development is facing an enormous challenge. A simple solution may consists of a close collaboration between R & D organizations, nuclear industry, and policy makers worldwide. A new construction focused on safety and security is needed. Economic efficiency may be only a consequence of standardization, modular design, improvements in fuel-use rates, reducing of the radioactive wastes amount, increasing the thermal efficiency, and power-output flexibility, etc. The majority of the nuclear reactors in operation today are large, use fuel as uranium dioxide pellets, use ordinary water to cool the cores and transfer the heat to the turbines with average efficiency.

Even the problem of spent fuel storage pool, revealed by Fukushima accident, may be solved in a simple manner if the spent fuel may be shipped (after 1-2 years) to a reprocessing plant in order to extract minor actinides to be burn in Generation IV reactors. But all this improvements needs time and intensive efforts for development.

On the other hand any decision to slow down nuclear-energy development cannot avoid the environmental consequences since at the moment the nuclear fission is in a real competition only with fossil fuels. Closing of some NPPs means more carbon dioxide in the atmosphere and a new pressure on climate change.

2. Romanian decision to host ALFRED

ALFRED (Advanced Lead Fast Reactor European Demonstrator) project aims to build a 125MWe lead cooled fast reactor demonstrator, connected to the electrical network, with a target date for operation start-up in 2025. The main design features of the demonstrator are ([3],[4]):

- Pool type configuration with reactor vessel and the cavity liner safety vessel,
- Hexagonal wrapped fuel assemblies extended to cover gas to simplify fuel handling
- Mechanical pumps located in the hot collector,
- Double-walled straight SG tubes with continuous monitoring of tube leakages.

The thermal cycle is completely consistent with the ELFR thermal cycle: primary lead temperature being between 400-480°C, secondary side pressure 180 bars, once through SGs with water/steam temperature range from 335 to 450°C in superheated conditions, the overall efficiency has been evaluated higher than 42%. ALFRED will also allow for testing the connection to the electrical grid, with a generated power of about 120 MWe. Based on the use of the defense in depth criteria, safety of ALFRED is extensively enhanced by the use of passive safety systems. Safety features of the LFR system is designed to face challenging conditions and events, due to the very forgiving and benign characteristics of the coolant. There is no need of off-site or emergency AC electrical power supply to manage the design basis accident conditions, the only action needed is the addition of water to maintain the level in the decay heat removal pools which are sized to guarantee at least three days of unassisted fully passive operation.

During the last decade INR was more and more invloved in the European efforts dedicated to Generation IV development [6], by participation in the Euratom FP projects like: ELSY, LEADER, ADRIANA, SEARCH, MATTER, STYLE, MAXIMA. At the same time the national support for Generation IV continuously increased. The main efforts covered aspects of core design, shielding calculations, instrumentation and control, Roadmap definition, material testing, planning of infrastructure.

As a consequence of these efforts and taking into consideration the international context for the development of Generation IV, the interest of Romanian policy-makers and nuclear stakeholders started a national debate for LFR development in Romania.

In February 2011 Romanian Government approved the Memorandum 2025/03.02.2011, "Romanian option to host ALFRED demonstrator", initiated by Ministry of Economy, Trade and Business Environment (METBE). The document declares the availability of Romania to host ALFRED demonstrator and nominates Institute for Nuclear Research (INR) to join the international efforts devoted to the ALFRED consortium construction at European level.

The decision process was facilitated by early stage discussions with some important Romanian stakeholders involved in nuclear development: National Nuclear Agency and for Radioactive Wastes, National Agency for Research and Development, Institute for Atomic Physics- Horia Hulubei, Center for Nuclear Engineering and Design, Regulatory Body.

In the next years the list of the stakeholders will be enlarged in order to include representatives of public, NGOs, and local authorities for the purpose of the necessary assessments of this nuclear installation siting.

The main advantages perceived for the construction of ALFRED demonstrator in Romania are derived from:

- implementation of a high technology
- supporting of the investment based on the existing EU structural/cohesion funds
- active involvement of the R&D organisations and industry in programmes of international interest
- consolidation of the position of the country in the nuclear sector
- creation of new jobs for nuclear sector
- hosting an important European demonstration infrastructure and improvement

- deep involvement of the country in Generation IV development

In February 2012 a MoU (Memorandum of Understanding) was signed by Ansaldo Nucleare, ENEA, and INR in order to prepare the future ALFRED consortium. MoU considers Romania as the reference option for the siting.

In April 2012 the meeting of the partners decided to form three working groups: WG1 Roadmap; WG2 Legislative and Financing framework; WG3 Costs.

In this context some tasks related to the siting was clearly defined and some activities are under development:

- exploring of the specificity of national regulations for site licensing and ALFRED licensing;
- evaluation of the influence of a specific site in the costs;
- exploring the framework of cohesion/structural funds at European and national level;
- Roadmap construction including aspects of the siting process.

In May 2012 the new Prime Minister of Romanian Government, Victor Ponta, attended "Nuclear 2012" the 5th Annual International Conference on Sustainable Development through Nuclear Research and Education hosted by the INR. Victor Ponta acknowledged the importance of ALFRED project for the sustainable development of nuclear power. He stated that on behalf of the Government he will ask the authorities at Brussels to consider Romania as hosting country for ALFRED reactor based on a structural funds scheme.

In May 2012 INR was accepted as member of ESNII [5]. Some lobby activities were performed at the level of European organisations including European Parliement in order to support Romanian option to host ALFRED.

3. Siting process

Based on the national decision and MoU activities, INR has started discussion with national organisation responsible with siting study, Center for Nuclear Engineering and Design (SITON) in order to produce a list of input data needed for siting evaluation, and also with the Regulatory Body (CNCAN) in order to discuss the licensing process.

A reference option for the siting was considered: a field included in nuclear platform Mioveni, near Pitesti. This option is shortly described bellow. The nuclear platform includes three organisations: INR, FCN (CANDU Fuel Plant), and a branch of AN&DR (National Nuclear Agency and for Radioactive Wastes). A dual core research reactors (TRIGA SSR, and ACPR), post irradiation examination laboratories, fuel fabrication buildings, waste treatment plant are the main facilities on the site.

The site benefits of the:

- electrical supply, including 110 kV electrical station
- water supply
- demineralised water
- waste water treatment plant
- radioactive waste facilities
- fire brigade

- heating plant
- natural gas supply
- physical protection
- access road to transport large equipment
- already investigated field (e.g. earthquake characterization)

A part of these capacities need to be extended for the purpose of ALFRED demonstrator operation. The site may benefit for the existing infrastructure, proximity of the INR departments, availability of the existing personell for different activities. The choice will avoid some expenses with services and construction of buildings for these services and help ensure the timely development of the project.

Estimated surface (total footprint area) for ALFRED site (LEADER-Task 3.6 Plant Lay Out coordinated by Empresarios Agrupados) 325m x 300 m is available and in property of the Romanian state. This surface is incorporated in the actual site and in physical protected area. Additional land is available close to the site.

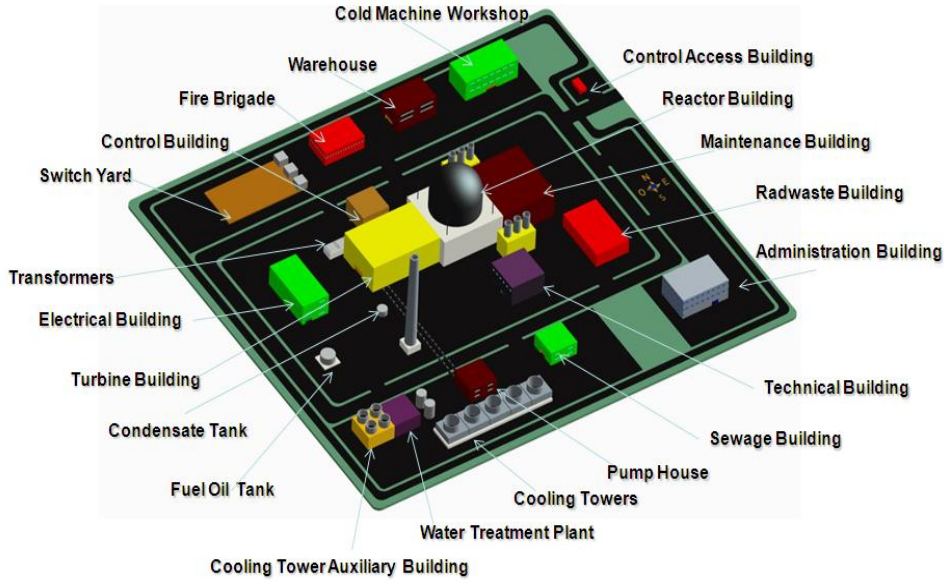

FIG. 1. ALFRED demonstrator – Plant Lay Out

In fig. 1 the plant layout proposed by LEADER project is presented [3]. In fig. 2 a possible adaptation of the lay out to the existing site (inside of security fence) is presented. A preliminary safety analysis is needed in order to produce the source term and define the exclusion zone according to national regulations. This exclusion zone needs to be correlated with other restrictions (TRIGA and FCN exclusion zones already defined on the nuclear site). Whole area represented in fig. 2 is at the moment free of any buildings. The proposed lay out maximize the distance from ALFRED to other nuclear installations.

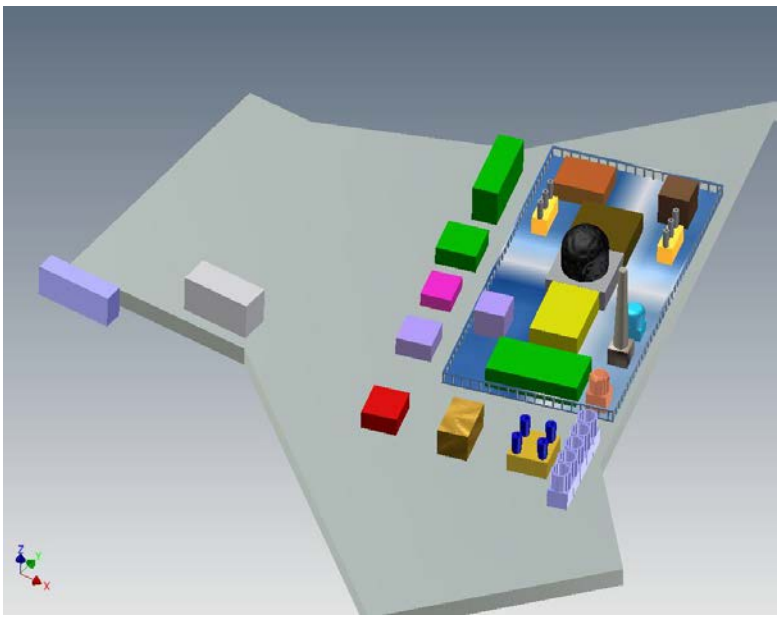

FIG. 2. Adapted Plant Lay Out to the Existing Site

4. Capabilities to Be Upgraded or to Be Built

The Institute for Nuclear Research from Romania is a complex R&D center with over 40 years of activity in the nuclear energy field, deeply involved in the management and execution of the R&D National Nuclear Power Program. The main activities cover a large spectrum of nuclear energy: nuclear safety, design, manufacturing and testing of nuclear fuels, ageing mechanisms of structural materials, irradiation technologies radioisotopes production, instrumentation and control, environmental protection, radioactive waste and spent fuel management. The main scope of the activities cover mainly CANDU technology. An important experience in operation of research reactors including operational safety, and also in CANDU NPP analysis, operation, and maintenance exists.

Also the institute acted as a pole of education by a strong collaboration with Romanian universities to support laboratory activities, fellowships, graduating disertation thesis or doctoral thesis.

From the point of view of the Generation IV R&D activities INR benefited by the expertise exchange and creation in the frame of Euratom projects (ELSY, LEADER, ADRIANA, SEARCH, MATTER, STYLE, MAXIMA) and IAEA projects (INPRO) and also by bilateral agreement. Activities performed by INR in the filed of core design, shielding design, instrumentation and control, and material testing proved real competences to contribute to LFR development. On the other hand the important experimental activities should be developed at INR in order to built the competences for lead technology.

Based on bilateral agreement INR-SCK·CEN a very useful expertise exchange are in progress with the aim to built two loops at INR: one for material testing (Fig. 3), and another for full scale ALFRED pump testing (Fig.4). The first loop is in the stage of construction and at the end of 2013 the start of the operation is expected. The second loop is in the design stage. Arrangements between INR and ENEA are planning in order to involve young scientists from INR in the field of lead corrosion and pump testing.

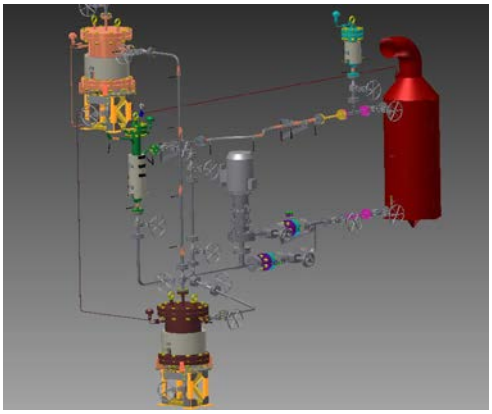

FIG. 3. Material Testing Loop

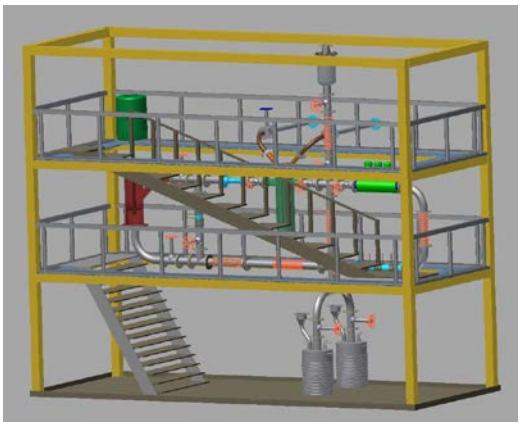

FIG. 4.Full Scale Pump Testing Loop

Another key issue is the safety analysis field in order to prepare the licensing documentation (both for siting process and ALFRED demonstrator itself), and the operational safety.

The sustainability and safety of the nuclear energy strongly depend on the sufficient and timely influx of highly educated, motivated and diverse workforce, and on creation or transfer of new knowledge. Research activities may support a mid term development of the competences for existing workforce and newcomers.

Taking into account ALFRED option INR considers a re-shaping of the organisational strategic development by increasing the LFR activities. For example in 2012 an increase of 1 mil. euro was produced. On the other hand a planning for hiring the appropriate workforce from the national market is prepared. According with this plan around 100 newcomers are expected to be hired until the end of 2016 (50 during the next 2 years), and around 300 until 2020.

The existence of the local competences is crucial for the safety of the operation. The accident of Fukushima revealed the importance of local competences during the progression of the accident. Also assimilation of a new technology requires local efforts and local competences building.

A great organisational effort is needed to train the newcomers for LFR field. Two approaches are considered in the INR vision: (1) international training at centers with high expertise in the field; (2) extending the training facilities at INR and use international and local trainers.

Another key aspect is the link between infrastructure development (especially related to experimental activities in lead technology) and training. This development is seen as a good school to upgrade and build competences and also as important tools for future trainings.

It should to be noticed that recent evolutions in the different countries, which include political decisions against nuclear power and a rather persistent economic crisis, might give rise to the deterioration of the sufficiency of national resources, both in terms of research capabilities and workforce. Potential consequences might include the long term deterioration of nuclear safety, which may jeopardize the sustainability of the nuclear energy.

Advancing sufficient and necessary diversity of the national and pan European nuclear safety research is therefore among the top strategic priorities of the Sustainable Nuclear Energy Technology Platform (SNETP). On the other hand SNETP promote the development of fast reactors with closed fuel cycle.

In this context Romania is determined to improve national capabilities for nuclear field including LFR development based on the next stage, ALFRED demonstrator.

5. Conclusions

(C1) Large and expensive infrastructures are planned to be constructed during the next 10 years in some New EU Member States (for example ALFRED in Romania, ALLEGRO in Czech Republic, Slovakia or Hungary). The costs of these investments cannot be covered only by traditional Euratom research funds, nor by national contributions. A mixed scheme with an important part of cohesion funds is expected.

(C2) Romania is determined to participate actively in LFR research and development by contributing to international projects and by its national programme. On the other hand Romania expressed the availability to host ALFRED demonstrator. A Memorandum of Understanding was built by INR, Ansaldo and ENEA considering Romania as the reference option for siting.

(C3) Local capabilities upgrading and building is an important issue for ALFRED development and development. INR planned the hiring of around 100 newcomers until 2016 (50 during the next 2 years) and provide their training by extending the domestic training facilities and by cooperation with high experienced centers in the field.

REFERENCES

[1] SUSTAINABLE NUCLEAR ENERGY TECHNOLOGY PLATFORM, Strategic Research Agenda (2009), http://www.snetp.eu/www/snetp/images/stories/Docs-AboutSNETP/SRA2009.pdf

[2] SNETP/EUROPEAN SUSTAINABLE NUCLEAR INDUSTRIAL INITIATIVE, A contribution to the EU Low Carbon Energy Policy: Demonstration Programme for Fast Neutron Reactors, Concept Paper (2010, under revision), http://www.snetp.eu/www/snetp/images/stories/Docs-ESNI/ESNII-Folder-A4-oct.pdf

[3] ALEMBERTI, A., et al., “The European Lead Fast Reactor Strategy and the Roadmap for the Demonstrator ALFRED”, International Conference on Fast Reactors and Related Fuel Cycles: Safe Technologies and Sustainable Scenarios (FR13), Paris, France (2013)

[4] ALEMBERTI, A., et al., “The Lead Fast Reactor – Demonstrator (ALFRED) and ELFR design”, International Conference on Fast Reactors and Related Fuel Cycles: Safe and Sustainable Scenarios (FR13), Paris, France (2013).

[5] TURCU, I., CONSTANTIN, M., “INR Contribution to LFR”, ESNII Task Force Meeting, Paris, May 2012.

[6] VALECA, S., PAUNOIU, C., TURCU, I., CONSTANTIN, M., “ALFRED: Current Status and Future Developments in Romania”, International Conference Nuclear 2012, Pitesti, Romania.

Status of the ASTRID core at the end of the pre-conceptual design phase 1

MS. Chenaud, N. Devictor, G. Mignot, F. Varaine, C. Vénard, L. Martin, M. Phelip, E. Brunon, D. Lorenzo, F. Serre, F. Bertrand, P. Richard, M. Le Flem, P. Gavoille, R. Lavastre
CEA, 13108 St-Paul-lez-Durance, France
Phone: +33 4 42 25 70 48 Fax: +33 4 42 25 36 35 E-mail: marie-sophie.chenaud@cea.fr

V. Garat, D. Verrier,
AREVA-NP, 10 rue J.Récamier, 69456 Lyon, France

D.Schmitt
EDF, Clamart, France

Abstract – *Within the framework of the ASTRID project, core design studies are being conducted by the CEA with support from AREVA and EDF. The pre-conceptual design studies are being conducted in accordance with the GEN IV reactor objectives, particularly in terms of improving safety. This involves limiting the consequences of 1) an hypothetical control rod withdrawal accident (by minimizing the core reactivity loss during the irradiation cycle), and 2) an hypothetical loss-of-flow accident (by reducing the sodium void worth).*
Two types of cores are being studied for the ASTRID project. The first is based on a 'large pin/small spacing wire' concept derived from the SFR V2, while the other is based on an innovative CFV design. A distinctive feature of the CFV core is its negative sodium void worth.
In 2011, the evaluation of a preliminary version (v1) of this CFV core for ASTRID underlined its potential capacity to improve the prevention of severe accidents.
An improved version of the ASTRID CFV core (v2) was proposed in 2012 to comply with all the control rod withdrawal criteria, while increasing safety margins for all unprotected-loss-of-flow (ULOF) transients and improving the general design.
This paper describes the CFV v2 design options and reports on the progress of the studies at the end of pre-conceptual design phase 1 concerning:

- *Core performance,*
- *Intrinsic behavior during unprotected transients,*
- *Simulation of severe accident scenarios,*
- *Qualification requirements.*

The paper also specifies the open options for the materials, sub-assemblies, absorbers and core monitoring that will continue to be studied during the pre-conceptual design phase 2.

Introduction

The first phase of the pre-conceptual design for the ASTRID[1, 2] prototype (Advanced Sodium Technological Reactor for Industrial Demonstration) is ending in 2012. This paper assesses the studies carried out at this date concerning the core design (at 1500MW) which falls under the responsibility of the CEA.

The pre-conceptual design phase 1 focused on a core concept with a low void effect, known as the CFV concept[3, 4], based on the use of a sodium plenum zone, an absorbing zone in upper shielding and an internal fertile zone in specific core geometry.

The first assessments carried out on version v1 of the CFV concept showed a promising safety improvement for this type of concept[5]. These studies were continued in 2012 with the aim of optimising this concept with respect to the ASTRID safety objectives by investigating the possibility of:

- increasing the safety margins in relation to the boiling point in the event of a total loss of power to the reactor without scram,
- increasing margins in relation to fuel meltdown in the event of an accidental control rod withdrawal,
- increasing margins in relation to the reactivity control requirements.

The options chosen to achieve these goals in version v2 of the CFV core were the following:

- Decreasing the fuel temperature at full rated power, which is favourable in the event of a total loss of power to the reactor without scram (reduction of the Doppler integral) while increasing the fusion margin in the event of a control rod withdrawal (increase in the ratio between the linear power to fusion and the initial linear power) obtained by:
  - Reducing the linear power by approx. 20%: increasing the number of fuel pins per sub-assembly (switching from 217 to 271 pins).
  - Reducing the power density by approx. 15%: increasing the number of fuel sub-assemblies (addition of an assembly ring).
- Adding shutdown rods to increase the margins between control requirements and available reactivity worth.

In addition, the design was optimised by 1) reducing the duct wall thickness and the inter-assembly gap according to the proposals resulting from the preliminary design studies on the fuel sub-assemblies, 2) using full fertile pellets (increased breeding gain and reduced loss of reactivity), and 3) minimising the quantity of B_4C in the upper neutron shielding (while respecting the negative sodium void worth criterion).

Performance

The following table summarises the characteristics of versions v1 and v2 of the CFV core.

Table 1: Summary of the characteristics of the cores studied during pre-conceptual design phase 1

	CFV-1500MW-v1	**CFV-1500MW-v2**
Number of fuel sub-assemblies (Inner zone / Outer zone)	291 (177 / 114)	355 (241 / 114)
Number of pins / sub-assembly	217	271
CSD/ DSD number	12 / 6	12 / 8
S/A pitch (cm)	17.5	17.17
Inner zone / outer zone fissile height (cm)	60 / 90	60 / 90
Inner fertile zone / lower axial blanket (cm)	20 / 30	20 / 30
Inner zone / outer zone Na plenum (cm)	40 / 30	40 / 30
Average PuO_2 enrichment (vol%)	21.6	22.7
Initial Pu loading (t)	4.9	5.8
Mass of Pu (t) per year	1.15	1.18
Circumscribed diameter of the core (cm)	340	367
Loss of reactivity per day (pcm/EFPD)	4.3	3.6
Core average power density (W/cc)	234	204

Maximum linear power (W/cm)	484	317
Average burn-up (GWd/t)	78	77
Conversion ratio	-0.02	-0.02
Sodium void worth at EOC ($)	-0.5	-0.6
Coolant Pressure drop across pin bundle (bar)	2.6	1.7

The CFV cores under study comply with the performance requirements of the ASTRID specifications in terms of fuel residence time, fuel cycle length, average burn-up and breeding gain.

In terms of the overall dimensions, the CFV v2 core has a circumscribed diameter which is slightly larger than that of the CFV v1. This is due to the design options (strong reduction in the power density and the linear power) which aim at reinforcing the intrinsic safety behaviour. This represents an economic penalty for the CFV v2. In the safety paragraph, the natural behavior of the two cores in prevention situations is compared.

It was checked that the CFV cores made it possible to achieve the performance levels expected in terms of transmutation for the ranges considered for the ASTRID project (up to 2% of homogeneous americium and 10% for minor-actinide-bearing blankets, known as MABB).

Lastly, the studies conducted on the cores at 3600 MW showed that the performance of the CFV cores could be extrapolated up to this level of power.

Safety

Severe accident prevention situations

As far as severe accident prevention is concerned, following conditions have been studied:

- Unprotected loss of flow (ULOF) sequences:
  - total loss of power without reactor scram resulting in the coast down of the primary and secondary coolant pumps and steam generators dry out. This was the reference sequence in the safety files for previous reactors,
  - coast down of all the primary pumps without reactor scram while the secondary coolant pumps remain operational to remove power. This sequence is an alternative to the previous sequence,
  - failure of a pump – diagrid connection without reactor scram. In this scenario, the behaviour of the core can be assessed with respect to fast flow losses.
- A sequence of unprotected loss of heat sinks (ULOHS): the secondary pumps are tripped and the steam generators dry out without reactor scram.
- Conditions involving control rod withdrawal (CRW), with or without detection.

The results and the analysis of two sequences are presented hereafter.

Modelling

The accident sequences are simulated with the CATHARE[6] code. The core, the entire primary system, the secondary circuit and the steam generators have been modelled. The water-vapour conversion system is represented by limit conditions at the inlet and outlet of the steam generators.

At the same time as the accident sequence calculations, work also focused on improving the modelling (modelling of the core and fuel pins based on GERMINAL[7, 8] calculations, modelling of the secondary circuit, etc.) during the entire pre-conceptual design phase 1, which will be continued during phase 2 of the pre-conceptual design.

Total loss of power transient

The following graphs represent the variations in the core outlet temperature (maximum temperature at the outlet of the hottest sub-assemblies) and in the core power during a total-loss-of-power transient for a SFRV2 core, as well as for the CFV v1 and CF v2 cores.

Figure 1 corresponds to a calculation in which the mechanical inertia of the primary pumps generates a semi-flow rate in the core within 10 s.

Figure 2 corresponds to a calculation in which the mechanical inertia of the primary pumps generates a semi-flow rate in the core within 24 s.

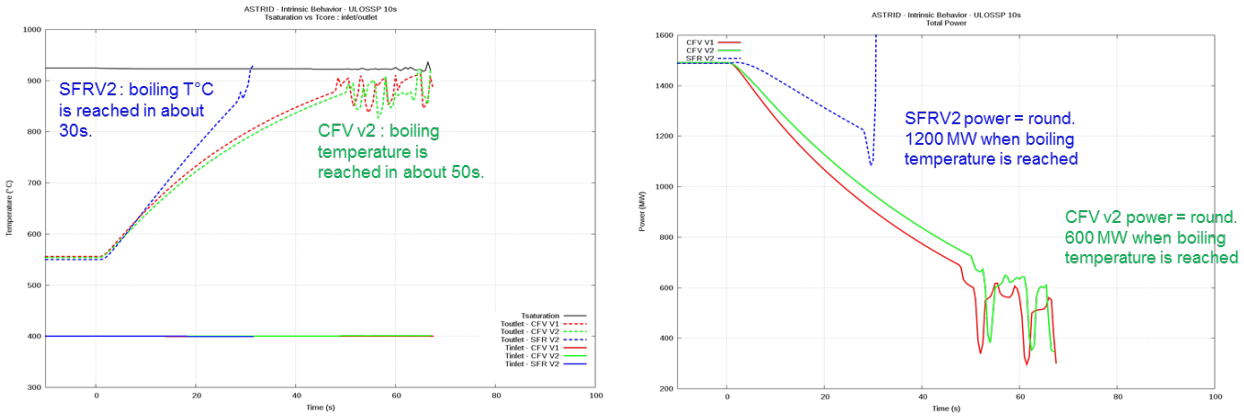

Figure 1: Total loss of power transient for CFV v1, CFV v2 and SFR V2 cores - Core semi-flow rate within 10s - Core outlet temperature and power

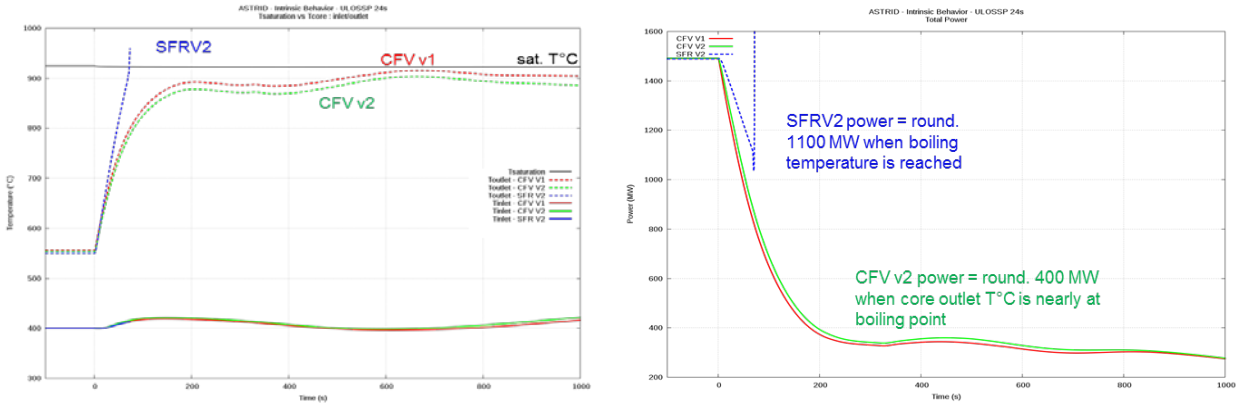

Figure 2: Total loss of power transient for CFV v1, CFV v2 and SFR V2 cores - Core semi-flow rate within 24s - Core outlet temperature and power

The results show that the specific characteristics of the CFV core (in particular, its set of neutron feedback and a low sodium void coefficient) lead to a behaviour scenario with different and more favourable kinetics than for the SFRV2.

For this transient, the CFV v2 core does not provide the gain expected with the selected design options (strong reduction in the linear power and the power density in particular) because the fuel analysis showed that part of the fuel did not fill in the pellet-cladding gap before the transient. The graphs in Figure 3 show the significant advantage of the CFV v2 design options in terms of Doppler feedback. However, 'free-fuel' operation modifies the neutron feedback related to fuel expansion, which reduces the positive impact of the reduction in the linear power and the power density. Overall, the sum of the feedback (Doppler + cladding expansion) varies little between the CFV v1 and the CFV v2 cores.

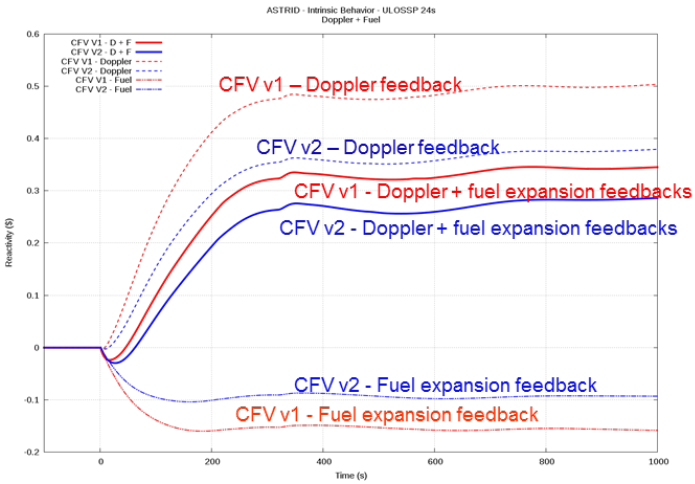

Figure 3: Total loss of power transient for CFV v1, CFV v2 cores – Doppler and fuel expansion feedbacks

Furthermore, the conditions (cold fuel, pellet-cladding gap equal to zero or very low, high power ramp) of pellet-cladding interaction due to a power increase during the accidental withdrawal of a control rod, are potentially met for certain CFV v2 core sub-assemblies located near the control rods. The examination of feedback from experiments conducted on accidental control rod ejection-type power transients leads to recommend that the linear power at the beginning of the life, in the maximum flux plane, is to remain above 300 $W.cm^{-1}$ so that the operating mode of the ASTRID core does not deviate from the known domain: this recommendation will be taken into account in the pre-conceptual design phase 2.

Unprotected-loss-of-heat-sink (ULOHS) transient

The graphs in Figure 4 show the temperature variations at the core inlet and outlet when the secondary coolant pumps are tripped without reactor scram, the steam generators are dried and the primary flow is maintained. The examined criterion is the isothermal temperature in the primary circuit at which the fission power is extinguished (without inserting the absorbers) thanks to reactivity feedbacks.

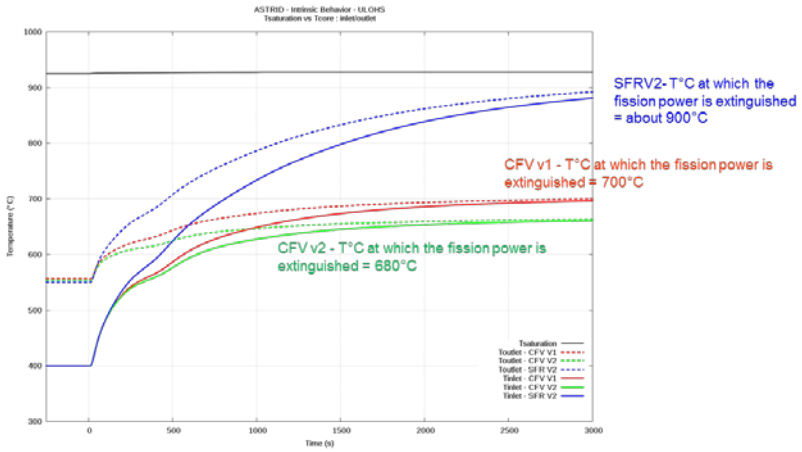

Figure 4: ULOHS transient for CFV v1, CFV v2 and SFR V2 cores - Core inlet and outlet temperatures

In a situation involving the loss of unprotected heat sinks (ULOHS), the CFV core shows a significant gain compared with a SFV2-type core. The CFV core reveals a substantial safety margin relative to the boiling point and a relatively low smothering temperature. This suggests a robust demonstration in terms of the resistance of the structures over several days, therefore providing more time for conducting operations and restoring safe conditions.

Other transients

Studying the initiators of transients of power (TOP) and control rod withdrawal (CRW) has not provided discriminating element between the CFV and SFR V2 core concepts.

Certain accidental control rod withdrawal assessments show low safety margins with respect to the criteria considered for the CFV cores. However, design optimisations have been identified.

Conclusion on prevention situations under study (total loss of power in particular) and orientation for the pre-conceptual design phase 2

In unprotected total loss of power conditions, according to certain assumptions concerning the chosen design options (e.g. the inertia of the primary pumps leading to a semi-flow rate within 24 seconds during the pump trip), the studies show that a CFV-type core can provide a positive safety margin in relation to the boiling point. However, the integration of uncertainties shows that this margin is insufficient vis-à-vis a robust demonstration showing that sodium does not boil. A robust margin will be ensured by adding an additional safety measure (which will be selected and designed during the pre-conceptual design phase 2) to cover these uncertainties and to achieve conditions which are compatible with the resistance of the structures.

Severe accident mitigation situations

These studies involve taking into account restrictive decoupling criteria to ensure a robust demonstration and an assessment that is as conservative as possible so it overrides any dependency in terms of the development of the scenario.

For a widespread core meltdown following an unprotected loss of power, the transient calculations show that, due to its intrinsic characteristics, the thermal power has already dropped significantly when the CFV core reaches the degradation phase, compared with the SFRV2 core (see Figure 1 and Figure 2). A reduced power, due to the negative sodium void effect in the event of sodium draining, would lead to a different phenomenological degradation sequence for the CFV core compared with the known reference sequences : the cladding would firstly melt and then the fuel.
The first assessments of theses conditions lead us to believe that there should be no major reactivity insertion and that the core behaviour would probably improve in terms of the release of mechanical energy compared with the SFR V2 core.
These conditions would lead to core degradation which is preferably controlled via the thermal conditions, and supports the assumption of a stratified geometry maintained for a certain period of time by the fertile plate in the inner core. As a result, it is expected to take significantly longer to reach molten pool conditions. This delay could be exploited to implement the additional mitigation measures.

The CFV core improved behaviour compared with the SFRv2 under these degraded conditions has to be confirmed in pre-conceptual design phase 2.

Qualification

In 2012, the various qualification requirements for the CFV core were analysed in the following fields: neutronics, thermohydraulics and core mechanics, fuel sub-assemblies and absorbers, core materials, core instrumentation, and safety. This analysis involved evaluating the feedback, identifying the lack of information in experimental databases, and validating computer codes for the various fields.

On the basis of this information, a preliminary qualification plan was established which mainly focused on identifying the qualification requirements that make it possible to differentiate between a CFV-type core concept and a homogeneous core (SFRv2), or potentially located on the critical path of the ASTRID master schedule.

The qualification data considered to be the most structuring with respect to the schedule are reviewed in the following section.

Neutronics

The need to complete the GENESIS neutronics programme on the critical MASURCA model has been confirmed, regardless of the core concept. These CFV and SFRv2 cores fall outside the scope of existing experimental qualification when considering the neutron spectrum, given their different characteristics compared with the previous core designs (such as Superphénix or the EFR) in terms of volume fractions of fuel and sodium. Due to its inventory of fissile material, the MASURCA model can be used to develop an experimental core that is representative of the physics of large cores (better representation of spatial effects), which is essential for the CFV or SFR V2 core concepts.

A prior experimental programme aiming at analysing effects of plenum addition and internal fertile zone insertion is starting in the BFS reactor of Obninsk IPPE in collaboration with Russia.

Fuel[10]

It is recommended to carry out a phase-3 qualification irradiation using a fuel prototype on the scale of the pin and bundle. The purpose of this irradiation using a fuel prototype is to validate the design,

manufacturing and operating process of the pin bundle in representative conditions. Indeed, the large pin/small spacing wire geometry is innovative compared to the pin bundle geometry of previous reactors.

The last qualification phase, known as phase 4, aims to qualify the industrial product and should be carried out in the ASTRID reactor during the transition from the start-up core to the equilibrium contractual core[9].

The level of qualification of both the CFV and SFR V2 fuel concepts are considered to be similar. For a heterogeneous CFV-type fuel, the examination of the ZEBRE irradiation programmes carried out in Phénix on heterogeneous pins showed that, in the fissile areas, the behaviour of the fuel remained similar to that of homogeneous fuel and that the interfaces with the fertile areas did not present particular phenomenologies.

Besides the ZEBRE program, it will be possible to mainly base the qualification of CFV fuel on the post-irradiation assessments of 1) the PAVIX 8 experiment carried out in Phénix in the nineties, consisting of full sub-assemblies of heterogeneous pins with an AIM1 cladding (cladding material selected for the first ASTRID core loadings) and 2) the CZAR 1 experiment, re irradiation at high rate of few pins of the ZEBRE experiment.

Absorbers

The following operations are strongly recommended in order to qualify the absorbers:

- Irradiation of specific materials to qualify the coatings of the guide parts exposed to the neutron flux.
- Irradiation of absorber elements, with design and flow conditions as representative as possible of the core upon start-up, to support the validation of the entire design-manufacture-service request process, the qualification of the carbo-thermal B4C, and the demonstration of the lifetime of a jacket.
- Optimisation of the integration schedule for the post-irradiation assessments of the Phénix rods by the LECI laboratory, in order to minimise the number of validation elements for the design, which are likely to be provided at a later date.

Materials

Concerning the materials, the first cores of ASTRID will be based on the choice of known materials, which have already been tested, even in Phoenix cores, such as for example EM10 for the material of the wrapper tube and AIM1 for the cladding. However, the CFV concept has design specificities which require a dedicated qualification program related to the welding of the plug/cladding subjected to a higher flux.

A program to acquire additional data of core material behaviour at high temperatures (up to 950°C) was initiated to complete the evaluation of the core behaviour under accident conditions.

Severe accidents

The possibility and relevance of conducting power excursion tests (with and without void conditions) and plugged sub-assembly tests to investigate severe accident issues are being examined with aim of supplementing the current database related to a pin bundle with a reduced hydraulic diameter (common option between the CFV core and the SFRv2 core).

Other test programmes of a more analytical nature are also being considered for the qualification of computational tools.

Conclusion on the qualification

The qualification of the fuel, absorbers and materials will mainly be based on the post-irradiation assessments of the irradiation experiments carried out in the Phénix reactor ('*Phénix treasures*' approach). A structured approach was implemented in 2012 to identify relevant objects worth examining for the ASTRID core, as well as to plan transport and the post-irradiation assessments[11].

At the current stage of the design studies, no discriminating element has been identified regarding the qualification needs of the two types of cores (CFV and SFRv2). It is therefore possible to consider commissioning the ASTRID reactor with a CFV-type fuel.

Designing in-core objects

Fuel sub-assemblies[12]

The overall concept of the fuel sub-assemblies is mainly based on feedback from Phénix and Superphénix, as well as on a design involving a sub-assembly with a shortened base (due to the compact pressure-reducing components), a closed leak tight wrapper tube made of EM10 steel and $UPuO_2$ fuel pin bundles with AIM1 cladding.

A specificity of the CFV concept is that it uses enriched B_4C in the lower part of the top neutron shielding in order to comply with the negative sodium void coefficient criterion. Taking into account certain cost and safety constraints, an approach for minimising this quantity is being pursued, including combinations with other absorbing materials such as hafnium.

Due to the risk of core compaction related to dynamic stress (earthquakes, pulse loads), the stiffness of the plates and the plasticity of the sub-assembly base will be optimised.

Absorber sub-assemblies[13]

It was decided to apply the same control rod and safety rod design principles employed for the French systems such as Phenix, Superphénix and the EFR, which include:

- Aligning the top parts of all the sub-assemblies (fuel and absorbers),
- Maintaining the mobile absorber inside the sheath.

With the aim of reducing the height of the sub-assemblies, the following major options have been retained for the absorbing devices:

- Control rods with a low level and a olive-shaped base,

- Safety rods with a low dashpot and unsegmented absorbing bundle.

A sheath base option involving a fool-proofing system is being studied to avoid the complete insertion of a fuel sub-assembly instead of an absorbing device and to limit and improve the safety demonstration with respect to handling errors.

The reference material for the absorbing components in the first cores is natural B_4C and/or B_4C enriched at 48% with ^{10}B.

Reflector sub-assemblies and lateral neutron shielding

The design of the reflector sub-assemblies and lateral neutron shielding is underway. This design is consistent with progress made in the field of the secondary sodium activation criteria, the acceptable tritium source term in the ASTRID reactor, and the primary system design requirements.

Various materials and design options are being considered for the reflectors and the lateral neutron shielding. They remain open at the present stage of the studies:

- For the reflector sub-assemblies: pins or rods made of Sic, MgO, $MgAl_2O3$ or $^{11}B_4C$.
- For the lateral neutron shielding: natural B_4C or alternative materials on a hafnium or steel base. The use of the natural B_4C makes it possible to minimise the thickness of lateral internal protective devices around the core.

During the AVP2 phase, the aim is to converge towards optimising the design/materials for the reflector sub-assemblies and the lateral neutron shielding, in relation to the ASTRID specifications described above.

Monitoring the core

A preliminary analysis of the parameters to be monitored during operation and for detecting incident/accident conditions (corresponding to categories 1 to 4 up to severe accident prevention situations) led to a first proposal for the core monitoring and protection system at the end of the pre-conceptual design phase 1. Hereafter are indicated the R&D options for the monitoring and protection of the ASTRID core:

- Controlling the core neutronics: High-temperature fission chambers with a high dynamic range positioned in the primary vessel on the edge of the core or possibly in the core cover plug. Neutron power chambers located outside the vessel are also being studied for post-accident management in particular.

- Detecting plugged fuel sub-assemblies: In addition to the thermocouples above each sub-assembly and fission chamber (by the detection of delayed neutrons), flux distortion meters are also being studied.

- Detecting an accidental control rod withdrawal via 2 approaches: Thermocouples above each sub-assembly and fission chamber inside the vessel located behind the lateral neutron shielding (to detect local deformation in the flux layer).

- Core movements: Poles with ultrasonic transducers for detecting radial geometry variations in the core.

- Handling errors: Measuring the temperature of the sub-assembly from the handling arm and implementing an identification system using bar codes on the sub-assembly and by ultrasonic readings.

The objective at the end of pre-conceptual design phase 2 will be to define an exhaustive list of reference options for the core protection and monitoring system by determining the chosen technologies and by defining the level of diversification, the overall performance expected and its location in the reactor block.

Conclusion

The pre-conceptual design phase 1 confirmed the safety potential of the CFV cores and the CFV concept is retained for pre-conceptual design phase 2. Its potential will have to be consolidated by:

- Characterising the core behaviour in all of the operating conditions (categories 1 to 4 and severe accident prevention situations).
- Defining the choice and the characteristics of the various additional safety measures in relation to prevention and mitigation measures.
- Reinforcing the studies during the sodium boiling phase and the primary and secondary phases of the core meltdown accident.

During the pre-conceptual design phase 2, a technical-economic optimization of the design of the CFV core will also be pursued, including a goal of reducing the core overall radial dimensions.

ACKNOWLEDGMENTS

The authors wish to thank all the teams involved in the core design at the CEA and AREVA.
Thanks also to Electricité de France for its support within the SFR framework.

NOMENCLATURE

CFV: French acronym for “Coeur à Faible Vidange” (low sodium void core)
CSD : Control and Shutdown Device
DSD : Diverse Shutdown Device
CRW: Control Rod Withdrawal
ULOF: Unprotected Loss Of Flow
ULOHS: Unprotected Loss Of Heat Sink

REFERENCES

1. P. LE COZ, et al., “Sodium-Cooled Fast Reactors: the ASTRID Plant Project” – Proceedings of ICAPP 2011, Nice, France, May 2-5, 2011

2. B. FONTAINE, et al., “Sodium-Cooled Fast Reactors: the ASTRID Plant Project” – Paper 432757, Proceedings of GLOBAL 2011, Makuhari, Japan, Dec. 11-16-5, 2011

3. P. SCIORA, et al., “Low void effect core design applied on 2400 MWth SFR reactor” – Proceedings of ICAPP 2011, Nice, France, May 2-5, 2011

4. P. SCIORA et al., “A break even oxide fuel core for an innovative French sodium-cooled fast reactor : neutronic studies results”, Global, Paris, Paper 9528 (2009)

5. F.VARAINE et al., “Pre-conceptual design study of ASTRID core” – Paper 432757, Proceedings of ICAPP 2012, Chicago, USA, June 24-28, 2012

6. G. GEFFRAYE et al., “CATHARE 2 V2.5_2: A single version for various applications”, Nuclear Engineering and Design, Volume 241, Issue 11, November 2011, Pages 4456-4463

7. L. ROCHE, M. Pelletier, “Modelling of the thermomechanical and physical processes in FR fuel pins using the GERMINAL code”, Paper IAEA-SM-358/25, Proceedings of Symposium on MOX fuel technologies for medium and long term deployment, Vienna, 2000.

8. M. LAINET “Recent modelling improvements in fuel performance code GERMINAL for SFR oxide fuel pins” IAEA-CN-199/241, this conference

9. G. MIGNOT “Preliminary considerations on the startup phase for the ASTRID core”, this conference

10. DOUGLAS C. CRAWFORD et al. “An approach for fuel development and qualification”, JNM 371, 2007

11. I. MUNOZ “ Recovery of materials from PHENIX to support the qualification of ASTRID design options”, this conference

12. E. BRUNON et al., “State-of-the-art of the conceptual design fuel sub-assembly for ASTRID ”, IAEA-CN-199/281, this conference

13. I. GUENOT-DELAHAIE et al., “State-of-the-art of the conceptual designs of control and shutdown rods for ASTRID”, poster IAEA-CN-199/285, this conference

IAEA-CN-199
Paris, France, 4-7 March 2013
Paper CN-199-261

The ASTRID Project : Status and Future Prospects

Pierre LE COZ (CEA), Jean-François SAUVAGE (EDF), Jean-Marie HAMY (AREVA), Vincent JOURDAIN (ALSTOM), Jean-Pierre BIAUDIS (COMEX NUCLEAIRE), Hiroyuki OOTA (TOSHIBA), Thomas CHAUVEAU (BOUYGUES), Philippe AUDOUIN (JACOBS), Daniel ROBERTSON (ROLLS-ROYCE), René GEFFLOT (ASTRIUM)

Abstract - The pre-conceptual design of the ASTRID project has been launched in 2010 by CEA. The objectives of this first phase are to consider innovative options to improve the safety level with progress made in SFR-specific fields. A few examples of these innovations are: a core with an overall negative sodium void effect, specific features to prevent and mitigate severe accidents, power conversion system decreasing drastically the sodium-water reaction risk, improvements in In-Service Inspection and Repair, etc. ASTRID will also be designed to pursue the R&D on sodium fast reactors and demonstrate the feasibility of transmutation of minor actinides.

CEA has concluded partnerships with industrial partners (EDF, AREVA NP, ALSTOM, BOUYGUES, COMEX NUCLEAIRE, TOSHIBA, JACOBS, ROLLS-ROYCE and ASTRIUM) and the total staff involved in the project is now about 500 people.

The paper describes the organization and the current status of the project, the mains results obtained during the pre-conceptual design and the objective of the conceptual design with the associated milestones.

Introduction

The future of mankind is confronted with increasing energy demands, the gradual exhaustion of fossil fuels, and the pressure to reduce greenhouse gas emissions. This is why more and more countries are considering nuclear energy as a viable element of their energy mix.

A wide spread ‘nuclear renaissance’ will put extra pressure on natural uranium stocks. A policy to preserve these resources must therefore be developed to sustain this renaissance. This is one of the main challenges facing Generation IV reactors and it will be the keystone on which the future of nuclear energy can be built.

This fourth generation will focus on fast reactors which are capable of converting a large majority of uranium-238 into plutonium-239 while producing electricity. In this way, it will become possible to exploit more than 90% of natural uranium to generate electricity, rather than only 0.5 to 1% in light water reactors. The large quantities of depleted and reprocessed uranium available in France could be used to maintain the current electricity production for several thousand years. The worldwide availability of primary fissile resources could thus be multiplied by more than 50. The construction of fast reactors will also open the door to unlimited plutonium recycling (multi-recycling) by taking advantage of its energy potential.

Radioactive waste management is yet another challenge facing Generation IV reactors which involves reducing the volume and the inherent long-term radioactivity of final waste. These reactors may in fact be capable of burning some of the long-lived radioactive elements contained in radioactive waste: minor actinides (americium, neptunium, curium, etc.).

The Generation IV International Forum (GIF) was born out of the desire to create an international R&D framework capable of boosting research in the different countries so that the most efficient technologies can emerge as quickly as possible.

Four main objectives have been defined to characterise the future reactor systems that must be:

– **Sustainable:** using a minimum natural resources and be environmentally friendly (limiting waste production in terms of radiotoxicity, mass, decay heat, etc.).

- **Cost-effective:** in terms of investment costs per installed kWe, the price of fuel, the cost of operating the facility, and consequently, the cost of electricity production which must be competitive in comparison with other energy sources.
- **Safe and reliable:** aiming for improvement compared with reactors currently in operation, while eliminating the need to evacuate the population from the site as much as possible, regardless of the cause and severity of the accident.
- **Proliferation resistant** and **protected against any external hazards**.

Furthermore, the French Act No. 2006-739 dated 28 June 2006 on the sustainable management programme for radioactive materials and waste stipulates the commissioning of a Generation IV reactor by 2020. The CEA therefore decided to launch – in cooperation with its industrial partners – the conceptual design of a sodium-cooled fast reactor (SFR). This is currently the only GEN IV reactor technology that is sufficiently mature and benefits from considerable feedback both in France and overseas, associated with the potential to meet the GEN IV criteria.

This project has been called ASTRID which stands for 'Advanced Sodium Technological Reactor for Industrial Demonstration'.

Specifications for ASTRID

To meet the above-mentioned objectives, Generation IV sodium fast reactor (SFR) concepts must be significantly improved, particularly in the following fields:

- Further reducing the probability of a core meltdown accident through improved preventive measures,
- Integrating the impact of a mechanical energy release accident as early as the design phase if the demonstration of its 'practical elimination' is not sufficiently robust,
- Taking into account feedback from the Fukushima accident,
- Improving the capacity to inspect structures in sodium, with efforts especially focusing on structures ensuring a safety function.
- Reducing the risks associated with the affinity between sodium and oxygen: sodium fires and sodium/water reactions.
- Achieving a better availability factor than previous reactors, while aiming for the performance levels required by current commercial reactor operators.
- Ensuring the transmutation of minor actinides if this radioactive waste management option is chosen by the French government.
- Being competitive in relation to other energy sources with equivalent performance levels.

As an integrated technology demonstrator, ASTRID has the main objective of demonstrating advances on an industrial scale by qualifying innovative options in the above-mentioned fields. It must be possible to extrapolate its characteristics to future industrial high-power SFRs, particularly in terms of safety and operability.

ASTRID will nevertheless differ from future commercial reactors for the following reasons:

- ASTRID will be a **1500 MWth reactor, i.e. generating about 600 MWe,** which is required to guarantee the representativeness of the reactor core and main components. This level will also compensate for the operational costs by generating a significant amount of electricity. A sensitivity study will be conducted on this power level.
- It will be equipped for experiments. Its design must therefore be **flexible** enough to be able to eventually test innovative options that were not chosen for the initial design. Novel instrumentation technologies or new fuels will be tested in ASTRID.

– It will be commissioned at approximately the same time as Generation III power plants, which means that its level of safety must be at least equivalent to these reactors, while taking into account the lessons from the Fukushima accident. Focus will nevertheless be placed on validating safety measures enabling the future reactors to ensure an even more robust safety level. This means taking into account core meltdown accident conditions from the design phase.

– ASTRID's **availability** objective is below that of a commercial power plant due to its experimental capacity. However, the options chosen must demonstrate that a higher level of availability can be reached when extrapolated.

– Without being a material testing reactor (MTR), ASTRID will be available for irradiation experiments like those conducted in PHENIX in the past. These experiments will help to improve the performance of the core and absorbers, as well as to test new fuels and structural materials, such as carbide fuel and oxide dispersion steel (ODS) cladding. ASTRID will be equipped with a hot cell for examining irradiation objects, built either in the plant or nearby.

– ASTRID will be able to **transmute radioactive waste** so as to go on with the demonstration of this technique at larger scales for reducing the volume and lifespan of final radwaste.

– Though future fast reactor plants intend to be breeders, ASTRID will be a self-breeder considering the current nuclear material situation, while being able to demonstrate its breeding potential.

– ASTRID must also integrate feedback from past reactors, especially PHENIX and SUPERPHENIX, while being clearly improved and belonging to Generation IV. It must take into account current safety requirements, especially in terms of protection against both internal and external acts of malevolence, as well as the protection of nuclear materials, while meeting the latest requirements in terms of proliferation resistance, and controlling its costs by following a value analysis approach from design.

Project organisation

- The CEA has been appointed by the French Government to manage the ASTRID Project. This involves:
  - Operational management by a project team which is also responsible for the industrial architecture, i.e. it defines the different engineering work packages.
  - Managing most of the R&D work and qualification of the options that will be chosen for ASTRID.
  - Assessment of studies carried out by its industrial partners in charge of technical work packages, or external engineering companies.
  - Direct responsibility of the core work package.

- The CEA has set up partnerships with French and foreign industry players who are providing both technical and financial support. These partnerships are based on bilateral contracts between the CEA and the relevant industrialist. To date, agreements have been signed with:

- EDF which provides the CEA Project Owner Team with support through its direct involvement in the team, as well as providing a team based in Lyon to deal with safety and technology matters. It contributes its skills in architecture and its expertise as an operator of PWRs and SFRs. EDF also brings the results of its own R&D works on SFRs (materials, core, severe accidents, in-service inspection and repair, socio-technology, etc.).

- AREVA NP, the only European Union OEM with know-how in the design of sodium-cooled fast reactors, is in charge of the engineering aspects of the nuclear island, the nuclear auxiliaries and I&C; based on its know-how and skills, AREVA NP also provides technical assistance to CEA in the frame of the core and fuel design workpackage led by CEA.

- ALSTOM, designer and manufacturer of energy conversion systems for power plants, is in charge of the power conversion systems studies for ASTRID.

- COMEX Nucléaire is contributing its mechanical design know-how to studies on various systems, especially robotic means for the in-service inspection of the primary system and the diversified design of control rod mechanisms, etc.

- TOSHIBA is responsible for developing and qualifying large electromagnetic pumps for the sodium secondary systems.

- BOUYGUES is essentially working on the civil engineering design of all the nuclear island buildings (including the reactor building, nuclear auxiliary buildings, fuel handling buildings), as well as the turbine hall housing the turbo-alternator unit.

- JACOBS Nucléaire is responsible for the engineering of the infrastructures and joint site facilities.

- ROLLS-ROYCE plc, designer and manufacturer of nuclear power systems and components is researching innovative sodium-gas heat exchangers and fuel handling.

- ASTRIUM is involved in applying methodologies to the ASTRID project that help to improve reactor availability; these methodologies have been developed on the basis of their experience in space launch vehicles and missiles.

About 550 people are currently working on the ASTRID project, half of which are provided by the industrial partners.

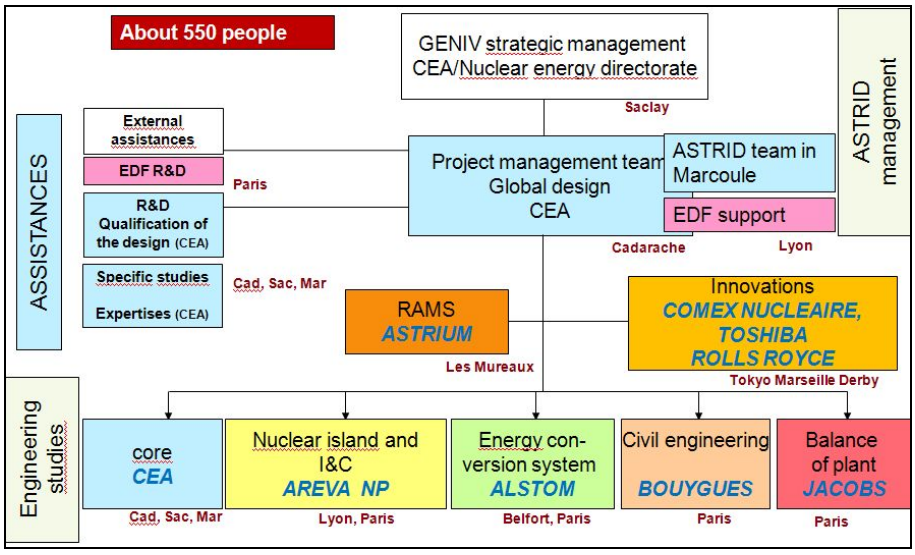

The project remains open to other partnerships, whether French or foreign.

Such partnerships enable the CEA to concentrate on the ASTRID pre-conceptual design by implicating key industrial players whose experience and skills in their respective fields will guarantee the project's success. The association of different industrial partners offers a number of advantages: it fosters innovation, ensures that the industrial issues are covered (operability, manufacturability, etc.) as early as the design phase, while providing a source of funding for the pre-conceptual design phases 1 and 2 since the partners have partially financed the project.
The project organisation is described in greater detail in a specific paper [1].

Current status and general schedule

The R&D actions performed within the scope of the three-party CEA-EDF-AREVA framework between 2007 and 2009 made it possible to establish the preliminary project orientations and to finalise a number of structuring concepts, e.g. the pool-type primary system and the UO_2-PuO_2 fuel. These actions provided the foundation for the project orientations file issued in September 2010, which lists the finalised structuring options and the remaining open options. By leaving some options open, this gives the project enough time to study a number of innovative solutions that could eventually be integrated into the ASTRID design with the aim at clearly positioning ASTRID as a Generation IV reactor.

The pre-conceptual design phase was launched in October 2010 [2] and involves 3 phases:

- A preparatory phase which served to structure the project, formalise the project requirements, and define the main milestones and lead-times. It ended with an official review which launched the following phase in March 2011.
- The pre-conceptual design (dubbed in AVP1 in French) aims at analysing the open options – particularly the most innovative – so as to choose the reference design by the end of 2012.
- The conceptual design (dubbed in AVP2 in French) is set to start in 2013 and aims at consolidating the project data to obtain a final and consistent conceptual design by late 2015. It will include a cost estimate and a more detailed schedule, facilitating the decision-making process for the next phases of the project.
- The basic design phase is planned from 2016 to 2018.

The reference project schedule retained by CEA is shown below.

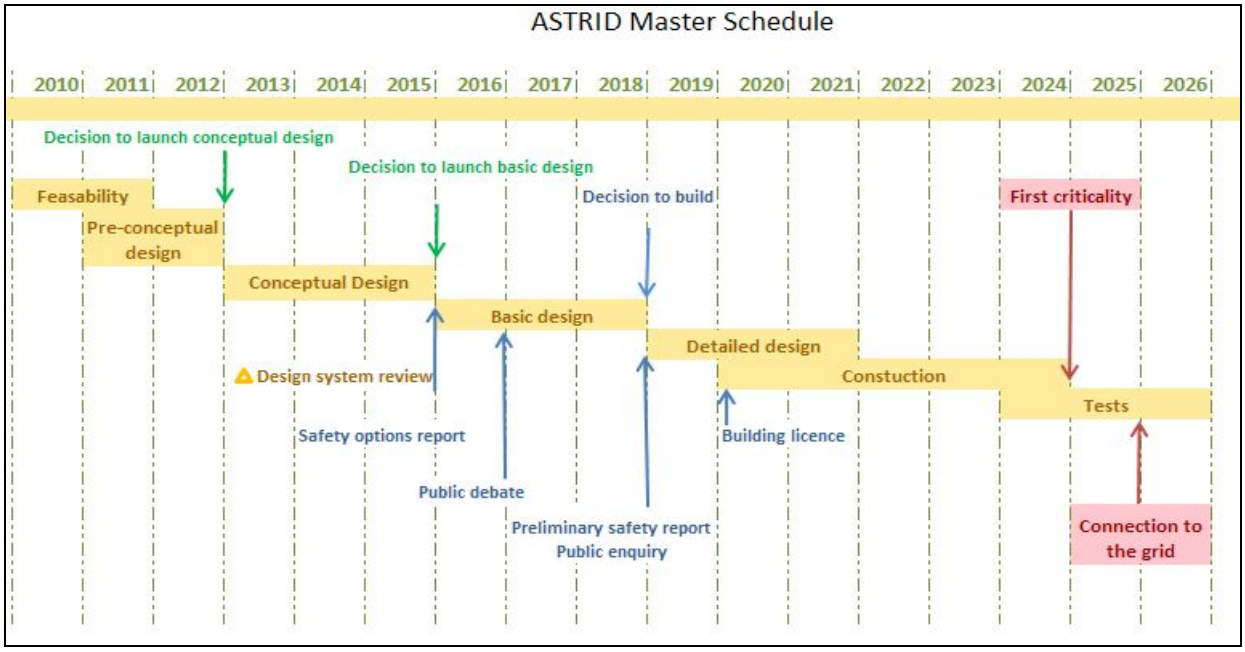

Several options were investigated in parallel during the pre-conceptual design. This involved examining a number of innovations with the potential to provide significant improvements compared with previous reactors. This phase was concluded with several design option reviews to finalise the project as much as possible before launching the second phase of the pre-conceptual design.

The end of the first phase also corresponds to the first milestone set by French Act No. 2006-739 dated 28 June 2006 on the sustainable management programme for radioactive materials. A file was

therefore submitted to the French government in December 2012 that makes the synthesis of the CEA vision regarding the future role of SFR GEN IV concepts to ensure nuclear energy sustainability thanks to closed fuel cycle.

Main options have been selected by the end of 2012. The conceptual design – lasting until late 2015 – will consolidate the first phase, allowing to optimize the design, confirm or question some options, and providing more information and greater consistency.
Dialogue has been instigated with the French Nuclear Safety Authority (ASN) during the first phase of the pre-conceptual design, which resulted in a "safety orientations report" submitted in June 2012. A formal examination of this report will be made by the French Safety Authorities in June 2013. The safety options report will be written and submitted to ASN at the end of the conceptual design (AVP2).

A few examples of options studied and decided during the pre-conceptual design

- ***Low void effect core***

  The CFV[1] core concept is based on a low sodium void effect. This core concept involves heterogeneous axial $UPuO_2$ fuel with a thick fertile plate in the inner core and is characterised by an asymmetrical, crucible-shaped core with a sodium plenum above the fissile area.

  The CFV core concept is focusing on optimising the core neutron feedback parameters (reactivity coefficients) so as to obtain improved natural core behaviour during accident conditions leading to the overall core heating. More specifically, the reactivity effect associated with sodium expansion achieved by design (sodium plenum and heterogeneous fertile plate) is negative in the event of a total loss of primary coolant, and can result in an overall negative void effect if a boiling phase is reached. This new specificity in relation to standard SUPERPHENIX- or EFR-type cores can be extrapolated and remains valid for high-power CFV cores. The preliminary studies on unprotected-loss-of-flow (ULOF) transients or unprotected-loss-of-heat-sink (ULOHS) transients without rod drop, show a potential for an acceptable natural behaviour of the CFV core which will remain to be confirmed in the remainder of the studies.

  The CFV concept also retains a low reactivity loss thanks to the fuel pins with a larger diameter. Generally speaking, the CFV core retains a number of key advantages in terms of longer cycles and fuel residence times, as well improved behaviour during an accidental control rod ejection transient with respect to conventional core designs.
  The CFV core has been chosen as the reference option for the conceptual design studies.

- ***Malevolent hazards***
  Hazards of both internal and external (aeroplane impact) origin are taken into account from design.

- ***Decay heat removal***
  The objective is to design decay heat removal systems that are sufficiently redundant and diversified so that the practical elimination of their total failure over a long period of time can be supported by a robust demonstration. To meet this goal, both water and air will be used as cold sources. Furthermore we will take advantage of the favourable characteristics of sodium reactors in terms of their high thermal inertia, large safety margins before sodium boiling and their capability to cope with natural convection flows. Different systems have been studied during the pre-conceptual design [4]. The final choice on decay heat removal systems will be made by mid-2013.

- ***Mitigation of potential core meltdown/ mechanical energy release accident:***

[1] French abbreviation for "*Cœur à Faible effet de Vide sodium", meaning low void effect core*

To provide defence in depth against scenarios such as the melting of the core, the ASTRID reactor will be equipped with a core catcher. It will be designed to recover the entire core, maintain the corium in a sub-critical state while ensuring its long-term cooling. As other equipments important for safety, it must be inspectable. At this stage, several options are being investigated in terms of the possible core-catcher technologies, locations (in-vessel or outside the vessel) and attainable performance levels. A sustained R&D effort will remain necessary in parallel on such subject, to help for the selection of the more promising technical solutions.

The choice of the technical orientations for the conceptual design studies will be made by the end of 2013.

- ***Containment***

  The containment will be designed to resist the release of mechanical energy caused by an hypothetical core accident or large sodium fires, to make sure that no countermeasures are necessary outside the site in the event of an accident.

- ***Capability to inspect structures in sodium***

  Contrary to the PHENIX and SUPERPHENIX reactors, the periodic inspection of the reactor block internal structures has been integrated at the early stage of the design. The design of these structures, and particularly those contributing to the core support, were conceived to make easier their inspection.

  Technologies now exist that enable this inspection either from outside or inside the vessel. They mainly use optical and ultrasonic methods; the technology will be chosen in relation to the primary system design [6].

- ***Architecture of primary and secondary circuits***

  Some choices have already been made during the pre-conceptual design phase: pool-type reactor with conical '*redan*' (inner vessel): a solution extrapolated from previous reactors and the EFR project. This solution has the advantage of being well-known; simplications have been made to allow for extended ISIR access.

  In terms of the reactor block, it has been decided to use three primary pumps together with four intermediate heat exchangers.

  Each intermediate heat exchanger is associated with a secondary sodium loop which includes modular stream generators or sodium-gas heat exchangers.

  The choice is currently focusing on electromagnetic pumps to equip the secondary loops, on the basis of one pump per loop [3].

  The nuclear island design is detailed in a specific document [4].

- ***Steam or gas power conversion system (PCS)***

In order to reduce the risks associated with the affinity between sodium and oxygen, studies have been carried out on 2 power conversion systems:

– To improve the safety and acceptability of the reactor with the *de facto* elimination of the risks associated with sodium-water reactions, an innovative energy conversion system is being considered that uses gas (nitrogen) for the thermodynamic transformations (Brayton cycle). This type of system has never been built for the pressure and power ranges required in ASTRID so it will first be necessary to make sure of its feasibility, cost and compatibility with SFR constraints. In any case, this concept would be coupled to the reactor through an intermediate sodium system, in order to exclude any risk of gas entrainment into the core.

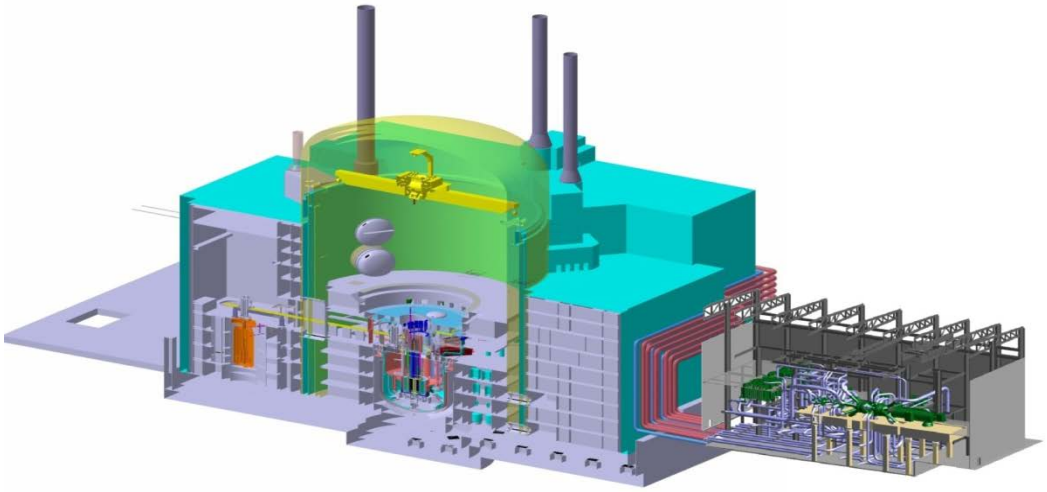

– If the water-steam PCS is chosen, the following improvements are to be considered [7]:
    - Modular steam generators whose size guarantee the integrity of the intermediate heat exchanger, and thus protect the primary system, the secondary system and the steam generator casing, even in the event of the sudden and simultaneous failure of all the steam generator module tubes; the heat exchange power of each module will be about 150 MWth.
    - Steam generator concepts ensuring better protection against wastage.
    - Reinforcement of the redundancy and performance of the leak detection systems.

  The steam generator will also be chosen on the basis of its cost and that of the intermediate system in sodium, which represent a significant portion of the power plant cost.

The selection among the 2 PCS concepts will be made by february 2013 [5].

- ***Fuel handling***

At the beginning of the ASTRID project, it was decided to use a sodium environment in which to load and unload the fuel sub-assemblies. This implies a sodium external vessel storage tank (EVST) whose capacity depends on whether a whole core unload is deemed necessary or not.

Different options are under consideration (ramp, cask, etc.) and the reference option for the conceptual design will be finalised in 2013.

- ***Hot cell***

ASTRID will be able conduct irradiation experiments to improve the performance of the core and absorbers, as well as to test new fuels and structural materials, and to demonstrate the industrial feasability of minor actinide transmutation.

The CEA existing or future hot cells have been investigated and it appears that a specific hot cell for ASTRID is necessary for the post-irradiation examinations.

It has thus been decided to build a hot cell in the nuclear island of ASTRID.

- ***Transmutation capabilities***

The transmutation of minor actinides is part of the ASTRID specifications. Only americium and neptunium are considered.

Studies were carried out during the pre-conceptual design to analyse the impact of minor actinides on the ASTRID design. Thresholds have been identified in terms of safety, reactivity loss, decay heat, radioprotection, and fuel handling, etc.

With a percentage of 2% of minor actinides in an homogeneous core or 10% in dedicated blankets, there is no major impact on the plant design.

Conclusion

By pursuing R&D and launching the ASTRID programme, France is clearly on the path to developing a concept of Generation IV reactors based on the sodium-cooled fast reactor technology, which could become operational at the industrial level, if necessary, in the middle of the 21st century to offer a sustainable use of the uranium and plutonium resources, based on the demonstration ensured by the erection, commissioning and operation of ASTRID in the mid term. The ASTRID reactor would also contribute to the R&D effort on the transmutation of minor actinides. With the objective of developing an innovative machine taking full advantage of the unique feedback from Phenix and Superphenix, France will be able to develop and offer a competitive and safe reactor technology.

References

[1] : An original and efficient project organisation for ASTRID
Marie LADURELLE, Pierre LE COZ
Proceedings of FR13, Paris France 4-7 March 2013; Paper CN-199-264

[2] : Sodium-cooled Fast Reactors: the ASTRID plant project
P. LE COZ, JP SERPANTIE, JF SAUVAGE
Proceedings of ICAPP'11, Nice France, May 2-5, 2011; Paper 11249

[3] : Large capacity EMP design for application in the ASTRID sodium-cooled fast reactor
Guy LAFFONT, Frédéric REY, Rie AIZAWA, Tetsu SUZUKI
Proceedings of FR13, Paris France 4-7 March 2013; Paper CN-199-263

[4] : Status of ASTRID nuclear island pre-conceptual design
Manuel SAEZ, Jean-Charles ROBIN, Bernard RIOU, Alexandre VILLEDIEU, Dominique DEPREST, Gérard PRELE
Proceedings of FR13, Paris France 4-7 March 2013; Paper CN-199-127

[5] : ASTRID power conversion system : assessment on steam and gas options
Guy LAFFONT, Lionel CACHON, Vincent JOURDAIN, Jean Marie FAUQUE
Proceedings of FR13, Paris France 4-7 March 2013; Paper CN-199-262

[6] : In-service inspection and repair in the ASTRID project: main stakes and considered options
F. JADOT, J. SIBILO, JM. AUGEM, V. DELALANDE, JL. ARLAUD
Proceedings of FR13, Paris France 4-7 March 2013; Paper CN-199-165

[7] : Sodium-Water Reaction approach and mastering for ASTRID Steam Generator design
Manuel SAEZ, Sylvain MENOU, Alexandre ALLOU, François BEAUCHAMP, Carole BERTRAND, Gilles RODRIGUEZ, Gérard PRELE
Proceedings of FR13, Paris France 4-7 March 2013; Paper CN-199-126

IAEA-CN-199
Paris, France, 4-7 March 2013
Paper CN-199/264

An original and efficient project organisation for ASTRID

Marie LADURELLE, Pierre LE COZ
CEA Cadarache, DEN/DER/CPA, 13108 Saint-Paul lez Durance Cedex, France
Contact author: Marie LADURELLE, +33442252814, ladurelle@drncad.cea.fr

Abstract. Specified in French Act published in 2006 before becoming reality in mid-2010, the ASTRID project needed to set up an efficient organisation to produce a pre-conceptual design package for the first important milestone in December 2012. As project owner and leader, the industrial political strategy followed by the CEA involved organising a "core design team" through a set of bilateral agreements with AREVA-NP, ALSTOM, BOUYGUES, JACOBS, COMEX Nucléaire, EDF, TOSHIBA, ROLLS ROYCE and ASTRIUM. The CEA is also responsible for the overall design, core, fuel and safety studies, while developing international partnerships for Research and Development (R&D) and experimental facilities to support design. Two years after its launch, the ASTRID project employs about 500 people. The paper will describe the specific measures required to coordinate studies and to take into account the opinion of partners when choosing the options.

1. Context

The ASTRID project was set up following the French Act No. 2006-739 dated 28 June 2006 on the sustainable management of radioactive materials and waste which stipulates the commissioning of a Generation IV reactor by 2020. It was decided to focus on a sodium-cooled fast reactor power plant.

After three years of studies and R&D jointly performed by the CEA, EDF and AREVA to investigate a range of innovative solutions, the project itself was launched in late 2009 and a project team was set up in the first half of 2010. The project is funded through an agreement between the French government and the CEA as part of the 'future investments' programme which was officialised in the French Official Journal in September 2010.

The main objective of the project is to finalise the conceptual design for the ASTRID prototype. The design process has been divided into two phases:

- Pre-conceptual design (AVP1) which aims at investigating innovative options that could be integrated into the reactor. At this stage of the process, the team is not looking to ensure coherence between the options nor provide a finalised conceptual design.
- Conceptual design (AVP2) will start with choosing the reference options for ASTRID and aims at providing a coherent, finalised conceptual design.

The pre-conceptual design started in 2010 and will be finalised at the end of 2012. It involved forming a project team within the ASTRID Project Unit (CPA). The number of people working for this team has gradually increased as the project has gathered steam. The project was officially launched when the agreement between the French government and the CEA was signed on 9 September 2010, providing the necessary funds. In compliance with the above act and this agreement, the CEA set up partnerships with French and foreign companies which are also investing in the project on both a technical and financial level.

2. Project organisation

2.1 General organisation with the engineering companies

The CEA was appointed the project owner under the French Act of 28 June 2006. It was also attributed the financial resources to cover the conceptual design phase (2010-2017) through the Future Investments programme (PIA).
The project is organised according to the following principles:

- The CEA is the project owner: This role is confirmed by the fact the CEA was given the funds via the above-mentioned agreement to launch the pre-conceptual design.
- As project owner, the CEA is responsible for drafting the safety reports and maintains dialogue with the French nuclear safety authority (ASN).
- The CEA has set up partnerships with industrial companies to carry out the conceptual design.
- The CEA chose to assume the role of architect engineer itself instead of using a prime contractor. For this reason, the CEA defined the different project engineering packages and then distributed them among the industrial partners.
- The CEA also decided to ensure the engineering of the reactor core during the pre-conceptual design phase.

The project was thus divided into different engineering packages which were entrusted to its industrial partners within the scope of bilateral collaboration agreements for this pre-conceptual design phase.

The relationships with the different partners in charge of the engineering packages are detailed in the management specifications (with each partner providing their own management plan in response). These specifications stipulate the following requirements:

- Project reviews as understood in the RG aero 0040 standard. These reviews correspond to the main hold points at the project's launch and at the end of the conceptual design (detailed design review).
- In-house design reviews by the different engineering companies, prior to the system design review and detailed design review in particular.
- Design option reviews organised by the ASTRID Project Unit with the participation of the strategic leader.
- Monthly progress meetings to assess: status of actions, analysis of schedules, production of deliverables, and physical progress of the project.
- Three-monthly progress meetings to discuss budget issues and actions designed to reduce project risks.
- Two-monthly coordination meetings with the ASTRID engineering teams to discuss: design change sheets, configuration management, interface coordination, performance integration activities, and integration of engineering mock-ups into the overall ASTRID mock-up.
- Reviews of consultation meetings with the management bodies, with the strategic leaders from each partner.

The general project organisation is illustrated in the diagram below.

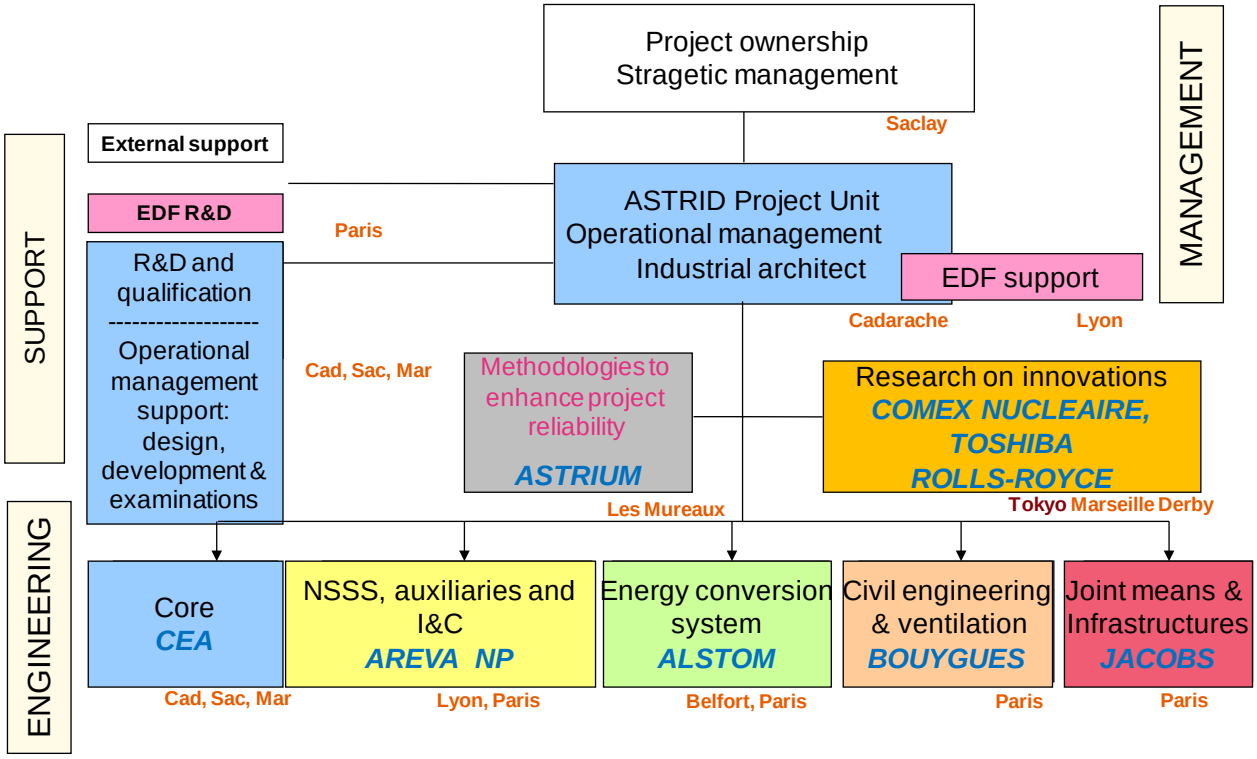

Figure 1: General organisation of the ASTRID project

As the project owner, the CEA ensures the strategic and operational management of the project. It is also responsible for drafting the safety reports and maintaining dialogue with the French Nuclear Safety Authority (ASN).

In order to integrate the safety and availability objectives as best possible while retaining as much flexibility to take into account innovative solutions during the design phase, the CEA has chosen a concurrent engineering design approach. This approach covers the product definition, the manufacturing processes and all other processes required during the reactor life cycle such as operation and in-service inspection. With this type of management system, cross-disciplinary units (R&D, modelling, operation, maintenance, etc.) can work towards the same objective in parallel right from the start. Dialogue between these different professions is simplified by the deployment of computerised means of sharing up-to-date and reliable information. The specific tasks performed within this innovative set-up are therefore taken into account by an entity called ‘industrial architect’. These tasks also help to coordinate the studies between the different engineering companies, as well as managing changes, configurations, interfaces, performance levels and the integration of designs and 3D mock-ups.

2.2 Organisation within the project team

The operational management of the project is ensured by the ASTRID Project Unit working within the Reactor Studies Department (DER) at the CEA/Cadarache Centre. A project manager heads this unit. The project manager relies on a support team which includes:

- Deputy-manager,
- Industrial architect, since the CEA decided to forgo a prime contractor, preferring to ensure the technical integration and engineering coordination aspects itself. It relies on external support for integration and configuration management tasks,
- A project management supervisor responsible for organisation, risk control, and schedule and cost tracking; this person relies on external support,
- Work package leaders responsible for cross-border functions related to the major issues of ASTRID, i.e. safety, operability, value analysis, experimental programmes, instrumentation and ISIR,
- Work package leaders responsible for managing the different engineering packages (site interfaces, NSSS, core, energy conversion system, nuclear auxiliaries and handing, I&C, electrical distribution, civil engineering),
- Secretary.

The ASTRID Project Unit also relies on a number work package leaders in the technical fields assigned to entities outside the DER, particularly in civil engineering, high voltage, I&C, fluids and ventilation.

In collaboration with its industrial partners, the ASTRID Project Unit also set up three groups of experts to cover the following themes throughout the design phase:

- Safety, with the ASTRID safety group (GSA) which is responsible for elaborating the project's safety approach and communicating the safety requirements to the designers,
- Operation, with the ASTRID operators group (GEA) which is responsible for analysing the design options in relation to the future operation of the plant,
- Malevolent acts, with the ASTRID technical protection group (GTPA) which is responsible for analysing the constraints associated with this issue and integrating them into the design.

The project management organisation is illustrated in the diagram below.

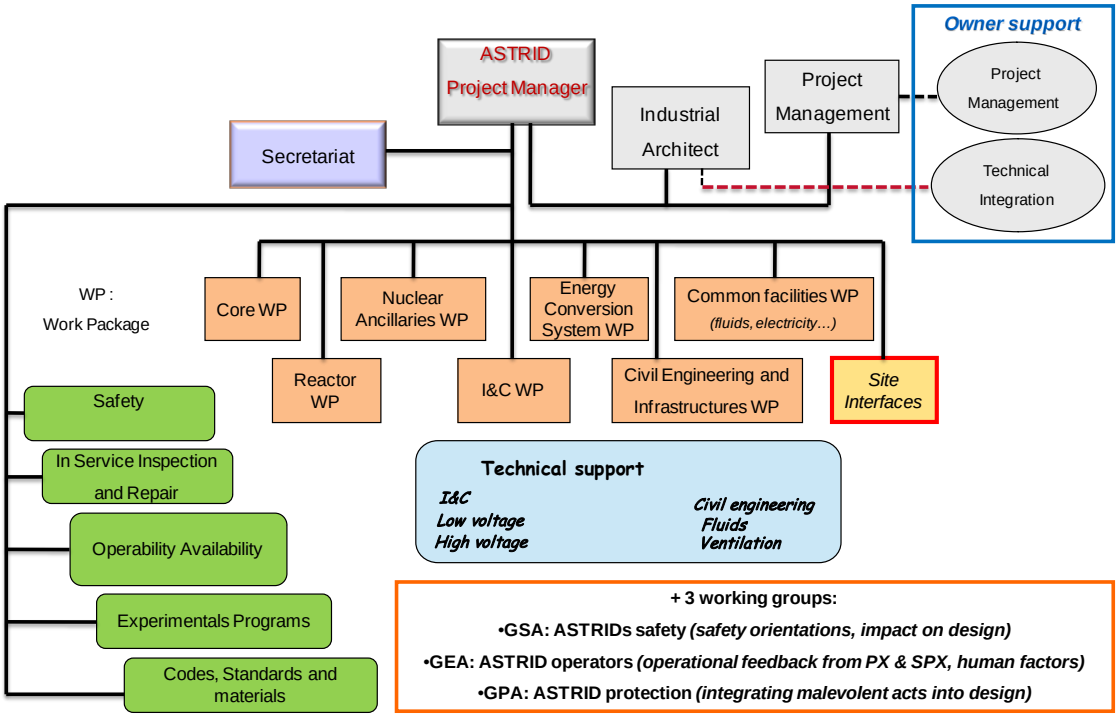

FIG.2. Organisation of the ASTRID project team

To prepare for the increased activity in the CEA and engineering teams during the pre-conceptual design, as well as to supervise and manager the interfaces between partners, the ASTRID Project Unit signed a number of commercial contracts for technical support in various fields: project management and technical integration, training, value analysis, cost assessment.

2.3 Partnerships

In compliance with the above act and the 'Future Investments' agreement, the CEA set up partnerships with French and foreign companies which are also investing in the project on both a technical and financial level. These partnerships are bilateral contracts between the CEA and the relevant industrialist. To date, agreements have been signed with:

- EDF/SEPTEN which provides the CEA Project Owner Team with support through its direct involvement in its team, as well as providing a team based in Lyon to deal with safety and technology matters. It contributes its skills in architecture and its expertise as an operator of Pressurized Water Reactors (PWRs) and Sodium Fast Reactors (SFRs).
- AREVA NP, the only European manufacturer with know-how in the design of sodium-cooled fast reactors, is in charge of the engineering aspects of the nuclear island,
- ALSTOM POWER SYSTEMS (signed on 26 May 2011), designer and manufacturer of energy conversion systems for power plants, is in charge of the Power Conversion System studies for ASTRID.
- COMEX Nucléaire (signed on 4 July 2011) is contributing its mechanical design know-how to studies on various different systems, especially robotic means for the in-service inspection of the primary system and the diversified design of control rod mechanisms, etc.
- TOSHIBA (signed on 13 April 2012) is responsible for developing and qualifying large electromagnetic pumps for the sodium secondary systems.
- BOUYGUES (signed on 27 April 2012) is essentially working on the civil engineering design of all the nuclear island buildings (including the reactor building, nuclear auxiliary buildings, fuel handling buildings), as well as the turbine hall housing the turbo-alternator unit.
- EDF (signed on 25 April 2012) extended the agreement signed with the SEPTEN to cover R&D activities and technical assessments to support the ASTRID project.
- JACOBS Nucléaire (signed on 21 June 2012) is responsible for the engineering of the infrastructures and joint site facilities.
- ROLLS ROYCE (signed on 24 September 2012) is researching innovative sodium-gas heat exchangers and fuel handling.
- ASTRIUM (signed on 19 October 2012) is involved in applying methodologies to the ASTRID project that help to improve reactor availability; these methodologies have been developed on the basis of their experience in ARIANE space launch vehicles and missiles.

To date, about 500 people are working on the ASTRID project, half of which have been provided by our industrial partners.
The project remains open to other partnerships, whether French or foreign.

Such partnerships enable the CEA to concentrate on the ASTRID conceptual design by implicating key industrial players whose experience and excellence in their respective fields will contribute to the project's success. The association of different industrial partners offers a number of advantages: it fosters innovation, ensures that the industrial issues are covered (operability, manufacturability, etc.) as early as the design phase, while providing a source of funding for the pre-conceptual design phases 1 and 2 since they have partially financed the project.

2.4 R&D activities

The ASTRID project aims at integrating a number of innovative options to meet the objectives of the Generation IV reactors while fulfilling its specifications. It is therefore relying on an important R&D programme at the CEA – SFR R&D. This was launched in 2006 as part of the three-party framework agreement with EDF and AREVA, to provide in due time the data required to qualify the ASTRID options. A progress report on all the actions performed is provided on a monthly basis.

Since 2007, the CEA has also been setting up a series of international partnerships to consolidate and develop its R&D efforts. These partnerships make it possible to share the development costs and the use of heavy experimental infrastructures.
The section below briefly describes these partnerships and their objectives.

On a European level, the SFR technology and the ASTRID prototype are covered by 1) the SNE-TP roadmap (*Sustainable Nuclear Energy Technology Platform*, www.snetp.eu) which aims at building a European research platform in the field of fission, 2) the European Sustainable Nuclear Industrial Initiative (ESNII) which is the industry's equivalent to SNE-TP, and 3) the European Energy Research Alliance (EERA, http://www.eera-set.eu).

On an international level, the CEA is a key player in the Generation IV International Forum (http://www.gen-4.org/) which federates 13 countries interested in sharing R&D efforts on six different systems including the SFR, as well as on transmutation, safety and technology issues. This International Forum – via its Risk and Safety Working Group – is actively involved in harmonising standards and safety references.
The CEA is also involved in a number of IAEA activities within the scope of the Technical Working Group on Fast Reactors (TWG-FR), and the International Project on Innovative Nuclear Reactors and Fuel Cycles (INPRO). These groups provide the opportunity to discuss the safety and technological developments of fast reactor systems, while sharing feedback from the construction, operation and dismantling phases of SFRs.

In parallel to these institutional collaborations, the CEA has signed a series of bilateral partnerships with R&D organisations involved in SFR development, such as Rosatom (Russia), the Indira Gandhi Centre for Atomic Research (IGCAR, India), Bhabha Atomic Research Centre (BARC, India), the Japan Atomic Energy Agency (JAEA), the Department of Energy (DOE, United States) and the Chinese Experimental Fast Reactor (CEFR).

2.5 Interfaces outside the CEA

Considering the feedback from the other projects run by the CEA Nuclear Energy Division (DEN) and the issues related to ASTRID, the CEA has maintained regular contact with the following entities very early on in the process since they play an important role in ensuring the smooth progress of the project:

- French National Assessment Committee (CNE). The strategic objectives and preliminary technical orientations of the project were presented to the CNE several times in the pre-conceptual design.
- French Nuclear Safety Authority (ASN). Discussions with the French regulator started as early as 2010 to present the project's safety objectives, the project's positioning in terms of the WENRA directives, the expected reactor performance, and the preliminary design data. Five technical meetings were held between 2011 and 2012. A safety orientations document (corresponding to a very preliminary version of the safety options file) which was sent to the ASN mid-2012 and which will be formally reviewed by a safety evaluation group ("Groupe Permanent") in mid-2013. This approach makes it possible to integrate the safety objectives as early as possible into the design, and to develop the technical solutions required to meet these objectives on the basis of a common vision.
- Senior Defence & Security Official. A similar approach is currently underway to integrate the security issues (theft, physical protection and malevolent acts) as early as possible into the design, and to draft an equivalent security file associated with each safety file.

3. Innovative industrial set-up

The innovative nature of this industrial set-up is due to several aspects:

- The design is not ensured by a single engineering company but several different engineering companies at the same time, with each having been chosen to work in its core field of excellence. This requires an industrial architect to ensure the technical coordination and integration of the different parts of the project.
- The signing of collaborative agreements with the different engineering companies rather than standard commercial contracts. This aspect has enabled the co-funding of studies by the industrial parties, which is additional proof of their desire to make this project a success.
- Continuation of R&D activities in parallel to the design studies carried out by the engineering companies. This guarantee of innovation demands highly efficient and flexible R&D (capable of integrating its activities in association with the key project milestones for the choice of options) that can be adapted to reorient or develop additional programmes in relation to the project's needs.

4. Efficiency and the key to success

4.1 Communications

Launching such a far-reaching project like ASTRID which involves about 300 people at the CEA, has had a significant impact of the working arrangements of the teams due to:

- The role of industrial architect that has been entrusted to the CEA (which is normally assumed by a prime contractor when there are several engineering companies involved),
- The CEA's decision to assume responsibility for the core design package,
- Changes affecting R&D activities. The R&D on Generation IV programme is now oriented by the project's design options, its constraints and its option qualification schedule.

A specific training course was set up to help the staff adapt to the changes in their working arrangements. It discussed the notion of project management involving simultaneous engineering activities, though focus

was placed on supporting the different parties within the context of the ASTRID project. It concerned everyone working on the project, from design engineers and managerial staff to functional staff.

In terms of internal communications, two technical conferences were organised in October 2011 and November 2012. Among others, they aimed at describing the project status and were open to all project contributors.

A chart presenting the main technical events, the status of the project milestone and cost tracking is broadly distributed every three months. A written internal communications document is also distributed. Several project presentations have already been given to a non-CEA public:

- French Nuclear Energy Society (SFEN) during conferences held in Paris, Marseille, Grenoble, Marcoule, Lyon and Aix-en-Provence,
- Various conferences, such as the International Conference on Advanced Power Plants (ICAPP) in Nice in May 2011 and in Chicago in August 2012.

Lastly, the entire project data is shared between the different CEA players via an electronic document management (EDM) system under Sharepoint, which is organised so it can be accessed by all the partner projects when necessary, while ensuring the necessary confidentiality of intellectual property.
The list of international publications issued during the pre-conceptual design is detailed in the References below.

4.2 Multi-level management of engineering companies

On such a far-reaching project with a complex industrial set-up, project management requires the proactive participation of the entire project owner team, each person assuming their responsibilities within their assigned scope, even if in the end, the project manager and programme manager make the final decisions (see Figure 3).

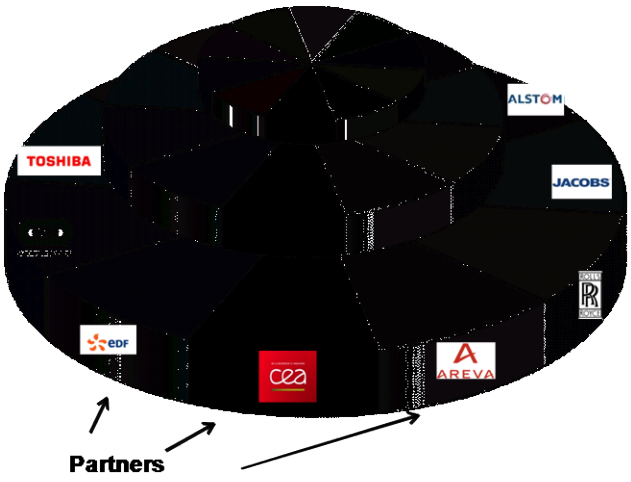

Strategic management
Who: strategic management on 4th generation reactor + project manager
When: two-party management committee meetings; multilateral coordination board meetings
What: governance programme, collaboration agreements, IP

Operational management
Who: project management + architects
When: monthly engineering meetings
What: technical barriers, physical progress, schedules, budgets, costs, project risks

Technical control
Who: Architects + work package leaders + project management unit + technical integration unit
When: technical meetings, two-monthly engineering coordination meetings
What: schedule integration, interface coordination, performance control, configuration management, 3D mock-up consolidation

FIG.3. Project management involvement of the different parties

4.3 R&D management

In order to assess the progress of R&D actions, to check their correspondence with the project needs and to ensure their reorientation or possible prioritisation, regular meetings are organised with the different technical work package leaders and with the relevant project managers.
Furthermore, a joint planning approach is used by the prototype investment project team and the R&D support team. This guarantees that the qualification needs and related deadlines are taken into account on both sides, while taking into consideration the schedules for regulatory procedures and engineering design studies.

4.4 Upstream continuous integration of external structuring interfaces

The continuous integration of external structuring interfaces upstream of the process is the result of feedback from other CEA projects. This is one of the main reasons why discussions were started with the French regulators as early as 2010, which made it possible to draft the first major document for the project, i.e. the safety orientations file submitted in mid-2012.

4.5 Partner involvement in strategic decisions

The agreements are bilateral collaborations between the CEA and the various industrial partners, thereby giving the CEA a central role in the industrial set-up.

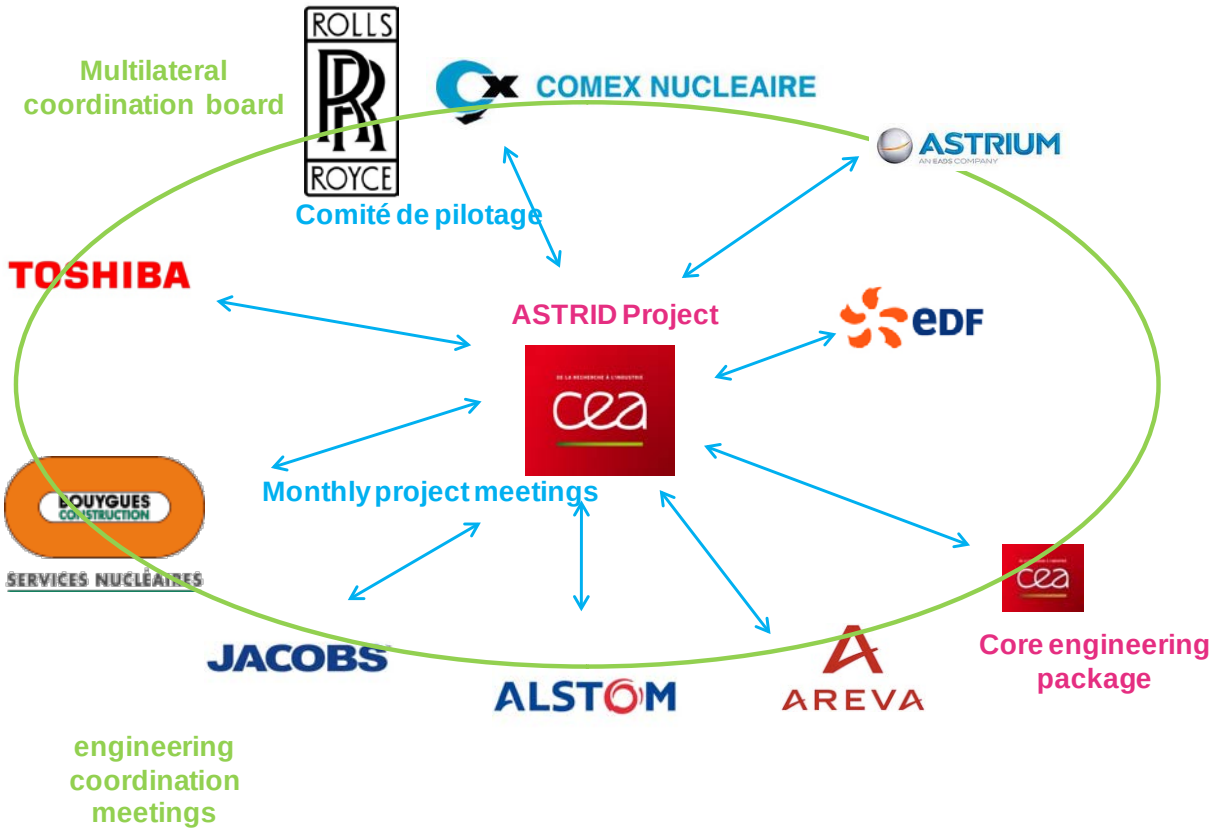

FIG 4. Industrial set-up

Nonetheless, a participative approach has been largely encouraged with partners, which required setting up a number of special bodies to discuss the strategic decisions, even if the CEA is responsible for the final decisions regarding ASTRID design.

- A multilateral coordination board meets on a two-monthly basis to collectively examine the technical subjects of major strategic relevance and to gauge the opinion of all the partners.
- The CEA involves its partners in the project reviews conducted before validating each important project milestone (project launch, choice of a strategic option such as the energy conversion system, etc.).

5. Conclusion

This paper describes the industrial set-up implemented through the series of collaboration agreements with the different project partners, thereby making it possible to take into account the interests of the industrial parties at a very early stage and to integrate recent feedback from other projects. Close coordination between the prototype construction project and the R&D support programmes will also contribute to the success of the project. Lastly, the CEA as project owner is managing the ASTRID project in a collaborative approach based on a series of concrete organisational methods. This organisation will function up to the end of the conceptual design. The relevance of the organisation will be re-assessed for the subsequent phases (basic design).

NOMENCLATURE

ASTRID Advanced Sodium Technological Reactor for Industrial Demonstration

REFERENCES

[1] F. Gauché; The French Prototype of 4th Generation Reactor: ASTRID; Annual meeting on nuclear technology, Berlin, May 17&18th; 2011.

[2] P. Le Coz *et al.*; Sodium-cooled Fast Reactors: the ASTRID plant project; Proceedings of ICAPP'11, Nice France, May 2-5, 2011; Paper 11249.

[3] M. Saez *et al.*; Assessment of pool type sodium fast reactor design options; Proceedings of ICAPP'11, Nice France, May 2-5, 2011; Paper XXX

[4] F. Jadot *et al*. "ASTRID sodium cooled fast reactor: Program for improving in service inspection and repair", ANIMMA 2011,

[5] P. Le Coz et al., Sodium-cooled Fast Reactors: the ASTRID plant project; Revue Générale du Nucléaire, Sept-Oct. 2011,

[6] M. Saez *et al.*; The pre-conceptual design of the nuclear island of ASTRID; Proceedings of ICAPP'12, Chicago United-States, June 24-28, 2012; Paper 12070.

A CORE DESIGN APPROACH AIMED AT THE SUSTAINABILITY AND INTRINSIC SAFETY OF THE EUROPEAN LEAD-COOLED FAST REACTOR

G. Grasso[a†], C. Döderlein[b], K. Tuček[c], K. Mikityuk[d], F. Manni[e], D. Gugiu[f]

[a] Technical Unit for Reactor Safety and Fuel Cycle Methods, Italian National Agency for New Technologies Energy and Sustainable Economic Development (ENEA-UTFISSM), Bologna, Italy

[b] Alternative Energies and Atomic Energy Commission (CEA), Cadarache, France

[c] Institute for Energy and Transport, Joint Research Centre (JRC-IET), Petten, The Netherlands

[d] Paul Scherrer Institute (PSI), Villigen, Switzerland

[e] Servizi di Ricerche e Sviluppo S.r.l. (SRS), Roma, Italy

[f] Institute for Nuclear Research (INR), Pitesti, Romania

Abstract. Among the Generation-IV fast reactor technologies, a Lead-cooled Fast Reactor concept is currently under development in Europe as a potential candidate for the deployment, to meet long-term objectives of European energy policies.

Within the Lead-cooled European Advanced DEmonstration Reactor (LEADER) project, co-financed by the European Union within the 7th EURATOM Framework Programme, the conceptual design of the reference Generation-IV European LFR (ELFR) industrial plant was developed, benefiting from and further optimizing the concept put forward during the ELSY 6th EURATOM Framework Programme project.

In order to embed in the design the safety and sustainability goals in the most effective way, an innovative, dedicated design approach was developed and applied to the design of the ELFR fuel pins, fuel assemblies and core. This new approach, together with the main analysis results supporting the design of the reference ELFR configuration, are presented and discussed in detail.

1. INTRODUCTION

While the current Nuclear Energy Systems (NES) designs already represent an economic, reliable and environment-friendly energy source, the desire to broaden the opportunities and to improve sustainability of nuclear energy stimulated a discussion on the development of new generation designs. According to this, the Generation-IV International Forum (GIF) [1] defined the four areas where substantial improvements might allow for an effective implementation of these advanced NES: sustainability of the entire fuel cycle – including waste management, increased safety, proliferation resistance and physical protection, while maintaining the economic competitiveness.

† giacomo.grasso@enea.it

This world-wide discussion matches also the aims of the European Union's energy policy as formulated in the Strategic Energy Technology Plan (SET-Plan) [2], to achieve whose goals the Sustainable Nuclear Energy Technology Platform (SNETP) [3] has been launched in 2007. Concerning the advent of Generation IV NES, SNETP established a Strategic Research Agenda (SRA) [4] currently being updated and a Deployment Strategy (DS). In 2009, an industry-led European Sustainable Nuclear Industrial Initiative (ESNII) [5] was also launched aiming at the demonstration of a new generation of fission reactors with increased sustainability for the year 2040.

Among the promising technologies identified in the SRA, the Lead-cooled Fast Reactor (LFR) has been included because of the fast-neutron spectrum – allowing the possibility for a closed fuel cycle for efficient conversion of fertile uranium and management of actinides, and the favourable characteristics of the inert coolant – allowing for a design with increased safety margins, even under the most severe accidental conditions. These features encouraged the constitution of a consortium of research centres, industrial partners and universities for exploiting the potentialities for an effective, Gen-IV compliant design of an industrial-size LFR.

The LEADER (Lead-cooled European Advanced DEmonstration Reactor) project [6] is a collaborative research initiative co-funded by the European Commission within the 7th EURATOM Framework Programme, dealing with the further development of the conceptual design of the European LFR (ELFR), starting from the achievements of the previous ELSY project (EU 6th FP) [7].

In order to fulfil the Gen-IV requirements, a comprehensive approach has been adopted for the preliminary design of the ELFR core: this strategy allows indeed to include from the very beginning all the options implying the achievement of the aimed performances, together with the technology constraints whose respect is envisioned mainly for safety and investment protection reasons. In this preliminary phase of the project, only sustainability and safety goals have been taken into account, to prove the effectiveness of the proposed approach, leaving optimizations to a more detailed project phase, in which goals of economics will be included in the comprehensive design strategy.

2. FROM ELSY TO THE ELFR

At the end of the ELSY project, an overall system layout was proposed for the industrial-scale LFR, relying on the favourable lead properties to comply with all the Gen-IV goals, while implementing simple engineered solutions to cope with the unfavourable lead properties [8].

The LEADER project, mainly aimed at the conceptual design of a small, representative reactor aimed at the demonstration of the lead technology chain (ALFRED, the Advanced Lead-cooled Fast Reactor European Demonstrator, described in a companion paper [9]), had to face the conflict between the unreadiness of the technological solutions proposed for ELSY (such as the use of ferritic-martensitic steels for the cladding or the spiral-tube steam generator), and the aim to build and commission the demonstrator in a short time. Consequently and to maintain the representativeness of ALFRED to the reference industrial-scale system, it was decided to review the design of ELSY critically and further update it, trying to solve the hard points through solutions representing a simple evolution of already available technologies, which – in its turn – would have been implemented in the demonstrator.

2.1. Impact on core design

The critical analysis of the ELSY core focused on two aspects: the layout of the Fuel Assemblies (FAs), and the mechanism for maintaining the geometry of the core and FAs [8]:

- the absence of a wrapper in favour of the "open lattice" concept, has been reckoned as an issue in particular with respect to the demonstrator: the lack of exact flow paths through the core does not allow for a precise monitoring of the coolant temperatures within each FA, eliminating an effective provision for the control of the reactor;

— the mechanism for tightening the FAs lattice – relying on a direct contact between the structures at the foot of the FAs – has been evaluated as a much weaker solution than a more traditional diagrid in which proper spikes in the FAs are engaged.

It was therefore decided to recover the core configuration investigated as backup solution in the ELSY project (characterized by hexagonal, wrapped FAs instead of the innovative ones with open square lattice of fuel pins, proper of the reference configuration), while adopting from the reference ELSY core all the solutions deemed to be adequate for implementation in the new ELFR core.

3. A SAFE AND SUSTAINABLE CORE

The design of the ELFR core, starting from the previous designs, has been aimed at exploiting from the very beginning the favourable coolant features to achieve the aimed objectives in terms of safety and sustainability, rather than relying on provisions to be successively implemented to target the desired performances.

To what concerns sustainability, aside the ELSY project it was shown that the given core configuration could have been suitable for both the management of the Minor Actinides (MAs) and the complete use of the uranium resources [10], through an adiabatic [11] operation of the reactor (Figure 1), that is: reprocessing the spent fuel so as to recover the entire inventory of actinides, and simply replacing the Fission Products (FPs) by natural or depleted uranium up to the reaching of a constant fuel composition characterized by every isotope in its equilibrium concentration.

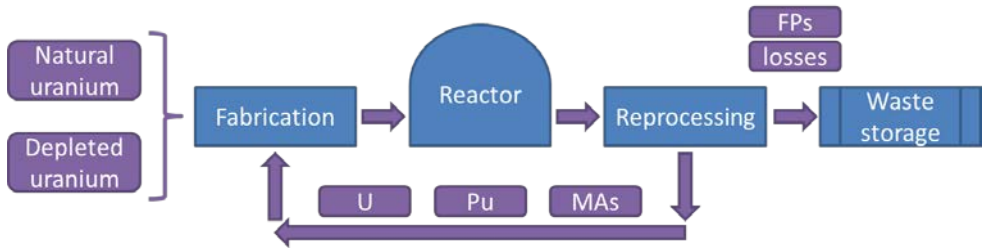

FIG. 1. Scheme of a fuel cycle implementing an adiabatic reactor.

The impact, in terms of sustainability, of operating adiabatically a reactor is clear: with the only exception of the reprocessing losses, the fission chain reaction has no net by-products – which are responsible for the long-term radiotoxicity of the waste –, all actinides being either fissioned or transmuted so as to maintain the production and removal rates in equilibrium along the whole fuel cycle (including cooling, reprocessing and fabrication). Such a reactor is therefore a net fissioner of either natural or depleted uranium, allowing for a complete exploitation of the uranium resources.

The main difference between this approach, and the so called multi-recycling strategy [12], is the a priori definition of the equilibrium core, to define a core able to sustain by design the adiabatic operation (details of this reverted design strategy can be found in [11]).

Concerning the aim of achieving a core able to stand in every possible accidental condition – including unprotected transients –, it is clear that the implementation of the safety features cannot rely simply on adding more and more devices, systems or protections, even if passive. Among the main evidences of the Fukushima accident, the inability to monitor the reactor and to operate the safety systems along an incredibly complex and lasting-in-time event, prove the need for a new approach to safety, based as much as possible on inherent features. Furthermore, reliability and economics have to be simultaneously faced, so that targeting simplicity becomes the leitmotif: it is always true indeed that *simple* is elegant, robust – thus safe – and cheap.

A strong effort has been therefore dedicated to the careful selection of design constraints, to be considered along with ensuring the compliance to the adiabatic core requirements. The

implementation of preliminary safety considerations from the very beginning allows indeed to rely on a strong robustness of the designed core to initiators, accommodating wide temperature excursions still below the safety margins, so as to effectively trigger the counteractions that intrinsically control the transients such that acceptable stable conditions are achieved, ensuring long grace times.

Aiming at this goal, the favourable features of lead are exploited to enhance the effective implementation of prevention and mitigation strategies in the most inherent and intimate level as possible.

4. THE ELFR CORE DESIGN

The comprehensive approach adopted for the design the ELFR core so as to target the safety and sustainability goals can be summarized by the scheme of Figure 2.

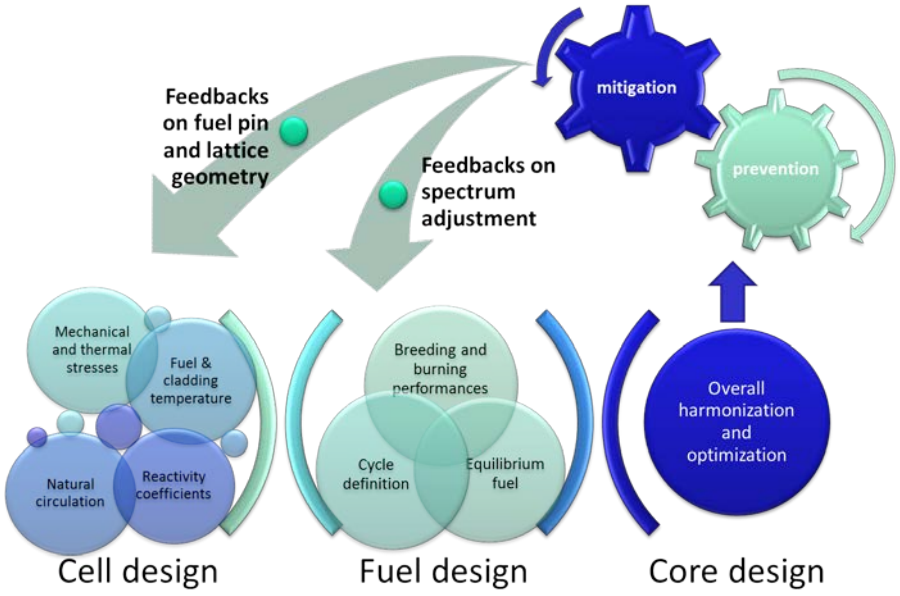

FIG. 2. Scheme of the comprehensive strategy used for ELFR core design.

At first, all the technological constraints, the implications of design goals and the impositions for the aimed safety behaviour are put together to design the elementary cell, i.e. the fuel pin and coolant sub-channel. The breeding and burning performances for plutonium and MAs, together with the in- and ex-core periods, are used to specify the boundary conditions for retrieving the fuel composition, which is set by the neutron spectrum defined by the volume fractions of fuel, structures and coolant. In the end a sufficient number of fuel pins are arranged to achieve criticality, so as to define the core configuration together with the dimensioning and positioning of control and safety rods.

The size of the core, defining the total power, together with the core behaviour during safety-related transients are used to retrieve feedback information for adjusting the elementary cell design and the fuel composition iteratively, until a final configuration is attained, complying with the design goals:

- maximum cladding temperature in normal operation below the limit of 550 °C for corrosion protection;
- maximum fuel temperature in nominal condition low enough (indicatively 2000 °C) to accommodate excursions in Unprotected Transients of Over-Power (UTOP), preventing fuel melting;
- elementary cell geometry providing pressure losses low enough to allow the setting of natural circulation during Unprotected Loss Of Flow (ULOF) at temperatures which ensure a time to clad failure of at least 30 minutes;

— maximum coolant velocity through the core below 2 m/s to protect the cladding against erosion;

— core configuration ensuring criticality with the fuel composition determined by the adiabatic operability of the reactor.

4.1. Cell design

The design of the elementary cell has to cope with the harmonized and intimate integration of all the features ensuring the intrinsic robustness of the safety capabilities of the core. The typical temperature behaviours set during unprotected transients are often characterized by a temperature peak due to the delay between the initiating cause and the response of the system, which is always followed by a plateau corresponding to the setting up of the final equilibrium thermal regime. The safety capabilities concerning the prevention pillar can therefore be formulated accordingly, in terms of both countermeasures for accommodating and recovering initiating events, and provisions for an affordable long-term stable passive control of reactivity and heat removal, so to:

— conceive a system able to passively/intrinsically react to every initiating cause, withstanding all conceived initiators (including unprotected transients) accommodating the initial peak before the reaching of the self-regulated semi-asymptotic condition (*short-term goal*);

— design the system to withstand, preserving the integrity of the structures, during the self-regulated stationary condition providing thus sufficient grace times for a manual operator intervention to shutdown the reactor (*long-term goal*).

Consistently with these aims, and taking into account the specific lead properties, the design of the elementary cell can be approached step by step.

The coolant temperature at core inlet is set to 400 °C to introduce a sufficient margin against lead freezing, and to avoid the embrittlement of ferritic-martensitic steels.

In order to respect the 550 °C limit on cladding temperature for corrosion protection, it is decided to target a relatively low coolant temperature at core outlet (480 °C) which introduces a high margin against structures melting (the coolant boiling being practically excluded). The cladding is also subject to erosion by flowing lead, so that a limit of 2 m/s must be set on the coolant velocity: this requires the adoption of large sub-channels around the fuel pins.

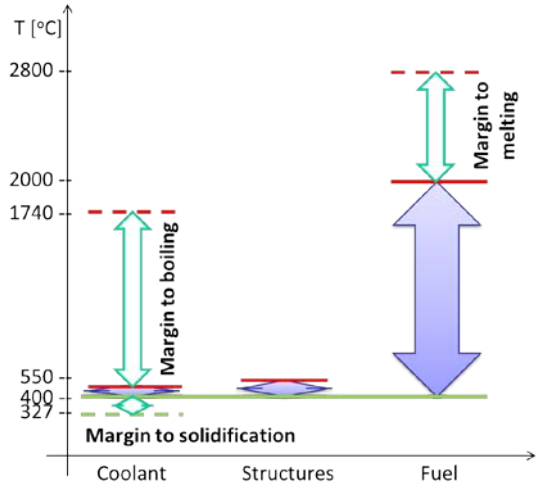

FIG. 3. Representation of nominal temperature ranges and margins for ELFR core design.

Aiming at introducing a margin sufficient to accommodate every possible transient of over-power protecting the fuel against melting, and having in mind also the constraints for the protection of the cladding, it was decided to lower the linear power rating. A lower linear power rating allows indeed to

respect the narrow interval between the average coolant outlet and the maximum cladding temperatures, and to contain the enlargement of the coolant flow area imposed by the low maximum coolant velocity.

A representation of the temperatures set for designing the ELFR core, and the respective margins which are derived from the latter, is shown in Figure 3.

To target all the above mentioned goals, and having in mind the needs coming from the successive steps, it was decided to maintain the large pin of the previous ELSY configurations, which counterbalances the wide lattice pitch, increasing the reactivity of the elementary cell[1] and tuning the neutron spectrum in the core. Also the active height and the coolant velocity are determined to contain the coolant volume fraction, while targeting a geometrical configuration favourable for the natural circulation to set at temperatures that yield to the aimed grace time.

Due to the homogeneous composition of the equilibrium fuel, two pellet designs with varying inner voids are envisaged for the fuel elements in the inner and outer core region, adjusting their reactivity according to the flux buckling, so as to flatten – as far as possible – the power/FA distribution, not to lower the average linear power too much, the maximum value being fixed by the maximum fuel temperature.

All these things put together, the resulting fuel pin and coolant sub-channel are represented in Figure 4.

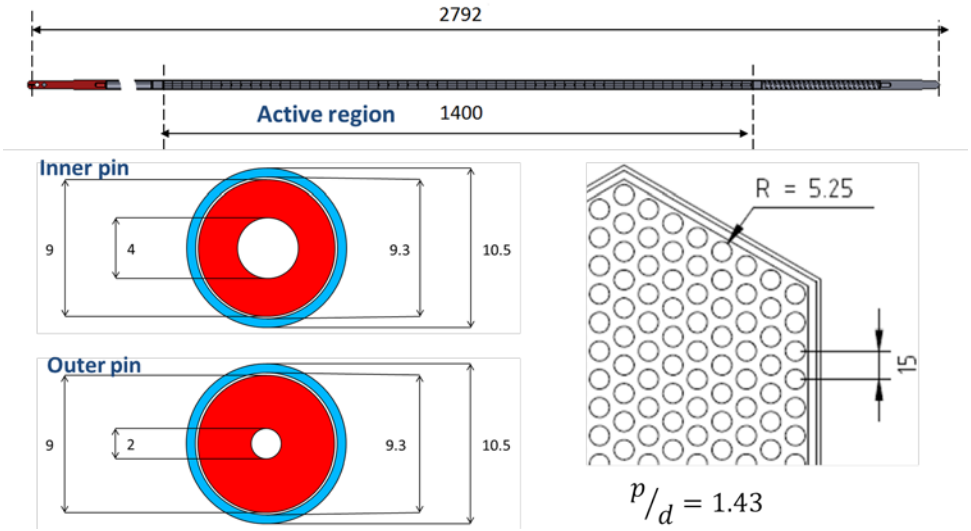

FIG. 4. Cross sections of the ELFR fuel pins and lattice pitch (dimensions in mm).

Finally, 169 fuel pins have been arranged in every FA. The latter has been redesigned trying to maintain the typical layout of fast reactors fuel elements, while extending the upper part such that it extends above the lead level in the reactor vessel to the cover gas, for simplifying the refuelling operations in full visibility.

To allow the lead exiting from the core, a restriction of the FA (*funnel*) has been introduced, together with holes in the wrapper and a nozzle to orient the outflow towards the main pumps sucking ducts, placed all around the Inner Vessel (IV). Despite the extension in the cover gas, the FAs would float in lead. A tungsten ballast has been introduced therefore to oppose buoyancy during refuelling, while preloaded springs are inserted in the top diagrid to both counterbalance the drag due to the pressure

[1] It should be kept in mind that the plutonium content is not a free parameter, being the fuel composition set in order to implement the adiabatic operation of the reactor, as stated in Section 3.

head driven by the primary pumps and to allow for differential thermal dilations of the elements. A view of the ELFR FA is shown in Figure 5.

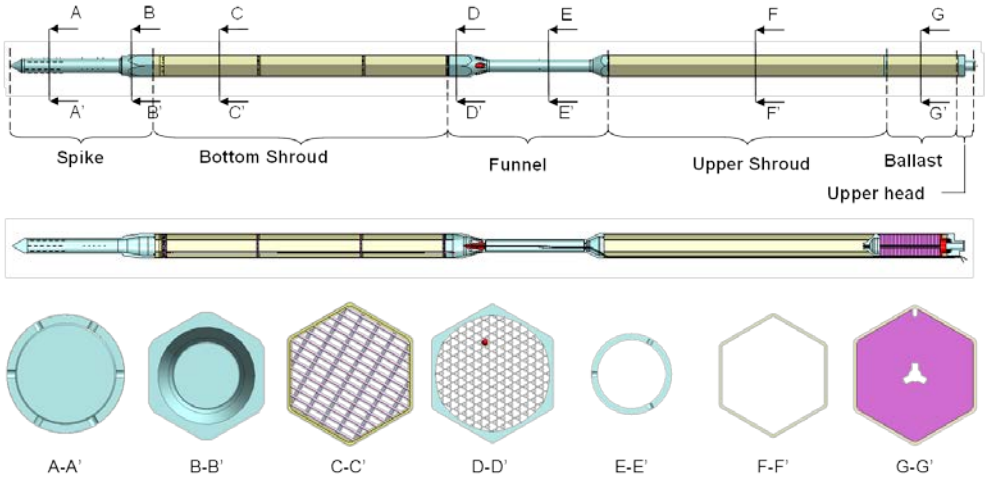

FIG. 5. Cross-section view of the ELFR Fuel Assembly.

4.2. Fuel design

The definition of the equilibrium fuel composition has been performed using the method described in [11], assuming an irradiation period of 5 y to achieve 100 MWd/kg as peak burn-up, and a total decay time for cooling, reprocessing and refabrication of 7.5 y. This assumption seems feasible with the present technology, and is based on the requirement to minimize the number of refuelling operations during the life of one fuel element, so as to maximize the availability factor of the plant. Tentatively the length of the irradiation sub-cycle has been set indeed to 2.5 y, to be confirmed later by more detailed criticality evaluations during the burn-up analysis (see also Figure 7).

Starting from the neutron spectrum evaluated in the ELFR FA, the equilibrium fuel composition is shown in Table 1.

Table 1. Composition of the ELFR equilibrium fuel.

Element	Fraction [%]
Uranium	80.56
Plutonium	18.15
Neptunium	0.11
Americium	1.02
Curium	0.16

4.3. Additional core design characteristics

For setting up the 1500 MWth ELFR core, the final ELSY configuration has been used as starting point. On this reference a redesign of the control and safety systems has been required, because of the insufficient shutdown margin provided by these systems in the original design. Furthermore, the design of the Control Rods (CRs) and Safety Rods (SRs) themselves has been completely changed, adopting the concept investigated in the frame of the Central Design Team project (CDT, 7th EURATOM Framework Programme) [13], in which two diverse, redundant and separate shutdown systems are foreseen:

(1) a control system, used for both normal control of the reactor (start-up, reactivity control during the fuel cycle and shutdown when actuated by motors) and for SCRAM (passively actuated in case of emergency);
(2) a safety system, passively actuated and used only for SCRAM.

The CRs are extracted downward and rise up by buoyancy in case of emergency insertion (SCRAM). The volume of the plenum in the rods (collecting the helium and tritium produced by nuclear reaction of ^{10}B) is optimized for tuning the insertion speed. The control mechanism pushes the assemblies down with a ball screw (for accurate positioning – like in BWR). The ball screw, its motor and resolver (or encoder) are placed atop the cover (at cold temperature), and are protected from radiation by a shielding block. The actuator is coupled to a long rod by an electromagnet. When the coupling electromagnet is switched off (in case of SCRAM), the rod is free to rise up. CRs use a 19 pins absorber bundle, cooled by primary lead.

The SRs are the redundant and diversified complement to the CRs for SCRAM. The absorber bundle – made of 12 absorbing pins – stays in the primary coolant. The rods are extracted above the core and inserted downward against the buoyancy force by means of a tungsten ballast at the top of the rods. Like CRs, the absorbers insertion is triggered by an electromagnet, the switching off of which results also in the actuation of a passive preloaded pneumatic system, which even though is not necessary for the insertion of the rods, further accelerates the SR movement.

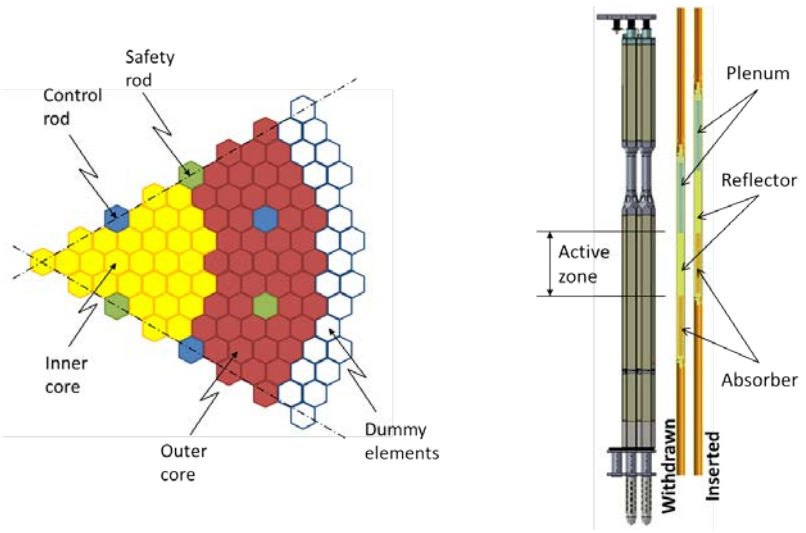

FIG. 6. The final ELFR core: core map (left) and CR concept (right).

The result of the zoning of the core map, for power distribution flattening, along with the positioning of the control and safety systems is shown in Figure 6 (one sixth of the core, left part), together with a scheme of the CR concept (right part).

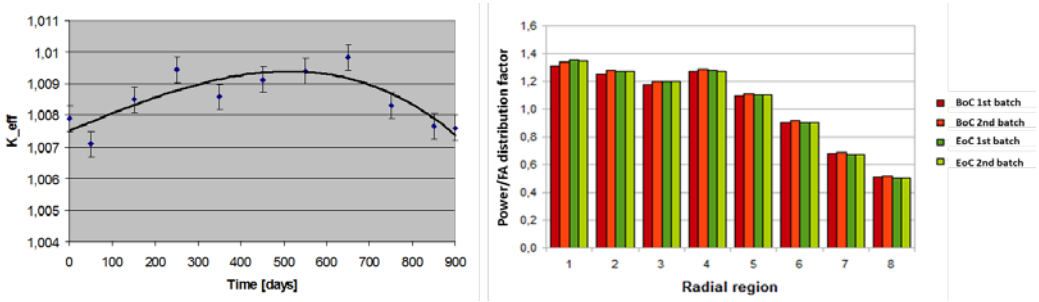

FIG. 7. Neutronic performances of the ELFR core: reactivity swing (left) and power/FA distribution factor (right) as evaluated by MCB [14].

The neutronic performances of the ELFR core are summarized in Figure 7, which shows how the final configuration complies with the respect of the design constraints and the achievement of the goals.

One of the most interesting facts achieved by the design of the ELFR core is the very modest reactivity swing along the 2.5 y sub-cycle: about 200 pcm. Being this value far below 1 $ (= 320 pcm), it can be easily compensated by the control system through a surface penetration of the rods which, besides implying a negligible distortion of the axial flux profile, makes the spurious withdrawal of the CR with the largest reactivity worth (about 30 pcm at maximum insertion during operation) an event that can be well accommodated by the system.

The thermal analysis of the hottest pin (Figure 8), verifying that fuel and cladding temperature constraints are respected, as well as preliminary safety analyses, presented in a companion paper , confirm the effectiveness of the comprehensive design approach adopted and here described.

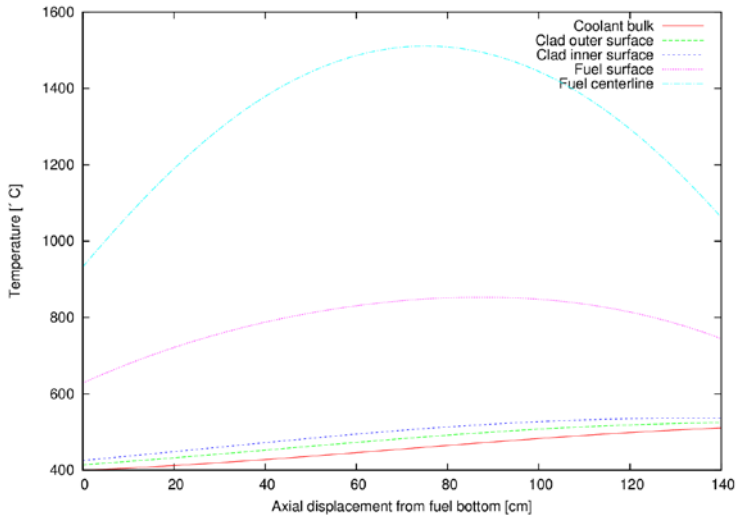

FIG. 8. Temperatures axial profile in the hottest fuel pin and coolant sub-channel.

5. CONCLUSIONS

The comprehensive strategy adopted for the design of the ELFR core, which ensures the ability to consistently implement goals and constraints from the beginning of the design process and thus to minimize the iterative feedback adjustments, has been presented along with its application to the specific safety and sustainability goals proper of Generation-IV NES.

A 1500 MWth core, operating along a 2.5 y sub-cycle with a reactivity swing of about 0.63 $, characterized by a wide pitch-to-diameter ratio encouraging the establishment of natural circulation at sustainable thermal regimes during Unprotected Loss Of Flow accidents, has been described and commented.

The results of the considerations and analyses performed in support of the abovementioned strategy have been also detailed. The studies shown the robustness of LFR in general, and the ELFR in particular, to support the adiabatic operation of a reactor, as well as to exploit the intrinsic safety allowed by the favourable characteristics of lead as coolant.

Finally, despite the many uncertainties affecting the definition of the boundaries for core design (criteria for the protection of the structures against dissolution in the lead, uncertainties in nuclear data, etc.) which are still the main R&D challenges for LFR systems, the proposed strategy seems robust enough to allow approaching the design of the ELFR core to comply with all the Generation-IV goals, including also economics, proliferation resistance and physical protection, not fully taken into account in the present work.

ACKNOWLEDGEMENTS

The Authors acknowledge the European Commission for funding the LEADER project in its 7th Framework Programme. Grateful acknowledgements are also due to all the researchers that collaborated in the LEADER "Core design" Work Package, performing the studies, analyses and computations shown in this paper.

REFERENCES

[1] UNITED STATES DEPARTMENT OF ENERGY NUCLEAR ENERGY RESEARCH ADVISORY COMMITTEE AND GENERATION IV INTERNATIONAL FORUM, A Technology Roadmap for Generation IV Nuclear Energy Systems, report (2002), http://www.gen-4.org/Technology/roadmap.htm.

[2] EUROPEAN COMMISSION, Towards a European Strategic Energy Technology Plan, communication to the council, the European parliament, the European economic and social committee and the committee of the regions (2007), http://ec.europa.eu/energy/technology/set_plan/set_plan_en.htm.

[3] DIRECTORATE-GENERAL FOR RESEARCH AND DIRECTORATE J – ENERGY (EURATOM) OF EUROPEAN COMMISSION, The Sustainable Nuclear Energy Technology Platform: A vision report, special report EUR 22842 (2007), http://www.snetp.eu/www/snetp/images/stories/Docs-VisionReport/sne-tp_vision_report_eur22842_en.pdf.

[4] SUSTAINABLE NUCLEAR ENERGY TECHNOLOGY PLATFORM, Strategic Research Agenda, report (2009), http://www.snetp.eu/www/snetp/images/stories/Docs-AboutSNETP/sra2009.pdf.

[5] SUSTAINABLE NUCLEAR ENERGY TECHNOLOGY PLATFORM, ESNII: The European Sustainable Nuclear Industrial Initiative, Concept Paper (2010), http://www.snetp.eu/www/snetp/images/stories/Docs-ESNI/ESNII-Folder-A4-oct.pdf.

[6] EURATOM SEVENTH FRAMEWORK PROGRAMME, Lead-cooled European Advanced DEmonstration Reactor (LEADER), Proposal/Contract no. FP7 - 249668 (2010), http://www.leader-fp7.eu/default.aspx.

[7] EURATOM SIXTH FRAMEWORK PROGRAMME, European Lead-cooled System (ELSY), Proposal/Contract no. FP - 036439 (2006), http://www.elsy-lead.com/.

[8] ALEMBERTI, A., et al., European lead fast reactor—ELSY, Nucl. Eng. and Des. **241** 9 (2011) 3470.

[9] GRASSO, G., et al., Demonstrating the effectiveness of the European LFR concept: the ALFRED core design, Fast Reactors and Related Fuel Cycles: Safe Technologies and Sustainable Scenarios (Proc. Int. Conf. Paris, 2013), IAEA, Vienna.

[10] GRASSO, G., et al., "The effectiveness of the ELSY concept with respect to minor actinide transmutation capability", Actinide and fission product Partitioning and Transmutation (Proc. 10th Information Exchange Meeting Mito, 2008), OECD-NEA-6420, Paris (2010).

[11] ARTIOLI, C., et al., A new paradigm for core design aimed at the sustainability of nuclear energy: the solution of the extended equilibrium state, Ann. Nucl. En. **37** (2010) 915.

[12] YUN, H., et al., Study on integrated TRU multi-recycling in sodium cooled fast reactor CDFR, Nucl. En. and Design **240** (2010) 3638.

[13] DE BRUYN, D., et al., " The FP7 Central Design Team project: towards a fast-spectrum transmutation experimental facility",Advances in Nuclear Power Plants (Proc. Int. Conf. San Diego, 2010), (CD-ROM paper 10114).

[14] CETNAR, J., Development and applications of MCB – Monte Carlo Contiunous Energy Burnup Code, AGH- WFiIS, Kraków (2006) ISBN 83-921064-4-X.

[15] BUBELIS, E., et al., LFR safety approach and main ELFR safety analysis results, Fast Reactors and Related Fuel Cycles: Safe Technologies and Sustainable Scenarios (Proc. Int. Conf. Paris, 2013), IAEA, Vienna.

IAEA-CN-199
Paris, France, 4-7 March 2013
Paper CN-199-275

Status of ASTRID architecture and pre-conceptual design

Philippe ALPHONSE[1], Jean-Lou PERRIN[1], Philippe GAMA[2]
[1]: CEA Cadarache, DEN/DER/CPA, 13108 Saint-Paul lez Durance Cedex, France
[2]: AREVA NP, 10 rue Juliette Récamier 69456 Lyon Cedex 06, France
Contact author: Philippe ALPHONSE, +33442253458, philippe.alphonse@cea.fr

Abstract. In the frame of the June 2006 French act on sustainable management of radioactive materials and wastes, the ASTRID (Advanced Sodium Technological Reactor for Industrial Demonstration) reactor aims to demonstrate, from the 2020's, at the industrial scale, improvements in the identified fields of progress of Sodium-cooled Fast Reactor (safety, operability, economy) and to perform transmutation demonstration. CEA (French Commission for Atomic Energy and Alternative Energy) is the leader of the ASTRID project, including ten industrial partnerships and EDF SEPTEN for architectural engineering design support.
This document presents the status of the ASTRID pre-conceptual and global industrial design. All of the options of processing systems studied by the industrial engineering partners are managed in configuration models, and monitored by a CEA ASTRID project management team.
Items addressed in this document include views of nuclear island buildings, other operational and process buildings, projected site layout with requirements and specific constraints (external hazards like earthquake, floods, airplanes crashes…)

1. Introduction

Sodium-cooled Fast Reactors (SFR) is one of the Generation IV reactor concepts selected to secure the nuclear fuel resources and to manage radioactive waste.
The French law from June 2006 on sustainable radioactive materials management and waste, requires that concerning transmutation of long-life radioactive elements, studies and investigations shall be conducted, in order to provide an assessment of the industrial prospects of those systems by 2012. Fast Reactor strategy was confirmed in May 2008 at Ministry level and in September 2010 an agreement was published between CEA and the French Government in order to conduct design studies of the ASTRID prototype and associated R&D facilities [1].
Input data for ASTRID pre-conceptual design are a sodium-cooled pool reactor of 1500 MWth generating about 600 MWe. The ASTRID lifetime target is of 60 years.
The main alternative conceptual design is the Power Conversion System (PCS) with two cycles to be studied in parallel to the end of the pre-conceptual design phase: Rankine steam cycle or Brayton gas based power conversion cycle. The ASTRID design is guided by the following major objectives compared to previous SFRs: improved safety, simplification of structures, improved ISIR (In Service Inspection & Repair), improved manufacturing conditions for cost reduction and increased quality, reduction of risks related to sodium fires and Sodium-Water Reaction (SWR), and improved robustness against hazards.
The first phase of the Preliminary Design Project, the pre-conceptual design phase, was conducted from mid-2010 till the end of 2012. Innovation and technological breakthroughs have been favoured, while maintaining risk at an acceptable level. However, the pre-conceptual design delivered by the end of 2012 still includes some open options. Upon completion of this phase it has been possible to obtain the first investment cost estimation, by the important deadline set by the June 2006 law. During the pre-conceptual design phase, interactions have been initiated with the Safety Authority on safety objectives and orientations. The conceptual design will be delivered by the end of 2014. During the conceptual design phase, the ASTRID design choices will be finalized and the Safety Option File will be submitted. Then from 2015 onwards, the basic design phase will start. The ASTRID demonstration prototype is to be commissioned in the 2020 decade [2].

3. Studies and interface data management

3.1. Concurrent engineering

At this time, the ASTRID project gathers 10 partners (cf. fig.1). The interfaces between the different entities involved in this concurrent engineering project are managed on 2 levels. First, in a general manner with meetings held every 2 months. During these meetings, all partner companies and project manager teams (CEA) share the project's progress, especially through the configuration status, recent developments in the planning of studies and performance evaluations of the solutions which are proposed.
In parallel, engineering companies with physical or functional interfaces in their studies regularly meet in pairs. They define the forthcoming needed data and plan their exchanges.

FIG.1: Partner companies for Astrid project

3.2. Configuration management

Due to the numerous possible solutions during the first part of this pre-conceptual phase, a robust configuration management has been put in place from the beginning.
In the first half the year 2011, 2 product breakdowns (one for each model) were defined down to the level of sub-assemblies, which lead to the creation of a reference configuration. Thereafter, following the technical options chosen between 2011 and 2012, this configuration has been updated to maintain an applicable configuration and to provide accurate data to the various partners for their studies.

3.3. Performance management

Performance management is an iterative process. It is based on expected performances and must be conducted from the beginning of the project to its end. For each configuration studied, a reassembly of the performances of all the systems is performed thanks to a validated methodology. This allows an evaluation of coherent combinations of solutions in order to classify them by performance.
Periodic reviews are made to estimate the global performance of each different selected design. It allows comparisons, in terms of performance, and it allows the assessment of target deviations. A classification is done according to essential discriminating criteria such as safety, cost and maturity/feasibility.

4. Plant layout and 3D CAD models

In this pre-conceptual phase, 2 models of the future ASTRID process have been studied. In both cases, the core and primary circuit structures are the same, and they are described in another document written by CEA and AREVA participants.

The first issues of both 3D models, based on 2 different power conversion systems were delivered at the end of 2012. In order to efficiently collect and consolidate the different designer's project databases; the implantation of this pre-conceptual design has been performed on suitable software for complex industrial facilities.

4.1. Steam model (PCS with steam turbine – Rankine thermodynamic cycle)

Figure 2 shows a cross section of the Nuclear (NI) and Conventional Islands (CI) of the model based on the Rankine cycle. The NI buildings housing the fuel storage tank, the electric premises and the steam generators are located on the same concrete slab in order to eliminate the differential shifting during an earthquake. This slab is also placed on seismic proof pads to reduce horizontal forces transmitted into the walls and floors. A second containment shell protecting against aircraft crash surrounds the reactor building and all the buildings with major safety functions. On the left side of the figure, there is the heavy components' maintenance building. On the opposite side, we can see the machine room with the turbo alternator standing on a slab linked with the main foundation of the turbine hall.

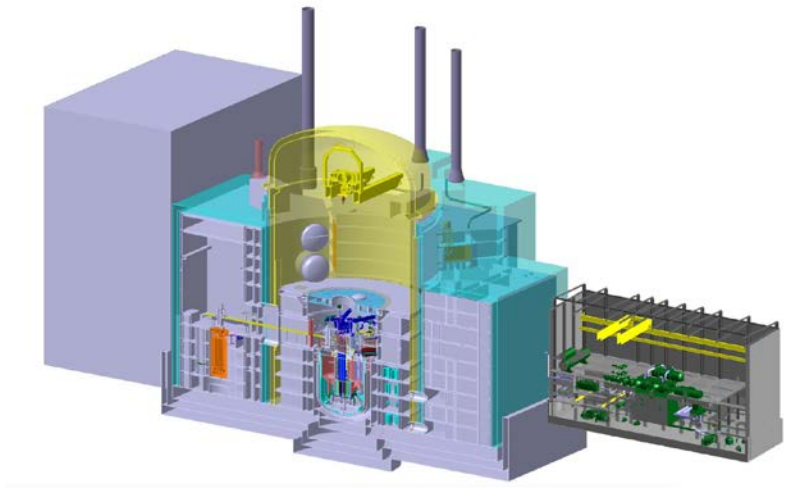

Fig.2: Nuclear and Conventional Islands – Steam model
ASTRID Project Business Confidential Information, CEA and AREVA NP and ALSTOM property designs

Safety considerations have guided the choice of a structure composed of 4 secondary loops equipped with 3 steam generators and an electromagnetic pump. Each circuit is located in a separate building with a strict separation between areas containing the sodium circuits from those with water/steam pipes. The studies have been focused on minimizing the length of sodium piping. Layout is guided by sodium leak risks management requirements. The 4 circuits of decay heat removal are each located in a different steam generator building.

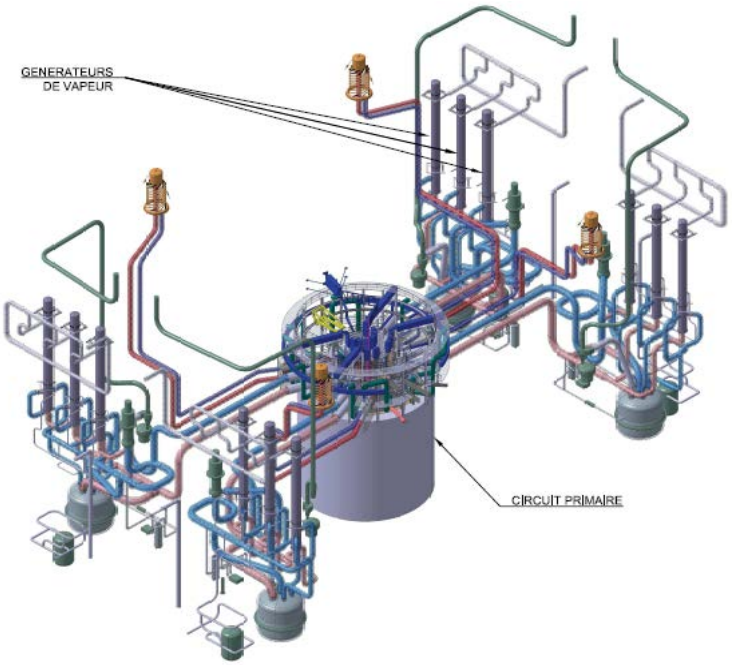

FIG.3: 3D layout of the primary/secondary circuits and steam generators
ASTRID Project Business Confidential Information, CEA and AREVA NP property designs

4.2. Gas model (PCS with nitrogen turbine – Brayton thermodynamic cycle)

At this level in the studies, the only specific features of the gas model are inside layouts of the Sodium/Nitrogen Heat exchangers (SNHx) buildings and of the machine room equipments. These buildings, however, are very comparable in size to their counterpart steam model. The layout of the SNHx buildings takes into account the benefits from the use of a non-reactive gas with sodium. It allows the elimination of a large amount of the partitions required to avoid the sodium/water reaction in the steam model. The heavy nuclear components' maintenance building does not appear on this figure, nevertheless it remains unchanged.

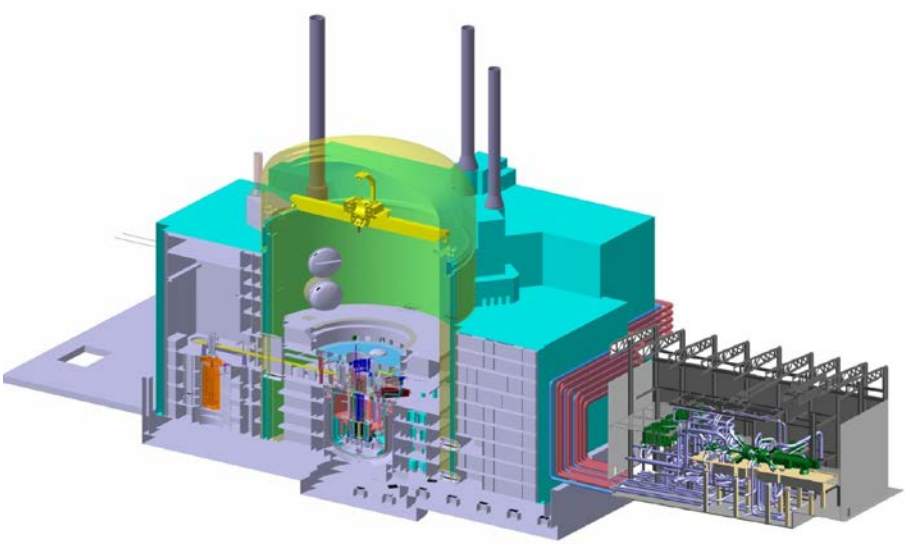

FIG.4: Nuclear and Conventional islands – Gas model
ASTRID Project Business Confidential Information, CEA and AREVA NP and ALSTOM property designs

The routing of the sodium pipes is preserved (cf. Fig.5). A structure with 4 loops serving 24 Sodium/Nitrogen Heat exchangers (SNHx) is studied as the reference configuration. In order to minimize the losses on the gas side, the designer chose to avoid output collectors upstream the SNHx and to link each gas pipe directly to the turbocharger. The electromagnetic pumps and the 4 segregated trains for the decay heat removal are also kept unchanged.

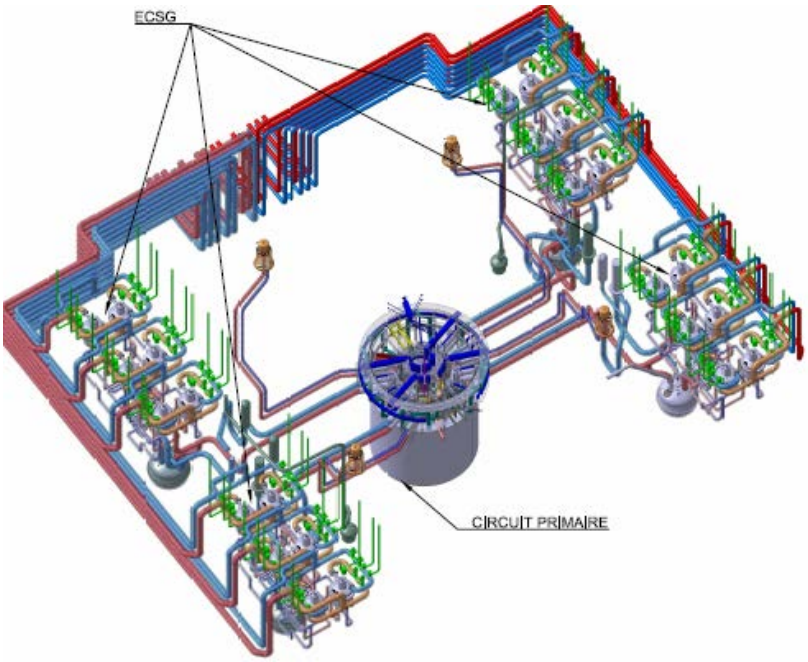

Fig.5: 3D layout primary/secondary circuit and sodium/gas heat exchangers
ASTRID Project Business Confidential Information, CEA and AREVA NP property designs

During the second phase of the pre-conceptual design, an optimization of the layout of the entire nuclear island will be carried out in order to reduce the lengths of gas pipes in connection with the conventional island.

4.3. Site layout

At this stage, a reference site has been selected for the project. In the current implementation, a special attention has been given to the protection of the nuclear island. Its position high over the river and the surrounding reliefs will help significantly to reduce the risk of external aggressions. The availability of water from the nearby river, from water reservoirs located above the plant or from independent drillings offers a wide variety of cold source.
The limited height of the forced draft cooling tower reduces the visual impact and favors the environmental integration of the ASTRID power plant.

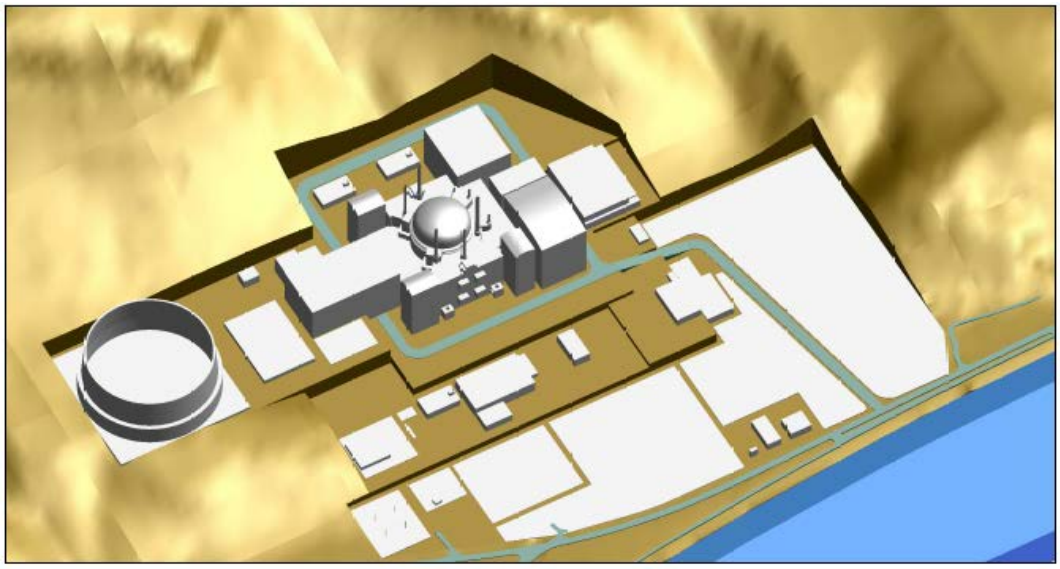

FIG.6: 3D site layout
ASTRID Project Business Confidential Information, CEA and AREVA NP property designs

5. Conclusion

This document presents a status of the pre-conceptual design and architecture of the ASTRID prototype. The configuration management is explained. The pre-conceptual design has been delivered at the end of 2012. The conceptual design will be delivered by the end of 2014.

REFERENCES

[1] F. Gauché; The French Prototype of 4th Generation Reactor: ASTRID; Annual meeting on nuclear technology, Berlin, May 17&18th; 2011.

[2] P. Le Coz *et al.*; Sodium-cooled Fast Reactors: the ASTRID plant project; Proceedings of ICAPP'11, Nice France, May 2-5, 2011; Paper 11249.

Preliminary Conceptual Design for a Multipurpose Experimental Sodium-Cooled Fast Reactor

M.H. Kim[a], H.H. Lee[a], T.K. Kim[b]

[a] Kyung Hee University, Gyeonggi-do, Rep. of Korea

[b] Argonne National Laboratory, Argonne, IL, U.S.A.

Abstract

A conceptual nuclear design was done for a 100MWe multi-purpose sodium cooled fast reactor core for both research and experiment as a pre-feasibility study. Challenging goals for a small sized core were set up. Cycle length should be longer than 4 month with low enriched uranium-only fuels in a U-Zr metal alloy form. Overall design features are chosen from previous design concept - advanced burner test reactor (ABTR). Number of fuel assemblies and reflector assemblies were increased from 54 to 66 and from 78 to 207 respectively, resulting in increase of core radius to 180cm. In the reflector zone, there was enough space to install three independent fuel test loops in which different type of coolants and fuels might be tested. Fuel pin size was selected to be 0.737cm through a parametric study with database for U-Zr metal fuels tested in EBR-II. Core height was optimized to be 87cm after a parametric study on core size. Target flux levels at both fuel test assemblies and material test assemblies were 3.0×10^{15}n/cm^2-sec. Most of performance parameters as well as safety parameters were satisfied with goals except a flux level at the MTA. Overall safety aspects of the reactor is better than any other previous SFR design concepts.

1. Introduction

For a sustainable energy option, recycling of spent fuel from both existing plants and future Gen-IV plants became an international concerns for research. Partitioning and transmutation of high-level long-lived minor actinide(LLMA) from spent fuel has been studied for two options; accelerator-driven subcritical reactors and critical reactors. Among many sub-options, sodium-cooled fast reactor(SFR) option was chosen by most of countries because of strong and wide technical infra-structures. Rep. of Korea also chose SFR as the Gen-IV reactor. Korean design for SFR is based on KALIMER-600 which is designed to burn LLMA without fissile breeding. It may be connected with collocated reprocessing plant with pyro-processing technique. New design concepts such as passive reactor core cooling systems were added, and they were arranged in a integral pool allowing in-service inspection. Recently Korean government changed a timeline goal of commercialization from 2030's to a later time, may be between 2030 and 2050. As a preliminary step for commercialization, a small prototype plant rating at 300MWt was planned to be constructed before 2028 for the building up of technical validation and industrial manufacturing infrastructure. Later on, domestic technology can move to the commercialization of the larger-sized SFR plants in future [1].

For the time being at least, pyro-processing of spent fuel and manufacturing of U-TRU-Zr fuel are not allowed even though TRU test fuel might be burned in a reactor with special safeguard measures. Therefore, a protopype SFR should be loaded with low enriched uranium(LEU) fuel in the form of U-

Zr alloy. The purpose of 100 MWe prototyp reactor must be the technical verification of SFR design concept with new design features and a test bed for an in-pile fuel irradiation with TRU fuels.[2]

Prototype reactor can have several different design concepts depending on the utilization purpose and functional scope. In this study, it is expected that a Korean prototype SFR should be used as an experimental tool as well as system design verification. In order to give functional variety, there must be many irradiation holes for fuel test assemblies(FTA) and material test assemblies(MTA). This is very crucial function of a test reactor designed to develop new fuels and claddings, especially new TRU samples should be burned for fuel research and license procedures. If there is a big design modification in size, material or operational condition, these irradiation holes cannot be used. Instead of them separate independent fuel test loops(FTL) can be used for test fuel irradiation. They can be located in the out of core, at the reflector zone. In this FTL, different reactor concepts also can be tested independently, such as MOX fuel with Pb-Bi coolant, square fuel array in high-temperature Na coolant, different size fuel assemblies, etc.

This work is an early-stage feasibility study on the nuclear design for SFR core in order to find a possibility of a Multipurpose Experimental Sodium-cooled Fast Reactor (MESOF) concept which can accommodate many kinds of experiments and testing of fuels and materials. Core concept was based on the Advanced Burner Test Reactor(ABTR) designed by Argonne National Laboratory(ANL) in 2006.

2. Design Targets & Requirement of MESOF

Based on the published data of some prototype and experimental fast reactors, design targets and requirements of MESOF were decided. The most functionable size for the prototype would be more than 600MWt (~250MWe) in order to have high neutron flux level with more than 4 months cycle length.[3] However, for the first kind of prototype reactor in Korea it should not be large considering the budget and engineering risk. The size goal was set up as 300MWt (100MWe) with fuel cycle length of 4 months. Target level of neutron flux was 3.0E+15n/cm^2-sec, but flux level may not be a prime design target for maximization. Instead of this, minimization of required uranium enrichment under the longer cycle length is more practical goals, because a MESOF core should be loaded with U-Zr fuel. Because target power level is almost same with the ABTR, design work was started with the same number of fuel and control assemblies, but larger number of reflector assemblies in order to maximize the neutron economy. In the early stage of operation of MESOF, a core cannot be loaded fully with TRU fuel assemblies. TRU test fuel should be loaded either in FTA locations or in FTLs.

Table 1. Design Targets of MESOF comparing with ABTR

Targets	MESOF	ABTR
Power	300MWt (100 MWe)	250 MWt
Flux Level	Avg. 3.0E+15 n/cm^2-s	Avg. 2.38E+15 n/cm^2-s
Cycle Length	> 4 months (120 days)	4 months
Fuel	LEU U-10Zr	U-20TRU-Zr (TRU: WG Pu only)
Alternative Core Options	LEU UO_2, LEU-TRU-10Zr (TRU: LWR SF Recycle)	Oxide, U-Zr & U-TRU-Zr

For the verification of fuel and structural material, required discharge burnup was targeted upto 150MWd/kg and peak fast fluence was targeted to be less than 3.0×10^{23}n/cm^2. The maximum Peak Linear Power value was limited to 33kW/m for the nuclear fuel safety. Reactivity worth inserted by ejection of one control rod assembly (CA) from critical condition should be less than 1$ in order to prevent from prompt critical. Therefore, in case of ABTR rod worth was designed to be less than 0.9$. However, reactivity addition by the rod ejection is one of the major initiating events for UTOP. For the safety concern, rod worth of one CA should be as low as possible. This requirement may be one of challenging guidelines in case of small size and small power reactor core. The Design requirement explained in the upper part was shown to Table 2.

Table 2. Design Requirements of MESOF comparing with ABTR

Requirements	MESOF	ABTR
Fuel	Driver: LEU U-10%Zr Fuel Test: U-TRU-10%Zr Fuel	Driver: U-20(WG-Pu)-Zr All kinds of Alternative
Burnup Rate	Target: 150 MWD/KgHM	Avg. 97.7 MWD/Kg
Worth of one Control Assembly	< 0.5$	< 0.9$
Cladding Temp. Limit	<650℃	<650℃
Fuel Temp, Limit	< 1,100℃	< 1,100℃
Peak LPD	(33) < 44.0 kWt/m	(38.5) < 44.0 kWt/m
Peak Fast Fluence	3.0E+23 n/cm^2 (E>0.1MeV)	3.24E+23 n/cm^2

3. Design Tools for Design

A computer code system used for design a core was validated by comparing with Monte Carlo code and transport code calculation because there has not been proper experimental data. [4] Since many years ago, TRANSX - DANTSYS - REBUS-3 code have been used for a design study for a lead-cooled fast reactors in Kyung-Hee University. Those were already benchmarked with MCNP with reasonable error size. KAFAX-F22 library published by KAERI has been used in this study. [5][6][7][8][9]. REBUS-3 code in Kyung Hee University has only one neutronic solver, a nodal diffusion module, DIF-3D, which showed relatively large difference compared with transport theory code, VARIANT.

4. Study on Optimization of Conceptual Core Design

ABTR inner core configuration was adapted in MESOF design because power level was similar each other. In addition, the same goals of flux level and burnup were set up with U-10Zr fuel. In order to compensate reactivity penalty from LEU fuel compared with TRU (WG-Pu), fuel assembly(FA) should have more fuel volume. The thicker fuel pin and larger core size may help to this direction. The fuel assembly design like the ABR-1000 was used for the assembly size increasing.[10] FA has 271 fuel pins instead of 217 pins of ABTR, and 16.14cm pitch instead of 14.6cm. In addition, to minimize the neutron leakage the number of reflector assemblies was chosen over 120 which reduces the reactivity loss. Since the nuclear fuel design should primarily depend on manufacturing feasibility,

fuel pin diameter of 0.63cm and 0.737cm were selected from database for U-Zr metal fuels tested in EBR-II.[11]

4.1. Preliminary Check through Parametric Study

Based on the core design of ABTR, a parametric study was performed to satisfy the cycle length by varying the fuel pin height and number of reflector assemblies around the core. Calculations were performed by varying the fuel pin height from 80 cm to 91 cm, which is EBR-II test data value, with 2 cm step increase in fuel pin height. Calculations were performed using REBUS-3 code. The calculations showed that the reactivity increase linearly with fuel pin height by 0.5% value at each step. The calculations were also performed by increasing the reflector assembly layers, surrounding the core, in multiple steps. The neutron leakage is reduced as the number of reflector assembly layers are increased but the anonymous increase in reflector assemblies will result in increased construction cost of core. Therefore, an optimized number of reflector assembly layers should be estimated through the parametric study. In reflector assembly parametric calculations it is observed that over the 3 layers of the reflector assembly the reactivity increase is negligible.

4.2. Proposed Conceptual Core Design

For an experimental reactor in prototype reactor class, there should be test assemblies for both fuels and materials for the purpose of in-pile irradiation tests. In this study, the same locations and number in ABTR were chosen. In addition, separate and independent irradiation loop is needed for the irradiation experiment of fuels under different coolant or at different operation conditions. Thus, separate test loop (independent fuel test loop) was placed in the outer reflector zone. Table 3 presents the design specification of the proposed design determined through the parametric study and Fig. 1 show the proposed core design. From parametric study, fuel pin diameter was determined as 0.737cm and fuel pin height was 87cm. Installation of separate test loop reduces some amount of excess reactivity. Therefore, in the case of the core with separate test loop, the numbers of fuel assemblies were increased up to 66, as well as the numbers of reflector assemblies, up to 207.

Table 3. Design Specification of the Proposed MESOF

	MESOF
Driver Fuel	U-10%Zr (with 19.5w/o enrichment)
Core Internals	66 Driver FA, 7 (Pri.) +3 (Sec.) CA 6 (Fuel) +3 (Material) TA 207 Reflector Assembly 3 FTL at Reflector Zone
Test Fuel	U-16.5%TRU-10%Zr (with LWR-SF-TRU)
Fuel Assembly	Pitch 16.14cm 271 pins Hex. Array
Fuel Pin Size	Radius (fuel+bond+clad) 0.2837+0.0438+0.041 =0.3685cm Pin Diameter =0.737cm wire-wrap diameter, 0.1585cm
	Length (shield+fuel+plenum) 60+87+120=267cm

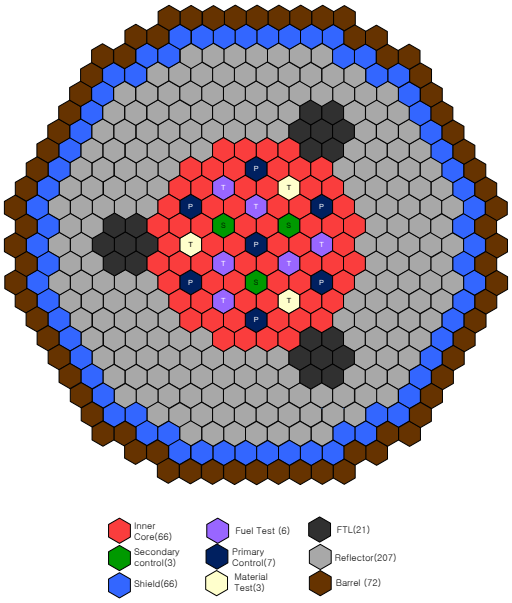

FIG. 1. Map of Separate Fuel Test Loop Loaded into the Proposed Core Design

4.3. Core Performance Check about Impact from Loading of Test Assemblies

Loading of U-TRU-Zr test fuel assemblies in all 6 FTA locations may lead a high excess reactivity, or unloading of test fuels from all FTA into vacancy may lead a loss of excess reactivity under criticality condition. In some cases, partly loading of FTA may cause a severe power shape anomalies resulting in local power peaking. In this study, probable extreme loading conditions of FTA, MTA are examined as a preliminary design check-up. Separate FTL in autonomous loop can be used as an independent test for the different core concept, such as U-N fuel in a lead-bismuth coolant. A feasibility test was also done for the various loading conditions to outer FTLs.

The following Table 4 showed calculation results from REBUS-3. Impact of U-Zr test fuel loading in FTA locations with TRU (WG-Pu) fuel loading on all FTL was tested in Case 2. Core excess reactivity value was increased a lot. Reactivity addition should remain within a total control rod worth in order to have sufficient shutdown margin. However, peaking factors are decreased by evenly loading of fuel throughout the core zone. Flux level at the MTA locations are decreased unexpectedly because of more heavy metal loading to the core. Even if the Pb-Bi coolant was flowing in FTL, flux level is similar to other cases of sodium coolant. This results showed the possibility for the irradiation experiment of fuels under different coolant or at different operation conditions. In Case 4 where no test materials are loaded into all 9 locations and also in all FTLs, core excess reactivity is low below the criticality condition as it is expected.

Table 4. Performance of Core Design under Investigation into Case Study

	MESOF			
	Case_1	**Case_2**	**Case_3**	**Case_4**
K-effective value [BOC /EOC]	1.00946/ 1.00042	1.07644/ 1.06900	1.05008/ -	0.95862/ 0.94907
Power Density of active Core, KW/l [Core /FTA/FTL]	219/ 137.3 / 0	171.6/0/139.1 / 0	191.7/ 211.0 / 0	231.53/ 0 / 0

Peak Power Density of active Core, KW/l	431.41	303.66	371.7	466.08
Peak linear power, KW/m	35.92	25.28	30.95	38.81
MTA average flux, 10^{15}n/cm^2-sec	2.05	1.64	2.27	2.07
Active Core average flux, 10^{15}n/cm^2-sec [Core /FTL]	1.73 / 0	1.35 / 1.0	1.5 / 1.48	1.77 / 0
Separate Test Loop average flux, 10^{15}n/cm^2-sec	0.636	1.17	1.75	0.588

In Case 3 where one out of 3 FTLs is loaded with U-TRU-Zr test fuels with asymmetric loading, peaking factor is not affected by FTL because they are located far from the core center. In this core, due to the small size of core, asymmetric effect was not shown considerably.

4.4. Control Rod Worth

Through the Case_1 of MESOF as described in Table 5, the control rod worth is evaluated as one of a safety analysis on core design proposed. The reactivity worth was calculated for various combinations of control assemblies inserted, and one stuck-rod worth was estimated for each control assembly. Table 5 presents the calculated control assembly worth for various combinations of control assemblies. Among the primary control assemblies, the central control assembly has the largest worth because of higher neutron flux in the core center. The estimated worth of the central assembly is 3.13$.

Table 5. Evaluation of Control Rod Wroth ($)

	Number of inserted CRs	Rod Worth ($)
Primary System		
- Central rod	1	3.13
- All CR's in 5th row	6	7.77
- Central and 5 CR's in 5th row	6	9.77
- All Primary rods	7	11.46
Secondary System		
- 2 CR's in 3rd row	2	5.13
- All Secondary rods	3	7.83
One Stuck Rod Worth		
- Central rod		3.69
- One of the 5th row		1.68
- One of the 3rd row		2.99

4.5. Optimized Core Design

In the previous case study, the flux level of all core design concepts under consideration showed lower value than the design target. For the purpose of irradiation experimental reactor, flux level at MTA location should be increased by design optimization. This may be achieved by some corrections such as 1) fuel enrichment increase, 2) core size increase, or 3) MTA location change with FTA, In order not to change the size of core, MTA location change was the easiest way. three MTA location were moved to the central part of the core. Figure 2 showed the optimized core design concept, MESOF-S.

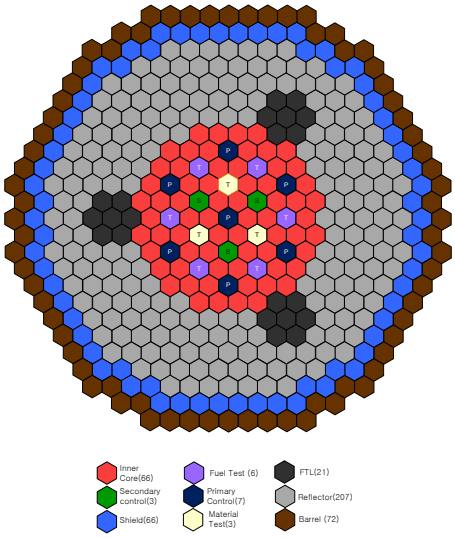

FIG. 2. Optimized Core Design, MESOF-S

Table 6 summarized REBUS-3 calculation results. K-effective value at the end of cycle(EOC) was less than 1.0. However, reactivity value from the diffusion model was always less than the real values or values from transport codes with constant deviation. Therefore, cycle length requirement would be satisfied without problem. The flux level was 2.54×10^{15} n/cm^2 but it was about 85% level of the design target. Therefore, iirradiation time should be increased for the desired irradiation performance. Peak linear power density(LPD) was 33.4kW/m within the limit value 44kW/m. The flux Level at the FTL was similar to the proposed core design.

Table 6. Result of Neutronic Calculations of the Optimized Core Design.

	MESOF-S
K-effective value [BOC /EOC]	1.00385/ 0.99482
Peaking Factor [BOC /EOC]	1.87359/ 1.93403
Power Density of active Core, KW/l [Inner core / TFA/ Separate test loop]	220.3/ 122.7/ 0
Peak Power Density of active Core, KW/l	412.89
Peak Fast Fluence, n/cm^2	2.16810E+22
Peak linear power, KW/m	34.4
MTA average flux, 10^{15}n/cm^2-sec	2.54
Active Core average flux, 10^{15}n/cm^2-sec [Inner core / Separate test loop]	1.72
Separate Test Loop average flux, 10^{15}n/cm^2-sec	0.643

5. Reactivity Control and Shutdown System

5.1. Temperature and Power Defects

As previously proposed in section 4, the MESOF-S design has been chosen to carry out further safety analysis with the DIF3D. A parametric study for the safety point of view such as the reactivity feedback coefficients resulted from Doppler broadening, radial expansion, axial expansion and sodium density variation is performed as shown in Table 7 where the comparison between the MESOF-S and ABTR is also presented.

Table 7. Temperature and Power Reactivity coefficients

	MESOF-S	**ABTR**
Delayed neutron fraction (beta)	0.006391	0.0033
Doppler Coefficient (cent/℃)	-0.12	-0.10
Radial Expansion Coefficient (cent/℃)	-0.23	-0.59
Axial Expansion Coefficient (cent/℃)	-0.075	-0.06
Sodium density (cent/℃)	-0.13	0.03
Coolant Void Effect ($)	-1.54	1.75

The effective delayed neutron fraction obtained 0.006391 through MCNP calculation. The Doppler coefficient represents the effect of the reactivity according to the fuel temperature change. The radial & axial expansion coefficients are calculated as the rate of expansion according to the fuel temperature change. By varying the sodium coolant density of all fuel assemblies loaded in the MESOF-S core design, the sodium density coefficients are evaluated to check subsequent reactivity insertion. Sodium void effect calculated that when the flowing sodium inside the assembly duct of all the fuel assemblies is voided in the core.

Effective delayed neutron fraction of MESOF-S is 0.006391, and ABTR is 0.0033. In case of the MESOF-S, the effective delayed neutron fraction is bigger than ABTR because of using LEU fuel. From the important safety aspects about reactor kinetics of the MESOF-S, the calculation results approve that larger value of the delayed neutron fraction of that design is obtained when compared to that value of the ABTR design. It implies that the design may have enough time to control the rapid reactivity insertion.

Doppler, radial expansion, axial expansion coefficient has the negative value as ABTR altogether. ABTR and MESOF-S have large neutron leakage due to small core size. However, in case the sodium voiding occurs in ABTR using the TRU (WG-Pu) fuel, the positive spectral hardening effect over-weighs the negative leakage effect. So, the sodium void worth and sodium density coefficient are positive. On the other hand MESOF-S using the LEU fuel has negative value because leakage effect is bigger.

Table 8. Temperature and Power Defects ($)

	Hot full power to hot standby ($)	Hot standby to refueling ($)
Fuel Doppler	0.344	0.181
Axial expansion	0.059	0.117
Radial expansion	0.177	0.354
Sodium density	0.107	0.214
Sum	**0.687**	**0.866**

Using the reactivity coefficients in table 8, reactivity defect is calculated from hot full power critical to zero-power refueling temperature. The refueling temperature was conservatively assumed 200℃. The calculated temperature and power defects are summarized in Table 9.

5.2. Reactivity Control Requirements

The primary system must be able to shut down the reactor from any operating condition to the refueling temperature, with the most reactive control assembly stuck at the out of core. The secondary system must be able to shut down the reactor from any operating condition to the hot standby, even in case the most reactive assembly is inoperative. Secondary control system should be capable of working as an exact substitute of primary control system. However, the compensation of burn-up related reactivity changes does not belong to its requirements. The uncertainties are not included in the secondary system requirements. The reactivity control requirements are summarized in Table 10. Values in Table 9 and 10 are evaluated for the optimized design in Fig.2. Therefore values are slightly different from those in Table 5.

Table 9. Reactivity Control Requirements ($)

	Primary	**Secondary**
Temperature defect	**1.553**	**0.687**
Full power to hot standby	0.687	0.687
Hot standby to refueling	0.866	
Overpower (15%)	**0.1**	**0.1**
Fuel cycle excess reactivity	**1.41**	
Uncertainties (RMS)	**3**	
Temperature defect (20%)	0.3	
Burnup reactivity (50%)	0.7	
Criticality prediction	1	
Fissile loading	1	
Reactivity fault	**0.5**	**0.5**
Total	**6.563**	**1.287**

Table 3. Reactivity Control Requirements and Available Reactivity Worth

	Primary	**Secondary**
Number of control assembly	7	3
Reactivity worth of system ($)	11.71	7.30
Worth of 1 stuck assembly ($)	3.48	2.25
Reactivity worth available ($)	8.23	5.05
Maximum requirement ($)	6.563	1.287
Shutdown margin	**1.667**	**3.763**

The estimated temperature and power defect from hot full power to cold shutdown at BOEC is 1.553$. The overpower margin is allocated to permit the reactor to operate at 115% of the rated power, which is equivalent to 15% of the power defect. The fuel cycle excess reactivity is 1.41$. Uncertainties is one of the unconsiderable factor in the conceptual design, it will be assumption. The uncertainties consist of 20% of total temperature defect, 50% of total burnup reactivity and an assumption of 1.00$ each for criticality prediction and fissile loading. In the simulation of the control rod insertion into that

proposed design, the reactivity fault only reaches 0.5$. In Table 11, the reactivity control requirements are compared with the available reactivity worth of the control systems. The shutdown margins of the primary and secondary systems were determined with the assumption that the most reactive assembly is stuck. The shutdown margin of primary system is 1.667$ and secondary system is 3.763$. Total shutdown margin of MESOF-S is 5.43$.

6. CONSLUSION

In this paper, a conceptual design model for an multi-purpose experimental sodium-cooled fast reactor(MESOF) was found. This model is different from ABTR, more versatile with separate FTL, having the same design performance with LEU fuel instead of TRU(with weapon-grade Pu) fuel. However, size of reactor became larger than ABTR because of large reflector zone outside of core. Flux level at the test assembly location was less than target by 15 %.

Preliminary study on the safety impact from hypothetical sample irradiation operations were done with satisfying results. Safety analysis was done only for the nuclear design aspects. Delayed neutron fraction was larger than ABTR and all reactivity feedback coefficients were negative. Sodium-cooled fast reactor using the fuel of composition of Pu in a large size core always have a positive sodium void effect. However, MESOF showed negative values. The reactivity control system showed large shutdown margin under all possible requirements with uncertainty penalties. There must be a detail design works with transport code for the preliminary core design. The results of this study showed there would be no significant problems except fine tuning design and design optimizations.

REFERENCES

[1] Personal Communication with Dr. Yeong-Il Kim, KAERI, Korea (2011)

[2] Personal Communication with Dr. Dong-Wook Cheong, NRF, Korea (2011)

[3] Fast Reactor Database 2006 Update, IAEA-TECDOC-1531, International Atomic Energy Agency (2006)

[4] Allen. K., et al., “Benchmark of Advanced Burner Test Reactor model using MCNPX 2.6.0 and ERANOS 2.1,” Progress in Nuclear Energy (2011)

[5] R. E. MacFarlane, "TRANSX 2: A Code for Interfacing MATXS Cross-Section Libraries to Nuclear Transport codes," LA-12312-MS, Los Alamos National Laboratory, NM, USA (1992)

[6] R. E. Alcouffe, et. al., "DANTSYS: A Diffusion Accelerated Neutral Particle Transport Code System," LA-12969-M, Los Alamos National Laboratory, NM, USA (1995)

[7] B. J. Toppel, "A users guide for the REBUS-3 fuel cycle analysis capability," ANL-83-2, Argonne National Laboratory, IL, USA (1983)

[8] J. D. Kim, C. S. Gil, "KAFAX-F22: Development and Benchmark of Multi-Group Library for Fast Reactor Using JEF-2.2-Neutron 80 Group and Photon 24 Group," KAERI/TR-842/97, Korea Atomic Energy Research Institute, Daejeon, Korea (1997)

[9] Jae-Yong Lim, Myung-Hyun Kim, "A New LFR Design Concept for Effective TRU Transmutation" Progress in Nuclear Energy, Vol.49, No.3, pp.230-245, April, (2007)

[10] E. A. Hoffman, W.S. Yang, and R.N. Hill, “Preliminary Core Design Studies for the Advanced Burner Reactor over a Wide Range of Conversion Ratios,” ANL-AFCI-177, Argonne National Laboratory (2006)

[11] D.C. Crawford, D.L. Porter, S.L. Hayes , “Fuels for sodium-cooled fast reactors: US perspective,” Journal of Nuclear Materials, Vol.371, pp.202-231, (2007)

Core Design Study of Ultra-Long Cycle Fast Reactor Concept

T. Tak[a], **D. Lee**[a], **T. K. Kim**[b]

[a] Ulsan National Institute of Science and Technology, Ulsan, Republic of Korea

[b] Argonne National Laboratory, Argonne IL, USA

Abstract. New designs of ultra-long cycle fast reactor with power ratings of 1000 MWe and 100 MWe (UCFR-1000 and UCFR-100) have been developed based on breed-and burn strategy. Low enriched uranium (~12.3 %) in the core bottom region plays a role of igniter. Fertile materials in the core upper region act as a blanket for breeding and the active core moves upward as the core burns. Natural uranium and pressurized light water reactor (PWR) spent fuel were used as the blanket materials in order to improve fuel utilization and mitigate the nuclear proliferation issues especially in Korea where the reprocessing of spent fuels is not allowed. HT-9 and sodium were used as structure and coolant materials, respectively, and metallic form was adopted for fuel. The design of UCFR-100 has advantages in terms of lower local power peaking, fuel/clad temperature, and peak fluence of high energy neutron. The core design study and performance evaluation were performed using a Monte Carlo code, McCARD, and it was confirmed that the 60-year operations of the UCFRs without refueling are feasible.

1. Introduction

The Ultra-long Cycle Fast Reactor (UCFR) concepts have been developed since it was introduced in 1950s and it is being actively investigated recently as a mean to improve uranium utilization and solve the nuclear proliferation issues [1-11]. Advanced materials for shielding, cladding, and structure are also under development to increase the fuel discharge burnup and thermal efficiency at high operating temperature [12]. Authors presented the 1000 MWe UCFR (UCFR-1000) design using U-10Zr metallic fuel in 2012 [13] and this paper presents further study since then on the nuclide conversion, shutdown margin (SDM) analysis, and incorporation of feedback from UCFR-1000 thermal hydraulic analysis [14]. The U-10Zr binary metallic fuel has inherent safety features proven in EBR-II [15], favorable behavior for a long refueling interval, and rapid deployment. In this paper, UCFR-1000 was designed with PWR spent fuel (SF), which could be one way to solve the issue of permanet spent fuel storage facility in Korea.

For the UCFR design, a core conversion ratio needs to be high and the fuel volume fraction is about 40~60 % of the core, which is relatively high comparing with conventional fast reactor design [16]. And it was investigated that the high reactor power rating combined with high axial peaking in UCFR-1000 could cause a very high local power and consequently violate the temperature limits of fuel and clad regions [17]. Another issue in the UCFR-1000 design was the high fast neutron fluence which violated the current irradiation experience of HT-9 clad. Hence, this paper also includes a new core design of small-size UCFR with the power rating of 100 MWe (UCFR-100), which was developed with an intention to lower the temperatures in the fuel region and the neutron fluence in the clad.

In this paper, a reactor core design study has been performed under the following conditions: liquid sodium cooled UCFR, tall and large core diameter for UCFR-1000, short and small diameter for UCFR-100, high temperature, and high fuel volume ratio. Many aspects of core design have been investigated and the core design and performance evaluation were performed by the Monte Carlo depletion code, McCARD [18].

2. Core Design of UCFR

In the following sections, core design requirements and key parameters for UCFRs will be presented. The detail core geomety and compositions will also be described.

2.1. Core Design Requirements and Key Parameters

Table 1 shows the primary design parameters. The design power of UCFRs are 2600 MWth/1000 MWe and 260 MWth/100 MWe and the thermal efficiency is assumed as 38.5 %. The metallic form of fuel material (SF-7Zr, U-5Zr) has been chosen due to its high thermal conductivity and liquid sodium has been chosen as coolant due to its low density.

TABLE 1. PRIMARY CORE DESIGN PARAMETER

Parameters	UCFR-1000 (NU)	UCFR-1000 (SF)	UCFR-100 (NU)
Thermal power (MWth / MWe)	2600 / 1000	2600 / 1000	260 / 100
Cycle Length (effective full power years)	60 (Once through)	60 (Once through)	60 (Once through)
Initial heavy metal loading (t)	201	216	36
Core Volume (kL)	32.1	32.1	4.6
Equivalent Core Diameter (m)	4.8	4.8	3.2
Fuel pin overall length (cm)	460	460	220
Active core height (cm)	360	360	120
Specific power density (MW/t)	12.0	12.0	7.3
Volumetric power density (W/cc)	81.0	81.0	56.7
Linear Power (W/cm)	210.0	210.0	147.0
Fuel form	U-10Zr	SF-7Zr	U-5Zr
Fuel density (g/cc)	15.98	15.91	17.38
Uranium enrichment (bottom-driver/upper-blanket) (%)	12.3 / NU	12.3 / Spent Fuel	11.55 / NU
Maximum Neutron Flux (#/cm^{2}sec)	8.8E+15	8.7E+15	1.7E+15
Fast Neutron Fluence (#$\times 10^{24}$/cm^2)	2.57	2.63	1.77
Average Coolant Velocity (m/s)	4.8	4.8	1.3
Average Discharge Burnup (GWD/t / %)	282.7 / 29.8	264.1 / 27.8	159.9 / 16.8

Since the target of this design is to achieve 60 years of operation without refueling, the breed and burn concept has been utilized along the axial direction [19, 20]. The low-enriched uranium (LEU) fuel is loaded in the lower part of the fuel region for igniting the reactor at beginning of cycle and spent fuel or natural uranium (NU) blanket is loaded in the upper part of the fuel region for completing breed-and-burn. The active core region will move from bottom to top of the fuel pin over the 60 year operation. The active core height of UCFR-1000 is 3.6 m and the core diameter was chosen to fit into core barrel diameter of 5 m including the radial reflectors of 50 cm thickness. Those of UCFR-100 are 1.2 m and 3.2 m each so that it is feasible for the core of 260 MWth to operate 60 years. The average fuel and coolant temperatures in calculation were assumed to be 900 K and 800 K, respectively.

2.2. Core Layout of UCFR

Figure 1 shows the core layout of UCFRs. There are three types of assemblies: driver assembly, control assembly, and reflector assembly. For the UCFR-1000, there are total 631 hexagonal assemblies in 15 radial rings and it consists of the fuel region of inner 12 rings and the reflector region of outer 3 rings. For UCFR-100, there are total 271 hexagonal assemblies in 10 radial rings and it consists of the fuel region of inner 8 rings and the reflector region of outer 2 rings.

There are total 19 control assemblies in UCFR-1000: 13 primary control assemblies and 6 secondary control assemblies. The number and the location of control assemblies were determined based on the evaluation of the control rod worth and shutdown margin. The control material in the primary control assemlies is natural boron and the control material in the secondary control assembly is 90 % enriched boron. In UCFR-100, there are 7 control assemblies with only natural boron.

Assemblies consist of pin, cladding, and duct. Figure 2 shows the each detail geometry of the three types of assemblies regardless of the core size. Pins are placed in hexagonal array as the assemblies in the core. The total number of pins in the fuel and reflector assembly is 91 in 7 radial rings while that of control assembly is 7 in 2 radial rings. The control assembly has double ducts and the inner one moves with the control rods together when controlling the reactivity of the core.

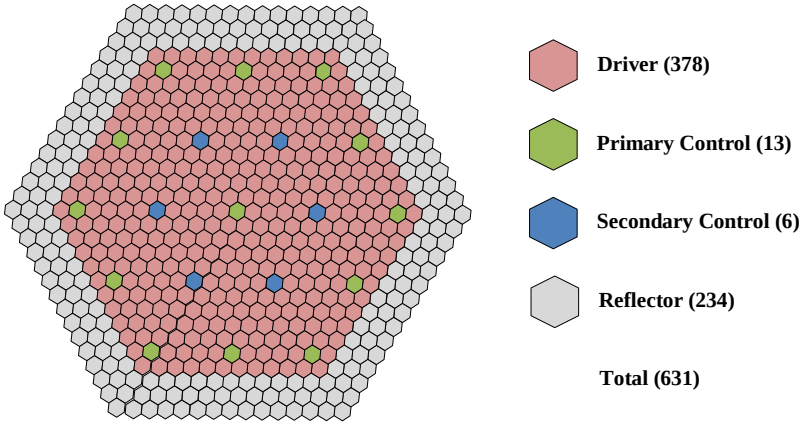

(a) UCFR-1000

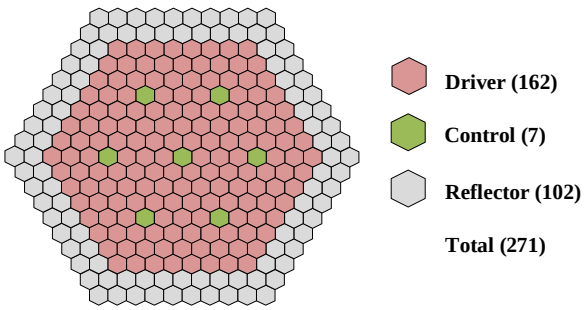

(b) UCFR-100

FIG. 1. Core layout of UCFRs.

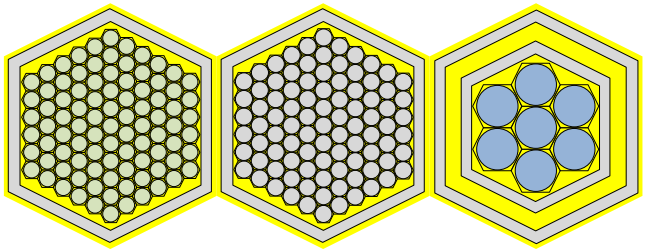

FIG. 2. Assembly geometry.

In the core design calculation of UCFR, the compositions were homogenized in each assembly based on the volume fractions. The composition variations in the axial direction of the pins are shown in Fig. 3: lower reflector, ignition zone with LEU, breeding zone with spent fuel or natural uranium and the upper reflector. The lengths of the ignition zone and the breeding zone were determined to achieve the desired cycle length of 60 years. The UCFR adopts fission gas vented fuel concept, in which the fission gases are directly released to the primary coolant during the reactor operation [21]. Due to the vented fission gas, the stresses in the cladding caused by fission gas buildups can be maintained at low level even at high burnups and the upper gas plenum region can be designed to be small size [22]. The fuel region is separated in two parts, spent fuel or natural uranium for upper part and LEU for lower part. It causes the active core movement along the axial direction from the bottom to the top gradually. The reflector and control pin has simple geometry but control pin has larger diameter.

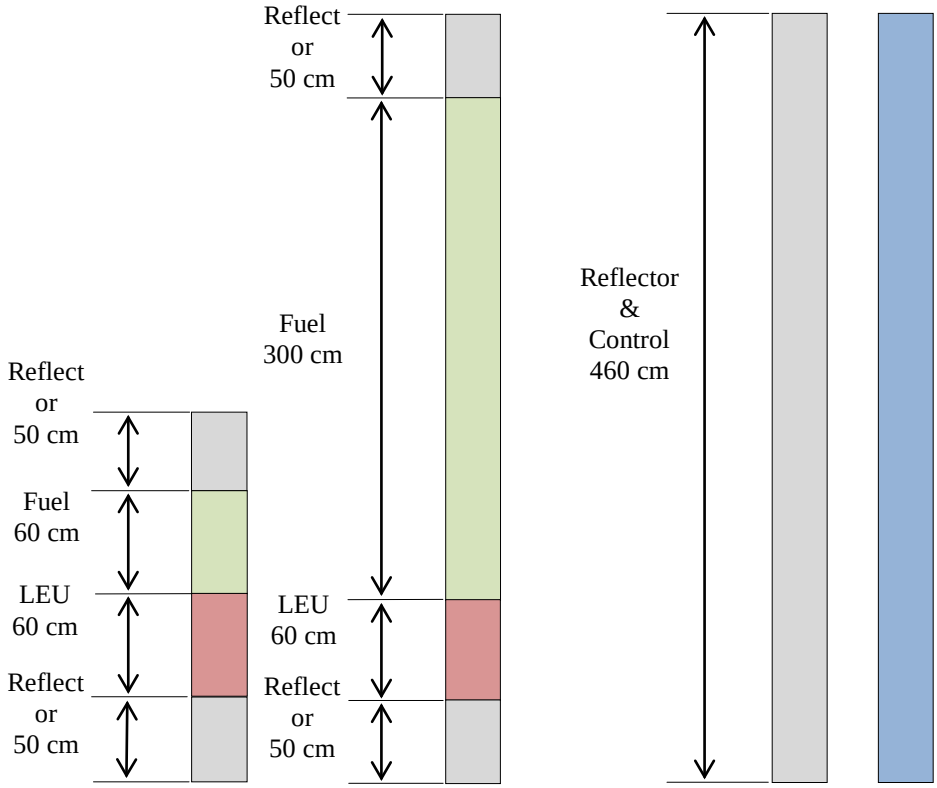

(a) Fuel pin in UCFR-100 (b) Fuel pin in UCFR-1000 (c) Reflector pin (d) Control pin

FIG. 3. Axial pin geometry.

Table 2 shows the PWR spent fuel composition which is used for the blanket in designing of UCFR. This data is result from depletion calculation by ORIGEN2 code with the assumptions: PWR discharge burnup is 50 GWD/MTU, cooling time is 10 years, No other process to change the actinide composition but fission products which has evaporation point of less than 1000 ℃ were removed [23].

TABLE 2. COMPOSITION OF PWR SPENT FUEL

Element/Isotope	wt.%	Element/Isotope	wt.%	Element/Isotope	wt.%
Ge	9.00E-05	Ba	2.47E-01	U-235	9.72E-01
Rb	1.00E-01	La	1.68E-01	U-236	5.89E-01
Sr	6.00E-02	Ce	3.22E-01	U-238	9.41E+01
Zr	5.10E-01	Pr	1.53E-01	Np-237	5.76E-02
Nb	5.50E-07	Nd	5.55E-01	Pu-238	1.94E-02
Mo	3.30E-01	Pm	1.50E-03	Pu-239	5.22E-01
Tc	1.05E-01	Sm	1.11E-01	Pu-240	2.47E-01
Ru	2.96E-01	Eu	1.71E-02	Pu-241	8.38E-02
Rh	6.00E-02	Gd	1.68E-02	Pu-242	6.27E-02
Pd	1.76E-01	Tb	3.00E-04	Pu-244	1.83E-06
Ag	9.30E-03	Dy	1.60E-04	Am-241	5.82E-02
In	3.80E-04	Ho	1.40E-05	Am-242	1.34E-02
Sn	1.10E-02	Er	3.10E-06	Am-243	1.35E-04
Sb	2.30E-03	U-234	1.95E-03	Cm-242	2.62E-07

Assembly design parameters are summarized in Table 3. The smeared density and bond parameters in the table are considered for the swelling of metal fuel due to high temperature and neutron irradiation. All the calculations in this paper are based on smeared density and volume fractions. The structure includes the duct and cladding.

TABLE 3. ASSEMBLY DESIGN PARAMETERS

	Driver (NU / SF / UCFR-100)			Reflector	Control
Assembly data					
-Number of pins	91	91	91	91	7
-Assembly pitch (cm)	16.5	16.5	16.5	16.5	16.5
-Inter-assembly gap (cm)	0.30	0.30	0.30	0.30	0.30
-Duct thickness (cm)	0.30	0.30	0.30	0.30	0.30
-Gap duct and interior duct (cm)	-	-	-	-	0.40
-Interior duct thickness (cm)	-	-	-	-	0.30
-Interior duct inside flat-to-flat (cm)	-	-	-	-	14.2

Pin data					
-Pin material and type	U-10Zr	SF-7Zr	U-5Zr	HT-9	B_4C
-Bond material	Na	Na	Na	-	He
-Active core height (cm)	360	360	120	-	-
-Smeared density (% TD)	74.5	74.5	75.8	-	84.3
-Cladding material	HT-9	HT-9	HT-9	-	HT-9
-Clad outer diameter (cm)	1.49	1.49	1.55	1.611	5.01
-Pin pitch-to-diameter ratio	1.075	1.075	1.038	-	1.028
-Cladding thickness (cm)	0.050	0.050	0.040	-	0.070
-Bond thickness (cm)	0.095	0.095	0.095	-	0.2
Volume fraction at fabrication (%)					
-Fuel or Absorber	43.7	43.7	49.7	-	46.6
-Bond	14.9	14.9	15.8	-	8.7
-Structure	15.7	15.7	14.3	85.7	16.6
-Coolant	25.7	25.7	20.2	14.3	28.1

3. Performance Evaluation of UCFR

The calculation methods and performance evaluation of UCFR will be presented in this chapter.

3.1. Computation Methods

The core design computations for this study were done using the McCARD code, which solves a continuous energy neutron transport equation based on Monte Carlo method. This code was written in C++ language and designed exclusively for neutronics analysis of multiplying media like fuel pins, fuel assemblies, and reactors. The code can handle arbitrary geometry by dividing it into three-dimensional unit cells that are defined using surfaces such as planes, cylinders and spheres.

Because McCARD is also designed for the depletion analysis of nuclear power reactors, it has built-in subroutines to solve the depletion equation while other Monte Carlo depletion codes need to couple with external depletion analysis codes. The depletion analysis capability can be activated simply by declaring burnup cell and then the code automatically generates burnup tallies.

McCARD code was validated using various benchmarks in the ICSBEP [24] which includes from thermal spectrum to fast spectrum critical experiments fueled with U and/or Pu fissile materials. The depletion capability of the code was validated with comparison against well-known burnup codes such as CASMO [25], HELIOS [26], and MVP-BURN [27][28].

3.2. Depletion Performance of UCFR

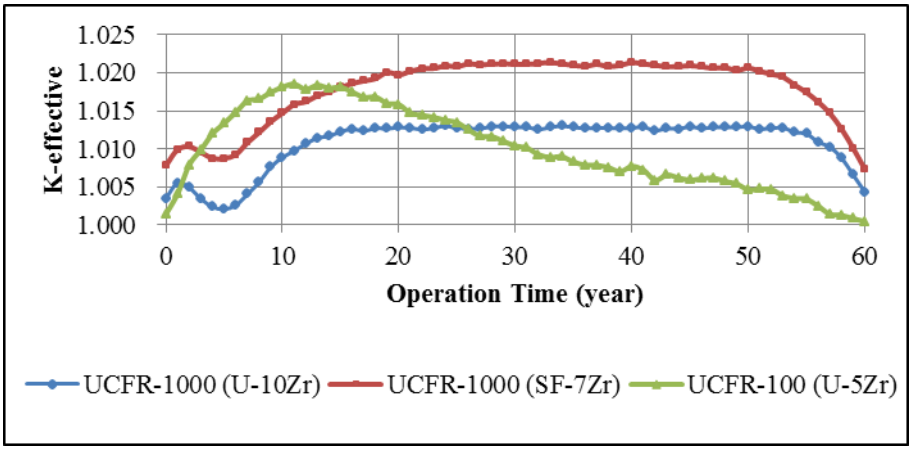

FIG. 4. k-effective vs. time.

Figure 4 shows the multiplication factors behavior over the depletion. All calculation in this paper used the following conditions: 1) all control rods out (ARO) state, 2) the depletion calculation step size is 1 year, and 3) the number of neutron histories is chosen such that the average standard deviation of all the steps is about 10 pcm. One can notice that the fluctuations of k-effective over the depletion can be decereased by using more neutron histories in each MC calculations, which implies the k-effective fluctuations over the depletion is caused by the statistical nature of the MC calculations.

It is noted that the core can maintain criticality for 60 years with full power rating with the discharge burnup of 264 GWd/t (27.8 %) and 160 GWd/t (16.8 %) for each. Overall, the multiplication factors are between 1.000 and 1.025 and the difference between the maximum value and the minimum value is about 1500 pcm. From several trials for adjusting core parameters, it was noted that the initial k-effective value and the slope of k-effective change in the initial 15 years of the core depletion could be controlled by adjusting the enrichment and/or height of LEU region.

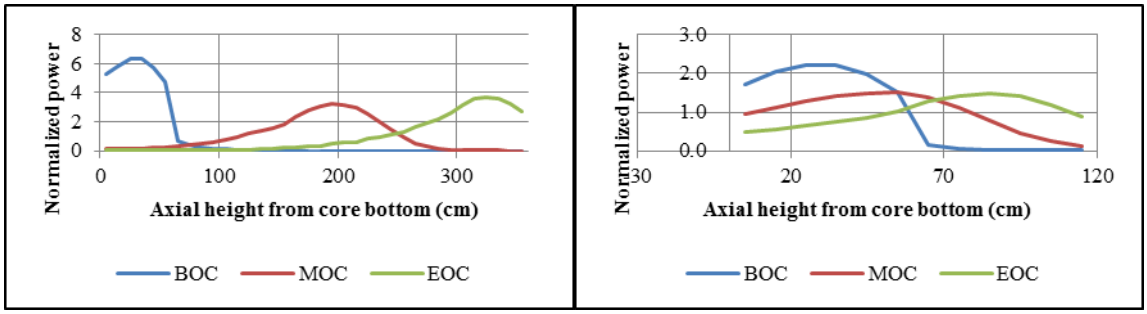

(a) UCFR-1000 (SF-7Zr) (b) UCFR-100

FIG. 5. Normalized axial power distribution.

Figure 5 presents normalized core axial power distributions in the beginning of cycle (BOC), middle of cycle (MOC), and end of cycle (EOC) of 60 year operation of UCFR. Axial mesh size of 10 cm was used for the core depletion calculation and axial power tallies. As shown in the figure, the active core

region is moving from the bottom to the top of the core as the core burns. At BOC, most fission reactions occur at the bottom LEU region due to the uranium enriched up to 12.3 w/o or 11.55 w/o. This LEU region is acting as an igniter of UCFR. While the bottom region is burning, the blanket region right above the LEU region breeds and eventually the active core region moves upwards in the core. The speeds of the axial movement of active core were measured to be 4.8 cm/year and 1.0 cm/year for each.

3.3. Kinetics Parameters and Reactivity Feedback Coefficients

Table 4 and Table 5 summarizes the core analysis parameters of UCFR-1000 and UCFR-100. The delayed neutron fraction at BOC is about 700 pcm and it decreases at MOC and EOC as TRU bulids up. As the core burns, the total control worth does not vary much in terms of pcm but it increases significantly in terms of dollar due to the decreased delayed neutron fractions. It is also confirmed that the control rod worth satisfies the required shutdown margin of the reactor. Reactivity parameters such as isothermal temperature coefficient (ITC), fuel temperature coefficient (FTC) are also summarized in the table. This is a synthetic effect of relatively large leakage at BOC and decrease of delayed neutron fraction. The fast neutron fluence (E > 0.1 MeV) was calculated to be 2.63 E+24/ cm^2 and 1.77 E+24/cm^2. Further study of power flattening by introducing another fuel type [29]. or shortening of refueling period could help reduce the fast fluence.

TABLE 4. SUMMARY OF UCFR-1000 PARAMETERS (NU)

Coefficients	Values(BOC/MOC/EOC)		
Leakage (%)	18.5	5.1	13.8
Delayed neutron fraction(beta) (pcm)	711	359	353
Total rod worth ($)	8.9	17.1	16.9
ITC (pcm/K)	-0.20	-0.81	-0.68
FTC (pcm/K)	-0.22	-0.48	-0.54
Peak fulence (10^{24} neutrons/cm^2)		2.63	

TABLE 5. SUMMARY OF UCFR-100 PARAMETERS (NU)

Coefficients	Values (BOC/MOC/EOC)		
Leakage (%)	19.8	17.2	20.2
Delayed neutron fraction(beta) (pcm)	708	434	377
Total rod worth ($)	8.1	13.3	15.1
ITC (pcm/K)	0.14	-1.18	-0.85
FTC (pcm/K)	0.15	-0.90	-0.83
Peak fluence (10^24 neutrons/cm^2)		1.77	

4. Conclusions

The design of UCFR has been developed to achieve the goal of 60-year full power operation without refueling during the core lifetime. The reactor power is 2600 MWth/1000 MWe for UCFR-1000 and 260 MWth/100 MWe for UCFR-100 and the thermal efficiency is 38.5 %. The active core is 3.6 m tall and the core diameter is 4.8 m including reflectors for UCFR-1000, while those of UCFR-100 are 1.2 m tall and 3.2 m.

The core depletion calculation using McCARD code confirms that 60 years of full power operation without refueling is feasible with respect to nuclear isotopics and criticality. This core utilize breed-and-burn concept along the axial direction. The evaluated core characteristics such as power feedback coefficient, power peaking factor, and multiplication factors show that the concept is implemented successfully. The active core region travels along the axial direction at the speed of 4.8 cm/year and the average core discharge burnup is 264 GWd/t for UCFR-1000 and those of UCFR-100 are 1.0 cm/year and 160 GWd/t. One of the advantages of UCFR relative to the other FBR designs is the complete avoidance of a nuclear fuel reprocessing and recycling industry for the reprocessing and recycling of spent FBR fuel. Kinetics parameters and reactivity feedback coefficients were evaluated. UCFR-100 has been developed to achieve lower the temperature and flux peaking. The core height decreased from 3.6 m to 1.2 m and therefore the axial power peaking factor was also decreased from 6.6 to 2.2. The peak fluence of fast neutron also decreased from 2.63 E+24/cm^2 to 1.77 E+24/cm^2 but it still higher than the HT-9 irradiation experience of ~4 E+23/cm^2. A safety analysis for a new design is required to confirm that the temperature limits are satisfied.

ACKNOWLEDGEMENTS

This research was supported by National Nuclear R&D Program through the National Reserch Foundation of Korea (NRF) funded by the Ministry of Education, Science and Technology.

REFERENCES

[1] T. KIM, T. TAIWO, “Feasibility Study of Ultra-long Life Fast Reactor Core Concept,” PHYSOR 2010, May 9-14 (2010).
[2] H. SEKIMOTO, K. RYU, Y. YOSHIMURA, “CANDLE: The New Burnup Strategy,” Nucl. Sci. Eng., 139, pp.306-317 (2001).
[3] T. ELLIS, et al., “Traveling-Wave Reactors: A truly Sustainable and Full–Scale Resouce for Global Energy Needs,” ICAPP 2010, San diego, CA, USA, June 13-17 (2010).
[4] C. AHLFELD, et al., “Conceptual Design of a 500 MWe Traveling Wave Demonstration Reactor Plant,” ICAPP 2011, Nice, France, May 2-5 (2011).
[5] N. UEDA, et al., “Sodium Cooled Small Fast Long-life Reactor “4S”,” Prog. Nucl. Energy, 47, No. 1-4, pp.222-230 (2005).
[6] N. UEDA, et al., “Current Design Status of Sodium Cooled Super-Safe, Small and Simple Reactor,” ICONE 10, Arlingon, VA, April 14-18 (2002).
[7] T. KIM, C. GRANDY, R. HILL, “A 100MWe Advanced Sodium-Cooled Fast Reactor Core Concept,” PHYSOR 2012, April 15-20 (2012).
[8] E. TELLER, et al., “Completely Automated Nuclear Reators for Long-term Operation II,” Proc. Int. Conf. Engineering Nuclear Energy Systems (ICENES’96), Obninsk, Russsia (1996).
[9] A. WRIGHT, et al., “Development of Advanced Ultra-High Burnup SFR Metallic Fuel Concept – project Overviw,” Nuclear Fuels and Structural Materials for the Next Generation Nuclear Reactors, Chicago, USA, June 24-28 (2012).
[10] T. TAIWO, T. KIM, “Fuel Cycle Performance Characteristics of Advanced Once-Through Nuclear Energy Systems,” ICAPP 2011, Nice, France, May 2-5 (2011).
[11] W. S. YANG, et al., “Neutronics Modeling and Simulation of SHARP for Fast Reactor Analysis,” Nucl. Eng. Technol., 42, No.5, pp.520-545 (2010).W. S. YANG, “Fast Reactor Physics and Computational Methods,” Nucl. Eng. Technol., 44, No.2, pp.177-198 (2012).
[12] FAST REACTOR DATABASE, IAEA-TECDOC-866, IAEA (1996).
[13] TAE WOO TAK, HWANYEAL YU, JI HYUN KIM, DEOKJUNG LEE, “Preliminary Design of Ultra-long Cycle Fast Reactor Employing Breed-and-burn Strategy,” PHYSOR 2012, Knoxville, USA, April 15-20 (2012).
[14] TAEWOO TAK, DEOKJUNG LEE, “Design of Ultra-long Cycle Fast Reactor Emplying

Breed-and-burn Strategy," to appear in Nucl. Technol., (2013)
[15] S. FISTEDIS, "The Experimental Breeder Reactor – II Inherent Safety Demonstration," Nucl. Eng. Des., 101, pp.1 (1987).
[16] W. S. YANG, "Fast Reactor Physics and Computational Methods," Nucl. Eng. Technol., 44, No.2, pp.177-198 (2012).
[17] H. SEO, S. KANG, I. BANG, "Safety evaluation of UCFR-1000 MWe with MATRA-LMR," Trans. Kor. Nucl. Soc. (2012).
[18] H. SHIM, C. KIM, "MCCARD user's manual," Version 1.0, Nuclear Design and Analysis Laboratory, Seoul National University (2010).
[19] A. NAGATA, N. TAKAKI, H. SEKIMOTO, "A feasible core design of lead bismuth eutectic cooled CANDLE fast reactor," Ann. Nucl. Energy, 36, pp.562-566 (2009).
[20] H. SEKIMOTO, S. MIYASHITA, "Startup of "CANDLE" burnup in fast reactor from enriched uranium core", Energy Convers. Manage., 47, pp.2772-2780 (2006).
[21] T. KIM, C. GRANDY, "Assessment of Fission Gas Vented Fuel Impact with Advanced Burner Reactor," PHYSOR 2010, May 9-14 (2010).
[22] W. BECK, R. FOUSEK, J. KITTEL, "The Irradiation Behavior of High-Burnup Uranium-Plutonium Alloy Prototype Fuel Elements," ANL-7388, May (1968).
[23] YONGHEE KIM, "Semi-direct Recycling of LWR Spent Fuel in Ultra-long-life Core Fast Reactor," ANS Winter Meeting, Las Vegas, USA (2010).
[24] "INTERNATIONAL HANDBOOK OF EVALUATED CRITICALITY SAFETY BENCHMARK EXPERIMENTS," NEA/NSC/DOC(95)03, OECD Nuclear Energy (2006).
[25] M. EDENIUS, B. H. FORRSEN, "CASMO-3 A Fuel Assembly Burnup Program User's Manual," Studsvik/NFA-89-3, Rev. 2, Studsvik AB (1992).
[26] R. J. J. STAMM'LER, "HELIOS Methods," Studsvik Scanpower (2002).
[27] K. OKUMURA, et al., "Validation of a Continuous-Energy Monte Carlo Burn-up Code MVP-BURN and Its Application to Analysis of Post Irradiation Experiment," J. Nucl. Sci. Technol., 37, 128 (2000).
[28] H. SHIM, et al., "MCCARD: Monte Carlo Code for Advanced Reactor Design and Analysis," Nucl. Eng. Technol., 44, No.2, pp.161-176 (2012).
[29] H. SEKIMOTO, et al., "Power Flattening for CANDLE Fast Reactor by Adding Thorium in Inner Core," ICAPP 2010, San Diego, CA, USA, June 13-17 (2010).

Physics Design and Safety Studies of a 320 MWt Experimental Metal FBR

K. Devan, Debanwita Paul, Abhitab Bachchan, A. Riyas, T. Sathiyasheela, P. Puthiyavinayagam, P. Chellapandi and S. C. Chetal

Indira Gandhi Centre for Atomic Research,
Kalpakkam, India

Abstract. *Fast reactors play a major role in the sustained growth of nuclear power in India. Metal fuelled fast reactors with high breeding ratio are essential to meet the rapid growth rate of energy demand. Several R&D programs have been initiated at IGCAR for establishing this technology with closed metal fuel cycle. Construction of a Metal Fuel Test Reactor (MFTR) at IGCAR has been planned to enable full-scale experimental testing of fuel sub-assemblies of a typical commercial power reactors before their launching. With the availability of MFTR, it is possible to experimentally validate various core physics design parameters of metal fuels. There would be a co-located pyro-reprocessing plant to demonstrate closing the fuel cycle. The discharged fuel from MFTR will be recycled after reprocessing and fuel fabrication. It is, therefore, desirable to have high burnup for mastering reprocessing of high burnup metal fuel sub-assemblies. MFTR will also be used to produce radio isotopes for medical applications and also for the development. Irradiation experiments towards validation of new fuel and structural materials, capable of achieving higher burnup and doses, are also planned in MFTR. In order to meet these objectives, the physics design of a MFTR core with breeding ratio ~1.1 is performed using sodium bonded ternary fuel (U-Pu-6%Zr). Core height is fixed to be 1000 mm. Design is performed to achieve a peak linear heat rating (LHR) of 450 W/cm and peak burnup of 150 GWd/t. Minimum power level satisfying the above requirements is found to be 320 MWt. Salient features of this core is discussed in this paper.*

1. INTRODUCTION

Fast reactors play a major role in the sustained growth of nuclear power in India. To meet the growing demand for electricity in India, studies [1] have shown that the share of nuclear power has to be increased from the current 3 % to 20 % by the year 2050. It is possible through the introduction of 1000 MWe metal FBRs with higher breeding ratio beyond 2025. Several R&D programs have been initiated at IGCAR for establishing the technology of closed metal fuel cycle with emphasis on fuel fabrication and reprocessing. Irradiation of metallic fuel pins and testing of metal fuel sub-assemblies (SAs) are planned in FBTR. Irradiation experiments of sodium bonded U-Zr alloy pins are already started in FBTR. Since FBTR has smaller core height, it is impossible to test SAs having 1000 mm fuel column. It is therefore planned [2] to construct a Metal Fuel Test Reactor (MFTR) at IGCAR to enable full-scale experimental testing of fuel sub-assemblies before launching commercial metal FBRs. It is realized that after FBTR, this facility would form the back bone of all R&D activities related to irradiation at IGCAR. In this paper, we discuss about the objectives of MFTR and the physics design of its core. It is to be noted that the MFTR core presented in this paper is only a

preliminary design. The final optimized core will be arrived at after taking into account all the design aspects including reactor safety.

2. PHYSICS DESIGN OF MFTR

2.1 The objectives of MFTR

The main objecive of MFTR [3] is to provide full-scale testing of metal fuel SAs of a typical commercial power reactors in a closed fuel cycle mode. The fuel column should be of 1000 mm with a linerar heat rating of 450 W/cm. It has to be a marginal breeder to enable fuel sustainability. In addition, MFTR has the following other objectives:

- To validate the reactor physics parameters of metal fuel.
- Demonstrating the safe operation of metal FBRs in closed fuel cycle mode.
- Mastering the industrial scale manufacture and re-processing of metal fuel SAs as a forerunner of large size metal FBRs.
- A facility for material irradiation for developing advanced fuels and structural materials for future reactors.
- A facility for production of radio isotpes for medical applications.

The MFTR is desired to to have the minimum thermal power for meeting all its objectives.

2.2 Design requirements

Following are the design requirements for the MFTR core:

- Minimum reactor thermal power.
- Relatively low critical mass for Pu.
- Marginal breeder to meet its own fuel requirements.
- Peak LHR of 450 W/cm at all time of irradiation.
- Single fuel enrichment.
- Hexcan size and clad diameter same as that of PFBR.
- Fuel column height of 1000 mm.
- Peak burnup of 150 GWd/t
- 6 CSRs and 3 DSRs
- 3 experimental locations
- Special experimental central assembly.

2.3 Design criteria

The design of a fast reactor core involves the optimization of various core parameters, viz. plutonium enrichment, power, LHR, burnup, cycle length, breeding ratio, absorber rod worth, sodium void coefficient etc. It is often difficult to achieve the optimum value for all the above parameters because they are, in general, inter-dependent. A series of neutronics calculations have to be performed in an iterative manner to arrive at an optimized core configuration.

The shutdown system contains two independent and diverse systems, namely CSR and DSR. The CSR system is used for reactor start up, control of reactor power, controlled shutdown and SCRAM of the reactor. The DSR system is not used for any reactivity control and is used only to SCRAM the reactor. The rods in DSR system are in fully raised position during reactor operation. The number of absorber rods and their location in the core are decided to provide the safe shutdown of the reactor during normal and accidental conditions.

Based on EBR-II irradiation experiments [4-6], a lower limit of 23 % plutonium is chosen for the ternary fuel (U-Pu-Zr). Recent neutronics studies by Riyas and Mohanakrishnan [7] have shown that breeding ratio increases by reducing Zr content and an optimum value of 6 wt %Zr is reccommended

for Indian nuclear power programme with the objective of higher breeding ratio. Fuel enrichment is adjusted to obtain peak LHR of 450 W/cm. The cycle length is fixed in the range of 300 effective full power days (efpd) such that peak burnup of 150 GWd/t is achieved. The excess reactivity of the core is adjusted to obtain the above cycle length.

2.4 Design data

Engineering design involves in sizing of sodium bonded fuel pin satisfying the given set of conditions:

a) Fuel centre temperature with all uncertainties shall not exceed its melting point at 115 % of the operating power (Over Power Margin (OPM)- 15%).
b) Clad inside temperature shall be less than 923 K (650°C) under hotspot condition.
c) Sodium temperature shall be less than its boiling point.
d) CDF limit is restricted to 0.25.

Design shall be such that the fuel shall always remain covered with sodium during its life and the Fission gas plenum length shall be sufficient to accommodate fuel swelling and sodium expelled for the target burnup. The diameter of fuel pin is maintained at 6.6 mm with thickness of 0.45 mm. To avoid lower temperature eutectic between fuel and the clad, modified 9Cr- 1Mo, T91 steel is selected as the clad material. The fuel smeared density is kept < 75 % of TD to avoid FCMI and to allow sodium infiltration into the fuel which helps in increasing the thermal conductivity of fuel. Fabricated fuel slug diameter is 4.90 $\pm$ 0.06 mm. The active core length is designed as 1000 mm. Since the commercial MFBRs are likely to have 1 m length active core, it is decided to test its behavior and fabrication feasibility in MFTR. To study the breeding potential, U- 6Zr, blanket slug with smeared density of 85 % TD is provided on either side of fuel column to a length of 300 mm each. A typical fuel pin is shown in Fig. 1. Fuel pin length is ~ 3260 mm. 217 pins would be arranged in a triangular pitch inside the hexcan made of modified 9Cr-1Mo (T91) material with width across flat of 131.3 mm and thickness 3.2 mm. The geometrical data of pin and SA are similar to that of PFBR (Table 1). The fuel slug is put inside a modified 9 Cr-1Mo steel (T91) clad of 6.6 mm outer diameter. The fuel expansion coefficient used is 1.905×10^{-5}/K. The core inlet and outlet sodium temperatures are 370 and 510 °C respectively. Clad mid wall mean temperature is limited to 650 °C during normal operation. The average fuel temperature considered is 750 °C, whereas it is 440 °C for both coolant and structural materials.

TABLE 1. Geometrical data of fuel and blanket sub-sssemblies

Parameters	Fuel	Radial Blanket
Fuel pin diameter (mm)	6.6	14.33
Fuel column length (mm)	1000	1600
Clad thickness (mm)	0.45	0.60
Sub-assembly pitch (mm)	135	135
Pins per sub-assembly	217	61
Spacer wire diameter (mm)	1.65	1.2
Hexcan width across flats/thickness (mm)	131.3 /3.2	131.3 /3.2

2.5 Method of calculations

The European Reactor Analysis Optimized calculation system called ERANOS [8] is used for the most of the calculations. The ERANOS 2.1, available at IGCAR, contains cross section libraries based on JEF-2.2, JEFF-3.1 and ENDF/B-VI. It also contains various procedures for the reference and design calculations of Liquid Metal Fast Reactor cores, with extended capabilities for Generation-IV type advanced fast reactors, Accelerator Driven Systems and Gas Cooled Fast Reactors. The cross

section libraries were available in different energy group structures for various applications. For fast reactor applications, 33-group library is provided for all the important nuclides. A fine group library in 1968 group structure is also available for 37 nuclides of interest to fast reactors. There are libraries in 172 and 175 energy group structures for thermal spectrum and shielding applications. Figure 2 gives the flowchart of calculations with ERANOS 2.1 system at IGCAR. The ECCOLIB library based on JEFF3.1 is used for the core calculations. The cell code ECCO is used to prepare the homogenized cross sections. It uses the subgroup method to account the resonance self-shielding effects. The preparation of cross sections for the absorber rod requires a special treatment due to very high coupling of heterogeneous absorber rod to the surrounding core cells. The method used is called the reactivity equivalence method, developed by Rowland and Eaton in 1978. Based on this method, there is a special procedure available in ERANOS 2.1 to homogenize the absorber rod cross sections which uses 2-D S_n transport theory code BISTRO and its associated perturbation modules. Three dimensional diffusion theory calculations are done for estimating the core physics parameters. To estimate the temperature and power coefficients, PREDIS [9] code is used.

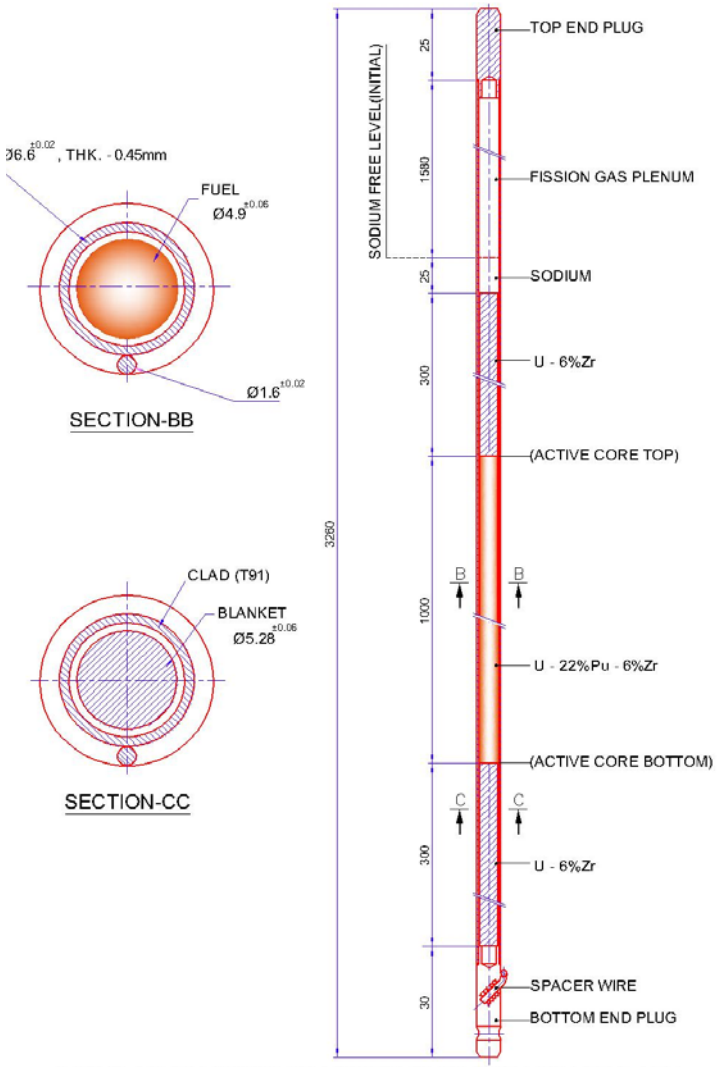

FIG.1. Sodium bonded fuel pin of MFTR

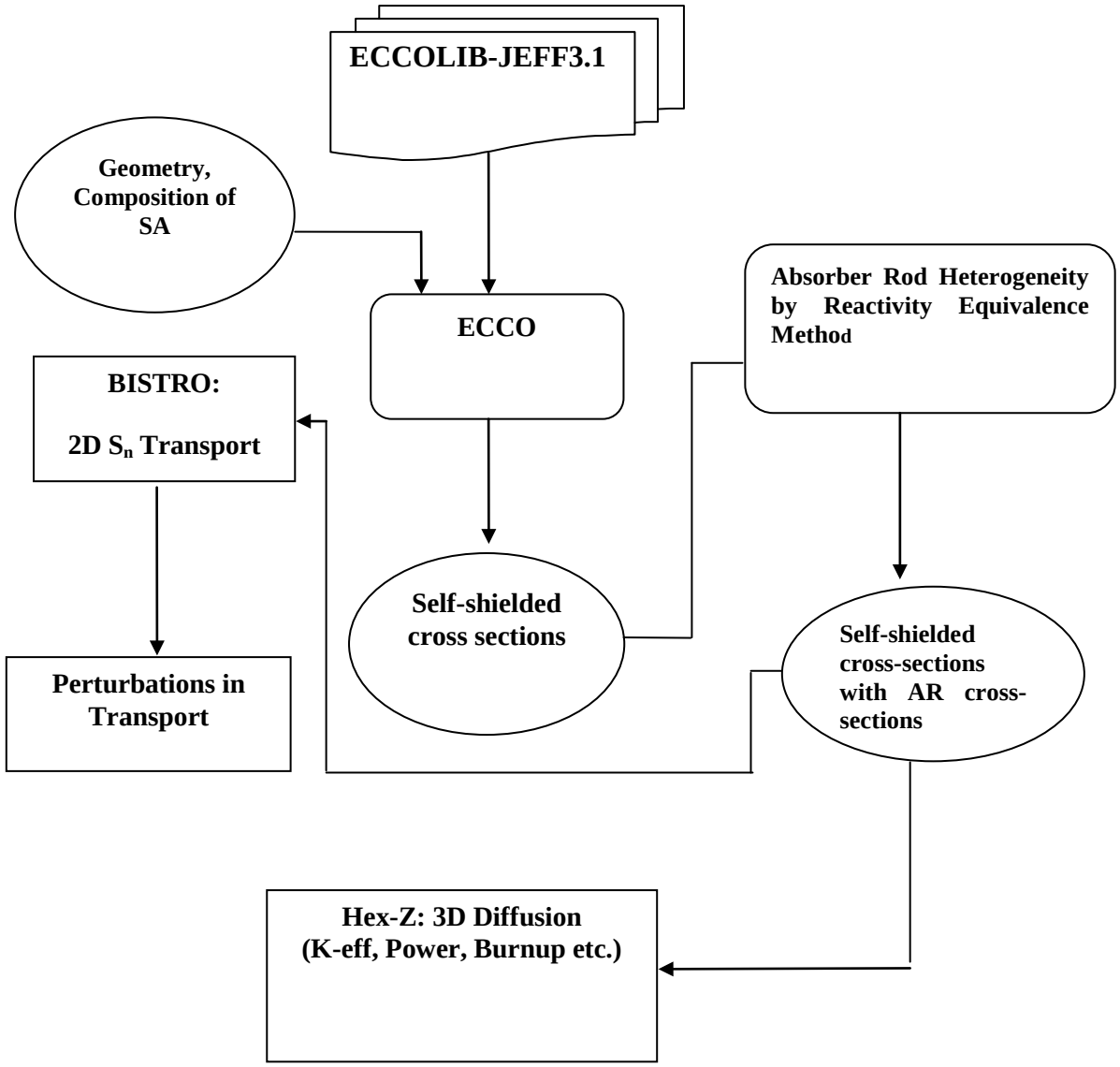

FIG.2. Flowchart of FBR core calculations with ERANOS 2.1 system

2.6 MFTR core

The minimum power of the core, satisfying all the designobjectives, is 320 MWt. An optimum core is arrived at with 60 fuel and 42 radial blanket SAs. The central location is reserved for a special assembly with 180 fuel pins to be utilized for irradiation experiments besides three other experimental locations in the fourth ring. There are 6 CSRs, 3 DSRs and 102 steel reflector SAs. The worth of absorber rods are not optimised. MFTR core is shown in Fig. 3. Plutonium enrichment is optimized as 21 %. The excess reactivity of the core is computed by taking into account the reactivity loses during reactor operation.

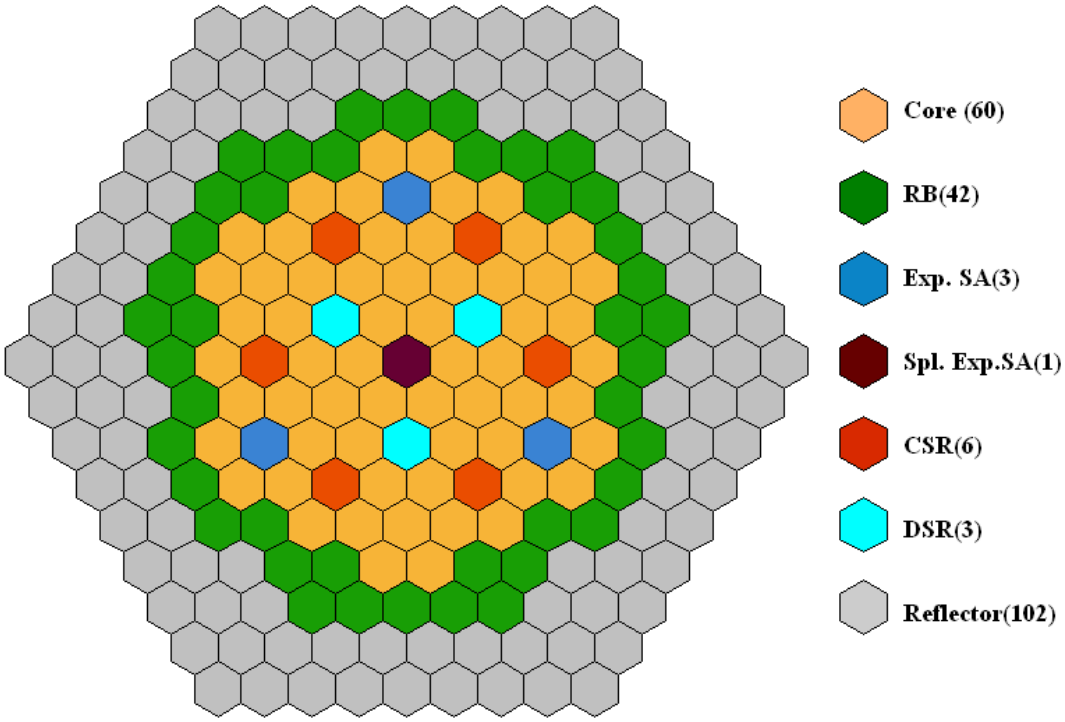

FIG.3. MFTR Core Configuration (Total Power 320 MWt)

TABLE. 2. Summary of MFTR core characteristics

Parameters	Value
Power (MWt)	320
Fuel	U-Pu-6 % Zr alloy
Fuel density (g/cm^3)	17.1 at 20 °C
No. of core zones	1
Pu enrichment (%)	21
Cycle length (days)	300
No. of batches	3
No. of blanket SA	42
No. of CSR/DSR	6/3
B_4C enrichment (%): CSR/DSR	Not optimised
No. of reflector SA	102
No. of experimental locations	4
Breeding ratio	1.12
Average core centre flux	4.5×10^{15} n/cm^2/s

The SA-wise power and LHR are given in Figs. 4 and 5 respectively. Fig. 6 gives the peak burnup after 3 cycles (1 cycle equals 300 efpd). The SA-wise neutron flux distribution is given in Fig.7. Average neutron flux at the central SA is 4.5×10^{15} n/cm^2/s, whereas it is about 1.7×10^{15} n/cm^2/s at the core boundary. The average neutron flux levels at the experimental locations is 2×10^{15} n/cm^2/s.

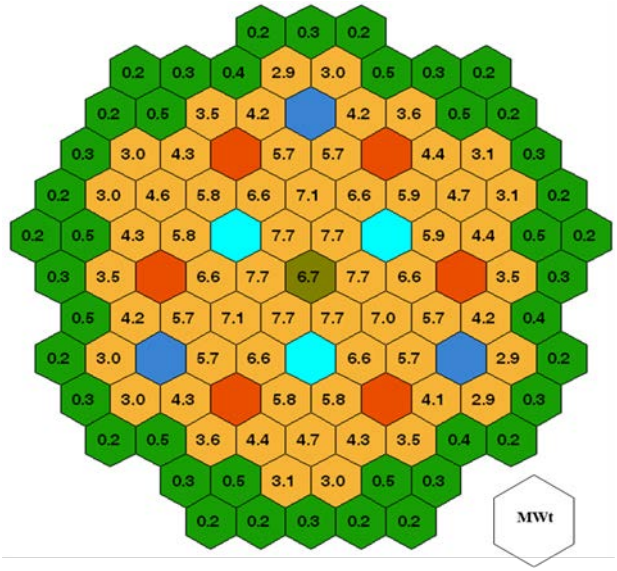

FIG.4. SA power of MFTR (all rods up)

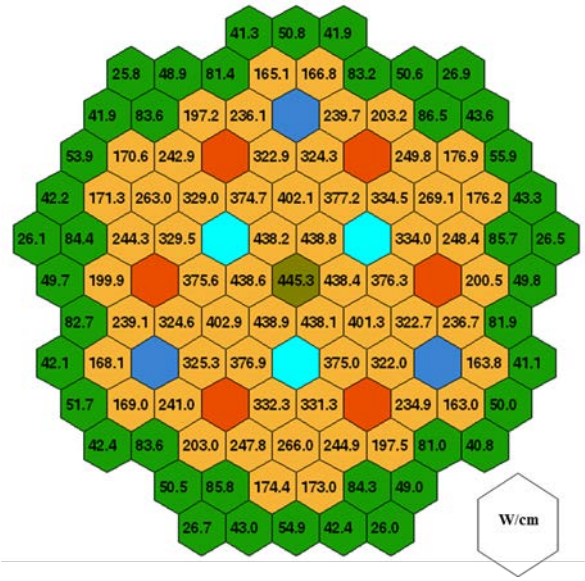

FIG.5: SA peak LHR of MFTR (all rods up)

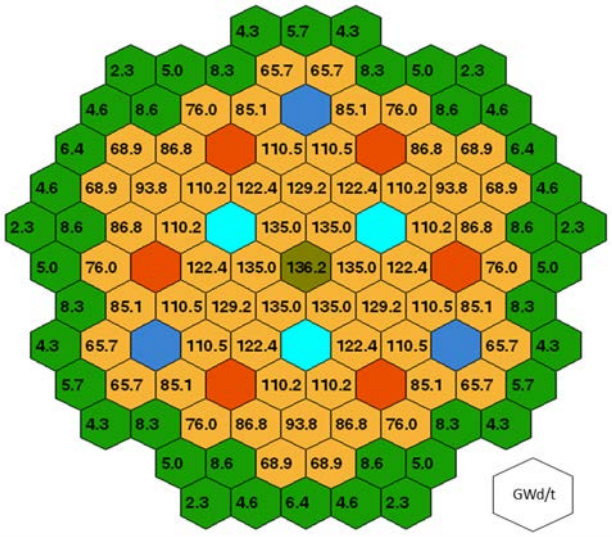

FIG.6. Peak burnup after 3 cycles

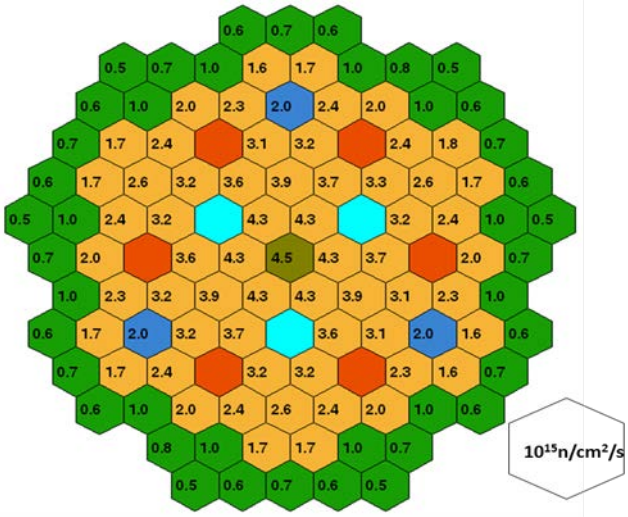

FIG.7. SA neutron flux of MFTR

The structural damage caused by the neutron fluence, ie. displacement per atom (dpa), is given in Fig. 8 for one cycle (300 efpd) of operation. The 33-group dpa cross sections of Fe based on NRT model is used for this study. It is seen that core centre has an average displacement dose of 44 dpa for 300 days of operation, whereas the experimental location at 4th ring has 27 dpa. To achieve dose of 150 dpa, central sub-assembly has to undergo irradiation for 3.7 years (75 % load factor) whereas it requires 6.2 years at experimental location in 4th ring to achieve the above dose.

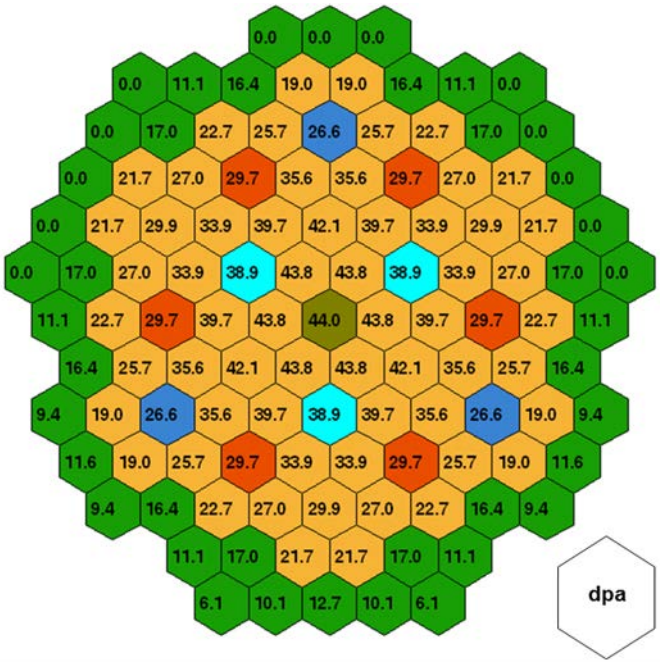

FIG.8. SA-wise average displacement dose for 1 cycle

3. SAFETY STUDIES

The knowledge of temperature and static reactivity coefficients of the reactor is useful in evaluating control rod worth, and the safety analysis of reactor. Any change in reactor power, inlet temperature and flow alters the temperature of the reactor materials, and in turn there will be a change in reactivity due to change in density of the reactor core material, axial and radial core boundary movement, and apparent insertion of control rod due to expansion of the control rod suspension and the removal of control rod due to reactor vessel expansion. So, it is necessary to determine the static power coefficient in order to evaluate the required reactivity compensation while taking the reactor power from zero power to nominal power. The reactivity loss due to burnup is 3785 pcm/cycle. The cycle length is 300 effective full power days.

Static power coefficient is defined as the change in reactivity of the reactor for a unit change in power from one steady state to another steady state, keeping all the other reactor parameters like coolant flow and inlet temperature constant. Static power coefficient calculated using the code PREDIS, which uses the effect of change in density of the reactor core material, axial and radial core boundary movement worth. Temperature reactivity coefficients of expansions are calculated by assuming thermal expansion coefficients of fuel and steel are constant. Isothermal temperature reactivity coefficients are given in Table 3. Lumped heat transfer model is used in determining power co-efficient. Lumped heat transfer model where the average temperature of the fuel pin is calculated by assuming the spatial temperature distribution across the fuel doesn't change with transient. Justification of lumped heat

transfer model can be made based on the better thermal conductivity of the metal fuel and liquid sodium bond gap material. Effective heat transfer coefficients are used in calculating the temperature gradients across fuel and clad. From the temperature gradients representative temperature of fuel and clad are determined. Static power power coefficient components of MFTR are summarized in Table 4. Temperature defect when the reactor is brought from hot critical to cold critical, and the power defect when it is brought to zero power from full power is given in Table 5.

TABLE 3. Isothermal temperature reactivity coefficients of MFTR

Reactivity Component	Temperature coefficient (pcm/C)
Doppler	-0. 731
Fuel Axial expansion	-0.616
Clad axial expansion	0.002
Coolant expansion	-0.130
Spacer pad expansion	-1.236
Total	-2.711

TABLE 4.: Static power coefficients of MFTR (Averaged over Zero to Full Power)

Reactivity Component	Power coefficient (pcm/MWt)
Doppler	-0.144
Fuel Axial expansion	-0.286
Clad & sheath axial expansion	0.005
Coolant expansion	-0.002
Spacer pad expansion	-0.274
Total	-0.701

TABLE 5: Temperature and Power Defects

Feedback Reactivity Component	Temperature Defect (pcm)	Power Defect (pcm)
Doppler	144.01	46.08
Fuel Axial expansion	121.35	91.52
Clad & sheath axial expansion	- 0.39	-1.6
Coolant expansion	25.61	0.64
Spacer pad expansion	243.49	87.68
Total	534.07	224.32

The number of absorber rods in the shutdown sytems and their positions in the core is being determined. The shutdown capability of each absorber rod system will be demonstrated for all the postulated normal and accidental conditions. It is to be noted to perform the Transient Over Power Accident (TOPA) analysis, it is essential to have the S-curve of the absorber rod worth. So, the absorber rod optimisation studies will be repeated in an iterative manner till the worth of absorber rods satisfies all the safety requirements. This work is currently in progress.

4. SUMMARY AND CONCLUSIONS

To meet the growing energy demand in India, the rapid growth of fast reactors with high breeding gain is proposed by the Department of Atomic Energy and laid a road map to achieve this task through the deployment of metallic fuel reactors of 1000 MWe beyond the year 2025. A comprehensive program has been started in India for mastering the various technologies of metal fast breeder reactors with closed fuel cycle. It includes fuel fabrication (sodium and helium bonded), full-scale irradiation of fuel sub-assemblies under operating conditions of a power reactor and reprocessing based on electro-

refining method. Construction of a small experimental fast breeder facility is envisaged to provide the necessary inputs to the above program.

Towards this, preliminary physics design of a reference MFTR core is performed with ERANOS 2.1 system such that this core satisfies the design requirements of: (a) Minimum reactor thermal power (b) Relatively low critical mass for Pu (c) Marginal breeder to meet its own fuel requirement (d) Peak LHR of 450 W/cm at all time of irradiation (e) Single fuel enrichment (f) Hexcan size and clad diameter same as that of PFBR (g) Fuel column height of 1000 mm (h) Peak burnup of 150 GWd/t (i) 6 CSRs and 3 DSRs (j) 3 experimental locations and (k) Special experimental central assembly with 180 fuel pins. Reactor power of 320 MWt is arrived at. This core provided the necessary inputs for making the preliminary layout for MFTR.

Future studies like absorber rod optimization, safety analysis (TOPA and LOFA), in-vessel shield design and fuel management scheme are needed to finalise the reference core configuration. It is likely that the number of absorber rods and their location in the core may get modified in the final optimised core which will satisfy the required shutdown margin during all the postulated normal and accidental situations.

5. ACKNOWLEDGEMENTS

The first author wishes to express his sincere thanks to Shri S. Clement Ravichandar, Head, CES/CDG for providing the engineering design of sodium bonded metallic fuel pin.

6. REFERENCES

[1] R. B. Grover and S. Chandra, Scenario for Growth of Electricity in India, Energy Policy, 34, 2834-2847 (2006).

[2] S. C. Chetal, A Perspective on Development of Future FBRs in India, Int. Conf. Fast Reactors and Related Fuel Cycles (FR09)-Challenges and Opportunities, Dec. 7-11, Tokyo, Japan (2009).

[3] K. Devan et al., Physics Design of Experimental Metal Fuelled Fast Reactor Cores for Full Scale Demonstration, Nuclear Engineering and Design, 241, 3058-3067 (2011).

[4] I. I. Chang, Technical Rationale for Metal Fuel in Fast Reactors, Nucl. Eng. Tech., 39 (3), 161-170 (2007).

[5] G. L. Hofman, L. C. Walters and T. H. Bauer, Metallic Fast Reactor Fuels, Progress in Nuclear Energy,Vol. 31, pp. 83-110 (1997).

[6] G. L. Hofman, Irradiation Behavior of Experimental Mark-II EBR-II Driver Fuel, Nucl. Tech., 47, 7 (1980).

[7] A. Riyas and P. Mohanakrishnan, Studies on physics parameters of metal (U-Pu-Zr) fuelled FBR cores, Ann. Nucl. Energy, 35, 87-92 (2008).

[8] (a). Gérald Rimpault et al., The ERANOS Code and Data System for Fast Reactor Neutronic Analyses, PHYSO 2002, Seoul, South Korea, October 7-10 (2002).
(b). J. M. Ruggieri et al., ERANOS 2.1 : International Code System for GEN-IV Fast Reactor Analysis, Proceedings of ICAPP'06, Reno, NV, USA, June 4-8 (2006).

[9] R.Harish, T. Sathiyasheela, G. S. Srinivasan and Om Pal Singh, KALDIS: A Computer Code System for Core Disruptive Accident Analysis of Fast Reactors, IGC-208 (1999).

Optimum design parameter studies on different power level of the small size SFR

M. H. Baek, J. Y. Lim, S. J. Kim

Korea Atomic Energy Research Institute,
111 Daedeog-daero 989,Yuseong-gu, Daejeon, 305-353, Rep. of Korea

Abstract. Core characteristics on different power levels were evaluated for technical support to determine the proper power level of the prototype SFR (Sodium cooled Fast Reactor) in Korea. The initial core will be constructed based on U metal fuel due to the insufficient TRU experiment database, and Uranium fuel will be substituted to TRU fuel. The various uranium cores were designed with same cycle length and the number of batches, and the performances of those cores were evaluated to decide the candidate core for each power levels at first. The selected power levels are 50, 75, 100, 125, 150, and 200 MWe. The fuel cost, irradiation time, and irradiation performance were compared among the candidate cores on different power level. As a different way, the core performance was also estimated by increasing the number of batches to reach the limit of fast neutron fluence at each power level. According to the evaluation of studies, the power capacity of the prototype SFR should not be less than 100 MWe from the neutronics viewpoint because the irradiation performance and the fuel economy became worse rapidly with decreasing power level.

1. Introduction

A prototype SFR (Sodium-Cooled Fast Reactor) has been planned to be developed at KAERI as a mid-term target for the commercialization of an SFR. The major roles of the prototype SFR are to provide an irradiation test environment for the fuel and structural materials and to prepare operational experience on T/H systems and mechanical components before the construction of demonstration SFR or commercial SFR.[1] The proper power level of prototype SFR should be decided with the consideration to achieve the major goal in the viewpoints of such as fuel cost, core performance and so on. To reduce the construction burden and the risk of investment, smaller power level is recommended if it can be satisfied with the main objectives of prototype SFR.

To figure out the appropriate power level, core performance should be compared with various points of view such as fuel cost, TRU irradiation time and so on. The core models which compared with each other should be optimized at different power level to compete with same condition.

In this paper, core designs were performed for 6 different power levels of 50 MWe, 75 MWe, 100 MWe, 125 MWe, 150 MWe and 200 MWe and two design approaches – same cycle length/batches and similar discharge burnup were tried to determine the optimized cores. The purpose of this study is to suggest and to evaluate the adequate range of power level in neutron aspect.

2. Candidate core design on different power level

2.1. Computational method

The core calculation was performed based on the K-CORE system, in which the fine-group(150 group) cross sections were generated based on Bondarenko f-factor method and collapsed into a 25-group structure using the fine-group fluxes obtained by the TWODANT code (R-Z model with P_3 scattering order and S_8 angular quadrature).[2][3] The equilibrium fuel cycle was analyzed by REBUS-3 which is based on the nodal diffusion theory with 25 group cross sections in a hexagonal-z geometry.[4] The pressure drop was calculated using the SLTHEN code, which is a multi-subassembly, steady-state subchannel analysis code based on a simplified energy equation model.[5] The flow distribution at the assembly inlet nozzle was first determined so that the maximum difference in power between subassemblies became 7 % within the same flow group.

2.2. Reference core

As the reference core, KALIMER-600 burner design was selected which was one of candidate design for the demonstration SFR.[6] The demonstration SFR has a transition from a uranium core to TRU loaded core after validating the fuel and structure material as follows. The first phase of the demonstration SFR is the uranium loaded core and then its fuel is replaced by the TRU fuel recycled from a light water reactor spent fuel (LTRU) in next phase. Finally, the core changed to the TRU core loaded with a self-recycled TRU fuel mixed with the external feed from a light water reactor spent fuel (MTRU). Because the prototype SFR is taken partially the role of the demonstration SFR, the main design parameters of KALIMER-600 was applied for the conceptual design of prototype SFR such as coolant inlet/outlet temperature, fuel smeared density, cladding thickness and so on.

Table 1. Basic design parameters of the reference core

Core type	Uranium core	LTRU core	MTRU core
Power (MWe)	600		
Cycle length (EFPD)	365		
The number of batches (inner/outer)	4/4	3/3	3/3
Core mixed mean inlet temperature (^oC)	365.0		
Core mixed mean outlet temperature (^oC)	510.0		
Fuel smear density (%)	75		
Fuel cladding thickness (mm)	0.56		
Duct wall thickness (mm)	3.7		
Duct gap (mm)	4.0		
The number of fuel pins in an assembly	271		
Active core height (cm)	106	85	85
Fuel type	U-10%Zr	U-TRU-Zr	

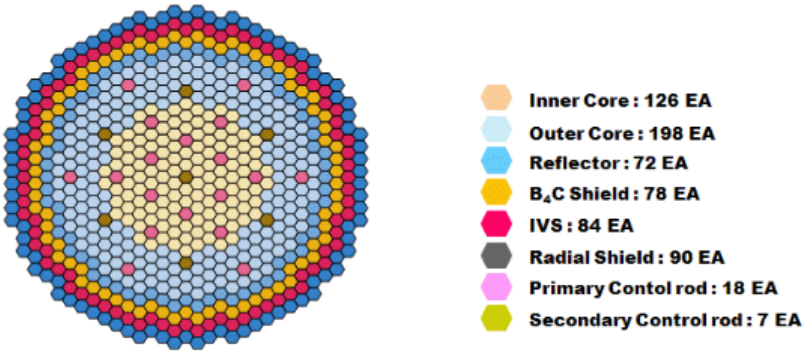

FIG. 1. Configuration of the reference core (U core)

The design specification and configuration of the reference core are shown in Table 1 and Fig. 1. The region of core consists of inner core, outer core, reflector, B4C shield, IVS (In-Vessel Storages) and radial shield.

2.3. Design constraints and design target

Design constraints of the prototype core are defined as follows;

1) The uranium enrichment is limited up to 20 wt.% owing to the non-proliferation.

2) The assembly bundle pressure drop should be below 0.25 MPa to remove residual heat by natural circulation.

3) The fast neutron fluence is limited up to 4.0×10^{23} n/cm^2 due to the irradiation tolerance of the cladding and structure materials.

4) The maximum cladding mid-wall temperature must be lower than the creep limit temperature (620 ^{o}C) including 2σ uncertainties.

Since the aim of the prototype SFR is to validate the irradiation performance of the TRU fuel and cladding material, the design target of a candidate core for the prototype SFR is to maintain the highest fast neutron flux level during reactor design life.

2.4. Core design procedure

The general design procedure of core design consists of numerous iterations between thermal, mechanical and nuclear design. Design parameters like fuel pin diameter, pitch-to-diameter ratio, core height, assembly size, etc., as well as core configuration and core dimension are being finalized in these iteration process. To simplify this procedure, the parameters of nuclear design took the same with reference core. The outer diameter of fuel pins is fixed to 0.74 cm and the number of fuel pins in an assembly is fixed to 271. As the ground rules for core design search, all core models were designed with single enrichment core (20 wt.%) and were modified to preserve the bundle pressure drop of 0.25 MPa. Additionally, reflectors of 2 layers were adopted to reduce the neutron leakage into the reactor structure as shown in Fig. 2. To exclude the effect of control rod, the same number of control rod and position were applied to all core configurations.

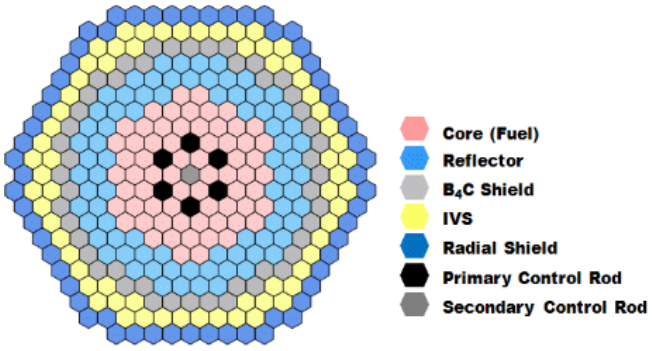

FIG. 2. Location of reflectors and control rods at the smallest core model with 66 fuel assemblies

Based on upper mentioned design rules, 14 core configurations were suggested to construct the cylindrical core shape by increasing fuel assemblies as shown in Fig.3. Several core models with different number of fuel assemblies were searched by changing P/D ratio and active core height to satisfy the design criteria at the same power level. This approach was also carried out for each power level – 50, 75, 100, 125, 150 and 200 MWe.

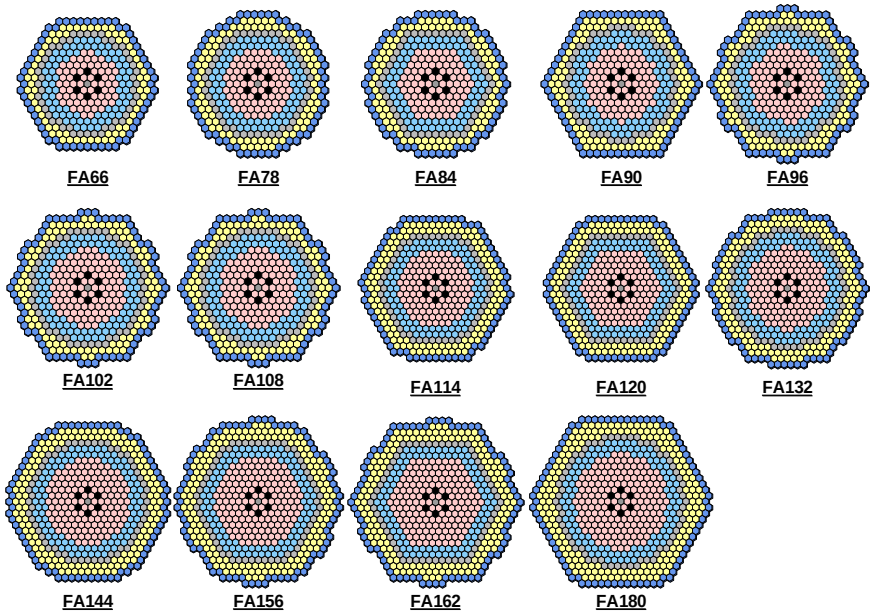

FIG. 3. Core configurations to search the candidate core at each power level

The fuel inventories of 3 ~ 6 core models at each power level were compared to decide the candidate core at each power level. The fuel inventory of several core models were varied with concave shape and the discharge burnups had convex shape oppositely for each power level. As shown in Fig.4, the core model with the lowest fuel inventory which had 132 fuel assemblies at 200 MWe was selected as the candidate core.

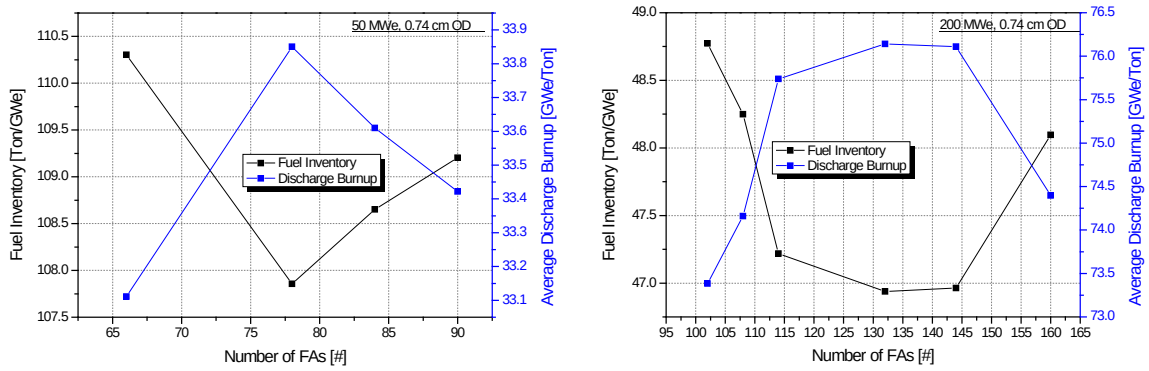

FIG. 4. Comparison with the fuel inventory according to the core models

3. Core performance evaluation on different power level

Assuming the annual fuel strategy with 80% of capacity factor, cycle length and batches were changed from 365 EFPD/4 batches of reference core to 290 EFPD/5 batches. The optimized core configuration and design parameters on different power level searched by equilibrium cycle calculation were listed in Table 2. To satisfy the criterion of bundle pressure drop, pitch to diameter ratio (P/D ratio) was adjusted for each power level and the core height was modified to match the limit of fuel enrichment. In case of reference core, enrichment split core was adopted to reduce power peaking and the U-235 enrichments were decided at 15 wt.% and 20 wt.% at inner core and outer core respectively. For smaller power level, single enrichment fuels with 20 wt.% were applied. When the reactor power increased, P/D ratio also increased to reduce the pressure drop which depended on the length of fuel rod – active core height.

Table 2. Design parameters of the small cores

Power (MWe)	50	75	100	125	150	200	600
Active core height (cm)	78.3	77.3	75.9	79.1	81.5	82.1	85.8
Eq. core diameter (cm)	139	151	163	170	177	194	304
Height to diameter	0.56	0.51	0.47	0.47	0.46	0.42	0.28
Number of FAs (#)	78	90	102	108	114	132	324
Assembly pitch (cm)	14.36	14.64	14.85	15.12	15.35	15.65	15.63
P/D ratio	1.073	1.094	1.110	1.131	1.149	1.172	1.17
Cycle length / Batches	290/5						
Outer diameter of fuel pins (cm)	0.74						
Fuel pins in an assembly	271						
Enrichment (wt.%) [Inner/Outer]	20						15/20
Pressure drop (MPa)	0.25						

Since the same cycle length and batches were applied to equilibrium core calculation, average discharge burnup became larger with increasing the power level. With large effect of neutron leakage, fuel loading at smaller power level should rise up to compensate the loss of neutrons. Therefore, the fuel inventory at 50 MWe had 2.3 times than that of 200 MWe as shown in Table 3. Average power density of 50 MWe power level should be reduced up to 44 % compared with that of 200 MWe oppositely.

Table 3. Core performance of the small cores

Power (MWe)	50	75	100	125	150	200	600
Fuel inventory (Ton/GWe)	107.9	81.5	67.8	59.6	53.9	46.9	40.0
Average discharge burnup (GWd/ton)	33.8	44.5	53.3	60.4	66.7	76.1	85.2
Average fast neutron flux ($\times 10^{15}$ n/cm^2·sec)	0.60	0.79	0.96	1.08	1.19	1.36	1.68
Peak fast neutron fluence ($\times 10^{23}$ n/cm^2)	1.2	1.6	2.0	2.2	2.5	2.9	3.3
Average power density (W/cm^3)	103	131	155	170	182	200	225
Peak linear power density (W/cm)	120	165	198	229	270	312	309
Average linear power density (W/cm)	69	91	109	124	142	157	176
Reactivity swing (pcm)	992	1,334	1,618	1,854	2,058	2,395	2,051
Neutron flux [>100 keV] (%)	71.4	70.5	70.2	69.7	69.2	68.5	67.7

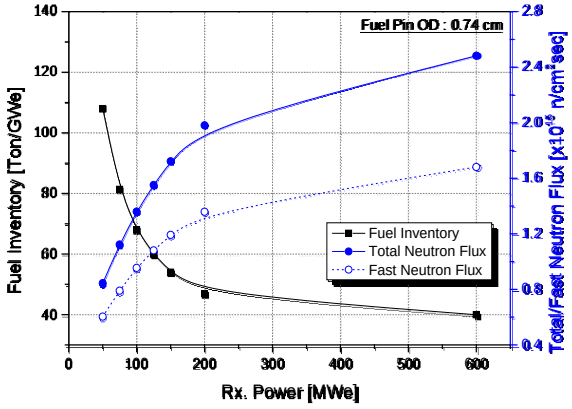

FIG. 5. Evaluation of fuel inventory and neutron flux on different power level

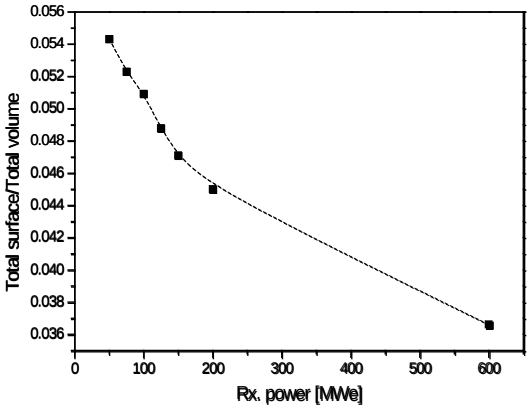

FIG. 6. Surface to volume fraction on different power level

The tendency of fuel inventory and neutron flux according to power level was shown in Fig. 6. The neutron flux and fuel inventory became worse rapidly with decreasing power level caused by the large leakage and low power density on small core. It was also confirmed that the leakage at 50 MWe had 20% larger than that of 200 MWe by comparing surface to volume ratio as shown in Fig. 7.

3.1. Evaluation of the fuel costs

Economic evaluation of operation cost was performed at each power level and resulting fuel cost was listed in Table 4. Total uranium fuel cost is the sum of conversion, enrichment and uranium ore costs. Conversion cost was 7 $/kgU, enrichment cost was 125 $/SWU, and uranium ore cost was 60.25 $/lb.[7] Fuel cost was evaluated as initial cost and annual cost. The fuel cost per unit power decreases with increasing power level, but the decrease becomes relatively insensitive in the power range from 150 to 200 MWe compared with that between 50 and 100 MWe.

Table 4. Uranium fuel cost on different power level

Power (MWe)	Uranium cost [million $]		Uranium cost per unit power [million $/MWe]	
	Initial cost	Annual cost	Initial cost	Annual cost
50	67.4	14.1	1.35	0.28
75	75.3	16.0	1.00	0.21
100	82.7	17.8	0.83	0.18
125	90.2	19.6	0.72	0.16
150	97.0	21.3	0.65	0.14
200	111.5	24.9	0.56	0.12
600	259.7	57.3	0.43	0.10

The initial cost and annual cost were increased about 0.18 million $/MWe and 0.04 million $/MWe with decreasing power level from 150 to 100 MWe, respectively. It showed about 2 times larger than the cost rate from 200 to 150 MWe. It also showed that the cost rate from 50 to 100 MWe was about 2.5 times compared with the value from 100 to 150 MWe.

3.2. Investigation of the TRU irradiation time

For the evaluation of irradiation and economic efficiency, TRU irradiation time and the consumption of the Uranium fuel to achieve the target neutron fluence were estimated and listed in Table 5. The target neutron fluence for the irradiation test should be close to the limit of fast neutron fluence for cladding and structure material. The fast neutron flux was assumed the half value between peak and average concerning the position of TRU test assembly.

Table 5. Irradiation time and consumption of the fuel on different power level

Power [MWe]	Irradiation time [years]	Consumption of the Uranium fuel [Ton/MWe]
50	20	0.55
75	15	0.33
100	13	0.24
125	11	0.20
150	10	0.17
200	9	0.13
600	8	0.10

It was shown that irradiation time required for obtaining the target neutron fluence gradually decreases with increasing power level. There was the difference of about seven years between 50 MWe and 100 MWe core, but only one year difference between 150 MWe and 200 MWe. The trend of the consumption of the uranium fuel was similar to that of the irradiation time.

3.3. Estimation of irradiation performance on the TRU core

To analyze the impact of change by replacing uranium fuel by TRU fuel, two types of TRU cores were evaluated in relation to the uranium core. Fig. 8 shows the average fast neutron flux when the uranium fuel of the prototype SFR is replaced by TRU fuel recycled from LWR (LTRU) or the self-recycled TRU fuel (MTRU). MTRU core was composed by reducing the core height for raising the charged TRU fraction up to 30 wt.%, which is the preliminary target enrichment for a TRU burner design. When the uranium core changed to the LTRU core, the irradiation performance was improved by about 20 % at each power level because of higher the number of fission neutrons per a fission of Pu increasing the contents of Pu. When the LTRU core changes to the MTRU core, the irradiation performance was improved by about 30 % due to the higher enrichment. Finally, when the uranium core changed to the MTRU core, the irradiation performance was improved by about 50 % at each power level. However, the ratios of flux change from U core to MTRU core between different power levels were maintained with same tendency.

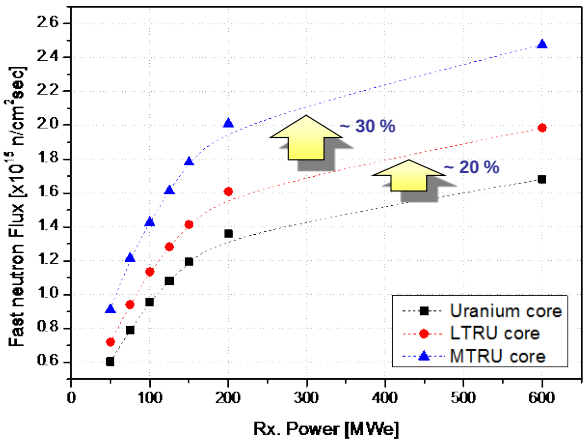

FIG. 7. Irradiation performance of the TRU cores on different power level

4. Study on the number of batches

In chapter 3, the cycle length and the number of batches kept same values to minimize the fuel inventory under the same core resident time. In this chapter, the different number of batches at each

power level was adopted to recognize the neutronic characteristic variation. The number of batches was decided by the limit of peak fast neutron fluence (around 4.0 x 10^{23} #/cm^2 for HT-9) as mentioned chapter 2.3. After determining the number of batches, core optimization was also performed by same procedure of chapter 3 and candidate cores were searched under same design constraints. The design parameters of cores with increasing the number of batches on different power level were listed in Table 6. When the number of batches increased from 5 to 19 at 50 MWe, the number of fuel assembly also increased extremely from 78 to 102 to supply additional fissile material for maintaining reactivity.

Table 6. Candidate core design parameters with different the number of batches at each power level

Power (MWe)	50	75	100	125	150	200	600
Active core height (cm)	78.4	87.4	82.8	89.0	81.4	84.5	89.4
Eq. core diameter (cm)	155.4	160.1	170.9	175.0	187.6	200.5	307
Number of FAs (#)	102	102	114	114	132	144	324
Assembly pitch (cm)	14.10	14.53	14.72	15.07	15.07	15.46	15.64
P/D ratio	1.05	1.09	1.10	1.13	1.13	1.16	1.17
Cycle length / Batches	290/19	290/15	290/12	290/10	290/9	290/8	290/6
Outer diameter of fuel pins (cm)	0.74						
Fuel pins in an assembly	271						
Enrichment (wt.%) [Inner/Outer]	20						15/20
Pressure drop (MPa)	0.25						

The performance of cores with increasing the number of batches on different power level was listed in Table 7. Peak fast neutron fluences at different power level are closed to 4.0 x 10^{23} #/cm^2 as mentioned design procedure. Thus similar discharged burnup showed at each power level 10±0.5 GWd/ton. As increasing core volume, fuel inventory was 21%, 9% less than the results of chapter 3 with same cycle length and batches at 50 MWe and 200 MWe respectively. It means that smaller core with same burnup should be required more fuel loading by higher effect of neutron leakage. Average power density also showed same tendency with fuel inventory comparison.

Table 7. Core performances of small cores which adopted different the number of batches at each power level

Power (MWe)	50	75	100	125	150	200	600
Fuel inventory (Ton/GWe)	136.0	100.8	80.2	69.0	61.0	51.7	41.3
Average discharge burnup (GWd/ton)	9.8	10.4	10.1	10.2	10.0	10.5	9.8
Average fast neutron flux (×10^{15} n/cm^2·sec)	0.51	0.68	0.85	0.97	1.09	1.28	1.64
Peak fast neutron fluence (×10^{23} n/cm^2)	4.0	4.2	4.1	4.0	4.0	4.0	3.9
Average power density (W/cm^3)	84	106	130	144	163	183	216
Peak linear power density (W/cm)	107	145	187	217	252	302	308
Average linear power density (W/cm)	54	72	91	106	120	141	171
Reactivity swing (pcm)	808	1,098	1,330	1,611	1,766	2,093	1,986

The tendency of fuel inventory and neutron flux compared with those of Chapter 3 according to power level was shown in Fig. 9. Red line represented the flux changes depend on power level from chapter 3 and blue line showed that from chapter 4. From these comparison, the fast neutron flux decreased 15 % and 6% at 50 MWe and 200 MWe respectively because of smaller power density. However, the variations of fuel inventory and neutron flux depend on power level change revealed same tendency with Fig. 6 that the reactor performance became worse at lower power level.

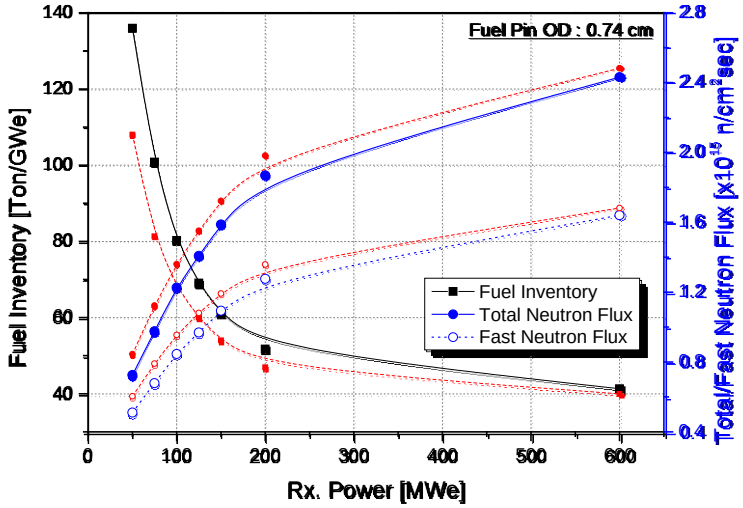

FIG. 8. Comparison of Fuel inventory and neutron flux on different power level

4.1. Estimation of the fuel cost

The fuel cost with increasing batches against that of same batches were listed in Table 8. Initial cost of different batch case was higher than that of same batch case due to the increase of fuel inventory to hold criticality up to EOEC. When initial costs were compared between different batch case and same batch case, the increase rate of different batch case showed 16, 15, 10, 8, 5 % at 50, 75, 100, 125, 150, 200 MWe, respectively. In case of annual cost, however, different batch case revealed lower annual cost because charged fuel assemblies per every cycle were reduced. Therefore, it was confirmed that the core with larger batch number was more profitable in fuel cost aspect except initial core loading.

Power [MWe]	Uranium cost [million $]		Uranium cost per unit power [million $/MWe]			
	Diff. Batches		Diff. Batches		Same Batches	
	Initial cost	Annual cost	Initial cost	Annual cost	Initial cost	Annual cost
50	784	48	15.7	1.0	13.5	2.8
75	865	68	11.5	0.9	10.0	2.1
100	922	90	9.2	0.9	8.3	1.8
125	990	116	7.9	0.9	7.2	1.6
150	1052	137	7.0	0.9	6.5	1.4
200	1182	174	5.9	0.9	5.6	1.2
600	2654	497	4.4	0.8	4.3	1.0

5. Conclusion

For determining the proper power level of a prototype SFR which will be developed by 2028, the comparison between various power levels under 200 MWe. First, candidate cores which were optimized at the minimum fuel inventory were searched on 14 core configurations for 6 different power levels – 50, 75, 100, 125, 150 and 200 MWe. To preserve the consistent comparison between each power level, the most of design parameter were fixed based on KALIMER-600 burner core. Two design parameters of P/D ratio and active core height were adjusted to be fittable the design constraints of pressure drop and fuel enrichment, respectively. As comparison ways, 3 core performance - fuel costs, TRU irradiation time and performance change by TRU fuel loading were observed between candidate cores with different power and same cycle length/batches. Second comparison was conducted at the similar core resident time by adopting different number of batches. Both of comparison showed that the fuel inventory became worse rapidly and the fast neutron flux

decreased at less than 100 MWe power level. TRU irradiation time also increased 2 times to reach the target neutron fluence when power level changed from 200 MWe to 50 MWe because the fast neutron amount was directly proportional to TRU irradiation time. After substituting U fuel for TRU fuel, TRU loaded core showed higher fast neutron flux – increase rate of 50% at every power level. As a conclusion of our entire study, the power capacity of the prototype SFR should not be less than 100 MWe, because of the large amount of neutron leakage on smaller core.

ACKNOWLEDGEMENTS

This study was supported by long term national R&D program of Ministry of Education, Science and Technology (MEST) in Korea.

ACKNOWLEDGEMENTS

REFERENCES

[1] Hahn, D., et. al, “Status of Fast Reactor and Pyroprocess Technology Development in Korea”, The Science Council for Global Initiatives Creating an Energy-Abundant Future 2012 (Proc. Int. Conf. California, 2012), California (2012).
[2] Macfarlane, R. E., “TRANSX 2: A Code for Interfacing MATXS Cross Section Libraries to Nuclear Transport Codes,” LA-12312-MS, Los Alamos National Laboratory (1993).
[3] Alcouffe, R. E., et al., “User’s Guide for TWODANT: A Code Package for Two-Dimensional, Diffusion-Accelerated, Neutron Transport, ” LA-10049-M, Los Alamos National Laboratory (1990).
[4] Toppel, B. J., “A User’s Guide to the REBUS-3 Fuel Cycle Analysis Capability,” ANL-83-2, Argonne National Laboratory (1983).
[5] Yang, H. S., An LMR core thermal-hydraulics code based on the ENERGY model, J. Korean Nucl. Soc. 29 (1997) 406.
[6] Kim, Y. I., et al, “Preliminary Conceptual Design Report of Gen-IV SFR Demonstration Plant,” KAERI/TR-4335/2011, Korea Atomic Energy Research Institute (2011).
[7] Nuclear Fuel Cost Calculator, http://www.wise-uranium.org/nfcc.html (2012).

Sample of EDF-R&D 2009-2012 core studies on heterogeneous sodium-cooled fast reactors with low sodium void effect.

D.Schmitt, D.Verwaerde, S.Poumérouly, P.Tétart, G.Darmet, B.Maliverney, S.Massara*

Electricité de France R&D, Clamart, France

* (currently working at NEA)

Abstract. *The unprotected loss of primary or/and secondary pumps transient is often used as a reference initiator to evaluate the intrinsic behaviour of SFR cores. Traditional designs show a major positive sodium reactivity feedback during this transient and many studies were led in the past to get rid of that effect. In 2009-2012, consistently with researches led at CEA and AREVA, cores with low sodium void effect were studied and optimized at EDF-R&D. The use of a sodium plenum with a boron carbide plate, a reduction of the fissile height, or a step-wise modulation of the fissile height can be used to reduce the sodium void worth. To go further, neutronic leakage can be enhanced using axial or radial heterogeneities. Axial heterogeneity is the basis of the CFV CEA concept. An analysis of this design using an EDF optimization methodology led to a better understanding and allowed to define core variants. As far as radial heterogeneities are concerned, various configurations featuring annular shapes, fertile sub-assembly rings and modulations of the fissile height are presented in this paper. One of these concepts is applied on a 600 MWe scale and compared to a CFV-like core. This paper aims at giving an overview of EDF-R&D core design studies on the time period 2009-2012, and concludes on perpectives for future work.*

1. INTRODUCTION

In the French cooperation framework, CEA, AREVA and EDF R&D are studying innovative sodium cooled fast reactors designs. These activities are backing the development of the ASTRID prototype, to be built around 2020. Safety objectives of this design are ambitious and improvements are expected from more traditional designs such as EFR or Super-Phénix. The current strategy aims at reducing the probability of a core degradation accident, relying as a priority on the natural behavior of the core. Mitigation measures only come in a second step, in case the neutronic feedback effects are not sufficient.

For that reason, conception studies led at CEA, AREVA and EDF R&D focus on improving the core intrinsic response to a set of reference unprotected transients, such as Unprotected Loss Of Flow (ULOF), Unprotected Loss Of Supply Station Power (ULOSSP), Unprotected Transient of Power (UTOP), and Unprotected Control Rod Withdrawal (UCRW).

In 2009, core design activities within the French framework were centered on the SFR_v2b concept ([1]). This core features a very low burn-up reactivity swing (~450pcm) but still a high sodium void worth (~5$). It was then decided to tackle this strong reactivity source. Conception studies started focusing on reducing the sodium void worth. A reduction of the fissile height, a sodium plenum and a boron absorber plate can notably decrease the sodium void worth on an homogeneous design. However; for large cores, more complex designs seem to be needed to reach a negative effective sodium reactivity feedback.

In particular, heterogeneous designs (including for instance fertile parts, step-wise modulation of the fissile height – called diabolo) can allow a strong reduction of the sodium void worth, leading to significant progress concerning ULOF behavior.

The CFV concept was first presented by CEA in 2011. Several versions were then issued ([2]). This concept achieves a good trade-off between sodium void worth (-0.5$), breeding gain (~ –0.02) and reactivity swing (~1550 pcm).

If CEA is in charge of ASTRID development, studies are also led at EDF R&D, as a support, on core concepts analysis and optimization, transient analysis and severe accident analysis.

In this paper, a sample of core design studies led at EDF R&D on the 2009-2012 period is presented. It is supported by previous publications such as [3], [4] and [5].

To begin with, some basics of low void core features are recalled. Some tools and methods used at EDF R&D, and evoked during this paper, are also mentionned.

The CEA concept CFV features an axial fertile plate in the inner core. This axial heterogeneity allows to increase neutron leakage and leads to interesting overall performances. Trade-offs on those performances must however be found, and an optimization method was used at EDF-R&D for that purpose [3]. The second section of this paper gives a quick overview of these results.

The use of an annular shape allows to increase neutron leakage. This effect can be combined with the inclusion of rings of fertile sub-assemblies. An EDF annular core with a modulation of fissile height allows to reach a negative value of the sodium void worth (-1$). Unlike the CFV, this core can be modeled with the current version of the SAS-SFR code[1], and gives some indications on low-void core behavior during the primary phase of a loss of flow transient ([6]). Variants of this annular core and other radially heterogeneous cores are presented throughout the third part of this paper. A 600 MWe core design with radial heterogeneities is selected and compared with a CFV-like core during a ULOF transient.

2. TOWARDS A NEGATIVE SODIUM REACTIVITY FEEDBACK

2.1. Behavior of a low-void effect core

When adding the local effects of a 1% decrease of sodium density, one usually gets a positive reactivity insertion. However, during a transient, the axial temperature profile of the sodium is such that the density decrease is stronger in the sodium plenum, where sodium reactivity feedback is negative. The overall resulting sodium reactivity feedback can then be negative, and hence drives the power down. The “effective” sodium feedback coefficient, calculated as a weighting of the sodium feedback coefficient distribution by the sodium temperature profile, is given on Tableau 2-1.

Reactivity feedback (pcm/K)	SFR_v2b like core	homogeneous core (reduced height/ sodium plenum)	annular/diabolo core	CFV like core
Global sodium feedback coefficient	0.496	0.287	0.159	0.165
Effective sodium feedback coefficient	0.531	0.093	-0.074	-0.090

Tableau 2-1 Effective sodium reactivity feedback

If this decrease is quick enough to counterbalance the sodium temperature increase, this can lead to a reduction of fuel temperature and hence to a positive Doppler feedback. In that case, the phenomenology of a ULOF is reversed : a negative sodium reactivity feedback is counterbalanced by a positive Doppler feedback (cf. results below : Figure 4-7).

[1] Analysis made in the framework of a collaboration with KIT-INR.

What's more, as the sodium density effect within the sodium plenum is not linear from 1% to 100% perturbation, low-void cores can provide a quick and strong decrease of the reactivity once boiling onset is reached ([6]).

2.2. Tools used

This work is supported by the use of the CEA code ERANOS ([7]) for neutronics and the CEA/EDF code MAT5DYN ([3]) for transient analysis. MAT5DYN is a multi-channel transient analysis code based on point-kinetics. Hot channels behavior and spatial distribution of reactivity feedbacks are taken into account.

For core designs studies an analysis methodology called SDDS allows to quickly scan a large set of different core designs. This tool is based on an interpolation of neutronic performances over a calculation data base, and on simple correlations about thermal and thermo-hydraulical behavior.

2.3. Core selection

Breeding gain and burn-up reactivity swing may be deteriorated when increasing the leakage contribution to sodium void worth. This effect can be limited if leakage is only increased when voided. Behavior during UCRW and UTOP transients can be worsened as well. Reducing fissile height or introducing fertile material within the core leads to higher fissile radius and impact vessel and primary circuit.

For a given sodium void reduction, various concepts can lead to various performance penalties. The core selection during neutronic studies or SDDS analysis ([1]) is based on several performances indicators such as burn-up reactivity swing, breeding gain, sodium void worth and sodium reactivity feedback. More complex safety indicators based on quasi-static asumptions are also used. A ULOF estimator (TULOF) is notably used in this paper. This correspond to a theoretical temperature asymptotically reached at the end of a ULOF transient with 12% final mass flow ([2]).

3. ANALYSIS OF THE CFV CONCEPT

3.1. CFV basics

The CFV concept is the reference option for the ASTRID core design ([2]). This core features a sodium plenum with an upper boron carbide plate and a step-wise modulation of the fissile height. The sodium plenum efficiency for sodium void reduction is strongly enhanced by an axial fertile plate, located just below the core mid-plane.

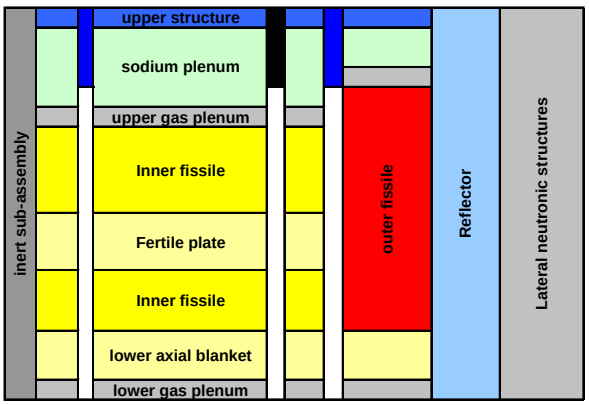

Figure 3-1 CFV concept 2D-RZ geometry

3.2. Design analysis using the SDDS methodology

The analysis of this concept was performed at EDF-R&D using the SDDS methodology [3], which allows to quickly sweep a large set of core variants defined by a set of geometric parameters (here : inner fissile radius, fissile volume, mean fissile height, position and thickness of the fertile plate, material fractions within the core). A special focus was given on the trade-off between a quasi-static estimator of the ULOF behavior and the burn-up reactivity swing. An objective of the study is to identify the Pareto front, i.e. the set of cores optimized in such a way that neither of these two performances can be improved without worsening the other one.

For instance, the impact of the position of the fertile plate on these two performances is given on the left side of Figure 3-2. It can be seen that the burn-up reactivity swing is minimum when the plate is at position[2] 0.5, i.e at the core mid-plane. On the contrary, the ULOF quasi-static estimator is more favorable when the fertile plate is in the lower part of the fissile height (corresponding to positions from 0 to 0.5). This can be easily understood : if the fertile plate is located at the top of the fissile core, the void effect does not benefit any more from the sodium plenum voiding. On the contrary, if the fertile plate is located below the core mid-plane, the flux axial profile is shifted toward the top. Axial leakage and control rod expansion effects are then enhanced.

On the right side of Figure 3-2 is plotted the distribution of the fertile plate position as a function of the two performances above mentionned, for all the cores of the design space. It can be seen that the plate is located in the lower part of the active height for all the cores of the Pareto front. Among these optimized cores, the plate position spans from 0.3 (for cores with a low ULOF quasi-static estimator) to 0.5 (for cores with a low burn-up reactivity swing). These results are consistent with the plot on the left side of Figure 3-2.

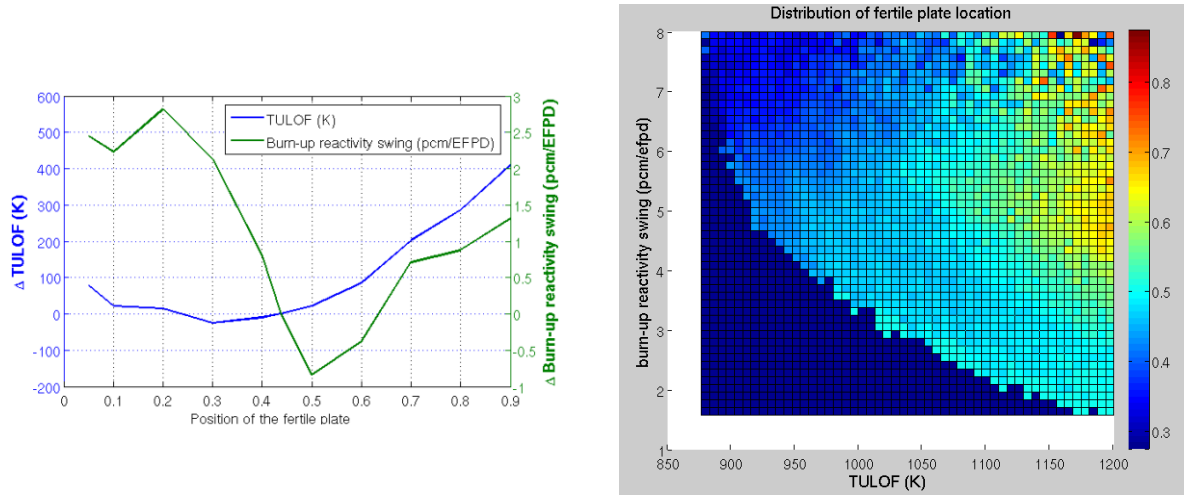

Figure 3-2 Impact of the fertile plate axial position on the ULOF quasi-static estimator and the burn-up reactivity swing.

Similar studies were led on each of the design parameters resulted in Figure 3-3. Design parameters can be separated in two sets. To be inside the Pareto front, a core must feature a thick fertile plate, a large fissile volume and no fissile height shift (first set of parameters). Within the Pareto front, a low fertile plate position and a low fissile height ensure a good ULOF behavior, whereas a centered fertile plate and a high fissile height grant a low burn-up reactivity swing (second set of parameters).

[2] The fertile position is calculated as x/h, where h is the inner fissile height and x the distance from the bottom of the fissile column to the center of the fertile plate.

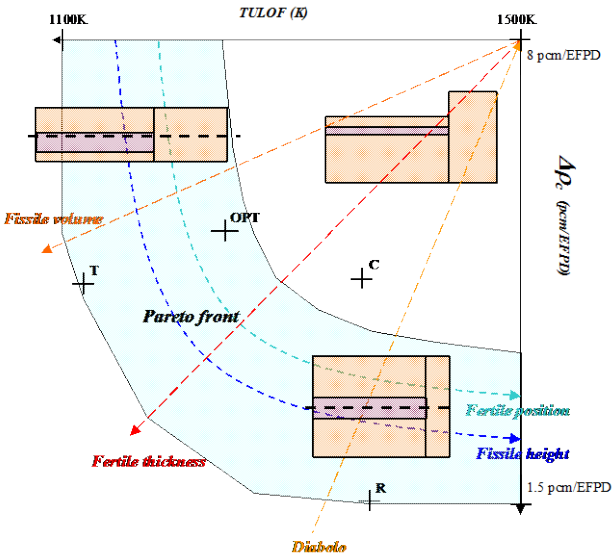

Figure 3-3 General overview of design parameter influence on the ULOF quasi-static estimator and on the burn-up reactivity swing. OPT, C, T and R are core variants.

This analysis also pointed out that the control rod expansion feedback can differ strongly from one core image to another, and that it has a clear influence on the results. In particular, the absence of the fissile height shift for optimized designs is linked to the choice of positionning control rods at the top of the outer core, at EOC. Control rod design and positionning should be chosen so as to enhance the control rod driveline expansion feedback. Actually, optimization of rods and core design should ideally be solved as a whole.

This work led to the definition of a core variant, called OPT (Figure 3-3). It features a thick fertile plate (25cm), located at position 0.42, a low fissile height (67cm), and a fissile volume of 5.5m^3. This core was compared with another CFV like design, called R. The quasi-static ULOF estimator used in the SDDS methodology foresaw a 100K difference between these two designs. This discrepancy was confirmed by finer calculations with the MAT5 DYN code ([5]). About 70K, out of 100K, are a consequence of the more negative differential control rod expansion of the OPT design.

4. STUDIES ON RADIALLY HETEROGENEOUS CORES

4.1. Annular core with diabolo shift

As previously mentionned, EDF R&D objective in 2009 and 2010 was to evaluate the safety benefits stemming from a negative sodium void worth. Core design studies began at a time when no data on the CFV concept was available at EDF R&D. An annular core with a diabolo shift was then designed. Parametric studies led with SDDS resulted in a final design with a power of 2880MWth ([4]). The global void worth is about -1$, and it is obtained without increasing too much the burn-up reactivity swing (1500pcm). However, the outer fissile radius is increased as a consequence of the annular shape. A radial scheme of this design is given in Figure 4-1.

New variants of this release were tested in 2011. These calculations were made with a simplified neutronic scheme (homogenenous cell calculation, transport 2D-RZ core calculation, once-through evolution). Six variants are mentionned in the next section : the reference annular core with diabolo shift (cf. §4.1, Case 1, Figure 4-1), an annular core with diabolo shift and a fertile ring within the intermediate core (Case 2) an annular core with diabolo shift and a low fertile ring within the intermediate core (Case 3,

Figure 4-2), a standard core (non-annular) with two diabolo shifts (Case 4), a standard core with two diabolo shifts and an inner fertile ring (Case 5, Figure 4-3), and an annular core filled with a small inner core (Case 6, Figure 4-4). They are all detailled hereafter.

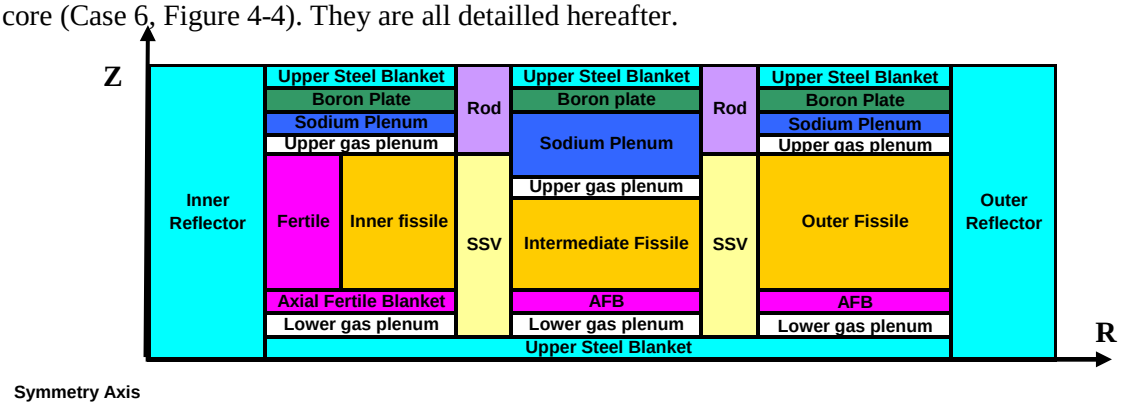

Figure 4-1 Radial scheme of the annular core with diabolo shift.

4.2. Introduction of a ring of fertile sub-assemblies.

The annular diabolo core comprises three fissile zones. The plutonium content is higher in the inner and outer zones, to make-up for leakage and flatten the power shape. The introduction of a ring of fertile sub-assemblies (S/A) in the intermediate zone allows to use only one plutonium content (Case 2, Tableau 4-1). If the fertile height is lower than the intermediate core fissile height (Case 3, Tableau 4-1 and

Figure 4-2), the sodium void worth is strongly decreased, at the cost of an increase of the burn-up reactivity swing. The inclusion of fertile S/A makes the outer core radius larger. This is a drawback of this feature and would penalize the vessel and primary circuit design.

			Case 1	Case 2	Case 3
			annular/diabolo core	annular/diabolo core with fertile ring	annular/diabolo core with fertile ring
outer core radius		cm	245	260	260
diabolo shift of the fertile zone		cm	/	0	20
Pu content	inner core	%vol.	19.65	21.9	21.8
	intermediate core	%vol.	18.35	21.9	21.8
	outer core	%vol.	19.65	21.9	21.8
maximum power density		W/cm3	326	308	312
burn-up reactivity swing		pcm	1424	1570	1777
EOC sodium void worth (total)		$	-0.99	-1.52	-2.49

Tableau 4-1 : Main results for variants of the annular/diabolo core with fertile ring.

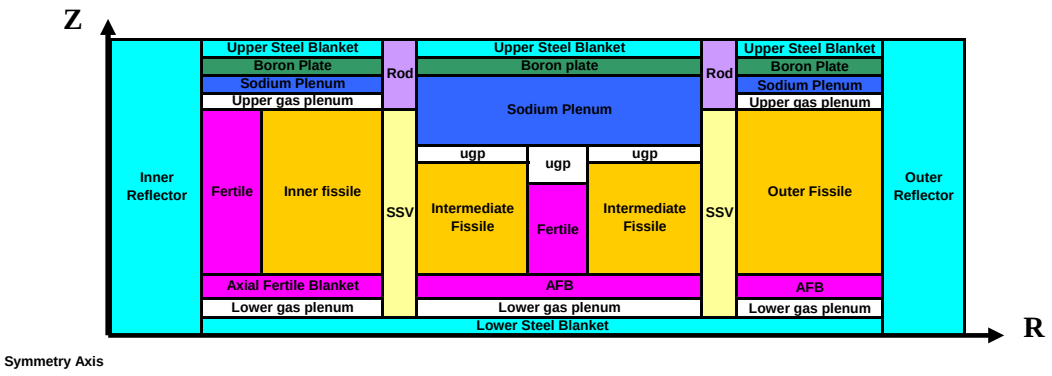

Figure 4-2 : Radial scheme of the annular/diabolo core with a fertile ring (Case 3) (scales not respected).

In the annular/diabolo core, the space lost at the core center results in a higher outer radius. Fertile S/A rings, combined with diabolo shifts, can be introduced in a non-annular core (cf. Figure 4-3). It appears that this feature allows to get a very good compromise between the reactivity swing and the sodium void worth (Case 5, Tableau 4-2). The outer radius is intermediate between that of a standard core and that of the annular/diabolo core. Nevertheless, the power shape of this design is harder to flatten, and this requires as many as four different plutonium content zones.

This core consists of an inner core separated from an outer core by rings of fertile S/A. For that reason, it can be compared to an annular core, with an inner fertile blanket, whose center would have been filled with a little inner core. This remark led to Case 6 (Tableau 4-2 and Figure 4-4). This design shows lesser performances than Case 5, but makes it possible to flatten the power shape with three plutonium content zones.

			Case 1	Case 4	Case 5	Case 6
			annular/diabolo core	standard core with 2 diabolos	standard core with 2 diabolos and fertile ring	annular core filled with a small core
outer core radius		cm	245	220	231	228
Pu content	core 1	%vol.	19.65	15.5	16.4	17.5
	core 2	%vol.	18.35	15.5	18	17.5
	core 3	%vol.	19.65	17.5	19.6	17.5
	core 4	%vol.	/	19	21.1	18.1
	core 5	%vol.	/	/	/	21.7
maximum power density		W/cm3	326	325	319	323
burn-up reactivity swing		pcm	1424	839	1103	939
EOC sodium void worth (total)		$	-0.99	-0.32	-1.84	-0.18

Tableau 4-2 : Main results for standard cores with diabolos and fertile ring.

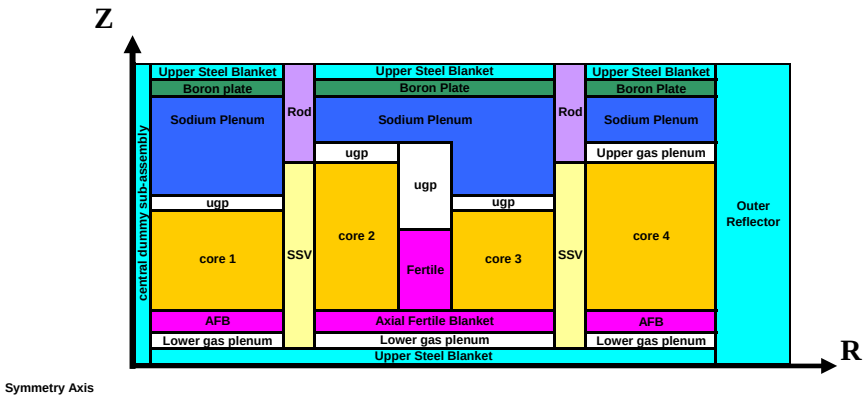

Figure 4-3 : Radial scheme of a core with double diabolo and a fertile ring (Case 5) (scales not respected).

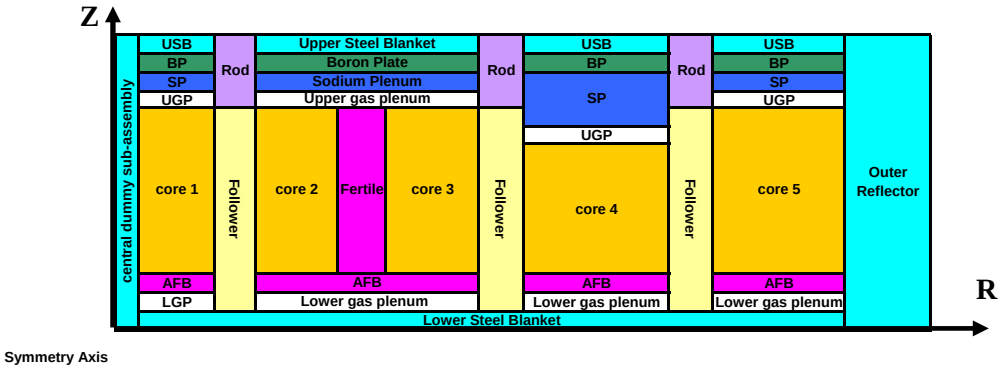

Figure 4-4 : Radial scheme of a annular core filled with a small inner core (Case 6) (scales not respected)

These results show that very complex designs can lead to very interesting safety performances. The cost and operating capacity would obviously be penalized with such complex designs. What's more, the safety gain obtained by reducing the total sodium void worth from –1$ (annular/diabolo core) to –1.8$ (case 5) or even to –2.5$ (case 4) should be evaluated during an unprotected loss of flow transient.

4.3. ASTRID-sized radially heterogeneous core.

Case 6 concept from previous section was used to design a 600 MWe core. Conception study included parametric calculations, an analysis of the design with the SDDS methodology, and the selection of a final release of the core.

The impact of the width and location of the fertile ring are plotted on Figure 4-5 (the inner radius of the fertile ring is determined by the radius of the inner fissile core). These results were obtained with the SDDS methodology (interpolation of a simplified neutronic calculations) and correspond to mean results over a set of core complying with a set of constraints (fixed burn-up, outer radius below a given limit, fissile heigth over fissile radius above a given limit). It can be seen (left) that a thick fertile plate is best for minimizing the sodium reactivity feedback, but increases the burn-up reactivity swing. Additionnally (right), a larger inner fissile core decreases the burn-up reactivity swing, but increases the sodium reactivity feedback.

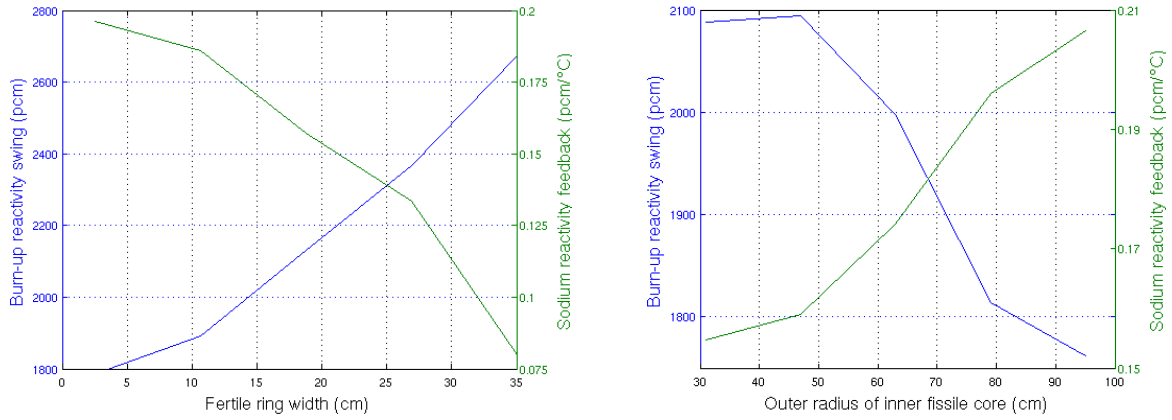

Figure 4-5 : Impact of the characteristics of the fertile ring (left : radial location ; right : radial width).

A design was selected as a trade-off between the burn-up reactivity swing and the ULOF asymptotic estimator, and called RD1. This design was chosen to comply with a set of constraints, among which a fixed burn-up, a maximum outer fissile radius, a minimum cycle length and a maximum sodium void worth. The width of the fertile ring on 2D RZ geometry is not very large on this design (~10cm). Actually, within the SDDS design spaces, cores without fertile ring can reach nearly similar performances. The interest of the inner fertile ring seems to be less interesting on a small design than it was on a 2880 MWth core.

This release was evaluated with a finer neutronic calculation scheme (heterogeneous cell calculation, 3D transport core calculation, evolution with reloading scheme). Some adjustments where also made when building a 3D geometry from the 2D RZ one got in SDDS. The shift on burn-up reactivity swing are related to change from rough to fine cell calculation scheme.

RD1		SDDS	rough ERANOS calculation	fine ERANOS calculation
mean Pu content	%vol.	20.43	20.43	21.23
burn-up reactivity swing	pcm	1528	1641	1806
total void worth	pcm	-11	-1	-58

Figure 4-6 : Performance drift from SDDS to fine ERANOS calculations

The main safety parameters of the selected core (RD1) are given on Tableau 4-3, and compared with the OPT core, derived from an optimization of the CFV design, and previously mentionned in this paper. It can be noticed that the voiding of the fertile ring has a positive impact on reactivity. The behavior of this core during a ULOF transient was evaluated with the MAT5 DYN code [5] (Figure 4-7).

		RD1	OPT core
Mean burn-up	GWj/(hmt fissile zones)	101	92
Mean power density (EOEC)	W/cm3	256	231
Max power density (EOEC)	W/cm3	333	305
Outer fissile radius	cm	163	168
Sodium reactivity feedback	pcm/°C	0.175	0.106
Control rod expansion feedback	pcm/°C	-0.415	-0.645
Total void worth (fertile plate/ring voided)	$	0.21	0
Total void worth (fertile not ring voided)		-0.16	/
Doppler constant			
fissile (from 1500K to 453K)	pcm	-752	-550
fertile (from 900K to 453K)	pcm	-166	-359
Beta effective	pcm	365	367
Burn-up reactivity swing	pcm	1806	1824

Tableau 4-3 : Main safety parameters of the design 3 core, compared to the OPT core.

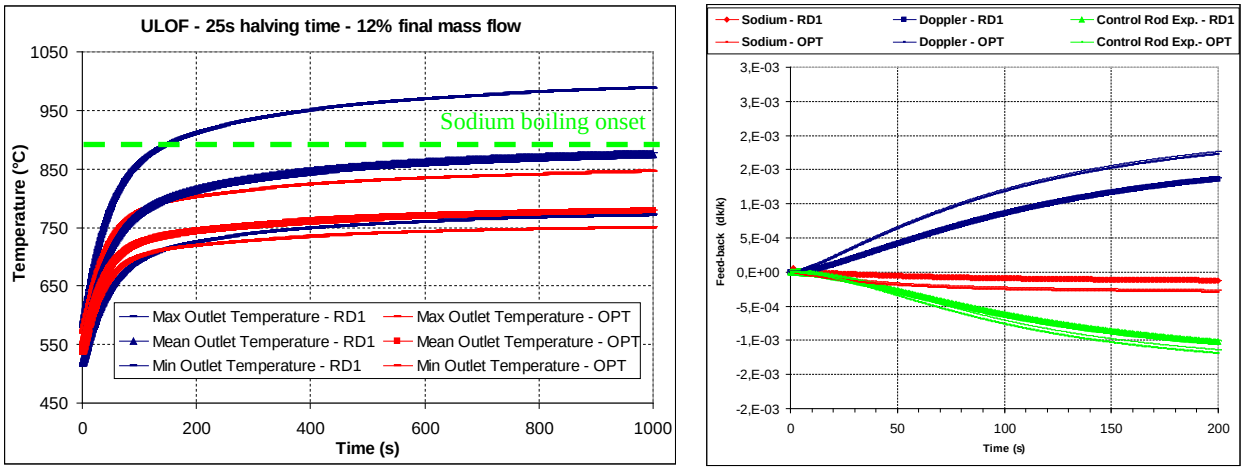

Figure 4-7 : Transient analysis : comparison of OPT and RD1 cores during ULOF (outlet temperature (left) – main reactivity feedbacks (right))

The RD1 core has a more positive sodium reactivity feedback and a lower control rod efficiency[3]. During an ULOF, these two discrepancies lead to a lesser negative reactivity insertion (Figure 4-7, right). For that reason, the power decrease is slower and more limited for the RD1 core than for the OPT core. This is the reason why the RD1 core experiences a smaller Doppler feedback. Because of these discrepancies, the sodium outlet temperature is higher by about 100°C (Figure 4-7, left). Even if the outlet temperature of the OPT core is below boiling onset on that graph, boiling cannot be excluded because of simplifications made and overall uncertainties. Even if the behavior of the RD1 core is less interesting than the optimized CFV-like OPT core, the temperatures reached are relatively

[3] This was a choice : as control rods were not redefined for this design, it was decided not to optimize this core on that aspect.

low. Nevertheless, at this stage of the studies, the OPT core overall characteristics are better than that of the RD1 core.

5. CONCLUSION

From 2009 to 2012, conception studies led to innovative designs with very low or even negative total void worth. Improvements were obtained by introducing strong heterogeneities within the geometry. The reference core design for ASTRID, CFV, is based on an axial heterogeneity, allowing to strongly decrease the sodium void worth without damaging other performances too much. Radially heterogenous cores allow very interesting performances as well, but sometimes requires complex configurations.

On the one hand, investigations must still be led on new core concepts. Some peculiar configurations with interesting performances could still be found. Optimization methods, such as SDDS, must be improved so as to gain precision and be able to include more safety indicators.

On the other hand, in the framework of ASTRID development, efforts should now be made on design simplification and economic performances improvement, on the basis of the CFV reference core design. Is should also be checked, as a back-up, if simpler designs can reach low sodium void worth as well.

Besides, transient analysis shows that sodium boiling cannot be avoided with certainty. For that reason, severe accident behavior should be taken into account on the same ground as transient analysis.

ACKNOWLEDGEMENTS

EDF R&D wants to thank the CEA for providing data on the CFV core concept.

REFERENCES

[1] P.Sciora et al., A break even oxide fuel core for an innovative french sodium-cooled fast reactor : neutronic studies results, Proceedings of GLOBAL 2009, Paris, France, September 6-11, 2009, paper 9528
[2] F.Varaine et al., Pre-conceptual design study of ASTRID core., Proceedings of ICAPP 2012, Chicago, USA, June 24-28, 2012, paper 12173.
[3] S.Poumérouly et al. Optimization of a heterogeneous fast breeder reactor core with improved behaviour during unprotected transients, proceedings of ICAPP 2012, Chicago; June 24-28, paper 12214.
[4] D.Schmitt et al., Design of a Sodium-cooled Fast Reactor with innovative annular geometry and very low sodium void worth proceedings of ICAPP 2011, Nice, France, Mai 2-5, paper 11073.
[5] G.Darmet et al., Dynamical analysis of innovative core designs facing unprotected transiens with the MAT5 DYN code, proceedings of ICAPP 2012, Chicago; June 24-28, paper 12245.
[6] S.Massara et al., Behavior of an heterogeneous annular FBR core during an Unprotected Loss of Flow accident : analysis of the primary phase with the SAS-SFR code, Proceedings of ICAPP 2012, Chcago, USA, June 24-28, paper 12213
[7] G.Rimpault et al, The ERANOS code and data system for fast reactor neutronic analyses, Proceedings of PHYSOR 2002, Seoul, Korea
[8] H.S.Khalil et al., Evaluation of Liquid-Metal Reactor Design Options for Reduction of Sodium Void Worth, ANL, Nuclear Science and Engineering, 109, 221-266, 03/04/1991.

DEMONSTRATING THE EFFECTIVENESS OF THE EUROPEAN LFR CONCEPT: THE ALFRED CORE DESIGN

G. Grasso[a†], C. Petrovich[a], K. Mikityuk[b], D. Mattioli[a], F. Manni[c], D. Gugiu[d]

[a] Technical Unit for Reactor Safety and Fuel Cycle Methods, Italian National Agency for New Technologies Energy and Sustainable Economic Development (ENEA-UTFISSM), Bologna, Italy

[b] Paul Scherrer Institute (PSI), Villigen, Switzerland

[c] Servizi di Ricerche e Sviluppo S.r.l. (SRS), Roma, Italy

[d] Institute for Nuclear Research (INR), Pitesti, Romania

Abstract. The "Lead-cooled European Advanced DEmonstration Reactor" (LEADER) project, approved by the European Union within the 7th EURATOM Framework Programme, was addressed with the twofold goal of further developing the conceptual design of the reference Generation-IV LFR for industrial use, and of conceiving the Advanced Lead-cooled Fast Reactor European Demonstrator. ALFRED is a 300 MWth pool system aimed at proving the viability of the design concept adopted for the European LFR systems, while demonstrating the effectiveness of the safety features that are implemented in a simple, passive, robust and economic way.

The reference ALFRED core configuration is presented, together with the rationales adopted in the design approach in order to outline from scratch a fuel pin, fuel assembly and core complying with the technological, safety and performance constraints/goals by design.

The results of the detailed neutronic and thermal-hydraulic analyses carried out to verify the proposed core design are also presented.

1. INTRODUCTION

The realization and successful operation of demonstration reactors is required for proving the industrial maturity of a new generation of Nuclear Energy Systems (NES), fully complying with the goals in the areas of sustainability, improved safety, economics and proliferation resistance and physical protection, as numbered in the Generation IV International Forum (GIF) Technology Roadmap [1]. This is also stated in the Strategic Research Agenda (SRA) [2], compiled by the Sustainable Nuclear Energy Technology Platform (SNETP) [3] in accordance with the dictates of the European Union's energy policy gathered by the Strategic Energy Technology Plan (SET-Plan) [4],

Among the promising technologies identified by the GIF [1], the Lead-cooled Fast Reactor (LFR) has been selected by the European Union, together with the Sodium-cooled and the Gas-cooled Fast Reactors. These systems, relying on a fast neutron spectrum, are indeed the most promising candidates for the closure of the fuel cycle, ensuring at once the efficient exploitation of the uranium resources, and the minimization of the long lived waste.

† giacomo.grasso@enea.it

The favourable nature of the inert coolant – allowing for a *forgiving* design of the system even under the most severe accidental conditions and a strong simplification of the overall plant layout, with a strong impact on robustness and economics – attracted the interests of industrial partners, research institutions and universities, who constituted a consortium for a Gen-IV compliant design of an industrial-size LFR. The European Lead-cooled System (ELSY) collaborative project [5] was therefore proposed, approved and co-funded by the European Union through its 6th EURATOM Framework Programme (EU FP6).

After that, the EU FP7 funded a new initiative, the Lead-cooled European Advanced DEmonstration Reactor (LEADER) project [6], with the twofold objective of further developing the ELSY design [7] towards a reference European LFR (ELFR) configuration (which is described in a companion paper [8]), and of setting up the configuration of a fully representative demonstration reactor, ALFRED (the Advanced Lead-cooled Fast Reactor European Demonstrator), as envisaged by the SRA.

2. THE DEMONSTRATION AIMS: RATIONALES FOR CORE DESIGN

The successful demonstration of the LFR technology chain is represented by the effective operation of an intrinsically safe, economic, sustainable and proliferation resistant First-Of-A-Kind (FOAK) of the industrial-scale ELFR. As described in the proposed LFR roadmap presented in a companion paper [9], the achievement of this ambitious goal by 2050 (as dictated by the SRA) requires the realization of the demonstrator by 2025. According to this, ALFRED has to rely on already proven technological solutions to speed up the design and the licensing phases: this requirement dictates the choice of the materials and of the components (e.g.: the proven 15-15 Ti steel for the cladding instead of ferritic-martensitic T91, or the double-wall bayonet-tube steam generator instead of the spiral one [7]).

In its demonstration role, ALFRED is called at proving, to the largest extent, the viability of the design concepts to be adopted for the European LFR systems. On the other hand, according to the limited size of the plant (required for the reduction of the initial risks), the demonstration aims have to be limited to the effectiveness of the safety features[1]. This point has furthermore assumed a paramount importance as a consequence of the Fukushima events.

According to these considerations, and keeping as reference the ELFR [8], the ALFRED core parameters have been organized into *families*, depending on their importance to what concerns the demonstration aim:

- Parameters that must be kept for demonstration:
  - materials (fuel, clad, coolant),
  - core inlet temperature;
- Parameters that should be kept, but not necessarily reached at their maximum:
  - peak burn-up,
  - plenum pressure,
  - maximum cladding temperature,
  - coolant velocity,
  - linear power rating (hence fuel temperature);
- Parameters that might be borrowed, but could not be kept:
  - core height,
  - core outlet temperature,
  - core pressure drops;

[1] As mentioned, the limited size of ALFRED will require an enrichment far above the one allowing the implementation of the adiabatic fuel cycle [22] envisaged for the ELFR [8]. Nevertheless, the operation of ALFRED will also serve the qualification of the tools and the methodology used for designing the core, providing in this way an indirect demonstration of the sustainable features of the ELFR.

— Parameters that could be different, but it is wiser keeping for more persuasive coherence:
  - fuel assembly concept;
— Parameters that do not need to be the same for validation:
  - pin diameter,
  - clad thickness,
  - gap thickness,
  - pins lattice pitch;
— Parameters that cannot be kept:
  - core power,
  - fuel enrichment,
  - breeding ratio.

2.1. Main constraints and recommendations

Following the presented logical scheme, a list of constraints and recommendations has been compiled to provide a reference for the design of the core (Table 1).

Table 1. Main technological constraints for the ALFRED core design.

Parameter	Unit	Limiting value
Thermal power	MW	300
Maximum inner vessel radius	cm	≈ 170.0
FA concept	-	Closed hexagonal
Fuel type	-	MOX
Maximum Pu fuel enrichment	%	30[a]
Maximum fuel temperature[b]	°C	≈ 2000
Peak BU	MWd/kg	100
Maximum plenum pressure	MPa	5.0
Clad material	-	15-15 Ti
Maximum clad temperature	°C	550
Maximum clad damaging	DpA	100
Coolant	-	lead
Coolant inlet temperature	°C	400
Coolant outlet temperature	°C	480
Maximum coolant velocity[c]	m/s	3.0
Maximum cladding temperature in ULOF[d]	°C	750

[a] This values has been set because of fabrication limits [10].

[c] The value of the maximum coolant velocity to contain erosion refers to the maximum allowable component of the lead velocity normal to structural surfaces. This limit must therefore be translated, by means of CFD analyses, in a corresponding limit on the coolant velocity through the pins bundle.

[d] The Unprotected Loss Of Flow (ULOF) accident has been selected, being the most penalizing for what concerns the cladding temperature.

[b] The limit on the maximum fuel temperature in operation is set to provide a margin against melting which is sufficient to accommodate temperature excursions during transients (with particular regard to Unprotected Transients of Over-Power, UTOP).

The only parameter that has been changed with respect to the ELFR is the cladding material: indeed, the expected time required for the full qualification of a T91 cladding (together with a suitable coating) in lead is not compatible with the roadmap for ALFRED. On the other hand, the temperature limit for the cladding is the same as for T91, because it is assumed that also the 15-15 Ti cladding tubes will be coated to enhance the protection against lead corrosion and erosion.

As can be seen from Table 1, the ALFRED design is challenging since the narrow temperature range to be respected, bounded by the 400 °C of coolant inlet temperature to prevent with sufficient margin lead freezing, and the 550 °C of cladding temperature in the hottest fuel pin.

3. ALFRED CORE DESIGN

A comprehensive core design strategy (analogous to the one used for the ELFR [8], Figure 1) has been adopted, approaching systemically, from a thermal-hydraulic, thermo-mechanic and neutronic point of view, all the aspects of the reactor core impacting on the safety and the robustness of the plant. As a matter of fact, such an approach allows for the *a priori* definition of a core which respects, at least in first approximation, all the technological constraints and fulfils all the performance objectives by design. Then the results are checked *a posteriori* with more detailed code calculations.

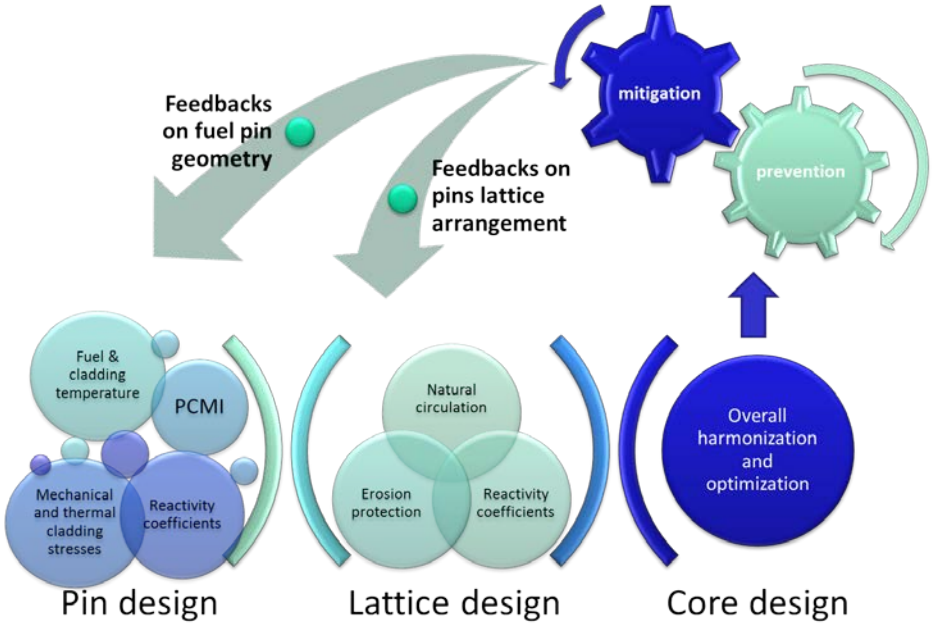

FIG. 1. Scheme of the comprehensive core design approach followed.

According to this, the ALFRED fuel pin, the fuel assembly, the control and safety systems, the reflector and the core have been designed. In particular, preliminary analyses have been performed to check whether the investigated fuel pin and the coolant sub-channel allow for an acceptable thermic of the pin and a sufficient natural circulation in ULOF conditions without exceeding some safety limits, mainly linked to the clad temperature.

3.1. Fuel pin and coolant sub-channel design

The first phase of the core design process foresees a preliminary thermal/hydraulic analysis to check the respect of the design limits to what concerns both the fuel and cladding maximum temperatures in the hottest channel. Since the latter – together with the coolant inlet and outlet temperatures – are the same as for the ELFR [8], the design of the fuel pin has been borrowed by this system, together with the maximum linear power rating (≈ 340 W/cm). The same assumption holds considering the target peak BU (≈ 100 MWd/kg), so that the hollowed fuel concept of the ELFR has been kept to accommodate the irradiation-induced swelling without incurring in Pellet-Cladding Mechanical Interaction (PCMI). The resulting (radial) fuel pin design is shown in Figure 2.

The design of the sub-channel cannot omit preliminary safety analyses to verify the respect of the cladding integrity for the desired grace time (30 minutes before SCRAM is manually actuated) in case of accident. To account for this constraint, the natural circulation regime during a ULOF transient has to be evaluated. Having this in mind, the sub-channel has to be designed so as to offer a hydraulic

diameter the pressure losses associated to which can be overtaken with a small prevalence, attained through acceptable coolant temperatures.

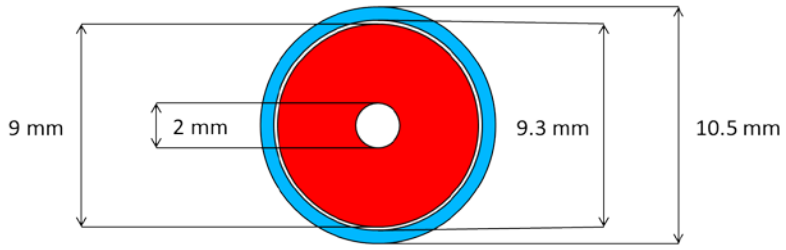

FIG. 2. ALFRED fuel pin cross-section.

On the other hand, the wider the pitch, the lower the fuel volume fraction in the elementary cell, to the detriment of the reactivity of the system. According to this, two values of the nominal coolant flow velocity have been therefore assumed for the present study, 1.4 and 1.5 m/s, supposing these as reasonable for achieving a sufficient natural circulation without affecting excessively the core reactivity. Furthermore the choice of the preliminary core configuration has to cope also with the constraint imposed for the inner vessel radius.

At last, two active heights (60 and 90 cm) have been considered in the present study not only to encourage the natural circulation by increasing the chimney height (since the shorter fuel and plenum length), but also to allow for keeping in the width of the lattice pitch, gaining in reactivity.

The natural circulation regime in case of ULOF has been then evaluated by means of the SIMMER code [11] for the four different configurations resulting by combining the two active height options with the two coolant velocities. According to the results of this investigation, the configuration corresponding to a coolant velocity of 1.4 m/s and 60 cm active core height has been chosen as reference, to which corresponds a value of the maximum cladding temperature during ULOF below 740 °C.

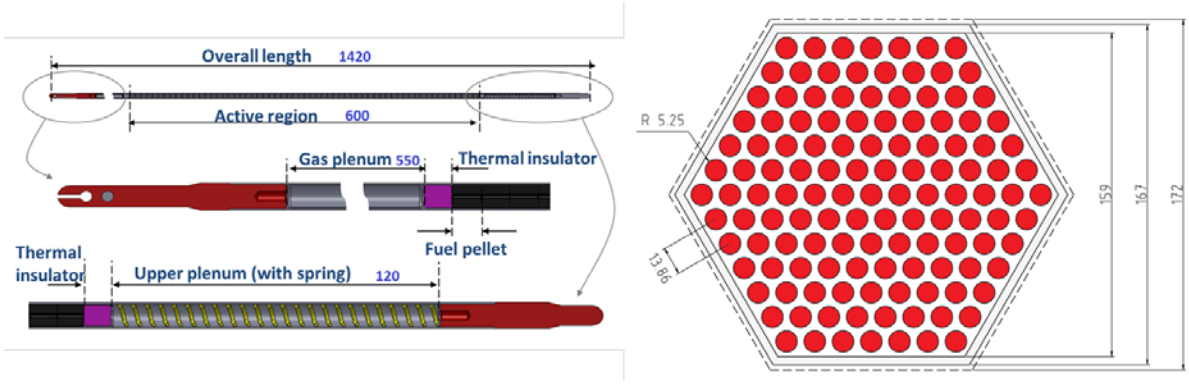

FIG. 3. Final ALFRED fuel pin (left) and FA cross-section (right). Dimensions in mm.

For the final dimensioning of the coolant sub-channel, the radial and axial power form factors had to be evaluated. Concerning the axial form factor, a value of 1.15 has been borrowed from the analyses performed on a similar system [12]. The radial power form factor has been set equal to 1.2, assuming a proper power/FA distribution flattening is achievable through suitable Pu enrichment zoning of the core. According to these assumptions – which automatically become recommendations for the neutronic design of the core – the corresponding pitch for the fuel pins lattice is set to 13.86 mm.

The mechanical design of the ALFRED Fuel Assembly (FA), borrowing the same concept adopted for the ELFR [8], started by completing the design of the fuel pin: the axial extensions of the plenum and the spring have been set in order to comply with the target pressure of the fission gases and to allow

for a free differential expansion of the fuel column and the cladding, respectively. Then, a wrapper with a sufficient stiffness has been added, enclosing 127 fuel pins arranged in a triangular lattice to form the bundle. The axial design of the ALFRED fuel pin and the horizontal cross-cut of the FA are shown in Figure 3.

3.2. Core design

Starting from the maximum linear power rating and the axial and radial power form factors, the average linear power rating is computed and used to define the number of fuel pins to be arranged to sum the aimed 300 MWth. The corresponding number of FAs (171) can be arranged to form a cylindrical core, together with 16 positions for Control and Safety Rods (CRs and SRs respectively), surrounded by two rings of dummy elements shielding the inner vessel within the imposed radius.

Extensive neutronic calculations – by means of both MCNPX [13] and ERANOS [14] codes with the JEFF 3.1 cross-sections library [15] – followed, to define the Pu enrichments and zoning, along with the positioning of control and safety elements, ensuring the aimed criticality level, a power/FA distribution flattening complying with the assumptions made for the design of the fuel pin and coolant sub-channel, and anti-reactivity worth for control and safety systems ensuring the respect of safety constraints. The underlying hypothesis is a fuel management according to a 5-batches cycle without reshuffling, with 5 y FA residence time in pile. The latter comes directly from the assumption on the maximum linear power rating and the chosen pellet geometry, to target the aimed peak burn-up of 100 MWd/kg.

The requirements for the control/safety systems are:

- a sufficient worth of the CRs to compensate the reactivity swing during the 1-year sub-cycle;
- the worth of each single CR when inserted to compensate the criticality swing not higher than 1 $;
- 5000 pcm for the refuelling status (k_{eff} = 0.95);
- about 2500 pcm for the SCRAM. This has been set according to:
  - some 500 pcm for the transition from hot to cold state;
  - 1000 pcm of sub-criticality, k_{eff} = 0.99 (value to be verified by kinetics analyses);
  - 1000 pcm of uncertainty (assumed).

The strategy to accomplish these requirements foresees:

- two redundant systems for SCRAM (2500 pcm each), one of which also devoted to the compensation of the reactivity swing during the cycle;
- the simultaneous use of both CR and SR systems during refuelling to reach k_{eff} = 0.95.

The design of the CRs and SRs has been borrowed from the one developed within the CDT-FASTEF project [16] for MYRRHA [17]. Accordingly, the CRs are made of a cylindrical bundle of 19 pins (left frame of Figure 4), cooled by primary lead and positioned into a guiding tube occupying a core position. Their withdrawn position is below the core, and are actuated by motors during operation (compensation, start-up and controlled shutdown), but are provided also of an electromagnetic connection whose release allows for a rapid insertion into the core by buoyancy for emergency shutdown. To tune the velocity of insertion, the volume of the plenum in the absorbing pins can be adjusted at will. The CRs are provided with a roller guiding mechanism to allow for the self-centring of the bundle within the guiding tube even in case of distortions of the tube itself (e.g.: in case of earthquake).

The SRs are similarly conceived: they are made of a bundle of 12 absorbing pins (right frame of Figure 4), cooled by primary lead and positioned into a guiding tube occupying a core position. During normal operation they stay still atop the active zone. Their only actuation is for SCRAM, through the

unlocking of an electromagnet. When the latter is turned off, it is also passively triggered a pneumatic system that pushes the SRs rapidly into the core. To face the failure of the pneumatic system, a tungsten ballast is added atop the SRs, providing a sufficient weight to contrast the buoyancy and ensure the insertion of the SRs into the core, even if at reduced speed.

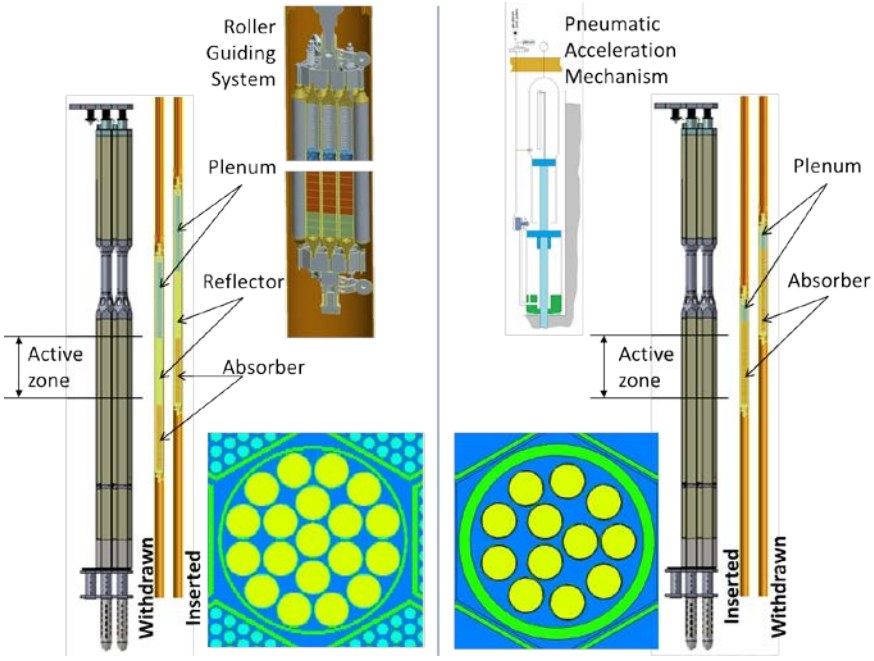

FIG. 4. Scheme and cross section of ALFRED CRs (left) and SRs (right).

The resulting core configuration is characterized by 57 FAs in the inner region, with a Pu enrichment of 21.7 wt.%, and 114 FAs in the outer region, with a Pu enrichment of 27.8 wt.%. 12 CRs are positioned within the outer region with the twofold goal of lowering the flux insisting on the most enriched FAs, while compensating the over-criticality along the cycle through a progressive withdrawal from their maximum-inserted position at BoC. 4 SRs are also positioned close to the core centre to minimize the shadow effect with the CRs. The ALFRED core, and the power/FA distribution at Beginning and End of Cycle (BoC and EoC) are shown in Figure 5.

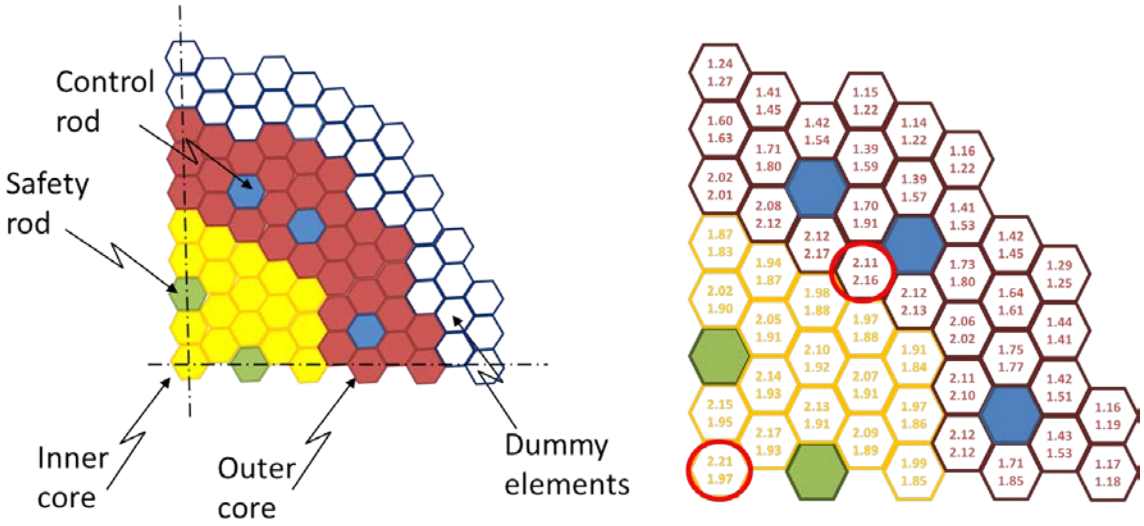

FIG. 5. Final ALFRED core configuration (left) and BoC (upper value) and EoC (lower value) power (in MW) per FA distribution (right).

For this configuration, a criticality swing of about 2600 pcm is found during the 1 year cycle. The worth of the control and safety systems is found to be –8500 pcm and –3300 pcm, respectively. Even in case of one SR stuck in withdrawn position, the anti-reactivity provided by the safety system is still about 2600 pcm. These values are found sufficient for the achievement – in every condition – of the required anti-reactivity margins for control, SCRAM and refuelling. To compensate the reactivity swing during the sub-cycle, a partial insertion of the CRs is sufficient at any power level. This is the main responsible for the radial and axial distortion of the power distribution in the core. Thanks to the high number of CRs, the limit for the maximum worth of 1 CR at BoC is also respected, being 220 pcm the maximum accidental reactivity insertion against 335 pcm of delayed neutrons fraction.

4. VERIFYING THE SAFE DESIGN OF THE ALFRED CORE

For the most powerful FAs in the two zones (the ones marked by a red circle in Figure 5), the detailed power/pin distribution has been computed by means of MCNPX. A complete thermal analysis of the fuel element followed, in order to verify the respect of the maximum fuel and cladding temperatures. This analysis has been performed by means of the ANTEO-LFR sub-channel code [18], originally developed in ENEA for fast reactors fuel assembly thermal/hydraulic studies, and adapted to lead-coolant.

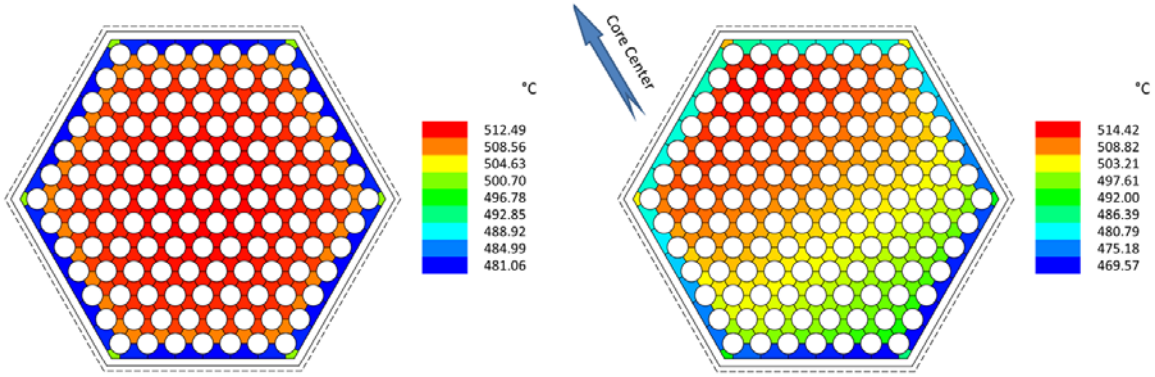

FIG. 6. Coolant outlet temperature distribution among the sub-channels of the most powerful FAs: on the left the central one; on the right the one in the outer core region.

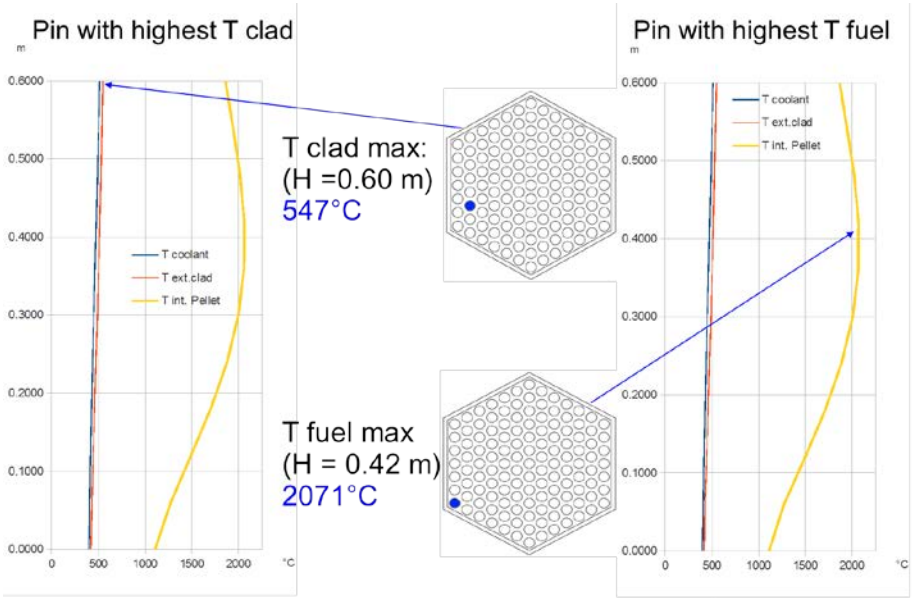

FIG. 7. Axial temperature profiles in the hottest pins of the most powerful FA.

The distribution of the coolant temperature at core outlet among the sub-channels of both these FAs is shown in Figure 6. For the FA in the outer region, since the most unfavourable power distribution within the FA itself, a complete analysis of the fuel pins followed, showing the respect of the design limits even for the hottest pins (Figure 7).

Finally, preliminary safety analyses have been performed for the proposed core configuration by means of several system codes, under the most penalizing Design Extension Conditions (DEC): ULOF, ULOF with simultaneous Unprotected Loss Of Heat Sink (ULOHS) and Unprotected Transient of Over-Power (UTOP). All the results (exhaustively presented in a companion paper [20]) seem to confirm the good implementation of the safety principles at code design level, with no temperature (cladding, fuel and vessel) exceeding the imposed limits for the assumed time before operators' intervention.

5. CONCLUSIONS

In order to fully prove the compliance of the systems of the LFR technology chain to the goals set for Generation-IV NES, the successful operation of a demonstration reactor is envisaged by the EU. According to this, ALFRED – the Advanced Lead-cooled Fast Reactor European Demonstrator – will be primarily called at proving the robustness of the safety approach which characterizes the LFR systems, based on, and fully exploiting, the forgiving nature of lead as coolant.

The comprehensive strategy adopted for the design of the ELFR core, which ensures the ability to intimately implement goals and constraints from scratch into the design process, has been therefore adopted also for the design of the ALFRED core.

A 300 MWth core, achieving most of the main performances envisaged for the ELFR, has been described and commented. The reference configuration, resulting from the application of the comprehensive design strategy, has been detailed, and the main results discussed in comparison to the design aims.

The results of thermal/hydraulic verifications for the proposed configuration and of preliminary safety analyses show the promising ability of ALFRED to resist, preventing core damage and ensuring the aimed grace times.

After the successful application of the described methodology to the preliminary design of ALFRED, a more detailed design phase is envisaged, which includes deeper investigations on the effect of uncertainties on the respect of the design limits, and on the approximations introduced by the codes in the evaluation of the core performances. As a matter of fact, proper operating margins will be required for ALFRED, given its demonstration role. Nevertheless, it is expected that the proposed comprehensive approach could be used again for the new design of the ALFRED core, complying with the more and more challenging constraints required for the advancement of the project.

ACKNOWLEDGEMENTS

The Authors acknowledge the European Commission for funding the LEADER project in its 7th Framework Programme. Grateful acknowledgements are also due to all the colleagues who contributed to the analyses of the LEADER "Core Design" Work Package, and to Dr. Giacomino Bandini of ENEA for the preliminary safety investigations in support to the design of the ALFRED core.

REFERENCES

[1] UNITED STATES DEPARTMENT OF ENERGY NUCLEAR ENERGY RESEARCH ADVISORY COMMITTEE AND GENERATION IV INTERNATIONAL FORUM, A Technology Roadmap for Generation IV Nuclear Energy Systems, report (2002), http://www.gen-4.org/Technology/roadmap.htm.

[2] SUSTAINABLE NUCLEAR ENERGY TECHNOLOGY PLATFORM, Strategic Research Agenda (2009), http://www.snetp.eu/www/snetp/images/stories/Docs-AboutSNETP/sra2009.pdf.
[3] DIRECTORATE-GENERAL FOR RESEARCH AND DIRECTORATE J – ENERGY (EURATOM) OF EUROPEAN COMMISSION, The Sustainable Nuclear Energy Technology Platform: A vision report, special report EUR 22842 (2007), http://www.snetp.eu/www/snetp/images/stories/Docs-VisionReport/sne-tp_vision_report_eur22842_en.pdf.
[4] EUROPEAN COMMISSION, Towards a European Strategic Energy Technology Plan, communication to the council, the European parliament, the European economic and social committee and the committee of the regions (2007), http://ec.europa.eu/energy/technology/set_plan/set_plan_en.htm.
[5] EURATOM SIXTH FRAMEWORK PROGRAMME, European Lead-cooled System (ELSY), Proposal/Contract no. FP - 036439 (2006), http://www.elsy-lead.com/.
[6] EURATOM SEVENTH FRAMEWORK PROGRAMME, Lead-cooled European Advanced DEmonstration Reactor (LEADER), Proposal/Contract no. FP7 - 249668 (2010), http://www.leader-fp7.eu/default.aspx.
[7] ALEMBERTI, A., et al., European lead fast reactor—ELSY, Nucl. Eng. and Des. **241** 9 (2011) 3470.
[8] GRASSO, G., et al., A core design approach aimed at the sustainability and intrinsic safety of the European Lead-cooled Fast Reactor, Fast Reactors and Related Fuel Cycles: Safe Technologies and Sustainable Scenarios (Proc. Int. Conf. Paris, 2013), IAEA, Vienna.
[9] ALEMBERTI, A., et al., The European Lead Fast Reactor Strategy and the Roadmap for the Demonstrator ALFRED, Fast Reactors and Related Fuel Cycles: Safe Technologies and Sustainable Scenarios (Proc. Int. Conf. Paris, 2013), IAEA, Vienna.
[10] WOAYE HUNE, A., AREVA fuel fabrication capabilities: minimum allowable pin diameter and maximum fuel Pu enrichment, CDT-FASTEF (Project meeting Brussels, 2009).
[11] MASCHEK, W., et al., SIMMER-III and SIMMER-IV safety code development for reactors with transmutation capability, Mathematics and Computation, Supercomputing, Reactor Physics and Biological Applications (Proc. Int. Conf. Avignon, 2005); Contributed paper (CD-ROM).
[12] BORTOT, S., et al., Conceptual core design study for a high-flux LFR demonstrator, Progr. in Nucl. En. **54** (2012) 56.
[13] MCKINNEY, G. W., et al., MCNPX Overview, Hadronic Shower Simulation Workshop (Int. Conf. Fermilab, 2006), AIP Conf. Proceedings **896** (2007) 178.
[14] RIMPAULT, G., et al., The ERANOS code and data system for Fast Reactor neutronic analyses, Physics of Reactors (Proc. Int. Conf. Seoul, 2002).
[15] JOINT EVALUATED FILE (JEF) PROJECT, The JEFF-3.1 Nuclear Data Library, JEFF Report 21 (2006), OECD/NEA, Paris.
[16] EURATOM SEVENTH FRAMEWORK PROGRAMME, Central Design Team (CDT) for a fast-spectrum transmutation experimental facility, Proposal/Contract no. FP – 232527 (2009), http://cdt.sckcen.be/.
[17] AÏT ABDERRAHIM, H., et al., MYRRHA, a Multipurpose hYbrid Research Reactor for High-end Applications, Nucl. Phys. News **20** 1(2010) 24.
[18] MATTIOLI, D., CEVOLANI, S., ANTEO-LFR: a pc code for thermal-hydraulic optimized core analysis in a Lead Fast Reactor, Technical Report UTFISSM-P000-005 (2012), ENEA, Bologna.
[19] ARTIOLI, C., et al., A new paradigm for core design aimed at the sustainability of nuclear energy: the solution of the extended equilibrium state, Ann. Nucl. En. **37** (2010) 915.
[20] BANDINI, G., et al., Safety results of representative DEC accidental transients for the ALFRED reactor, Fast Reactors and Related Fuel Cycles: Safe Technologies and Sustainable Scenarios (Proc. Int. Conf. Paris, 2013), IAEA, Vienna.

CP ESFR: Collaborative Project for a European Sodium Fast Reactor

L. Buiron, A. Vasile,
CEA Cadarache, BP 1 13108 St. Paul Lez Durance, France
R. Sunderland *AMEC*, G. Glinatsis *ENEA*, J. Krepel, K. Mikityuk *PSI*, A. Rineiski, B. Vezzoni, F. Gabrielli *KIT*,
N. Garcia Herranz, R. Ochoa *UPM*, F. Martin Fuertes *CIEMAT*, F. Polidoro *RSE*, H. Tsige-Tamirat *JRC*, S. Massara *EDF*

Abstract – *The Collaborative Project for a European Sodium Fast Reactor (CP ESFR) is performed (2009-2012) in the 7th European Framework Programme. It is devoted to the identification and study of innovations to be considered for the future in the core design, safety, reactor architecture, components and the dissemination of knowledge related to this technology among young European professionals.*

I. INTRODUCTION

The Collaborative Project for a European Sodium Fast Reactor (CP ESFR, 2009-2012, see logo in Figure 1) merges the contribution of 23 European partners. It is being carried out under the aegis of the 7th Framework Programme (FP) in the area - Advanced Nuclear Systems.

CP ESFR follows the 6th FP project named “Roadmap for a European Innovative SOdium cooled FAst Reactor – EISOFAR” further identifying, organizing and implementing a significant part of the needed R&D efforts [1]. The main areas of CP-ESFR are:

- Management (administrative and technical issues),
- Consistency and assessment,
- Fuel, fuel element, core & fuel cycle,
- Safety concept, Proliferation Resistance & Physical Protection (PR&PP) issues,
- Innovative reactor architecture and components,
- Education & training.

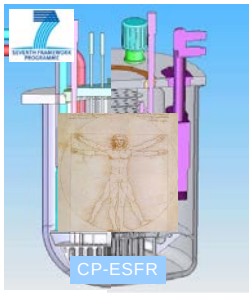

Fig. 1. CP ESFR logo

The inputs for the project are the key research goals for fourth generation of European sodium cooled fast reactors which can be summarized as follows:

(1) An improved safety. Attention is focused on the achievement of a robust architecture with respect to hypothetical accident conditions, and the robustness of the safety demonstrations;
(2) The guarantee of a financial risk similar to that of the other means of energy production;
(3) The flexible and robust management of nuclear materials, waste reduction through Minor Actinides (MAs) burning.

In this paper, the main attention is devoted to activities on the optimization of cores loaded with oxide and carbide fuels. Safety-related optimization options for the oxide core are described only briefly as these activities are presented in detail in [2]. Optimizations for the carbide core have been done by following the approach proposed for the oxide core.

In the project, different options for utilizing MAs have been investigated. The results obtained for the optimized configurations with different MA loading options are summarized in this paper.

II. OBJECTIVES

The key research objectives addressed by the project for fourth generation of European sodium cooled fast reactors can be summarized as follows:

(1) An improved safety. The expected progress of the Sodium Fast Reactors (SFR) safety architecture should allow this technology reaching a level at least equivalent, or even higher, to that of the third generation's reactors. The system behavior under hypothetical accident conditions is a key issue to be considered.

(2) The guarantee of a financial risk similar to that of the other means of energy production. Reducing the electricity production cost to a level similar to those of the third generation light water reactors by simplifying the system, reducing the mass of steel, and improving the performances, by increasing the level of energy conversion efficiency and/or by increasing the fuel burn-up.

(3) A flexible and robust management of the nuclear materials. The management of the nuclear materials allows the minimization of the impact on the environment. This impact has to be as low as practicably achievable. The reduction of the impact on the environment includes on one hand the possibility of transmuting the radioactive long life waste (mainly MAs) and, on the other hand, progressing in the reduction of the quantity of effluents and the staff radiological exposure.

In addition to the mentioned objectives, the project has been considered as a platform for re-building the European expertise on sodium fast reactors with participation of young engineers.

III. PARTICIPANTS

The European research institutes, utilities, universities, reactor industrial providers and other organizations participating in the project are listed in Table 1.

Table 1: Participants of the CP ESFR project

CEA	France
AMEC	United Kingdom
ANSALDO	Italy
AREVA NP	France
RSE	Italy
CIEMAT	Spain
EDF	France
Empresarios Agrupados	Spain
ENEA	Italy
EVM	Czech Rep.
KIT	Germany
FZD	Germany
JRC - ITU	Europe
JRC - IPSC	Europe
JRC - IE	Europe
NRG	Netherlands
NRI	Czech Rep.
PSI	Switzerland
SENER	Spain
Univ.Roma	Italy
Univ. Politecnica Madrid	Spain
IRSN	France
ENSA	Spain
ACCIONA	Spain
IPUL	Latvia

IV. CORE STUDIES

The development of the ESFR core took place in two phases.

In the first phase, lasting two years, the study has been based on “working horse” cores (with oxide and carbide fuels) provided at the beginning of the project by CEA. These cores were considered to have a reasonable performance and thus adequate as a starting point. In this phase, technologies for improving the core performance have been studied, particularly on safety and MA transmutation. The majority of the studies in this phase have been based on the oxide core because of a larger experience obtained in the past on oxide fuel cores. Therefore the oxide “working horse” core was in a more mature state of development than the carbide one. A detailed analysis of the results obtained during optimization of the oxide core in order to improve its safety-related parameters, in particular the sodium void effect is presented in [2].

In the second phase, the optimized oxide core has been finalized and the same approach has been applied to the carbide core, a more speculative design with respect to the oxide one. Whilst optimisation work was carried out on the carbide core, it was not achieving the same level of development as that for the oxide one. In this second phase, the MA transmutation performance of the optimized oxide core has been studied. The present paper focuses in particular on this second phase of the project.

A major objective for the optimization procedure described in [2] is improving the safety performance compared to earlier fast reactor concepts. The following main issues have been considered:

1. Compared to the previous generation of fast reactor concepts, a reduction in the sodium void reactivity worth is required to improve the core performance during hypothetical unprotected transients, particularly those involving the Unprotected Loss Of coolant Flow, ULOF, and the Total Instantaneous Blockage of a flow in single subassembly, TIB. More details are provided in [2, 3].
2. The amount of reactivity held up by the control rods (CRs) should be small in order to limit the impact of accidental CR withdrawal. Since a major function of the CRs is taking up the excess reactivity of the core, which is largest at beginning of the cycle, the best way for limiting the amount of reactivity held up in the CRs is a reduction of the reactivity loss of the core during fuel during irradiation. This requires the core to be designed with low fuel enrichments (Pu content in the range of 12%-14%). This leads to a core with a large inventory loaded with fuel pins having large diameters (>10 mm) and with an appropriate P/D ratio to avoid a pressure drop penalisation. This objective for the CRs is also consistent with an almost zero internal breeding gain (active core only), i.e. the reactor is self-sufficient in plutonium without requiring fertile blankets. No detailed analysis on CSD and DSD was performed.
3. The core should be capable of transmuting MAs. Whilst the inclusion of minor actinides will tend to worsen reactivity coefficients, their introduction should be done in such a way as to limit the impact on safety.

The last two points are particularly addressed in the following.

IV.1 Oxide Core

The Oxide Working Horse Core and the modified configuration

As mentioned above, the optimisation process started from the oxide “working horse” core. The core (Figure 2) has a power output of 3600 MWth, a fissile height of 1m, and contains upper and lower axial blankets made of steel.

The fuel sub-assembly consists of 271 pins, with ODS steel cladding with an outer diameter of 10.73 mm and containing oxide fuel pellets of 9.43 mm outside diameter. The fuel pins are surrounded by 4.5 mm thick hexagonal EM10 wrapper tube of 206.3 mm outside across flats. The sub-assembly pitch is 210.8 mm.

The oxide “working horse” core contains larger diameter fuel pins as compared to previous designs. The adopted low fuel enrichment implies a low reactivity loss with burn-up over the cycle, meeting already the goal concerning CRs. Therefore, the optimization has been devoted to reduce the positive sodium void reactivity worth.

Major options considered for optimizing the sodium reactivity void worth are discussed in [2]. As a result of the work a recommendation was made for inclusion of an upper sodium plenum, 600 mm high, with a 300 mm thick absorber layer (natural boron carbide) above the plenum and the adoption of a lower fertile blanket. This new core, referred as CONF2, differs from the “working horse” core only axially (Figure 3).

Some additional work on sodium void reactivity worth reduction has been undertaken (by EDF) while considering different active core heights in the inner and in the outer core zones to increase the neutron leakage. The analysis demonstrated a possible further reduction in the sodium void reactivity worth, but concluded that more detailed 3D neutronics analyses and transient studies would be required to confirm the effectiveness of these measures.

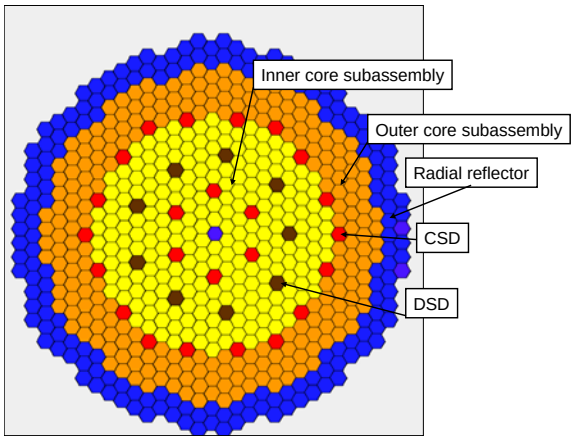

Fig. 2. Working Horse core oxide.

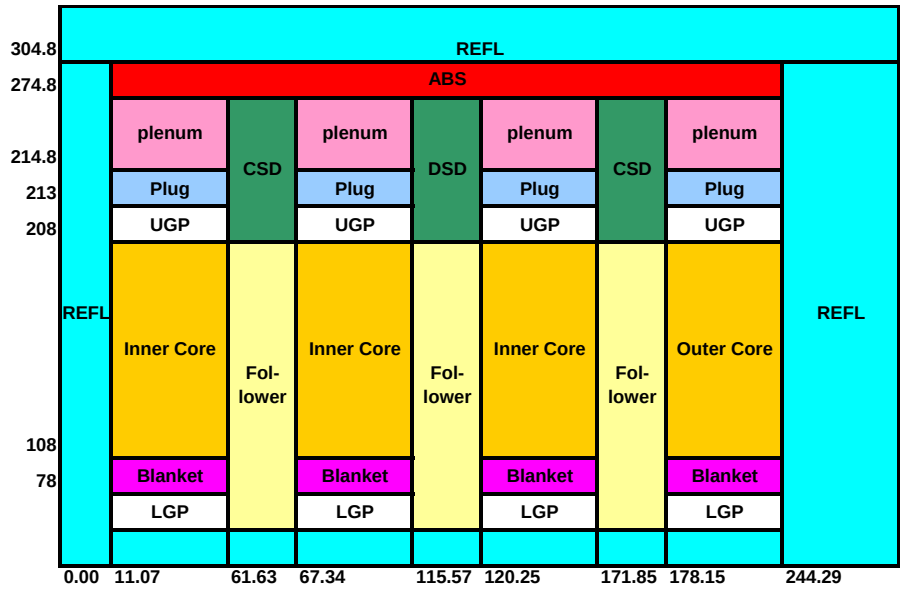

Fig. 3. Transverse section of CONF2: optimized oxide configuration

Control Rods Worth for the oxide CONF2 configuration

Even though the core has a low reactivity loss per cycle compared with the past cores, an assessment of the CR worth has been undertaken to ensure that a sure shutdown can be achieved. The assessments have been performed by using MCNP [4] for the Beginning of Equilibrium Cycle (BOEC) condition.

The determination of the S-curves (reactivity variation due to CR movement) has been carried out by considering separately (due to their different functions) for Control and Shutdown Device (CSDs) and for Diverse Shutdown Device (DSDs). The calculated reactivity worth is 4535 pcm for CSDs (1 rod) and 1260 pcm for DSDs (1 rod).The requirement to

shut down the core at cold temperatures (100 °C) conditions has been also assessed. The related reactivity introduction is 2084 pcm.

The CSDs have also to be able to cover the reactivity loss with burn-up. It was assessed that, even for a single batch refuelling scheme, the reactivity loss is approximately 200 pcm, see Table 2.

The results have shown that the bank of CSDs is able to accommodate with a significant margin the total requirement of ca. 2300 pcm (considering burn-up effect and shutdown to cold state). This margin (ca. 2000 pcm) allows for uncertainty on the calculated values.

The function of DSDs is to shut down to sodium inlet temperature rather than cold and they do not need to take up the reactivity loss with burn-up since that is done by the CSDs. The requirement for DSDs has been evaluated to be of rather less than 2000 pcm. With the array of 9 DSD rods used at present this is not possible. Therefore, it is judged likely that some transfer of rods from the CSDs group to the DSDs group would allow the DSDs to meet the requirements without affecting the ability of the CSDs to meet theirs (because of the significant margins available in the current CSDs array).

Table 2: Equilibrium open cycle core parameters for one-batch approximation.

	BOL	**BOL**		**EOC**	
Core reloading pattern	**all**	**One-batch**	**One-batch**	**One-batch**	**One-batch**
Equivalent burn up position (EFPD)	**0**	**820**	weighted	**1230**	weighted
K_{eff}	1.01201	1.01197	1.01054	1.01043	1.00812
Reactivity (PCM)	1187	1183	1042	1032	803
Breeding gain	0.196	0.143	0.144	0.120	0.120
$^{239}Pu/^{238}U$ mass ratio	0.066	0.081	0.080	0.087	0.087
Void ρ in AC and plenum (PCM)	512	884	854	1017	1001
Doppler const. (PCM)	-1169	-1020	-1028	-959	-967
Void ρ in AC and plenum at Dopp. temp. (PCM)	638	991	962	1116	1101
Doppler const. by voided AC and plenum (PCM)	-921	-810	-816	-764	-771
β_{eff} (JEF 2.2) (PCM)	393	372	374	364	365
Λ (JEF 2.2) (μs)	0.446	0.418	0.422	0.409	0.413
β_{eff} (JEFF 3.1) (PCM)	401	380	381	372	373
Λ (JEFF 3.1) (μs)	0.446	0.418	0.422	0.409	0.413
Diagrid expansion (PCM/°C)	-0.847	-0.834	-0.838	-0.834	-0.835
Fuel expansion (PCM/°C)	-0.153	-0.141	-0.145	-0.142	-0.144
Cladding & wrapper expansion (PCM/°C)	0.137	0.168	0.165	0.178	0.177
Global coolant expansion (PCM/°C)	0.145	0.304	0.292	0.362	0.356
Global coolant expansion (PCM/g/cm^3))	602	1260	1210	1498	1473

Minor Actinide Transmutation for the oxide CONF2 configuration

During the first phase of the project, a wide range of both homogeneous and heterogeneous options for MA transmutation were studied on the basis of the “working horse” core. The options covered a wide range of transmutation rates.

For the optimised CONF2 core, two options have been considered among those from the previous phase: the first one refers to a low minor actinide transmutation rate and the second one to a high transmutation rate. These options are known as the HET2 configuration (low transmutation rate) and the HOM4 configuration (high transmutation rate).

As a minimum option for recycling of MAs, the ESFR core should be able of transmuting its own MAs. The configuration meeting this requirement is the HET2 configuration, where one ring of 84 radial blanket sub-assemblies containing fuel composed of 20 wt.% MA and 80 wt.% depleted uranium is added at the periphery of the core (Figure 4). For this configuration, addition of MA target sub-assemblies outside the active core will have a small impact on the reactivity coefficients of the core.

A high level of minor actinide consumption is provided by the HOM4 configuration. This configuration, indeed, is able of transmuting not only the MAs produced within the ESFR core but also the MAs accumulated by the thermal reactors. The HOM4 configuration consists of 4 wt.% of MA homogeneously dispersed in the core fuel. This configuration will have a greater impact on reactivity coefficients than the HET2 configuration.

These two boundaries configurations (HET2 and HOM4) allow covering a wide range of MAs transmutation capabilities and they also are able to cover the full range of impact of MAs transmutation on the safety performance.

More detailed analysis of the MAs transmutation capabilities of the oxide core for the HET2 and HOM4 configurations, using the CONF2 axial configuration, has been undertaken in the second phase of the work. The impact of MAs loading on safety, particularly sodium void reactivity worth and Doppler constant, in addition to the cores' efficiency in transmutation of MAs has been considered.

In addition to the standard HOM4configuration, which did not include MAs in the lower axial blanket, the CIEMAT analysis also considered loading of 4 wt.% of MA in the lower axial blanket (HOM4' case in Table 3) to further improve MAs consumption. The MAs loaded in the lower axial blanket does not have further impact on safety-related parameters, such as sodium void effect with respect to HOM4 configuration.

In Table 3, the actinide mass balance per isotopes and core regions are presented, while the impact of MAs loading on reactivity coefficients is summarized in Table 4.

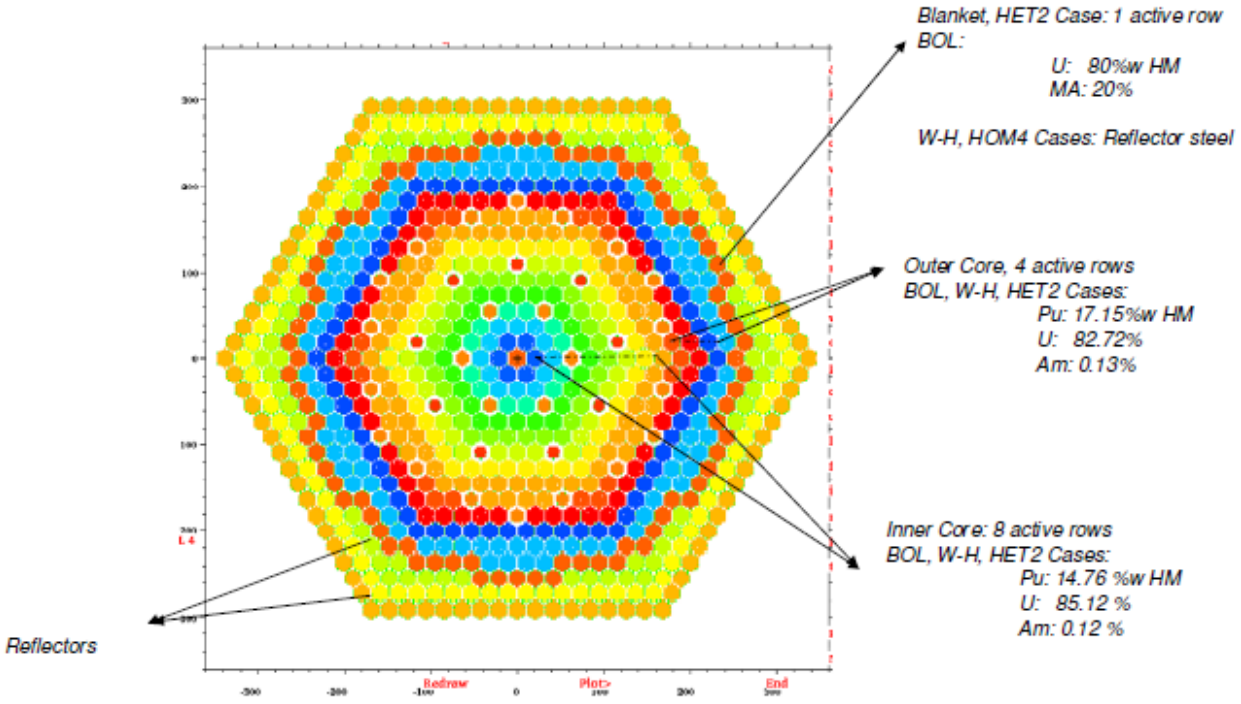

Fig. 4. MCNPX model, cross section view of the core: HET 2

The following conclusions can be drawn from this analysis:

- The HET2 configuration consumes approximately all self-produced MAs. In other words, this configuration is approximately neutral as concerns the MA balance: incineration/production. In more detail, there is a small net consumption of Neptunium and Americium and a small net production of Curium (see Table 3), this balance being affected by cooling time after uploading the fuel.
- The impact on safety of MAs in the HET2 configuration, as judged by the sodium void reactivity and Doppler constant, is minimal (see Table 4). As expected, the HOM4 configuration has a much higher MA consumption. After 2050 EFPDs, end of life of the fuel, the mass of transmuted MAs is about 870 kg within the active core. Including 4% MA in the lower axial blanket would increase the mass further by 175 kg. There is, however, a net Curium production in the core and lower blanket of approximately 214 kg at zero cooling time. It is important also to remark that the HOM4 reactivity variation due to burnup shows that the addition of MAs makes an important effect on the reactor breeding ratio, and hence on the reactivity swing (even making it positive) as a result of the increment of the amount of Pu, in particular due to the Am241-to-Cm242-to-Pu238 chain (see Figure 5).
- Homogeneous loading (HOM4) has a detrimental effect on the sodium void reactivity worth and Doppler constant: sodium void reactivity is increased by approximately 100 pcm (which means only 13% deterioration at EOC in terms of absolute reactivity) and the absolute value of the Doppler constant is reduced by approximately 140 pcm. It should be noted that with the reduction of the total sodium void reactivity in CONF2 as compared to the working horse design and the low

enrichment of the fuel, the absolute values of the sodium void reactivity and Doppler constant with homogeneous minor actinide content may still be acceptable. Transient analysis would be required before a final judgment could be made.

Table 3: Actinide mass balance per isotopes and core regions are presented

Mass balance (kg) (EOL-BOL)	**CONF2**			**HOM4'**			**HET2**			
	Inner Core	**Outer Core**	**Axial blanket**	**Inner Core**	**Outer Core**	**Axial blanket**	**Inner Core**	**Outer Core**	**Axial blanket**	**Radial blanket**
Total U	-4557.61	-3426.60	-1225.80	-3993.37	-3109.90	-951.30	-4649.62	-3206.60	-1223.90	-314.00
U234	5.10	6.67	0.01	11.02	12.50	2.23	5.04	6.88	0.55	4.67
U235	-52.72	-43.38	-21.80	-47.75	-39.93	-16.70	-53.31	-41.00	-21.61	-5.48
U236	11.77	10.29	5.58	10.80	9.50	4.21	11.84	9.76	5.51	1.33
U237	0.12	0.07	0.02	0.11	0.07	0.01	0.12	0.07	0.02	0.01
U238	-4515.88	-3401.10	-1207.10	-3968.15	-3093.30	-942.90	-4607.43	-3184.90	-1208.30	-313.00
Total Np	21.83	17.41	4.06	-112.18	-95.23	-31.33	21.98	16.84	0.07	-59.07
Np237	15.26	13.58	2.04	-118.25	-98.70	-32.94	15.46	13.17	-1.99	-59.55
Np238	0.02	0.01	0.00	0.14	0.09	0.05	0.02	0.01	0.01	0.08
Np239	6.55	3.82	2.02	5.91	3.38	1.57	6.50	3.66	2.00	0.41
Total Pu	415.47	-63.30	1007.20	575.67	105.65	930.64	415.63	-63.71	1048.15	549.50
Pu238	-85.63	-84.80	0.30	170.85	152.25	105.89	-86.85	-80.53	26.04	210.60
Pu239	680.99	306.34	943.01	569.23	214.73	753.08	683.24	304.59	947.47	262.62
Pu240	89.67	8.65	60.78	51.76	-11.80	50.41	91.47	-0.87	67.26	37.70
Pu241	-173.74	-204.89	2.96	-178.28	-208.81	1.76	-174.50	-204.04	2.83	0.79
Pu242	-95.89	-88.67	0.10	-37.37	-40.60	19.53	-97.93	-83.13	4.56	37.80
Total Am	112.04	132.89	0.23	-483.89	-372.39	-170.05	112.01	131.46	-39.60	-335.10
Am241	28.63	50.84	0.22	-468.91	-373.45	-149.91	27.82	54.67	-35.70	-297.90
Am242	0.03	0.02	0.00	0.15	0.10	0.05	0.03	0.02	0.01	0.08
Am42M	3.67	3.91	0.00	26.46	26.60	13.02	3.64	3.78	3.52	27.01
Am243	79.70	78.11	0.00	-41.69	-25.74	-33.23	80.50	72.99	-7.40	-64.49
Total Cm	37.58	27.97	0.01	106.11	81.50	26.27	38.51	24.87	-0.61	33.64
Cm242	5.04	4.09	0.01	30.09	20.96	10.16	4.96	3.95	2.16	16.80
Cm243	0.47	0.35	0.00	2.69	1.81	0.41	0.48	0.31	-0.09	0.06
Cm244	28.56	21.38	0.00	59.44	48.55	12.71	29.40	18.78	-3.05	13.20
Cm245	3.25	2.03	0.00	9.30	6.73	1.99	3.40	1.72	0.17	1.85
Cm246	0.24	0.12	0.00	4.07	3.08	0.91	0.26	0.10	0.17	1.55

Table 4: Impact of MAs loading on reactivity coefficients

	CONF2		HOM4’		HET2	
	BOC	**EOC**	**BOC**	**EOC**	**BOC**	**EOC**
Doppler (pcm)	-827	-772	-594	-629	-783	-717
βeff	370	362	346	338	368	359
Core void worth (pcm)	1516	1654	1712	1746	1517	1626
Core void worth ($)	4.10	4.57	4.95	5.17	4.12	4.53
Reactor void worth (pcm)	767	922	1061	1095	743	875
Reactor void worth ($)	2.07	2.55	3.07	3.24	2.02	2.44

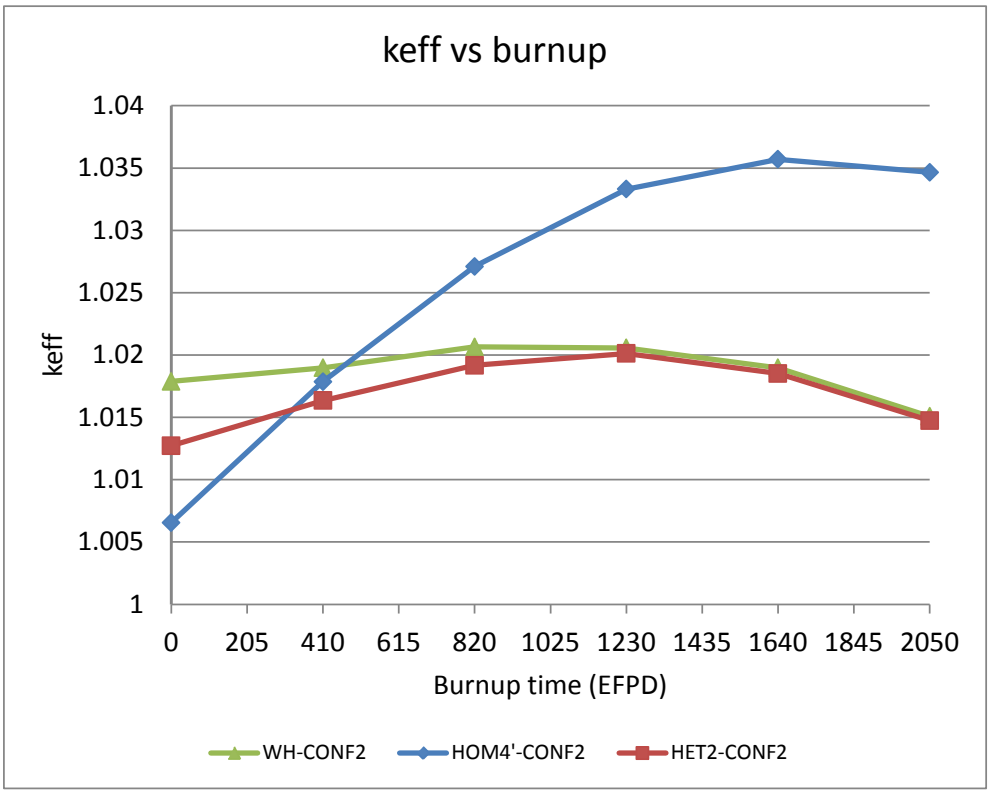

Fig. 5 Keff estimation with the single-batch approach in 2050 burnup days.

The impact of recycling options and corresponding actinide loadings on core decay heat and the design of decay heat removal systems were not included in the study.

IV.2 The Carbide Core

The Carbide Working Horse Core

A “working horse” carbide core was proposed by CEA at the beginning of the project. This core has a power output of 3600 MWth. Axially the core has a fissile height of 0.8m and contains upper and lower axial blankets made of steel. The fuel sub assembly consists of 331 pins in ODS steel clad with an outer diameter of 8.0 mm and containing a carbide fuel pellet of 6.87 mm outside diameter. The fuel pins are surrounded by a 4.5 mm thick hexagonal EM10 wrapper tube of 178.7 mm outside across flats. The sub-assembly pitching is 183.2 mm.

The performance of the carbide “working horse” core is rather different from that of the oxide core: it has a significantly higher reactivity loss with burnup and a much lower internal breeding gain.

Therefore, further modifications, in addition to the ones considered for the oxide core, were added. The more optimized carbide core is discussed in the followings.

Initial Optimization of the Carbide Core

The carbide “working horse” core is a less mature design than the oxide core and required further optimisation. The limits on fuel residence time were defined in the “working horse” core by the maximum clad damage permitted by ODS, which is 200 dpa. This leads to a peak fuel burnup in excess of 20%, which is rather optimistic for a type of fuel for which there is much less irradiation experience than for oxide. This should be considered to be an interim position until more information becomes available on carbide fuel performance.

The particular criteria for optimisation of the carbide core were as follows:

1. The reactivity loss between beginning and end of cycle should be reduced to a low level to limit the amount of reactivity that can be injected into the core on accidental withdrawal of one or more control rods.
2. The internal breeding gain of the core should be increased to a level similar to that of the oxide core (~0.02). This is consistent with the previous criterion.
3. Reduce the peak burnup of the fuel to ~15%, as already discussed.
4. Retain the safety advantages of the carbide core which arise from the high thermal conductivity of the fuel, i.e. normal operational fuel temperatures should be lower than those of the oxide core. This can be achieved by ensuring that peak linear ratings do not exceed those of the oxide core.

To reduce the large reactivity loss with burnup, the optimised core height was increased from 0.8m to 1.0m (like that of the oxide core) and the fuel pin outer diameter was increased from 6.87 mm to 8.5 mm. These two modifications have allowed the fuel enrichment to be reduced significantly with advantages in terms of reactivity loss with burnup: between start and end of equilibrium cycle, considering 3-batch fuel cycle, the reactivity loss is only 440 pcm.

The reduction of sodium void reactivity, studied particularly for the oxide core, would be expected to be equally applicable to the carbide core. A CONF2-like axial configuration has therefore been adopted for the carbide core.

The advantages of using carbide fuel arise from its higher density and greater thermal conductivity compared to the oxide option. The higher fuel pellet density permits low enrichment to be attained with a smaller fuel pin diameter than the oxide core. The higher thermal conductivity provides greater margin to fuel melting under hypothetical accident conditions, provided that normal operation linear ratings are maintained at similar levels to those of the oxide core. Both of these advantages have been retained in the optimised core design.

The specification of the optimised core is given in Table 5, where the design parameters are compared to those of the carbide “working horse” core.

The optimised core layout is given in Figure 6. Because the subassembly pitch has been reduced slightly, minor modifications have been made to the CSD and DSD rods designs. The revised dimensions have been determined by scaling of the carbide “working horse” core control rod dimensions.

Table 5 Optimised Carbide Core and Comparison with Carbide “working horse” Core

	Working Horse Core	Optimised Core
Number of Inner core S/A	168	225
Number of Outer Core S/A	246	228
Number of CSD	24	24
Number of DSD	12	9
Active Core Height (m)	0.8	1.0
SA Pitch (mm)	183.2	176.3
Sodium gap width inter assembly (mm)	4.5	4.5
Wrapper tube outer flat-flat width (mm)	178.7	171.8
Wrapper tube thickness (mm)	4.5	4.5
Wrapper tube material	FM Steel (EM10)	FM Steel (EM10)
Wire wrap spacer diameter (mm)	1	1
Wire wrap helical pitch (mm)	225	225
Wire wrap spacer material	ODS Steel	ODS Steel
Number of fuel pins per sub-assembly	331	271
Outer clad diameter (mm)	8.0	8.5
Inner clad diameter (mm)	7.0	7.5
Cladding material	ODS Steel	ODS Steel
Fuel pellet diameter (mm)	6.87	7.37
Fuel pellet material	(U, Pu)C	(U, Pu)C
Inner Core Fuel Enrichment (atom%)	17.8	14.05(1)
Outer Core Fuel Enrichment (atom%)	24.5	18.35(1)

Rod Worths for the carbide optimized core

An initial assessment of the control rod worth of the ESFR carbide core has been undertaken to ensure that shutdown can be achieved. Assessments of control rod worth for the primary (CSD) and secondary (DSD) were performed using MCNP [4] and include the determination of the worth curves as a function of rod bank insertion. As for the oxide configuration, the assessments were performed for Beginning of Equilibrium Cycle (BOEC) condition.

The results obtained are the following: 4875 pcm for CSDs (1 rod) and 2046 pcm for DSDs (1 rod).

The requirement to shut down to cold temperatures (100 °C) the optimized carbide core was calculated to be equal to 1585 pcm. The reactivity loss with burnup, that has to be taken into account by CSDs, is approximately 650 pcm, even for a single batch refuelling scheme.

Therefore, the total requirement to be managed by CSDs is about 2300 pcm. The results have shown that with the actual configuration, the CSDs have a significant margin even when allowing for uncertainty on the calculated values. The DSDs do not need to take up the reactivity loss with burnup since that is done by the CSDs but they have to shut down to sodium inlet temperature rather than cold condition. The requirement for DSDs calculated is less than 1600 pcm. With the array of 9 DSD rods used at present (2046 pcm in total) it is possible respect this requirement, allowing also for uncertainties on the calculated values.

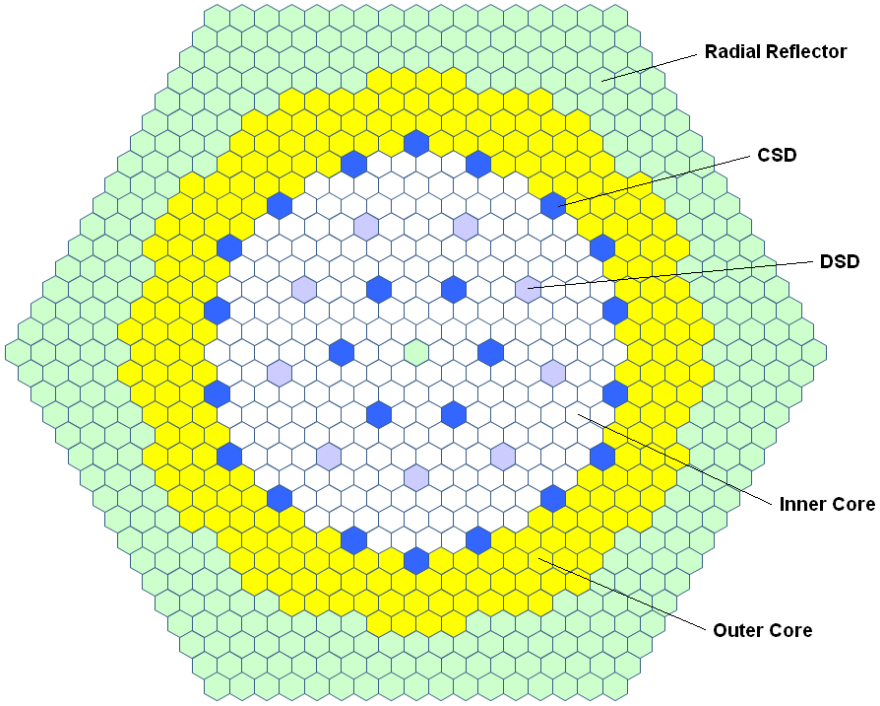

Fig 6. Radial view of optimised carbide core (225 IC + 228 OC assemblies)

IV.3 Comparison between the Oxide and Carbide Cores

With respect to the “working horse” carbide core, the optimized core has undergone significant changes to bring its performance closer to that of the oxide core. The adopted modifications have resulted in lower fuel enrichments, nearer to those of the oxide core, with a low reactivity loss over the fuel cycle. The similar performance of the oxide and carbide cores is achieved with a significantly smaller fuel pin diameter and fuel S/A pitch in the carbide core due to the higher density of the carbide fuel. However, at this stage the carbide core has not undergone the same level of optimization as the oxide core.

When comparing safety performance, characterized by sodium void and Doppler constant the carbide core is close to that of the oxide but not quite as good, even for CONF2-like optimized design with carbide fuel. CSDs absorber rod worths are similar but the DSDs array worth is higher in the carbide core than that for the oxide core. Modifications in the number of CSDs/DSDs for the oxide core were proposed.

Whilst fuel temperatures have not been assessed, the carbide core can be judged to have lower fuel temperatures during normal operation, because of the greater thermal conductivity of the carbide fuel, giving larger margins to fuel melt.

V. CONCLUSIONS

Significant progress has been made in optimising both the oxide and carbide ESFR cores.

The oxide “working horse” core already had a low reactivity loss over the fuel cycle, a benefit as concerns control rod withdrawal faults, so the optimisation process concentrated on the reduction of the sodium void reactivity effect and on the evaluation of MA burning performances. The CONF2 axial configuration has provided a significant overall reduction of the sodium void reactivity effect [2]. The working horse oxide core with the CONF2 axial configuration has been adopted as the optimised oxide core. With respect to this configuration, investigations of transient behaviours (i.e. ULOF, TIB) have been performed in the project (e.g. [3]) and supported conclusions made by reactor physics analyses.

The “working horse” carbide core had a significantly higher reactivity loss over the fuel cycle compared to the oxide one. By increasing slightly the fuel pin diameter, whilst still retaining the advantages of lower fuel temperatures of carbide fuel,

and making some changes in the core layout, the reactivity loss over the cycle has been reduced to a level similar to that of the oxide core. By adopting the CONF2 axial configuration initially developed for the oxide core, the sodium void reactivity of the carbide core has also been reduced appreciably.

The MA transmutation performances of the optimized ESFR oxide core have been investigated with respect to two boundary configurations. The HET2 configuration (where high content of MA are loaded at the periphery of the core in blanket SA) shows a low MA transmutation rate sufficient to burn the MA produced by the ESFR core (making the core neutral in MA production) without affecting the safety parameters. The HOM4 configuration (where 4%wt. MA are loaded homogeneously in each core SA) is the most challenging configuration due to its impact on safety coefficients but it shows an high MA burning rate suitable for burning also MA accumulated by a thermal reactor fleet.

REFERENCES

[1] G. L. Fiorini et al., Roadmap for a European Innovative SOdium cooled FAst Reactor – EISOFAR, EUR 23732, 2009.
[2] A. Rineiski, B. Vezzoni, D. Zhang, M. Marchetti, F. Gabrielli, W. Maschek, X.-N. Chen, L. Buiron, J. Krepel, K. Sun, K. Mikityuk, F. Polidoro, D. Rochman, A.J. Koning, D.F. DaCruz, H. Tsige-Tamirat, R. Sunderland, “ESFr core optimization and uncertanties studies”, Proc. Inter. Conf. FR13, Paris, France, March 4-7, (2013).
[3] M. Flad, D. Zhang, C. Matzerath Boccaccini, F. Gabrielli, B. Vezzoni, W. Maschek, H. Bonneville, “ESFR Severe Accident Analyses with SIMMER-III”, Proc. Inter. Conf. FR13, Paris, France, March 4-7, (2013).
[4] X-5 Monte-Carlo Team. MCNP—A General Monte Carlo N-Particle Transport Code, Version 5; Tech. Report; LANL: New Mexico, USA, 2003.

The European Lead Fast Reactor Strategy and the Roadmap for the Demonstrator ALFRED

Alessandro Alemberti[a], Luigi Mansani[a], Giacomo Grasso[b], Davide Mattioli[b], Ferry Roelofs[c], Didier De Bruyn[d]

[a] Ansaldo Nucleare, Genova Italy

[b] ENEA, Bologna Italy

[c] NRG, Petten The Netherlands

[d] SCK-CEN, Mol Begium

Abstract. The development of the technology for a new reactor must follow a chain of gradual and progressive steps to reach maturity. This paper presents the strategy for the development of a nuclear fast reactor with closed fuel cycle and based on lead coolant technology for economical electricity production: the European Lead Fast Reactor (ELFR). This reactor has the potential to multiply by two orders of magnitude the energy output from a given amount of uranium while improving the safety of the plant and the management of high level radioactive waste (HLRW) through the transmutation of minor actinides. The roadmap of ELFR is based on the progressive up-scaling from a zero power facility to the commercial deployment of the first-of-a kind plant. The intermediate steps are a Technological Pilot Plant (MYRRHA), a Demonstrator (ALFRED) and a Prototype (PROLFR). The roadmap of the demonstrator ALFRED is also presented.

1. Introduction

1.1.Nuclear energy potential to satisfy world energy needs

Today more than 2 billion people worldwide have no access to electricity. Current forecasts show that the world population will increase up to 9 billion people by 2050. All these people have an inalienable right to have better conditions of life, which primarily includes energy supply. Moreover demand for electricity is likely to increase significantly in the near future, as current fossil fuel applications are replaced by processes using electricity, for example in the transport sector. At the same time, the threats to the Earth's climate have never been so strong; sustainable development to address the future needs of humankind requires non CO2 emitting sources of energy. In that regard, while nuclear energy (as any other form of energy generation) will not be the whole solution, it has the chance to play a significant role, being an important part of the solution for the coming years and decades. Therefore, a strong and concerted action is required to develop appropriate technologies from the short term to the long term. Today, nuclear energy represents about 16% of electricity production in the world and about 30% in the European Union. More than 30 countries have already expressed to the IAEA their interest in getting support for the definition and realization of a nuclear program. The main nuclear reactor technology available today is the Light Water Reactor one, which relies on more than a thousand reactor-years of accumulate operation. For those countries already equipped with Generation II nuclear reactors, the main issue is to properly manage plant aging and power upgrades, in order to obtain the best economic value from their fleet, while keeping the highest standards of safety. New reactors (Generation III) are being built, decided upon, or planned in countries which are extending their nuclear fleet and in countries that are "new comers" to nuclear energy.

1.2.Need for fast reactors

The competitiveness of nuclear fission technologies, together with the questions raised on the management of spent fuel and radioactive waste, being key short- and medium-term issues and are addressed by the Strategic Energy Technology Plan of the European Union (SET Plan). The present known resources of cheap uranium represent about 100 years of consumption with the existing reactor fleet. However, depending on the growth rate of nuclear energy worldwide, the question of uranium resources will be raised; therefore, it is reasonable to anticipate, as foreseen by the SET Plan, the development of fast neutron reactors with closed fuel cycle. These technologies have the potential to multiply by a factor of 50 to 100 the energy output from a given amount of uranium (with a full use of U238), while improving the management of high level radioactive waste, through the transmutation of minor actinides. Fast reactors are therefore potentially able to provide energy for the next thousands of years, with the already known cheap uranium resources. Fast reactors attractiveness has been recognized since the beginning of the nuclear era, so that Fast Reactors have quite a long history of research and development. Together with United States, Russia, Japan and India, Europe supported an active development of Sodium cooled Fast Reactors (SFR) from the 1960s to 1998. No less than seven experimental demonstration and prototype reactors were built and operated over this period in France, United Kingdom and Germany. However, the industrial development of SFRs stopped in Europe when the political decision was taken in February 1998 to abandon Superphénix. It had stopped earlier in the United States with the Non Proliferation Act promulgated in 1978. Russia proceeded with the development of SFRs in spite of budget constraints and it is expected to put BN-800 (750 MWe) in service in 2014 and BREST-OD-300 (300MWe) in 2020. India and China, both have aggressive agendas to develop light water reactors and SFRs. India has plans to start a prototype fast reactor (PFBR, 500 Mwe), expected to start commissioning in 2013. China has built an experimental reactor (CEFR, 20 MWe), which has reached the first criticality in 2010.

1.3.Generation IV Fast reactors

European stakeholders have agreed to develop Generation IV fast neutron reactors. These Generation IV reactors will explore the opportunities of providing an economically and publicly acceptable electricity supply in many markets and broadening the opportunities for the use of nuclear energy. Generation IV reactors are required to reach high standards in the areas of sustainability, proliferation resistance and physical protection, safety and economics. Recently, the European Union launched the Sustainable Nuclear Energy Technology Platform (SNE-TP) to propose a vision for the short, medium and long term development of nuclear fission energy technologies. The Strategic Research Agenda of SNE-TP explicitly refers to fast reactors developments as follows: for the longer term objectives of ensuring that Europe will have a low carbon energy mix and a more secure energy supply by 2050, the next technological path identified in the SNE-TP Vision Report and being further elaborated in the Strategic Research Agenda is the development of Generation IV fast neutron reactors with closed fuel cycle. Also the European Sustainable Nuclear Industrial Initiative (ESNII) focusing on the preparation of a more sustainable nuclear energy scenario refers to the development of fast nuclear reactors. The main advantages of such systems over current reactor technology are their improved use of resources, and the reduced volume, long-term radio-toxicity and thermal load of final waste, which is to be disposed in geological repositories. The research efforts for Generation IV technology are already underway in different EU countries, but they need to be strengthened and focused to achieve major technological breakthroughs, notably through the construction of technology demonstrators and reactor prototypes. European stakeholders, part of ESNII, have identified three fast spectrum systems that were the most likely to meet long-term Europe’s energy needs in terms of security of supply, safety, sustainability and economic competitiveness: the Sodium-cooled Fast Reactor (SFR) as a first track, aligned with Europe’s prior experience, a short term alternative fast neutron reactor technology the Lead-cooled Fast Reactor (LFR) and the Gas-cooled Fast Reactor (GFR) as a long term alternative. Even though only SFRs led to prototype so far, all types of fast reactors have been selected for their comparable potential for making an efficient use of uranium and minimising the production of high level radioactive waste.

1.4.Lessons from the Fukushima evenst

As world-wide known, the incredible earthquake and the following tsunami that destroyed the north-east costs of Japan on March 11th, 2011, also stroke the Fukushima Dai-ichi NPP, originating a complex accident sequence on the three operating reactors, out of the six the site hosts. Despite the huge efforts – based on competence and real heroism actions of the emergency personnel against the complexity of the situation – spent to achieve a slow, but progressive control of the reactors, the consequences of this severe accident are in front of everybody: about two hundred thousands of people have been evacuated from their houses, a lot of them continuing to live in improvised shelters with low comfort and privacy. Two orders of lessons must be gathered from the analysis of the accident causes and effects, on public and technical levels. A great emotional reaction has turned anti-nuclear sentiment in the public opinion, which is no more disposed to accept the consequences of any kind of accident to a nuclear facility. Concerning the technical aspects, the Fukushima events showed that an accident sequence might be more complex, or lasting in time than foreseable, requiring the need for stressing the simplicity and reliability of safety systems and emergency procedures. It is definitely clear that the nuclear scientific community is therefore asked to pay a major attention to the safety aspects at large. In this frame, research and development for Generation IV systems should offer the required answers to the legitimate concerns of the general public, providing the aimed perspective that today is necessary for the further development of nuclear energy in the future.

1.5.The Lead Fast Reactor (LFR)

In the Generation IV technology evaluations, the LFR system was top-ranked in sustainability because of its capacity at effectively employing a closed fuel cycle, and in proliferation resistance and physical protection thanks to the possible operation of long-life cores. It was rated good in safety and economics. The safety was considered to be enhanced by the choice of a relatively inert coolant. The LFR was primarily envisioned for missions in electricity, hydrogen production and actinide management. In Europe, a major step in favor of the LFR development occurred when EURATOM decided to fund ELSY (the acronym for the European Lead cooled System) – a Specific Targeted Research Project of the 6th European Framework Programme (FP6) – proposed to investigate the economical feasibility of an industrial size (600 MWe) Lead-cooled Fast Reactor for electricity production with closed fuel cycle. This project developed a very innovative pre-conceptual design of an industrial plant, that met most of the design objectives originally proposed.While it solved some of the key technological and design issues, others still remained open and needed further investigations.

1.6.The LFR safety features

Among Generation IV requirements there is the possibility to avoid an off-site management plan: it implies that even very low probability events will have to be considered in future reactors design. LFRs have peculiar characteristics that facilitate the management of emergency situations. First of all the Fukushima events have shown how in case of loss of ultimate heat sink, for instance due to natural disasters, very few resources are readily available for emergency cooling of reactors: among these, air and water are the most readily available in any nuclear site. As lead does not react with these fluids emergency cooling is greately facilitated. As a second point, complete station blackout events can be effectively managed in LFRs thanks to the design of passive systems for decay heat removal which is permitted by the physical and chemical properties of the lead coolant. Finally, the need to avoid chemical reactions, that lead to hydrogen formation, can be easily met in LFRs, by employing structural materials that are inert in lead environment. In synthesis, the combination of lead coolant inherent characteristics and plant design features, specifically developed to face identified challenges, show a large potential for a very robust and forgiving design, even in very extreme conditions.

2. R&D needs

2.1.Need for technology breakthroughs

Technology breakthroughs and innovations are needed for all Generation IV fast reactors. Innovative design and technology features are needed to achieve high safety and security standards, to minimise waste and enhance non-proliferation through advanced fuel cycles, as well as to improve economic competitiveness, especially with a high availability factor. In particular, structural materials and innovative fuels are needed to sustain high fast neutron fluxes and high temperatures, as well as to comply with innovative reactor coolants. The development and qualification of new fuels also requires significant R&D effort in terms of resources and time.

2.2.Key R&D topics

To achieve the commercial availability of all Fast Reactors technologies by 2040, it is vital to continue and accelerate R&D on key topics, primarily: primary system design simplification; improved materials and innovative fuels; improved safety (safety standards not inferior to Gen III ones); innovative heat exchangers and power conversion systems; advanced instrumentation and in-service inspection capabilities; reduction of the plant costs; partitioning and recycling processes; plant availability improvement. In particular the work in the area of partitioning and transmutation with innovative fuels, core performance and associated fuel cycle studies will lay the groundwork for assessment of future sustainable nuclear fuel cycle strategies. Whether and to what extent it should involve transmutation in dedicated waste-burning Accelerator Driven Systems or in future Generation IV power plants needs to be assessed. Specifically focusing on LFRs, the main challenges for their feasibility are: corrosion and erosion of structural materials; erosion in primary pump; seismic risk due to large mass of lead; in-service inspection of core support structures and possibility of replacing internal components; refueling at high temperature in lead; spent fuel management by remote handling; managing of the Steam Generator Tube Rupture inside the primary system; prevention of flow blockage and mitigation of core consequences; radiation damage (at high temperatures); development of measuring devices.

Corrosion and erosion - The use of existing industrial materials for the primary system is possible by limiting the core outlet temperature but new materials need to be used for special components (e.g. pump impellers). The present technological solutions are the use of low carbon grade austenitic steels for components at relatively low temperatures and low irradiation fluence, e.g. the reactor vessel, and the use of ferritic-martensitic steels for fuel cladding and core structures. Techniques for coating of steam generators tubes, fuel cladding and core structures operating at high temperature need further development. R&D needs come from the qualification of: an austenitic steel for the reactor vessel, a lead corrosion and erosion resistant material for the in vessel structure, a protective coating for fuel cladding and steam generator tubes, special materials corrosion and erosion resistant for the impeller of the mechanical pumps.

Seismic risk - The mass of lead can be kept low by means of an innovative layout (e.g. Steam Generating Units and Primary Pumps installed in the reactor vessel). In such a configuration seismic loads defined by the European Utility Requirements can be accommodated by means of 2D seismic isolators of the reactor building. An application of the existing seismic isolators technology to LFR is ongoing in a specific FP7 project (SILER) started on 1st of October 2011 [1].

Refuelling - The fuel assemblies can be fitted with an extended stem to permit fuel handling, using a simple handling machine that operates in the cover gas under full visibility. This eliminates in-vessel fuel transfer equipment which has never been designed or tested in lead. The problem of refueling can be considered solved by design, so no specific research activities are needed.

Purification and inspection - The use of molten lead as coolant implies also research focused: i) on the development and validation of a technique for lead purification before reactor vessel filling and with reactor in operation to prevent/control slag/aerosol formation, ii) on the development and calibration

of instrumentation operating in lead and under irradiation, iii) on the development of techniques and instrumentations for in-service inspection of the steam generator tubes and the reactor vessel and iv) on the development and validation of oxygen control techniques for regulating oxidation kinetics.

Fuel cycle - Significant R&D efforts should be focused on innovative fuels and fuel cycle (minor actinides bearing fuels, homogeneous reprocessing techniques). In the near term an essential goal is to confirm that ready-to-use technical solutions exist, so that fuel can be provided in time with the operation of the first installation. In the mid-term, it is necessary to confirm the possibility of using advanced MA (Minor Actinide)-bearing fuels and to confirm the possibility of achieving high fuel burn-ups. In the long term, it is important to confirm the potential for industrial deployment of advanced MA-bearing fuels and the possibility of using fuels that can withstand high temperatures to exploit the advantage of the high boiling point of lead.

Research and testing facilities - To meet the R&D challenges presented in the previous section, several facilities are necessary. Therefore the following actions are required: i) design, construction and operation of the necessary irradiation tools and devices to test materials and fuels; ii) design, construction and operation of the necessary fuel fabrication workshops, dedicated to uranium-plutonium fuels, and MA-bearing fuels; iii) design, construction, upgrading and operation of a consistent set of experimental facilities for component design, system development, code qualification and validation, that are essential to perform design and safety analyses of the demonstration program (e.g. hot cells, gas loops, liquid metal loops).

Experimental irradiation capacities - There is a clear need to update European irradiation facilities, given that existing facilities are close to end of life. New facilities are currently in construction or design phase in Europe: i) JHR, the Jules Horowitz Reactor (Cadarache, France) dedicated to materials testing for nuclear fission; its construction has started in March 2007, the start of operation is foreseen in 2014. ii) PALLAS (Petten, The Netherlands), a 'tank-in pool' reactor with a high neutron flux, a power of 45-80 MW and an annual degree of utilisation of more than 300 full-power days, equipped to meet the demand for both nuclear knowledge and services and the production of essential medical isotopes. PALLAS will substitute the existing HFR. According to the present plans, PALLAS could be in full operation in 2023. iii) MYRRHA (Mol, Belgium), a flexible fast neutron irradiation facility, able to test both lead coolant systems and accelerator-driven sub-critical systems (ADS) for transmutation.

Beyond the availability of these irradiation capacities, it is necessary to develop new experimental devices taking into account cutting-edge progresses in modelling, instrumentation and modern safety standards.

Experimental facilities for reactor physics - Development of dedicated experimental facilities for reactor physics in fast reactor systems for component design, system development and code qualification and validation is necessary. GUINEVERE, a zero power lead reactor already in operation in Belgium, and ELECTRA, a lead-cooled education and training reactor in its design phase in Sweden, are such kind of machines.

Other experimental facilities - R&D demands further experimental facilities for: i) LFR materials, coolant physics-chemistry and corrosion/erosion studies; ii) LFR safety experimental studies; iii) LFR studies of moving mechanisms, instrumentation, maintenance, in-service inspection and repair; iv) LFR studies in thermal hydraulics and heat transfer.

Fuel reprocessing capacity - Existing large research facilities (ATALANTE at CEA in France, ITU at JRC in Germany, the Central Laboratory at NNL in the United Kingdom) offer effective potentialities at lab-scale in the short term. They should be used in the future to develop suitable processes and to perform demonstration runs on samples of spent fuel, or on irradiated targets up to pin-scale. For oxide fuel processing, minor actinide recovery processes, under development at lab-scale, mainly rely on well-known and industrially mature solvent extraction technologies. The important background coming from industrial plant feedback, or from the very important work carried out over past decades

to design modern reprocessing plants, make extraction a well-mastered technology. Therefore, considering that there are no important issues for scaling-up hydro-metallurgical processes, the requirements in this field could be postponed. The present reprocessing capacity may represent a bottleneck in the future, due to the overlapping of the time schedules for the development of the SFR and LFR (MYRRHA and ALFRED).

Fuel manufacturing capacities - Beside existing facilities (ATALANTE, ITU, Central Laboratory facility), it is important to improve capability in the field of experimental fuel fabrication. A Prototype Core Facility (PCF) will be needed in a short time, for the production of the MOX fuel to be loaded into the core of the fast reactors prototypes, demonstrators and experimental. An industrial facility is under preliminary design in France by AREVA and CEA. A pin-scale facility will be also needed, able to provide in an efficient manner the (very diverse) experimental pins to be irradiated in experimental facilities during the early phases of the design of possible future fuels (MA-bearing fuel, other than oxide fuel). Such a facility could be located in existing hot labs. The goal is an efficient, modern and flexible tool with the capacity to produce from a few pellets up to a few pins per year, to address the many and diverse experimental needs expected from the R&D fuel research community.

3. The LFR Road Map

The main drawback facing the industrial deployment of a LFR fleet in Europe is the lack of operational experience gathered so far. Whilst a satisfactory technological readiness has been achieved in Russia in the past century, driven by military research, the aim at filling the technology gap in Europe requires the setting up of a complete R&D roadmap, in complete analogy with what has been done in France for the development of the SFR technology chain, whose readiness is almost proven.

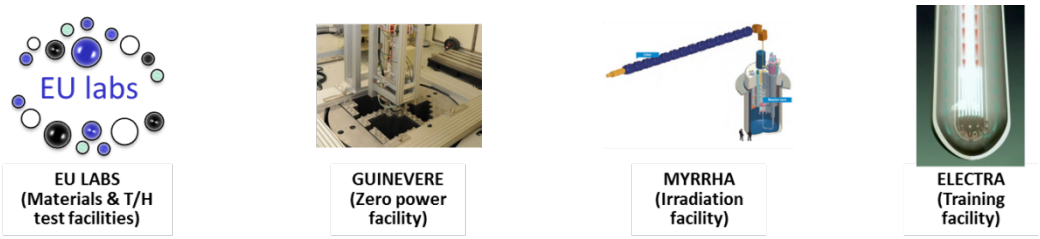

FIG. 1. Facilities for LFR technology development.

Besides all the existing and planned EU lead labs, as well as the further facilities envisaged for fullfilling the technology gaps in thermal/hydraulics, materials development and corrosion testing, a complete set of nuclear facilities is needed to bring the LFR technology to industrial maturity (Fig. 1). In this frame the following facilities are well fitting: GUINEVERE, the zero-power facility operating in Mol (Belgium) since 2010; MYRRHA, the irradiation facility to be built and operated in Mol and the European training facility ELECTRA, planned for realization in Sweden.

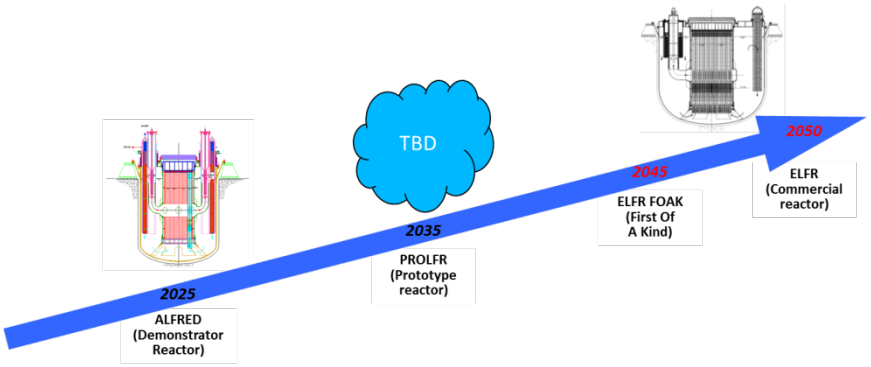

FIG. 2. LFR Roadmap towards industrial deployment.

In this sense, the approach to the industrial maturity is based on the concept of progressive upscaling, assuming the zero-power GUINEVERE as the starting point. The LFR development roadmap (see Fig.

2) requires at first a small Demonstrator reactor (ALFRED) for proving the viability of reliable electricity production for LFR systems. A Prototype reactor (PROLFR) is then envisaged, for testing the scaling laws at an intermediate step – according to a common approach focused both on plant size and representativeness of the target reference system – before moving to the First-Of-A-Kind (FOAK) representative of a commercial ELFR fleet. A brief description of the main nuclear facilities envisaged in the LFR roadmap is presented below.

LFR Zero Power Facility (GUINEVERE) - GUINEVERE is a test fast reactor coupled with an accelerator, already in operation since 2010 and constructed by SCK•CEN in cooperation with European partners. It is a zero power facility designed for core design qualification and reduction of design uncertainties (critical mass, power distribution as well as reactivity coefficients).

LFR European Technology Pilot Plant (MYRRHA) – MYRRHA [2] is a research fast reactor cooled by Lead- Bismuth Eutectic (LBE) with a power of 70 MWth when operated in sub-critical mode (as an accelerator driven system) and a power of 100 MWth when operated in critical mode. It employs a MOX fueled core. The main mission of MYRRHA is to test both technologies of fuel and heavy liquid metals, and the endurance of materials, in-service inspection and repair, components and systems to control industrial risks (obtain reactivity feedback at power) for the PROLFR and the ELFR. Comparing the scope and specifications, the calendar and the current status of the project MYRRHA will fulfill the role of the LFR European Technology Pilot Plant (ETPP, with no need for electricity production). The realization of MYRRHA will include several phases (2010-2024): Front End Engineering design, tendering and procurement, construction of component and civil engineering, on site assembly, commissioning, progressive start-up and finally full exploitation. The completion of the design phase is planned for 2015. The construction and commissioning is expected in 2022 with full operation in 2025. In parallel, the support R&D program will provide during the 2010-2014 period the necessary answers to the remaining technical challenges. After 2014, the fuel qualification and to a lesser extent the material qualification will remain the main topics of the R&D support program. The completion of fuel and material qualification processes is expected in 2020.

LFR European Technology Demonstration Reactor (ALFRED) – ALFRED, as LFR ETDR, will have to demonstrate the viability of the LFR technology for use in a future commercial power plant, construction and operation to the largest extent. It is also expected to significantly reduce uncertainties in construction and licensing. It will be the first system of the technology chain connected to the electric grid, hence allowing global evaluations on the plant responses to the grid needs. To fully exploit its role, taking the maximum advantage possible while respecting the tight schedule for the full development of the LFR technology in due time, two operating phases are envisioned, thus acting also as multipurpose research infrastructure. The first one, starting in 2025, will be devoted to proving the technology at large, with technological solutions already available to speed up the construction and licensing so to anticipate as much as possible the retrival of feedback for the design of the other systems in the technology chain, with a specific focus on the PROLFR. The second operation phase, starting in 2035 after a refurbishment of the facility, will be devoted to the specific mission of proving the more advanced solutions to be implemented in the industrial scale ELFR. A more detailed description of the ALFRED roadmap is provided in the following dedicated section.LFR prototype (PROLFR) – The need for this intermediate step emerged within the LEADER project from the consideration to limit as much as possible any big step in the power upscaling. Its power, of the order of 300-400 MWe, and its characteristics will be therefore between the ones of ALFRED and the ELFR.

First Of A Kind European industrial size LFR (ELFR FOAK) – Design and construction of the first of a kind 600 Mwe industrial reactor is foreseen in 2035 to start with LFR industrial plants building up at the horizon of 2040-2050. The reactor design parameters and characteristics are the same as in ALFRED with few exceptions. Electric power is 600 MW. Fuel is MOX with equilibrium MA content and an enrichment ensuring the isobreeding of Pu. The target value for maximum discharge burnup is 100 MWd/kg-HM. The target secondary system efficiency is close to 42%.

LFR Education and Training facility (ELECTRA) – ELECTRA is a low power fast neutron reactor cooled by liquid lead whose design has been presented by KTH. Application of (Pu,Zr)N fuel permits to design a core with very small volume and fuel column height, resulting in highly negative coolant, fuel and structure temperature coefficients and very low channel pressure drop. Full design power of 0.5 MWth can be completely removed by natural circulation in the primary circuit, thus eliminating the need for pumps. Analysis of flow stability and performance under unprotected transients show that the suggested design is highly safe. ELECTRA's mission is in training and education. In particular it could be employed for training operators and staff of the other LFR systems in the roadmap, such as MYRRHA and ALFRED. In addition it could be employed for research on reactor dynamics. The main milestones for ELECTRA completion include the construction and operation of an electrical mockup at KTH in scale 1:1 in 2013-2014; the completion of the engineering design in 2016; the carrying out of irradiation experiments for licensing of cladding and fuel in 2012-2020 and the licensing for operation of ELECTRA in 2022.

Fig. 3 shows how all the components of LFR development described above combine to an overall LFR roadmap.

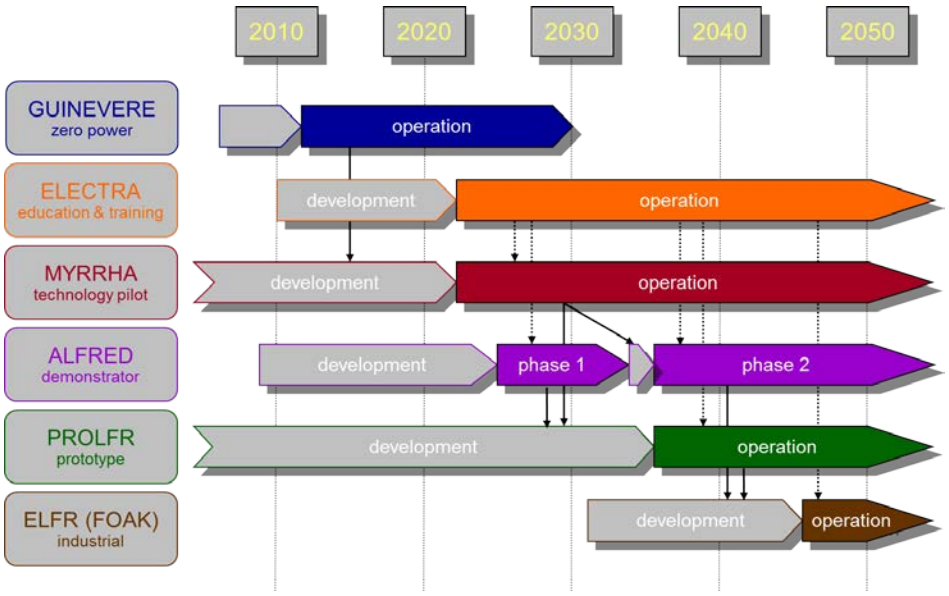

FIG. 3. Overall roadmap for deployment of a European LFR.

4. The ALFRED Roadmap

As widely described in two companion papers [3] [4], ALFRED (see Fig. 4) is a pool type LFR of ~125 MWe (300 MWth). Being the demonstration of economical and reliable electricity generation a key goal, the reactor core and primary coolant path should be as prototypical as possible, as well as the secondary circuit and the Balance of Plant (BoP). The primary coolant is pure lead in forced circulation. It can be cooled by natural circulation in emergency conditions. The core inlet temperature is 400°C and the average core outlet temperature is 480°C. The secondary coolant is water-superheated steam with the feed-water temperature of 335°C, the steam temperature of 450°C and the pressure of 18 Mpa. The secondary system efficiency is about 41%. The reactor vessel is in austenitic SS. The safety vessel is anchored to the reactor pit. The core barrel – cylindrical and integral with the core support grid and the hot collectors – is designed so as to be removed. The steam generators – at least for the first operation phase – are bayonet type with double walls and they are integrated in the reactor vessel and removable. Primary pumps are mechanical, installed in the hot collector and removable as well. The fuel assembly is closed hexagonal, extended up to the cover gas to allow its weighting down when primary pumps are off; when primary pumps are on, a spring coupling with the top diagrid forces the FAs in position. The fuel is traditional MOX (Pu enrichment below 30%), designed to comply with the aimed maximum discharge burn-up of 100 MWd/kg-HM. The cladding

material for the first operation phase is coated 15-15/Ti, to speed up the qualification of the fuel elements. For the second operation phase, advanced cladding materials (like ferritic-martensitic steels or oxide-dispersed steels, ODS) are envisioned, as for the ELFR. Control/Shutdown systems are two, diverse and redundant, derived from the MYRRHA design developed in the FP7 Central Design Team (CDT) project: the 1st system is made of pneumatically inserted absorber rods to be passively actuated by depressurization from the top of core; the 2nd system is made of buoyancy-driven absorbers rods passively inserted from the bottom of the core.

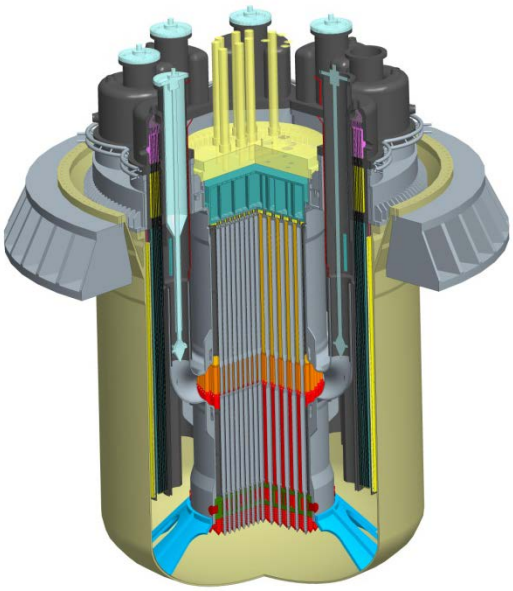

FIG. 4. 3D view of the ALFRED reactor block.

Within the LEADER project the design of the ALFRED is on going while the main suitable characteristic and design guidelines for the facility have been identified. A scaled demonstrator fully representative of the industrial size reactor is being designed, using components/technologies already available in the short term, to be able to proceed in the near future to a detailed design followed by the construction phase. The realisation of ALFRED will include several phases (2010-2025), as shown in Fig. 5. The first step is identified in the set-up of an international consortium (2013), while the choice of a dedicated site for construction has been already performed (Pitesti in Romania). In parallel several design activities should be running: basic design, siting and pre-licensing in the period 2013-2016 and detailed design and licensing in the period 2016-2019. Finally construction of components and civil engineering, on site assembly and commissioning (2019-2025). The completion of the design phase is presently planned for 2019 to be able to exploit the synergies with the design of MYRRHA. In parallel, the support R&D program will provide, during the 2011-2018 period, the necessary answers to the remaining technical challenges.

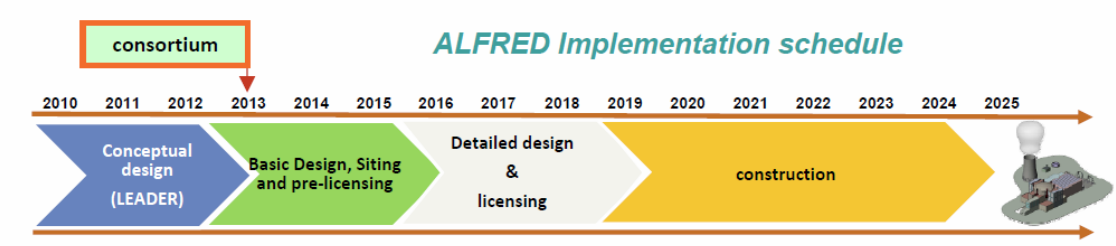

FIG. 5. ALFRED Implementation schedule

5. Expected Impacts

A huge potential increase in the sustainability of nuclear energy will be achieved through demonstrating the technical, industrial and economic viability of Generation IV fast neutron reactors,

thereby ensuring that nuclear energy can remain a long-term contributor to a low carbon economy. This demonstration program will play a key role by involving European industry and maintaining and developing European leadership in nuclear technologies worldwide. It will also make possible the further commercial deployment by the European industry of these technologies by 2040 and beyond. This is the prime goal for industry, which in the mean time will seek to maintain at least a 30% share of EU electricity from currently available reactors for the benefit of the European economy (the industrial needs for nuclear energy could be enhanced with an expansion towards co-generation of process heat for industrial applications when such markets develop). With the construction and operation of a LFR ETPP (MYRRHA) and ETDR (ALFRED), Europe will be in an excellent position to secure the development of a safe, sustainable and competitive fast spectrum technology. The program will allow to investigate and address the main technological issues that can then be implemented in the LFR prototype around 2020-2035. This LFR prototype, in turn, will pave the way for industrial deployment of industrial LFRs by 2050, and hence contribute significantly to the development of a sustainable and secure energy supply for Europe from the second half of this century onwards.

ACKNOWLEDGEMENTS

The authors acknowledge the European Commission for funding the LEADER project in its 7th Framework Programme. Acknowledgment is also due to all the colleagues of the participant organizations for their contributions in many different topics.

REFERENCES

[1] Forni M. et al., “SILER: Seismic-Initiated events risk mitigation in Lead-cooled Reactors”, International Congress on Advances in Nuclear Power Plants (ICAPP’12), Chicago, Illinois, 24-28 June 2012, American Nuclear Society.

[2] Aït Abderrahim, H., et all., “MYRRHA, a multi-purpose fast spectrum research reactor”, Energy Conversion & Management, Volume 63, 4-10, 2012

[3] Alemberti A., et al., “The Lead fast reactor - Demonstrator (ALFRED) and ELFR design”, International Conference on Fast Reactors and Related Fuel Cycles: Safe Technologies and Sustainable Scenarios (FR13), Paris, France (2013).

[4] Grasso G. et al., “Demonstrating the effectiveness of the European LFR concept: the ALFRED core design”, International Conference on Fast Reactors and Related Fuel Cycles: Safe Technologies and Sustainable Scenarios (FR13), Paris, France (2013).

A New Design Option for Achieving Zero Void Effect in Large SFR Cores

D. Verrier, A.-C. Scholer, M. Chhor

AREVA NP, Lyon, France

Abstract. *Sodium void effect reduction is a leading objective when designing a fast reactor core. Core design solutions allow reaching a global zero void effect, for instance the CFV concept recently promoted by CEA in France. With the same objectives AREVA has identified and developed an alternative design option, called TOPAZ, which is favorable for achieving a zero void effect in large power cores while preserving core performances and core size. TOPAZ design involves asymmetrical axial zoning of Pu content in the fuel column. Neutron studies have showed that TOPAZ is effective in case of usual fissile height values around one meter like typically applied in large power Fast Reactor cores.*

The paper presents the principle of the new TOPAZ design option and its application in the case of a 3600 MW SFR core. Main core performances are presented and benefits are exhibited.

1. Introduction

In France a coordinated R&D program [1] on Sodium-cooled Fast Reactor (SFR) technology has been launched in 2006 by CEA, AREVA and EDF. The technical program is consistent with the Gen IV International Forum guidelines. During the past six years progress was made in the field of core design with the objective to improve core safety, especially by minimizing the risk of inadvertent reactivity insertion. Consequently main core design efforts have been focused on the minimization of two parameters: the reactivity excess necessary to operate the reactor and the sodium void reactivity. A first stage of progress has been achieved by using an innovative fuel pin bundle based on a very compact bundle of fat pins. This resulted in the SFR V2b core design [2] developed by CEA. As such the SFR V2b design fully answers the minimal reactivity excess requirement and improves the sodium void reactivity; nevertheless void reactivity still remains positive at about 5$. In that regard a second dramatic stage of progress has been completed by CEA in 2010 with the development of the CFV core concept [3]. This innovative concept allows reaching a zero or negative sodium void effect, even in large cores, while preserving other neutronic performances. As such it offers a real opportunity to strengthen the safety demonstration of future SFR cores.

AREVA is directly involved in and contributes to this R&D program since 2006. Since the development of the CFV concept by CEA, AREVA has been working on its optimization especially for its application to large power commercial SFRs. In 2011 AREVA has identified a design variant to the original CFV concept which could ease its implementation on large cores: this is the TOPAZ concept which is presented hereafter. Prior to the presentation of TOPAZ, a summary of the CFV concept is given. Then the TOPAZ principle is introduced and illustrated with an example of implementation on a large power SFR. Before concluding identified open issues are mentioned.

2. Reminder: original CFV design

The following is largely based on technical data presented by CEA in papers [3] and [4].

2.1. A strong reduction of void worth

The sodium void worth can be broken up into the absorption and leakage components. The absorption component is basically positive in plutonium fueled cores, all the more since the core volume is large. The leakage component is negative. In very small cores it can compensate for the absorption component but usually, above one cubic meter core volume, it cannot. Consequently in standard power SFR reactors the void worth is positive.

The CFV concept consists of a core design with a reinforced leakage component. The principle is to enhance neutron leakage when necessary, that is in voiding condition: neutron propensity for escaping from the active core is strongly favored when coolant density decreases. The CFV concept is successfully achieving that through the combination of three essential design features: first the use of a thick sodium plenum closely above the core fuel zone; second the use of an absorbing zone just above the sodium plenum; third an axial heterogeneous fuel zone with an appropriately disposed internal fertile slab. The latter is related to the very fuel column design while the two formers concern the design of the region above the active core zone.

The sodium plenum is placed where sodium coolant is hot and where boiling is expected to occur first in case of a heat-up transient. A sufficently thick plenum placed a the top of the fuel zone is known to strengthen neutron leakage when voiding. The presence of an absorbing material just above the plenum prevents escaping neutrons to return to the core and thus optimizes the role of the plenum. In the following the sodium plenum topped with an absorbing material is called *optimized sodium plenum*. The role of the fertile slab in the fuel column is to axially distort the flux distribution so as to increase the importance of the flux at the Core / Sodium Plenum interface. This last option really magnifies the sodium plenum effectiveness.

Base core geometry of the CFV is illustrated in Fig. 1 [3]. A different fuel column height with an homogeneous axial arrangement is considered in the outer core zone in order to complete the optimization of core performances but this plays a little part in the void effect. The very benefit of the CFV on void effect really lies in the axial arrangement of the inner core zone.

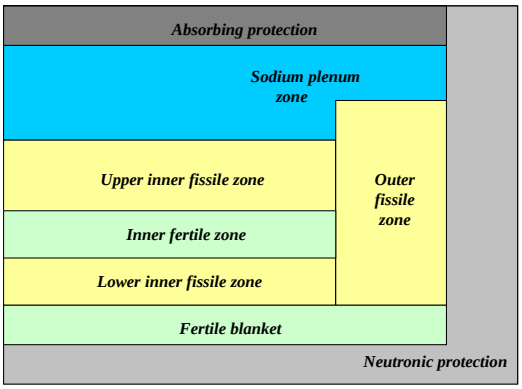

FIG. 1.Core geometry of CFV design

Examples of application of the CFV are given in [3] in case of a 2400 MWth SFR and in [4] in case of a 1500 MWth SFR. Compared to standard homogeneous cores the CFV solutions show a strong reduction of the total sodium void worth from about +5$ to less than -1$. Details [3] of the void components given in Table 1 clearly exhibit that the change comes from the leakage component which contribution is roughly multiplied by five while the absorption component remains almost unchanged.

Table 1. Comparison of sodium void reactivity distributions depending on core type

(10^{-5} Δk/k)	Absorption component	Leakage component	Total void worth
Homogeneous core	2359	-621	1738
CFV core	2709	-3439	-730

The strong gain on the sodium void effect reflects in the core natural behaviour in case of accidental transients. For this reason the CFV concept is currently considered as the reference option for the ASTRID 1500 MW SFR project in France [4].

2.2. Constraint on core height

Effectiveness of the CFV solution has been assessed depending on the axial arrangement of the fuel column: thickness and position of the internal fertile slab and core height. According to [3] the thickness of the fertile slab should be between 15 and 35 cm to generate flux distortion while not decoupling the lower and upper fissile zones. As for the core height, that is from the bottom of the inner lower fissile zone to the top of the inner upper fissile zone, it should be about 80 cm. Details [3] of the assessment show that the negative void worth cannot be indeed maintained for larger heights, e.g. 90 or 100 cm.

Limiting the core height to 80 cm is not unacceptable. Nevertheless it can become inconvenient when extrapolating the concept to very large power reactors. With such a constraint the only way to increase core volume, i.e. core power, is indeed to enlarge core diameter. Geometrically it can have undesirable repercussions on reactor vessel diameter. From a neutron physics point of view it leads to very flat cores with possible risk of radial instability due to neutron decoupling between core regions, which is undesirable as well.

For those reasons AREVA considered that solutions should be looked for to improve the CFV concept so as to maintain the negative void worth even in the case of larger core heights, typically around 1 m.

3. The TOPAZ design option

3.1. Principle

The effectiveness of the CFV concept lies in the possibility to distort enough the axial flux shape. In CEA's original design it is generated by both the optimal thickness and axial centring of a fertile slab within the fuel column. The alternative option followed by AREVA does not consider any fertile slab but involves axial zoning of the fissile content in the fuel column. Practically the TOPAZ concept consists in placing higher fissile content fuel at the top of the fuel column where flux level is to be increased. TOPAZ principle is illustrated in Fig. 2. The example shows a fuel column with two different fissile contents but it is clear that several contents could be used. Whatever the number of axial fissile contents, the principle remains that the fissile content shall increase when going from the bottom to the top of the fuel column.

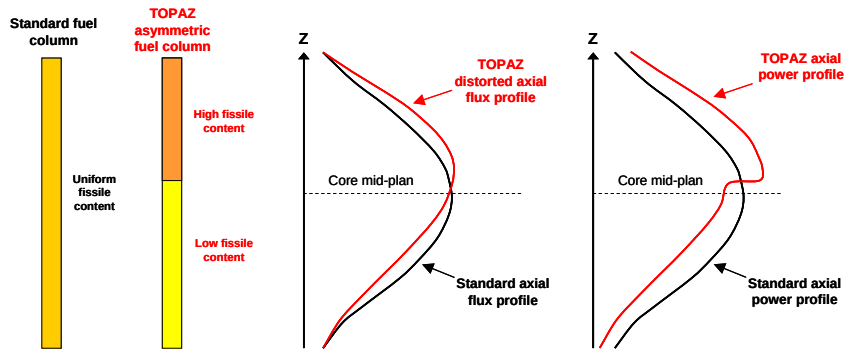

FIG. 2. Principle of TOPAZ design and expected behaviour

Combined with the optimized sodium plenum like in the CFV such a fuel column arrangement is expected to provide a global negative void worth as long as a similar axial flux distortion is obtained.

Fuel zoning is not a new option except that it is generally used to flatten the power distribution. In TOPAZ, power flattening is definitly not the objective, quite the reverse. Moreover TOPAZ zoning results in high asymmetry of the flux and power which is unusual. For these reasons TOPAZ option is really innovative.

3.2. Anticipated issues

Apart from the desired flux distortion, introducing the axial discontinuity in the fissile content is going to generate a local step in the axial power profile at the interface between the two fuel materials, as illustrated on the right part of Fig. 2. Such a step on power profile is not an issue in itself. The same happens, with a higher magnitude, in case of the presence of a fertile slab in a fuel column, like in the CFV design for instance. What could be an issue is the consequential rate of peak linear power at which the upper part of the fuel column will operate. It will depend on where the interface of fissile content is located in relation to the axial flux profile. In the case of Fig. 2. the peak linear rating would be higher for the TOPAZ configuration. Depending on margin to limits, an increase of the cumulated length of fuel pins over the core might be necessary as compared to the homogeneous case. That will have to be taken into account.

4. Testing TOPAZ on a simple model

First investigations have consisted in verifying the effectiveness of the option. Starting from a CFV like core configuration with 80 cm fissile height [3] the fuel column has been changed for a two axial zones fuel column. A thick sodium plenum topped with an absorbing material is placed above the fissile zone. Fissile height is kept for this first stage. A sodium plenum height of 40 cm is selected. The objective of the exercice was to determine the respective heights and fissile contents of the two zones leading to a total negative void worth like in the CFV design. Void worth is to be calculated when removing all sodium from the bottom of the active core to the top of the sodium plenum.

The assessment of sodium void effect being the key parameter the choice of an appropriate calculation tool was essential. For SFR neutronic applications AREVA historically relies on the ERANOS deterministic code system [5] developed by CEA. If necessary stochastic Monte Carlo tools can be deployed. The 2D Sn Transport code of ERANOS has been selected because of the presence of the sodium plenum above the core. It is consistent with CEA's works and recommendations [3]. That code is able to properly evaluate the strong leakage effects taking place in the upper regions of the core and provide a reliable estimate to the void worth. JEFF3.1 nuclear data library has been used.

A simplified core model has been built in 2D RZ geometry. Although simplified attention has been payed to the axial description of the design and to the meshing particularly in the upper core regions

where flux gradient is pronounced. Core simulations and void worth calculations have been made after fuel depletion up to an average burnup high enough to be representative of an end of equilibrium cycle configuration, the worst-case configuration.

Preliminary results have rapidly confirmed that the TOPAZ option was able to generate the necessary flux distortion and provide a negative void worth like with the CFV fertile slab option. A design solution has been identified consisting of a split of the fuel column in a 55 cm lower part and a 25 cm upper part, with plutonium (Pu) contents of 14.5% and 22.4% respectively. The core design also includes a radial outer core region which single Pu content is equal to that of the upper part in the inner core. Flux and power profiles in the axial direction are illustrated in Figure 3 at beginning-of-cycle (BOC) and end-of-cycle (EOC) in the inner core region. Differences in levels between BOC and EOC are only due to a change of radial power balance during the equilibrium cycle (the opposite being observed in the outer core region). They are not relevant to the void worth assessment, they are just related to the simplified RZ model. Steps in power density at the interface between low and high Pu content fuel zones are of +29% at BOC and +24% at EOC. It is more than +50% in fresh fuel. This downward trend with burnup illustrates Pu depletion in the upper fuel zone while it is almost constant in the lower fuel zone where initial conditions are close to self-sustainability.

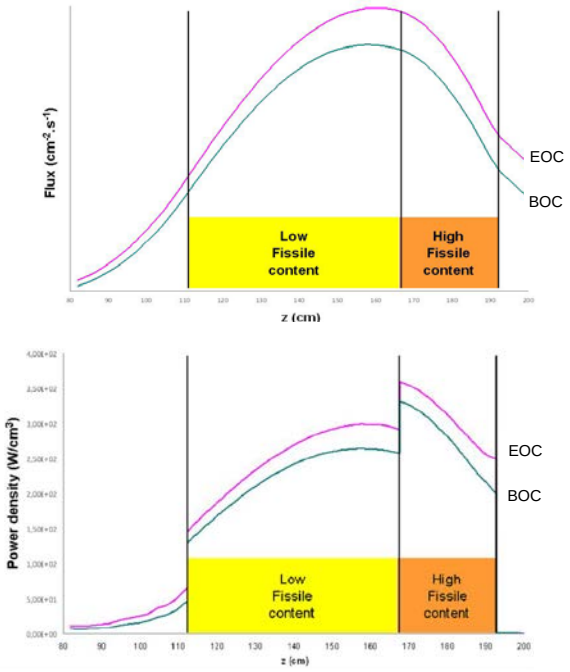

FIG. 3. Axial flux and power profiles – 80cm TOPAZ core

Considering the previous favourable result with the initial 80 cm fuel column, the testing has been continued envisaging 90 cm and then 100 cm fuel columns. RZ core models has been modified with the appropriate fissile height with reduction of the core diameter to maintain the active core volume constant. Other core regions are not changed. Then investigation of many configurations of axial fuel zones and fuel contents have been launched, seeking for negative void worth at EOC. In both cases favourable results have been obtained with three axial fuel zones instead of two in the previous case. Main results are given in Table 2.

Table 2. Main characteristics of simplified TOPAZ models

Parameter	80	90	100
Average Pu content (%)	19.1	18.0	18.0
Axial fuel zones in inner core	2	3	3
Pu contents* inner core (%)	14.5	14.5	12.2
	22.4	20.3	23.5
	-	32.2	28.5
Fuel zone heights* inner core (m)	0.55	0.70	0.75
	0.25	0.10	0.15
	-	0.10	0.10
Axial fuel zones in outer core	1	1	2
Pu contents* in outer core (%)	~22	~19	~20
	-	-	~26
Fuel zone heights* outer core (m)	0.80	0.90	0.75
	-	-	0.25
Sodium void worth ($)	-0.9 $	-0.4 $	-0.4 $

* from bottom to top of the fuel column

The 90 cm case includes an outer core region which single Pu content is close to that of the intermediate fuel zone in the inner core. The 100 cm case also includes an outer core region but with two axial fuel zones. Predictably, the increase of fissile height requires to implement higher and higher fissile contents at the top of the fuel column to sufficently increase the flux distortion upward. At 100 cm the implementation of axial zoning seems also necessary in the outer core region in order to better flatten the power distribution.

That first stage of TOPAZ design testing proved to be very encouraging: the possibility to adapt the number of fuel zones, their respective thickness and Pu content, provides the flexibility to implement it at different fuel column height. It was time to move from simple academic core models to a more detailled and representative core configuration.

5. TOPAZ implementation on a 3600 MWth SFR core

The appropriate basis for final testing of TOPAZ was the SFR V2b core [2] developed during the first phase of the French R&D collaborative programme (cf. 1.). It is a 3600 MW thermal core based on oxide $UPuO_2$ fuel and presenting sound performances. It features a 100 cm fuel column height and sodium void worth of about +5$, which correspond to the desired demonstration case. Finally, it has been largely studied in AREVA and reference calculation schemes and detailled results were available.

Main design core and fuel assembly characteristics, geometry and materials, and specifications of the SFR V2b core have been published in [2]. Necessary design modifications to implement the TOPAZ concept have been the introduction of an optimized sodium plenum above the active core and the TOPAZ type axial zoning of Pu content in the fuel column. The optimized sodium plenum consists of the same axial dimensions as for the testing phase, that is 40 cm. It is introduced as close as possible to the top of the fuel column taking into account the necessary presence of a small expansion volume and a steel plug at the top end of fuel pins. Axial zoning of Pu content is discussed farther but studies have been initiated based on the findings of the 2D RZ models. Reference SFR V2b core layout is maintained, see Figure 4.

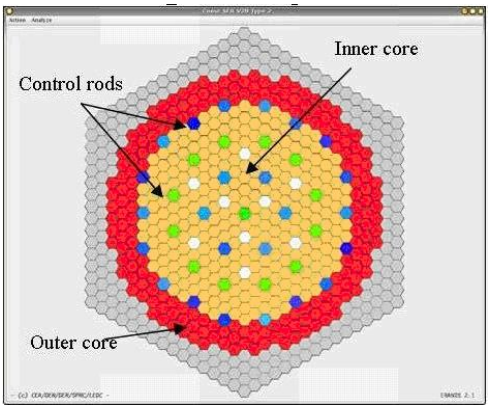

FIG. 4. SFR V2b core layout.

Core calculations are performed with both the 2D Sn transport code BISTRO and the 3D Pn transport code VARIANT. BISTRO Sn solver is used for void worth calculation. This is the same approach as in [3]. That means that two models are used: a 3D hexagonal one and equivalent 2D RZ one.

Best performances have been obtained with a three Pu content split in both the inner core and outer core. Details of the axial zoning results and main core performances are given in Table 3. Flux and power profiles in the axial direction are given in Figure 5 and Figure 6 respectively. Figure 7 shows radial power profiles in the three axial fuel zones at BOC.

Table 3. Main performances of the 3600 MW TOPAZ core

Parameter	V2b Reference	V2b TOPAZ
Core power (MWth)	3600	3600
Fuel residence time (EFPD)	2050	2050
Core batches	5	5
Core diameter (m)	4.9	4.9
Core fissile height (m)	1	1
Sodium plenum height (m)	no	0.4
Axial fuel zones	1	3
Average Pu content (%)	15.8	16
Fuel zones heights* (m)	1	0.80
		0.10
		0.10
Pu contents* inner core (%)	-	12.3
		22.5
		28
Pu contents* outer core (%)	-	15.8
		23.5
		27
Average burn-up (GWd/t)	99	99
Peak burn-up (GWd/t)	139	
Peak neutron dose (dpa)	148	-
Internal breeding gain	+0.04	0.00
Power density (W/cm^3)	207	207
Peak Power density (W/cm^3)	294	350
Peak linear power (W/cm)	420	550
Sodium void worth ($)	+4.9	-0.7**

* from bottom to top of the fuel column

** including sodium plenum

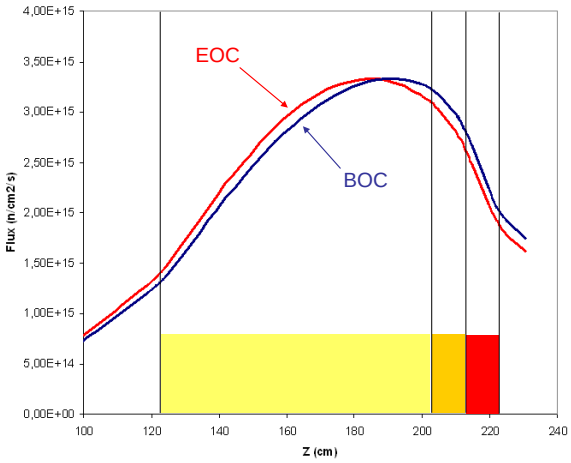

FIG. 5. Flux axial profiles in inner core.

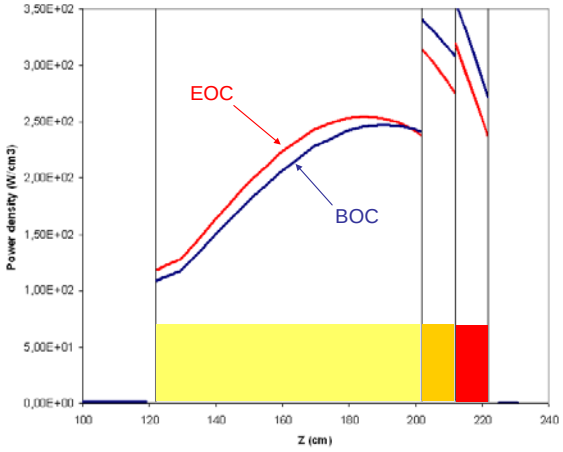

FIG. 6. Power axial profiles in inner core.

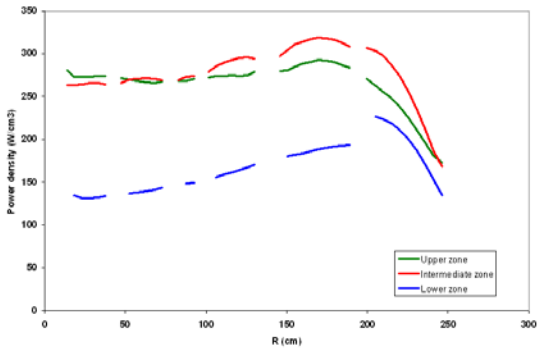

FIG. 7. Power radial profiles at BOC.

A slightly negative void worth at EOC is reached by means of a boost of Pu contents in the upper fuel zones. This is necessary to maintain the required flux distortion even after fuel depletion up to the EOC. High Pu content values remains however in the range of experienced values for Fast Reactor fuels. As a result a strong power peaking takes place in the upper part of the fuel column. Peak power density is about 350 W/cm^3 at BOC and estimated around 385 W/cm^3 for a fresh fuel assembly. Considering the initial design of the SFR V2b fuel assembly with 271 pins, it means around 550 W/cm peak linear rating in fresh fuel. Thermomechanical behaviour of the fuel pin has not been verified but it is probably too high for normal operation. The fuel assembly design would require a 331 pin bundle for TOPAZ. The impact of such a modification will be investigated in future studies but it is not expected to change completely the results.

The implementation of the TOPAZ option in the SFR V2b core design allows reaching a slightly negative sodium void worth while the initial core features a usual +5$ void worth. The sole implementation of the sodium plenum above the core is known to improve the figure but it is not enough particularly for a 1 m height core. The axial Pu zoning appears as the design complement which amplifies the negative effect of the optimized sodium plenum.

Since the physics is based on the same neutron principle, a TOPAZ type core is expected to provide the same improvements as the CFV as regard the behaviour in case of accidental transients [4].

6. Conclusion

AREVA has developed the TOPAZ design option as a solution to further minimize the sodium void worth in large SFR cores. The purpose of the TOPAZ option is to amplify the favourable negative component of an upper sodium plenum by means of an asymmetrical axial zoning of Pu content in the fuel column.

Neutron studies have demonstrated that the TOPAZ option was effective even in the case of a large SFR core. Applied on the 3600 MW SFR V2b core design with 1 m fissile height and an upper sodium plenum, the TOPAZ option allows reaching a slightly negative sodium void effect. Obviously this will be considered for the development of future SFR core designs with reinforced safety features.

The validation of present TOPAZ results relies on current CEA validation works performed for validating the CFV concept. Although involving similar physics phenomena to the CFV, a specific validation programme has to be planned in AREVA in order to fully confirm the gain on sodium void effect with TOPAZ.

In parallel to neutron studies, performances of the TOPAZ design should be now further assessed in regard to fuel behaviour and accidental transients.

ACKNOWLEDGEMENTS

The authors wish to thank CEA teams involved in SFR core design for their constructive support.

REFERENCES

[1] CARBONNIER, J.L., et al., “French Program for Sodium Fast Reactors”, ICAPP’2007, Nice, France, paper 7600.
[2] SCIORA, P., et al., “A Break-even Oxide Fuel Core for an Innovative SFR”, GLOBAL 2009, Paris, France, paper 9528.
[3] SCIORA, P., et al., “Low void effect core design applied on 2400 MWth SFR reactor”, ICAPP’2011, Nice, France, paper 11048.
[4] VARAINE, F., et al., “Pre-conceptual design study of ASTRID core”, ICAPP’2012, Chicago, USA, paper 12173.

[5] RIMPAULT, G., et al., “The ERANOS code and data system for fast reactor neutronic analyses”, PHYSOR 2002, Seoul, Korea.

Fuel Handling Systems : some technical orientations for ASTRID project

C. Courcier[a], **G. Laffont**[b]

[a] AREVA NP, 10 rue Juliette Récamier 69006 Lyon, France

[b] CEA Cadarache, 13108 Saint-Paul-lès-Durance, France

Abstract – This article deals with the technical orientations considered for fuel handling management in ASTRID (Advanced Sodium Technological Reactor for Industrial Demonstration) project. Its purpose is to present the orientations proposed by AREVA to solve the technical and economical issues involved by sodium fast neutrons reactors and by ASTRID specificities.

In the reactor vessel, the fuel handling is carried out under rotating plugs by means of a direct lift charge machine and a fixed arm charge machine.

To unload a minor actinide assembly as quick as required by ASTRID objectives, a sodium way has been chosen for core loading - unloading. A spent fuel/new fuel exchange device is implemented inside the reactor vessel to increase core loading - unloading efficiency and to improve the global plant availability.

The technical feasibility of an external storage in sodium is discussed and a first design proposed.

Management of new, spent and failed fuel from external storage to the outlet of the nuclear island is also described and a general architecture is proposed.

ACKNOWLEDGEMENTS

Thanks to E. Guillemin (AREVA NP), B. El Aslani (AREVA NP), C. Penigot (AREVA NP), D. Basset (AREVA NP), P. Gauthier (AREVA NP), F. Dechelette (CEA) and F. Morin (AREVA NEP) for their implaction in fuel handling studies on ASTRID project.

1. Introduction

The ASTRID project aims to design and build an industrial prototype of a 4th generation nuclear reactor which could answer to the objectives listed below:

- Preserve natural resources
- Ensure a safety level at least equal to the previous generation of reactor
- Ensure an availability at least equal to 90% (which involves the reduction of outages duration and a high reliability
- Be competitive compared to other energy production facilities (which involves a controlled cost during realization and during exploitation)

- Carry on experimentations concerning minor actinides burning and demonstrate its feasibility at a large scale

The important feedback available on Sodium cooled fast reactors over the past 40 years in France and worldwide shows that fuel handling systems are essential for designing the plant due to their strong impact on the operability and the availability of the reactor plant. These systems will ensure:

- the reception of new fuel assemblies, their storage and then their loading in the reactor core during outage,

- the unloading of spent and failed fuel assemblies during outage and then their washing and storage before their evacuation outside the power plant for reprocessing.

Fuel handling systems directly impact the general design of the core vessel and the nuclear island, their construction cost and the availability factor of the plant. They shall comply with operational requirements (efficiency and quickness) and safety requirements (for example, prevention of cladding failure or melt risk, radiological protection, …).

The purpose of this paper is the presentation of the technical orientations studied for ASTRID project. After a presentation of the general architecture of the fuel handling chains, the different equipements involved are described and the management of new, spent and failed fuel assemblies explained. The presented data are preliminary, which could evolve in the future.

2. General architecture

The figure 1 presents the general architecture of fuel handling systems.

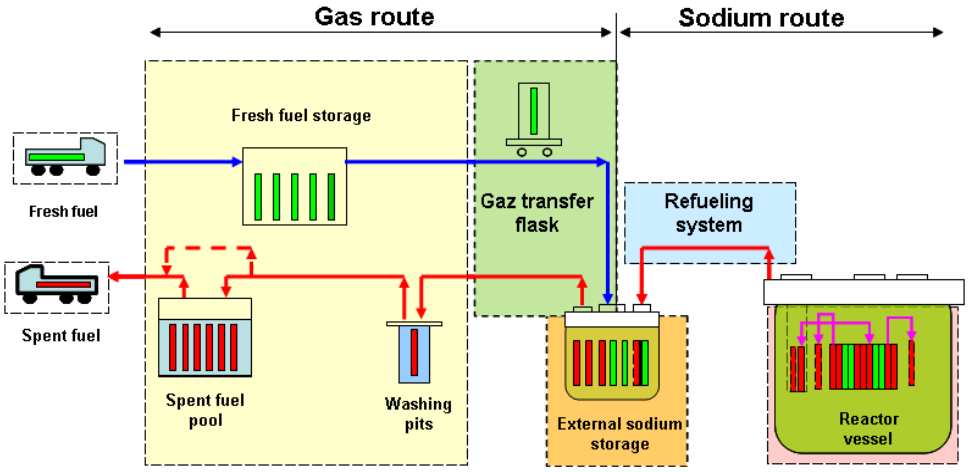

FIG. 1.: general description of fuel handling systems architecture

The general architecture is based on two types of handling route :

- *A sodium route :* this route requires an external sodium storage which permits the unloading of high powered fuel assemblies (in case of minor actinides management and quick whole core discharge) and gives an important flexibility during operations by decoupling fuel handling operations downstream and upstream the external storage.

- *A gas route :* this route complies with the interfaces characteristics of washing pits, spent fuel pool and new fuel storage.

In order to prevent common failure modes, the external sodium storage is not installed in the same building as the reactor primary vessel. This storage is installed in the "sodium" fuel building (HKS), built beside the reactor building (HR). Fuel assemblies' transfer between the two sodium vessels is ensured by the refueling system, which goes through the HR confinement.

Process devices supplied by water have been installed outside the sodium area, to avoid any risk of water/sodium interaction. That's why a specific "water" fuel building (HKL) has been installed, not far from the HKS, for washing pits and the spent fuel pool. To simplify the plot plan of the nuclear island, it has been decided to install the new fuel storage in the HKL too. Fuel assemblies' transfer between the external storage and facilities of the HKL is ensured by a gas transfer flask, which goes through the HKS confinement.

A hot cell is also considered in our architecture. This hot cell is installed in the HKL and aims to manage experimental assemblies (mounting, dismounting, NDT) and failed fuel assemblies, which shall be dismantled and prepared before washing.

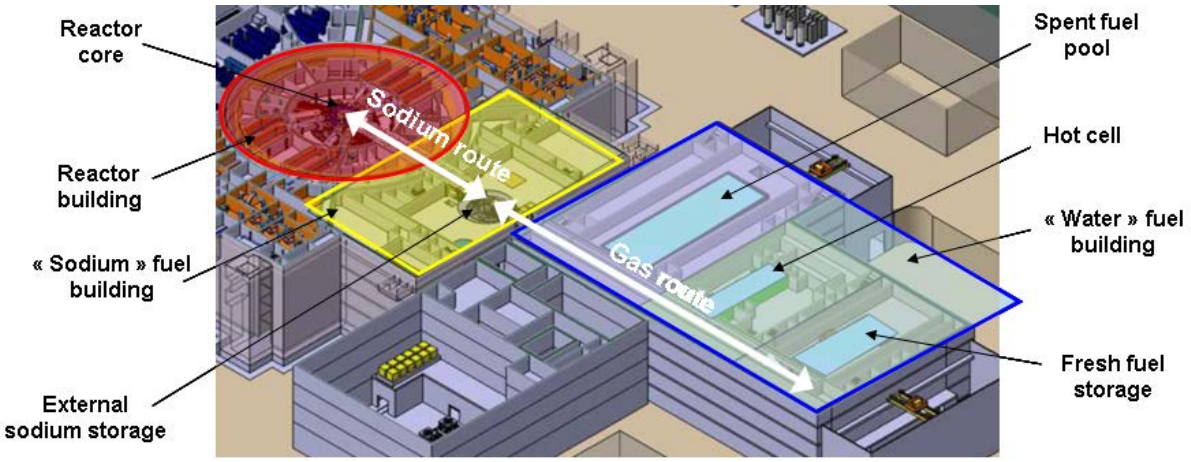

FIG. 2. Implantation of buildings involved in fuel handling activities

3. Sodium fuel handling route

The sodium fuel handling route concerns the following handling systems : in-vessel handling system, refueling system and external storage.

In-vessel fuel handling system provides the means to transfer sub-assemblies to and from all in-vessel positions during a reactor shutdown period. Equipments involved are *two rotating plugs* (a large one named LRP and a small one named SRP), *a direct lift charge machine* (DLCM), *a fixed arm charge machine* (FACM) and *a discharge position*. Access to any core positions is achieved by rotation of both rotating plugs, and in the outer handling zone also by rotation of the FACM (see figure 3). The discharge position ensures the interface between the FACM and the refueling system. In the reference configuration of ASTRID project, the DLCM is fixed on the SRP and the FACM on the LRP (the circulation area is bigger than the core diameter and the discharge position can be more distant from the core center).

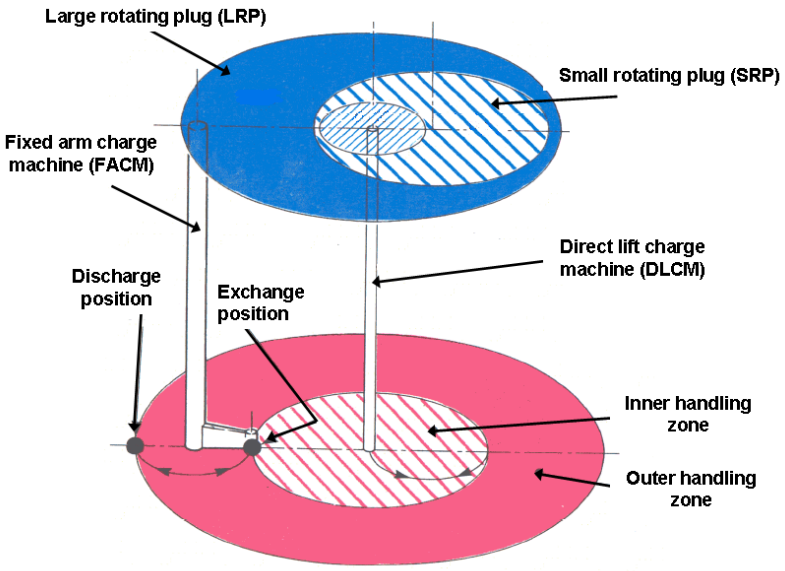

FIG. 3. : principles of in-vessel handling under rotating plugs

The refueling system transfers fuel assemblies between the core vessel and the external sodium storage. As explained in the section 1, a transfer in sodium is considered. For that, the assemblies are put in a sodium pot which is lifted and transferred by the refueling system. This kind of transfer permits the unloading of high powered fuel assemblies. To improve the efficiency of refueling operation, a pot with two positions is considered. This design allows new/spent fuel assemblies to exchange in each of the two vessels (reactor vessel and external sodium storage).

Two designs are currently studied for the refueling system (see figure 4) :

- The first one consists in *a flask*. This flask travels between the HR and the HKS on a railways track located at the level of flask body gravity center. The crossing of HR confinement is performed through a hatch. A docking valve is installed at the flask bottom to make possible a guided docking of the flask on the reactor vessel and on the external sodium storage. A reliable hoist ensures the lifting displacements of the sodium pot in the vessels. The biological shielding is obtained by the steel thickness of the flask body shell.

- The second solution consists in *a mix of 2 double ramps and a transfer cell*. The two double ramps ensure the communication between the vessels and the transfer cell. Each ramp is equipped with a shutoff valve to isolate the transfer cell from the vessels atmosphere. A conveyor in the cell receives the sodium pot from the ramps to transfer it between the HR and the HKS. The biological shielding is obtained respectively for ramps and cell by the steel and concrete thicknesses.

One can note that, for each solution, the cladding failure is prevented passively: natural convection and radiation phenomena are sufficient to respect thermal critera on cladding.

Currently the two solutions are still under investigation. A technical and economical analysis is ongoing to determine which systems shall be conserved for future ASTRID developments.

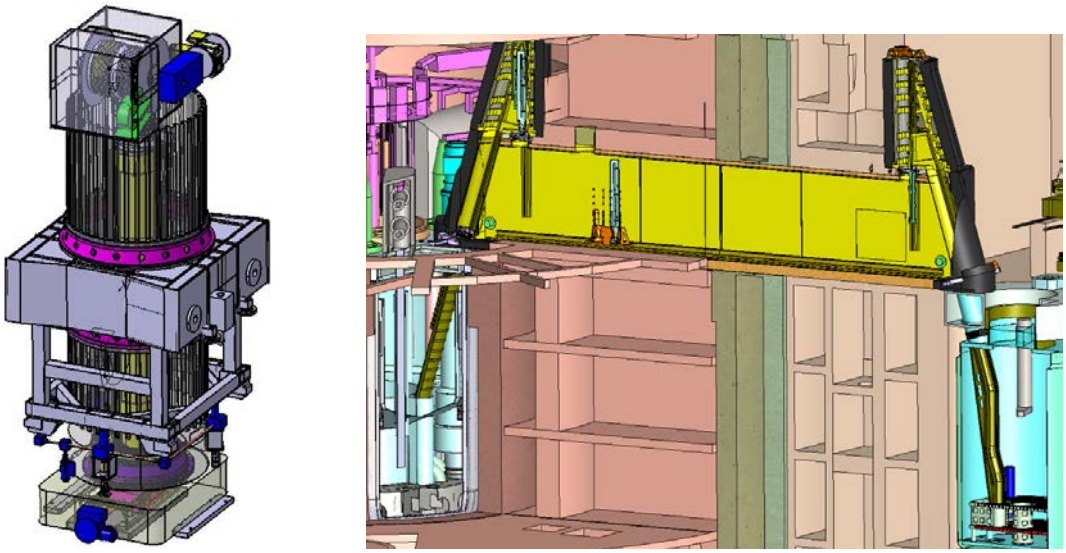

FIG. 4. :"flask" and "mixed" solutions

The external sodium storage (see figure 5) allows the decrease of assemblies residual power after refueling operations until a power compatible with the gas fuel handling route and the washing process. It consists in a primary vessel equipped with storage racks, a secondary vessel to collect sodium in case of primary vessel leak, and a thick and empty metallic slab.

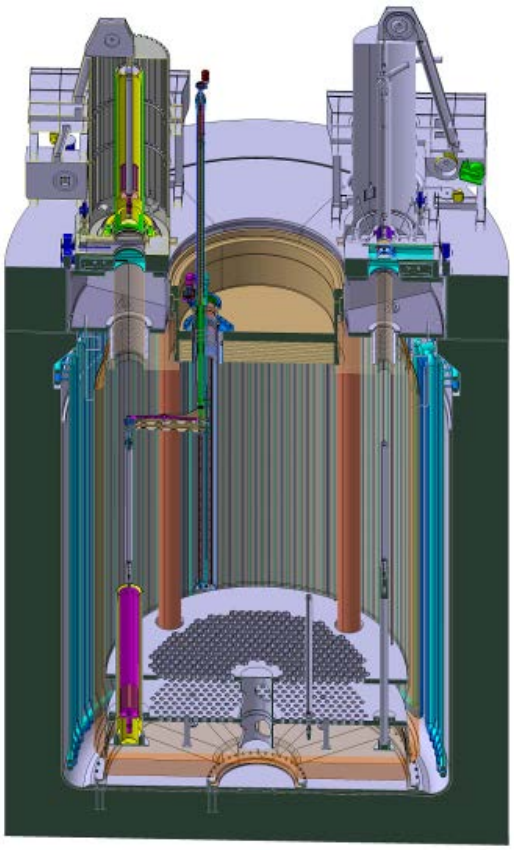

FIG. 5. : external sodium storage

The number of storage positions corresponds to 4/3 of the total core assemblies number to make a whole core discharge possible. The storage pitch is limited by the insertion of fixed absorbing assemblies which ensure the sub criticality.

The in-vessel handling operations are performed by means of a unique rotating plug and a FACM.

The sodium temperature is controlled by diversified in-vessel heat exchangers. Some additional facilities are installed in the sodium strorage pit to evacuate the residual heat by radiation in case of loss of the in-vessel heat exchangers.

4. Gas fuel handling route

The gas fuel handling route ensures the interfaces between the external sodium storage and front/back end fuel cycle facilities (new fuel manufacturing and spent fuel recycling).

2 specific and independent blocks, placed in the HKL, are considered :

- Spent fuel management facility, which manages spent fuel assemblies before their evacuation to back end facilities,

- New fuel management facility, which receives new fuel assemblies from front end facilities and prepares them before their transfer to the external sodium storage.

A hot cell is also implemented in the HKL. It ensures mounting, dismounting and examinations of experimental assemblies. It is also dedicated to dismantling and repacking failed fuel assemblies before their washing.

The crossing of the HKS confinement is done by a gas transfer flask (named “gas transfer flask 1”) through a hatch. Another gas transfer flask (named “gas transfer flask 2”) ensures internal transfers in each block.

4.1. Gas transfer flasks

As for the flask considered for the refueling system, the gas transfer flasks main components are:

- A thick metallic shell whose thickness ensures a sufficient biological shielding for operators,

- A docking valve at the basis of flask body to permit a guided docking on the operating stations,

- A railway track positioned at the level of gravity center of the flasks bodies (the track is common for the two gas flasks),

- A fiabilized hoisting device which ensures the lifting displacements of fuel assemblies

It has been decided to demonstrate the capability to unload high-powered fuel assemblies from the external sodium storage. To prevent any cladding failure by respecting thermal criteria, some redundant cooling devices, based principally on forced conduction by in-assembly blowing, are integrated in the gas transfer flasks. In case of failure of cooling systems, the assembly melt is prevented passively (natural convection and radiation phenomena).

4.2. Spent fuel management facility

This installation combines 2 washing facilities, a spent fuel pool equipped with a spent fuel mast bridge and storage racks, a conveyor and a spent fuel cask transfer facility.

The spent fuel assembly is put in a washing pit by means of the gas transfer flask 1.

Several processes have been tested for removing the residual sodium on fuel assemblies. The basic principle considered is an interaction between residual sodium and water. For ASTRID, the washing facilities are based on slow immersion or atomization processes.

After washing, the spent fuel assembly is lifted in the gas transfer flask 2, which is transferred and docked above the transfer pit.

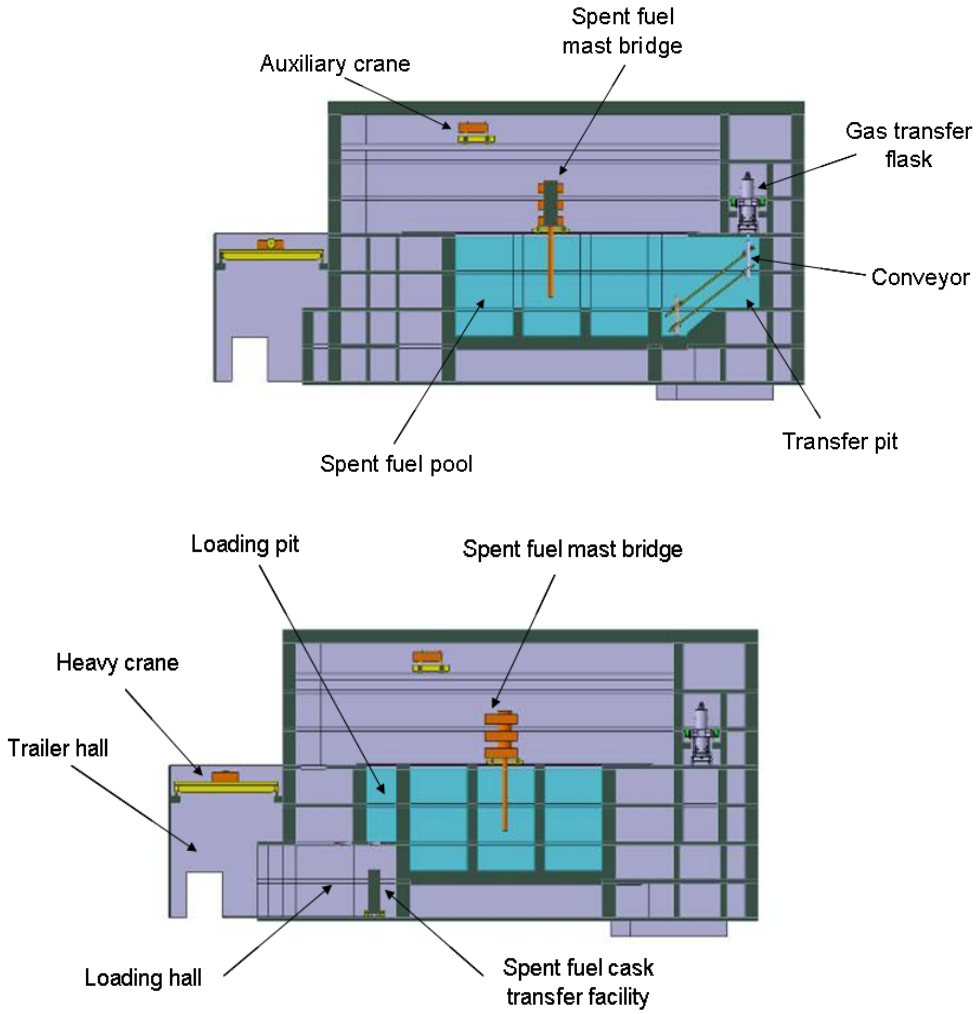

FIG. 6. : spent fuel management facility – spent fuel pool area

The transfer pit communicates with the spent fuel pool by the way of a combination of swivel and slot gates. The spent fuel assembly is put in the conveyor basket of the transfer pit. This conveyor transfers the assembly until a level compatible with the spent fuel mast bridge characteristics. This bridge lifts the assembly and transfers it into the spent fuel pool to be stored in stainless steel storage racks for a power decay time.

The sub-criticality of the spent fuel pool is obtained by the pitch between racks. The dose rate on the spent fuel pool operating floor is ensured by the water layer thickness above the handled spent fuel assembly's head.

The evacuation of spent fuel assemblies after power decay is performed by means of the spent fuel cask transfer facility. This facility, installed in the loading hall, ensures the following operations :

- Delivery and opening of the cask as well as its preparation before its loading with spent fuel assemblies,

- Automatical loading of cask with the transfer machine docked to the loading pit (which communicates with the spent fuel pool by the way of a combination of swivel and slot gates) through a penetration (loading performed by the spent fuel mast bridge),

- Closing/conditioning and preparation of the cask before its transport out of the “water” fuel building,

- Transfer of the cask between the “water” fuel building and the trailer hall (equipped with a heavy crane for lifting the spent fuel cask).

One can note that an auxiliary crane is implemented to perform tools and equipments handling operations. It can be also used as back-up of the spent fuel mast bridge in case of failure (specific handling tool designed in that way).

4.3. New fuel management facility

The proposed design is mainly based on the spent fuel management facility design: this facility combines a conditioning pit, a storage pit equipped with storage racks and a spent fuel mast bridge, an inspection pit, a conveyor and a new fuel cask transfer facility.

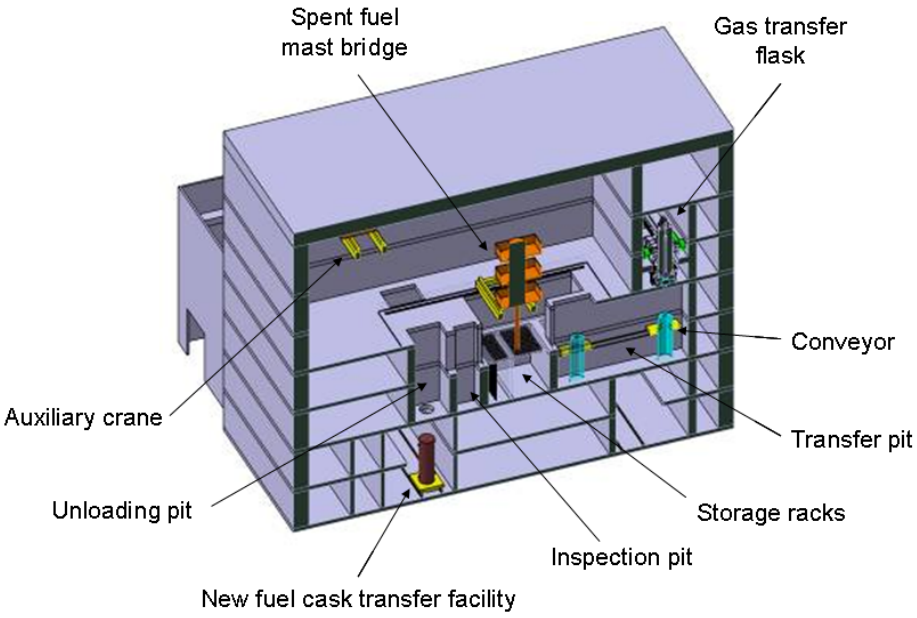

FIG. 7. : new fuel management facility – new fuel storage area

The reception of new fuel assemblies is performed by the new fuel cask transfer facility. This facility, installed in the unloading hall, ensures the following operations:

- Delivery and opening of the cask as well as its preparation before its new fuel assemblies unloading,

- Automatical unloading of cask with the transfer machine docked to the unloading pit through a penetration (unloading performed by the spent fuel mast bridge),

- Closing and preparation of the cask before its transport out of the “water” fuel building,

- Transfer of the cask between the “water” fuel building and the trailer hall (equipped with a heavy crane for lifting the spent fuel cask).

Before being put in a rack of the storage pit, each new fuel assembly is automatically controlled in the inspection pit.

The sub-criticality is obtained by the pitch between racks. The dose rate on the storage pit operating floor is ensured by the biological shielding of the mast of the spent fuel mast bridge and the distance with operator for the handled new fuel, and by one removable shielded slab on each storage position.

After storage, the new fuel assembly is put by the spent fuel mast bridge in the conveyor basket of the transfer pit. This conveyor transfers the assembly under the gas transfer flasks way. The gas transfer flask 2 lifts the fuel assembly and transfers it in the conditioning pit. After conditioning, the fuel assembly is lifted in the gas transfer flask 1 and finally transferred into the external sodium storage.

One can note that, as for the spent fuel management facility, an auxiliary crane is implemented to perform tools and equipments handling operations. It can be also used as back-up of the spent fuel mast bridge in case of failure (specific handling tool designed in that way).

4.4. Management of failed fuel assemblies

Failed fuel assemblies can be detected in reactor vessel, in external sodium storage and during the washing process.

To prevent the contamination of washing pits, failed fuel assemblies identified before the washing process are not directly washed. They are oriented to the hot cell to be conditioned. This conditioning consists in dismantling the assemblies to detect the failed fuel rods. Then the failed fuel pins are dry cleaned, over-cladded and their tightness tested. Over-cladded pins are placed in a holder which is transferred by the gas transfer flask 2 in the spent fuel pool. Intact pins are placed in the same kind of holder. This holder is transferred to the washing pits by the gas transfer flask 1 for cleaning and is treated as a normal spent fuel assembly.

Failed fuel assemblies detected after washing (cracks closed by sodium and so not detected) are treated as normal spent fuel assemblies. It is still possible to bring them to the hot cell for examination and conditioning.

5. Conclusions

Developments performed during first preliminary design phase of ASTRID project led to propose a general architecture of fuel handling chains and some basic designs of the handling systems. This paper summarizes the main orientations. One can note the important role of the external sodium storage as decoupling device between activities performed during reactor shutdown (sodium route) and those accomplished during core burn up (gas route).

Studies of the second preliminary design phase shall confirm the proposed orientations according to the input data evolution.

BREST-OD-300 Project Status and Basic Design Features

Yu. Dragunov, V. Lemekhov, V. Smirnov, O. Yarmolenko
Joint Stock Company "N.A. Dollezhal Research and Development Institute of Power Engineering" (JSC "NIKIET")

1. Introduction

Large-scale nuclear power of the future, based on fast reactors operating in a closed nuclear fuel cycle (NFC), can stop the growth in fossil fuel consumption, take up most of the increase in the electricity generation and solve the problem of energy supply for ensuring sustained evolution of the humankind, nonproliferation of nuclear weapons and improvement of the environment on the planet Earth. Such nuclear power will however prove to be socially acceptable when it satisfies to requirements of high safety and economic competitiveness with alternative sources of energy, with safety to be understood in this case in a broad sense of the word, specifically as:

- no limits on fuel resources;
- avoidance of dangerous accidents involving radioactive and toxic emissions to require evacuation of public and formation of exclusion areas;
- technological strengthening of nonproliferation resistance;
- environmentally safe closure of the fuel cycle in RW handling.

In recent years, Russia has made a number of steps in this direction of evolution to build a technological platform of nuclear power intended to support the closure of the nuclear fuel cycle (NFC) and deployment of fast reactors. A federal target program, “Nuclear Power Technologies of a Next Generation” (FTP hereinafter), was launched in 2010. 2011 saw the approval of the consolidated project “Proryv” which integrates the FTP’s conceptual issues of the nuclear fuel cycle (NFC) closure and fast reactors. For 2010-2015 and up to the year 2020, the FTP envisages the elaboration of three fast reactor technologies with different coolants and fuel designs, including fast reactors with lead, sodium and lead-bismuth coolants.

The report presents a concept developed as part of the FTP, a nitride-fuel fast reactor (BREST-OD-300) cooled by a heavy liquid-metal lead coolant operating in a closed uranium-plutonium cycle. This technology of naturally safe fast reactors, which is based on the experience of nuclear power evolution and the research conducted in Russia in recent decades, meets the requirements for large-scale nuclear power and is not very far from the state of the art in nuclear power.

The BREST-OD-300 reactor is a pilot demonstration fast reactor of the thermal power 700 MW and the electric power 300 MW with two heat removal circuits which use a water-steam mixture of subcritical parameters as the secondary circuit fluid. The BREST-OD-300 reactor is also viewed as a prototype of future BREST-type commercial reactors for large-scale nuclear power of natural safety. Therefore, the reactor’s key designs and technical data, including the BREST-OD-300 power, have been selected not only to demonstrate, in the course of pilot operation, the natural safety features of this reactor technology but also to take into account the requirement for preserving the key designs in reactor facilities of a higher power to be developed in the future.

The use of a high-boiling (>2000 K), radiation-resistant and low-activated lead coolant in the BREST reactor, which is inert when contacting water and air and does not require high pressure inside the circuit, excludes accidents with fires or steam and hydrogen explosions.

The use of a compact (γ=14.3 g/cm^3), highly heat-conducting ($\lambda\approx$20 W/(m·deg)) nitride fuel, which is compatible with the lead coolant and the fuel cladding steel, enables reactor operations with a relatively low average working temperature of fuel (T≤1000°C), a small thermal energy reserve and a minor release of gaseous fission products from the fuel and a low pressure of these on the cladding.

The combination of the lead coolant and nitride fuel properties creates conditions for achieving the complete breeding of fissionable nuclides in the core and stabilization of the reactor's breeding properties, which makes it possible to operate the reactor with a small and stable reactivity margin, exclude power runaway accidents, fuel failure and release of radioactivity. Minor moderation of neutrons by heavy lead makes it possible to extend the fuel element lattice pitch and so increase the coolant flow cross area in the core and the level of the power removed from the core by natural lead circulation without worsening the reactor's physical characteristics. The time-unlimited passive heat removal from the lead by the natural circulation of air with the heat released into the atmosphere excludes accidents with the lead circuit overheating during cooldown. A long-term reactor trip during loss of auxiliary power and low atmospheric temperature (down to -40^{o}C) does not result in the lead coolant fully freezing around the air heat exchangers (Field tubes) with the loss of lead natural circulation through the core. The tube spacing has been chosen by calculations from the condition that the formation of the lead skull on the tubes resulting in a greater thermal resistance and a decreased heat flow from the lead to the air in the tubes does not result in the lead flow path clogging and the loss of heat removal from the core. In a fact the lead skull turns into the feedback whose heat resistance prevents the lead circuit from freezing.

Therefore, two classes of the most severe accidents (with power runaway and loss of heat removal) are naturally excluded not through building up engineered barriers and safety systems but largely thanks to the natural laws of the chain reaction running in a fast reactor, the properties and qualities of the coolant and the fuel, the BREST reactor's main components, and the designs which enable these to be realized. This approach is exactly what fundamentally defines the ***natural safety*** of this reactor in extremely severe accidents.

2. Design features of the reactor

The reactor facility has a pool-type design with an integrally arranged lead circuit comprising a core with reflectors and CPS control rods, steam generators, pumps, components of the refueling system, the lead treatment system and the oxygen content control system, as well as other auxiliary components contained in one central and four peripheral (according to the number of the lead coolant circulation loops) steel-lined plenums of the reinforced-concrete vessel with a thermal blanket and a cooling system (Fig. 1). The concrete temperature is kept in the permissible limits by natural air circulation.

Combined with the selected lead circulation pattern and emergency steam dump from the reactor vessel during an SG break via rupture membranes into the localization system and further, via filters, into the atmosphere, such circuit arrangement excludes the entry of a hazardous steam quantity into the core and overpressurization of the reactor vessel.

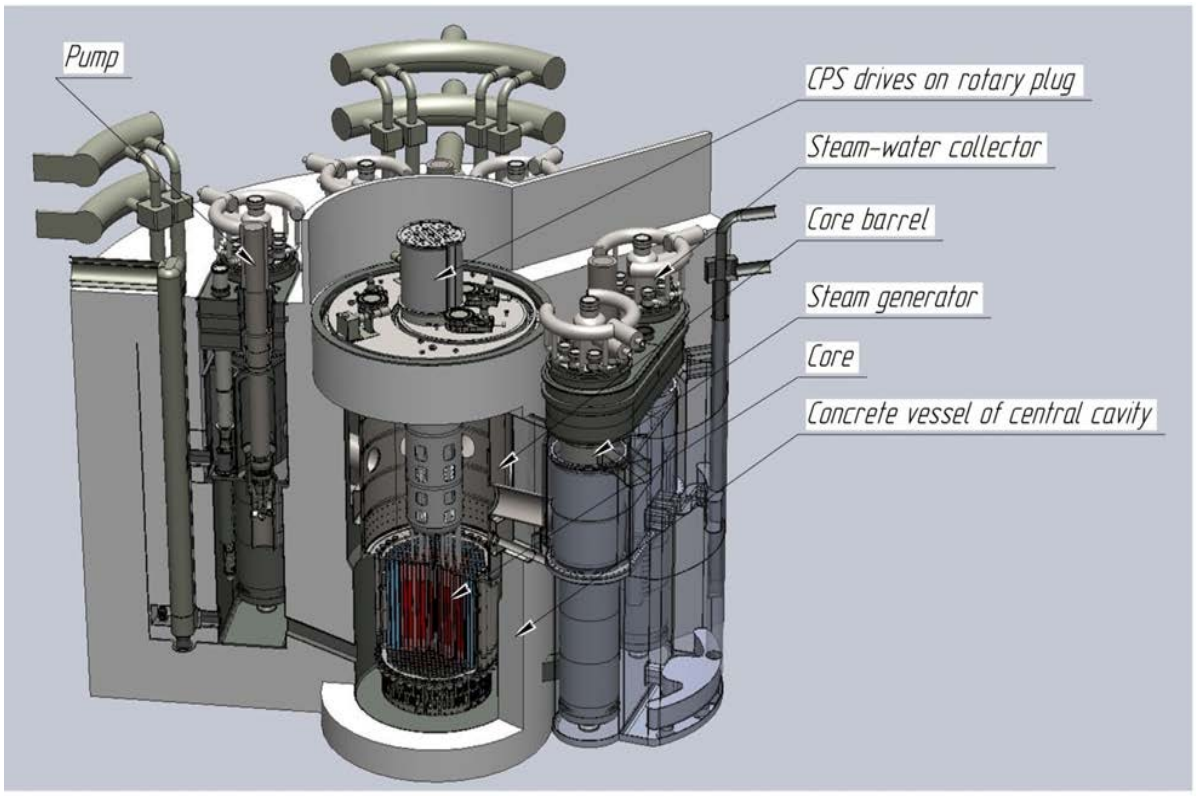

Figure 1 – A spatial model of the BREST-OD-300 reactor unit.

Upward lead circulation through the core has been selected and is ensured by the difference in the ‘cold’ and ‘hot’ coolant levels created by pumps (Fig. 2).

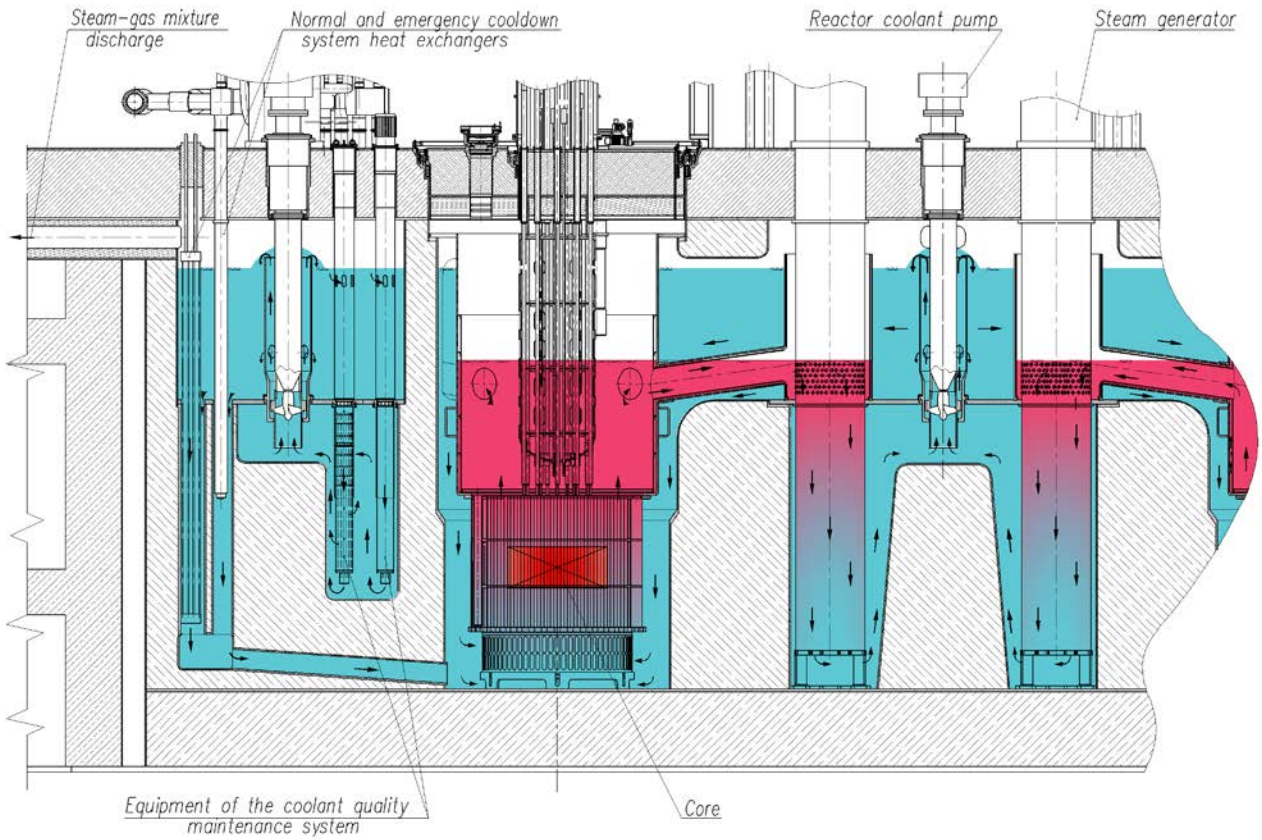

Figure 2 – Coolant circulation diagram.

The lead cooled in the SG to T=420°C is pumped to the upper level and further flows over the circuit's downcomer leg to enter the core, where while flowing upwards, it is heated to T=540°C and then enters the SG over the hot lead inlet branch tubes and goes further back to the suction chambers of the pumps. When such circulation pattern is used, the lead coolant, as it flows out of the pump, contacts the gas circuit where the steam and gas entrapped by the lead are separated. Such arrangement excludes their entry into the core together with the coolant, which could lead to an uncontrolled reactivity and power growth under certain conditions. This solution also reduces the irregularity in the coolant flow rate when one or more pumps are out of operation and ensures the inertia of the coolant flow rate through the core thanks to a difference in the levels when all pumps are shut down rapidly.

A low pressure in the reactor's concrete vessel and a relatively low temperature of the lead freezing (600 K), which contributes to the self-healing of potential cracks in concrete, excludes major lead leakage, loss of coolant and fuel melting.

Rotary plugs, an in-core refueling machine and a set of ex-core refueling mechanisms are used for refueling and reloading the fuel assemblies (FAs) and reflector blocks.

The core is composed of hexagonal canned FAs with fuel rods. All FAs have the same composition of fuel and the same fuel element spacing. The radial leveling of the FAs power and the coolant heating is ensured through the profiling of the fuel batch and the lead flow rate thanks to using fuel elements of a smaller diameter in the central FAs and of a greater diameter in peripheral ones. Using fuel of one and the same composition in all FAs, provided the core breeding factor is ~1, ensures the stability of the leveled-off distributions (Fig. 3).

Around the core there are rows of changeable blocks of the side lead reflector designed as compact steel hexagonal cans filled with the flowing coolant lead of a small flow rate. Some of the side reflector blocks adjoining the core are designed as vertical channels with columns of lead plugged at the top. The level of the lead columns follows the coolant flow rate (lift) and influences the neutron leakage. As the result, the channels with the lead columns form a passive feedback system (PFS) that links the reactor reactivity (and power) with the coolant flow rate (lift) in the core, which is an important factor of reactor safety and control.

The elimination of uranium blankets, which are traditional for fast reactors, and the replacement of these for a lead reflector exclude generation of weapon-grade plutonium (a technological measure which strengthens the nonproliferation resistance) and introduction of positive reactivity in response to a lead level reduction. High albedo qualities of lead reduce the critical mass of the fuel load and level off the core neutron flux and power density distributions.

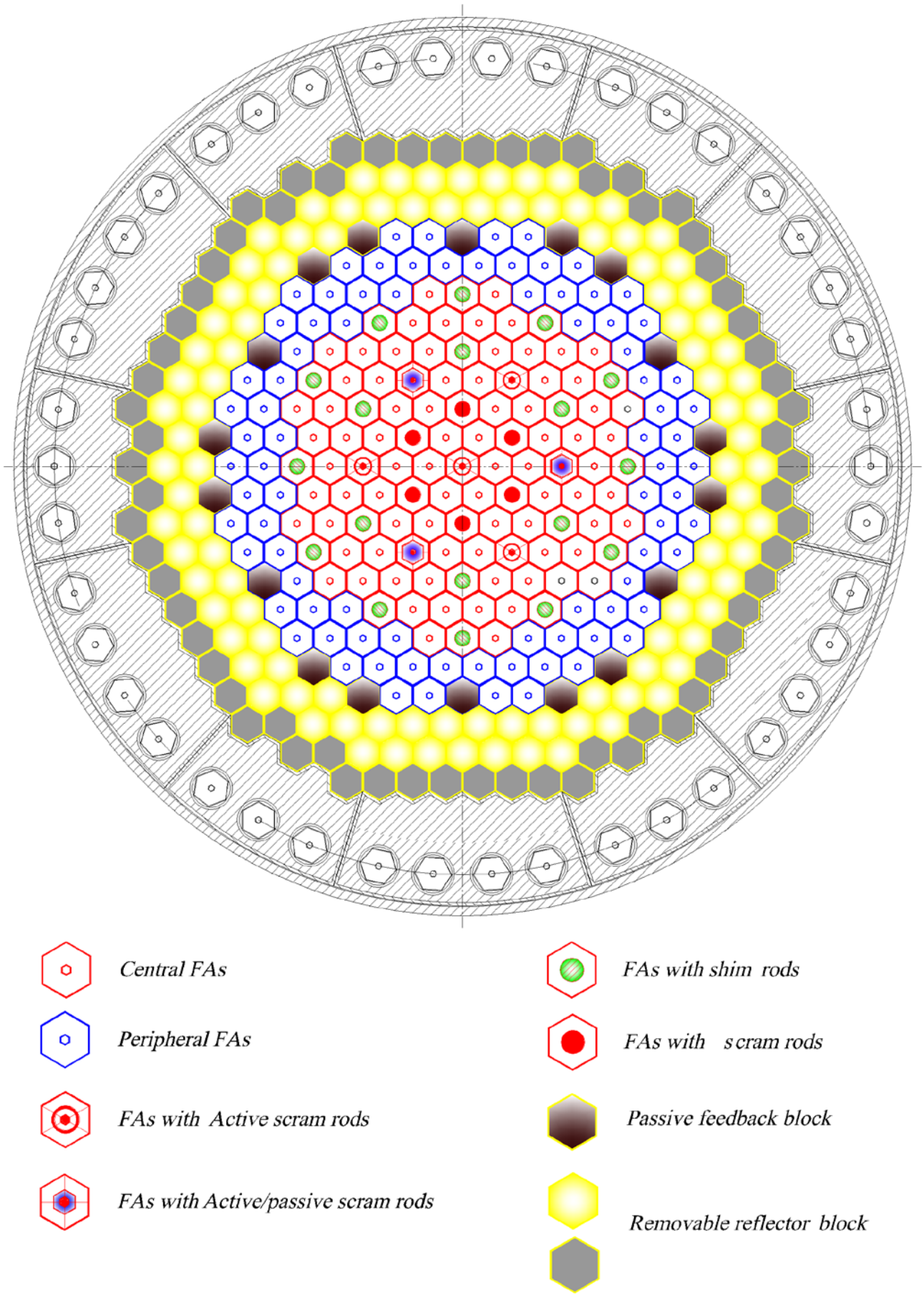

Figure 3 – A map of the core with CPS control rods and reflector blocks.

3. Anticipated economic performance of the BREST reactor facility

A great share of specific capital costs in the total cost of modern NPPs is primarily the price of the NPP safety. The avoidance of accidents which are hazardous to human life and the environment in the BREST reactor facility thanks to the required combination of inherent safety features rather than thanks to building expensive engineered features and protection systems has provided the solution to the safety and economic efficiency harmonization problem.

The expected economic competitiveness of the NPP with the BREST reactor facility against other NPPs is achieved primarily thanks to simpler safety systems and high efficiency of utilization of nuclear fuel and generated heat (efficiency). A low pressure in the lead coolant circuit makes it possible to use the reactor facility of a pool design and with a high heat capacity of the lead circuit, while the circuit components are deployed inside a concrete vessel lined with corrosion resistant steel. This not just enables a reduction in the cost of the reactor facility construction but also makes it safer during transients and emergencies thanks to a higher thermal inertia of the circuit. The planned onsite deployment of the CNFC components will be also economically reasonable because of a reduction in the SNF cooling time, transportation time and cost. It will ultimately lead to a reduction in the amount of fuel circulating in the CNFC, which is one of the major fuel cycle cost components.

4. Current status of activities on the BREST-OD-300 reactor facility

In accordance with the FTP, the pilot demonstration NPP with the BREST-OD-300 unit is developed and built in Russia in the following cooperation of major contractors:

- NIKIET – chief designer of the BREST-OD-300 reactor facility and head developer of the NPP with the BREST-OD-300 unit;
- Institute of Physics and Power Engineering (IPPE) – scientific supervisor for the effort;
- VNIPIET – general designer of the NPP with the BREST-OD-300 reactor facility.

The Siberian Chemical Combine has been chosen as the site for the construction of a pilot demonstration power complex to comprise the BREST-OD-300 reactor facility, the onsite nuclear fuel cycle, and integrated facilities for production of compact fuel for fast reactors.

The novelty of the tasks involved in the BREST project requires a great deal of research and development (R&D) activities which have been under way since the early 2000s. The program of R&D to validate the serviceability of the reactor facility components envisages the entire set of activities:

- Development of the core components mockups, accomplishment of hydraulic, thermal, strength and vibration testing, irradiation of fuel and absorbing materials;

- Creation of a small-scale bench and a mockup of the main circulation pump. Testing based on the small-scale bench. Creation of a full-scale bench and a mockup of the main circulation pumping set and their testing.
- Creation of small-scale work areas and equipment mockups for the integrated refueling system (IRS).
- Creation of small-scale work areas and mockups for testing the steam generator components in lead for the study of safety during SG tube ruptures.
- Development, manufacturing and testing of equipment mockups to ensure the coolant quality.
- Launch into manufacture, development of welding technologies and determination of long-term and lifetime mechanical properties of semi-finished items and their welded joints.
- Development, manufacturing and testing of full-height circuit models for verifying the software for dynamic calculations of the circuit thermal-hydraulic processes.

This work involves scientific and educational centers, as well as dozens of nuclear power enterprises and associated industries.

The project includes the following key events:

Development of the power unit design	2014
Obtainment of the construction license	2015
Launch of the unit construction	2016
Unit startup	2020

The results so far obtained from irradiation tests of fuel elements with mononitride fuel, studies into the impacts of lead on the structural steel components and tests of equipment mockups give every reason to believe that the goal of the activities carried out to validate and implement the BREST project will be achieved. The reactor’s structural components in the lead circuit are protected against corrosion through the control and maintenance of the respective oxygen conditions in the circuit. Experiments showed that even long-term (~1000 hours) deviations from the optimal oxygen concentration in the lead (~by a factor of 10) did not result in major corrosive damage.

Progresses made in the BREST-OD-300 design during the last 5 years:.

1.With calculational and experimental means the limits of hydrodynamic stability of steam generator were established.

2. The value of the heat transfer coefficient of the fuel rods in the fuel assembly of the projected geometry was found.

3. The completion of the mockup of main circulation pump flow section is on the way.

4.The completion of concrete vessel model element is on the way

MOX fuel optimization for a MYRRHA-based SMR

Alberto Ottonello[a], Gert Van den Eynde[a], Hamid Ait Abderrahim[a]

[a] SCK•CEN (STUDIECENTRUM VOOR KERNENERGIE, CENTRE D'ETUDE DE L'ENERGIE NUCLEAIRE)

Abstract. A key aspect of the SMR (*Small Modular Reactors*) is a long fuel cycle without re-shuffling, with a reactivity swing close to β. In our work we set the guidelines of a procedure of optimization for MOX fuels. We identified two parameters to control the burn-up reactivity swing and the excess of reactivity at BOL at fixed geometry, that enable to skip the details of the Pu vectors: the equivalent fraction of ^{239}Pu, *a*, as defined in our report, and the fissile to fertile ratio *f*. Starting from a required excess of reactivity one can select an interval for *a* from an empirical relationship. The enrichment to have an optimized fuel is then estimated with another empirical curve between the enrichment and *a*. The excess of reactivity can be refined changing *f* at constant *a*. MCNPX 2.6.0, and ALEPH burn-up code were used in the simulations.

At SCK•CEN a well-known project for a lead-bismuth cooled MOX fuelled reactor is on-going (MYRRHA [1]). How the present foreseen fuel could be optimized in order to be applied to a MYRRHA-based SMR with a long fuel cycle without re-shuffling, and with a reactivity swing close to the neutron delayed fraction β (about 400 pcm in a MOX fuel) was the starting point of this study.

In general, a longer fuel cycle, regardless of the reactivity swing, can be achieved by a larger initial excess of reactivity, which means raising the enrichment at fixed isotopic fuel vectors. This procedure is clearly bound to raise safety issues and in the end, a high enrichment leads to a very unfavourable breeding ratio (BR) and thus to a smaller and smaller gain in fuel cycle length.

Let's start by sketching some guidelines:

- a high fuel volume fraction is desired: this means fewer neutron leakages and a harder spectrum, which implies more neutrons produced per neutron absorbed, and also a decrease of the capture to fission ratio. Therefore the coolant area should be made minimal thus also gaining in reactivity. However the coolant flow must be obviously able to evacuate all the heat generated in the fuel rods;
- a too high fuel volume fraction means high reactivity excess (that raises safety issues and leads to a poor neutron economy to keep the power constant);
- a too high fuel volume fraction can make the coolant outlet temperature exceed the foreseen limit.

From a pure neutronic point of view it can be shown [2] that in a homogenized cylindrical core, in the limit of a one neutron group diffusion theory, the most convenient height to diameter ratio is close to one. Such result has been proven also in the case of a realistic geometry in the study made on PASCAR [3], where the total mass of the heavy metal fuels and the power were conserved.

However other needs put constraints on the choice of this ratio. We remember the request of small pressure drops in the core to enable a natural circulation of the coolant and the limits on the linear power according to the materials used. One might also have the temptation to shorten the active height in the hope to make the coolant voiding reactivity coefficient negative. In a fast reactor this in fact requires that the neutron leakages prevail on the spectrum hardening positive reactivity effect. However, all these considerations are outside the scope of this preliminary study.

Obviously, traditional power flattening by means of different enrichments (or less frequently by changing the geometry such as the fuel assembly size [4] or the hole of the fuel pins when present) will also be useful for a better fuel utilization which respects the material design limits and therefore to enable longer fuel cycles.

1. Fuel choice: our case

Several on-going projects of advanced lead or lead bismuth-cooled SMRs are using innovative metal or nitride fuels: PASCAR [3], PBWFR [5], SSTAR [6], SUPERSTAR [7], New Hyperion Power Module, TerraPower, and the Russian BREST-300 [4] and SVBR-100 [8]. In this work we want to stay on the side where more experience dwells, as done for SVBR-100, that is using MOX. Therefore we have to think about low enrichments compatible with the small size of the SMRs and the improvement of the fertile to fissile conversion is a mandatory step.

The conversion performance mainly depends on the number of neutrons that are not necessary to sustain the fission chain, that is $\eta - 1 = {}^{\nu\Sigma_f}/_{\Sigma_a} - 1$ in a one neutron group theory, if leakages are neglected and absorption is entirely due to the fuel.

^{233}U has the highest value of η in the thermal range (E< 1eV), and therefore in thermal reactors the fuel cycle ^{232}Th - ^{233}U is the most convenient. For energies above 50 keV instead, the best fuel for breeding purposes is represented by the cycle ^{238}U-^{239}Pu.

In MYRRHA [1] and LEADER [11] projects the MOX composition is extracted from the spent uranium dioxide fuel from a PWR with an original enrichment of 4.5% in ^{235}U, unloaded at a discharged burn-up of 45 MWd/kg HM and cooled for 15 years [9].

This MOX fuel has the chemical formula $(U_{1-y}\ Pu_{\ y})\ O_{1.97}$, where y % is the value of the plutonium enrichment we talk of. The isotopic vectors are those of Table 1.

Isotope	reference MOX	Isotope	reference MOX
^{234}U	0.003	^{238}Pu	2.348
^{235}U	0.409	^{239}Pu	57.015
^{236}U	0.010	^{240}Pu	26.952
^{238}U	99.578	^{241}Pu	6.069
^{238}Pu	2.348	^{242}Pu	7.616

Table 1 The U and Pu vectors for the reference MOX fuel from which we started. These atomic percentages correspond to a UO_2 (4.5 % enriched) spent fuel, from a PWR at a discharged burn-up of 45 MWd/kg HM and after 15 year cooling time.

The first thing we can try is to keep the composition fixed and simply reduce the enrichment to improve the breeding ratio. We must check how low we can go if we want a core of reasonably small size slightly supercritical at the Beginning Of Life (BOL). The minimum amount of excess of reactivity at BOL can be estimated as some times beta (about 400 pcm [10] in a typical MOX core), since our target is a reactivity swing of about this value. As long as the single absorbing rod is asked to provide not more than beta pcm of anti-reactivity, safety requirements against the occurrence of prompt criticality due to unforeseen single rod ejection are fulfilled.

To test the reactivity excess of the fuels at BOL we used a modified version of ALFRED, LEADER demonstrator reactor [11], whose active dimensions (H= 120 cm and D=2.56m) are similar to a SMR and whose geometry, besides, is quite similar to MYRRHA.

If we work at 100 MWth, the power density q''' turns out to be equal to 63 W/cm^3. To test the burn-up behavior of the optimized fuels, instead, we used a semplified geometry: a cylinder of fuel, with H/D=1 and H=84 cm. The fuel is surrounded by a lead axial and radial reflector, 20 cm thick. The simulations were run using MCNPX 2.6.0, JEFF. 3.1.1 nuclear data library and the burn-up code ALEPH [12].

	^{238}Pu	^{239}Pu	^{240}Pu	^{241}Pu	^{242}Pu
Min#1	2.40	57.33	27.30	5.38	7.59
Min#2	2.40	53.8	27.30	8.91	7.59
Max#1	0.88	64.31	22.30	9.66	2.85
Max#2	0.88	68.20	22.30	5.77	2.85
MAGNOX	0.10	71.90	23.00	4.00	1.00
AGR	1.00	60.00	30.00	4.00	5.00
MOX PWR	2.35	57.01	26.95	6.07	7.62

Table 2 The Pu vectors originally available, corresponding to different levels of discharged burn-up. The numbers are weight percentages. MOX PWR is the reference composition.

The result was that an enrichment in Pu of 14.6% is required to the MOX fuel to make the test core critical, however, all the available fuels of Table 2, besides the reference one (Table 1), corresponding to different discharged burn-up levels, have a negative burn-up reactivity swing in time with this enrichment. The reference MOX fuel (labelled MOX PWR) requires an enrichment of 12.4 % in Pu to have a burn-up evolution in time almost flat over about 7 years. AGR, instead, is successfully flattened with a Pu enrichment of 13.1 %, but the test core is subcritical with this fuel.

A modification of the isotopic vectors of these fuels is therefore required and in this work we decided to modify the Pu vector only for the moment. That means that the U vector is kept as that of our reference MOX fuel.

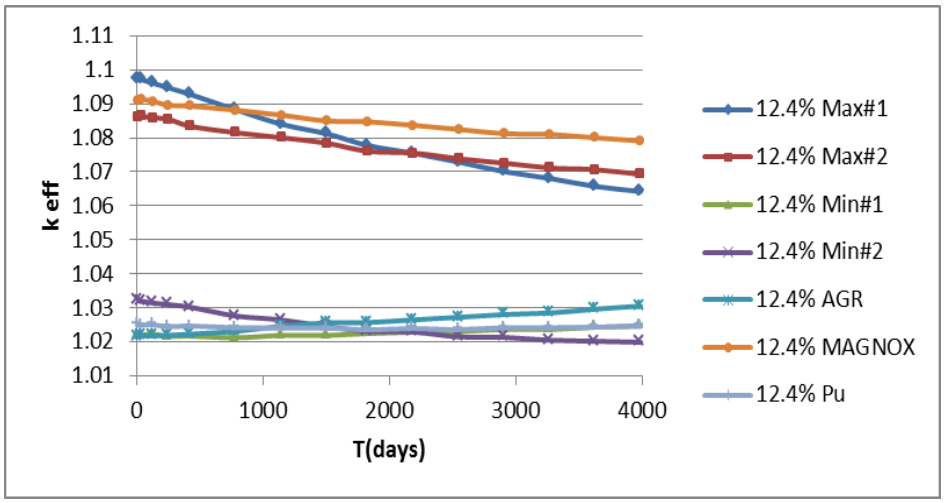

Figure 1 The time evolution of k_{eff} for the previous fuels. 12.4% Pu is the reference MOX, as specified above. The system simulated is always a cylinder of fuel with H=D=84 cm, surrounded by an axial and radial lead reflector, 20 cm thick. Being the geometry fixed here the absolute values of k_{eff} can be compared.

2. Pu vector optimization

The evolution of the fuel composition in time is ruled by the Bateman equations. A procedure of fuel optimization has to face them. However, by simply comparing the behaviour of fuel compositions differing just in the content of a couple of isotopes, for instance Min#1 and Min#2 or Max#1 and Max#2, we can draw some conclusions.

Looking for instance at Min#1 and Min#2, Figure 1, that have the same fissile to fertile ratio, it stands out that the fissile to fertile ratio doesn't explain alone the breeding or burning behavior of a certain fuel. ^{241}Pu and ^{239}Pu are not equivalent as we will justify later.

At equal weight percent of the other isotopes (Max#1, Max#2) a higher value of the ratio of ^{239}Pu to ^{241}Pu content means more breeding, although at the expense of the initial excess of reactivity. This last consequence can be explained by the fact that the fission cross section of ^{241}Pu is higher than that of ^{239}Pu almost at all energies lower than about 0.6 MeV and also the number of neutrons produced per fission is slightly higher in the case of ^{241}Pu at all energies [13]. This fact can be seen even more clearly from then behaviour of η with energy for the principal fissile nuclei.

By comparing Max#1 and Max#2 in particular we also see that increasing the ^{239}Pu to ^{241}Pu ratio it is possible to achieve a smaller total reactivity swing during burn-up.

A reason of this can be seen in the accumulation of ^{240}Pu and ^{242}Pu (something that happens also during recycling) that leads to more parasitic absorptions. ^{242}Pu, deriving from ^{241}Pu neutron captures, in particular, transmutes weakly into ^{243}Pu that has a low fission cross section, therefore ^{242}Pu behaves essentially as a parasitic absorber. While ^{240}Pu neutron absorption can be useful in terms of transmutation and safety (Doppler effect), we can try to reduce the ^{242}Pu content in AGR.

When we think of increasing the content of ^{241}Pu, we must also take into account the decay of ^{241}Pu into ^{241}Am, that has a very large thermal capture cross section and a large capture resonance integral, which lead to an inherent reactivity loss in time.

Some more precise hints can be derived from the production/destruction balance equations for the concentrations of the different isotopes, by making some reasonable assumptions.

We start by requiring that the number of fissile nuclei remains constant in time. We indicate quantities referring to an isotope by means of a *nm* superscript, where *n* is the last digit of the atomic number Z and *m* the corresponding one in the mass number A of that isotope. For instance n^{49} is used to indicate the atomic concentration of ^{239}Pu.

In case of ^{239}Pu we have $\frac{\partial n^{49}}{\partial t} = \lambda^{39} n^{39} - \sigma_a^{49} \phi n^{49} + \sigma_\gamma^{48} \phi n^{48} = 0$. Neglecting ^{239}Np contribution we would have $\frac{n^{49}}{n^{48}} = \frac{\sigma_\gamma^{48}}{\sigma_a^{49}} \approx 0.05$, where we made a rough estimation of the fast one group constants by averaging the JEFF 3.1.1 tabulated cross sections on a typical fission spectrum, getting a good agreement with those found in [2].

By neglecting ^{239}Np contribution we are making a very poor guess of the optimum ^{49}n/^{48}n ratio as long as the ^{39}n is varying rapidly with time. The equation describing the time behavior of ^{239}Np can be easily solved analytically, since it results in a system of only three differential equations involving also ^{239}U and ^{238}U, one of which, that for ^{238}U, is even uncoupled, since this isotope can only disappear by absorbing neutrons and no one transmutes or decays in it. Being ^{239}Np half-life very short compared to our time scale, ^{39}n can be expected to be rather constant over most of the time, with the exclusion of a time interval of the order of magnitude of some tens of days after BOL, and after the reactor shut-down when ^{39}n respectively grows to a nearly stationary value and rapidly drops to zero. This behavior can be confirmed by analyzing ALEPH output file or referring to some previous work on MOX burn-up, as [14].

Our first guess will very likely lead to an excessive breeding, as it appeared in our first simualtions. We can correct this problem in two ways, either increasing ^{49}n/ ^{48}n ratio keeping Pu enrichment constant or by increasing the Pu enrichment preserving the original ^{49}n/ ^{48}n ratio .

As regards ^{241}Pu, we can write: $\frac{\partial n^{41}}{\partial t} = \sigma_\gamma^{40} \phi n^{40} - (\lambda^{41} + \sigma_a^{41} \phi) n^{41} = 0$. That means $\frac{n^{40}}{n^{41}} = \frac{\lambda^{41} + \sigma_a^{41} \phi}{\sigma_\gamma^{40} \phi}$,

that in case of 10^{14} n/(cm^2 s) gives $\frac{n^{40}}{n^{41}} \approx 190$.

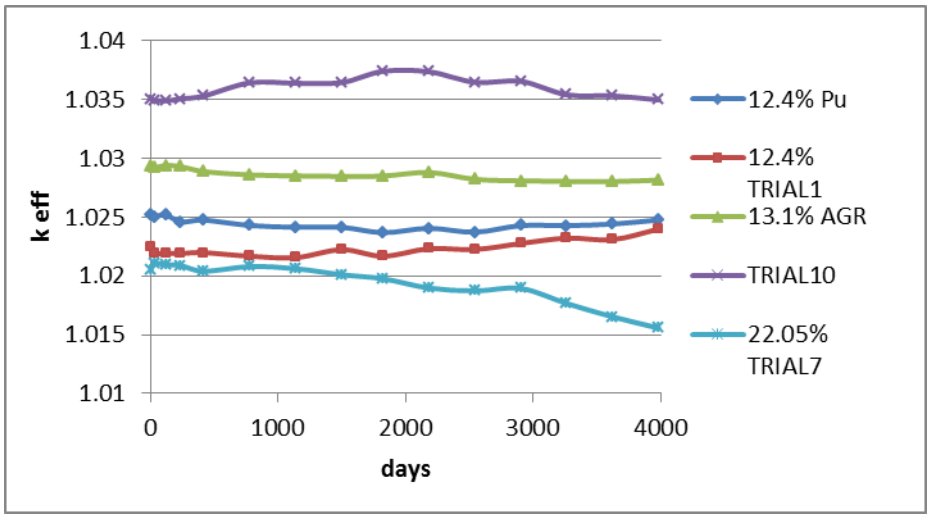

Figure 2 Time evolution of k_{eff} for some of our modified fuels. In this plot we isolated the best candidates.

We must notice that this value again is very approximate, since this ratio, as long the neutron flux is not much bigger than $\lambda^{41}/\sigma_a^{41} \approx 10^{15}\ n/cm^2 s$, is strongly dependent on the exact value of the flux. It would be almost independent and close to an asymptotic value of about 21 for very intense fluxes, but unfortunately this is not the case.

As a general guideline, we finally remind that ^{242}Pu is a parasitic absorber (^{243}Pu has a weak fission cross section), therefore its concentration should be kept low.

A similar procedure can be applied to the U vector, but we neglect this topic at the moment.

Using this strategy we were able to define optimized fuel vectors, such as the one that we called TRIAL 10, 18.5 % enriched in Pu, that are able to make our test core critical. However with this procedure we end up with unmanufacturable Pu vectors as we have to consider their full details and it is very difficult to avoid a loss of reactivity at constant plutonium enrichment and volume.

Table 3 Detailed isotopic composition of the most promising fuel candidates. The U vector is the same of the reference MOX. The numbers are atomic percentages.

isotope	TRIAL10	TRIAL7	isotope	TRIAL10	TRIAL7
^{234}U	0.003	0.003	^{238}Pu	29.616	58.200
^{235}U	0.409	0.409	^{239}Pu	31.557	3.019
^{236}U	0.010	0.010	^{240}Pu	33.826	33.785
^{238}U	99.578	99.578	^{241}Pu	0.059	0.059
			^{242}Pu	4.942	4.937

2.1. The equivalent fraction of ^{239}Pu.

So far we have done several steps toward a solution of our problem of optimizing the MOX fuel composition for a long burning core with a reactivity swing close or lower than beta. Yet, to solve the problem, we need to identify one or a few parameters that are able alone to control both the burn-up reactivity swing and the excess of reactivity at BOL at fixed geometry.

We already know that the fissile to fertile ratio alone can't control the burn-up evolution with time. The idea is then to try to give to the main plutonium and uranium isotopes a reactivity weight based on their fast one group absorption and fission cross sections and on the average number of neutrons produced per fission.

Precisely the quantity we will average on a fast spectrum is $\sigma_i \equiv \nu\sigma_{fi} - \sigma_{ai}$, where *i* is the index of the different isotopes.

Consider the plutonium and uranium isotopic vectors of our fuel, each with its atomic fractions a_{fi}. We would like to convert the real composition to an equivalent one where only ^{239}Pu and ^{238}U are present, with atomic fractions *a* and *1-a* respectively. The two compositions are assumed to differ just because of the absorption and fission cross sections. The equivalence is valid at the first perturbation order if the difference, integrated over the lethargy variable *u* $\int\{\sum_i a_{fi}\sigma_i^+ - [a\sigma_{49}^+ + (1-a)\sigma_{28}^+]\}\Phi^+(u)\Phi(u)du$ vanishes.

The one in the relation above can be conveniently written as $\sum_i a_{fi}$. Defining $\int \Phi^+(u)\sigma_i^+\Phi(u)du \equiv \bar{\sigma}_i^+$,we have $\sum_i(\bar{\sigma}_i^+ - \bar{\sigma}_{28}^+)\, a_{fi} = (\bar{\sigma}_{49}^+ - \bar{\sigma}_{28}^+)a$.

Therefore, $= \sum_i a_{fi}w_i$, where the weights w_i are defined as $w_i = {(\bar{\sigma}_i^+ - \bar{\sigma}_{28}^+)}\Big/{(\bar{\sigma}_{49}^+ - \bar{\sigma}_{28}^+)}$.

Isotope	Weight
^{235}U	0.8
^{238}U	0
^{239}Pu	1
^{240}Pu	0.1
^{241}Pu	1.5
^{242}Pu	0

Table 4 The values of the reactivity weights defined in the text above, averaged over a fast spectrum.

If the plutonium enrichment is ε, the expression for the plutonium equivalent fraction *a,* can be also written as

$$a = \varepsilon \sum_{Pu} a_{fi}w_i + (1-\varepsilon)\sum_{U} a_{fi}w_i . \qquad (2)$$

In Figure 3 we show a plot of the values of the plutonium equivalent fraction *a* for the optimized fuels TRIAL7 22.05%, TRIAL10 18.5%, AGR 13.1% and MOX 12.4%, versus their plutonium enrichment. Extrapolating from this curve the proper values of *a* it was possible to set compositions with different Pu enrichments (16%, 15%), still satisfying our requests about the burn-up behaviour, either modifying for instance AGR or TRIAL10 original compositions, to get the aimed value of *a*. These points were also added to Figure 3.

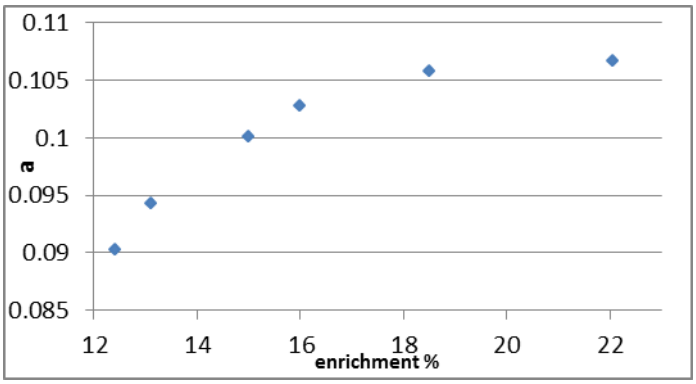

Figure 3 The behaviour of the equivalent ^{239}Pu fraction of the fuel compositions whose k_{eff} has been flattened over 11 years as a function of their plutonium enrichment. From this empirical curve it is possible either to choose a value of enrichment and to calculate the value of the parameter *a* of the corresponding optimized fuel, or to estimate the enrichment required to a fuel with a given value of *a* to have a burn-up reactivity swing almost zero over at least 10 years.

This proved the effectiveness of this parameter to select the burn-up behaviour. If the value of *a* for a certain fuel at a given Pu enrichment lies above the curve in Figure 3, it means that burning prevails over breeding, and the opposite in case of a too low value of *a*. This is quite reasonable if we consider first of all the physical meaning of this parameter and then the way it is calculated.

At this point we are able to estimate a convenient composition of the Pu vector once the enrichment is set or vice versa. In order to get the desired value of *a* it is very useful to recollect the previous discussions about the effect of the main isotopes in the Pu vector in terms of burn-up performance. We will analyse in a future work the impact of the equivalent fraction of ^{239} Pu on the fuel cycle length at fixed Pu-enrichment.

A first chance to exploit what we have learnt so far can be found soon. Having a look at Table 3, we notice that the content of ^{238}Pu is very high; it could be difficult to manufacture such a fuel if we consider the enormous heat output of this isotope. We could try to reduce this quantity preserving the value of *a.* This led to TRIAL10 M composition, 18.5% enriched, of Table 6, where the content of ^{238}Pu is the same as in the reference MOX (atomic fraction: 2.348%).

If this new fuel is charged in our test core at BOL we have k_{eff} = 1.03282 ± 0.00036, when the active height is 120 cm. With this last check we can state that the composition we called TRIAL10 18.5 % M (see Table 6) is the best at our disposal at the moment.

Now we increase our ambitions. Since whenever you change the Pu vector the risk of losing too much in reactivity at fixed geometry is always implied, we would like to be able to control not only the burn-up behaviour but also the reactivity of our fuel. We can see if simply the fissile to fertile ratio, that before proved unable to distinguish between different burn-up behaviours, is sufficient to tell apart more and less reactive fuels. By plotting for instance the k_{eff} values at BOL for the fuels of Table 2 (fixed enrichment and geometry) versus this ratio, one soon realizes that again these two quantities are nearly uncorrelated (scattered points).

Fuel	K_{eff} BOL
AGR 15%	1.08791 ± 0.00037
TRIAL10 16%	1.11016 ± 0.00044

Table 5 The k_{eff} at BOL for a cylinder of fuel with H=D=84 cm, surrounded by a 20 cm thick axial and radial lead reflector.

Can then the equivalent ^{239}Pu fraction be the solution of our problem once again? If we plot the values of k_{eff} for the optimized fuels versus the equivalent ^{239}Pu fraction, Figure 4, we get quite confident since the relation appears linear.

Name	^{238}Pu	^{239}Pu	^{240}Pu	^{241}Pu	^{242}Pu
MOX 12.4%	2.35	57.01	26.95	6.07	7.62
TRIAL7 22.05%	58.20	3.02	33.79	0.06	4.93
TRIAL10 18.5% M	2.35	49.74	42.91	0.06	4.94
TRIAL10 16%	7.04	54.11	33.84	0.06	4.95
AGR 13.1%	1.01	60.13	29.94	3.98	4.94
AGR 15%	10.80	54.31	29.94	0.00	4.95

Table 6 The Pu vectors (atomic fractions) of the fuels used to make the plot of Figure 4. All of them show the desired behavior of k_{eff} along burn-up over 11 years.

However the linear relation is different if we instead plot the fuels of Table 2, all of them with an enrichment of 12.4%, as one can see from Figure 4.

In order to understand the situation we have to see how k_{eff} behaves at fixed geometry in cases of different compositions resulting in the same value of *a*. Unfortunately it turns out that different k_{eff} can be obtained for the same equivalent ^{239}Pu fraction.

We can try to take this into account by re-introducing the fissile to fertile ratio that reasonably should play some role in this problem. If we impose that the equivalent ^{239}Pu fraction remains constant and the normalization condition upon the atomic fractions of the plutonium vectors, when we choose a particular value of the fissile to fertile ratio *f*, we end up with 2 degrees of freedom.

If we now, for instance, set the atomic fractions of ^{242}Pu and ^{238}Pu to a fixed value and vary the others to select different fissile to fertile ratios we discover that at fixed equivalent ^{239}Pu fraction, the resulting k_{eff} varies linearly with the fissile to fertile ratio. Once a proper couple of enrichment and equivalent ^{239}Pu fraction is chosen to have a fuel with an optimized burn-up behaviour, we can then increase the k_{eff} by raising the fissile to fertile ratio *f*. Notice that the interval of values within which *f* can vary is univocally determined by the choice of the two remaining degrees of freedom of the problem, in this case the atomic fractions of ^{242}Pu and ^{238}Pu. In turn these quantities can have some constraints, in the case of ^{238}Pu, for instance, we have an upper limit, because of the huge thermal output of this isotope.

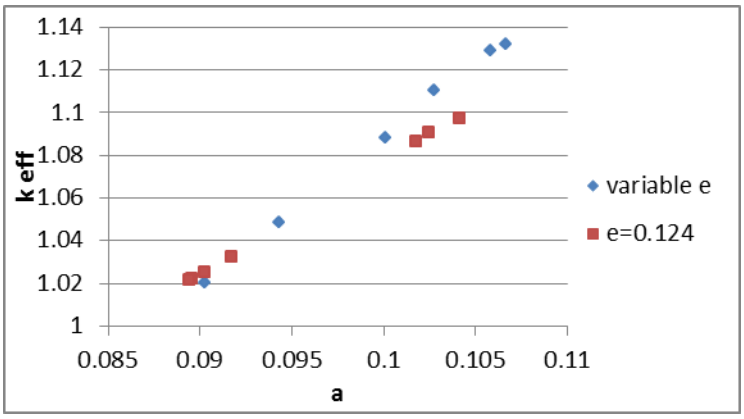

Figure 4 The behaviour of k_{eff} versus the equivalent ^{239}Pu fraction. In blue we plotted the optimized compositions of Table 6, while in red the case of the fuels of Table 2, all with an enrichment of 12.4%, is shown. The system is a cylinder of fuel with H=D=84 cm, surrounded by a 20 cm thick axial and radial lead reflector.

By conveniently varying the atomic fraction of ^{238}Pu, it is possible to get two or more compositions that have the same value of *a* and where *f* is allowed to assume values in intervals at least partially overlapping. What we discovered is that it is possible to have slightly different relations between k_{eff} and *f,* at fixed equivalent ^{239}Pu fraction. This result is shown in Figure 5. It simply means that in reality the reactivity excess depends in a more complicated manner upon the exact composition of the Pu vector. This is not surprising since both *a* and *f* are clearly just approximate parameters and can't alone include all the physical details of our system. If we want to keep all these effects into account we are forced to consider the isotopic vector in detail.

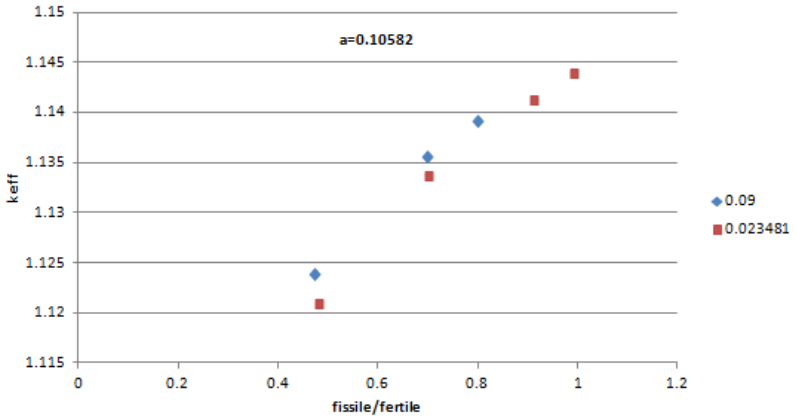

Figure 5 For a fixed value of the equivalent fraction of ^{239}Pu we plotted the behaviour of k_{eff} for different fissile to fertile ratios. The blue dots correspond to an atomic fraction of ^{238}Pu of 9%, the ones in red instead to a content of 2.35%, as in the case of MOX. In both cases the atomic fraction of ^{242}Pu is 4.94%, while the atomic fractions of the other isotopes of Pu are univocally defined by the request of fixed equivalent fraction of ^{239}Pu, by the condition of normalization of the atomic fractions, and by the choices of the atomic fraction of ^{238}Pu and of the fissile to fertile ratio. The system is a cylinder of fuel with H=D=84 cm, surrounded by a 20 cm thick axial and radial lead reflector.

To summarize, we have discovered that once we have optimized the burn-up behaviour of our fuel by a careful choice of the values of the enrichment and of the equivalent ^{239}Pu fraction, by means of Figure 3, we can then adjust the reactivity excess by varying the fertile to fissile ratio *f*. In doing this we have to remember that it is possible to get slightly different values of k_{eff} even if the value of *f* is the same, depending on the detailed compositions of the Pu vectors. Now that we are aware of this limit we can realize that the consequences are not so tragic. Even if we can't have an empirical relation between the reactivity excess and the fissile to fertile ratio at fixed equivalent ^{239}Pu fraction, we know that as long as we keep constant the value of *a,* the burn-up behaviour doesn't change significantly.

Even if we have just concluded that an unique relation between k_{eff} and the equivalent ^{239}Pu fraction even in presence of a fixed fissile to fertile ratio doesn't exactly exist, the plots of Figure 4 can be still of some utility.

In fact, by taking them into account, we could proceed in the optimization of our fuel as follows:

1) with a targeted value of k_{eff} in mind, we can choose around which value of *a* it is convenient to work from Figure 4; knowing that this is little more than an initial guess and that later we can always refine the amount of reactivity excess by modifying the value of *f* keeping *a* constant;

2) extrapolate from Figure 3 the enrichment necessary to optimize the burn-up behavior of the fuel.

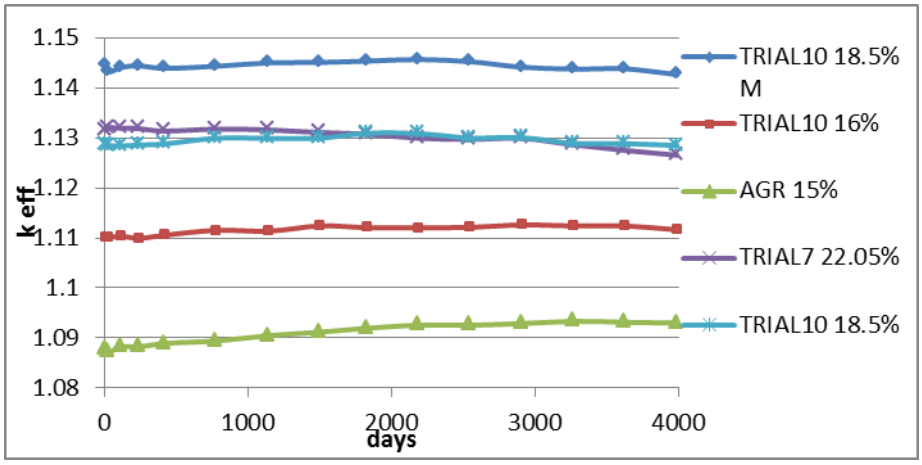

Figure 6 k_{eff} evolution in time for the two initial best candidates TRIAL10 18.5% and TRIAL7 22.05% and the new compositions. The system is always a cylinder of fuel with H=D=84 cm and 20 cm of axial and radial lead reflector. TRIAL10 18.5 % M is now the best solution since it both provides a very flat time profile of k_{eff} and the highest reactivity excess at fixed geometry. Besides the ^{238}Pu content has been reduced in this composition to that of the reference MOX, in order to keep into account the enormous thermal output of this isotope.

Let's face now the problem of how we can produce the fuel we would like to have. In practice it is not possible to manufacture a fuel exactly in accordance with the vectors so far specified; what would be very useful is to make the vectors of interest correspond to a certain level of discharged burn-up from any kind of existing NPP. Mixtures of the real discharged fuels to get the desired isotopic vectors could be also foreseen.

	^{238}Pu	^{239}Pu	^{240}Pu	^{241}Pu	^{242}Pu	$\sum_{Pu} a_{fi} w_i$
Min#1	2.40	57.33	27.30	5.38	7.59	0.699
Min#2	2.40	53.8	27.30	8.91	7.59	0.717
Max#1	0.88	64.31	22.30	9.66	2.85	0.817
Max#2	0.88	68.2	22.30	5.77	2.85	0.798
MAGNOX	0.10	71.90	23.00	4.00	1.00	0.803
AGR	1.00	60.00	30.00	4.00	5.00	0.698
MOX PWR	2.35	57.01	26.95	6.07	7.62	0.705

Table 7 The isotopic vectors from which we started our optimization. The term in the equivalent fraction of ^{239}Pu due to the plutonium isotopes is included.

In reality we have shown that it is not crucial to know in detail the plutonium vector composition, since the reactivity swing and the excess of reactivity at BOL can be controlled rather well by means of a couple of parameters, the equivalent fraction of ^{239}Pu and the fissile to fertile ratio, that provide an integral information. Therefore, instead of declaring the full isotopic vectors of our best performing fuel, TRIAL10 18.5% M, as in Table 6, we can simply say that if one is interested in a plutonium enrichment of 18.5% he has to use a fuel with an equivalent fraction of ^{239}Pu (calculated as specified by (2)) of about 0.1058. Then the excess of reactivity can be set by choosing a convenient value of *f*. For different enrichments one refers to Figure 3.

By a direct calculation we know that the k_{eff} of a fuel in the shape of a cylinder with H=D=84 cm, surrounded by 20 cm of axial and radial lead reflector, must not be lower than about 1.09, in order to be able to make our test core at least β pcm over-critical. From Figure 4 we can then estimate the corresponding value of the ^{239}Pu equivalent fraction as equal to about 0.1. Finally, using Figure 3, we find that the corresponding optimum enrichment is around 15%.

In general, starting from the targeted excess of reactivity it is possible, using both Figure 3 and Figure 4, to estimate the equivalent ^{239}Pu fraction and then the value of the plutonium enrichment of the optimized fuel, although with all the limits that we stated in the previous paragraphs. In this way one defines a fuel

composition with both the wanted excess of reactivity at fixed geometry and a nearly flat k_{eff} evolution over a long period of time.

Let's now try to work around the minimum excess of reactivity: as we said the corresponding value of *a* is of about 0.1 and the required enrichment is around 15%. However one can verify that all fuels in Table 2, when the enrichment is set to 15%, have values of *a* of at least 0.107 (higher than the optimum value and therefore these fuels have negative burn-up swings). This situation can only get worse if we increase any further the enrichment (*a* is a growing function of the enrichment[1], while the optimum value of *a*, up to an enrichment of about 22%, was never found higher than 0.107). This unfortunately means that it is not possible to get an optimum fuel composition by simply mixing the vectors of Table 2, unless one reduces the plutonium enrichment, but with our present test core we know that we are not allowed to go lower than 14.6%. If it was instead possible to work at lower enrichments, we know already that AGR composition could be optimized with a plutonium enrichment of 13.1%, while all the other fuels of Table 2 are optimized at lower enrichments.

3. Preliminary results on dpa rates

Preliminary studies on the neutron-induced damages (dpa) on the steel structures we made using our modified ALFRED model working at a power of 100 MWth. If we consider the same limits as in the LEADER project (the structural materials are the same), after about 19 years of exposure the fuel rods would have to be removed. As regards the reactor vessel a core life-time of 50 years is achievable. However, with a proper power flattening by using zones of different enrichments a lifetime of at least 25 years for all components is expected to be achievable.

4. Conclusions

In this paper we studied a procedure of nuclear fuel optimisation in order to have a long burning core without reshuffling and with a reactivity swing close to β, that in a MOX fuel is around 400 pcm. By selecting two parameters, the fissile to fertile ratio *f* and the equivalent fraction of ^{239}Pu *a,* we were able to control both the burn-up behaviour and the reactivity excess at BOL. Thus, it was possible to sketch a process of fuel optimization.

One can start from the requested reactivity excess at BOL and by using an empirical curve between k_{eff} and *a* (Figure 4), a range of values for the equivalent fraction of ^{239}Pu can be selected. At this point the enrichment needed to have an optimized fuel can be estimated since *a* is known, by means of another empirical curve, showed in this paper (Figure 3). As a final step, the excess of reactivity at BOL can be varied changing *f* but preserving *a.*

In this way we defined some optimized fuels, with both a small reactivity swing along a period of burn-up of 11 years and able to make critical a modified version of ALFRED core, assumed as a good approximation of a SMR. To define our fuel we need no more to specify the details of the isotopic vectors, but only the values of *a*, *f* and of the Pu enrichment.

Discussion with fuel-cycle specialists has now to confirm that the manufacturing of fuels according to our specifications is realistic. Born in the frame of the MYRRHA project, this work will continue with the definition of a detailed MYRRHA-based SMR core, cooled in natural circulation in all operating modes, to which our optimization procedure will be applied. The possibility of the insertion of fertile material in the form of axial heterogeneities or of a blanket, as currently studied in other on-going GEN-IV projects, will be investigated.

[1] This is true until $\sum_{Pu} a_{fi} w_i > \sum_{U} a_{fi} w_i$; the inequality is verified in our cases.

REFERENCES

[1] *MYRRHA-A multi-purpose fast spectrum research reactor*, Aït Abderrahim Hamid, Baeten Peter, Fernandez Rafaël, De Bruyn Didier, Energy Conversion and Management, Volume 63, November 2012, pages 4-10.

[2] *Nuclear Reactor Physics*, Weston M.Stacey, John Wiley and Sons, 2007.

[3] *PASCAR: Long burning small modular reactor based on natural circulation,* Sungyeol Choi, Jae-Hyun Cho, Moo-Hoon Bae, Jun Lim, Dina Puspitarini, Ji Hoon Jeun, Han-Gyu Joo, Il Soon Hwang, Nuclear Engineering and Design, Volume 24, Issue 5, March 2011.

[4] *Design features of BREST Reactor and experimental work to advance the concept of BREST Reactors*, A.I. Filin, V.V. Orlov, V.N. Leonov, A.G. Sila-Novitski, V.S. Smirnov, V.S.Tsikunov.

[5] *Design study on reactor structure of Pb-Bi-cooled direct contact boiling water fast reactor (PBWFR)*, Minoru Takahashi, Shoji Uchida, Yoshiyuki Kasahara, Progress in Nuclear Energy, Volume 50, Issues 2-6, March-August 2008.

[6] *SSTAR: The US lead-cooled fast reactor (LFR),* Craig F. Smith, William G.Halsey, Neil W. Brown, James J. Sienicki, Anton Moisseytsev, David C. Wade, Journal of Nuclear Materials, Volume 376, Issue 3, 15 June 2008.

[7] *Core design investigation for a SUPERSTAR small modular lead-cooled fast reactor demonstrator*, S. Bortota, A. Moisseytsevb, J.J. Sienickib, Carlo Artioli, Nuclear Engineering and Design, Volume 241, Issue 8, August 2011.

[8] *SVBR-100 module-type fast reactor of the IV generation for regional power Industry*, A.V. Zrodnikov, G.I.Toshinsky, O.G.Komlev,V.S.Stepanov, N.N.Klimov, Journal of Nuclear Materials, Volume 415, Issue 3, 31 August 2011.

[9] *Preliminary Fuel Pin and Hexagonal Assembly design*, V. Sobolev *et al*., ELSY, European Lead-cooled SYstem, D5, September 2007.

[10] *Alfred Core*, Alberto Ottonello, Edouard Malambu, presentation in the frame of the LEADER project, WP2, Genoa, May 2011, restricted access on www.leader-fp7.eu.

[11] Lead-cooled European Advanced DEmonstration Reactor (LEADER) project. Annex I – Description of Work. EURATOM, FP7-249668, Theme II.2.2 – Reactor Systems - 7th Framework Programme. 2009. See also www.leader-fp7.eu.

[12] *ALEPH 2.1, a Monte Carlo Burn-up Code*, Alexey Stankovskiy, Gert Van den Eynde, Open Report, SCK•CEN-BLG-1075, ISSN 1379-2407, October 2011.

[13] NEA, Nuclear Energy Agency database, for example by means of Janis 3.3, the Java-based nuclear information software, *www.oecd-nea.org/janis.*

[14] *Initial Core design Static, Dynamic and Safety parameters (BOC/EOC)*, Edouard Malambu, DEL/09/007, ELSY, European Lead-cooled System, May 2009.

BN-1200 reactor power unit design development

B.A. Vasilyev, S.F. Shepelev[a], M.R. Ashirmetov[b], V.M. Poplavsky[c]

[a] JSC "Afrikantov OKBM", Nizhny Novgorod, Russia

[b] JSC "SPbAEP", St. Petersburg, Russia

[c] FSUE "SSC RF-IPPE", Obninsk, Russia

Abstract. In February 2010, the RF Government has approved the Federal Target Program "New Generation Nuclear Power Technologies for the Period of 2010-2015 and for the long-term up to 2020". Within this Program, the R&D work for new generation 1200MWe sodium fast reactor is provided.

The BN-1200 design is based on the combination of approved and innovative technical decisions, which allow:

- reliable power unit with large BN reactor to be developed in a short period of time for commercial construction as a part of closed nuclear fuel cycle;
- qualitatively new technical level of power unit to be provided according to generation 4 NPP requirements.

The paper characterizes the activities performed now for the power unit design in various areas:

- power unit design;
- reactor plant (RP) detailed design development;
- R&D work to validate the RP system and equipment;
- code upgrading and verification;
- safety validation.

1. Introduction

BN-1200 power unit is being developed under the Federal Target Program "New Generation Nuclear Power Technologies for the Period of 2010-2015 and for the long-term up to 2020" and under the long-term action program of "Rosenergoatom" Concern to develop a competitive fast neutron reactor with enhances safety.

Since the middle of the last century, the Soviet Union, upon which the Russian Federation has developed the extensive capabilities for sodium fast reactors (BN).

In addition to the experience gained at BR-5/10 and BOR-60 [1], operation of BN-350 reactor (1973 – 1998) showed that, the long-lived equipment operation is ensured when using sodium as a coolant. The results of BN-350 reactor [2] development and operation were fully applied to develop BN-600 reactor together with implementation of more perfect decisions. The main decision is the integral layout, i.e., primary circuit equipment arrangement in the reactor vessel. In spite of large number of new decisions [3], BN-600 reactor operates successfully during more than 30 years starting from 1980.

BN-350 and BN-600 reactor design development and implementation allowed the effective design, production and operation infrastructure to be created, which is the base for further development of BN technology.

BN-800 reactor construction is now the most important phase of this process. The new decisions adopted in BN-800 design are aimed, first of all, at safety enhancement and improvement of economic indices [4]. BN technology development required much time and financial expenditure. A long way was travelled from small research reactors to large commercial power units. Based on well-developed BN technology, the commercial 1200 MW power unit with sodium fast reactor is now under development in Russia [5][6].

2. Main Goals and Provisions of BN-1200 design

The main goals of BN-1200 design are:

(1) development of reliable new generation reactor plant for the commercial power unit with fast reactor to implement the first-priority objectives in changing over to closed nuclear fuel cycle;
(2) improvement of technical and economic indices of BN reactor power unit to the level of those of Russian VVER of equal power;
(3) safety enhancement up to the level of the requirements for the 4th generation RP.

Main conceptual provisions used to develop BN-1200 design:

(1) maximum possible use of well tried scientifically proven technical decisions, implemented in russian BN;
(2) use of new engineering decisions to improve power unit safety and efficiency as well as fuel effectiveness;
(3) selection of electric power equal to that one of AES-2006(add explanation or references) to use general approach for NPP site selection and unification of turbogenerator and other electric equipment of electric energy generation system;
(4) provision of large-size equipment transportation by railway.

3. Main characteristics of BN-1200 power unit

Main technical characteristics of BN-1200 power unit as compared with BN-600 and BN-800 are given in Table 1.

Table 1. Main technical characteristics of BN-600, BN-800 and BN-1200

Reactor	BN-600	BN-800	BN-1200
Nominal thermal capacity/gross electric power, MW	1470/600	2100/880	2800/1220
Number of heat generating loops	3	3	4
Primary circuit temperature at IHX inlet/outlet, °C	535/368	547/354	550/410
Secondary circuit temperature at SG inlet/outlet, °C	505/318	505/309	527/355
Live steam temperature, °C	505	490	510
Live steam pressure, MPa	14	14	17
Feed water temperature, °C	240	210	275
Efficiency, gross/net, %	42.5/40	41.9/38.8	43.5/40.7

4. Design decisions on BN-1200 reactor and RP layout

The BN-1200 reactor block and RP layout diagram are given in Fig. 1, Fig. 2 respectively.

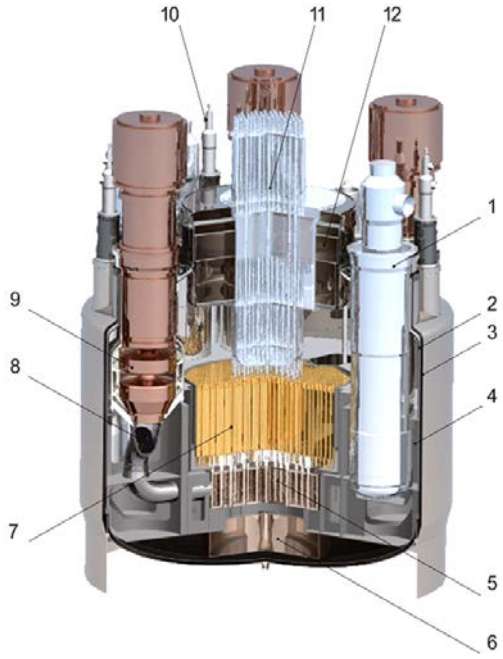

FIG. 1. BN-1200 reactor block:

1 – intermediate heat exchanger (IHX); 2, 3 – main and guard vessels respectively; 4 – support belt; 5 – pressure chamber; 6 – core debris tray; 7 - core; 8 – pressure pipeline; 9 – primary circuit main circulating pump (MCP-1); 10 – FA refuelling mechanism; 11 – control rod drive mechanisms (CRDM); 12 – rotating plugs.

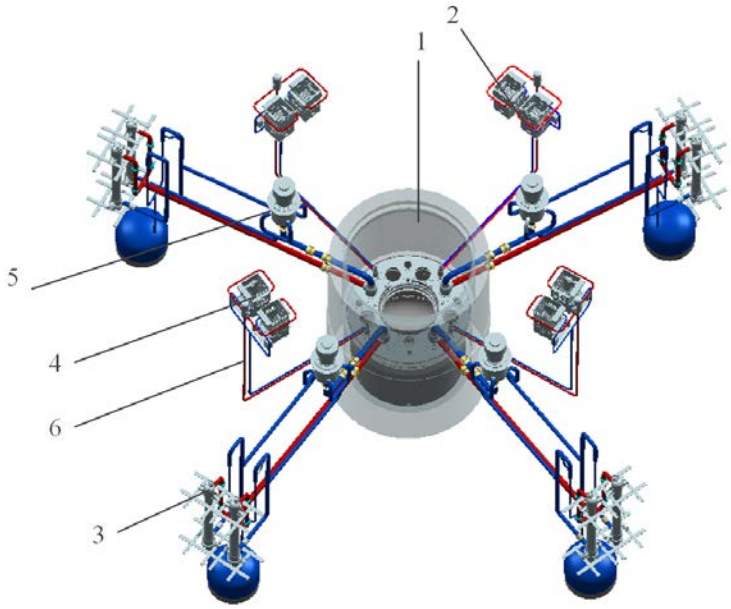

FIG. 2. BN-1200 RP layout diagram:

1 – reactor; 2 – secondary circuit main circulating pump (MCP-2); 3 – steam generator (SG); 4 – air heat exchanger (AHX); 5 – secondary circuit main pipelines; 6 – emergency heat removal system (EHRS) pipelines. (Figure index needs to be modified, 5:Secondary pump, 2:AHX)

BN-1200 development is based on maximum possible use of technical decisions, which showed good results in BN-600, and used in BN-800:

(1) primary circuit integral layout with guard vessel and main vessel supported in its lower part;
(2) rotating plugs of in-reactor refuelling system with sealing hydraulic locks based on tin-bismuth alloy;
(3) separate suction cavities of primary circuit pumps with check valves at pump discharge, which allow one of four RP heat removal loops to be disconnected in case of equipment failure without reactor shutdown;
(4) in-reactor storage for spent fuel assemblies (FA).

The design decisions adopted for some BN-1200 equipment (MCP-1, MCP-2, IHX, CRDM, autonomous heat exchangers) are taken close to those ones for BN-600 and BN-800 [6].

New technical decisions introduced in BN-1200 design are aimed to improve power unit safety and efficiency as well as fuel effectiveness.

The principally new decision is placement of the EHRS equipment and primary sodium purification system equipment inside the reactor vessel. This made possible not only to avoid the radioactive sodium leaking outside, but to reduce the number of auxiliary systems.

It is planned to aggregate substantially the BN-1200 SG (in view of demonstrated high reliability of sodium-water SG) to reduce RP specific material consumption. In addition, in order to increase the SG lifetime, they provide to use a new structural material – steel 12Cr-Ni-Mo-V-Nb, which has higher temperature and corrosion resistance as compared with steel 2Cr-Mo used in BN-600 and BN-800.

In BN-1200 design, the neutron irradiation of in-reactor structures is reduced to ensure the increased reactor service life up to 60 years.

BN-1200 refuelling system is considerably simplified due to some new decisions accepted and due to reduced residual energy release in the unloaded FAs because of the increased storage time up to 2 years in the in-reactor storage. Specifically due to the last decision, the sodium store for spent FAs intermediate storage before washing and transportation to the water pool is excluded.

Application of bellows thermal expansion compensators will allow reducing the sodium pipeline length of the secondary circuit as compared with BN-600 and BN-800 that will result in decrease of total structural volume and power unit material consumption.

RP parameters have been optimized. Feed water temperature and steam pressure increase resulted in efficiency increase (gross) by 1.5 %. The corresponding turbine generator is under development.

BN-1200 unit power increase as compared with BN-800 and implementation of new decisions brought to reactor vessel diameter increase (from 13 to 15.9 m) and aggregation of main equipment (IHX, MCP, SG, pressure chamber, rotating plugs, pipelines). However, the equipment fabrication process does not basically change relative to that one proven during BN-800 equipment fabrication, including reactor vessel assembling at the site. The only novelty is assembling of the large rotating plug at the site, as far as its dimensions exceed the railway shipping clearances.

5. Core Design Characteristics

The reactor cores with two types of fuel (MOX and nitride) are under development for BN-1200 reactor. The objective of nitride fuel implementation is complete satisfaction of the requirements for inherent safety of the Russian project “Proryv” [7]. Measures are taken to accelerate the experimental data obtaining, which shall ensure the possibility to use the nitride fuel starting from the first loading of BN-1200 reactor. MOX fuel is developed as a backup option in case of any difficulty or delay in nitride fuel validation.

The core layout is characterized by the upper sodium cavity to limit sodium void effect and by application of fuel of same enrichment. Main core characteristics are given in Table 2.

Table 2. BN-1200 core characteristics

Characteristic	Nitride fuel	MOX fuel
Number of FAs in the core	432	432
FA width across flats, mm	181	181
Fuel element diameter, mm	9.3	9.3
Core height, mm	850	850
Fuel loadings, t	59	47
Main fuel FA residence time [*] , year	4	4
Average burnup [*] , MW·day/kg	90	112
Breeding ratio	up to 1.35	up to 1.2

[*] FA residence time and fuel burnup meet the basic design option with achievement of maximum damage dose of ~ 140 dpa using new structural materials for fuel element claddings. During the initial operation stage, less fuel burnup is possible.

6. Power unit design decisions

By now, the following has been performed:

- integrated engineering investigations and ecological studies have been performed for the option of prototype power unit location at Beloyarsk NPP site;
- development of various schematic layout design options for the case of RP power and overall dimensions variation, RP equipment design, parameters of the third circuit and the turbine generator facility;
- studies in space and planning designs to select the optimum option of main vessel components;
- studies in optimization of handling, installation and maintenance equipment of NPP nuclear fuel handling system;
- development of options for general layout and BN-1200 power unit site.

As a result of development of various reactor building layout options (from rectangular to round shape), the round shape option has been accepted with reactor cavity in the centre and diametrical arrangement of RP equipment.

The SGs, EHRS heat exchangers for four RP loops and support system equipment are arranged in the round auxiliary building.

The adopted layout meets the modularity requirements for the equipment and process systems. All four process loops are arranged in the structural units absolutely identical in plan and along the height.

The cylindrical building with the dome above the RP can take load up to 20 t in case of air crash, shock-wave pressure of 30 kPa and maximum design earthquake of magnitude up to 8.

The selected option will allow taking of 400 t load in case of air crash without changes in main systems layout. In addition, only the outer building structures shall be strengthened.

Sectional elevation of BN-1200 power unit reactor building is given in Fig. 3.

Turbine building is made of cast reinforced concrete.

Now, the turbine building option of metal structures is considered to accelerate the construction work.

Further, the cost of civil and installation work as well as fire safety of the turbine building will be analyzed.

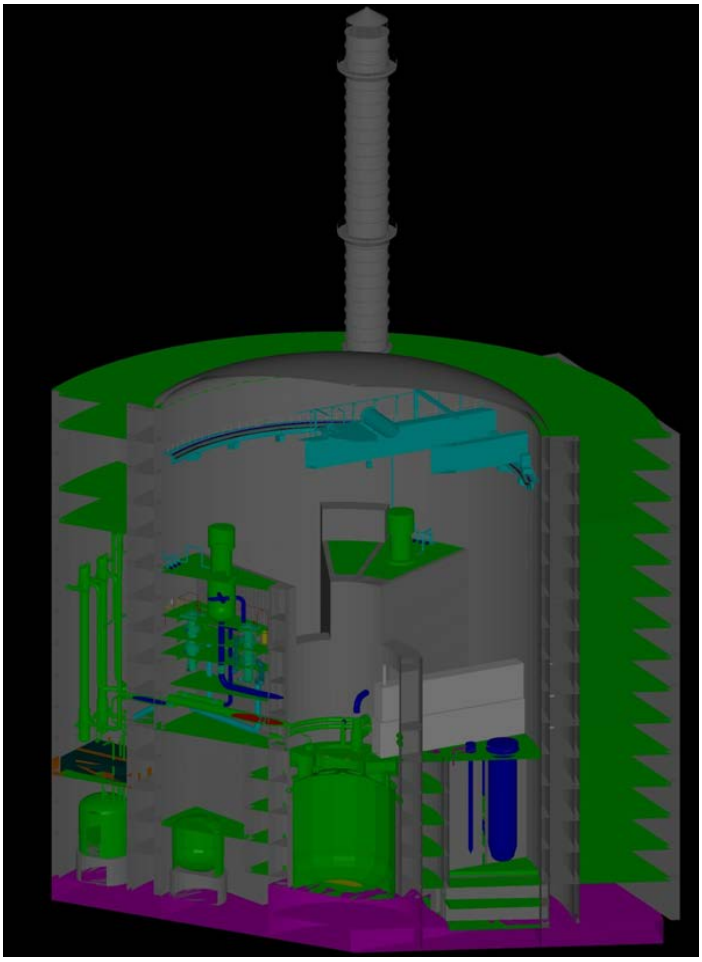

FIG. 3. Sectional elevation of BN-1200 power unit reactor building.

7. Economic indices improvement

Application of new RP design decisions, including the core, and updating of power unit design allowed substantial improving of BN-1200 technical-and-economic indices (Table 3). As a result, RP material consumption decreased by 40% as compared with BN-800. RP design simplification allowed the entire set of auxiliary systems to be excluded. Together with new design decisions application, it became possible to reduce considerably the reactor building overall dimensions (main building). It is planned to improve BN-1200 technical-and-economic indices owing to service life increase up to 60 years that seems to be real in view of experience gained when validating BN-600 service life extension up to 45 years. It is estimated that BN-1200 technical-and-economic indices are comparable with those ones for new LWR VVER-1200 (AES-2006) of same power, which is developed for commercial construction. In future, BN-1200 electricity generation cost shall become less than that one for VVER because of anticipated price increase for natural uranium.

Table 3. BN-1200 technical-and-economic indices as compared with BN-600 and BN-800

Reactor	BN-600	BN-800	BN-1200
RP specific materials consumption, t/MWe	13.0	9.7	5.6
Specific volume of the main vessel, m^3/MWe	1150	750	560
Continues(Continuous) reactor operation between refuelling intervals, eff. day	20-70	155	330
Average fuel burnup, MW·day/kg	70	70-100	up to 138
Plant capacity factor	0.77-0.8	0.85	0.9
Service life, year	45	45	60

Table 4 presents data on service life of BN RP main replaceable equipment, achieved at BN-600 and designed in BN-800 and BN-1200.

Table 4. BN RP replaceable equipment service life

Equipment	Main equipment service life before replacement, minimum, year:		
	BN-600	BN-800	BN-1200
MCP-1/MCP-2 removable part (impeller)	6.5/15	5/5*	15
Primary circuit cold trap	Replacement is not required		10-30**
CRDM (bottom part)	15	15	30
SG	15/30***	23	30

* Specified service life is less than in BN-600 because of more intensive operation conditions;

** The service life of new cold trap built-in the primary circuit depends on the decisions, which will be made as per the results of R&D;

*** Evaporator / superheater .

8. Technical decisions for BN-1200 safety enhancement

In the course of design development, first attention was focused on neutralization off sodium negative properties and plant self-protection properties improvement. The following decisions were made for that:

- instead of the outer sodium pipelines, cold traps are arranged in the reactor vessel that eliminates the most dangerous design-basis accidents with radioactive sodium leaks;
- secondary circuit sodium pipelines are enclosed and their length is reduced because of bellows used to compensate thermal expansions;
- emergency heat removal from the reactor is performed by special system connected directly to the primary circuit via the independent heat exchangers built-in into the reactor vessel. System connection and operation is based on passive principle (natural circulation of heat-removing

fluids in all circuits). Owing to that, the system reliability increases by more than 10 times as compared with BN-800;

- passive emergency protection system, which is actuated in case of core outlet coolant temperature increase, is provided in addition to the passive system on the hydraulically suspended rods, which are inserted into the core in case of primary MCP shutdown;
- the design provides above-reactor leaktight room for confinement of emergency releases from the reactor vessel during beyond-design accidents. After the accident and required decay storage, gas is released to special ventilation system.

Table 5 shows technical decision variations to provide safety as applied to BN designes.

Table 5. Technical decision evolution to enhance BN design safety

Technical decisions on safety	BN-600	BN-800	BN-1200
1 Decisions on sodium circuits:			
- sodium/sodium intermediate circuit	+	+	+
- enclosing of vessels with radioactive sodium	+	+	+
- enclosing of pipelines with radioactive sodium	+	+	pipelines with radioactive sodium are excluded
- enclosing of secondary circuit pipelines	+ (partially)	+ (partially)	+
2 Emergency protection:			
- active	+	+	+
- passive, based on hydraulically suspended rods	-	+	+
- passive, based on temperature principle of operation	-	-	+
3 Emergency heat removal system:			
- as a part of the third circuit	+		
- air heat exchanges are connected to the secondary circuit	-	+	
- air heat exchanges are connected to the primary circuit	-	-	+
4 Melted fuel confinement system	-	+	+
5 Emergency release confinement system	-	-	+

Owing to the adopted decisions, it is planned to achieve safety indices put forth to generation 4 NPP power units. The main requirement is to avoid evacuation of population in case of any technically possible accident.

9. Main R&D Work Areas and Technological Tasks to Implement the Design

BN-1200 reactor design is based on the results of R&D and technological work for validation of previous BN designs; and new decisions will be proven additionally using available test facilities, as well as, BN-600 for fuel testing. Basically, the design development and prototype BN-1200 construction is completion of main R&D work set for mastering of sodium fast reactors.

Main R&D work areas for BN-1200 design validation:

(1) validation of RP equipment (MCP-1, 2, entrainment filter, refuelling complex, SG, bellows compensators);
(2) validation of physical and thermohydraulic characteristics of the core; fuel element lifetime tests using BN-600 reactor;
(3) mastering of passive safety systems (EHRS, hydraulically- and temperature-actuated emergency protection rods);
(4) development of new structural materials to ensure RP service life up to 60 years, to increase lifetime of the replaceable equipment and fuel burnup;
(5) feasibility studies in fuel cycle closing (including minor actinides transmutation);
(6) computer code verification and certification.

10. Progress and plans for BN-1200 design

By 2014, it is planned to determine and validate the main design decisions for the power unit, and to develop the RP final design with validating R&D work, and by 2016, to complete the verifying R&D work. The Beloyarsk NPP, where BN-600 reactor is operated, and BN-800 reactor is constructed, is the optimum site to construct the prototype BN-1200 power unit. Partially, the infrastructure required for new power unit is already available at this site. BN-1200 RP equipment can be completely fabricated at the national production facilities developed for BN-800 RP. It is panned to decide on BN-1200 power unit construction at the stage of RP and power unit final design development based on power unit safety and cost analyses.

11. Conclusion

The experience gained in sodium fast reactor development and operation in Russia shows this technology maturity and possibility to develop BN-1200 design for commercial construction.

Due to optimum combination of reference and new decisions, high technical and economic characteristics and safety indices of BN-1200 design, as well as, possibility of fuel breeding make possible to attribute this design to the fourth generation of NPP power units.

There are necessary productions in Russia to ensure prototype BN-1200 reactor construction at the beginning of 21^{th} and further transition to the commercial construction.

If possible, it is recommended to add design characteristcs of instrumentation and controls, safety analysis and expected cost for electric generation.

REFERENCES

[1] Machinery encyclopedia, vol. IV-25 Nuclear engineering machinery. M.: Mashinostroenie, 2005, p. 589-620, p. 710-712.
[2] Progress in liquid metal fast reactor technology, IAEA-TECDOC-876, April 1996
[3] OSHKANOV, N.N., SARAEV, O.M., BAKANOV, M.V., et al. 30-year experience in operation of BN-600 sodium fast reactor // Atomnaya energia, 2010, vol. 108, issue 4, p. 186-191.
[4] SARAEV, O.M., NOSKOV, YU.V., ZVEREV, D.L., et al. BN-800 power unit design validation and construction progress // Atomnaya energia, 2010, vol. 108, issue. 4, p. 197-201.
[5] RACHKOV, V.I., POPLAVSKY, V.M, TSIBULYA, A.M., et al. Advanced power unit concept with sodium fast reactor // Atomnaya energia, 2010, vol. 108, issue 4, p. 201-206.
[6] VASILYEV, B.A., KAMANIN, YU.L., GLADKOV, V.V., et al. Fast reactor plant equipment upgrading // Atomnaya energia, 2010, vol. 108, issue 4, p. 241-245.
[7] VASILYEV, B.A., EVSEEV, V.I., KUZAVKOV, N.G., et al. Inherent safety principle implementation in BN-1200 RP design// Nuclear and Environmental Safety // International Journal, 2012, No. 1, p. 62-65.

A Simple Recycling of PWR Spent Fuel in a Breed-and-Burn Fast Reactor

Y. Kim and D. Hartanto

Department of Nuclear & Quantum Engineering, KAIST,
Daejeon, Republic of Korea

Presented by Y. Kim

Abstract. The breed-and-burn fast reactor (B&BR), also known as TWR, is attractive in terms of the core performances, economics, and non-proliferation. The B&BR has the capability to breed the fissile fuels and use the bred fuel in situ in the same reactor. In this work, a long-life breed-and-burn type fast reactor has been investigated from the neutronics points of view in order to re-utilize the PWR spent fuel. Feasibility of a compact sodium-cooled B&BR using PWR spent nuclear fuel as blanket material has been studied. In order to derive a compact B&BR, a tight fuel lattice and relatively large fuel pin are used to achieve high fuel volume fraction. The core is initially loaded with a LEU (Low Enriched Uranium) fuel and a metallic fuel is used in the core. For a very high fuel burnup, the smear density of the metallic fuel is burnup-dependent in this work. The Monte Carlo depletion has been performed for the core to see the long-term behavior of the B&B reactor. Several important parameters such as reactivity coefficients, delayed neutron fraction, prompt neutron generation lifetime, fission power, and fast neutron fluence, are analyzed through Monte Carlo reactor analysis. Evolution of the core fuel composition is also analyzed as a function of burnup. Although the long-life small B&B fast reactor is found to be feasible from the neutronics point of view, it is characterized to have several challenging technical issues including a very high fast neutron fluence of the structural materials.

1. Introduction

In recent years, the alternative concept of the fast concept reactor called Breed-and-Burn Fast Reactor (B&BR) has gained more attention and is currently under development [1][2]. The B&BR is unique because of its capability to breed its own fuel for a longer lifetime. The B&BR core consists of 2 fuel regions: the initial core and the blanket region. The active core, which is the initial core in the beginning, moves slowly toward the un-burned blanket. During this process, the fertile fuels in the blanket region are slowly converted into fissile fuels. Consequently, the theoretical lifetime of the B&BR core could be proportional to the height of the blanket in the axial direction.

The initial core is ignited to achieve criticality by using an LEU (Low-Enriched Uranium) fuel, and either natural or depleted uranium is used as the blanket fuel. The preliminary study of the B&BR reactor using the natural uranium blanket has been studied by the author [3]. The PWRs (Pressurized Water Reactors) spent fuel can also be used as the blanket fuel in this type of reactor. A study of using spent nuclear fuel in a 2600 MWth B&BR has been performed [4], but the analyses were based on a rather simple homogeneous modeling of the complex core. In the University of California, Berkeley, the study of neutron balance analysis for the sustainability of 3000 MWth B&BRs using depleted uranium has been investigated [5][6]. A study for recycling the PWRs spent fuel has also been performed by the authors in a small and compact sodium-cooled 250 MWth B&BR [7].

It was found in the previous study [7] that several concerns should be solved in order to realize the small and compact B&BR for recycling PWRs spent fuel. The most concerning problem is the capability of the cladding to withstand the high fast neutron fluence during long irradiation time. With the increased neutron fluence, the material properties usually degraded, which combined with increased stress on the cladding, could lead to the cladding breaching. One of the potential solutions to this problem is to do periodic re-cladding of the fuels when the peak fast neutron is near the allowable limit [5,6]. Another solution is to shuffle the fuel assembly located in the inner core to the outer core and vice versa because the peak fast neutron fluence is located around the center of the core. The other potential solution is to use a vented fuel concept [8][9]. If the fuel rods are vented and the fission gas

pressure does not increase within the rod, the stress load on the fuel cladding will be relieved and the allowable fast neutron fluence limit should be increased.

The local peak discharge burnup is also one of the main concerns. It was found that the peak discharge burnup in the initial LEU region is around 35%, and 20% for the blanket region. When irradiated, the metallic fuel swells. At high burnup, an important swelling could lead to an unacceptable fuel/cladding mechanical interaction (FCMI).To accommodate this swelling, the smeared density concept is applied to the metallic fuel in the fast reactor. It is concluded in the Ref. [10] that the 75% smeared density will allow the fuel to achieve burnup up to ~20% without any unacceptable FCMI occurring. In previous work [7], a uniform 75% smeared density was used for the both fuels in initial LEU core and blanket region. In this work, to deal with over 20% local burnup, different smeared densities for the initial LEU core and blanket region are proposed. Several important reactor parameters are also characterized to identify the major technical issues and challenges.

For the neutronic analysis, the continuous energy Monte Carlo code McCARD [11] was used. It also has a built-in depletion routine, thus it can be used in a stand-alone mode for the core depletion analysis. In a Monte Carlo depletion calculation, it is important to consider as many fission products as possible. In the current McCARD depletion calculation, all actinides and over 160 fission products are considered.

2. Compact Breed-and-Burn Reactor Concept

The compact sodium-cooled B&BR core configuration is identical to the one in Ref. [7]. Figure 1 shows the core configurations devised and considered in this work. The core consists of 78 hexagonal fuel assemblies, 78 hexagonal reflector assemblies, and 7 control rod assemblies. The equivalent core radius is about 115 cm. The reactor power is set to 250 MWth so that the electrical output should be about 100 MWe. The 7 control rod assemblies can be grouped into primary and secondary control rods since the burnup reactivity swing in the B&BR can be very small.

In Fig.2, the basic configurations of the fuel and the reflector assemblies are shown. It is assumed that the modified HT-9 is used as the structural material of the fuel and the reflector assemblies. Unlike the conventional sodium-cooled fast reactors, Pb (lead) is used as the radial reflector in the current B&BR since the superior neutronic performance of the Pb reflector results in a smaller core size than the conventional steel reflector [12]. In addition, a Pb reflector can be more favorable in terms of the temperature coefficient of reactivity due to its higher thermal expansion [3].

A sodium-bonded U-Zr metallic fuel is used in this small B&BR. In general, a high fuel volume fraction is required for the B&BR type reactor to achieve a long-life core. Consequently, the fuel volume fraction should be maximized in the case of a compact B&BR. In order to increase the fuel fraction, a relatively large pin and a tight lattice are utilized, as in Ref. [13]. Through a sensitivity analysis of the neutronic performance, the diameter of the fuel pin and the P/D were determined to be 1.9 cm and 1.064, respectively. The HT-9 cladding thickness is assumed to be 0.06 cm. As shown in Fig. 2, a fuel assembly consists of 127 fuel pins. The space wire is not shown in Figure 2. The thickness of the assembly duct is 3 mm and the flat-to-flat distance of the fuel assembly is 23.72 cm. The resulting volume fraction of fuel, coolant, and structure is 63.494%, 22.533%, and 13.970%, respectively.

As shown in the Fig. 1, the axial configuration of the small B&BR is quite typical of the axially-moving CANDLE-type reactor. The initial criticality is achieved by loading LEU into the bottom region of the core and the blanket fuel is placed above the initial LEU region. In this preliminary work, both the lower reflector and the upper plenum regions are modeled as shown in Fig. 1. In the conventional metallic fuel design, a long gas plenum is usually placed above the core to accommodate the fission gas. In the current work, only a short 40 cm-high gas plenum is modeled and it is assumed that the gas plenum is filled with the displaced bonding sodium. In the B&BR core, the maximum excess reactivity strongly depends on the initial LEU core size. If the initial LEU core is too high, the excess reactivity can be too high during a depletion period of the B&BR core. On the other hand, the

power density can be too high when the initial LEU core is too small. Since 2 types of smeared density are applied to the core, the initial LEU core height search was performed and the optimal height is shown in Section 3.

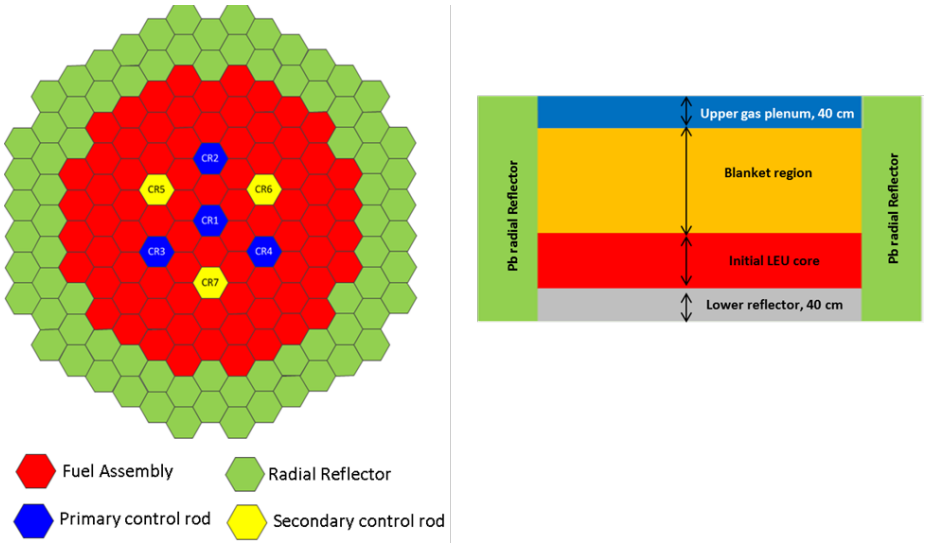

Figure 1. Radial and axial layout of the reactor.

In the radial reflector assembly, a tighter lattice is adopted and 91 reflector pins are placed in each reflector assembly. The Pb-containing reflector pin diameter is 2.32 cm and the thickness of the HT-9 cladding is 0.10 cm. The cladding of the reflector pin is thicker than of the fuel pin in order to accommodate the corrosive behavior of the lead. In the reflector assembly, the volume fraction of lead, coolant, and structure is 64.693%, 17.605%, and 17.702%, respectively. The melting temperature of lead is about 327.5 °C and lead is liquid during the normal operation of the reactor.

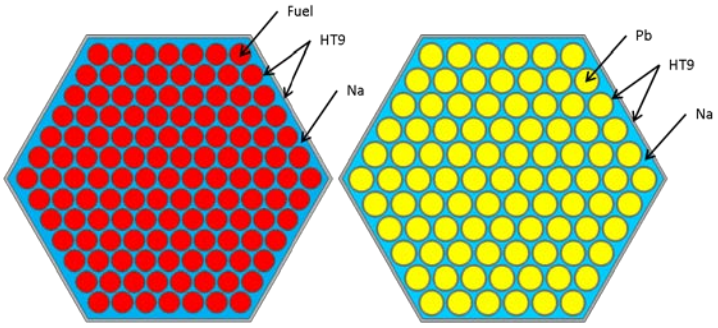

a) Fuel assembly b) Radial reflector

Figure 2. Fuel assembly and radial reflector configurations.

To achieve a high burnup of the metallic fuel, a smeared density of 70% and 75% is adopted for the initial LEU core and blanket region, respectively. In the typical U-Zr metallic fuel design, the Zr content is 10 wt%. However, it is well known that the Zr content can vary a little from the typical value [14]. In this work, the Zr content is adjusted to change the fuel fraction in a fuel assembly.

The PWR spent nuclear fuel (SNF) is used as the blanket fuel material in this work. For the fabrication of the blanket metallic fuel only, a very simple treatment is considered in this work in order to minimize the associated costs and improve the proliferation resistance of the SNF handling process. At the moment, it is assumed that the SNF can be metallized through a reduction process and the resulting metallic material is melted to fabricate a SNF-Zr metallic fuel. In the SNF treatment process, no fission products are intentionally removed from the original SNF and the resulting metallic SNF should contain many kinds of fission products. To determine the metallic SNF composition, it is assumed that the fission gases and fission products with a low boiling temperature (1000°C) can be removed from the original SNF.

Table I. Blanket fuel composition from PWR spent fuel

Element or Isotope	wt.%	Element or Isotope	wt%
Ge	8.94E-05	Ce	3.22E-01
Sr	1.08E-01	Pr	1.53E-01
Y	6.36E-02	Nd	5.55E-01
Zr	5.10E-01	Pm	1.54E-03
Nb	5.46E-07	Sm	1.11E-01
Mo	4.59E-01	Eu	1.71E-02
Tc	1.05E-01	Gd	1.68E-02
Ru	2.96E-01	Tb	3.18E-04
Rh	6.01E-02	Dy	1.56E-04
Pd	1.76E-01	Ho	1.38E-05
Ag	9.36E-03	Er	3.10E-06
In	3.84E-04	U	9.56E-01
Sn	1.10E-02	Np	5.76E-02
Sb	2.35E-03	Pu	9.35E-01
Ba	2.47E-01	Am	7.18E-02
La	1.68E-01	Cm	3.16E-03

Table I shows the composition of the metalized PWR SNF which is obtained by assuming that the discharge burnup is 50 GWd/MTU and the cooling time is 10 years. From the Table I it is worthwhile to note that the fraction of the remaining fission products is still significant, about 3.4 wt%. In the metallic SNF, the U content is about 95.6 wt% and the TRUs fraction is about 1.04% and the most of the TRUs is Pu, 0.93%.

3. Analysis Results and Discussion

3.1. Core lifetime and Breeding Ratio

Monte Carlo depletion analyses have been performed several B&BR cores to investigate essential characteristics of the core. In the first step, several calculations were performed to determine the optimal initial LEU core height and the Zr content of the metallic fuel. The fuel temperature used in this calculation is 800 K, and the temperature for the cladding, structural materials, and coolant, are determined to be 700 K. Because this study is kind of a scooping study, 150 cycles and 25,000 neutron histories per cycles were used in the McCARD calculation.

In these calculations, the active core height was fixed to be 150 cm. Two weight fractions of the Zr in the fuel for the initial LEU core and the blanket region are considered: 7 wt% and 8 wt%. It is also noted that the 7 wt% of the Zr in the fuel is the minimum requirement to achieve good performance of the metallic fuel. The appropriate Zr weight fraction is 9~10% when the natural U is used in the blanket material [3]. In the case of the SNF blanket fuel, a higher content of fuel loading is necessary due to neutron absorption of the fission products. Therefore, a lower weight fraction of zirconium in the fuel is considered.

The change of the multiplication factor for the 7 wt% and 8 wt% Zr in the fuel are shown in Fig. 3a and 3b as the function of the initial LEU core height. Table II shows the required enrichment and the mass of the LEU for the 7 wt% and 8 wt% Zr in the fuel, respectively. From Fig. 3, it is clearly shown that the higher the initial core, the excess reactivity is also higher, which is not favorable. It is also shown that the higher content of the Zr in the fuel, the shorter core lifetime is due to the poor neutron economy. Also from Table II, it is noticed that the higher the initial core, the necessary enrichment to ignite the reactor decreases, despite the increase of the amount of the LEU in the core.

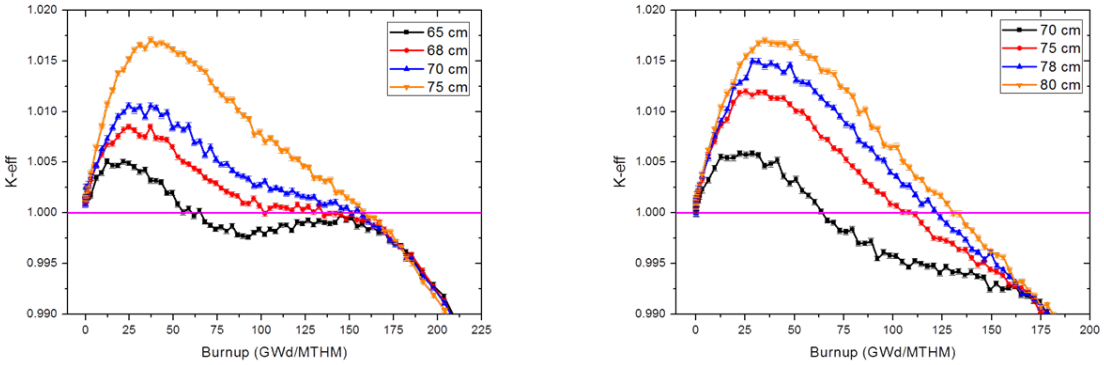

a) For 7 wt% Zr fuel b) For 8 wt% Zr fuel

Figure 3. Evolution of k-eff as function of the initial core height for 7 wt% and 8 wt% Zr fuel.

Table II. Required enrichment for the 7 wt% and 8 wt% Zr fuel.

For 7 wt% Zr fuel			**For 8 wt% Zr fuel**		
Initial core height (cm)	Enrichment (%)	Mass of LEU (ton)	Initial core height (cm)	Enrichment (%)	Mass of LEU (ton)
65	12.330	17.21	70	12.160	18.03
68	12.090	18.01	75	11.845	19.32
70	11.950	18.54	78	11.660	20.09
75	11.630	19.86	80	11.548	20.61

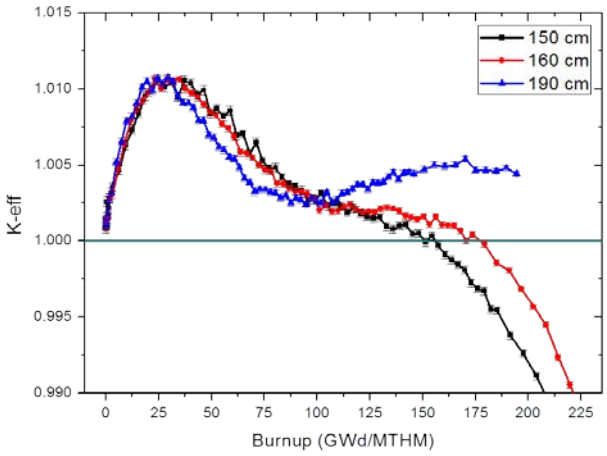

Figure 4. Evolution of k-eff as function of the total active core height for 7 wt% Zr fuel.

The B&BR core with 70 cm initial LEU core and with 7 wt% Zr in the fuel provides the best performance in term of low excess reactivity and long core lifetime. The achievable burnup of this configuration is about 154.46 GWd/MTHM or around 68.45 EFPY (effective full power years). Since in the B&BR, the core lifetime and fuel burnup increase with the core height, the total active core height is increased to 160 cm and 190 cm while the height of the initial LEU core is 70 cm. The result of these new configurations is shown in Fig. 4. It is shown that with the rather high blanket region, the B&BR core can achieve the quasi equilibrium core state. But with that core configuration, the sodium reactivity coefficient is more positive due to less neutron leakage. On the other hand, this result shows there may be a possibility to continue the operation of the reactor after one lifetime. This can be done by putting back the reprocessed fuel from the B&BR and adding fresh blanket fuels into the core. The reprocessed fuel will ignite the new B&BR core.

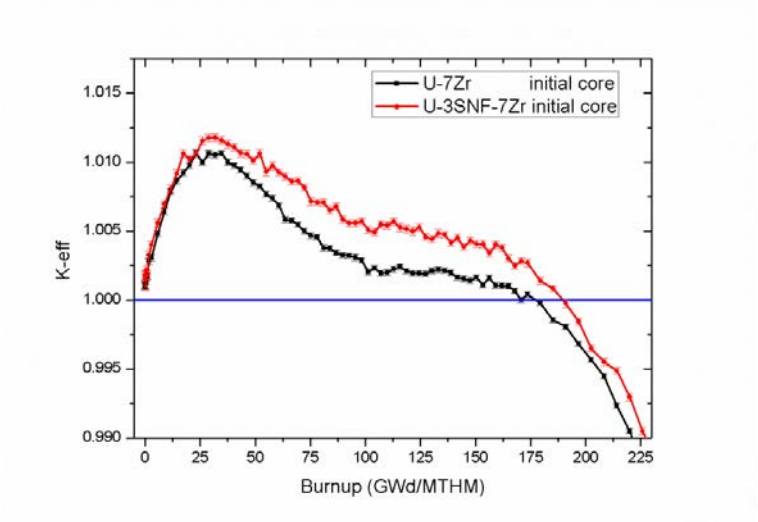

Figure 5. Evolution of k-eff as function of the initial core composition.

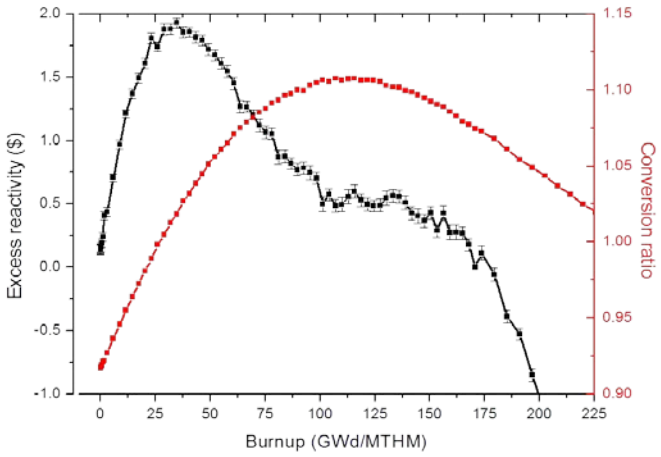

Figure 6. Excess reactivity and conversion ratio.

By adding the 10 cm blanket, the core lifetime is increased by about 14 years, from 68.45 years to 82.14 years and the achievable discharge burnup is now increased to 173.59 GWd/MTHM. The 160 cm B&BR with 70 cm initial LEU core and using 7 wt% Zr in the fuel is the reference core in this study and is used to characterize the important reactor parameters which are discussed in the following section.

Another feasibility study using the mixture of the SNF and LEU for the initial core was also performed using the reference core configuration. The weight fraction of the LEU, SNF, and Zr is 90 wt%, 3wt%, and 7 wt%, respectively. The necessary uranium enrichment to achieve criticality is 12.30% and the mass of the required LEU in the mixture is around 17.94 ton. The comparison of the k-eff between the U-3SNF-7Zr and U-7Zr is shown in Figure 5. The excess reactivity is higher for the mixture initial core because of the Pu-239 in the initial core. It is also observed that transition of the active core from the initial core to the blanket is rather smooth for the mixture initial core. The achieveable burnup is also higher in the mixture initial core case, around 185 GWd/MTHM or equal to 87.59 years.

The excess reactivity and the conversion ratio of the reference core are plotted as the function of irradiation time in Fig. 6. The excess reactivity is still higher than the design target (1$) and this optimization will be considered in a future study. The conversion ratio is defined as the ratio of the fissile produced and the fissile destroyed at the same time. In order to achieve the true breed-and-burn capability, the conversion ratio should be larger than 1.0 in an equilibrium core which can be achieved

with a high core. In the initial core, the conversion ratio is smaller than 1.0, and it is increasing because of the hard neutron spectrum and the higher η value of the bred Pu-239. The low conversion ratio during near BOC (Beginning of Cycle) is because the initial core is loaded with LEU. After it reaches the maximum point, the conversion ratio gradually decreases. The monotonic decrease of the conversion ratio is because the core height is rather short.

3.2. Beta effective and reactivity coefficients

Time evolution of important safety parameters are evaluated for the reference core, including the delayed neutron fraction (β_{eff}) and prompt neutron generation lifetime (l), and the reactivity coefficients. These parameters are calculated at 3 core burnup points: at BOC (Beginning of Cycle), at MOC (Middle of Cycle), and at EOC (End of Cycle).

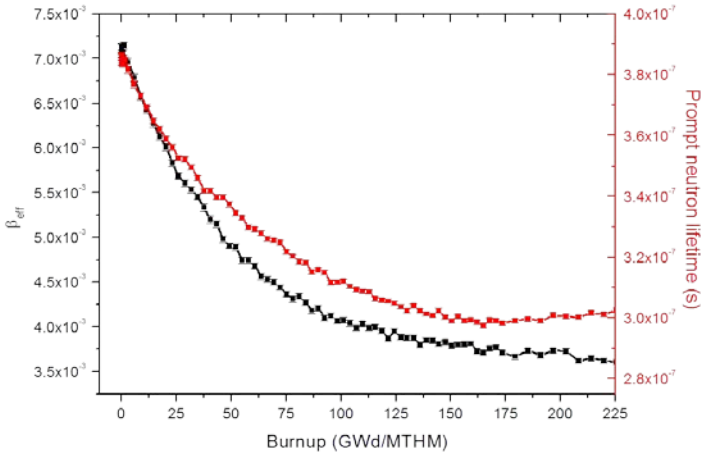

Figure 7. β_{eff} and l, as a function of burnup.

The effective delayed neutron fraction and prompt neutron generation lifetime as function of burnup are shown in Fig. 7. The β_{eff} at the BOL is high because the core is basically uranium core and gradually the fraction of U fission rates become smaller as the core converts to Pu-239-dominating core. The prompt neutron generation lifetime shows the same trend over the irradiation period. In general, the neutron spectrum becomes harder with the fuel burnup due to the buildup of the Pu fuel.

Table III. Burnup-dependent temperature coefficient of reactivity

Parameters	BOC (0 GWd/ MTHM)	MOC (86.8 GWd/MTHM)	EOC (173.6 GWd/MTHM)
β_{eff}	7.10E-3 ± 3.17E-5	4.24E-3 ± 2.39E-5	3.73E-3 ± 1.57E-5
l, s	3.85E-7 ± 1.36E-9	3.15E-7 ± 9.21E-10	2.98E-7 ± 8.95E-10
α_D α_D, cents/K	-0.033 ± 0.005	-0.066 ± 0.006	-0.069 ± 0.013
α_{Na} α_{Na}, cents/K	-0.064 ± 0.001	0.157 ± 0.001	0.165 ± 0.001
α_{Void} α_{void}, cents	-59.01 ± 3.59	556.53 ± 4.72	832.74 ± 5.50
α_H α_H, cents/K	-0.027 ± 0.006	-0.067 ± 0.008	-0.054 ± 0.009
α_R, cents/K	-0.312 ± 0.007	-0.508 ± 0.009	-0.534 ± 0.011

Five reactivity coefficients were analyzed: Doppler coefficient α_D, sodium density coefficient α_{Na} α_{Na}, sodium void worth α_{Void} α_{void}, axial expansion coefficient α_H α_H, and radial expansion coefficient α_R α_R, as shown in Table III. The Doppler coefficient, axial expansion coefficient, and the radial expansion coefficient remain negative for the whole lifetime. However, the sodium density coefficient

is positive, as is usually the case in the sodium-cooled fast reactor. The sodium void worth and the sodium density coefficient are slightly negative at the BOC because the core is uranium-dominated. At EOC, the sodium void worth is relatively high, about 8$, which is mainly ascribed to the axial dimension of the B&BR. It is noted that the fuel temperature coefficient is always slightly negative. Although the sodium density coefficient is slightly positive when the core is dominated by Pu-239, both fuel expansion coefficients are slightly negative, and the radial expansion of the core results in a strong negative feedback. The negative expansion coefficient is an important safety attribute of the fast reactor core.

3.3. Power distributions

Figure 8 shows the normalized axial power distribution of the B&BR core. As shown in the Fig. 8, the axial peak power at BOC is substantially higher than that of the MOC and EOC since the core height is quite small at BOC. It is noted that as the active core travels upward slowly with time, the active core region becomes wider and wider with the fuel burnup. Consequently, the axial peak power decreases with burnup. The EOC axial power shape is rather close to an equilibrium one which would be obtained with a very high B&BR core.

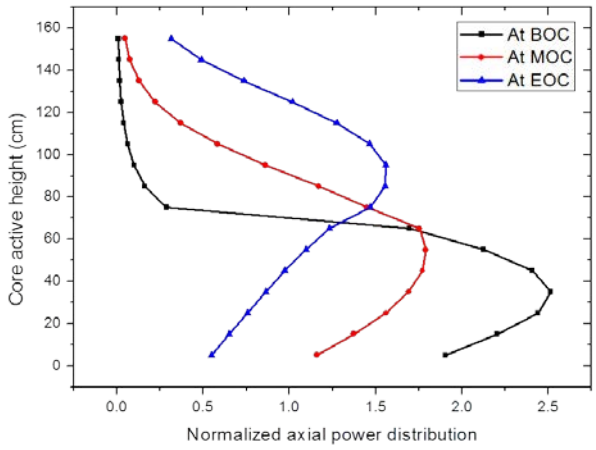

Figure 8. Axial power profile at BOC, MOC, and EOC

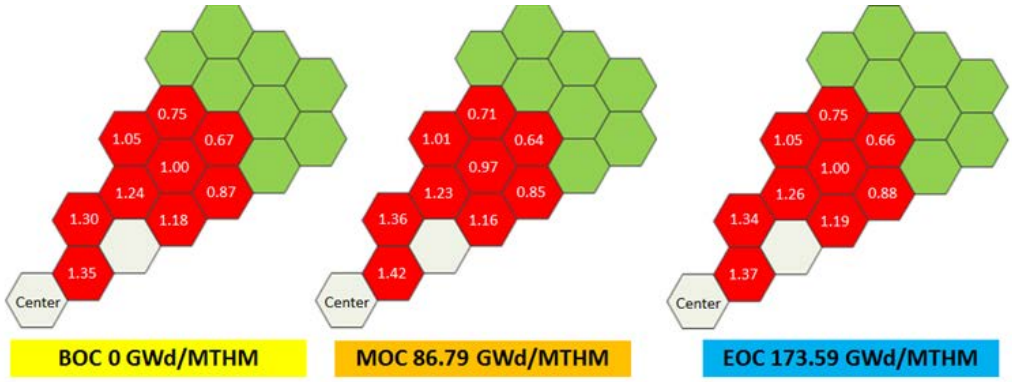

Figure 9. Normalized assembly-wise power distribution at BOC, MOC, and EOC.

In Fig. 9, the normalized radial power profiles are provided for the 3 burnup points. It is clear that the fission power density is noticeably higher in the inner core than in the outer region at BOC, MOC, and EOC. This is mainly because an identical U enrichment is used for the initial core.

3.4. Fast neutron fluence

One of the most challenging technical problems is the extremely high fast neutron fluence in the long-life B&BR. The fast neutron fluence is calculated at two axial locations for the assembly near center of the core and the results are shown in the Fig. 11. At EOC, the fast fluence is 4~5 times higher than the typical allowable limit of HT-9 structural material, 4.0×10^{23} neutrons/cm^2. It is generally agreed that either a new material should be developed or the potential solution mentioned earlier before should be adopted for the realization of the B&BR reactor.

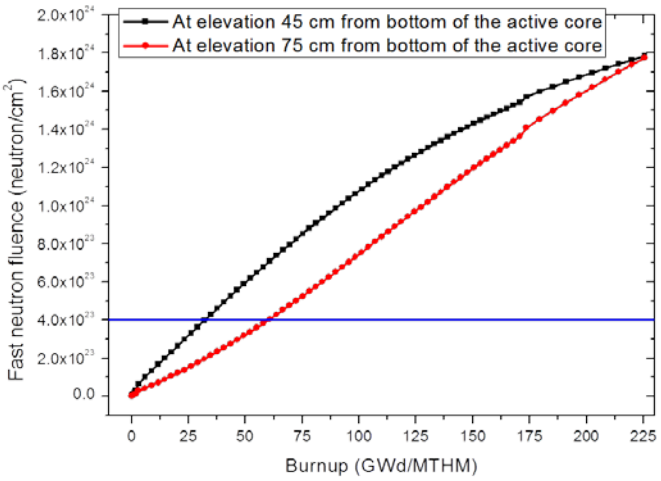

Figure 11. Evaluation of peak fast neutron fluence in the core.

3.5. Discharge burnup composition

The fuel composition at the end of lifetime is also analyzed for the reactor. This analysis will provide an insight of whether the lower weight fraction of the zirconium is allowable or not, which depends on the content of the plutonium in the fuel. Normally, for 20 wt% of plutonium, ~10 wt% of zirconium is recommended for the high performance of the fuel. The average discharge burnup is shown in Figure 12. The fuel compositions was analyzed for each 10cm-thick axial layer of the core and it was found that the maximum Pu fraction is about 12.02%, which may indicate that a lower Zr content (e.g., 7 wt%) may be allowable for the metallic fuel of the B&BR.

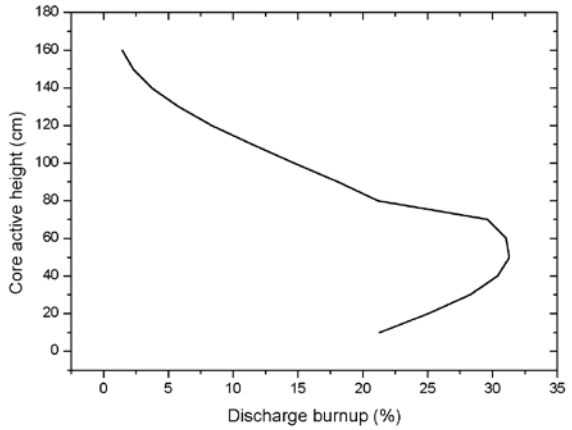

Figure 12. Average discharge burnup

Obviously from Figure 12, the purpose of utilizing 2 types of the smeared density for both initial LEU core and blanket region is satisfied. The fuel discharge burnup is less than 20% for the top of the core, and it is very high in the middle of the core, ~30%, due to the long depletion under a high neutron flux, which has been accommodated using a lower smeared density.

The plutonium vector at discharge burnup was also calculated. The fissile plutonium fraction (wt% Pu-239 + wt% Pu-241) for initial active core (layer 1 to layer 7) is around 78% to 81%, and it increases to ~88% in the blanket region.

4. Concluding Remarks

It has been shown that the PWR spent fuel can be reused, in terms of the neutronic feasibility, in a B&BR after a simple melt-refining processing. For a small B&BR recycling the PWR spent fuel, the Zr content in the metallic fuel should be minized to achieve the B&B condition. Benefit of mixing the SNF with LEU for the initial core is rather small. An heterogeneous smear density can be used to cope with a locally high burnup. The core lifetime can be very long depending on the core height. It was found that the sodium void reactivity is relatively large, ~8$, at the end of core lifetime of the B&BR. This is due to the relatively low neutron leakage in the B&BR core and the very high fuel burnup. The very high fuel burnup results in a very high fast neutron fluence exceeding the current limit of the structural materials. It is obvious that an innovative fuel design should be developed for the realization of the B&BR and the sodium void reactivity should be reduced a lot. An optimization study will be performed to improve the safety of the B&BR.

REFERENCES

[1] ELLIS, T. et al., Traveling-Wave Reactors: A Truly Sustainable and Full-Scale Resource for Global Energy Needs, Proceedings of ICAPP'10, San Diego, CA, USA (2010) (CD-ROM).
[2] SEKIMOTO, H., RYU, K., YOSHIMURA, Y., CANDLE: The New Burnup Strategy, Nucl. Sci. Eng. 139 (2001) 306-317.
[3] KIM, Y., HARTANTO, D., A Compact Sodium-cooled Traveling Wave Reactor, Transactions of Korean Nuclear Society Autumn Meeting, Gyeongju, Korea (2011) (CD-ROM).
[4] KIM, Y., Semi-direct Recycling of LWR Spent Fuel in Ultra-long-life Core Fast Reactor (UCFR), Trans. Am. Nucl. Soc. 103, Las Vegas, Nevada, USA (2010) (CD-ROM).
[5] HEIDET, F., GREENSPAN, E., Neutron Balance Analysis for Sustainability of Breed-and-Burn Reactors, Nucl. Sci. Eng. 171 (2012) 13-31.
[6] GREENSPAN, E., HEIDET, F., Energy Sustainability and Economic Stability with Breed and Burn Reactors, Progress in Nuclear Energy 52 (2011) 794-799.
[7] HARTANTO, D, KIM, Y., A Compact Breed and Burn Fast Reactor Using Spent Nuclear Fuel Blanket, Proceedings of PHYSOR 2012, Knoxville, Tennessee, USA (2012) (CD-ROM).
[8] AHLFELD, C. E. et al. Nuclear Fission Reactor, a Vented Nuclear Fission Fuel Module, Method Therefor and a Vented Nuclear Fission Fuel Module System, US Patent Application (2011).
[9] VITILLO, F., TODREAS, N.E., DRISCOLL, M.J., A Vented Inverted Fuel Assembly Design for an SFR, Proceedings of ICAPP'12, Chicago, USA (2012) (CD-ROM).
[10] HOFMAN, G.L., WALTERS, L.C., and BAUER, T.H., Metallic Fast Reactor Fuels, Progress in Nuclear Energy 31 (1997) 83-110.
[11] SHIM, H. J., KIM, C. H., McCARD User's Manual Version 1.0, Seoul National University (2010).
[12] KIM, Y., HARTANTO, D., A Physics Study on a LEU-Loaded Small Modular Fast Reactor, Trans. Am. Nucl. Soc. 105, Washington, D.C., USA (2011) (CD-ROM).
[13] CHANG, Y. I. et al., Small Modular Fast Reactor Design Description, Argonne National Laboratory (2005).
[14] HWANG, W., The Feasibility Study on Fuel Types for the KALIMER, Korea Atomic Energy Research Institute (1997) (in Korean).

Advanced Fast Reactor - 100 - Design Overview

C. Grandy, T. K. Kim, E. Jin, M. Farmer, H. Belch, J. Grudzinski, T. Sumner, Y. Momozaki, L. Krajtl, C. Gerardi, Y. Tang, T. Moran, A. Moisseytsev, R. Vilim, T. Wei, R. Seidensticker, C. Youngdahl

Argonne National Laboratory,
9700 South Cass Avenue
Argonne, IL, 60439
United States of America

Presented by Christopher Grandy

Abstract. The Advanced Fast Reactor-100 (AFR-100) is a small modular sodium-cooled fast reactor with an electrical power output of 100MWe. The AFR-100 has a long-lived core that does not require refueling for 30 years. The concept contains various innovations such as a small compact modular core (both vented and non-vented fuel pins), advanced core shielding materials, a compact fuel handling system, advanced electromagnetic pumps, compact intermediate heat exchangers, and a direct reactor auxiliary cooling system. These advanced systems and components were adopted in order to reduce the overall size of the primary heat transport system (and therefore the overall commodities and cost), enhance safety, and to improve overall plant performance. This paper presents the summary results of a year-long study that culminated in the design of two primary heat transport configurations for the AFR-100. The paper describes those innovations and shows how they are integrated into the overall AFR-100 primary heat transport system design.

Introduction

An Advanced Fast Reactor with 100 MWe power rating (AFR-100) was developed at Argonne National Laboratory to target emerging markets where a clean, secure and stable electricity resource is required, but a large-scale plant cannot be accommodated. The AFR-100 is targeted for small local grids, transportable from pre-licensed factories to remote plant sites for affordable supply, and operated for a long period without refueling. To achieve these strategic goals, several design requirements were proposed for the AFR core development; i.e., a power rating of 100 MWe that is equivalent to 250 MWth for a target thermal efficiency of at least 40%, a long refueling interval (30 years or more) with small burnup reactivity swing, a core barrel diameter of less than 3.0 m, and an active core height of less than 1.5 m.

Under the US-DOE programs, several options and innovative fast reactor technologies have been investigated or are being developed for improving overall core performance, achieving capital cost reductions, and increasing inherent safety. These features include the following:

- a compact long-lived core design with fission-gas vented (and non-vented) fuel
- advanced shielding material
- advanced structural materials that reduce commodities

- advanced cladding materials that allow higher burnup levels to be achieved beyond the current range of existing cladding performance
- compact intermediate heat exchangers
- compact fuel handling system
- self-cooled electromagnetic pumps
- advanced supercritical carbon dioxide power conversion system with superheated steam backup
- increased core outlet temperatures that increase the overall plant thermal efficiency

These innovative fast reactor technologies are not currently available, but it is expected that they will be available when the AFR-100 is deployed. Thus, the AFR-100 concept developed herein incorporated these technologies in order to investigate the effect on overall primary plant compactness which directly impacts economics while maintaining an inherent safety approach. Some of these technologies are also applicable to other fast reactor designs with the same expected benefit.

AFR-100 Core Design

U-10Zr binary metallic fuel was selected as the primary fuel form for the AFR-100 because of its inherent safety characteristics, favorable performance for long refueling intervals, and finally because it can be rapidly deployed due to its extensive use in fast reactors such as EBR-II. In order to specify the design parameters, the feasible design domain of the small fast reactor was explored through sensitivity studies. The specific power density was determined so as to maximize the cycle length and the assembly pitch [1]. The active core height and number of driver assemblies was selected to ensure that the core fits within the 3.0 m diameter core barrel and that the active core height is less than 1.5 m.

An enrichment zoning strategy was adopted for the AFR-100 core for which the low enriched fuel is surrounded axially and radially by higher enriched fuel. This enrichment zoning strategy allows for a 30-year refueling interval with a minimal burnup reactivity swing and a flat power distribution. The core performance characteristics, kinetics parameters, reactivity feedback coefficients, and the reactivity control requirement were calculated using the ANL suite of fast reactor analysis codes.

Orifice design calculations and steady-state thermal-hydraulic analyses were performed using the SuperEnergy2-ANL code. Thermal margins were evaluated by comparing the peak temperatures to the design limits for parameters such as the fuel melting temperature and the fuel-cladding eutectic temperature. The inherent safety features of the AFR-100 core were assessed using the integral reactivity parameters of the quasi-static reactivity balance analysis. The resultant core design is shown in Figure 1. Information on the detailed core design and its analysis can be found in Reference [1].

The AFR-100 core uses fission-gas vented fuel as one option (Figure 2). Since the vented pins doe not need the gas-plenum above the fuel slug, the overall length of the fuel assembly could be decreased from 421 cm to 302 cm. This fuel form does not affect the core performance characteristics, but does affect the radioactivity levels in the primary coolant and cover gas space. The volumetric activity of the primary coolant increases slightly because of the reduced primary coolant and the additional activation products from dissolved fission gas. However, additional biological shielding can be incorporated to maintain dose levels below the design constraint. An on-line primary sodium purification system is installed to remove various impurities in the

sodium coolant during reactor operations.

Advanced Shielding Materials

Advanced shielding material was used to reduce the thickness of the radial reflector. This reduces capital cost by decreasing the core (and thereby reactor vessel) diameter. The core was designed with one row of shielding made from zirconium hydride (ZrH_2) and boron carbide (B_4C). These advanced shielding materials were selected because extensive irradiation experience has been gained with their use in commercial and research reactors. For the AFR-100, the fractional loading in the radial shielding assembly was selected as 75% for zirconium hydride and 25% for boron carbide.

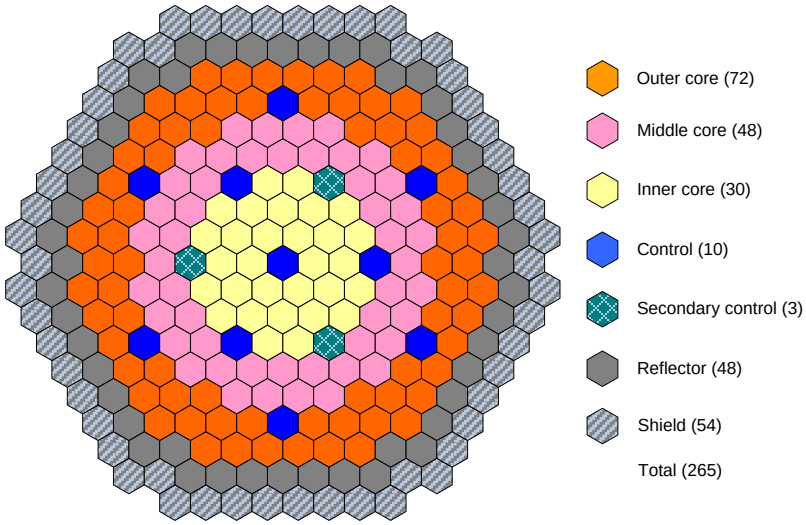

Figure 1 - Radial Core Layout for the AFR-100 Core

With this advanced shielding material, the fast neutron fluence beyond the core barrel was reduced below the reference core concept due to the moderating effect of the hydrogen in the zirconium hydride despite the fact that one reflector row was removed. Furthermore, the thermal neutron flux beyond the core barrel was significantly reduced by neutron absorption in the boron.

Advanced Materials

The U.S. is pursuing advanced structural materials as a way to reduce the overall steel commodities used in the primary and intermediate heat transport system of fast reactor technology. The U.S. has been investigating a number of austenitic and ferritic/martensitic stainless steels for sodium fast reactor applications during the past three years. During a recent down-selection process, two candidate alloys have been selected for detailed testing and analysis. These alloys are grade 92 ferritic-martensitic (FM) steel and NF709 austenitic steel. The U.S. believes that the superior performance of these advanced steels will improve reactor design flexibility, safety margins, and economics. These alloys are currently used in other energy applications, but not in nuclear service.

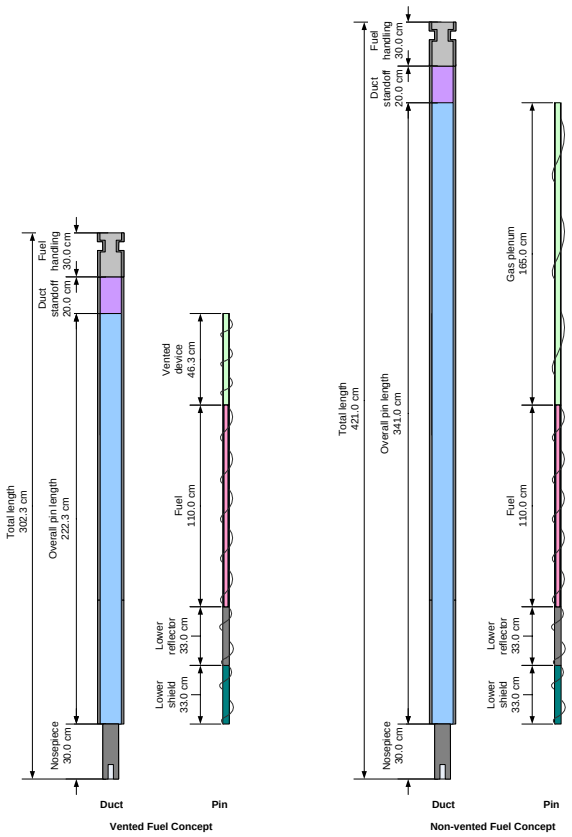

Figure 2 - AFR-100 Vented and Non-Vented Core Assemblies

Core Restraint System Approach

Bowing of core assemblies can cause significant changes in reactivity during start-up, overpower, and loss-of-flow without scram transients. A key performance objective is to maximize inherent safety; in particular, to assure net negative reactivity insertion during transients. The core restraint system controls core assembly bowing so as to ensure negative reactivity feedback during transients.

The NUBOW-3D software package was originally developed to analyze core bowing over the life of the reactor due to thermal/irradiation creep as well as swelling using duct temperature and neutron fluxes calculated with core physics codes as input. In addition, NUBOW-3D calculates the net reactivity change due to duct bowing displacements using reactivity displacement worths calculated from the physics codes. These features allow NUBOW-3D to be used as an analysis and design tool for core restraint systems.

In order to support the development of the AFR-100 vented and non-vented core design concepts (see Figure 2), NUBOW-3D was used to analyze the preliminary core restraint system. As part of the input, NUBOW used duct temperatures, flux, and displacement reactivity worths obtained from the core physics codes SE-II, DIF-3D, and VARI-3D. The vented and non-vented core designs are identical with the exception that the non-vented core has a gas plenum above the fuel that increases the overall core height. As a result, the core physics analyses were only carried out for the vented core design. The temperature and flux profiles from the vented core analysis were thus applied to the non-vented case since the difference in the core design begins above the active core region.

In terms of design approach for the AFR-100, two common methods were considered for the core restraint system; namely, the *free flowering* and *limited free bow* concepts. In previous Argonne studies, the limited free bow system has been shown to provide better inherent safety characteristics and was thus selected for the AFR-100.

Compact Fuel Handling System

A conceptual pantograph-type fuel handling machine (FHM) has been developed for the AFR-100 (see Figure 3). This fuel handling mechanism will be removed during power operations and used at other AFR-100 sites for the removal and insertion of fuel. The design was developed to reduce the height of the mechanism to suit a smaller sized primary vessel. The figure shows the overall assembly of the pantograph mechanism concept in the fully extended and retracted positions. Although preliminary, enough detail has been incorporated to simulate and evaluate overall operational characteristics.

The main design goal for the pantograph FHM was to reduce the size of the assembly both inside and outside the reactor vessel in order to reduce overall costs of the primary reactor system as well as the containment building.

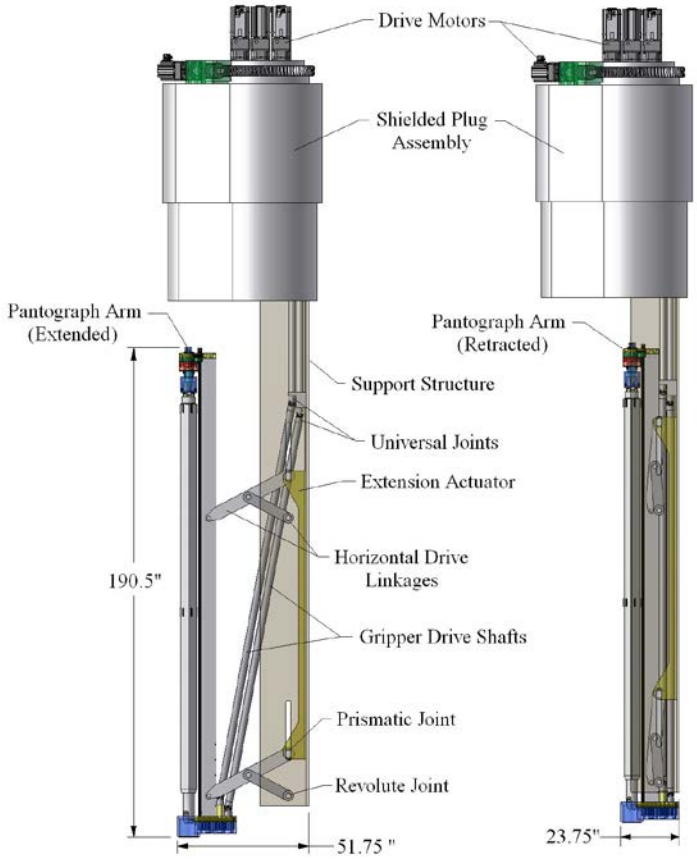

Figure 3 - Pantograph Fuel Handling Mechanism (arm extended and retracted)

The pantograph is controlled by a computerized drive system which provides several distinct and isolated motions to manipulate the fuel, control rod, reflector and shielding assemblies inside the reactor vessel. The drive motors utilize planetary reduction gear sets to achieve the required

torque to move the simulated core assembly while under maximum design loads. The calculated maximum forces required to operate the mechanism have been used to determine the size of various components based on expected frictional resisting forces. Actuation of any single isolated motion does not affect other component positions or orientations.

The pantograph FHM is supported from a shielded plug which fits into a port in the reactor vessel rotatable cover. A stepped shielded circular plug located inside this housing rotates on a set of bearings that support the entire weight of the mechanism from the shielded plug. Bi-directional servo gear motors that drive the mechanism motions are placed above this shielded plug for ease of maintenance, manual control access and increased reliability. Manual connections for operating the pantograph (in case of computer or electrical failure) are located on the top of the stepped circular plug. Mechanical and electronic visual indicators show the positions and orientations of all mechanism components during transfer operations. Refueling of the AFR-100 core is accomplished once every 30 years. The entire core is replaced during this outage and thus there is no in-vessel storage of fresh or spent core assemblies. During reactor operations, a plug is installed in the upper internal structure (UIS) that contains the same functionality in monitoring core outlet temperatures as the main portion of the UIS.

Primary Pumps

Electromagnetic pumps have some advantages over mechanical pumps as follows:

- Design using no penetration through the boundary between working fluid and ambient, thus a design without seals is possible,
- No moving parts are involved,
- Installation in any orientation is possible,
- Thermal distortion tolerant.

On the other hand, EM pumps have some disadvantages over mechanical pumps.

- Lower pumping efficiency (~40 %)[1],
- Lesser reactor plant experience, especially for large EM pumps

Because of these advantages, self-cooled EM pumps were adopted for the AFR-100. EM pump design optimization studies were carried out using an ANL code based on a calculational procedure developed to estimate the performance of various annular linear induction pumps (ALIPs). For the AFR-100 pool plant concept, the ALIPs are suspended from the reactor vessel enclosure in the pool of Na coolant. In the current design, the ALIP requires no active cooling because advanced high temperature windings are used, heat removal by surrounding sodium is excellent, and the sodium pool temperature is low (< 800 K). At the nominal design operating condition and a given pump length, the code estimates the diameter of the pump without return duct, mass, and efficiency of the ALIP. Figure 4 shows a schematic of an ALIP. Figure 5 provides the pump performance curve.

Intermediate Heat Exchanger

One of the objectives of this work was to develop an innovative IHX concept that minimizes the impact on the overall size of the reactor while maintaining key functional requirements. Since this advanced concept study has focused on pool-type plant configurations the design was evaluated from the viewpoint of the feasibility for deployment in this type of system. Three design options were identified that reduce the space that IHXs occupy in pool plant

[1] The lower pumping efficiency can be overcome in part by using a self-cooled EM pump in which the waste heat is rejected direclty into the sodium cold pool.

configurations: i) high thermal conductance materials, ii) kidney-shaped planar construction, and iii) IHXs that are part of the permanent structures of the primary heat transport system. The concept proposed herein builds upon these bases while extending the approach to consider a full annular design that is integrated into the redan. This approach effectively mandates that the units are permanent installations. Finally, the units are assumed to be made from ferritic steel (e.g. 9Cr-1Mo) that has a thermal conductivity ~ 40 % higher in comparison to stainless steel at 500 ºC.

The conventional shell and tube type heat exchanger design has been deployed in many fast reactor applications, but not in an annular configuration as investigated as part of this work. This concept consists of a number of round tubes attached to a tubesheet inside a cylindrical vessel, with tube size, length, and total number of tubes varying depending on system thermal requirements. The tube bundle normally contains a number of baffles to accomplish the dual objectives of providing a support structure for the tubes, and to direct the shell-side flow across the tubes rather than along the tubes. The resulting cross-flow on the shell side yields a relatively high pressure drop because energy is used to reverse the flow rather than to enhance heat transfer.

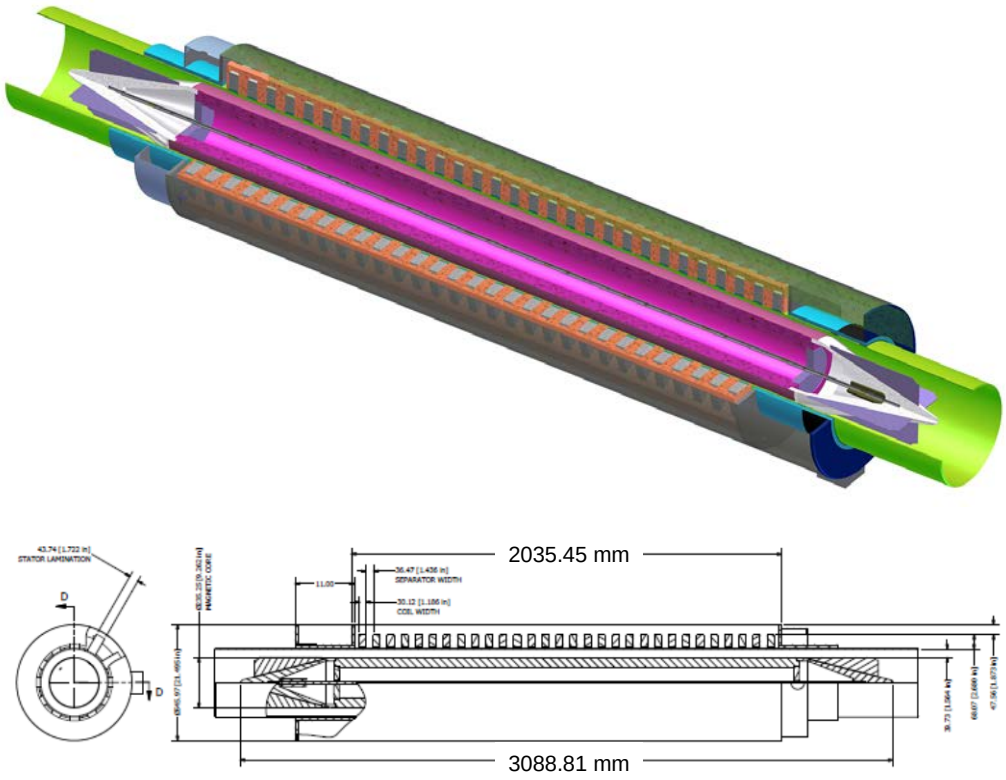

Figure 4 - Primary Annular Linear Induction Pump

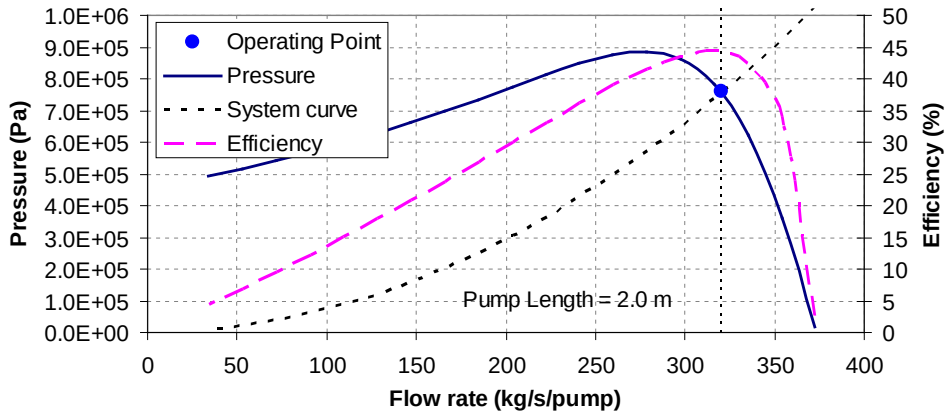

Figure 5 - Primary Pump Performance Curve

The Twisted Tube® heat exchanger originated in Eastern Europe and became commercially available in Sweden in the mid 1980's [3]. This concept was developed to overcome inherent limitations with conventional shell and tube designs described above. The twisted tube concept consists of a tube bundle assembled from uniquely formed tubes in an arrangement that does not use baffles; see http://www.kochheattransfer.com/products/twisted-tube-bundle-technology. The tubes are formed into an oval cross section with a superimposed helical spiral in the axial direction of the bundle. The forming process ensures that tube wall thickness remains constant and the material yield point is not exceeded thereby retaining mechanical integrity. The tube ends are round to allow conventional tube-to-tubesheet joints. The tubes are assembled into a bundle on a triangular pitch one row at a time with each tube oriented to align the twists at every plane along the bundle length. This alignment results in tubes contacting adjacent tubes at many points along the length of the bundle, and this minimizes flow-induced vibration. The shell-side flow path is complex and predominantly axial in nature. Typically, the shell side flow area is approximately equal to the tube side flow area. The twisted tube design imparts a swirl flow on both the shell and tube sides of the unit that enhances the heat transfer coefficients relative to those achieved in a traditional parallel flow heat exchanger designs. To the best of our knowledge, the twisted tube concept has not been previously employed in fast reactor applications. This is the current IHX design innovation that is incorporated into the advanced IHX design for the AFR-100.

In-vessel Primary Heat Transport System Configuration

Two main primary heat transport system configurations were used in this study; i.e., the open hot plenum pool concept and the cold pool concept. Both of these concepts have their advantages and disadvantages. The open hot plenum generally results in a smaller reactor vessel. However, the effects of the large mass of hot sodium on the reactor vessel head, the redan, and the upper internal structure must be addressed. The cold pool concept, which is very similar to EBR-II, results in an isothermal pool of sodium (at the core inlet temperature) that greatly reduces thermal stresses and long-term creep that would otherwise result if the system was held at the core outlet temperature. Both of these configurations are considered for use in the AFR-100 plant concept.

Plant Design Options

Various system and component hardware options were evaluated in the development of the AFR-100 concept. These options are summarized below for reference:

- Compact Core – Vented and Non-Vented Core

- Advanced Shielding Materials
- Compact Fuel Handling Systems
- Electromagnetic Pumps
- In-vessel PHTS configuration
    - Redan – Open Plenum Configuration – 4TT
    - Core Cover with cold pool – 3TT
- Reactor vessel and core support configurations
- Intermediate Heat Exchanger
    - Replaceable kidney-shaped tube-and-shell twisted tube HX
    - Integral twisted-tube and shell IHX integrated within the Redan
- Direct Reactor Auxiliary Cooling System – cold pool
- Containment options
- Advanced S-CO_2 Brayton Cycle System with a superheated steam Rankine cycle as backup

As a result of the above selected plant design options, two primary plant configurations were developed and evaluated. These concepts were developed to show the results of integrating the different plant systems and components. These two main concepts were referred to as 3TT and 4TT. These two configurations were compared with the Advanced Burner Test Reactor (ABTR) developed previously at ANL [4] to illustrate changes in size and commodities of the various systems and components as an indicator of relative cost. The ABTR is also an innovative plant that has the same thermal power level (250MWth) as the AFR-100, but the ABTR has a more conventional refueling cycle and does not incorporate all the innovations of the AFR-100.

Table 1 provides a summary of the characteristics of Concepts 3TT and 4TT, while Figures 6 through 9 show key primary system design features for these two concepts.

Table 1 – Summary of Fast Reactor Concepts 3TT and 4TT

	Concept 3TT	**Concept 4TT**
Core	UZr metal fueled core, 30 year life	UZr metal fueled core, 30 year life
Core Venting	Optional	Optional
Primary Pumps	Electromagnetic	Electromagnetic
PHTS Configuration	Core Cover – Cold Pool	Hot Open Plenum - Redan
Core Support	Top Supported with redundant support rods	Top Supported with redundant support rods
Intermediate Heat Exchanger Configuration	Kidney-shaped Removable IHX – Straight twisted tubes®	Annular IHX around core barrel – fixed in place – twisted tubes®
Reactor Vessel Support	Conical Ring – Top Support	Conical Ring – Top Support
Emergency Decay Heat Removal	Direct Reactor Auxiliary Heat Exchanger in cold pool – Twisted Tube® HX	Direct Reactor Auxiliary Heat Exchanger in cold pool – Twisted Tube® HX
Primary Purification System	Integrated cold trap within reactor vessel	Integrated cold trap within reactor vessel
Power Conversion System	S-CO_2 Brayton Cycle with superheated steam backup	S-CO_2 Brayton Cycle with superheated steam backup
Containment	Steel Containment with separate plane impact shield	Steel Containment with separate plane impact shield

In-Vessel Fuel Handling Mechanism	Single Rotatable Plug with pantograph FHM	Single Rotatable Plug with pantograph FHM

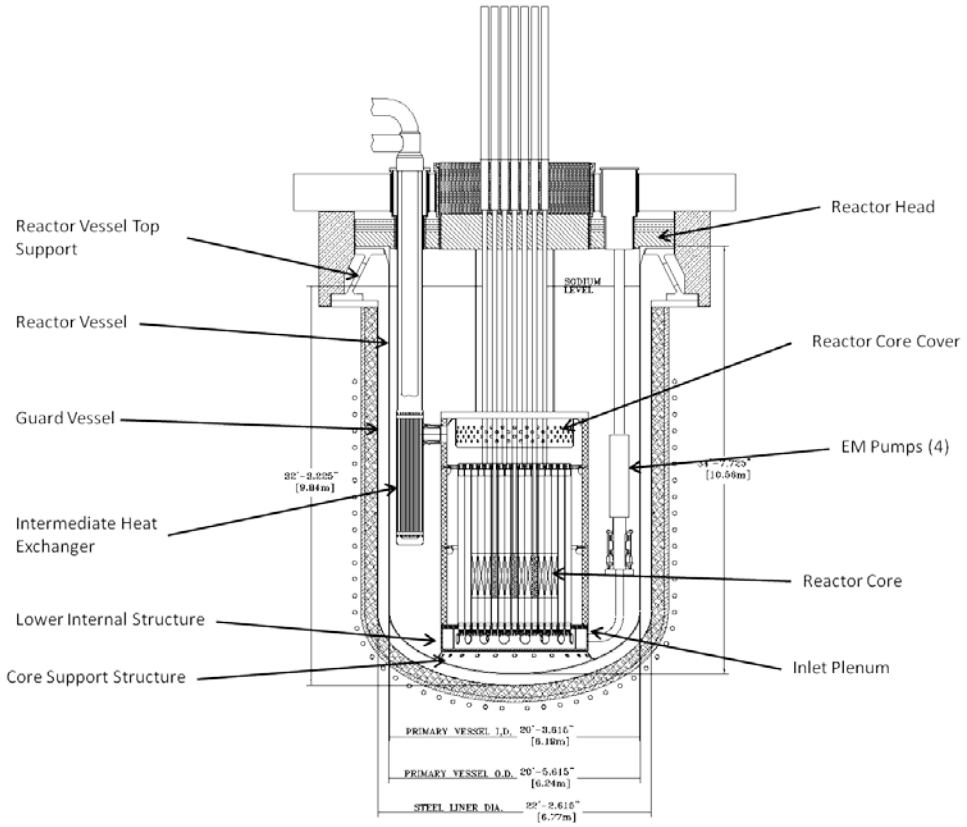

Figure 6 - AFR-100 Concept 3TT - Elevation View, Non-Vented

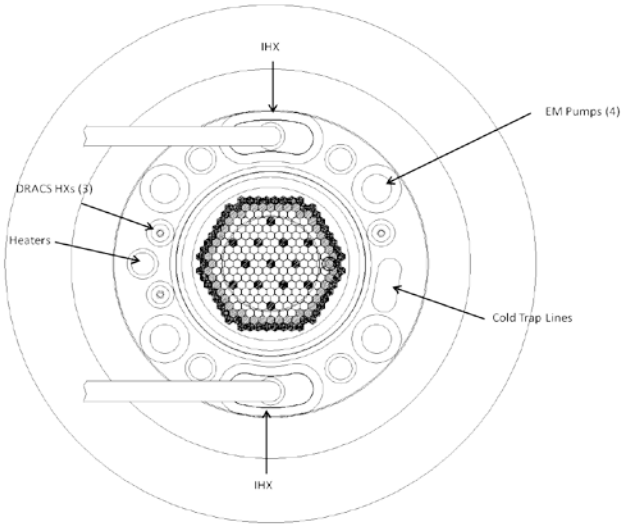

Figure 7 - AFR-100 Concept 3TT - Plan View

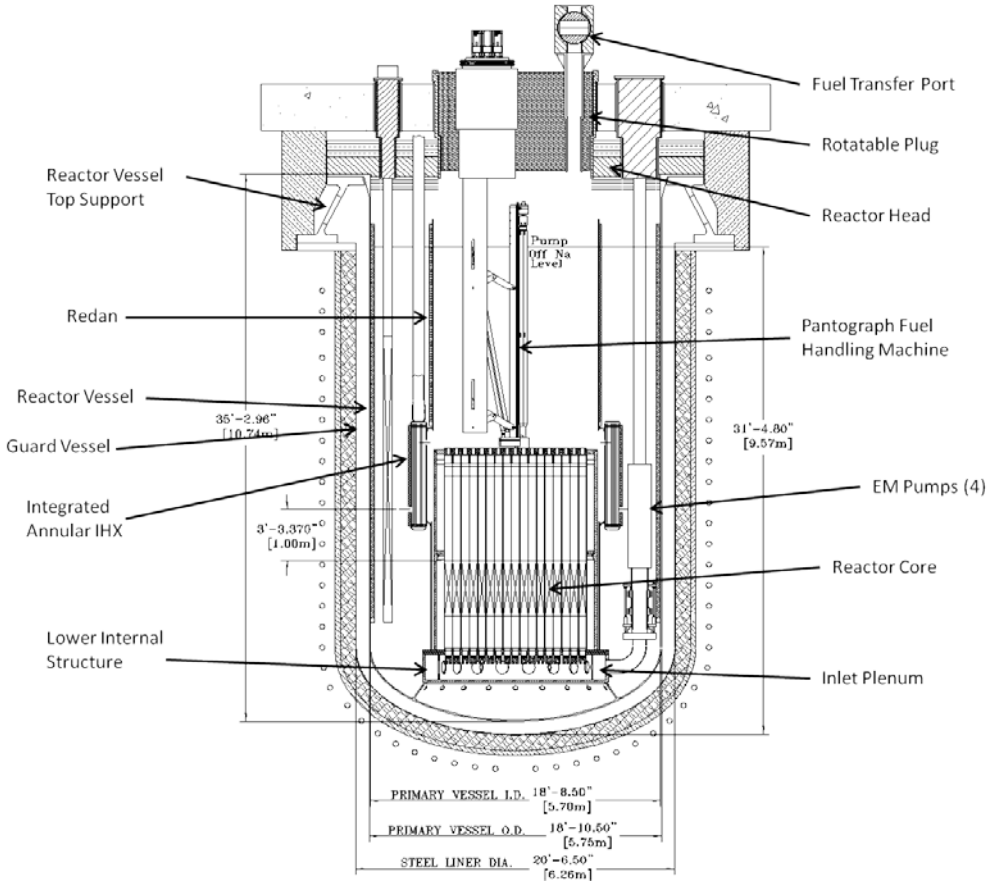

Figure 8 - AFR-100 4TT Hot Pool Concept - Elevation View, Non-vented, shown in Refueling Mode

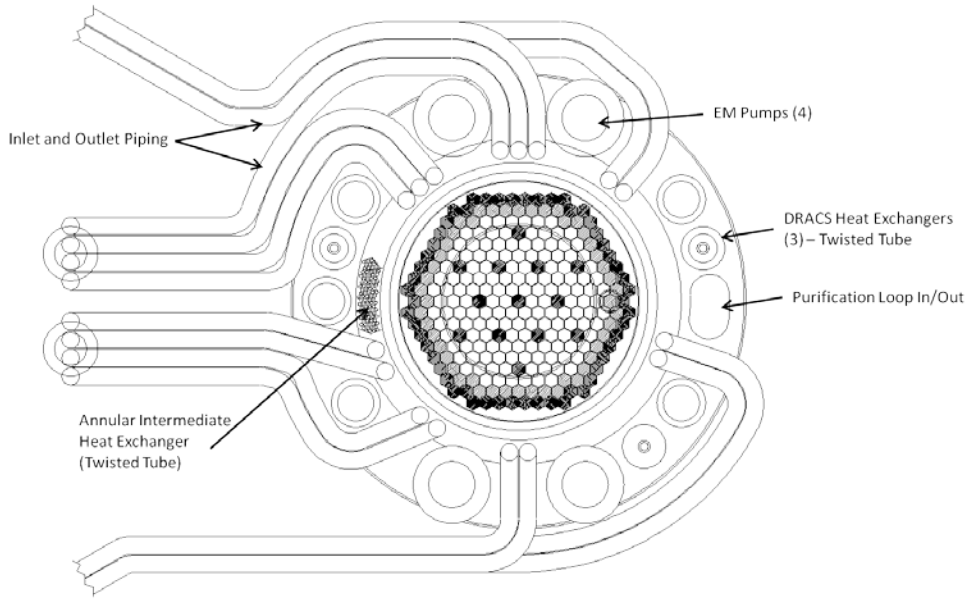

Figure 9 - AFR-100 4TT Concept - Plan View

AFR-100 Safety Analysis

A series of accident sequences that focused on the AFR-100's ability to provide protection against reactor damage during low probability accident sequences resulting from multiple equipment failures were examined. Protected and Unprotected Loss of Flow (PLOF and ULOF) and Unprotected Transient Over-Power (UTOP) accidents were simulated using the SAS4A/SASSYS-1 safety analysis code. The overall negative reactivity feedbacks in conjunction with the large heat capacity of the sodium in the pool-type concept allows the AFR-100 to absorb large amounts of energy during a PLOF with relatively small temperature increases throughout the system. During a ULOF with a 25-second flow halving time, coolant and cladding temperatures peak around 720ºC within the first minute before negative reactivity feedback effects decrease power to match the flow. Core radial expansion and fuel Doppler provide the necessary reactivity feedback during the UTOP to bring the system's reactivity back to zero before system temperatures exceed allowable limits. Simulation results indicate that adequate ULOF safety margins exist for the AFR-100 design with flow halving times of twenty-five seconds. Significant safety margins are maintained for PLOF accidents as well as UTOP accidents if a rod stop is used. The AFR-100 safety analyses are reported in more detail in Reference [5].

Conclusion

Argonne's AFR-100 is an advanced 100MWe sodium cooled fast reactor that can provide electricity to the grid for 30 years without refueling. The design incorporates various innovative systems and components that allow it to be smaller and more compact than Argonne's reference ABTR design while overcoming the physically larger derated long-lived core. The 4TT primary plant concept is considered the most innovative and is more compact than the 3TT configuration due to the annular configuration of the twisted-tube® intermediate heat exchanger.

ACKNOWLEDGEMENTS

The AFR-100 design work was performed under the auspices of the U.S. Department of Energy's Advanced Reactor Concepts program. The authors greatfully acknowledge the support provided by DOE especially our sponsors Brian Robinson, Craig Welling, and Thomas O'Connor.

REFERENCES

[1] T.K. Kim, C. Grandy, and R. N. Hill, "A 100MWe Advanced Sodium-Cooled Fast Reactor Core Concept", PHYSOR 2012 – Advances in Reactor Physics – Linking Research, Industry, and Education.

[2] T. L. Sham, et. al., "Development of Advanced 9Cr Ferritic-Martensitic Steels and Austenitic Stainless Steels for Sodium-Cooled Fast Reactor, FR13 Conference

[3] http://www.kochheattransfer.com/products/twisted-tube-bundle-technology

[4] Y. I. Chang, et al, "Advanced Burner Test Reactor Preconceptual Design Report," Argonne National Laboratory, ANL-ABTR-1.

[5] T. Sumner, A. Moisseytsev, T. Wei, "AFR-100 Safety Analyses", Proceedings of ICAPP '12.

ESFR core optimization and uncertainty studies

A. Rineiski[a], B. Vezzoni[a], D. Zhang[a], M. Marchetti[a], F. Gabrielli[a], W. Maschek[a], X.-N. Chen[a], L. Buiron[b], J. Krepel[c], K. Sun[c], K. Mikityuk[c], F. Polidoro[d], D. Rochman[e], A.J. Koning[e], D.F. DaCruz[e], H. Tsige-Tamirat[f], R. Sunderland[g]

[a] Karlsruhe Institute of Technology (KIT), Germany

[b] Commissariat à l'énergie atomique et aux énergies alternatives (CEA), Cadarache

[c] Paul Scherrer Institute (PSI),Villigen , Switzerland

[d] Ricerca sul Sistema Energetico (RSE), Milan, Italy

[e] Nuclear Research And Consultancy Group (NRG), Petten, The Netherlands

[f] Joint Research Centre (JRC), Institute for Energy, Petten, The Netherlands

[g] AMEC, Knutsford, United Kindom

Abstract. In the European Sodium Fast Reactor (ESFR) project supported by EURATOM in 2008-2012, a concept for a large 3600 MWth sodium-cooled fast reactor design was investigated. In particular, reference core designs with oxide and carbide fuel were optimized to improve their safety parameters. Uncertainties in these parameters were evaluated for the oxide option. Core modifications were performed first to reduce the sodium void reactivity effect. Introduction of a large sodium plenum with an absorber layer above the core and a lower axial fertile blanket improve the total sodium void effect appreciably, bringing it close to zero for a core with fresh fuel, in line with results obtained worldwide, while not influencing substantially other core physics parameters. Therefore an optimized configuration, CONF2, with a sodium plenum and a lower blanket was established first and used as a basis for further studies in view of deterioration of safety parameters during reactor operation. Further options to study were an inner fertile blanket, introduction of moderator pins, a smaller core height, special designs for pins, such as 'empty' pins, and subassemblies. These special designs were proposed to facilitate melted fuel relocation in order to avoid core re-criticality under severe accident conditions. In the paper further CONF2 modifications are compared in terms of safety and fuel balance. They may bring further improvements in safety, but their accurate assessment requires additional studies, including transient analyses. Uncertainty studies were performed by employing a so-called Total Monte-Carlo method, for which a large number of nuclear data files is produced for single isotopes and then used in Monte-Carlo calculations. The uncertainties for the criticality, sodium void and Doppler effects, effective delayed neutron fraction due to uncertainties in basic nuclear data were assessed for an ESFR core. They prove applicability of the available nuclear data for ESFR optimization studies.

1. Introduction

Within a Collaborative Project on European Sodium Fast Reactor (CP-ESFR) realized in the EUROATOM 7th Framework Programme, innovative large sodium-cooled fast reactor concepts have been investigated and optimized [1]. Two core designs (called Working Horses, WHs), with oxide and carbide fuels, proposed by CEA have been analyzed and modified for improving their safety. Both cores are self-breeder ones without fertile blankets in agreement with expected European needs. In the present paper, we focus on the oxide core as it was done within the project. In fact, the main effort has been done for the oxide core and the proposed modifications have been then applied to the carbide

one. Starting from the WH core, possible modifications and their influence on neutronics, thermal-hydraulics, core behaviour under severe accident conditions, have been studied, the main goal being the safety performance.

The main attention was on the initiation phase of a hypothetical severe accident and therefore on the sodium void reactivity effect reduction. In addition, the adoption of special pins and special subassemblies (SAs) have been proposed and analyzed in order to facilitate melted fuel relocation from the core in case of an accident, thus limiting potential for fuel compaction and related re-criticalities [2].

An optimized core, called CONF2, has been established as the first milestone in the optimization studies and served as the basis for additional modifications aiming at improving the core safety performance and analyzing minor actinide (MA) transmutation potential. CONF2 includes a limited number of modifications leading to a reduction of the reactivity variation at a sodium boiling onset without affecting appreciably other core characteristics. Additional modifications reduce the sodium void effect further, but they influence strongly other core characteristics, in particular the power profile.

Different codes, data libraries and methodologies have been applied by the project partners. In order to evaluate uncertainties (due to uncertainties in basic nuclear data) in the computed criticality values, sodium void and Doppler effects, the Total Monte-Carlo method (TMC) has been applied. The method and obtained results are presented in the paper.

1.1. Rationale for the WH oxide core

The oxide WH core is a result of CEA optimization studies in order to establish a core design with a low (as compared to large European SFR designs proposed in the past) sodium void effect and a near zero breeding gain leading to a low reactivity loss per cycle [1]. The WH design is based on the experience gained with the PHENIX, SUPERPHENIX and European Fast Reactor (EFR) projects [1]. In order to reduce the sodium void reactivity effect and the reactivity loss due to burnup, the WH core contains tight grid pin bundle SAs, so that the fuel volume fraction is maximized and the sodium volume fraction is reduced. With respect to the previous designs, the fuel pellet diameter is enlarged and the spacer wire (1mm in diameter) is slightly reduced (FIG. 1). Such dimensions could be envisaged if Oxide Dispersion Strengthened (ODS) steels were used for the clad [3]. With the optimized pin dimension, the power density and the maximum fuel temperature are reduced.

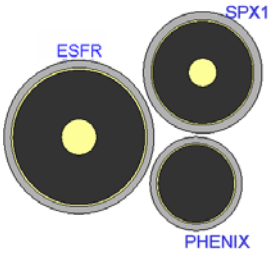

FIG. 2. ESFR pin dimensions with respect to PHENIX and SUPERPHENIX (SPX1) cores

1.2. The reference core

The WH oxide core is a 3600 MWth core composed of 453 SAs subdivided into two, inner and outer, fuel zones, with 14.5%wt. and 16.9%wt., averaged Pu content, respectively. The different enrichments are chosen for flattening the power profile at equilibrium (FIG. 2-a). Concerning the axial structure (FIG. 2-b), the following SA parts are above the active zone (100 cm): the upper steel axial blanket (UAB), 7.6 cm high, the upper gas plenum (UGP), 15 cm high, the plugs, the Na plenum, 15 cm high, and the upper steel structure. The lower SA part is composed of the lower steel axial blanket (LAB), 30 cm high, and a lower gas plenum (LGP), 91.3 cm. The average burnup is 100 GWd/tHM reached

after 2050 Equivalent Full Power Days (EFPDs) for the power density of 206 W/cm^3. In FIG. 2-a, nine Diverse Shutdown Devices (DSDs, containing B_4C with 90% of ^{10}B) and 24 Control and Shutdown Device (CSD, containing natural B_4C) are also displayed.

For this core the Sodium Void Reactivity Effect (SVRE)[1] is about 4$ at the Beginning of Life (BOL) while the extended effect (extended SVRE)[1] is about 3$ at BOL. These high SVRE values are governing the initiation phase of hypothetical transients like an Unprotected Loss Of coolant Flow (ULOF) or the Total Instantaneous Blockage (TIB) potentially leading to a core disruption. The SVRE values are higher by about 1.5$ at the Beginning of Equilibrium Cycle (BOEC) as compared to BOL.

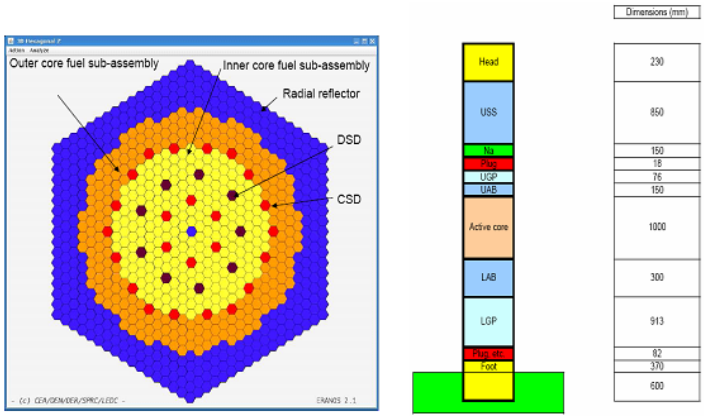

(a) *(b)*

FIG. 2. WH oxide configuration: (a) core layout, (b) axial structure

2. Rationale for optimization

Core modifications were done mainly for SVRE reduction. Note, that the void effect reduction is only part of a broader activity on accident prevention and mitigation. Another option is, e.g., introduction of specific devices, such as Curie-point latches or gas expansion modules [4]. In the study, the attention was focused on core geometry optimization, rather than on specific devices. Possible options for reducing SVRE have been extensively investigated in the past and some of them have been considered for modification of the ESFR core. Past studies did also show that modifications leading to a void effect reduction could often worsen other reactor characteristics, e.g., reactivity variations per cycle. Therefore, a parametric study has been performed in the CP-ESFR project as a first step to identify the most promising options. The obtained results confirmed the conclusions made in the past.

According to the literature [5], 6, 7], modifications for reducing SVRE can be subdivided into two main categories: (1) those to increase the neutron leakage, in particular, under voided conditions as the introduction of a large sodium plenum in the BN-800 design [6] and (2) those oriented to soften the neutron spectra and/or to reduce the spectrum hardening after the sodium voiding (e.g., by inserting moderator materials).

The modifications to increase the neutron leakage are often the most promising ways for reducing the SVRE. Within the project, the following options have been checked separately: 1) rearrangement of the axial SA structure above the core, in particular by increasing the sodium plenum height and placing an absorber layer above, different heights being considered both for the plenum and the

[1] With SVRE, we refer to the reactivity effect due to the voiding of the fissile height in the inner and outer fuel zones. For the extended SVRE, we refer to the voiding in addition of the above core structures (UGP, UAB, plugs and Na plenum regions). Sodium is assumed to be removed only inside the SA wrapper, (i.e., sodium between SAs is not removed).

absorber layer, 2) modification of the height over diameter (H/D) core ratio for increasing the axial neutron leakage, 3) introduction of different materials in the lower blanket to increase the neutron leakage from the core downwards, and 4) introduction of an internal fertile layer to create an axially heterogeneous core and increase the neutron leakage from the fuel into this layer.

Other options oriented to a SVRE reduction have been considered too, i.e. 1) adoption of different numbers/arrangements of pins with moderator materials (several materials have been checked) and 2) adoption of SAs with 'empty' pins, i.e. those filled with helium. The first modification is mainly for neutron spectrum softening leading to a SVRE reduction, while the second may also help to facilitate melted fuel relocation from the core in a late phase of a hypothetical severe accident to avoid core re-criticalities, similar to ideas of earlier studies [8].

The most effective way to reduce the extended SVRE was to increase the core leakage under voided conditions by modifying the region above the core [9, 10, 11]. With some additional modifications below the core, it resulted in an optimized core called CONF2, used then for further core optimizations and also in other CP-ESFR activities, in particular in safety studies, as a reference optimized configuration. CONF2 includes a large Na plenum moved close to the core with an absorber layer above the plenum, while the lower steel blanket is replaced by that with depleted uranium or absorber. Other measures, as introductions of special SAs, of an internal fertile layer, or modifications of the H/D ratio have been considered as additional options, and discussed in the paper after introducing CONF2.

3. The optimized core: CONF2

As previously mentioned, the region above the core has been modified to increase the neutron leakage under voided conditions. The core layout in plane remains unchanged, only the axial structure, as shown in FIG. 3, has been modified:

(1) The Na plenum height has been increased from 15 cm to 60 cm (the value found to be close to the asymptotic one obtained by analyzing further plenum enlargements).
(2) An absorber layer (natural B_4C) of 30 cm has been placed above the Na plenum.
(3) The Na plenum has been moved closer to the core by eliminating the UAB and reducing the UGP height (from 7.6 to 5 cm).
(4) The lower axial reflector (LAB) is replaced by fertile material (depleted uranium) in order to reduce the neutron reflection back to the core, the alternative being the use of an absorber material.

The introduction of a fertile LAB reduces also reactivity losses with burnup and improves the Pu balance as illustrated also in scenario studies [10]. The proliferation issues can be avoided by adding AmO_2, with Am containing ca. 75% of Am241 and ca. 25% of Am243, to the blanket. The amount of AmO_2 should be about of 5% or more to get a "dirty" Pu in the blanket after its irradiation, i.e. Pu with a large Pu238 content about 10% or more [12]. Note that adding of AmO_2 into the blanket does not affect SVRE. The MA introduction in the lower blanket can also be considered as an option for managing MAs [10]. For maintaining nearly – within the range of 200 pcm - the same criticality level at BOL and compensate the neutron leakage augmentation under nominal conditions, the Pu content has been homogeneously increased in CONF2 to 14.76%wt. and 17.15%wt. for the inner and outer zones, respectively.

These measures help to reduce the extended SVRE at BOL by about 2$ to 3$ (β_{eff} = 393 pcm) as shown in Table 1. More precisely, the extended SVRE value is reduced from +1211 pcm to +496 pcm in CONF2 according to the calcuations. The void effect for the core is also reduced, thanks to the introduction of the lower blanket, but the blanket contribution is not very large (ca. 100 pcm). As in the original WH design, the SVRE and Doppler constant values deteriorate with burn-up, see Table 1. At 1230 EFPDs (End of Cycle 3, EOC3, i.e. a representative time to evaluate the reactivity effects at

BOEC), SVRE is higher by 600 pcm and the extended SVRE value is higher by 750 pcm as compared to BOL.

The effects of the adopted modifications are negligible for other core characteristics, including the radial power distribution, see FIG. 4. Therefore, thermal-hydraulics assumptions adopted for the WH case can be applied to CONF2 without big changes. The CONF2 option has advantages also in terms of the reactivity swing as compared to WH. The reactivity decrease between BOL and the End of Irradiation (EOI, after 2050 efpd) is about 2500 pcm for WH and 1950 pcm for CONF2, thus allowing a lower reactivity weight of control rods and potentially reducing a reactivity increase in case of an inadvertent control rod withdrawal event. Lower SVRE values for the CONF2-type configuration were also shown for the carbide core.

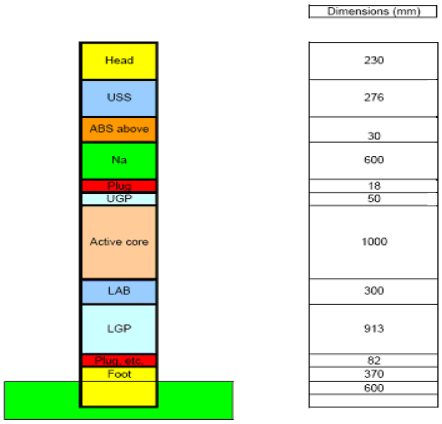

FIG. 3. Optimized configuration CONF2: axial structure

Table 1. Reactivity coefficients for WH and CONF2 core

Configurations	**WH (REF)**	**CONF2**		
	BOL	**BOL**		**EOC3**
Codes		**ERANOS**	**MCNP**	**ERANOS**
SVRE (pcm)	+1532	+1423	+1365 ± 60	+1951
Extended SVRE (pcm)	+1211	+496	+422 ± 60	+1170
Doppler constant, K_D (pcm/K)	-1239	-1158	-	-843
keff	1.00930	1.01141	1.01264	1.00414

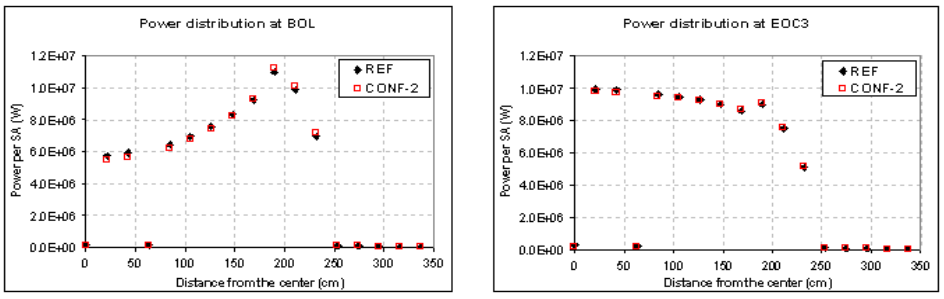

(a) *(b)*

FIG. 4. Radial power distribution comparison between WH (REF) and CONF2: (a) BOL, (B) EOC3

3.1. Introduction of MAs

The ESFR potential for managing its own MA wastes has been investigated both for the WH and the CONF2 cores. Two main options, homogeneous and heterogeneous loadings, have been compared, while analyzing the related advantages and associated drawbacks.

For homogeneous loadings, a maximum amount of 4% of MAs in the actinide content of the core has been considered, while for the heterogeneous loading, up to 20% of MAs, the rest being depleted uranium, were put into SAs placed at the periphery of the core instead of the initially proposed radial steel reflector or included in the LAB. These modification influence core transmutation performance in a fuel cycle.

A detailed study of fuel cycle strategies is beyond the scope of the present paper. However, in order to give an idea about the impact of MAs on reactivity coefficients in case of homogeneous loadings, Table 2 shows the comparison of CONF2 parameters for two cases, in which Am is loaded in the core and axial blanket; namely CONF2-2%Am, where ca. 2%wt. Am is introduced in the core and LAB, and CONF2-4%Am, where ca. 4%wt. Am is introduced in the core and LAB [10][11].

Table 2. Impact of Am loading in core and axial blanket on reactivity coefficients

Configurations	**CONF2**		**CONF2-2%Am**		**CONF2-4%Am**	
	BOL	**EOC3**	**BOL**	**EOC3**	**BOL**	**EOC3**
			Pcm			
SVRE (pcm)	+1423	+1951	+1636	+2029	+1821	+2104
Extended SVRE (pcm)	+496	+1170	+781	+1290	+1031	+1407
Doppler constant, K_D (pcm/K)	−1158	−843	−904	−785	−712	−600
β_{eff} (pcm)	393		377		361	
Λ (μs)	0.4406		0.3816		0.3345	
keff	1.01141	1.00414	1.00963	1.01330	1.00796	1.02105

The homogeneous introduction of Am in the core deteriorates the SVRE (and extended SVRE) at BOL by about 0.5$ (ca. 1$) for 2%wt. case and by ca. 1$ (ca. 2$) for 4%wt. case[2]. The extended SVRE value at BOL for the most challenging configuration (CONF2-4%Am) remains below the extended void effect for WH (+1211 pcm) at BOL, showing once more the advantages gained with the introduced core modifications. Variations of SVRE due to the introduction of MAs in the LAB are negligible. On the other hand, the introduction of Am in the core deteriorates SVRE, the Doppler constant, effective delayed neutron fraction (β_{eff}) and mean neutron generation time (Λ). More details can be found in [10][11]. One of the most attractive options is the loading of a high content of MAs in the lower axial blanket only (i.e. 10-20%wt.), not affecting SVRE appreciably, but allowing to burn MAs, that has been investigated in [10] for a simplified fuel cycle.

3.2. Preliminary transient analyses

In the ESFR project, the WH and CONF2 cores have been compared also in terms of transient behavior. In particular, in order to verify advantages of CONF2 with respect to WH, an ULOF accident has been simulated. ULOF analyses have been performed at KIT with the SIMMER III ver. 3D code [13][14]. In agreement with analyses made with static neutronics codes, CONF2 shows a better behavior at the initiation phase of the transient. In CONF2, reactivity drops down, see FIG. 5, when Na boiling starts. As shown in FIG. 6, representing the core material distribution obtained with SIMMER, Na boiling starts in the upper part of the hottest channel, where the local sodium void reactivity effect is negative due to the strong neutron leakage component, but then the void area spreads axially and radially (FIG. 6-b) leading to a positive reactivity insertion both for WH and

[2] Table 2 show lower variations at EOC3, as expected due to the MAs burning during irradiation.

CONF2. The studies have shown that further reduction of SVRE is needed to avoid potential power excursions in case of ULOF accident, in a particular for the core with irradiated fuel.

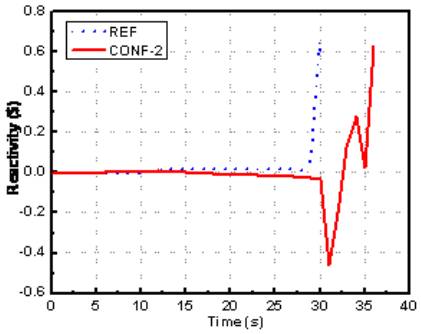

FIG. 5. ULOF transient: total reactivity variation versus time (SIMMER results)

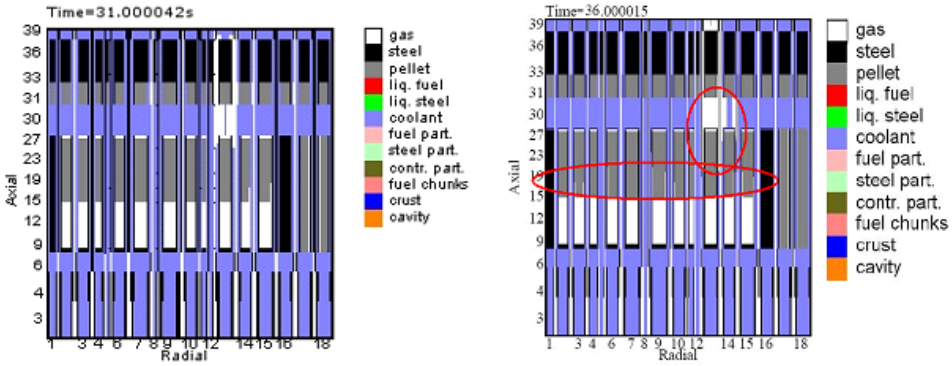

FIG. 6. Material distribution in CONF2 at Na boiling onset (ca. 31 s after ULOF starts)

4. Further optimizations

Additional modifications were performed on the basis of CONF2. A large number of studies were done on the introduction of SAs containing pins with moderators (such as zirconium hydride or B-11 carbide) softening the neutron spectrum or empty pins, increasing the neutron leakage from the core. Several materials and configurations (with different numbers of moderator and empty pins, different special pin arrangements within SAs), including those with SAs without pins inside, similar to control rod followers, were compared. The introduction of empty pins or empty SAs proposed at KIT was considered attractive also in view of the improved core potential for melted fuel relocation during a hypothetical Core Disruptive Accident (CDA) in order to prevent re-criticalities.

Options with empty pins and SAs were studied at KIT. Though these options reduce SVRE to a smaller extent as compared to moderators, they require no additional material to be introduced and considered in safety analyses, also as concerns its behavior under accident conditions, and help to avoid re-criticalities. A few modified configurations studied in more detail were similar to CONF2, but with 18 special SA in the inner core, replacing the inner core fuel SAs, and with 18 extra fuel SAs at the outer core periphery. Two most interesting cases in these studies were: 1) with 18 special SAs only with Na (wrapper with Na inside), a configuration called CONF3B, and 2) with 18 SA with empty pins (271 pins, same dimensions of for fuel SAs, with only helium inside), a configuration called CONF3C, the configuration layouts being shown in FIG. 7.

The next option was the introduction of an internal fertile layer (depleted uranium oxide) in a CONF3-like design, the layer being introduced only in the inner core zone, leading to a so-called CONF4 configuration. The fertile layer height was 10 cm (no optimization study on the location and thickness of the layer being performed) at the axial core mid-plane, the total core height remaining the same, i.e. 100 cm. Then starting from CONF4, the H/D ratio has been changed by reducing the core height (from

100 cm to 80 cm) while adding fuel SAs to the inner and outer core zones in order to maintain the total fuel mass of the reference model, resulting in CONF5. For each step, the Pu content was adjusted in order to maintain the multiplication factor of the system close to that of the reference model at BOL. These additional configurations, CONF3, CONF4, CONF5, reduce SVRE further, but their core characteristics, in particular, the power radial profile, would differ appreciably from those for CONF2 and WH if no additional optimization, as concerns enrichments, is done.

4.1. CONF3

The CONF3 modifications help in reducing the core SVRE void effect, but the main objective of CONF3 is to facilitate melted fuel relese from the core in case of CDA and avoid core re-criticalities. Both configurations, CONF3B and CONF3C, help in reducing the SVRE and extended SVRE values by about 100 pcm, as shown in Table 3. In case of using empty SAs, i.e. SAs with only Na inside the wrapper, an additional phenomena was observed: if voiding of empty SAs happens, e.g., during a late phase of a transient, a large negative reactivity effect, similar to that of a gas expansion module [4], is introduced, see Table 3. In order to enhance the SVRE reduction, a larger, than 18, number of special SAs, i.e. 30, can be introduced in the core, with additional outer core SAs increasing the core diameter.

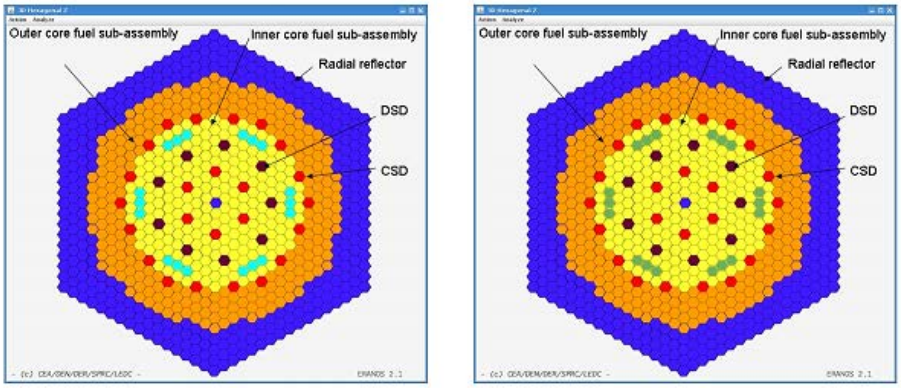

(a) *(b)*

FIG. 3. Additional optimizations: (a) CONF3B, (b) CONF3C

Table 3. Core and extended sodium void at BOL computed with the ERANOS and MCNP codes.

Configurations	**CONF2**		**CONF3B**		**CONF3C**	
Code	**MCNP**	**ERANOS**	**MCNP**	**ERANOS**	**MCNP**	**ERANOS**
SVRE (pcm)	1365 ± 60	1423	1325 ± 60	1317	1206 ± 60	1320
Extended SVRE + Special SAs (pcm)			125 ± 60	-209	327 ± 60	164

4.2. CONF4 and CONF5

The introduction of an internal fertile blanket of 10 cm (CONF4) in the inner core causes a reduction of the SVRE by 0.5$. The radial power distribution is highly influenced by this modification. In order to compensate this effect, the inner Pu content has to be significantly increased (more than by 15%) to approach the WH radial distribution at BOL.

The reduction of the core height from 100 cm to 80 cm, while increasing the core diameter by adding SAs to the inner and outer fuel zones (CONF5), can help in reducing the SVRE further by 100 to 200 pcm. Additional studies are needed for evaluating the impact of the CONF3, CONF4 and CONF5 options on reactor safety.

5. Uncertainty evaluation

In order to assess uncertanties in the computed parameters, such as sodium void and Doppler reactivity effects, due to uncertainties in basic nuclear data, the Total Monte-Carlo method (TMC) has been applied at NRG to a WH core with 4%wt. MA homogeneous loading.

The TMC methodology has been extensively applied at NRG in the past for criticality-safety benchmarks, fusion benchmarks and to a SFR reactor with metal fuel, KALIMER, uncertainty assessment [15]. The methodology is based on variations of 20 to 30 parameters employed in analytic models used to compute neutron cross-sections and related nuclear data required for neutronics analyses. The variations are performed within pre-determined ranges in order to create inputs for a code generating "random" nuclear data files in the ENDF format, converted further to the ACE format. The ACE files are used in MCNP core calculations. On the basis of this methodology, uncertainties in the computed values of criticality, SVRE, Doppler constant, and effective delayed neutron fraction, have been assessed. These uncertainties are shown in Table 4. The reader should be aware that the employed delayed neutron data were not random, but taken from an evaluated nuclear data file, thus leading to very low uncertainties in the computed effective delayed neutron fraction. In general, one may conclude that the evaluated uncertainties in the computed reactor parameters are rather small and the assumed uncertainties in nuclear model parameters/data do not influence appreciably those in the reactor ones, thus supporting application of modern data libraries to ESFR core optimization studies.

Table 4. Uncertainties evaluated with the TMC for the WH core with 4% MAs homogeneous loading

Parameter	SVRE	Full Na keff	Voided keff	βeff	Doppler
Value	5.86$	0.98298	1.00481	371 pcm	-0.60 pcm/C
Uncertainty	≅ 5%	≅100 pcm	≅ 15 pcm	< 1 pcm	≅ 7-13%

6. Conclusions

The paper summarises activities performed in the CP-ESFR project on core optimization for achieving favourable reactivity feedback coefficients and improving core safety performances. Different options have been investigated. In order to reduce the sodium void effect, the most effective option, in agreement with past studies, is to incorporate a large Na plenum above the core and add an absorber layer above the plenum, thus increasing the neutron leakage from the core, in particular under voided conditions. A lower fertile or absorber blanket brings an additional advantage, the former also in terms of breeding and reactivity swing. As a result, a CONF2 configuration was adopted by the project for the oxide core as it keeps almost all parameters unchanged, while reducing substantially, by 2$ to 3$ the reactivity effect due to sodium boiling in the core in case of a hypothetical accident.

CONF2 has been compared with the WH core also in terms of transient behaviour. Advantages of the optimized core with respect to WH have been confirmed by ULOF transient simulations. Lower SVRE values for the CONF2-type configuration were also shown for the carbide core. Additional core modifications lead to new core layouts and require additional studies. One of the most interesting options is the introduction of SAs with empty pins or empty SAs, i.e. with only sodium inside the wrapper, leading to CONF3-type configurations. They are favourable as concerns the sodium void effect, but also show a potential to facilitate melted fuel relocation in case of a hypothetical accident and prevent core re-criticalities. Further modifications, including an internal fertile layer and lower H/D ratios may also improve SVRE, their studies and studies of CONF3 requiring additional efforts to better assess possible advantages and drawbacks.

An evaluation of uncertainties due to those in nuclear data has been performed. The studies show a relatively small impact of assumed uncertainties in nuclear data on parameters relevant for ESFR safety, thus confirming the applicability of the available nuclear data for ESFR optimization studies.

ACKNOWLEDGEMENTS

The described activities were part of the CP-ESFR project, contract number 232658.

REFERENCES

[1] Fiorini, G.L., The Collaborative Project on European Sodium Fast Reactor (CP ESFR). In *Proceedings of the Int. Conf. on Euratom Research and Training in Reactor Systems (FISA2009)*, Prague, Czech Republic, June 22–24, (2009).

[2] Vezzoni, B., Gabrielli F., Rineiski A., Marchetti M., Chen X.-N., Flad M., Maschek W., Matzerath Boccaccini C., Zhang D., Safety-Related Optimization and Analyses of an Innovative Fast Reactor Concept, Sustainability, 4(6):1274-1291, (2012).

[3] Sciora, P., Buiron, L., Rimpault, G., Varaine F., Hourcade, E., Scholer, A.C., Ruah, D., Verrier, D., Massara, S., Lecarpentier, D., Jourdheuil, T., A break even oxide fuel core for an innovative French Sodium-cooled fast reactor: neutronic studies result, *Proceedings of the Int. Conf. GLOBAL2009*, Paris, France, September 6-11, (2009).

[4] Tentner, A.M., Parma, E., Wei, T., Wigeland, R., Severe Accident Approach—Final Report Evaluation of Design Measures for Severe Accident Prevention and Consequence Mitigation, ANL-GENIV-128, ANL: Chicago, USA, (2010).

[5] Barthold, W.P., Beitel, J.C., Lam, P.S.K., Orechwa, Y., Su, S.F., Turski, R.B., Low Sodium Void Cores. *In Proceedings of the Int. Conf. ENS/ANS Topical Meeting on Nuclear Power Reactor Safety*, Brussels, Belgium, October 16-19, (1978).

[6] "Evaluation of Benchmark Calculations on a Fast Power Reactor Core", Final Report of an International Benchmark Program, IAEA-TECDOC-731 (1994).

[7] Hill, R.N., Khalil, H., An Evaluation of LMR Design Options for reduction of Sodium Void Worth. In *Proceedings of the Int. Conf. on the Physics of reactors: Operation, Design & Computation*, Marseille, France, April 23-26, (1990).

[8] Sawada, T., Ninokata, H., Tomozoe, H., Endo, H., A re-criticality-free fast reactor core concept. Nucl. Techn. Vol 130, (2000).

[9] Sun, K., Chenu, A., Mikityuk, K., Krepel, J., Chawla, R., Coupled 3D-Neutronics/Thermal-Hydraulics Analysis of an Unprotected Loss-of-Flow Accident for a 3600 MWth SFR Core. *In proceedings of the Int. Conf. Advances in Reactor Physiscs (PHYSOR2012)*, Knoxville, Tennessee, TN, USA, April 15-20, (2012).

[10] Vezzoni, B., Gabrielli, F., Rineiski, A., Marchetti, M., Maschek, W., Zhang, D., Salvatores, M., Schwenk-Ferrero, A., Romanello, V., Forasassi, F., Analysis of Minor Actinides Incineration adopting an Innovative Fast Reactor Concept. *In Proceedings of 12th International Exchange Meeting on Partitioning and Transmutation, NEA/OECD*, Prague, Czech Republic, September 24-27, (2012).

[11] Rineiski, A., Vezzoni, B., Zhang, D., Chen, X.-N., Gabrielli, F., Marchetti, M., Sodium Void Effect Reduction and Minor Actinide Incineration in ESFR. *In Proceedings of the Int. Conf. ANS Annual Meeting 2011*, Hollywood, USA, June 26-30, (2011).

[12] Rineiski, A., Kessler, G., Proliferation-resistant fuel options for thermal and fast reactors avoiding neptunium production. Nucl. Eng. Des., 240, 500-510, (2010).

[13] Kondo, S., Tobita, Y., Morita, K., Brear, D.J., Hamiyama, K., Yamano, H., Fujita, S., Maschek, W., Fischer, E.A., Kiefhaber, E., *et al*. Current Status and Validation of the SIMMER-III LMFR Safety Analysis Code. In *Proceedings of the Int. Conf. ICONE-7*, Tokyo, Japan, April 19–23, (1999).

[14] Yamano, H., Fujita, S., Tobita, Y., Kamiyama, K., SIMMER-IV: A Three-Dimensional Computer Program for LMFR Core Disruptive Accident Analysis, JNC TN9400 2003-070; Japan Nuclear Development Institute: Tokyo, Japan, (2003).

[15] Rochman, D., Koning, A.J., DaCruz, D.F., Archier, P., Tommasi, J., Nucl. Inst. and Methods A612, 374 (2010).

Preliminary Analysis of Natural Circulation Characteristics of China Lead-based Research Reactor (CLEAR-I)

Tao ZHOU, Pengcheng ZHAO, Zhao CHEN, Yunqing BAI, Hongli CHEN, Yong SONG, FDS Team

Institute of Nuclear Energy Safety Technology, Chinese Academy of Sciences, Hefei, Anhui 230031, China

Presented by Tao ZHOU

Abstract. A large science project named "Advanced Nuclear Fission Energy-ADS Transmutation System" has been launched by Chinese Academy of Sciences. China LEAd-based Research Reactor (CLEAR-I) as a verification facility reactor will be developed in the first phase of the ADS program. In CLEAR-I, the liquid Lead-Bismuth eutectic (PbBi) was chosen as coolant in primary cooling system and driven by natural circulation since the power at a low level about 10MWt. The natural circulation of primary coolant system is a coupling of thermal-hydraulic problems of the core, upper and lower plenums of the reactor, reactor internal parts. Therefore, understanding the natural circulation flow capability and characteristics of CLEAR-I is very important, which can significantly improve the security features of the reactor. In this work, natural circulation characteristics and flow distribution at steady state in primary system of CLEAR-I were preliminary evaluated and discussed. A numerical simulation was conducted by using CFD code. The flow characteristics was illustrated and discussed. The temperature and pressure distribution were evaluated.

1. Introduction

The accelerator driven system (ADS) is an important approach to incinerate the radioactive waste for its good inherent safety and high transmutation support ratio [1-3].The project of "Advanced Nuclear Fission Energy-ADS Transmutation System" is promoted by Chinese Academy of Sciences since 2011, aimed at building series ADS transmutation system from research reactor to DEMO, and developing related key technologies. China LEAd-based Research Reactor (CLEAR-I) as a verification facility reactor is the first step of the ADS program, designed by Institute of Nuclear Energy Safety Technolgy, Chinese Academy of Sciences (INEST • FDS Team, CAS) which has designed a series of lead-based materical cooled sub-critical reactor systems [5-12]. The reactor power of CLEAR-I is about 10 MW at a low level, liquid Lead-Bismuth eutectic (LBE) was chosen as coolant in primary cooling system because of good neutronic and thermal physical properties. The reactor will be operated in critical mode at the first phase and then update to the sub-critical mode. The

primary system of CLEAR-I is pool type configuration, considering the current research and development status of material and manufacture technology, a key characteristics of CLEAR-I is that the primary system is driven by natural circulation, four primary heat exchangers (PHX) are located in the pool, and the hot barrier divides the LBE coolant into hot and cold pool. The cold LBE from the lower plenum is heated in the core region and driven by the natural circulation force caused by the density difference between hot and cold pool, and then collected and mixed in the hot plenum. The hot LBE pass through the inlet of primary heat exchanger, and flow downward to the cold lower plenum. Table.1 shows the main parameters of CLEAR-I.

Table 1. Main parameters of CLEAR-I

Parameter		**Values**
Core	Thermal power (MW)	10
	Activity height (m)	0.8
	Activity diameter (m)	1.05
	Fuel (^{235}U enrichment)	UO_2 (19.75%)
Cooling system	Primary coolant	LBE
	Total LBE mass (t)	~530
	Inlet/Outlet temperature (℃)	260/390
	Coolant drive type	Natural circulation
	Second coolant	Water
	Heat sink	Air cooler
Material	Cladding	316 Ti
	Structure	316L

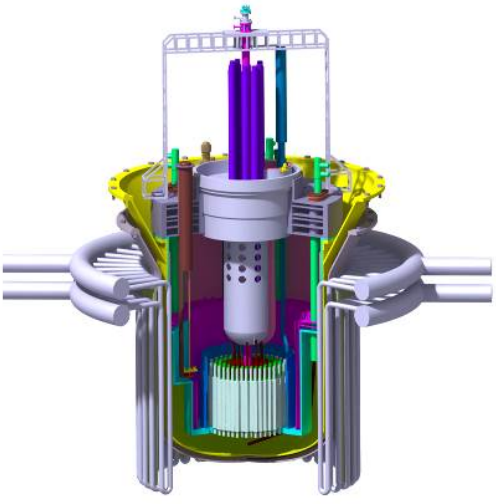

Fig. 1 The structural illustration of China lead–based research reactor CLEAR-I

Since the driven mode of primary coolant system of CLEAR-I is natural circulation, the core power density, the height of the coolant-circulating, the heat transfer capacity of the heat exchanger and other factors have a significant impact on the natural circulation capability. The natural circulation of primary coolant system is a coupling of three dimensional thermal-hydraulic problems of the core,

upper and lower plenums of the reactor, reactor internal parts. Therefore, understanding the natural circulation flow capability and characteristics of CLEAR-I is very important, which can significantly improve the security features of the reactor.

In this paper, natural circulation capability and flow pattern at steady state in primary system of CLEAR-I were preliminary evaluated and discussed. Two-dimensional model was built, and a numerical simulation was conducted by using CFD code. The flow field and the pressure distribution were illustrated. The effects of the core power density, the height of the coolant-circulating, the heat transfer capacity of the heat exchanger were investigated.

2. Description of the model

As a preliminary analysis, 2D half model of the CLEAR-I reactor pool was considered. All the components in the reactor pool were simplified to toroidal volume zones, and the half traverse cross section along the core axis was extracted as 2D reactor model. The model includes reactor core, up plenum, core above structure, primary heat exchanger and lower plenum.

In CLEAR-I reactor, all the assemblies in the core are hexagonal. There are 61 fuel assemblies, 8 control rod, surrounded by three layers reflector assemblies and one layer shielding assemblies. Each fuel assembly consists of 61 UO_2 fuel pins with an active length about 0.8m, and the pins are fixed with wire wrap. A simplified core model was used to do the simulation. All the assemblies in the core were treated as the radial variation zone according to the core power distribution along the radial directions, in the central of the core, the central dummy zone was considered, and along the outward of the radial direction, the zones represented fuel assemblies, reflector assemblies and shield assemblies, respectively. Fig. 2 shows the power density distribution of CLEAR-I. Since the reactor model were simplified 2D toroidal, it was impossible to resolve all the pins in the fuel assemblies, so the fuel assemblies were considered as the porous medium, and heated with the volumetric power of the core, that is assembly zones dependent on an radial power distribution, different power density were set in different core zones according to the neutronic analysis results. Because of the same reason of the core model, the pipe structure in the primary heat exchanger must be modified, and also treated as porous medium. For the nominal operation conditions, each primary heat exchanger should remove 2.5 MW, the frictional coefficient and neglect volumetric heat source were given for the primary heat exchanger model.

The porous medium approach was used to calculate the pressure losses of core and heat exchanger. The advantage of this approach is the possibility to create a temperature dependent pressure loss relation. Two important coefficients include viscous pressure loss coefficients and

inertial pressure loss coefficients should be gained during the use of this approach. With the method provided in FLUENT user's guide [13], the coefficients of core and heat exchangers were gained and presented in Table.2.

Table 2. Coefficients of porous medium approach

Calculate zone	Di(1/m2)	Ci（1/m）	Δn(m)
Core	1.728×106	11.35	0.8
Heat exchanger	5.35×105	1.04	1

For the numerical considerations, second order upwind scheme was chosen to discrete the convective term in the momentum equation, energy equation and Reynolds stresses equations. SIMPLE method was used to resolve the linear pressure-velocity coupling. Because the free lead surface was not taken into account, the top of the model was treated as a simplified free-slip adiabatic wall. As an preliminary investigation, all model boundaries except the vessel wall were considered as adiabatic. The thermal-physical properties of referred to the LBE handbook [14]. ANSYS FLUENT was used to carry out the simulation.

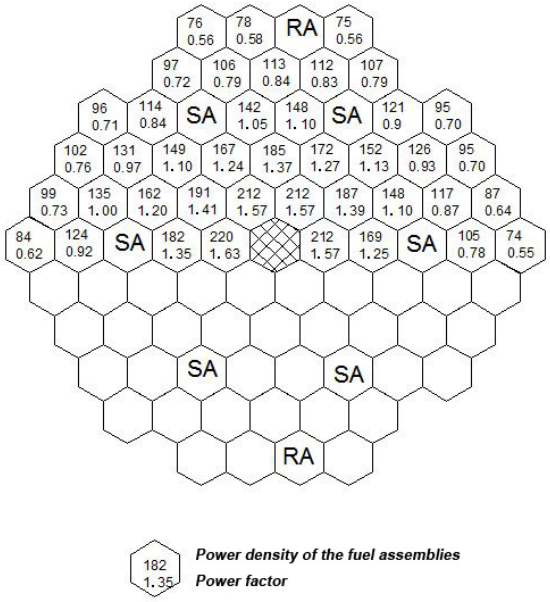

Fig. 2 the power density distribution of CLEAR-I (in KW)

3. Results and discussion

Fig.3-Fig.6 show the results of the steady state simulation. The temperature distribution was shown in Fig.2. There are temperature gradients in each assembly zone in axis direction since the LBE is heated in the core. The maximum temperature occurred at the assembly which adjacent to the neutron source assembly. Along the radial direction we can see that the temperature also varies because the LBE are

heated by the different power densityin each zone.. In the reflector assemblies and shield assemblies, the LBE almost not heated, and the temperature is relatively low. Temperature field in the hot pool is not homogeneous, this phenomena will be discussed below. Compared with that in hot pool , the temperature homogenization in the cold pool is better.

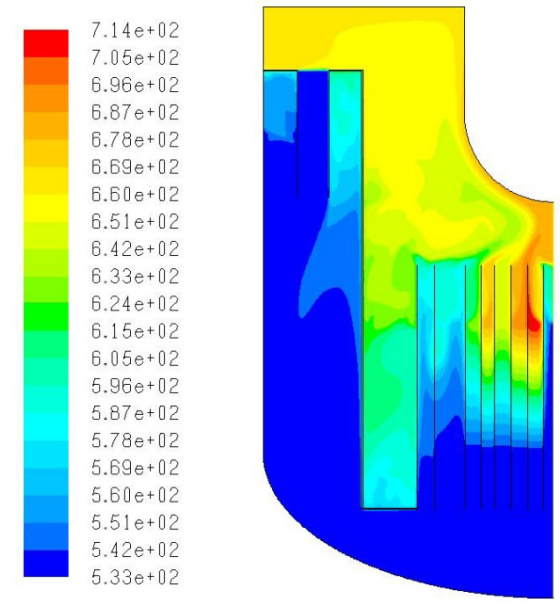

Fig.3 Temperature distribution in CLEAR-I reactor pool (in Kelvin)

Fig.4 shows the contour field of the velocity magnitude, Fig.5 shows the vector field of the velocity and the color express the pressure magnitude in the reactor pool. Since the LBE is only heated at the active region, the heated LBE is driven by the natural circulation force caused by the density difference between hot and cold pool, and flow upward, then collected at the hot pool. At the outlet of the reactor core, most of the heated LBE from core central region flow upward to the above core structure. And since the surrounding LBE is driven by natural convection force and flow upwards and towards central region of the hot pool, this phenomena lead to most of the high velocity hot LBE is distributed around the above core structure, and the temperature in this area is also relatively high as shown in Fig.4 and Fig.5. Thus, the coolant is not well mixing in the upper region of the core, and the temperature field in the hot pool is not homogeneous. In the other area of the hot pool, the temperature homogenization is better, and the macroscopic scale nature convection is not dominating, some vortexes are occurred, shown in Fig.5, and it is of benefit to the LBE mixing and heat transport. This should be considered in the structure optimize design.

In the lower plenum, since the LBE pass through the primary heat exchanger, and the LBE bulk flow down from the primary heat exchanger and turn the flow direction, finally collected in the lower plenum, a large LBE flow vortex is occurred, especially near the inlet area of the core, the flow is not stable, since the primary system is natural circulation, the unstable flow field at the core inlet region

has adverse impact on the core flow distributions. It seems that it may be necessary to modify the design of the the lower plenum, in order to make the LBE flow stably in this area.

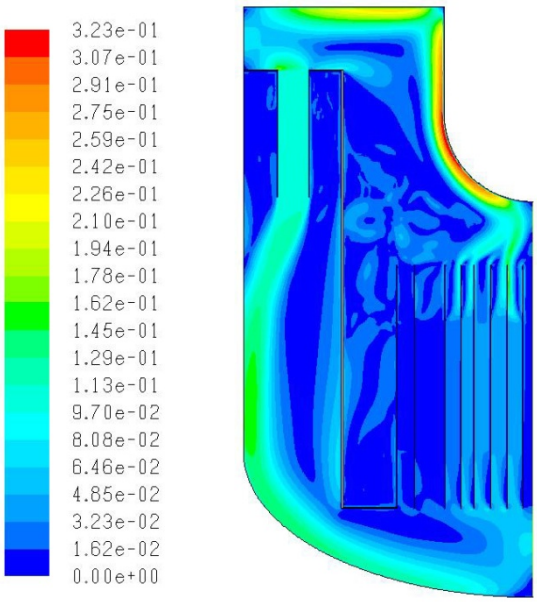

Fig.4 Magnitude distribution of velocity in CLEAR-I reactor pool (in m/s)

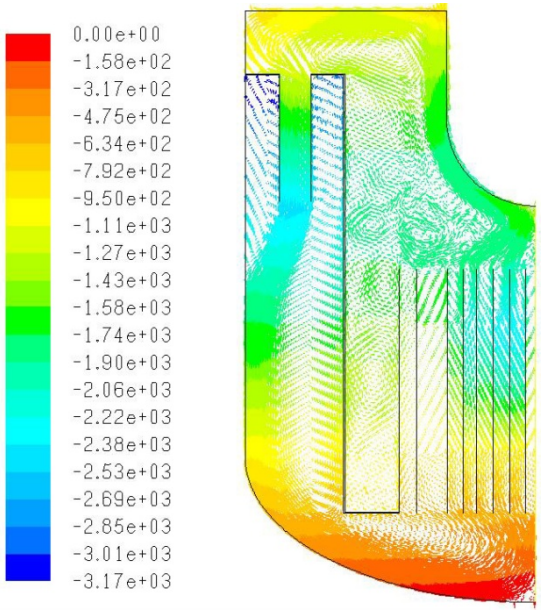

Fig.5 Vector field of velocity and pressure distribution in CLEAR-I reactor pool

Fig.6 shows the mass flow rate in different assemblies. The power density is relatively higher in the central area of the core and become lower gradually in other area. In the hot core region, the LBE is more heated, and a larger natural circulation force is produced because of the larger density difference. This leads to higher mass flow rate at high power density region. And the flow distribution in the core

is adjusted automatically, it is a good feature to safety considerations, and if the nutronics and structure design are appropriate, it seems that there is no need to design the additional flow distributers.

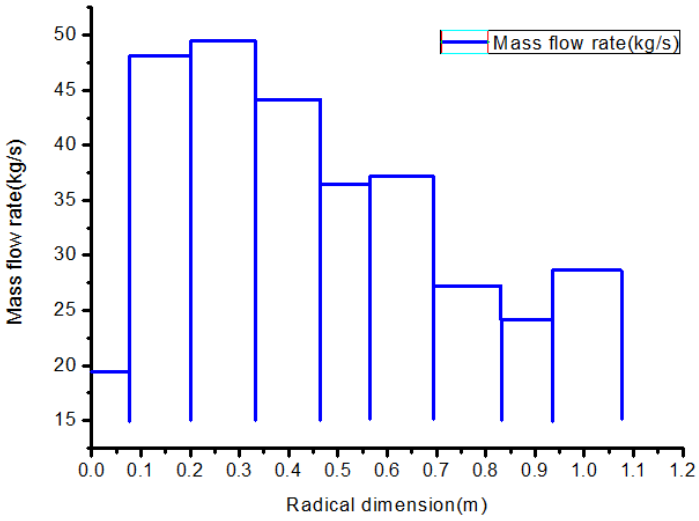

Fig.6 Mass flow rate distribution in reactor core

4. CONCLUSIONS

Natural circulation characteristics and flow distribution in primary system at the steady state of CLEAR-I were preliminary evaluated and discussed. A numerical simulation was conducted by using CFD code. The effects of the core power density, the height of the coolant-circulating and the heat transfer capacity of the heat exchanger were investigated. The results show that the natural circulation can be formed in the reactor pool. Homogenization of the temperature in the hot plenum should be carefully considered. The volume of the lower plenum should be enlarged in order to make the flow field stability in this region. Mass flow rate can be adjusted automatically and it is good to safety considerations. Since the flow and heat transfer phenomena in the reactor pool is very complex, the detailed 3D analysis should be carried out, and the result will be given soon.

ACKNOWLEDGEMENTS

This work was supported by Strategic Priority Research Program named “Advanced Nuclear Fission Energy-ADS Transmutation System” launched by Chinese Academy of Sciences and Natural Science Foundation of China under grant No.51076166. And thanks to the support of FDS team.

REFERENCES

[1] A Roadmap for Developing Accelerator Transmutation Accelerator Transmutation of Waste (ATW) Technology, A Report to Congress [R]. USA. October 1999
[2] IAEA-TECDOC--985: Accelerator driven systems: Energy generation and transmutation of nuclear waste. Status report [R]. November 1997.
[3] Won S. Park, et.al. HYPER (Hybrid Power Extraction Reactor): A system for clean nuclear energy [J]. Nuclear Engineering and Design 199 (2000) 155–165
[4] Y. Wu, et al, Overview of China LEad Alloy cooled Rector Development and ADS Program in China, NUTHOS-9
[5] Y. BAI et al., "Conceptual Design of Lead-Bismuth Cooled Accelerator Driven Subcritical Reactor (LEBCAR)," presented at the 15th International Conference on Emerging Nuclear Energy Systems (ICENES-15), May 15-19, 2011, San Francisco, USA.
[6] Weihua Wang, et al., "Structure Design and Analysis of Accelerator Driven Subcritical Reactor for China Nuclear Waste Transmutation", presented at the 15th International Conference on Emerging Nuclear Energy Systems (ICENES-15), May 15-19, 2011, San Francisco, USA.
[7] Y. Wu, FDS Team, Conceptual Design Activities of FDS Series Fusion Power Plants in China. Fusion Engineering and Design[J], 2006, 81(23-24): 2713-2718.
[8] Y. Wu, the FDS Team. Design Status and Development Strategy of China Liquid Lithium-Lead Blankets and Related Material Technology. Journal of Nuclear Materials[J], 2007, 367-370, Part B-2: 1410-1415.
[9] Y. Wu, S. Zheng, X. Zhu, et al., Conceptual Design of the Fusion-driven Subcritical System FDS-I. Fusion Engineering and Design[J], 2006, 81, PartB: 1305-1311.
[10] WU Yi-can. A Fusion Neutron Source Driven Sub-critical Nuclear Energy System : A Way for Early Application of Fusion Technology. Plasma Science and Technology, 2001, 3 (6): 1085-1092.
[11] Yican Wu. Progress in Fusion-driven Hybrid System Studies in China. Fusion Engineering and Design, 2002, 63-64: 73-80.Y. Wu, the FDS Team. Design Status and Development Strategy of China Liquid Lithium-Lead Blankets and Related Material Technology. Journal of Nuclear Materials, 2007, 367-370, Part B-2: 1410-1415.
[12] Y.C. Wu, J.P. Qian, J. N.Yu. The Fusion-Driven Hybrid System and Its Material Selection. Journal of Nuclear Materials, 2002, 307-311:1629-1636.
[13] FLUENT user's guide
[14] Handbook on Lead-bismuth Eutectic Alloy and Lead Properties, Material Compatibility, Thermal-hydraulics and Technologies, OECD NEA 6195, 2007 Ed.

SFR core design : a system-driven multi-criteria core optimisation exercice with TRIAD

Edouard HOURCADE[a], Frédéric JASSERAND[a], Karim AMMAR[a], Cyril PATRICOT[b]

[a] Commissariat à l'Energie Atomique et aux Energies Alternatives (CEA)

[b] Ecole Polytechnique

Presented by Edouard HOURCADE

Abstract. In the framework of Sodium cooled Fast Reactor (SFR) development, new core design strategies are proposed. For example, designers aim at demonstrating the absence of severe consequences in case of a pump loss (ULOSSP and ULOF accident). These new design objectives imply a deep re-shuffling of design parameter covering a large area of possible configurations.

Classic methodologies for core design consist of sequential analysis of neutron physics, core shielding, fuel behavior, sub-assembly mechanics and thermal-hydraulics (core and system), often performed by separates experts/services. This iterative scheme can be a lengthy process especially in the early stage of design when parameters are subject to frequent changes. Beside, this design approach is mainly feed-back oriented and final options are neither optimal nor "rigorously" justified with macroscopic indicators.

A complementary approach is a systematic and multi-physics exploration of design parameter space [3][4]: it implies the integration of reactor physics code systems and correlations into platforms dedicated to multi-physics and sensitivity/parametric analyses. Exploration can also be completed with either single or multi-criteria optimization processes with use of correlation techniques such as neural networks, kriging or polynomials. TRIAD (Tools for Reactor optImization Analysis and Design) is a code package developed at CEA which offers all features for core designers to implement these methods.

In this paper an example of system-driven core optimization will be made for next generation SFR heterogeneous core. Optimization will include shielding performance, as well as system Unprotected Loss of Flows transients.

1. Background, presentation of TRIAD

Within the framework of new reactor developement, the aim of TRIAD is to provide the core designers and project managers with an integrated multi-physics tool for core optimisation. An other objective is also to consider the possibility for non specialists of core physics to integrate economical performance indicators at early stage of core design.

Eventually, compromises within 10 performances indicators correlated to 20 parameters design space must be accessible to non specialists of data mining frameworks within reasonable time frame. In particular main possible design routes must be made obvious so that switch can be rapidly made in case of un-expected project event (safety reviews, technological deadends).

The main steps necessary and associated TRIAD tools for the whole process are the following :

- ***TRIAD-S*** (Simulation). Setting a multi-physical evaluation scheme with chained simulations (core and system (shielding) Neutronics, fuel physics, core and system thermal-hydraulics, etc.). Global caculation should not exceed 1 hour or 2 on standard CPUs, data exchange format

between codes is using SALOME mesh standards and tools (MED Coupling) [5]. Codes and models used in TRIAD-S are described in §2 but are summarized bellow:

- Neutronics : ERANOS [13], APOLLO3 [1] and TRIPOLI4 [12]
- Fuel Physics : GERMINAL V1.5 [2]
- Core and System Thermal-hydraulics CATHARE [14], TETAR

— ***TRIAD-L*** (Launch). Plan of experiments over design parameter space are performed using for example LHS (Latin Hypercube Sampling) method. Depending on variable ranges, up to several tens of thousands calculation must be run on parallel modes on calculation clusters.

— ***TRIAD-M*** (Meta-modelling). Based on results of plan of experiment, construction of meta-models aims at replacing codes at optimisation process step (TRIAD-O). This can be performed in several steps :

- Determining most influential parameters on performances (using expert judgment and sensitivity analysis methode like Morris [10] and Sobol [11])
- Most influential parameters are used to fit meta-models such as Neural Networks [9], kriging [8] or polynomials.

— ***TRIAD-O*** (Optimisation). Genetic algorithms are used in our case to perform multi-criteria optimisation. Results expected are best compromises for core configuration. Those are gathered on so called “Pareto front”. An example is given on §3.

TRIAD-L, M and O are mainly using CEA statistical analysis, data-mining and optimisation framework (URANIE [6])

2. Calculation Scheme

The essential task in a multi-physic optimization process is to obtain a sensible trade-off between precision and simulation time. As far as “best-estimate” codes are concerned, unitary runs rarely take less than a few minutes which lead to either physical modeling simplification or construction of meta-models (Neural networks, Kriging or polynomials in our case). The choice between these 2 options will essentially depend on the level of precision required in physical description which is often related to the development stage of the core design. Also, in case of coupled methods the accuracy level of models must be consistent between disciplines (neutronics and fuel mechanics for example).

Models for core Neutronics, Fuel thermal-mechanics, system thermalhydraulics and shielding implemented in the framework of French fast reactor core design are presented in this section.

2.1. Core neutronics

Core Neutronics is analysed using ERANOS code system with multi-groups (33) approximation using either diffusion or SN transport methods. Cross sections are calculated using several subgroups methods steps on homogeneous cells.
Core geometry is described using RZ assumption but accounting for main axial and radial core heterogeneities except control rods. Impact of latter assumption for unprotected loss of lows transients calculation will be further discussed (§2.2 and §3).

Criteria of interests for neutronics can be listed as follow:

— Reactivity swing: it corresponds to the variation of core reactivity between beginning and end of cycle (BOC, EOC). This value is important since this reactivity is compensated by rod insertion. This value has to be minimized to prevent from power excursion in case of incidental control rod withdrawal.

— Breeding gain: often expressed in equivalent Pu239

- Power distribution: minimizing the power total form-factor is favorable for steady state and transient behavior.
- Pu inventory: the objective is to minimise Pu mass in order to facilitate a potential fleet deployment.
- Void Coefficient : the objective is to justify that global reactivity stays negative when core sodium is voided.

Feedback coefficients such as Doppler (fertile and fissile), sodium dilatation (plenum and bulk), clading dilatation (with fuel-cladding bonding assumption) and core support dilatation are calculated at this stage to feed core thermal-hydraulics with data for point kinetics. Assumptions for flux calculation (diffusion or transport) is made according to the type of coefficient calculated (for example, transport model is used for all sodium dilatation perturbation).

TRIAD is also able to compute neutronics criteria of interest with 3D SN APOLLO3 solver or with TRIPOLI 4 (critical mode). For now, computation times of these models are too high for extensive plan of experiments but can be used for performance validation of selected cores.

2.2. Core and System Thermal-hydraulics

Within TRIAD-S, Core and system thermal-hydraulic can be performed using best-estimate system code (CATHARE) or simplified modelling. In the application presented in this paper, simplified system code TETAR developed within TRIAD framework is used. The objective is to estimate maximum sodium temperature reached during Loss Of Flows transients (LOF). In particular ULOSSP (Station Supply Power) and ULOF transient are considered. TETAR can handle diphasic flows but this feature is not activated for core design calculation scheme. One phase sodium characteristics are simply extrapolated in case temperature is above vaporisation threshold.

For core calculation, multi-1D modelling with closed chanels is considered. For initialisation, flow rates within chanels are estimated within an iterative process aiming at equilibrating pressure drop. A preliminary step is the setting of flow rate regions (zoning process) that are supposed to satisfy with criteria such as :

- maximum cladding temperature (620 °C is considered here)
- maximum temperature gradient between adjacent chanels (50 °C in our case)
- mean core temperature elevation target (150 °C in our case)

Core power evolution through LOF transient is calculated with point kinetic assumption. Most feedback coefficients are deducted from ERANOS neutronic calculation (see §2.1). Feedback due to differential dilatation of core, vessel and control rods is imposed to a fixed value from reference 3D calculation. Impact over core optimisation process is discussed in §3.

The rest of the system is modelled as one “loop” containing Hot and cold pools (can be modeled with either 0D or 1D elements), pump (caracterised with Flow rate vs time characteristics) and heat exchangers (sodium-sodium) modeled as a counter-flow device.

For transient calculation such as ULOF, pressure drop coming from the pump decreases and natural circulation can be assessed through a global pressure balance.

2.3. Fuel Physics

Developed by CEA, GERMINAL (V1.5) allows to simulate Fast Neutron reactor oxide fuel thermal and mechanical behavior under irradiation. It can be user under steady-state condition or transient conditions (Rod withdrawal transients for example). His domain of validation covers high burnup fuels up to 25 at%. It includes specific modeling for :

- Fuel evolution : central hole and porosity evolution, Plutonium redistribution, O/M radial profile, ransient gas swelling, melting fuel behaviour, minor actinides production
- High burn-up models (fission gas, volatile fission products and JOG formation)
- Fuel-cladding heat transfer
- Fuel-cladding mechanical interaction.

GERMINAL has a validation database of more than 40 experiments (PHENIX, PFR, CABRI) reactors with special emphasis on :

- local fission gas retention and global release,
- fuel geometry evolution, radial redistribution of plutonium for high burn-up fuels
- solid and annular fuel behaviour during power ramps including fuel melting,
- helium formation from MA (Am and Np) doped homogeneous fuels.

We have to keep in mind that we're within a core pre-design process; hence all core fuel pins cannot be calculated. One fuel pin per type of fuel is selected. Geometry is deducted from common geometric data and Flux profile, maximal linear power as well as DPA are extracted from neutronic results. As described in §3 fuel performance of interest are fusion margin, internal pin pressure and cladding constraints.

2.4. Shielding

One of the objective of current designs is to bring plant lifetime to the extent of current GEN3 level. This objective implies a minimization of main structure damaging (such as core plug).

An other objective is to facilitate heat removal systems maintenance in order to maximize plant availability factor. This implies minimization of secondary sodium activation for example.

However, current core design also rely on core leakage to maximize safety parameters such as void coefficient or ULOx behaviour. This design path may not be compatible with above objectives, consequently, a shieding model was developed for TRIAD (see FIG 1).

This model is based on TRIPOLI 4, and can described as follow :

- Two neutron transport runs are considered, one for core plug and the other one for intermediate heat exchanger
- Isotopic concentration as well as sources distribution are generated automatically from ERANOS RZ model
- Automatic biasing using TRIPOLI functions as well as additional ad-hoc procedures are used

One run of such simulations take a few hours and is not compatible with large plans of experiments. An equivalent ERANOS model running in less than a hour CPU is under study. The objective is to integrate core shielding as a design constraint within the optimisation process.

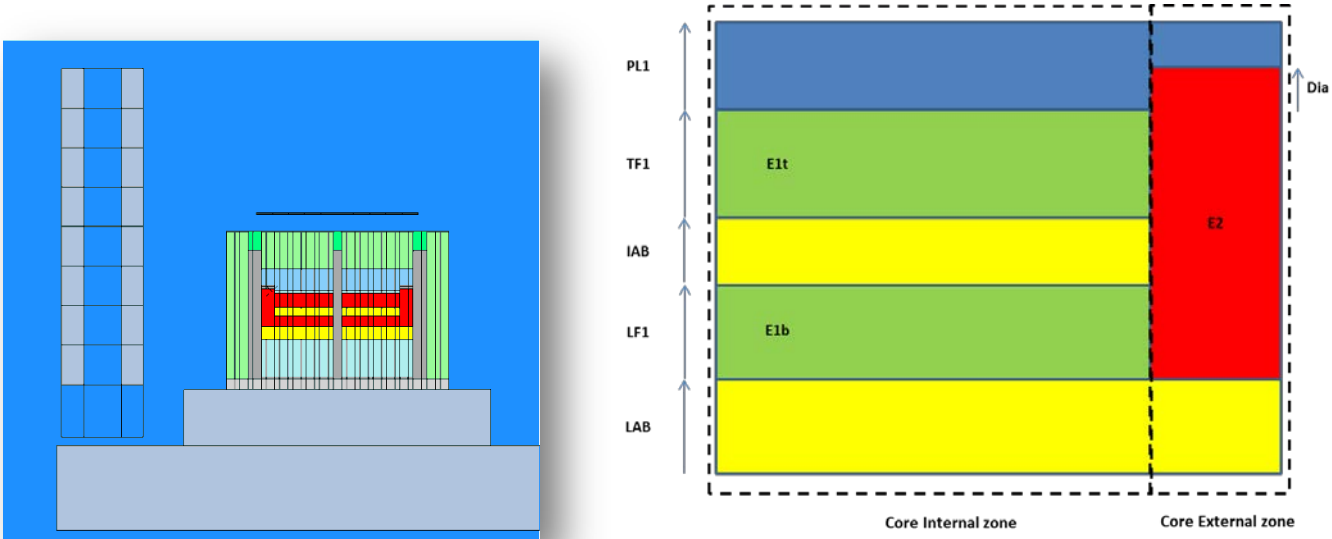

FIG. 1. On the left, TRIPOLI 4 model, on the right radial cut of core (central axis on the left)

In this paper, we used TRIPOLI model to calculate a few hundreds of core configuration selected from Pareto front (see §3). It is important to note that lateral protection configuration have little impact on core neutronics which was the first aim of our optimisation. Consequently, protections chosen in this study are not deducted from any preliminary core shielding design. Quantitative results for secondary sodium activation is not to be considered as reference values.

2.5. Calculation scheme

For each core configuration from the plan of experiment (several thousands of cores), core neutronics, core thermal-hydraulics and hot spot fuel thermal behaviour assessment are performed.

Calculation scheme is presented on FIG 2. ERANOS code is used twice : one run is dedicated to critical Pu mass search. The second run is performed on critical core (at end of cycle) and is used to finely caracterize core performance (Void coeficient etc.) and extract necessary results for core thermal-hydraulic calculation (feedback coefficients) and hot spot fuel thermal analysis (flux, DPA etc.)

TETAR is used to evaluate core zoning and pressure drop, estimate necessary diaphragms, and perform ULOF transient. Main performance indicator is maximal sodium temperature reached through ULOF transient. Flow rates are transmited to GERMINAL for hot spot fuel thermal analysis.

GERMINAL calculations are performed on one pin per type of fuel (typically one for internal core and one for external core). Selected pins are those with the highest mean linear power through irradiation. Performance indicators are margin to fuel melt and fuel internal pressure. Clad constraints indicators are also calculated but are not used for now as an optimization constraint.

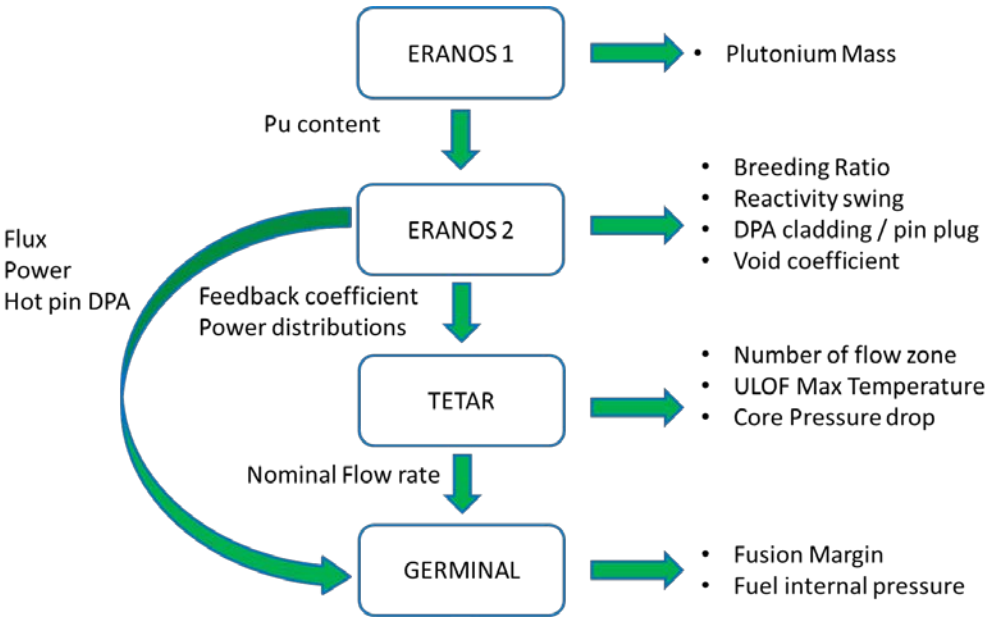

FIG. 2. Core calculation Scheme for plan of experiment

Shielding performances with TRIPOLI4 are calculated starting from core data and output from ERANOS calculation. For computation time reasons this model is not for now included in plan of experiment calculation scheme.

All space dependant datas (flux, powers) are handled with SALOME [5] mesh structure (MED_Coupling). Averaging and P1 & P0 interpolations are performed on 1D or 3D meshes.

3. Optimisation exercice

The objective in this section is to illustrate an “ab initio” approach using genetic algorithms of TRIAD as core designers. Our goal is to :

- Visualize core design compromises
- Select “extreme” core configurations to understand possible core design routes

3.1. Design parameters and performance objectives

For this exercice we mainly use design recipes of CEA CFV core [7] with AIM1 cladding. These type of cores rely on maximizing core leakage using heterogeneous axial structures. Heterogeneities are layers of fertile and fissile pellets, presence of sodium plenum and height difference between radial Pu enrichment zones (also called Diabolo). An illustration of design parameters as well as range of variation for optimisation studies are gathered on FIG 1 and FIG 3. Note that global core power (1500 MW Thermal), irradiation time (4 X 400 EFPD) as well as mean core inlet and outlet temperature (respectively 400°C and 550°C) are fixed.

Performance objectives for core design are gathered in FIG 4. Those performances can be seen either as design constraints like :

- DPA (displacement per atom) for AIM1 cladding should be less than 120.
- Core diameter without rod should be less than 4,5 m for economical reasons.

It can also be seen as criteria like :

- Minimizing maximum temperature through ULOF transient, the objective is to avoid boiling during such an extreme situation.
- Reactivity swing should be minimized, the objective is to minimize single rod worth or minimize total number of rods used.

Parameters			
E1t : Top Fissile Pu content (Mass %)	18 - 32	LAB : Lower Axial Blanquet (mm)	100-500
E1b : Bottom Fissile Pu content (Mass %)	18 - 32	DIAB : Diabolo (mm)	0-200
E2 : External Fissile Pu content (Mass %)	18 - 32	Core Outlet Temperature (°C)	550
CH : Fuel pellet central hole (mm)	0 - 3	PL : Plenum (mm)	10-600
FUEL : Fuel Diameter (mm)	5 - 11	Number of rings per assembly	7-12
CLAD : Cladding width (mm)	0.5	Number of internal assembly	123-350
TF1 : Top Fissile (mm)	200-500	Number of external assemblies	75-200
IAB : Internal Axial Blanket (mm)	10-400	Irradiation Time (EFPD)	1600
LF1 : Lower Fissile Layer (mm)	200-400		

FIG. 3. : Core and fuel design parameters

Constraint	**Condition**	**Criteria**	**Objective**
DPA cladding (pcm/irradiation)	<120	Core Diameter	Minimize
Ratio between external fuel height and core diameter	> 0.1	Plutonium Mass	Minimize
Fuel assembly pitch (mm)	> 100	Reactivity swing	Close to zero
Fuel width (mm)	> 2.5	Void effect	Minimize
Fuel smearing	> 0.8	ULOF Max T°	Minimize
Total number of FAs	> 216	Breeding Ratio	Close to zero
Core Diameter (no rods) (mm)	< 4500		
Fusion Margin (°C)	> 200		
Core pressure drop (bars)	< 5		

FIG. 4. : Optimisation criteria and constraints

3.2. First Optimization results

TRIAD-O is used to perform multi-criteria optimisation process.

Optimisation result is a 6 dimensions Pareto front (for 6 criteria of FIG 4) with 60000 core configurations is given on FIG 5. As a reminder, Pareto front gathers the best compromises cores within design parameter space : none of these core performance can be upgraded without downgrading another. Four 2D cuts of this Pareto front are presented on FIG 5. Compromises between void coefficients, maximum Na temperature through ULOF, reactivity swing ang breeding ratio are highlighted.

Performance of selected cores range from -1800 pcm to 1000 pcm for void coefficients, -4000 pcm to 0 pcm for reactivity swing, 700°C to 1070°C for ULOF sodium maximum temperature and -0.15 to 0.15 for breeding ratio.

We have to keep in mind that ULOF results are obtained using differential dilatation of core, vessel and control rod feedback from litterature. As a consequence, only relative values of maximum sodium temperature must be considered as relevant. This can be justified by the fact that a great uncertainty is associated with this coefficient which relies on differential rods insertion when temperature of sodium raises. Robust demonstration for ULOF transient should make a strongly conservative assumption on its value.

One can see on top graphs that Minimizing Void coefficient and Maximum temperature through ULOF transients are not compatible with minimizing reactivity swing. This is easily explained by the fact that CFV type core are mainly relying on leakage to minimize sodium dilatation coefficient which is not a favorable feature for neutronic balance. Consequently Pu content has to be increased with a negative effect on core breeding (shown on bottom right graph) and on reactivity swing.

Bottom left graph shows that some antagonism exist between void coefficient and ULOF sodium maximum temperature. A thorough analysis of results show that minimizing ULOF sodium maximum temperature can be done in two ways : minimizing sodium dilatation reactivity coefficient (compatible with sodium void minimisation) and lowering fuel nominal temperature (to minimize positive doppler effect related to power decrease during ULOF). This latter design path leads to minimizing fuel diameter hence potentially increasing sodium fraction in the core which is not compatible with void coefficient reduction.

To highlight technological paths behind performances compromises, a cobweb representation of our problem can be made (see FIG 6). In this representation, correlation between design parameters (X) and performances (Y) for each configuration is represented by a green broken line connecting parameters and criteria values. Precise core configurations can be determined using filters on performances to extract corresponding design parameters. For example, on FIG 6 core configurations identifying 3 different design routes or “best compromises” are highlighted (in blue, red and pink).

First design trends show that « compact » core configurations with no diabolo and small volumes of fertile can be rather good compromises. These designs tend to minimizing core leakage hence Pu content. Then Breeding ratio is satisfied with small fertile height which favors low core pressure drop, natural circulation and low ULOF maximum temperatures. Selection of pin size will highly depend on “acceptable” reactivity swing, which is determined on both economical (number of control rods) and safety consideration (Rod Withdrawal transients for example).

From this stage, complementary “best estimate” simulations, accounting for rods (precise ULOF evaluation, calculation of anti-reactivity margin at each step or core life etc.), potential diluents (flattening of power distribution), must be engaged before these core configurations are considered relevent.

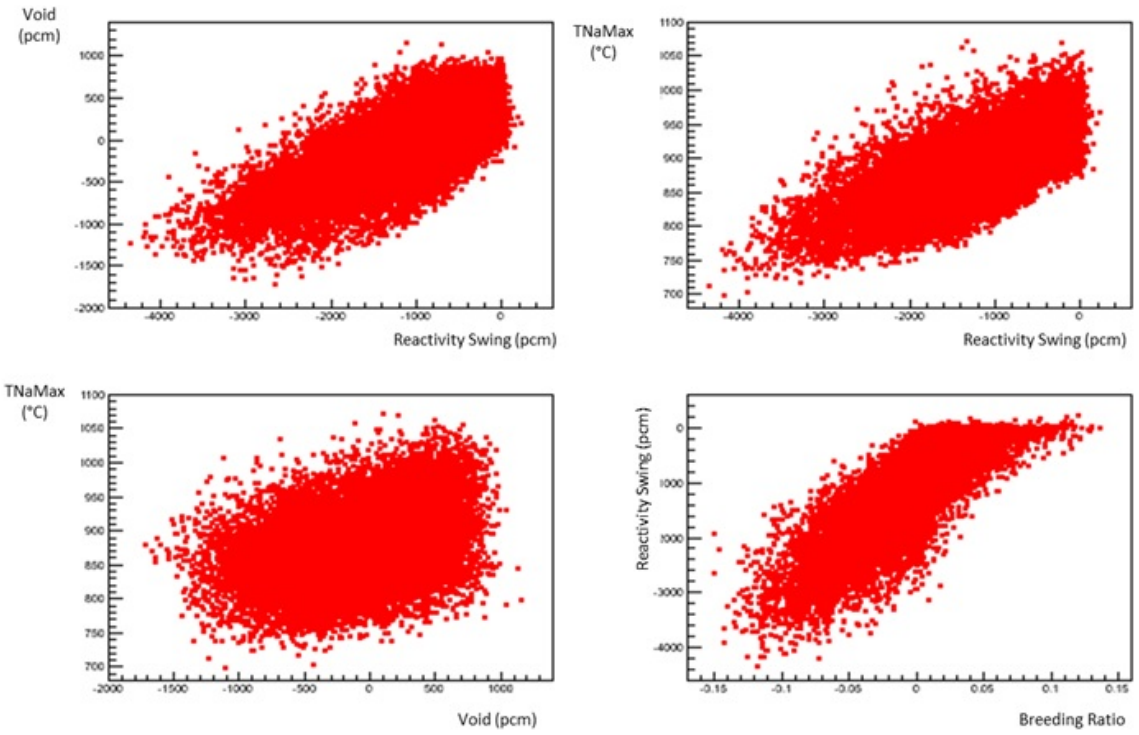

FIG. 5. Visualization of a fraction of Pareto Front for 4 performances : Void coefficient, Reactivity swing, Maximum sodium temperature through ULOF and Breeding ratio

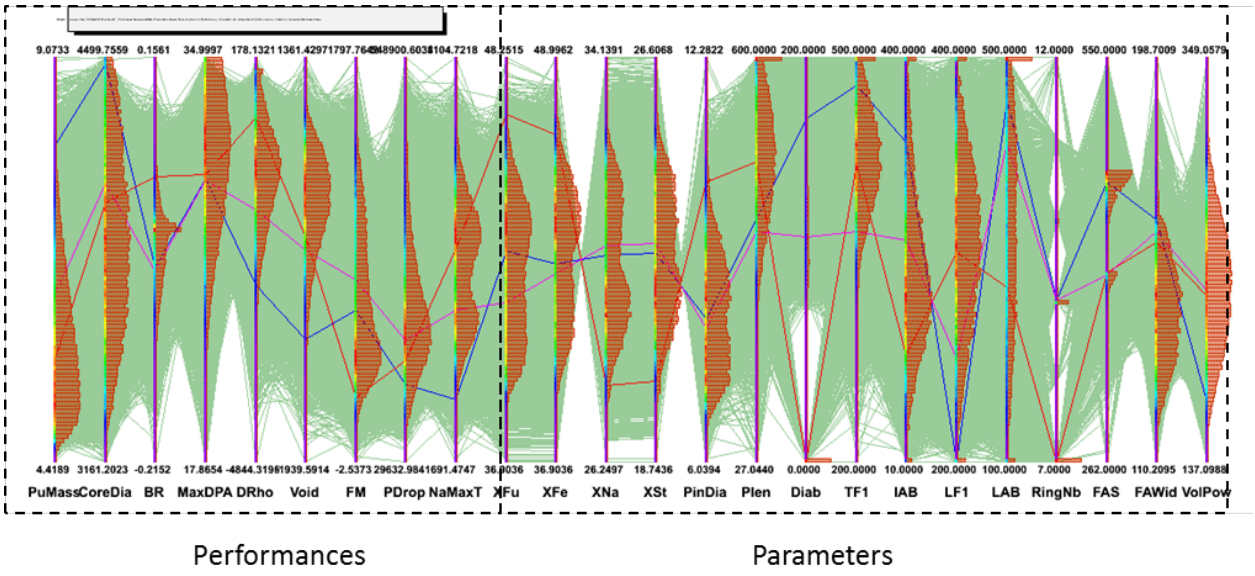

FIG. 6. Cobweb representation of parameter values (X, 14 right columns) and performances (Y, 9 left columns)

3.3. Impact of core design on shielding

Shielding performances of few hundreds of core configuration selected from Pareto front (FIG 5) were estimated with TRIPOLI 4 model. In our case lateral reflectors and neutron shields are not parameters for core design. Beside, as already mentioned (§2.4) lateral core protection considered here are smaller than realistic shielding configurations. This has a strong impact over order of magnitude of secondary sodium activation. Consequently, the objective is rather to assess the impact variation of core design itself on secondary sodium activation :the question raised is on the optimisation range accessible through core modification.

FIG 7 shows statistical repartition of secondary sodium activation over selected core “population”. This performance ranges from 10000 Bq/cm3 to 200000 Bq/cm3. With this first analysis we can consider that a gain of a factor 2 to 4 on secondary sodium activation is easily accessible through core design modification.

At this stage, no recommendation of structure for core design was issued. This will have to be confirmed with further detailed analysis on selected cores.

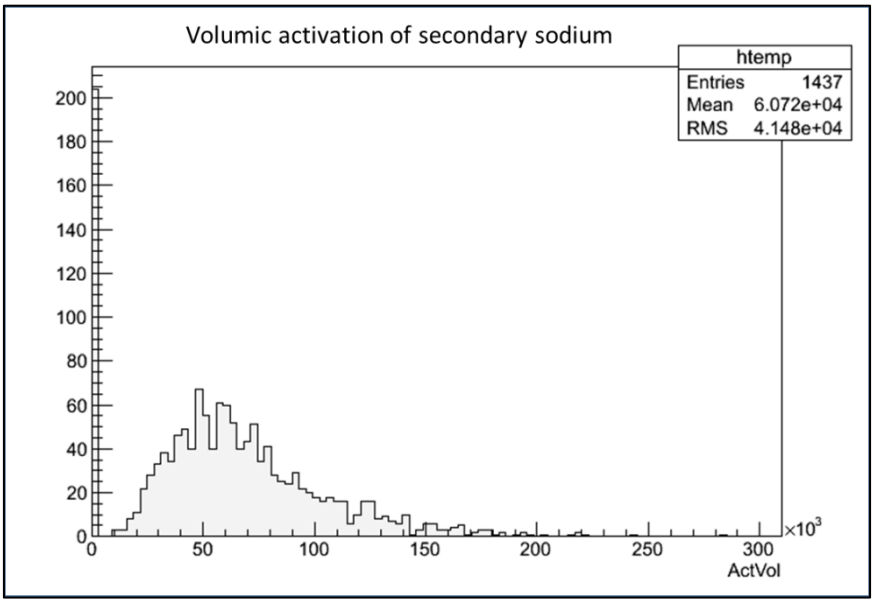

FIG. 7. Statistical repartition of secondary sodium activation for 1400 core randomly selected on Pareto Front

4. Conclusions

For a one team of experts, multi-physics design of heterogeneous core design, under constraints and with antagonist performances target is a challenge. In presented case, it amounts to optimising within a 17 dimensions design space with the objective of simultaneously optimizing 6 criteria. Beside, this process can be performed under more than 10 design constraints.

In this paper, we’re presenting TRIAD (Tools for Reactor optimIsation analysis and Design) as a tool to help with this difficult process. In one environment based on CEA Salome and Uranie softwares, it gathers core and systems multi-physics tools and offers super-computing, data-mining and optimizing facilities.

Results of the exercice show that TRIAD can be a powerful tool for multiphysical core design process. Core neutronics, system thermal-hydraulics, fuel behaviour as well as core shielding can be evaluated in one simulation run to serve core performance assesment and feed the genetic optimisation process. Once best performing core configurations are selected, highlighting of compromises between various performances is made easily accessible and tendancies for core design technological options can be proposed.

Perspectives are the integration of best estimate models in TRIAD-S, including a deterministic shielding model, a 3D neutron transport model and a reference system thermal-hydraulics model. This will allow accounting for finer effects in the optimization process such as core internal structure impact on core shielding or rod effect on transients. Also a graphical user interface for TRIAD-O is under development. The objective is to spread the tool amongst non expert of softwares including project managers. It will include features for integration of user defined core performance (economics for example) within the optimisation process.

REFERENCES

[1] "APOLLO3: a common project of CEA, AREVA and EDF for the development of a new deterministic multi-purpose code for core physics analysis" H. Golfier et al., International Conference on Mathematics, Computational Methods & Reactor Physics (M&C 2009)

[2] "Modelling of the Thermomechanical and Physical properties in FR Fuel pins using GERMINAL code", L. Roche, M. Pelletier, IAEA-SM-358/**25**

[3] "Innovative methodologies for Fast Reactor core Design and Optimization" E. Hourcade et al. ICAPP 2011

[4] "FARM: A New Tool for Optimizing the Core Performance and Safety Characteristics of Gas Cooled Fast Reactor cores" X. Ingremeau, P.Dumaz, G. Rimpault, M. Zabiego, S. David, D. Plancq. ICAPP 2011

[5] Salome Platform : "www.salome-platform.org/user-section/documentation/current-release"

[6] "Fuel loading pattern for heterogeneous EPR core configuration using evolutionary algorithm" J.M DO et al. M&C 2009

[7] "Low void effect core design applied on 2400 MWth SFR reactor" P. Sciora et al. , ICAPP11

[8] "Design and analysis of computer experiments." J. Sacks, W.J. Welch, T.J. Mitchell, and H.P. Wynn.Statistical science, 4, 1989.

[9] "Réseaux de neurones, méthodologie et applications" Gérard Dreyfus, Jean-Marc Martinez, Manuel Samuelides, Mirta B.Gordon, Fouad Badran, Sylvie Thiria, Laurent Hérault, Eyrolles, 2004

[10] "Factorial sampling plans for preliminary computational experiments" M. MORRIS, Technometrics, 33:161–174, 1991.

[11] "Sensitivity estimates for non linear mathematical models. Mathematical Modelling and Computational Experiments", I.M. SOBOL 1:407–414, 1993

[12] "TRIPOLI-4 version 8 User Guide", TRIPOLI-4 Project Team, CEA-Saclay, CEA-R 6316, 2013

[13] "The ERANOS code and data system for fast reactor neutronic analyses", G. Rimpault et al, Proceedings of PHYSOR 2002, Seoul, Korea (2002)

[14] "CATHARE 2 V2.5_2: A single version for various applications", G. Geffraye et al, Nuclear Engineering and Design A. 2010

Study on Asymmetric Parfait Cores with Low Void Reactivity and Recycled MAs for the Fast Reactor

A.Nagata[a], A. Hara[a], Y. Moriki[a], M. Kawashima[b], M. Yamaoka[a], T. Yokoyama[b]

[a] Toshiba Corporation Power Systems Company

[b] Toshiba Nuclear Engineering Services

Abstract. The minor actinides (MA) recycling is important for environmental harmonization. Fast reactor is useful for burning MA. It is important to discuss the safety performance, especially sodium void reactivity. From such viewpoints, Toshiba had studied axially heterogeneous cores named as "Asymmetric Parfait Core (APC)" which has different internal zones asymmetrically located in axial, and concave core with upper sodium plenum in the past. In this paperlow sodium void reactivity core with MA burning based on APC has been studied. Inner core height is discussed by sodium void reactivity and burnup reactivity points of view, and the difference of those by using two types of fuel composition are compared. Finally, the APC for high efficient MA burning with low sodium void reactivity and burnup reactivity is evaluated.

1. Introduction

A fast spectrum reactor is one of the good answer to recycle MA for environmental harmonization because MA can be burnt as fuel by fast neutron. In this paper, reactor core concepts which has enhanced safety feature and achieves high efficient MA burning at the same time, are discussed. Regarding safety feature, sodium void reactivity and burnup reactivity are focused. Generally sodium void reactivity should be low in terms of ULOF (Unprotected Loss of Flow) accident. Also, buruup reactivity should be low in terms of UTOP (Unprotected Transient of Power).

However, sodium void reactivity increases by MA because of neutron spectrum hardening for the fission cross section at high energy. Therefore, the reactor core concept to choose needs to have negative sodium reactivity as much as possible, when not loading MA.

From such viewpoints, Toshiba had studied axially heterogeneous cores named as "Asymmetric Parfait Core (APC)" which has different internal zones asymmetrically located in axial [1][2], and concave core with upper sodium plenum[3] in the past. And separately, CEA has been studying the low void reactivity core for large power SFR and an application to ASTRID as well [4].

Considering to contribute an optimization of this concept of core as well, low sodium void reactivity core with MA burning based on APC core has been studied in this paper. Inner core height is parametrically decided by sodium void reactivity and burnup reactivity points of view. After decision of inner core height, two types of fuel composition are used while keeping low sodium void reactivity and burnup reactivity, and difference of MA burning chalacteristics is evaluated.

2. Description of Core Design

Table 1 shows design specification and Fig. 1 and Fig. 2 show core layout and RZ geometry of the APC, respectively[3][4][5]with partial data coming from CEA papers. Coolant is sodium. Same Pu enrichment is used in inner core and outer core for easy fuel fabrication. MA is loaded in inner blanket. The volume fraction are assumed by considering the conventional FBR fuel assembly and reference, and fuel volume fraction is over 50% to increase the loading amount of MA in the core.

Two types of fuel composition are used in this study. 31 Control rod is homogeneously positioned[6]. Table 2 shows the isotope ratios of actinides for the high and low Pu-fissile cases[4][7]. In this evaluation, two dimentional RZ diffusion calculation code STANBRE[8] and two dimentional transport calculation code TWODANT[9] for sodium void reactivity are used. Nuclear data library used is the 70-group JFS-3-J3.3[10] processed from the JENDL 3.3[11].

Table 1. Design Specification

Item	Specification
Thermal Power	2400MWt[5]
Cycle Length	400EFPD[4]
No. of Refueling Batch	5
Core Type	U-APC*[3],[4] (Internal Blanket,One Pu Enrichment for core-fuels)
Core Height (Inner Core / Outer Core)	60, 70, 80, 90cm (parameter) / 100cm[3]
Axial Blanket Thickness(Upper / Lower)	0 / 20cm
Axial Shielding Material	B_4C
Radial Blanket	0
Core Diameter	428cm
Fuel Type	MOX
Fuel Volume Fraction	50.5%[4]
Structure Volume Fraction	21.9%[4]
Sodium Volume Fraction	27.6%[4]
Sodium Plenum Length (Inner Core / Outer Core)	78, 68, 58, 48cm (parameter) / 38cm

*Uranium-Type Asymmetric Parfait Core

Table 2. Isotope Ratio of Actinides for High and Low Pu-fissile Cases

Element	Isotopes	Mass content (%)		Element	Isotopes	Mass content (%)	
		High Pu-fissile [7]	Low Pu-fissile [4]			High Pu-fissile	Low Pu-fissile
U	U235	0.3	0.3	MA	Np237	49.1	16.9
	U238	99.7	99.8		Am241	30.0	60.6
Pu	Pu238	0.0	3.6		Am242m	0.1	0.2
	Pu239	58.0	47.4		Am243	15.5	15.7
	Pu240	24.0	29.7		Cm242	0.0	0.0
	Pu241	14.0	8.2		Cm243	0.1	0.1
	Pu242	4.0	10.4		Cm244	5.0	5.1
	Am241	0.0	0.8		Cm245	0.3	1.3
					Cm246	0.0	0.1

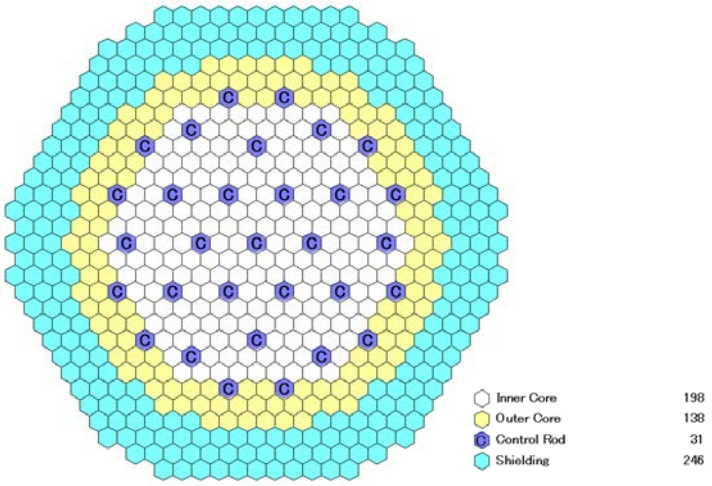

FIG. 1. Core Layout of APC[3],[4],[6]

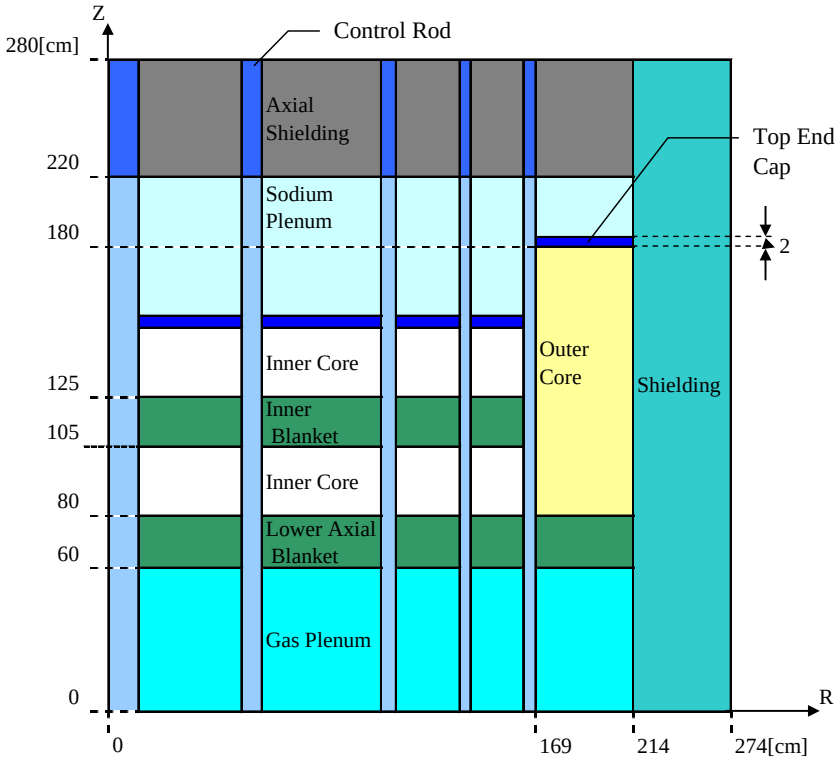

FIG. 2. Typical RZ Geometry of APC [3],[4]

3. Evaluation Results

Adding MA in core affects sodium void reactivity and burnup reactivity. Generally, sodium void reactivity increases and burnup reactivity decreases by MA. Before evaluating MA burning, influence to void reactivity and burnup reactivity by core geometries is surveyed, and the reference core of APC without MA is determined. Here, inner core height region, especially upper inner core region, is determined as a parameter of core geometry because neutron flux in upper inner core strongly affects these reactivities. Outer core height is not changed this for surveying.

Inner core height (IC) and sodium plenum length are changed, keeping lower inner core and inner blanket thickness. Others are same geometries written in Table 1 and Fig. 2. Sodium void reactivity is evaluated in EOEC and assumed as void condition in inner core and outer core, blanket, and sodium plenum regions. Burnup reactivity is evaluated in equilibrium cycle. Low Pu-fissile composition is used in this parameter survey.

Table 3 and Fig. 3 shows these results. Sodium void reactivity decreases along lowering inner core height because neutron leakage from upper inner core increases. This is because sodium plenum is used as reflector in normal condition and neutron leaks to sodium plenum region in sodium void condition. Sodium void reactivity becomes less than zero from IC=80cm. On the other hand, burnup reactivity increases along lowering inner core height.

Cases of IC=60 and 70cm are negative for sodium void reactivity. The value of IC=60cm is larger than one of IC=70cm however difference of these sodium void reactivity is about 0.001dk/kk'. Difference of burnup reactivity is about 0.4%δρ. Maximum power density in case of IC=70cm is smaller. In this paper, IC=70cm is selected as reference core of this study.

Table 3. Core Characteristics of Each Inner Core Height

	Inner Core Height [cm]			
	60	70	80	90
Pu Enrichment [%]	23.9	22.7	20.9	19.3
Max. Power Density [W/cc]	380	352	304	309
Sodium void Reactivity [dk/kk']	-0.0077	-0.0063	-0.0028	0.0094
Burnup Reactivity [%δρ]	2.22	1.82	1.16	0.67

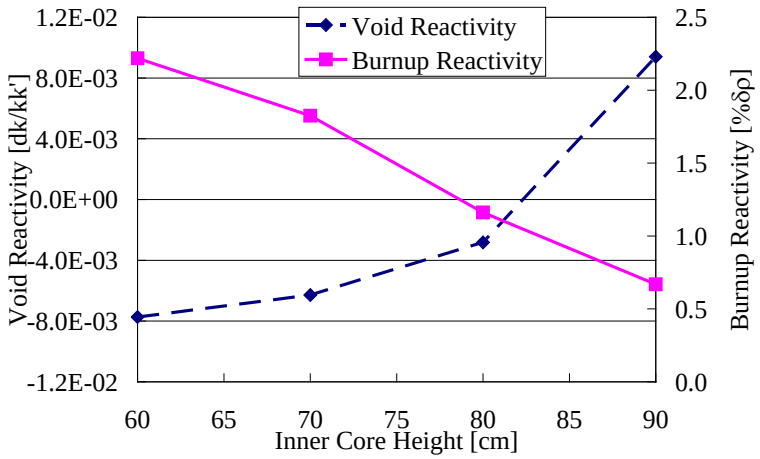

FIG. 3. Sodium Void Reactivity and Burnup Reactivity Changes vs. Inner Core Height

Sodium void reactivity and burnup reactivity changes are evalated in case of MA loaded to inner blanket of reference core. Here, three MA fractions (20, 30, 35%) are used. Figure 4 shows these results using high and low Pu-fissile compositions. In case of high Pu-fissile composition, sodium void reactivity becomes negative around 25% of MA fraction, however, in case of low Pu-fissile composition, sodium void reactivity is positive in all cases.On the other hand, burnup reactivity decreases along increasing MA fraction. This is because of fission reaction of Pu238 and Am242m by capture reaction of Np237 and Am241 respectively.

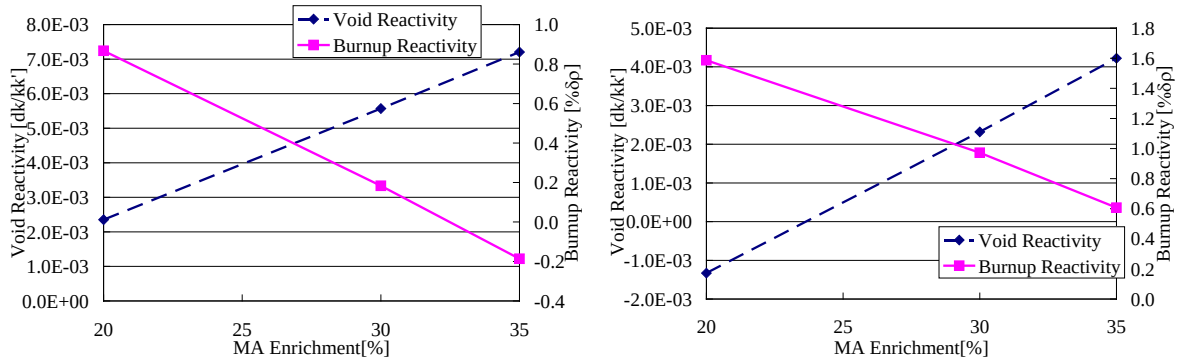

FIG. 4. Sodium void reactivity and Burnup Reactivity Changes (Left: Low Pu-fissile Right: High Pu-fissile)

Table 4 and 5 shows mass balance in low and high Pu-fissile compositions, respectively. In case of no MA to inner blanket, amount of MA increases 300% by produced MA during operation. In case of MA loaded to inner blanket, amount of MA especially Np237 and Am241 decreases. More MA in inner blanket is effectively burnt. By low Pu-fissile composition, a burnt MA fraction hardly changes with high Pu-fissile composition. Figure 5 shows power density distribution of axial direction on central of core. If MA fraction is larger, power density in inner blanket increases because fissile materials increase in the region.

Table 4. Mass Balance (Low Pu-fissile composition, IC=70cm)

Isotopes	No MA		20%		30%		35%	
	Load(kg)	Unload(kg)	Load	Unload	Load	Unload	Load	Unload
Np237	0	15	229	135	345	194	403	222
Np Total	0	15	229	135	345	194	403	222
Am241	66	127	900	520	1321	710	1532	797
Am242m	0	6	3	33	5	46	6	53
Am243	0	87	218	204	329	261	385	288
Am Total	66	219	1122	757	1655	1018	1923	1138
Cm242	0	6	0	26	0	36	0	41
Cm243	0	0	1	3	1	4	1	4
Cm244	0	21	72	120	108	168	126	191
Cm245	0	1	18	18	27	27	31	31
Cm246	0	0	1	4	2	5	2	6
Cm Total	0	29	92	171	138	239	162	273
MA Total	66	263	1442	1064	2138	1451	2487	1633
Burnt MA Fraction [%]	-296.0		26.2		32.1		34.4	

Table 5. Mass Balance (High Pu-fissile composition, IC=70cm)

Isotopes	20%		30%		35%	
	Load(kg)	Unload(kg)	Load	Unload	Load	Unload
Np237	670	368	1008	547	1179	632
Np Total	670	368	1008	547	1179	632
Am241	415	313	626	409	732	455
Am242m	1	18	2	25	2	28
Am243	217	151	326	210	382	238
Am Total	633	483	954	644	1116	721
Cm242	0	15	0	20	0	23
Cm243	1	1	1	2	1	2
Cm244	70	107	106	154	123	177
Cm245	4	14	6	20	6	23
Cm246	0	1	0	2	0	2
Cm Total	74	138	112	198	131	227
MA Total	1377	989	2075	1389	2426	1580
Burnt MA Fraction [%]	28.2		33.1		34.9	

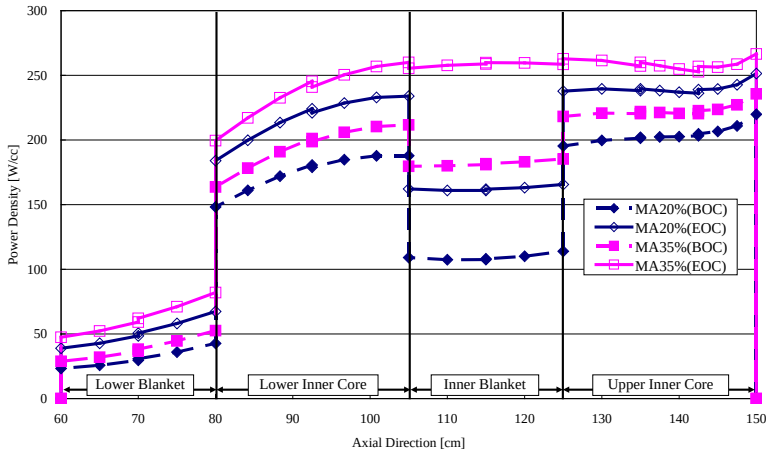

FIG. 5. Power Density Distribution on Central of Core (MA20%, 35%)

In case of low Pu-fissile composition, sodium void reactivity is positive in all cases. Here, a position of inner blanket moves to lower position for achieving negative void reactivity because neutron flux becomes large by heightening upper inner core and the leakage becomes also large. Figure 6 shows comparison of sodium void reactivity and burnup reactivity between normal position and inner blanket 10cm down position. Thus, sodium void reactivity becomes zero around MA fraction 25%.

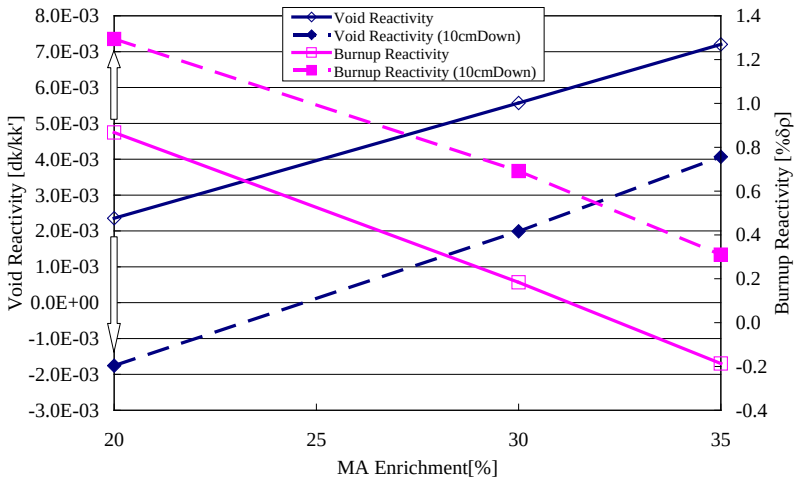

FIG. 6. Sodium void Reactivity and Burnup Reactivity Changes in Different Inner Blanket Positions

Table 6 shows MA mass balance comparison of the reference position and inner blanket 10cm down. Amount of burnt MA in both cases are close. Figure 7 shows power density distribution in both cases. Power distribution becomes large when an inner blanket is down.

Table.7 shows core characteristics of each MA fraction. Sodium void reactivity decreases by inner blanket 10cm down and becomes negative in case of 20% MA fraction. Breeding gain keeps positive in all cases.

Table 6. Mass Balance of MA (20%) in Each Inner Blanket Positions (Low Pu-fissile composition)

Isotopes	Reference		IB 10cm Down	
	Load(kg)	Unload(kg)	Load	Unload
Np237	229	135	229	140
Np Total	229	135	229	140
Am241	900	520	900	536
Am242m	3	33	3	33
Am243	218	204	218	209
Am Total	1122	757	1121	778
Cm242	0	26	0	26
Cm243	1	3	1	3
Cm244	72	120	72	120
Cm245	18	18	18	18
Cm246	1	4	1	4
Cm Total	92	171	92	171
MA Total	1442	1064	1442	1089
Burnt MA Fraction [%]	26.2		24.5	

Table 7. Core Characteristics of Each MA Fraction (IC=70cm, Low Pu-fissile)

	MA Fraction [%]			
	0	20*	30*	35*
Pu Enrichment [%]	22.7	21.7	21	20.5
Ave. Power Density [W/cc]**	235	227	220	216
Max. Power Density [W/cc]	352	332	318	337
Breeding Ratio	1.01	1.02	1.03	1.05
Burnt MA Fraction [%]	-296	26.2	30.1	32.3
Sodium void Reactivity [dk/kk']	-0.0063	-0.0018	0.0020	0.0041
Burnup Reactivity [%δρ]	1.82	1.29	0.69	0.31

* Position of inner blanket 10cm down

** Core only, BOC

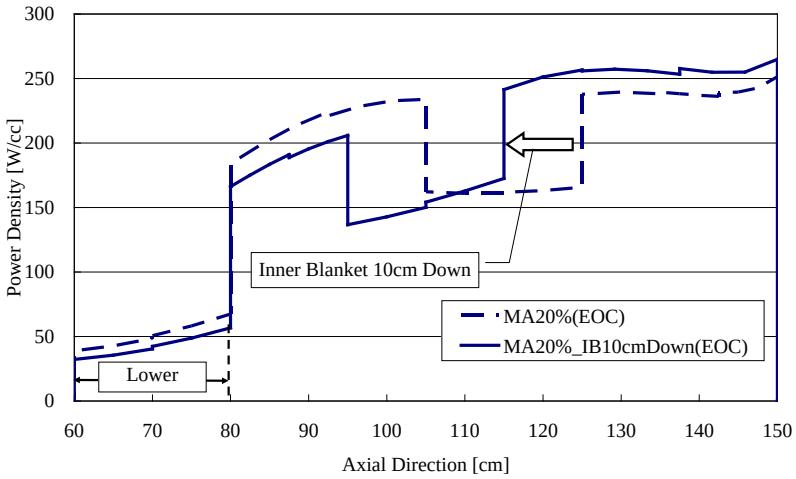

FIG. 7. Power Density Distribution on Central of Core (Normal, IB 10cm Down)

4. Conclusion

Fast spectrum reactor core which has high safety feature and high efficient MA recycle are discussed based on the APC concept for environmental harmonization.

As the conclusion, at first, it is clarified that negative sodium void reactivity can be achieved by 70cm of inner core height for the APC without MA. Regarding MA loaded core, about 25% MA can be

loaded while keeping negative sodium void reactivity and low burnup reactivity for the high Pu-fissile composition case. In case of the low Pu-fissile composition case, also 25% MA can be loaded with keeping the similar core characteristics such as sodium void reactivity by lowering inner blanket position. Thus, the APC for high efficient MA burning with low sodium void reactivity and burnup reactivity has been confirmed.

In this paper, MA fraction and inner core height are used as parameters for the survey. However, there are many other points to be evaluated. For example, core radius and height of inner blanket have to be also evaluated. Additionally, MA is loaded to only inner blanket in this paper and homogeneous loading in core has to be considered for more burning MA and increasing safety characteristics. Heterogeneous effect of sodium plenum has to be discussed because sodium plenum is treated as homogeneous in this paper and heterogeneous effect may be large. Not only core characteristics but also manufacturability of fuel assembly for high MA content fuel, fuel performances, how to control criticality using control rod, and so on, have to be discussed. In future, those items will be evaluated to investigate more preferred core.

REFERENCES

[1] T. Kamei et. al., “An Axially and Radially Two-Zoned Large Liquid-Metal Fast Breeder Reactor Core Concept”, Nucl. Technol., **71**, pp.548-556 (1985)

[2] M. Kawashima and Y. Moriki, “An Evaluation of Minor Actinide Transmutation Capability in a Large APC Fast Breeder Core”, Proceeding of International Conference on Design and Safety of Advanced Nuclear Power Plant (ANP’92) (1992)

[3] T. Yokoyama et. al., “A Study on Reactivity Insertion Controlled LMR Cores With Metallic Fuel”, Prog. In Nucl. Energy, **47**, pp.251-259 (2005)

[4] L. Buiron et. al., “Transmutation Abilities of the SFR low void effect core concept “CFV” 3600MWth”, Proc. of ICAPP’12, 12029 (2012)

[5] P. Sciora, et. al., “Low void effect core design applied on 2400 MWth SFR reactor”, Proc. of ICAPP’11, 11048 (2011)

[6] B. Fontaine, et. al., “The French R&D on SFR core design and ASTRD Project”, Proc. of GLOBAL 2011, 432757 (2011)

[7] T. Wakabayashi, “Study on Minor Actinide Transmutation in a Fast Reactor, Summary of Core Study”, PNC TN9410 93-226 (1993)

[8] OECD-NEA, “Calculations of Different Transmutation Concepts, An International Benchmark Exercise”, (2000)

[9] R. E. Alcoffe, et. al., “User’s Guide for TWODANT: A Code Package for Two-Dimensional, Diffusion-Accelerated, Neutral-Particle, Transport”, LA-10049-M, Los Alamos National laboratory, (1990)

[10] M. Nakagawa, et. al., “A Code for Cell Homogenization of Fast Reactor”, JAERI 1294 (1984)

[11] K. Shibata, et. al., “Japanese Evaluated Nuclear Data library Version 3 Revision-3: JENDL-3.3”, J. Nucl. Sci. Technol. Vol. 39. [11], 1125 (2002)

Neutron and gamma flux characterization in a pool-type SFR vessel with Monte Carlo codes

Nicolas Chapoutier[a], Marie Charlotte Ricol[a], Sylvain Boulley[a], Christian Jammes[b]

[a] AREVA NP, 10-12 rue Juliette Recamier, 69456 Lyon, France

[b] CEA, DEN, DER, Instrumentation, Sensors and Dosimetry Laboratory, Cadarache

Abstract. In the case of a pool-type Sodium-cooled Fast Reactor, neutron and gamma flux calculations are performed in order to optimize the design of the neutron shielding surrounding the core, select the best locations for in-vessel neutron flux monitoring, and assess absorbed doses for equipment qualification. Particles propagation is conducted over wide range of distance with several decades of attenuation and along multiple particle pathways. Monte Carlo method is used for these calculations: TRIPOLI and MCNP models are implemented to deal with these propagation cases. Adequate biasing methods are needed to reach statistical convergence. The neutron and gamma flux are assessed at different power stages: full power, partial power and shutdown phases and taking into account appropriate source terms (core, gamma induced neutron, activated coolant and structures, etc…).

1. Introduction

In France a coordinated R&D program [1] on Sodium-cooled Fast Reactor (SFR) technology has been launched in 2006 by CEA, AREVA and EDF. The technical program is consistent with the Gen IV International Forum guidelines. That future advanced SFR prototype was named ASTRID: Advanced Sodium Technological Reactor for Industrial Demonstration. In the frame of the pre-design of the ASTRID vessel, extensive neutron and gamma flux calculations are performed in order to answer to several engineering needs of the projects. Monte Carlo method is used for these calculations. The topics which are dealt with are:

- The design of neutron shielding surrounding the core,
- The assessment of absorbed doses for the qualification of sensors and equipment dedicated to the In Service Inspection and Repair (ISIR),
- The design of the core monitoring system.

2. Computational models

Particles propagation is conducted over wide range of distance with several decades of attenuation and along multiple particle pathways. Monte Carlo method is used for these calculations: TRIPOLI [2] and MCNP [3] models are implemented to study these propagation cases.

The key factors of success for the calculations are: fine geometrical modeling, detailed source terms (in power and shutdown states), and the ability to master the variance reduction techniques of the calculations codes.

The core and its near components in the vessel are modeled. The heterogeneous characteristics of the core are taken into account: radial reflector, upper and radial neutron shielding. Equipments like Rotating Core Plug (RCP), Primary Pump (PP) and Internal Heat Exchanger (IHX) are also modeled.

The source term is calculated by different codes depending on the cases. During power operation the neutron source from the core is calculated with the deterministic code ERANOS [4] developed by the CEA. The 3D power shape and the total neutron intensity of the core are imposed in the Monte Carlo models in order to run propagation of sources calculations. Shutdown states need specific models because of the sub-critical conditions. A sequence of calculations with ERANOS and the evolution code DARWIN-PEPIN [5] generates the source term of spent fuel assemblies (spontaneous fission and alpha-n reaction) and their isotopic composition as well. Those data are used as inputs for the Monte Carlo calculations in shutdown states. Other source terms are taken into account depending on what is studied: primary coolant activation, structures activation, etc…

Adequate biasing methods are needed to reach statistical convergence in areas of interest, e.g.: source is biased in order to propagate more particularly fast neutrons generated from peripheral assemblies in the vicinity of the areas of interest. The stochastic behavior of neutrons propagation in matter is also biased with specific options which are enabled in the codes: *Weight Windows* and *exponential transform* for MCNP or *Ponderation* for TRIPOLI.

3. Focus on applications

3.1.Design of neutron shielding

The design of the neutron shielding surrounding the core has a direct impact on:

- The neutron activation of the secondary coolant,
- The damages and the Helium production rate on structural equipments,
- The neutron activation of components (this leads to the minimization of shielding requirements for exceptional handling).

Several types of materials are studied to reach to the best configuration with alternatively moderators and absorbers assemblies. A benchmark between the French Monte Carlo code from CEA: TRIPOLI and MCNP is performed, resulting in a good accordance between the two codes.

3.2.ISIR – Dose assessment for sensors and equipment

Both gamma and neutron calculations are performed regarding the qualification of sensors and equipments. The absorbed doses are assessed at different power stages: full power, partial power and shutdown phases. The appropriate source terms (core, gamma induced neutron, activated coolant and structures, etc…) is taken into account. An overview of the kind of calculations performed is given in the following figure. This figure illustrates on the right the neutron flux calculated from the core to the outside of the vessel. On the left, the layout drawing is juxtaposed. The order of magnitude of neutron flux varies from 1E+15n/cm²/s to few decades. Independent calculations with appropriate variance

reduction techniques are needed in each area of interest to reach statistical criteria after a dozen hours of calculation.

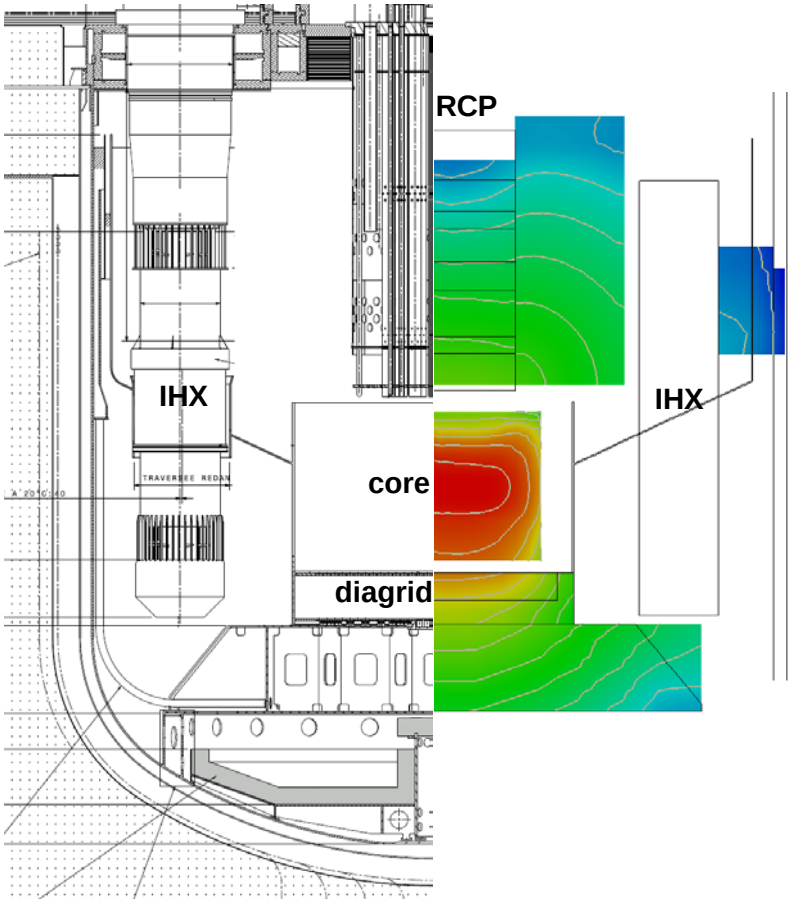

FIG. 1. In-vessel Neutron flux mapping during power operation

3.3.Design of core monitoring system

Several locations are considered to implement the High Temperature Fission Chamber (HTFC) in the vessel. One criterion for the selection of these locations is the capability to detect local deviations. Two accidents are studied: the refueling errors during shutdown and the unprotected accidental control rod withdrawal (ACRW) during power operation.

The study of refueling errors is performed with the shutdown state model. Deviations of detectors response are calculated in case of several control rods withdrawal or the replacement of a control rod by a fresh fuel assembly.

The capability to detect ACRW is assessed in every location foreseen by comparing fission rates between normal operation and ACRW states.

Each potential control rod withdrawal is calculated with ERANOS to generate tilted 3D power shapes. The MCNP model of the 3D power shape is fine enough to be able to fit with the variations of the core source.

The calculations show that the deviations of fission rates are significant during ACRW. Those calculations foreshadow the definition of reactor trip criteria to prevent ACRW. The following figure illustrates calculations of tilted flux induced in the first grid of RCP by ACRW.

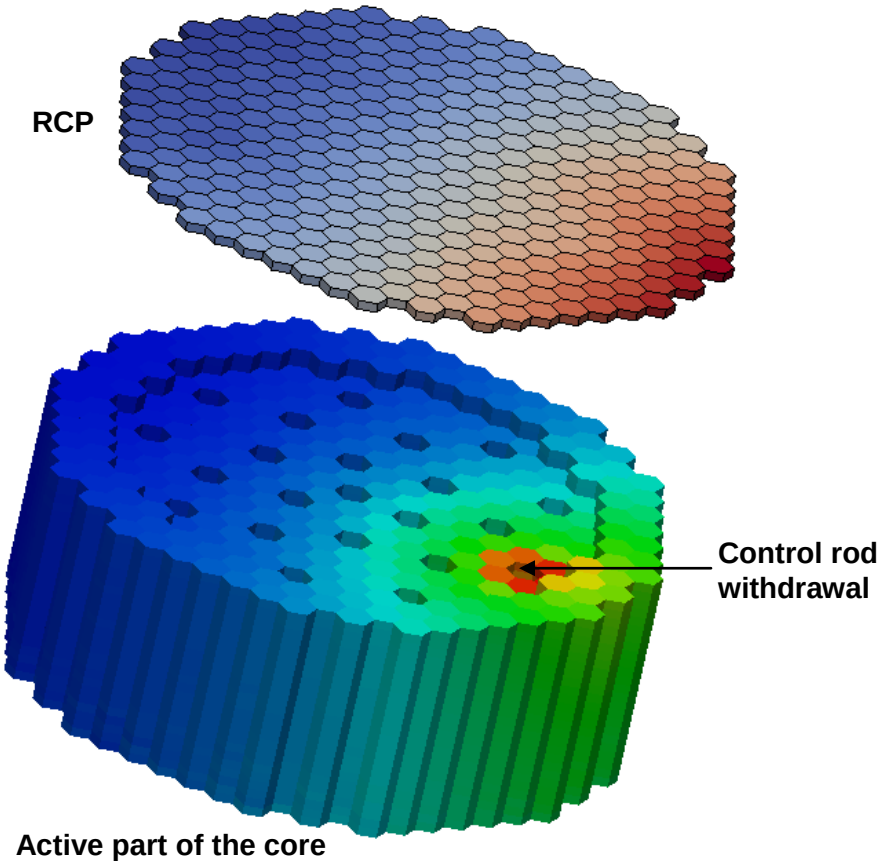

FIG. 2. Variation of neutron flux in RCP 1st grid due to power shape tilt induced by ACRW

REFERENCES

[1] MARTIN, Ph., et al., “French Program Towards An Innovative Sodium-Cooled Fast Reactor”, ICAPP’2007, Nice, France

[2] J.-P. Both et al. Tripoli4 - A three dimensional polykinetic particle transport Monte Carlo code. In SNA’2003, Paris, France, 2003

[3] F. B. Brown, et al. "MCNP5-1.51 Release Notes," LA-UR-09-00384, Los Alamos National Laboratory, 2009

[4] G. Rimpault et al., “The ERANOS code and data system for fast reactor neutronic analyses”, Proceedings of the International Conference on the Physics of Reactors, PHYSOR 2002, Seoul, Korea, October 7-10 (2002)

[5] A. TSILANIZARA et al, « DARWIN: an evolution code system for a large range of applications », Journal of Nuclear Science and Technology. Supplement 1 p 845 - 849. March 2000

Petri Net approach for a Lead-cooled Fast Reactor startup design

R. Ponciroli, S. Lorenzi, A. Cammi, L. Luzzi

CeSNEF Nuclear Division, Department of Energy, Politecnico di Milano, Milano, Italy

Presented by R. Ponciroli

Abstract. A preliminary approach to the development of the startup mode design for the Advanced Lead Fast Reactor European Demonstrator (ALFRED) currently under development within the European FP7 LEADER (Lead-cooled European Advanced Demonstration Reactor) Project has been undertaken. The reactor startup is the operational mode in which all the operating systems of the plant are brought from the *cold shutdown condition* to the full power operating status, close to power-frequency control. In this phase, the working conditions radically change and it is fundamental that the several control actions are properly coordinated. These aspects deserve a particular attention in a new generation reactor, whose management is not fully defined and for which the control strategy has to be finalized. In the development of the ALFRED reactor control system, it is then necessary to provide an adequate formalization of the sequence of the several control actions to be performed. For this purpose, Petri net approach has been employed in this work, since it represents a useful formalism for the modelling and the analysis of discrete event systems and it allows to identify the events coming from the plant that enable the switches among the several feedback controllers. In the first part of the paper, the issues characterizing the startup mode are described and some solutions to bring the reactor to full power mode (fulfilling the technological constraints) are provided. Finally, the results of the simulations related to the ALFRED output variables and control variables are discussed.

1. INTRODUCTION

The Lead-cooled Fast Reactor (LFR) has been selected by the Generation IV International Forum as one of the candidates for the next generation of nuclear power plants (NPPs) [1]. Advanced reactor concepts cooled by Heavy Liquid Metal (HLM) coolants ensure a great potential for plant simplifications and higher operating efficiencies compared to other coolants [2], introducing however additional safety concerns and design challenges. These features assume a particular relevance when the system operates in very different conditions from the nominal ones, such as during the *reactor startup* [3]. In this work, the development of a suitable startup procedure for the Advanced Lead-cooled Fast Reactor European Demonstrator (ALFRED) is presented. ALFRED is a pool-type, small power reactor [4] conceived to be fully representative of the industrial scale reference system, and thus it is provided with a Balance of Plant (BoP) and envisaged to be connected to the electrical grid.

The term reactor startup refers to the procedure whereby all the operating system (i.e., core, primary circuit, pressurizer, steam generators, turbines, etc.) are brought from a cold shutdown to a hot operating status. In particular, the procedure described in this work deals with the first criticality attainment starting from the first core configuration, taking into account the several control steps to achieve nominal power conditions. Despite the startup sequence of Nuclear Power Plants (NPPs) is a complex process that varies with each plant and combination of selected systems, the need for integrated pressure and temperature controller is a common requirement. Consequently, this first attempt to the definition of a startup procedure for a LFR begins from the experience gained in acknowledged reactor concepts, such as Light Water Reactors (LWRs) and Sodium-cooled Fast Reactors (SFRs), trying to adapt the conventional startup paradigm to the constraints and the needs of ALFRED reactor.

In common practice, the reactor startup procedure is described by defining the initial conditions of the several components of the plant and listing a set of operations that must be performed to bring the system to full power mode. Even though this schematic approach allows to point out the main operations to perform, it does not provide accurate and quantitative information on the regulators that allow to achieve the desired behaviour. In this work, a quantitative representation of this procedure has been carried out by adopting the Petri net modelling tool [5], since it represents a useful formalism for

the modelling and the analysis of discrete event systems. The application of this formalism to describe the procedure of the reactor startup allows to:

- Identify the different steps to be taken and establish the necessary system conditions so that suitable control actions can be performed;
- Verify the possibility to perform two or more operations in parallel in the system, in order to make more efficient the startup sequence;
- Represent the desired evolution of the system in order to obtain hints for the development of the related control system.

The paper is organized as follows. In Section 2, an introduction to the ALFRED reactor is provided and its main features are reported. In Section 3, the main steps to be taken in the startup procedure are described. In Section 4, the formalism of the Petri nets is briefly introduced. Finally, in Section 5, the proposed procedure has been simulated and the obtained results are reported and discussed.

2. REFERENCE REACTOR DESCRIPTION

The Advanced Lead Fast Reactor European Demonstrator (ALFRED) currently under development within the European FP7 LEADER (Lead-cooled European Advanced Demonstration Reactor) Project has been undertaken as reference reactor [4]. ALFRED is a small-size pool-type LFR. In Fig. 1, the current configuration of primary system is depicted. All the major reactor primary system components, including core [6], primary pumps and Steam Generators (SGs), are contained within the reactor vessel, being located in a large lead pool inside the reactor tank. The coolant flow coming from the cold pool enters the core and, once passed through the latter, is collected in a volume (hot collector) to be distributed to eight parallel pipes and delivered to as many SGs. After leaving the SGs, the coolant enters the cold pool through the cold leg and returns to the core. In Table 1, the major parameters of the system are resumed.

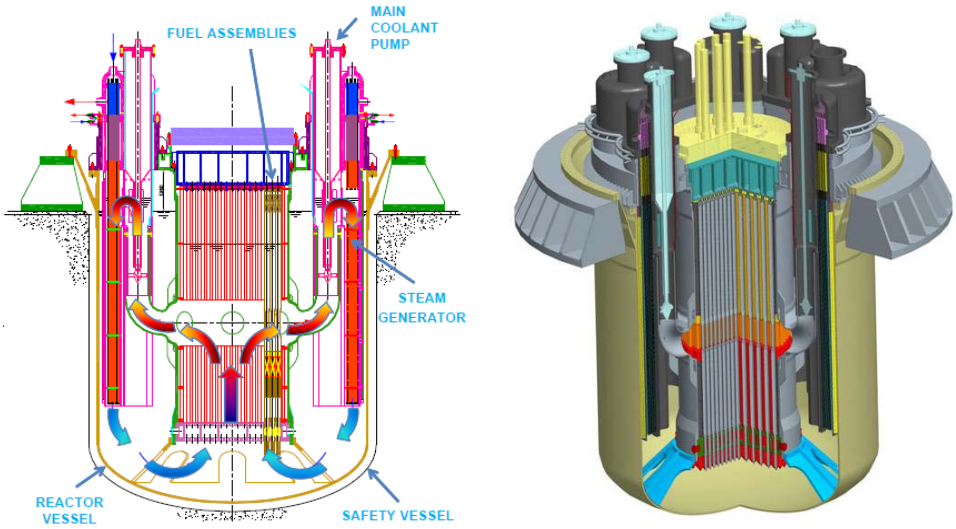

FIG. 1. ALFRED primary system and core layouts [4].

Table 1. ALFRED system parameters.

Parameter	Value	Units
Thermal power	300	MW_{th}
Coolant mass flow rate	25984	$kg \cdot s^{-1}$
Coolant core inlet temperature	400	°C
Coolant core outlet temperature	480	°C
Pool temperature during cold shutdown	380	°C
Feedwater mass flow rate	192	$kg \cdot s^{-1}$
Water inlet temperature	335	°C
Steam outlet temperature	450	°C
SG pressure	180	bar

3. STARTUP PROCEDURE DEFINITION

In order to simulate the entire operational sequence, a non-linear one-dimensional model of ALFRED has been developed by adopting an object-oriented approach [7] based on the Modelica language, realized in the Dymola environment [8]. In Fig. 2, the layout of the model is represented to point out the main components of the plant and the respective control variable (blue triangles) and outlet variables (white triangles).

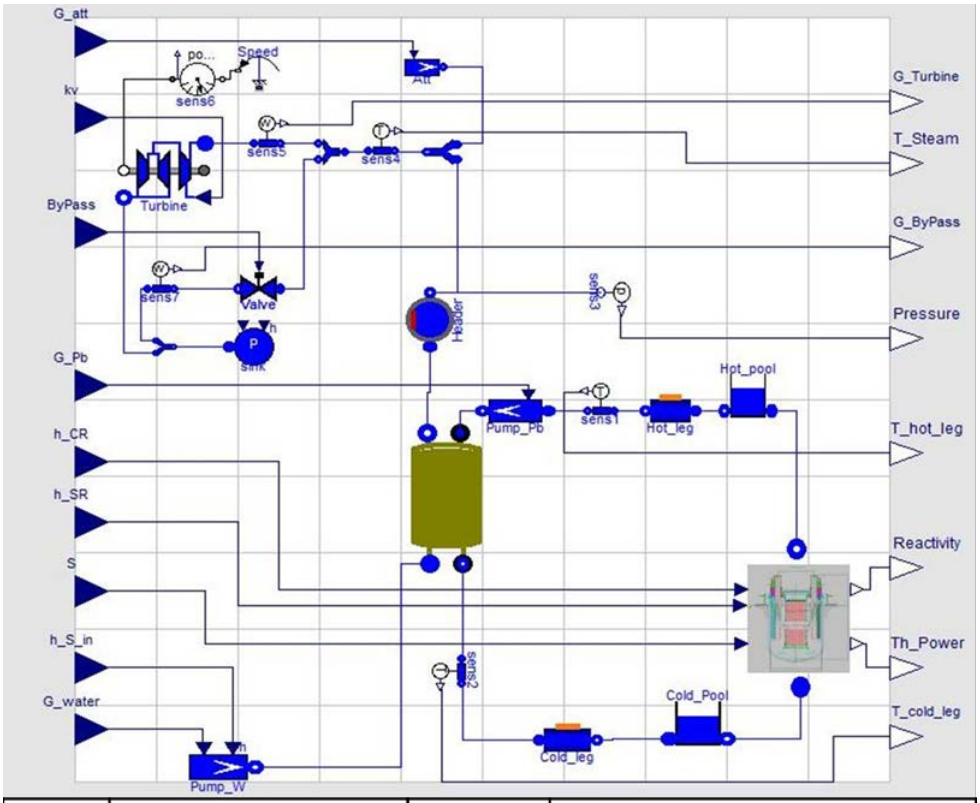

Input	Definition	Output	Definition
G_att	Attemperator mass flow rate	*G_Turbine*	Turbine admitted mass flow rate
Kv	Turbine valve coefficient	*T_Steam*	Turbine inlet steam temperature
Bypass	Bypass valve coefficient	*G_Bypass*	Bypass discharged mass flow rate
G_Pb	Lead mass flow rate	*Pressure*	SG pressure
h_CR	Control rod height	*T_hot_leg*	Temperature of lead flowing out the core
h_SR	Safety rod height	*Reactivity*	Multiplying system reactivity
S	Neutron source	*Th_Power*	Thermal power produced within the core
h_S_in	Feedwater inlet enthalpy	*T_cold_leg*	Temperature of lead flowing into the core
G_water	Feedwater mass flow rate		

FIG. 2. Model of the ALFRED plant.

The system simulator has been realized by connecting several dedicated models (see Ref. [9] for details):

- *Core model*: it is composed by three subsystems. The model *Kinetics* describes the dynamics of the neutron generation processes in the core implementing a point reactor kinetic model, with one neutron energy group and six delayed precursor groups. The coupling between neutronics and thermal-hydraulics is achieved by means of the reactivity feedbacks. The model *FuelRods* is adopted to represent the thermal behaviour of the fuel pins, which are discretized in five radial regions (i.e., the cladding, the gap and three concentric zones within the pellet). The model *LeadTube* represents the coolant flowing through the core channels adopting one-dimensional mass, momentum and energy conservation equations.
- *SG Model*: as far as the water side is concerned, a two-phases homogeneous model (i.e., same velocity for the liquid and vapour phases), has been adopted. On the lead side, the core component *LeadTube* is reused, describing the behaviour of a single-phase fluid.

- *Primary model*: the dynamics effects of the coolant cold pool have been represented by employing a free-surface cylindrical tank component on which mass and energy balances are taken into account, assuming that no heat transfer occurs except through the inlet and outlet flows. In order to consider the time delay due to the transport phenomena between the core and the SG, two dedicated models have been implemented. As far as the integrated primary pump is concerned, an ideal mass flow rate regulator has been employed.
- *Secondary side model*: the component selected for the turbine model describes a simplified steam turbine unit, in which a fraction of the available enthalpy drop is assumed to be converted by the High Pressure (HP) stage, while the remaining part to be converted by the Low Pressure (LP) one, with different time constants. The steam mass flow rate is considered proportional to the inlet pressure and governed by operating on the turbine valve admission (k_v), not by throttling. Downstream of the steam temperature sensor, the steam mass flow rate can follow two ways. The former is a pipe that leads to the turbine, whereas the latter constitutes a bypass, which leads directly to the condenser. Thanks to the adoption of a bypass, it is possible to employ this model to simulate the startup phase. Indeed, when the thermal power from the primary circuit is not sufficient to ensure the steam nominal conditions, the flow is directly disposed to the condenser to avoid jeopardizing the integrity of the turbine.

3.1. ISSUES AND CANDIDATE PROCEDURE

In the development of the reactor startup procedure, the sequence of operations to be performed and their synchronization are fundamentally determined by the fulfilment of certain technological constraints. As far as the LFRs are concerned, the most challenging issue regards the lead temperature in the cold pool. Besides the lower limit fixed by the coolant solidification (327°C), the lead temperature in the cold pool has to be set in a narrow range. In particular, the vessel temperature should not exceed 420°C (limit due to thermal creep issues), whereas the minimum temperature is fixed at 380°C due to the embrittlement of the structural materials enhanced by the fast neutron irradiation. Another troublesome aspect concerns the coupling between the primary and the secondary circuit during the startup and the role played by the latter in this initial phase. For LFRs, this aspect turns out to be more challenging than in other ones. The use of in-vessel heaters, which can control the lead temperature in the cold pool, may be useful for this purpose but their adoption in a such aggressive environment may be hazardous. The alternative solution adopted in this work is the use of an *auxiliary system* that feeds the SG with a reduced overheated steam mass flow rate, preventing lead from freezing at the interface between the primary and secondary systems. Since the pool temperature in cold shutdown is around 380°C, the water inlet temperature has to be fixed at 380°C and 180 bar (nominal pressure) when the auxiliary system is used. After having achieved the criticality condition and having reached a certain level of power, the feedwater inlet temperature is gradually reduced to 335°C. In this case, the control system has to deal with the problem of switching the SGs operational condition from the auxiliary mode to the normal one. Hence, the inlet conditions at secondary side are not modified anymore, the auxiliary system is switched off and the secondary system begins to operate in normal mode, according to the full power scheme. The advantage of this solution is using water flows, temperatures and pressures which are close to the nominal ones, becoming easier to perform the switch. As far as the following power rise is concerned, the procedure is quite similar to the one followed in acknowledged reactor concept extracting the absorber rods to achieve criticality. In ALFRED, two different, independent and redundant systems are envisaged to control the reactivity. The Safety Rods (SRs) are dedicated only to shutdown the system, whereas the Control Rods (CRs) are devoted both to shutdown and to control the reactor power level. However, before this stage, a suitable neutron source is inserted within the core to initiate the chain reaction and to monitor the neutron flux, which may be so low as not be detectable. Indeed, even small movements of the control rods can determine large reactivity insertion, i.e., the power can rise to unacceptable levels which compromise the integrity of the reactor before the safety systems may operate. At this point, once attained criticality, the reactor power level can rise and, after the power has reached 20% of the nominal value, the control system switches to the full power mode, which allows to get the operating nominal conditions. As far as the overall plant behaviour simulation is concerned, the initial conditions are such that the primary circuit is already filled with the molten lead at cold shutdown temperature,

whereas the secondary system turns out to be already pressurized at the nominal value and the feedwater inlet temperature is equal to 380°C. On the other hand, the previous stage of the reactor startup requires the filling of the vessel with the molten lead and the verification of the operating conditions of the several devices in the primary circuit. Afterwards, it is necessary to pressurize the secondary circuit avoiding overcooling concerns. At this stage of the reactor conceptual design, these operations have not been fully characterized.

3.2. SYSTEM EVOLUTION DURING REACTOR STARTUP

Before describing the modelling tool adopted to represent the candidate procedure, the system *desired behaviour* during the first startup is described. An ordered sequence of the control that has to be performed to bring the reactor up to full power mode in critical condition has been defined, ensuring the compliance with the technological constraints related to the safety of the system. In Table 2, the different phases of the startup procedure are reported. Due to the control-oriented purpose of this paper, the commissioning tests to be performed before core loading and at zero power conditions are not explicitly taken into account. These aspects and safety calculations will be analysed and performed at a later stage.

Table 2. Different phases of the startup procedure and respective descriptions.

System state	State Description
M0	The primary circuit filled with lead is kept at 380°C (cold shutdown conditions). Primary pumps are switched off. The secondary system is pressurized at 180 bar, the temperature of the feedwater at the SG inlet is equal to 380°C and a reduced water mass flow rate is circulating (20%). These conditions are necessary to avoid local lead solidification.
M1	At the beginning, the core is constituted entirely by dummy elements in order to test the primary circuit devices in the filled vessel configuration. The loading of the core with fuel assemblies (FAs) is gradually performed. First of all, the neutron source is inserted in order to monitor the neutron flux. Afterwards, most of the dummy elements are replaced with the fuel assemblies in order to get the BoL (Beginning of Life) configuration.
M2	Once obtained the BoL configuration, the pumps achieve the nominal operational condition.
M3	The SRs are slightly extracted in order to reduce the subcritical level of the reactor.
M4	The CRs are extracted in order to achieve the criticality. Then, a power ramp from 0 to 0.1 MW_{th} is given.
M5	When the core reaches 0.1 MW_{th}, the feedwater inlet temperature is lowered to bring it gradually up to 335°C.
M6	Once the feedwater inlet temperature reaches the nominal condition (i.e., 335°C), it is no longer modified and a suitable controller to keep it constant is adopted. In the meantime, the power continues to rise up to 60 MW_{th}.
M7	Once the thermal power produced in the core reaches 60 MW_{th}, the water mass flow rate that circulates in the secondary circuit is updated by using a mixed control feedforward-feedback. The feedforward is necessary to gradually increase the mass flow rate in a programmed way until the nominal conditions are reached, whereas the feedback loop is used to govern the lead temperature in the cold leg. Up to this moment, the SG pressure has been controlled by using the bypass valve. At this point, since the steam quality at the SG outlet is good enough to be admitted in the steam turbine, the bypass valve is gradually closed in accordance with a user-defined ramp, whereas the turbine admission valve begins to be opened allowing steam to flow into the turbine. Henceforth, the secondary side pressure is governed by using a Proportional-Integral (PI) controller on the turbine inlet valve.
M8	On the secondary side, once the bypass valve is completely closed, the steam mass flow rate flows entirely in the turbine, and the flow of the circulating water is continuously updated according to the adopted control scheme. CRs are progressively extracted up to reach nominal power conditions. At this point, an attemperator is employed to control the condition of the steam temperature at the turbine inlet.

4. ALFRED STARTUP FORMALIZATION

In the perspective of developing the ALFRED reactor control system, it is necessary to provide an adequate formalization of the sequence of the several control actions to be performed during the startup phase. In this way, once having rigorously defined the desired behaviour that the system has to follow, designing and developing the startup mode for the control system can be straightforwardly achieved. The most diffused mathematical models for such kind of problems are the *Discrete Event Systems* (DES) [10], in which the state changes when certain events and operating conditions take place. In the following section, a brief introduction of DES is given.

4.1. STARTUP: A DISCRETE EVENTS SYSTEM

In the representation of the startup procedure as a Discrete Event System, the state of the system is characterized by discrete variables that change value in an asynchronous way correspondently to the occurrence of certain “events”. In spite of the apparent simplicity of these systems (e.g., the state variables assume only discrete values, the time variable is not explicitly modelled, etc.), the study of DES is made complicated by some issues. In particular:

- *Dimension*: a considerable number of states and transitions must be managed, also in case of elementary systems. In order to properly describe industrial processes with DES models, it is necessary to adopt formal tools, following a rigorous approach.
- *Representation*: there is no convergence on the standards of representation and manipulation of DES, because of the wide field of applications and needs. Moreover, DES constitute an abstraction of physical systems that does not necessarily derive from first principles of mass, energy and momentum conservation. For these reasons, it is possible to derive for the same plant very different models, according to the controlling and simulating requirements.
- *Definition of the control problem*: unlike time-dependent control systems, in the control of DES it is not possible to define neither set-points nor parameters that allow to quantify the desired behaviour of the closed-loop system. On the other hand, the desired behaviour (indicated with Σ) is usually specified in terms of DES and represents a specified sequence of discrete states that allows to reach the established final state. Since a not-controlled system could evolve reaching not-acceptable states and operating conditions, Σ constitutes a restriction of the dynamic behaviour of the system. Therefore, the controller can be seen as a set of rules and constraints, which can be obtained from Σ and the initial state of the system itself.

4.2. PETRI NET CONCEPT

In this work, the quantitative description of the ALFRED startup procedure has been studied by adopting the Petri net, which constitutes a useful formalism for the modelling of the DES dynamic behaviour and control, with particular attention to the description of causal relationships between events [11]. Petri net has been proposed as a tool for formal modelling useful both to eliminate any source of ambiguity in the representation and to perform analysis and verification on the system behaviour. In addition, it is characterized by an intuitive graphical representation, which makes it easy to be used, besides representing a significant extension of the concept of automaton [12]. The Petri net, compared with an automaton, can be considered as a distributed system in which the overall state is composed of multiple states related to partial and independent subnets. In this way, it is possible to represent the occurrence of two independent events through two net transitions that can *fire* in a "competitor" way, whereas in the finite-state automaton [12] possible state transitions are mutually exclusive to each other. A *net* is characterized by a set of *places*, *transitions* and the connections between them, namely the *flow relations*, which are the set of ordered couples of places and transitions allowed, for example (p_1,t_1) or (t_1,p_3). The elements of the flow relations represent the characteristic structural links that rule the system evolution. The net can be graphically represented using a *bipartite graph* (Fig. 3), in which there are two distinct kinds of nodes (places and transitions) connected by oriented arcs that indicate the existing flow relations.

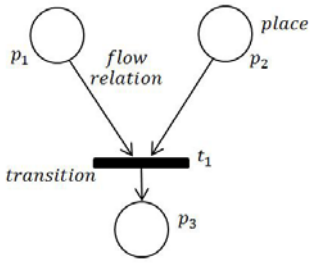

FIG. 3. Graphical representation of net elements.

Starting from these "static" definitions, several "dynamic" models have been proposed, which allow to describe the dynamic evolution of the net. The provided definitions refer to the topological aspects of a net, which are necessary to represent the structural links among its elements.
In a Petri net, the places represent the partial state of the system, which is identified by integer numerical values (*tokens),* whereas the transitions are associated with events that change the state. An initial marking defines the set of partial states that describe the system at the beginning of its evolution. The dynamic behaviour of a Petri net is determined by the occurrence of one or more events which can take place and the corresponding net evolution is achieved by changes in the place marking, following dedicated rules (Fig. 4). An event is modelled by representing the possibility of occurrence (*transition enabling*) and the effect on the system (*firing rules*). The former is established according to the marking of the places in the net. On the other hand, a change in state of the system is represented by a change in the marking when a transition fires. The firing rules define the change in the number of tokens, whose total number is not necessarily unchanged. Since the firing of a transition represents a local event in the net, the occurrence has only local effects and cannot influence components of the net that are not directly connected.

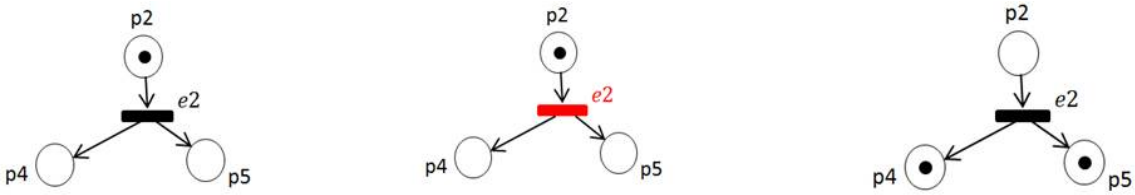

FIG. 4. Example of a Petri net evolution.

4.3. PETRI NET FOR ALFRED STARTUP

In the development of the controller, a fundamental role is played by the *synchronized Petri net*, i.e., an extended version of a Petri net to which a new element, the *event*, is added. Indeed, in this kind of Petri net, an external event e_i is associated to each transition t_i and the latter t_i fires only if it is enabled when the external event occurs. Therefore, an additional logical condition (i.e., the occurrence of the related event) must be verified to permit the transition firing. The logical condition is typically expressed as a function of the controller input variables (i.e., measures coming from the plant). The synchronized Petri net for the ALFRED startup sequence is shown in Fig. 5 along with the associated places and events, described in Table 3 and Table 4, respectively.

Table 3. Description of the places in the Petri net.

#	Place	Description
p0	Primary circuit filled	Primary circuit filled with lead, secondary system pressurized
p1	Source insertion	The source is being inserted
p2	FAs core loading	The core is loaded with FAs in order to reach the BoL configuration
p3	G_{Pb} ↑	The lead mass flow rate increases
p4	→ → Γ_{Pb} G_{Pb} nominal value	The lead mass flow rate is kept at the nominal value
p5	SRs extraction	The Safety Rods are being extracted
p6	P(t) ↑ by CRs	The increase of power is regulated by the Control Rod PI controller
p7	→ $T_{feedwater}$ = 380°C	The feedwater temperature is kept constant at 380°C
p8	P(t) = 0.1 MW_{th}	The power is kept constant at 0.1 MW_{th}
p9	P(t) ↑↑	The power rise continues
p10	$T_{feedwater}$ ↓	The feedwater temperature is being decreased
p11	→ $T_{feedwater}$ = 335°C	The feedwater temperature is fixed at 335°C
p12	P(t) = 60 MW_{th}	The power is kept constant at 20% of the nominal value
p13	→ p_{SG}(Bypass) = p_{nom}	The pressure is kept constant with the bypass valve PI controller
p14	→ G_{water}=$G_{water,0}$/5	The feedwater flow rate is kept constant at 20% of the nominal value
p15	P(t) ↑↑	The power rise continues
p16	P(t) = 300 MW_{th}	The power is kept constant at nominal value
p17	→ p_{SG} (k_v) = p_{nom}	The pressure is kept constant operating on the turbine admission valve
p18	G_{water} ∝ P(t)	The feedwater flow rate is controlled by a feedforward-feedback scheme

$$G_{water} \propto P(t)$$

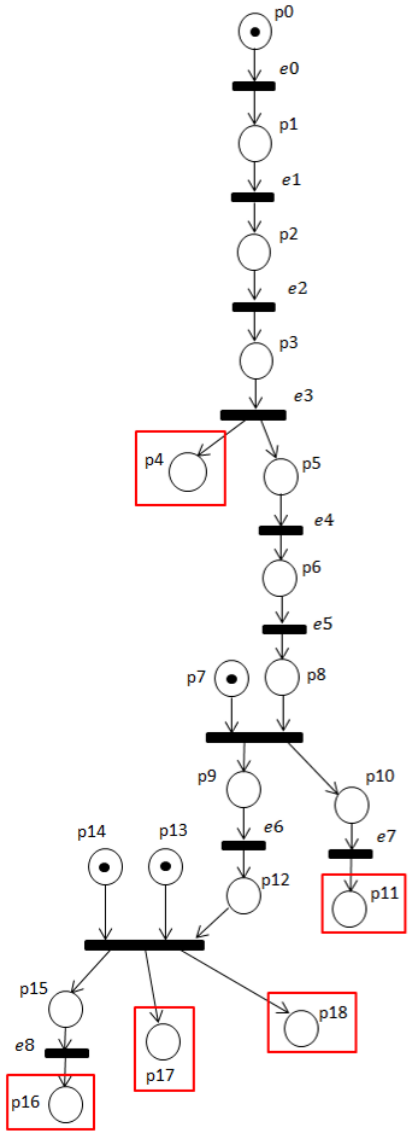

FIG. 5. System desired behaviour during the startup sequence (the squared red places refer to the conditions held in the full power mode).

Table 4. Description of the events in the Petri net.

#	Event	Description
e0	User-defined	Beginning of startup procedure decided by the user
e1	Source inserted	The source is completely inserted
e2	Core loaded	The BoL configuration is reached
e3	$G_{Pb} = G_{Pb,0}$	The lead mass flow rate reaches its nominal working point
e4	SRs extracted	The Safety Rods are totally extracted
e5	P(t) = 0.1 MW_{th}	The measured thermal power is 0.1 MW_{th}
e6	P(t) = 60 MW_{th}	The thermal power reaches 20% of the nominal value
e7	$T_{feedwater}$ = 335°C	The feedwater temperature reaches 335°C
e8	P(t) = 300 MW_{th}	The reactor is at full power

5. SIMULATIONS AND RESULTS

The proposed procedure for the ALFRED startup has been implemented in SIMULINK® [13], in which the plant behaviour has been simulated by means of a special block that allows to connect SIMULINK® with the Dymola simulation environment (Section 3). In more detail, the plant behaviour is simulated using the object-oriented model [9], while the controller actions are performed by means

of the Simulink block. The main purpose of these simulations is to demonstrate the feasibility of the proposed startup procedure and verify that all the main constraints during the power rise are satisfied. Furthermore, it is possible to track all the main control and controlled variables during the startup sequence. The overall procedure takes 150.000 s (almost 42 hours). This time is only indicative and it can be optimized reducing some "dead times" and establishing the maximum rate for the controlled variables. During the startup sequence the lead temperature in the pool (Fig. 6) does not exceed 410°C, respecting the limit imposed by corrosion problem on the vessel steel. As far as the lead temperature is concerned, at the core outlet the constraints are respected since the temperature does not exceed the nominal value of 480°C (Fig. 7).

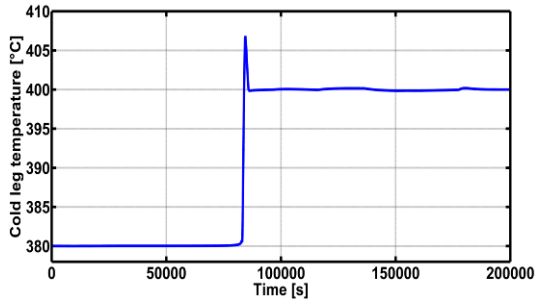

FIG. 6. Lead temperature in cold pool.

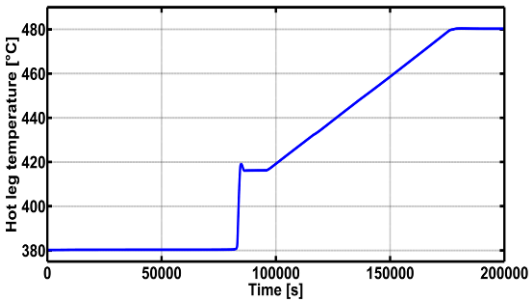

FIG. 7. Lead temperature at the core outlet.

The power evolution is divided in two stages (Fig. 8). The first one is devoted to reach and maintain 60 MW_{th} (20% of the nominal power) so as to keep the condition of the primary side constant during the switch between auxiliary and normal mode of the secondary circuit. The level has been chosen since it has been considered sufficient to produce steam to be admitted in turbine. In the second stage, the nominal conditions are gradually reached in order to avoid strong reactivity insertion. Starting from a subcritical level, the reactivity (Fig. 9) does not exceed 0.4$ throughout the startup procedure.

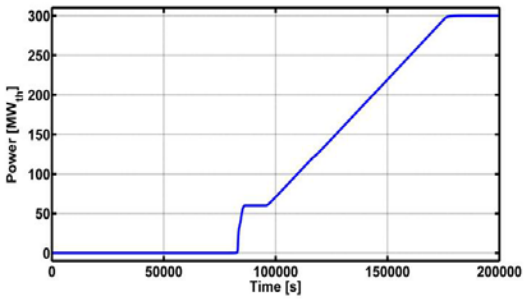

FIG. 8. Reactor power evolution.

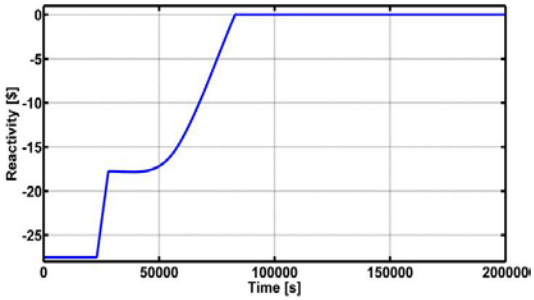

FIG. 9. Reactivity evolution.

In Fig. 10, the position of the control rods is represented and it is possible to observe how after the initial extraction performed to achieve criticality, in following stages the rods are progressively removed to reach the nominal conditions. From the simulation on the secondary circuit behaviour, it can be stated that the steam temperature (Fig. 11) cannot be properly controlled until the thermal power reaches 250 MW_{th}. This is due to the fact that the feedwater mass flow rate (Fig. 12) has already been employed to control the lead temperature in the cold pool and cannot be used to satisfy the control requirements of the balance of plant, i.e., keeping the steam temperature close to its nominal value. This aspect has to be taken into account for the secondary system operation since the steam temperature is 30°C/40°C lower than its nominal value when the steam starts to flow in the turbine. Finally, the pressure shows a very good trend (Fig. 13) since the variation are minimal, limiting mechanical stresses on the secondary components. These results are achieved by means of an appropriate tuning of the controller parameters, which allow to limit elongation (overshooting or undershooting) during operational transient.

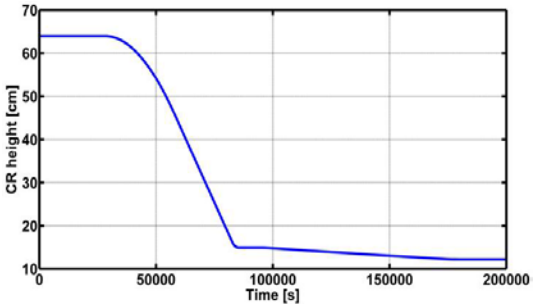

FIG. 10. Control Rod position evolution.

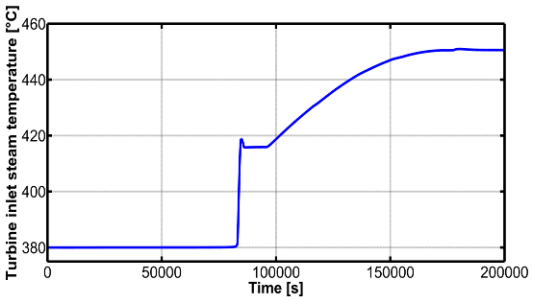

FIG. 11. Steam temperature evolution.

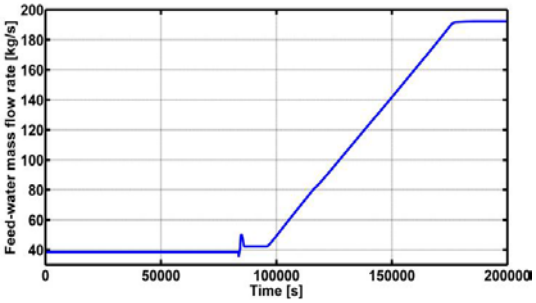

FIG. 12. Feedwater mass flow rate evolution.

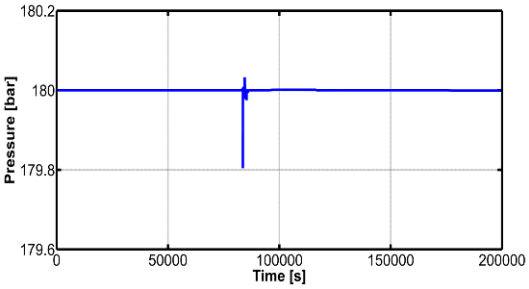

FIG. 13. SG pressure evolution.

6. CONCLUSIONS

Commonly, the adopted procedure to bring a nuclear power plant from zero power conditions to the full power mode is not suitably formalized with a quantitative description. On the other hand, it is evident how the startup phase deserves a particular attention in a new generation reactor, such as the LFR, whose operation is not fully defined and for which the control strategy has not been finalized yet. For the operation modelling of the ALFRED nuclear power plant, the present work has employed the Petri net approach, a widely used tool in the control of industrial processes that allows to coordinate and manage the transitions that take place in Discrete Events Systems. This tool has permitted to define exhaustively and unambiguously the sequence of the several control steps that must be taken so as the system evolution can proceed in the desired way. By adopting the Petri net approach, it was possible to easily obtain the sequence of the controllers to be used during the startup and to identify the set of events coming from the plant that enable the switches among the several feedback controllers within the control system architecture. As a major outcome of this work, the simulation results of the ALFRED reactor startup related to both the output and the control variables were presented.

As a further development, the formalized procedure will be implemented in the *supervisory system*, in order to coordinate the switching of the different operational modes (i.e., startup, full power, shutdown, etc.). In this way, by representing the overall control system architecture by means of a synchronized Petri net, it would be possible to analyse and represent every operational stage of ALFRED by adopting the same effective and functional formalism.

ACKNOWLEDGEMENTS

The authors acknowledge the European Commission for funding the LEADER project in its 7th Framework Programme. Acknowledgment is also due to all the colleagues of the participant organizations for their contributions in many different topics, in particular to Dr. Alessandro Alemberti and Dr. Luigi Mansani (Ansaldo Nucleare, Italy) for their fruitful criticism in developing the reactor startup procedure. The authors are also grateful to prof. Luca Ferrarini (Politecnico di Milano, Italy) for his suggestions about the formalism and the development of Petri net.

REFERENCES

[1] GIF, 2002. A Technology Roadmap for Generation IV Nuclear Energy Systems. Technical Report GIF-002-00.

[2] TUCEK, K., et al, "Comparison of sodium and lead-cooled fast reactors regarding reactor physics aspects, severe safety and economical issues", Nucl. Eng. Des. 236 (2006) 1589–1598.

[3] KOK K.D., "Nuclear Engineering Handbook", CRC Press, Taylor & Francis Group (2009)

[4] ALEMBERTI, A. et al, "The Lead fast reactor Demonstrator (ALFRED) and ELFR design", International Conference on Fast Reactors and related Fuel Cycles: Safe Technologies and Sustainable Scenarios (FR 13), Paris, France (2013).

[5] PETRI, C., "Kommunikation mit Automaten", Ph.D. Thesis, Darmstadt University of Technology, Germany (1962)

[6] GRASSO, G., et al, "Demonstrating the effectiveness of the European LFR concept: the ALFRED core design", International Conference on Fast Reactors and related Fuel Cycles: Safe Technologies and Sustainable Scenarios (FR 13), Paris, France (2013).

[7] FRITZSON, P., "Principles of Object-Oriented Modelling and Simulation with Modelica 2.1", Wiley IEEE Press (2004).

[8] ELMQVIST, H., et al, "Object-Oriented Modeling of Hybrid Systems", European Simulation Symposium (ESS'93), Delft, Netherlands (1993).

[9] PONCIROLI, R., et al, "Object-Oriented Dynamics Modelling and Simulation of the ALFRED plant", Prog. Nucl. En., (submitted).

[10] CASSANDRAS C.G., LAFORTUNE, S., "Introduction to Discrete Event Systems", Springer (2010).

[11] PETERSON, J. L., "Petri Net Theory and the modelling of systems", Prentice Hall (1981).

[12] HOPCROFT, J., et al., "Introduction to Automata Theory, Languages, and Computation (2nd ed.), Reading Mass: Addison-Wesley (2001).

[13] SIMULINK® Software, Version 7.1, The MathWorks Inc (2008).

Advanced Structural Mechanics Design of 500MWe Commercial SFRs

Gagan Gupta, S. Jalaldheen, P. Chellapandi, S.C. Chetal

Reactor Design Group, Indira Gandhi Center for Atomic Research, Kalpakkam, India

Abstract. In future 500 MWe SFRs, innovative design features have been incorporated in the reactor assembly components, to achieve improved economy and enhanced safety. The major design changes are: (1) innovative configuration of main vessel bottom dished head, (2) dome shaped roof slab with conical support, (3) thick plate for the rotatable plugs instead of box type structure, (4) welded grid plate with reduced number of sleeves, reduced diameter of intermediate shell and reduced height, (5) increased number of seamless primary pipes, (6) inner vessel with single radius torus welded with the grid plate, (7) integrated liner and safety vessel with thermal insulation arrangement, (8) innovative core support structure, (9) introducing in-vessel purification (10) integration of control plug and small rotatable plug and (11) straight pull fuel handling system. These features also help to shorten the construction time significantly. To validate the innovative design features, structural analysis for the geometrical optimization, investigation of buckling of thin shells, integrity assessment of integrated reactor assembly components were carried out. Further, to demonstrate the manufacturing feasibility of the new designs, technology development activities have been completed successfully. These developments are (i) thick tri junction forging for dome shape roof slab, (ii) welded grid plate, (iii) thick plate narrow gap welding for rotatable plugs, (iv) doubly curvature inner vessel sector, (v) embedded safety vessel with thermal insulation panel and (vi) large diameter bearing. The presentation brings out clearly the main structural features of the innovative concepts, which have been incorporated in future designs, application of advanced structural mechanics analyses carried out to comply the RCC-MR (2010), design requirements, challenges and achievements of technology development exercises completed.

1. Introduction

In India Prototype Fast Breeder Reactor of 500 MWe sodium cooled, the first large size fast breeder power plant is under advanced stage of construction at Kalpakkam. Following the construction of PFBR, it is planned to construct six 500 MWe Commercial Fast Breeder Reactors (CFBR) by adopting twin unit concept (three 2x500 MWe reactors). Among these one twin unit would be built at Kalpakkam. Since these units are intended as part of commercial program, there is a need for cost competitiveness and enhanced safety. Therefore, many innovative design & safety features are incorporated in reactor mainly in reactor assembly in addition to the proven concepts of PFBR components. To validate these design features, structural analysis of reactor assembly components were carried out. Further, to demonstrate the manufacturing feasibility of the new designs, technology development activities have been completed successfully. These new design, structural analysis and technology development for the reactor assembly of CFBR are discussed in this paper.

2. Innovative Design in CFBR Reactor Assembly Components

The reactor assembly components of CFBR were designed with many innovative features to improve economy and enhance safety as shown in Fig. 1. The diameter of main vessel, thermal baffles and inner vessel have been reduced through various optimization measures taken on the layout of components in main vessel and top shield and introduction of innovative design features. Number of primary pipes has been increased from four to eight with reduced size, which provides enhanced safety margin in case of one pipe rupture event. With this modification, the height of grid plate has been also reduced. Also, by introduction of spigots welded to top plate of grid plate to support most of the shielding subassemblies instead of sleeves, the diameter of grid plate shell and bottom plate are reduced. Inner vessel upper shell diameter is reduced and its redan is of single toroidal shape as compared to conical shape in PFBR. This improves the buckling strength, reduces thickness and in

turn weight of inner vessel. Roof slab has been made dome shaped with a conical skirt support which is in compression under the reactor assembly load.

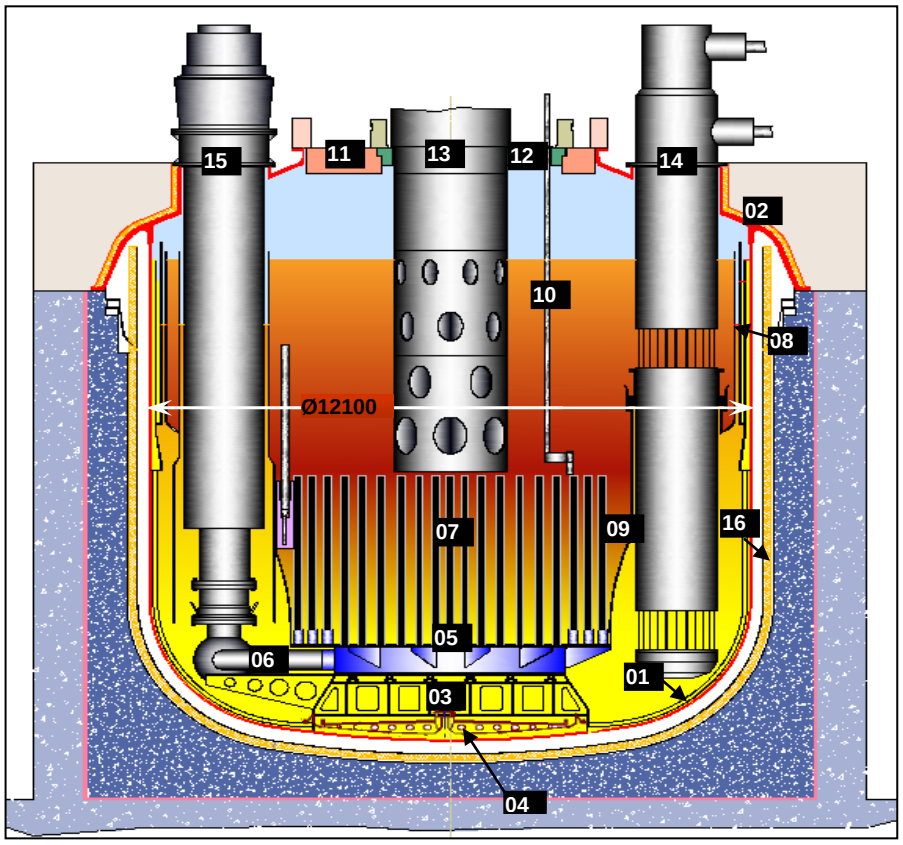

Sl. No	Components
01	Main Vessel
02	Roof Slab
03	Core Sup. Structure
04	Core Catcher
05	Grid Plate
06	Primary Pipe
07	Core
08	Thermal Baffle
09	Inner Vessel
10	Transfer Arm
11	LRP + Support
12	SRP + Support
13	Control Plug
14	IHX- 4 Nos.
15	Primary Pump- 2Nos.
16	Safety Vessel + Thermal Insulation

Fig. 1 Reactor Assembly of CFBR

2.1. Innovative Configuration of main vessel bottom dished head

The shape of the dished head and the triple point location where the CSS transmits the load including its self weight are optimized with respect to buckling and plastic collapse failure modes as shown in Fig. 2 . The optimized shape has three portions viz. knuckle, crown and a frustum of conical shell in-between as depicted in Fig.3 compare to two portions viz knuckle and crown in PFBR. Apart from this, in the design stage the vertical displacement is limited to 3 mm to ensure certain minimum natural frequency so as to avoid high dynamic amplifications during vertical seismic excitations and in turn high reactivity oscillations.

2.2. Dome shaped roof slab with conical support

In PFBR, roof slab **is** large box type structure as shown in Fig. 4 with many penetrations and is made of carbon steel of special grade (A48P2) posed a lot of difficulties during manufacturing, in particular due to lamellar tearing and found to be time consuming. In CFBR, roof slab has been conceptualised with dome-shape structure resting on conical skirt, which is under compression, supporting the entire reactor assembly as shown in Fig. 5. Material of construction for the shell is chosen as SS 304 LN to avoid the bi-metallic joint. Analysis of dome structure was carried out under normal load conditions to meet the design requirements of maximum deflection of 3 mm (Fig. 6 & Fig. 7) at inner edge and maximum global Von-Mises stress. Further, the slope of support flanges for major components like pump, IHX and LRP need to be restricted to ensure the verticality of components within acceptable limits. The model is meshed with shell elements having six degrees of freedom. Several geometrical features like radial stiffeners, circumferential stiffeners between penetration shells, gussets for penetration shells etc. were added to the basic structure to increase the rigidity of the dome and in-turn to reduce the central deflection. The air cooling system is integrated over the top surface of the dome so that the stiffening effect due to air cooling box is also accounted in the analysis. Due to change in

the concept, the net reduction in the weight of the roof slab will be ~80 t which is around 35% of present roof slab.

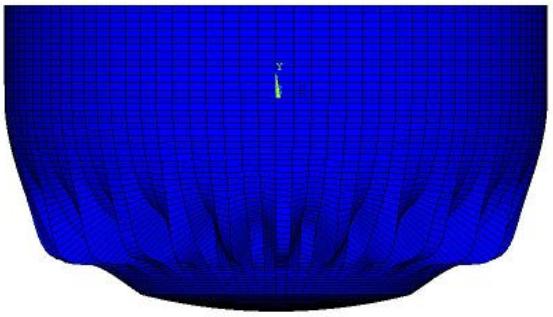

Fig. 2 Critical buckling mode shape of Main Vessel

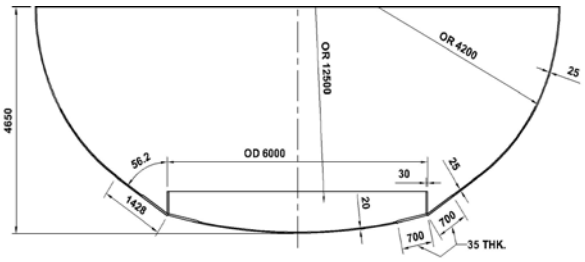

Fig. 3 Innovative Main vessel Bottom dished head

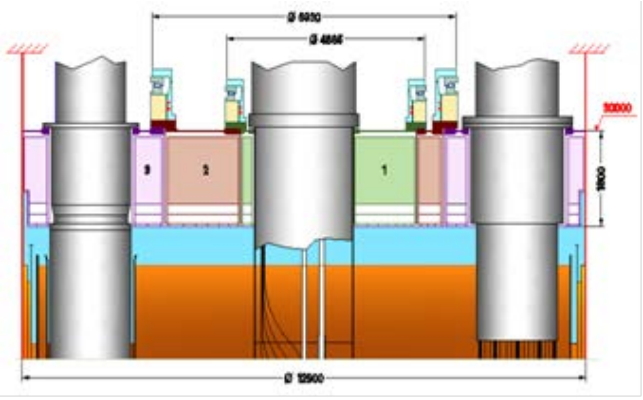

Fig.4 Box type structure of roof slab, large rotatable plug and small rotatable plug

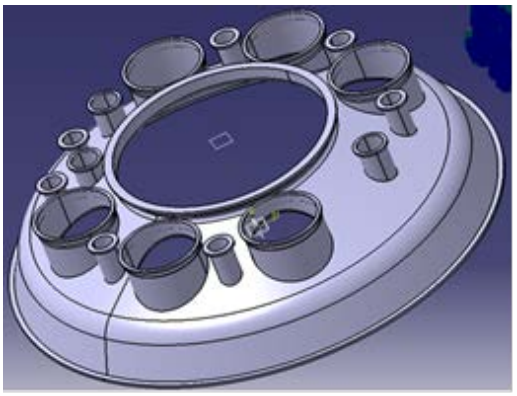

Fig. 5: Dome shaped roof slab with conical support skirt for CFBR

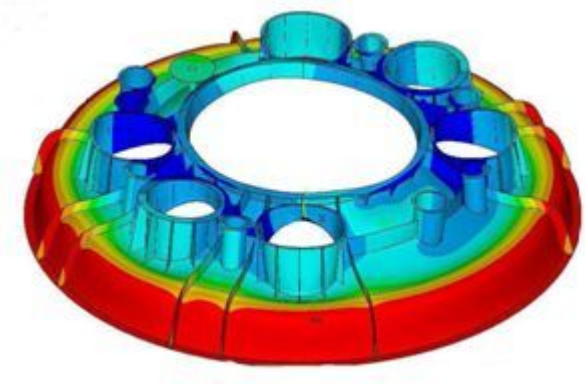

Fig. 6: Typical Plot of Vertical Deflection of Dome Shaped Roof Slab

Fig. 7: Typical Plot of Von mises stress in Dome Shaped Roof Slab

To enhance the reliability of dome shaped roof slab, it is proposed to use a forged piece at the tri-junction joint of main vessel, roof slab, and its support shell (Fig. 8). The major challenge in the realization of dome shaped roof slab, is ensuring the indigenous supplier base for the critical tri-junction forging in stainless steel which is ~12 m in diameter having an overall cross sectional dimension of ~500 mm x 500 mm.

The indigenous technology development of the tri-junction forging (in the form of 30° sectors) was undertaken and the same was completed successfully (Fig. 9) after overcoming several challenges.

One of the major challenges faced is in-complete filling of material within the cavities of the dies (Fig. 10). This was resolved by adopting pre-forming of the ingot to favorable shape with external means and then feeding the pre-formed shape to the forging hammer.

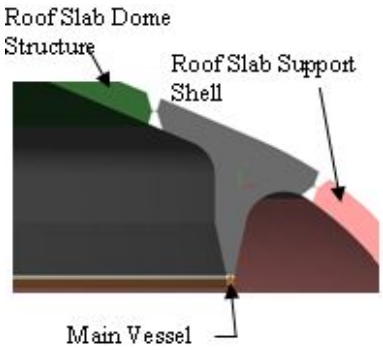

Fig. 8 Tri-Junction of roof slab, main vessel and support shell

Fig. 9 View of forged tri-junction sectors

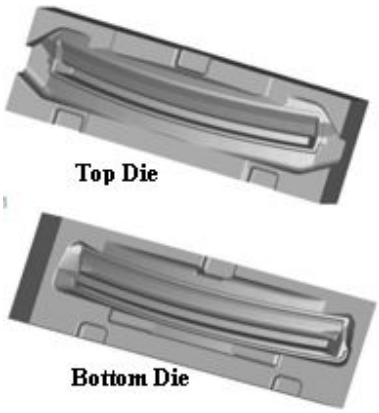

Fig. 10 3D view of forging dies

This process involved many brainstorming discussion with the industry. Another major challenge faced was Ultrasonic Examination of complex shaped tri-Junction. This was overcome by identifying multiple locations for scanning with shear wave and normal wave probes in parallel. 1 MHz probes were used at locations where depth of material is very high.

2.3. Thick plate for the rotatable plugs instead of box type structure

In PFBR large rotatable plug (LRP) and small rotatable plug (SRP) as shown in Fig. 4 are box type structure and made of carbon steel which have same manufacturing difficulties as roof slab and found time consuming. In CFBR, thick plate concept is conceived for SRP and LRP as shown in Fig. 11. The advantage of thick plate are (a) the only type of weld required will be butt weld between sectors of thick plates and the possibility of lamellar tearing will be eliminated (b) The component penetrations will be machined and hence the annular gaps will be less than 5 mm (compared to ~20 mm in case of PFBR). This will drastically reduce the complementary shielding requirement above SRP and LRP. Annular gaps less than 5 mm will also result in substantial reduction of cellular convection in the annular gaps and hence less circumferential temperature asymmetricity and thus reduced thermal stresses. Smaller annular gaps also mean less deposition of sodium aerosols in the gaps and less amount of sodium ejected into the top shield in the unlikely event of core disruptive accident. Furthermore, the reduction in annular gaps will contribute towards reduction in top shield/main vessel diameter and (c) The thickness of top shield would be reduced, thereby the length of components penetrating the top shield gets reduced (about 1 m length reduction is possible).

Their outer support flange will be machined from thick forged rings. In order to determine the thickness required for SRP and LRP of CFBR, finite element analysis was performed considering both structural and thermal loads. The thickness requirement is governed by rigidity consideration rather than strength consideration. The deflection contours for LRP (Min. 0.17 & Max. 2.5 mm) and SRP (Min. 0.17 & Max. 1.9 mm) are shown in Fig. 12 and 13 respectively. The thickness of SRP and LRP required is 300 mm and 500 mm respectively.

Diameter of thick plate for SRP and LRP is large and commercially these plates are not available hence a project for the development of narrow gap welding technology of 800 mm thick welds plates as shown in Fig. 14 was carried out. Narrow Gap Welding (NGW) as shown in Fig. 15 utilises weld groove preparation having very small included angle (less than 4^{o}) in contrast to the conventional weld grooves (U and V types). The advantages of the NGW technique compared to the conventional groove welds are as follows. Smaller cross-section of the weld groove requires less filler material and less heat input during welding. The residual stresses are reduced and distortion is less due to low heat input

and smaller volume of molten weld metal. High quality of the weld is obtained as a result of low heat input, extremely narrow heat affected zone (HAZ) and fine grained weld metal. Therefore improved-

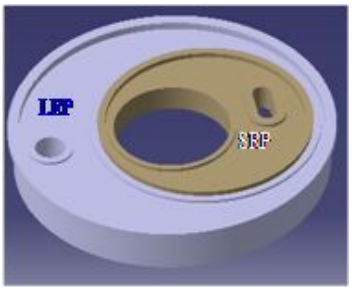

Fig. 11: Thick Plate SRP & LRP of CFBR

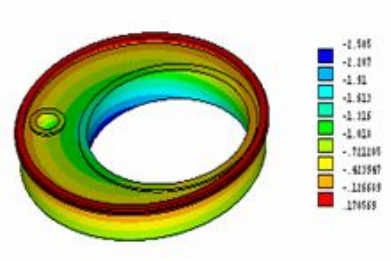

Fig. 12 Deflection contour of LRP

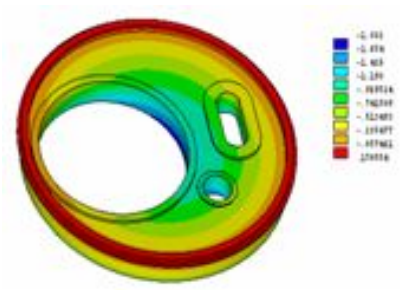

Fig. 13 Deflection contour of SRP

-fracture toughness and fatigue strength of the welded joint is realized. The aforementioned advantages are more pronounced in case of welding very thick plates as is the case for fabrication of thick plate rotatable plugs. Before carrying out welding of actual plates, mock-up welding was conducted. Three mock-up welds were made. During the course of mock-up welding, valuable experience was gained regarding the shrinkage behavior of narrow gap welds, effect of precambering and stiffeners / restraints. Three welds were carried out after mock-up welding. Repair procedures were also demonstrated for the welds both for defects at the end of the plate and the defects near the middle of the plate. For repair, narrow groove similar to that used for original welding was used (Fig. 16). This minimised the volume of base metal and previously deposited weld metal to be removed for repair. The welds have successfully passed all the non-destructive examination (NDE) and destructive testing requirements of the technical specifications.

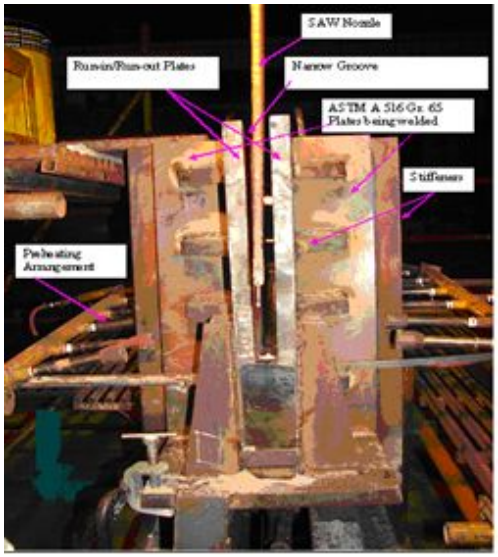

Fig. 14: SAW Set-up for NGW of 800 mm thick welds at L&T, Hazira

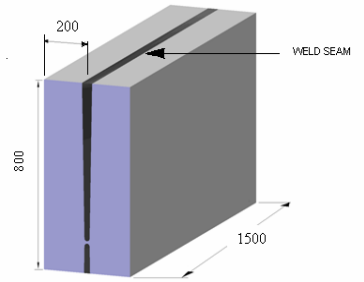

Fig. 15: Schematic of 800 mm thick Narrow Gap Weld

Fig. 16: Narrow groove for repair

2.4. Welded grid plate with reduced number of sleeves, reduced diameter of intermediate shell and reduced height

In PFBR, grid plate has circular box type structure where sleeves are provided for all core subassemblies as shown in Fig. 17. It has fully bolted construction between shell to plate joint and sleeve to plate joint. It is connected to pumps via four primary pipes (two pipes from each pump). In CFBR, grid plate is fully welded box-type / shell structure as shown in Fig. 18 in which sleeves are provided only for subassemblies that require forced cooling and two/three rows of other subassemblies (outer shielding) for required flow distribution inside the grid plate plenum. For remaining shielding

subassemblies spikes are provided on the top plate for supporting. Hence, diameter of shell & bottom plate reduced to 4600 mm. It is connected to pumps via eight primary pipes (four pipes from each pump) hence, overall height of grid plate reduced to 685 mm. The net weight reduction of new grid plate is estimated as 55%. To check the slope, deflection and stresses in grid plate during normal operating condition, structure analysis was carried out as shown in Fig. 19 and Fig. 20.

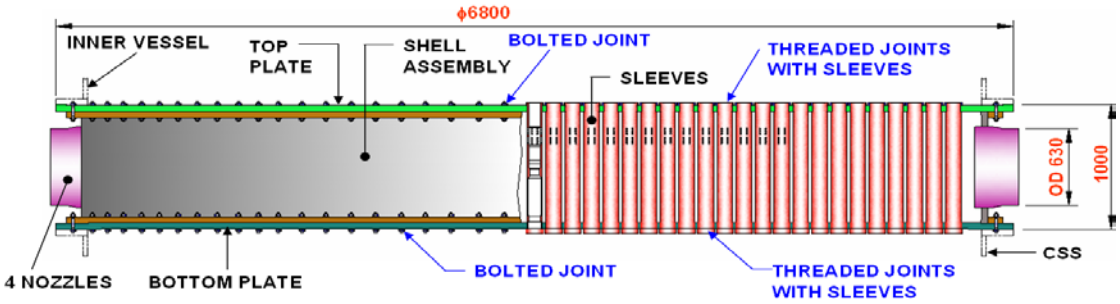

Fig.17: PFBR Grid Plate fully bolted structure

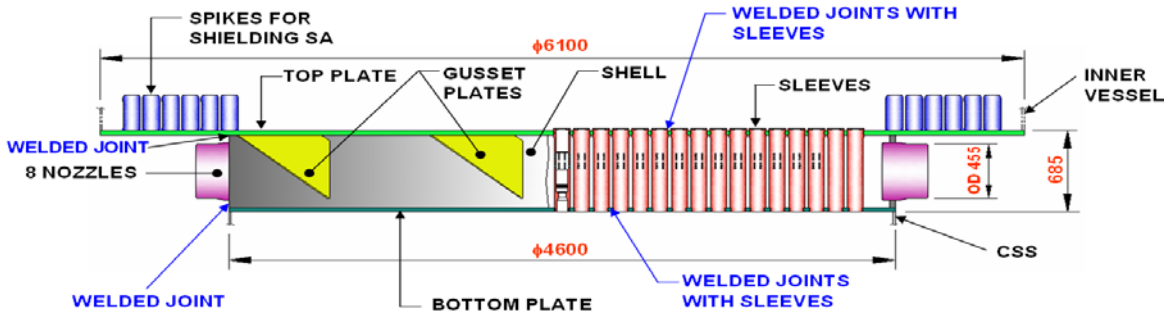

Fig.18: CFBR Grid Plate fully welded structure

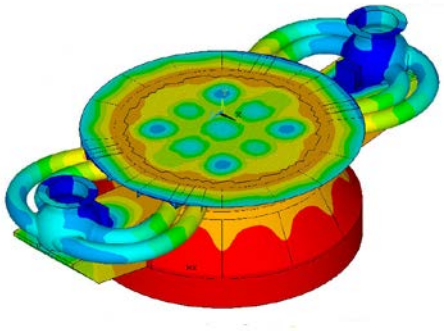

Fig.19: Deflection in Grid Plate

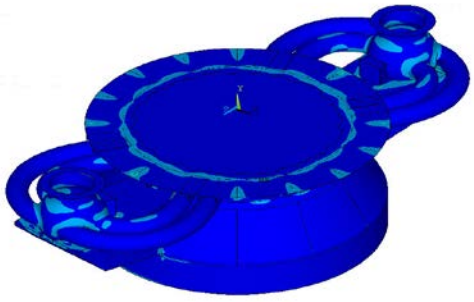

Fig.20: Stress distribution in Grid Plate

For technology development of welded grid plate (Fig. 18), a full size component having selected number of sleeves and spikes was manufactured (Fig. 21 & 22). During the process of development, various technical challenges were faced. The successful resolution of them resulted in fine tuning of the design. Manufacturing procedures were evolved during the course of development based on numerous mock-up & trials. Some of them are related to (a) innovative joint configuration for shell-plate weld eliminating the need for welding & grinding inside the box structure with limited space between top & bottom plates, (b) sleeve-plate & spike-plate weld joint configurations, (c) procedures for various heat treatments and machining of the individual parts and assembly, (d) suitable distortion control measures, (f) procedure for measuring the verticality of sleeves, (g) procedure for examination of sleeve-plate joints etc. The successful completion of technology development activities has demonstrated the manufacturing feasibilities and given confidence for the design improvements.

Fig. 21 Box structure (in inverted position) after assembly of top & bottom plates and shell

Fig. 22 Final machining of spikes on assembly of welded grid plate

2.5. Increased number of seamless primary pipes

In PFBR, four numbers of branch pipe are supplying sodium from the outlet of the primary sodium pump (PSP) to grid plate as shown in Fig. 23. Each branch pipe (outside diameter 630 X 10 thickness.) is made of three segment, two straight pipes and one bend pipe having welded joint. In case of one pipe rupture the core flow reduces to 30 %. and the maximum clad hotspot temperature will reach to 1346 K. To increase the safety margin & reliability in CFBR, eight seamless pipes are provided, i.e. four per pump, thereby reducing the diameter of pipes from 630 mm to 455 mm (Fig.-24). The increased number of pipes increases the safety margin under pipe rupture event, i.e. the flow reduction is 43 % (core flow is 57 % of nominal flow) and maximum clad hot spot temperature is 1110 K. The seamless condition will increase the reliability of pipe.

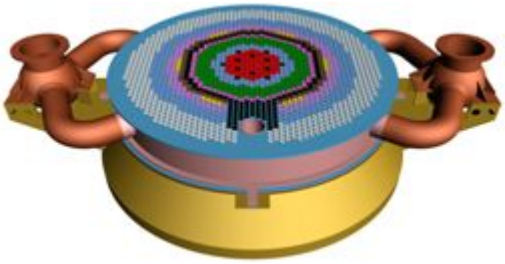

Fig. 23 Primary Pipe Configuration in PFBR

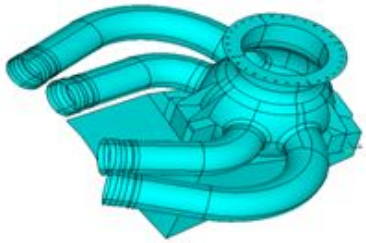

Fig. 24 Primary Pipe Configuration in CFBR

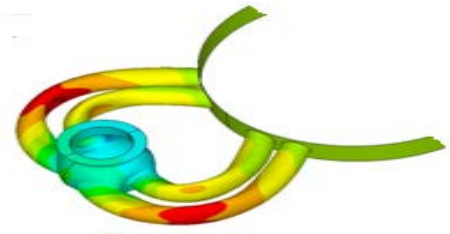

Fig. 25 Displacement in Radial

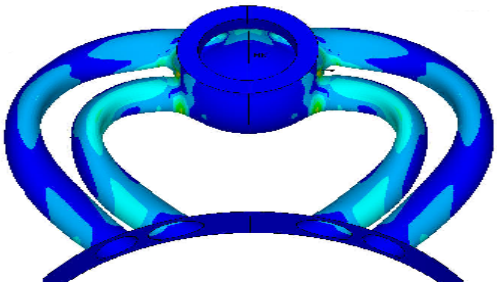

Fig. 26 Von-Mises Stress in Primary pipe

Flexibility analysis for primary pipe was carried out for various layout configurations and optimum layout was conceived as shown in Fig. 25 and Fig. 26. A technology development project is under progress to check the hot bending of seamless pipes under desired bend radius

2.6. Inner vessel with single radius torus welded with the grid plate

In PFBR, inner vessel consists of the 3 thin shells, a lower cylindrical shell surrounding the core subassemblies, an intermediate toroidal-conical-toroidal shell called redan which provides opening for

stand pipes through which IHX, PSP, sodium purification line and CPLD enter into cold pool and an upper cylindrical shell of large diameter, surrounding the stand pipes as shown in Fig. 27. The redan joins the upper shell and lower shell. There is a bottom flange that is bolted to the grid plate. In CFBR, the shape of inner vessel as shown in Fig. 28 is optimized with reduced upper & lower shell diameter and double curvature single toroidal redan, which results in higher buckling strength and reduced thickness and hence reduced weight. Additionally in-vessel transfer port (IVTP) which is used as intermediate port during transportation of fuel from core to outside the reactor was also accommodated in toroidal redan which was in the grid plate of PFBR. Inner vessel is welded to grid plate. Inner vessel was analysed (Fig. 29) for pressure load due to differential level between hot & cold pools and thermal load including through-thickness thermal gradient. The optimized thickness of 15 mm is arrived at for the single toroidal redan, with respect to buckling mode of failure (20 mm in case of PFBR). The weight saving is about 12%.

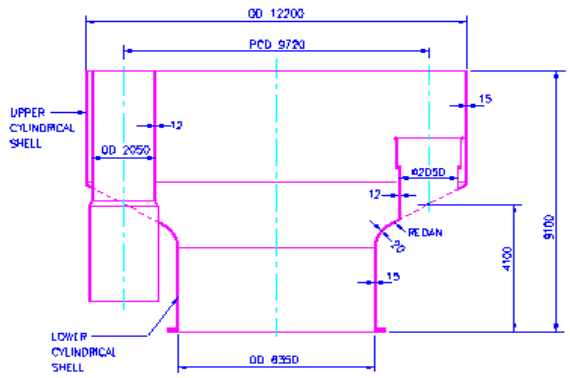

Fig. 27 PFBR inner vessel

Fig. 28 CFBR inner vessel

.

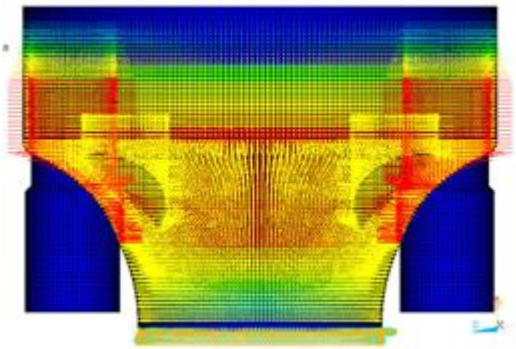

Fig. 29 FE Model with Boundary Conditions

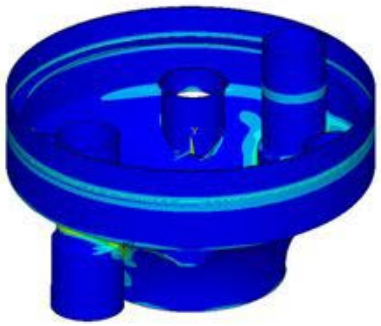

Fig. 30 Overall Vonmises Stress Distribution

For the technology development of inner vessel, a sector of doubly curved toricone with a portion of upper cylindrical shell was manufactured. The major activities involved are the development of suitable die & punch, pressing the job and inspection of the profile. Weight of the die and punch made of carbon steel is around 22 tonnes. Pressing of the toricone was carried out gradually on 4000 t capacity press (Fig. 31). A number of trials and mock up were carried out, first on carbon steel and then on stainless steel blanks. After each trial, the dimensions achieved were reviewed and based on the feedback, the profiles of die and punch were suitably modified. The finalized die & punch were used for pressing the actual job. The dimensional inspection was carried out using the conventional swing arm template & local templates and ECDS methods (Fig. 32). The achieved profile of the toricone satisfies the design requirements.

2.7. Integration of control plug and small rotatable plug

In PFBR, control plug is supported over SRP and radial gap between them is around 25 mm. In CFBR, innovative concept of thick plate SRP with integrated control plug is conceived. This will reduce the main vessel diameter as well as complementary shielding requirement.

Fig.31 Forming of toricone of inner vessel sector using die and punch

Fig. 32 Profile measurement of inner vessel sector using swing arm arrangement

2.8. Integrated liner and safety vessel with thermal insulation arrangement

In PFBR, the gap between safety vessel and inner reactor vault is provided around 250 mm due to heat transfer consideration as shown in Fig. 33. In CFBR, the thickness of safety vessel is reduced to 6 mm and the gap between safety vessel thermal insulation and liner is eliminated (very small 30 mm only compare to 250 mm in PFBR) as shown in Fig. 34. This has reduced the weight of safety vessel and concrete requirement for reactor vault. To enhance the strength of the safety vessel in particular during the seismic events where main vessel is under leaked condition, the gap between the free end of insulation support studs and the inner concrete wall is optimised to transfer the seismic load from safety vessel to concrete while allowing for thermal expansion of vessel under normal operating conditions.

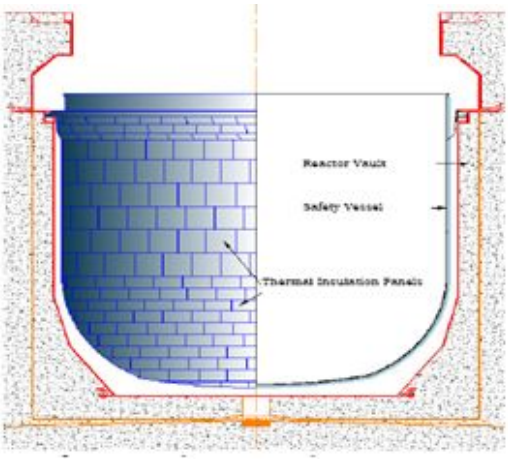

Fig. 33 Arrangement of safety vessel and reactor vault

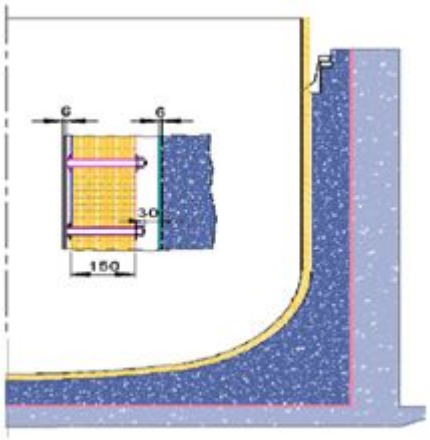

Fig. 34 Integrated liner and safety vessel with thermal insulation

2.9. Innovative core support structure

In PFBR, the Core Support Structure (CSS) is large diameter and bolted with grid plate. In CFBR, CSS is modified to suit the bottom of grid plate and welded with it. The grid size at the top plate of CSS was optimized based on normal loading condition as shown in Fig. 35, 36 and 37. The location of support pads between the CSS plate and grid plate were also modified.

2.10. Introducing in-vessel purification

In PFBR, primary sodium was purified outside the reactor vault as shown in Fig. 38. Sodium purification line is provided in inner vessel to cold pool, which transfer the radioactive cold sodium from main vessel to outside the reactor vault and after purification in cold trap it will be transferred back. This circuit is very expensive. In CFBR, it is planned to carryout in-vessel purification as shown in Fig. 39. From the safety point of view, keeping the radioactive sodium within the reactor is

preferred. This concept will eliminate the requirements of shielding, thermal insulation and leak collection trays.

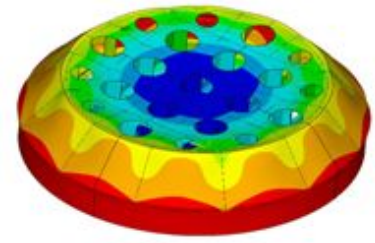

Fig. 35 Displacement plot in CSS

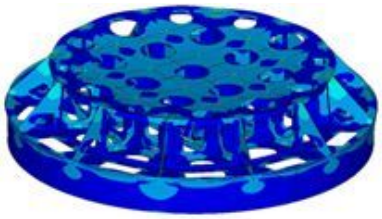

Fig. 36 Vonmises stress plot in CSS

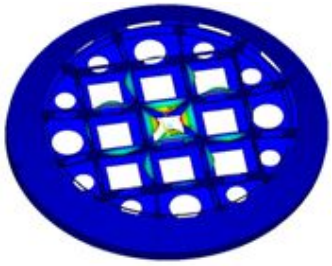

Fig. 37 Buckling Analysis of CSS

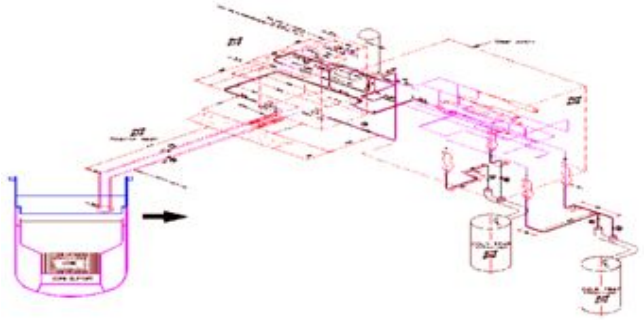

Fig. 38 Sodium purification circuit in PFBR

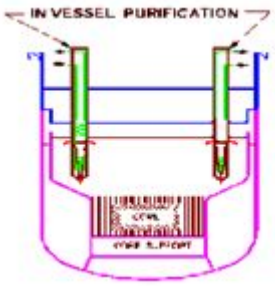

Fig. 38 Sodium purification circuit in CFBR

2.11. Straight pull fuel handling system

In PFBR, Inclined fuel transfer machine (IFTM) is used for transferring fuel inside the reactor to outside. Many difficulties were faced during manufacturing of IFTM and time spent was huge. In CFBR it is preferred to use a straight pull machine in top shield which will transfer the fuel from In vessel Transfer Port (IVTP) to outside the reactor. The transfer of subassembly between the respective location in the core, storage location and IVTP are achieved through two transfer arms one each in SRP & LRP. The scheme for fuel handling in CFBR is shown in Fig. 40.

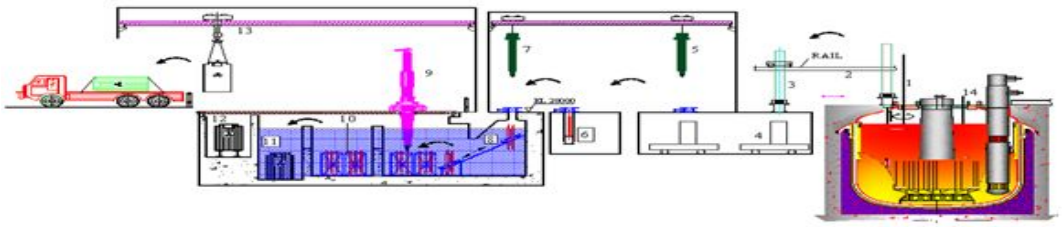

Fig. 40 Simplified fuel handling schem

3. Acknowledgements

Contributions by engineers in the Reactor Design Group are gratefully appreciated.

4. References

[1] Chellapandi, P., Puthiyavinayagam, P., Balasubramaniyan, V., Ragupathy, S., Rajan Babu, V., Chetal, S.C., and Baldev Raj, 'Design Concepts for Reactor Assembly Components of 500 MWe Future SFRs', Nuclear Engineering and Design 240 (2010) pp 2948–2956.

[2] Chellapandi, P., Puthiyavinayagam, P., Balasubramaniyan, V., Ragupathy, S., Rajan Babu, V., Chetal, S.C., and Baldev Raj, 'Design of innovative reactor assembly components towards commercialization of future FBRs, Enegry Procedia

Advanced Thermal Hydraulics Design of Commercial SFRs

Juby Abraham, M. Asokkumar, M. Rajendrakumar, K.Natesan, R.Arul Baskar, K.Velusamy, P.Selvaraj, P.Chellapandi

Thermal Hydraulics Section, Reactor Design Group, Indira Gandhi Centre for Atomic Research, Kalpakkam – 603102, INDIA.

Abstract. Prototype Fast Breeder Reactor (PFBR) is a 500 MWe pool type sodium cooled fast reactor, which is in an advanced stage of construction in India. As a follow-up to PFBR, six commercial sodium cooled fast reactors (Commercial SFR) of similar capacity are to be constructed, wherein the focus is improved economy and enhanced safety. These reactors are envisaged to have twin-unit concept. Design and construction experiences from PFBR provided the motivation to achieve an optimum design for the Commercial SFR with significant design changes. Some of the changes include, (i) provision of four primary pipes per primary sodium pump, (ii) inner vessel with single torus, (iii) dome shaped roof slab supported on reactor vault, (iv) machined thick plate rotating plugs, (v) reduced main vessel diameter with narrow-gap cooling baffles and (vi) safety vessel integrated with reactor vault. Advanced computational fluid dynamic studies have been performed towards thermal hydraulic design of these components. This paper covers thermal hydraulic design validation of the chosen options, including hot pool thermal hydraulics, influence of control plug shape on pool hydraulics, flow requirement for main vessel cooling, safety analysis of primary pipe rupture event and thermal management top shield and reactor vault.

1. Introduction

Prototype Fast Breeder Reactor (PFBR) is a 500 MWe pool type Sodium cooled Fast Reactor (SFR), which is in an advanced stage of construction in India[1]. As a follow-up to PFBR, six commercial SFRs of similar capacity are planned to be constructed, wherein the focus is on improved economy and enhanced safety. Commercial SFRs [2] are envisaged to have a twin-unit concept. The design and construction experiences from PFBR have guided the centre to achieve an optimized design for commercial SFRs (FIG. 1) with significant design changes for many components. Some of the changes include, (i) provision of four primary pipes per primary sodium pump, (ii) inner vessel with single torus lower portion, (iii) dome shaped Roof Slab (RS) supported on Reactor Vault (RV), (iv) machined thick plate rotating plugs, (v) reduced main vessel diameter with narrow-gap cooling baffles and (vi) safety vessel integrated with RV. Advanced computational studies have been carried out towards thermal hydraulic design of these components. The present paper covers thermal hydraulic design validation of the chosen options with respect to hot pool thermal hydraulics, influence of control plug shape on pool hydraulics, flow requirement for main vessel cooling, safety analysis of primary pipe rupture event and thermal management of top shield and reactor vault.

2. Thermal Hydraulics Design Limits

This section deals with some of the thermal hydraulic design limits, derived from detailed analysis of various thermal hydraulic phenomena of relevance to sodium cooled fast reactors.

2.1. Free Level Fluctuation

The height of inner vessel above the mean hot pool sodium level is arrived at from the amplitude of free level oscillations to avoid overflow of sodium. Also, the structures which are partly immersed in the sodium hot pool and partly exposed to cover gas region are subjected to high cycle fatigue due to

temperature oscillations at the interface of sodium and argon. Hence, the amplitude of fluctuations is limited to ±50 mm.

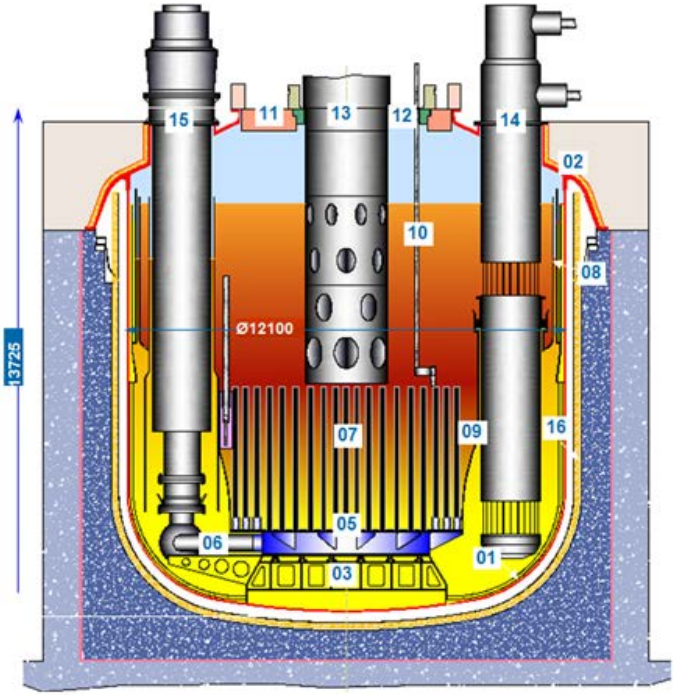

Sl. No	Components	Weight in t		
		PFBR	CFBR	Average in %
01	Main Vessel	134	85	- 36
02	Roof Slab	275	110	- 60
03	Core Sup. Structure	45	35	- 22
04	Core Catcher	21	15	- 28
05	Grid Plate	85	34	- 60
06	Primary Pipe	5	5	0
07	Core	513	420	- 18
08	Thermal Baffle	65	75	+ 15
09	Inner Vessel	61	55	-10
10	Transfer Arm	22	22	0
11	LRP + Support	73	106	+ 45
12	SRP + Support	45	40	- 11
13	Control Plug	78	78	0
14	IHX- 4 Nos.	172	172	0
15	Primary Pump- 2Nos.	143	143	0
16	Safety Vessel + Thermal Insulation	154	122	- 20

FIG. 1. Schematic of reactor assembly of Future SFR

2.2. Free Surface velocity in the Pool

The argon gas entrainment into the sodium pool can be a serious issue as it can cause a change in the value of net reactivity of the core. The free surface velocity plays a crucial role in gas entrainment phenomenon. Higher the velocity more is chance of gas entrainment. The studies on gas entrainment reveal that the free surface velocity has to be limted to 0.5 m/s to avoid gas entrainment.

2.3. High-cycle Temperature Fluctuation

Thermal stratification and thermal striping are the other two thermal hydraulic phenomena which can influence the integrity of structures immersed in the sodium pool. The thermal stratification in the pool is governed by the ratio of buoyancy force to inertia force as it influences the temperature gradients seen by the immersed structures. Higher value of this ratio leads to large temperature gradient in the pool. The maximum permissible gradient should be limited to < 300 K/m from structural mechanics point of view. Also, from thermal striping considerations, peak to peak temperature fluctuation on structures has to be limited to 60 K for control plug and 40 K for main vessel [3].

2.4. Heat Loss to Top shield and Reactor Vault

A thermal shield plate provided below top shield reduces the heat load to top shield by ~ 50 %. But it increases the bulk temperature of argon and associoated circumferential variations in component penetrations. The temperature in penetrations of the roof slab should be greater than 120°C to avoid sodium aerosol deposition and the circumferential temperature difference in component shells should be less than 30°C. To maintain structural integrity of reactor vault concrete, its temperature should be limited to 65^{o}C for normal operation and 90^{o}C during transients [4].

3. Hot Pool Thermal Hydraulics

The reduction in grid plate diameter makes lower shell of the inner vessel smaller by 250 mm in diameter. Also reduced pitch circle diameter and corresponding annular gaps in the Top Shield (TS)

benefits reduction in diameter of the upper shell by 360 mm. The redan which connects the upper and lower shells is designed to have a single torus shell, which inherits higher buckling strength. Thermal stratification, thermal striping and gas entrainment are the some of the unfavorable phenomena during the reactor operation under normal and transient conditions.

3-Dimensional hot pool thermal hydraulic analysis of Future SFR has been carried out by adopting a 90° symmetry sector of hot pool to estimate critical parameters, viz., axial thermal gradient in the hot pool, velocity distribution near Intermediate Heat eXchanger (IHX) inlet and sodium velocity in free surface. Predicted sodium flow pattern in the pool (FIG. 2) shows that sodium from the core outlet flows towards the control plug and nearly 75 % of flow takes a 90° turn below lattice plate due to the resistance offered by the anti-stratification skirt. The anti-stratification skirt is a 10mm thick shell with 10% porosity which is hanging from control plug as depicted in FIG. 2. The sodium then flows horizontally till it meets the inner vessel wall and then rises vertically upwards. Part of this flow finds its way to the IHX inlet directly while the remaining part continues to flow further up to the free surface and makes a circulation loop before entering the IHX. About 15% core flow enters into the control plug through the annular gap between the absorber rods and their shrouds and it exists from the control plug to join with the main flow. There is a mild recirculation flow in the cavity region between shielding subassemblies and torus portion of the inner vessel. The study indicates that with the aid of anti-stratification skirt, favorable flow conditions can be achieved in the bottom regions of the hot pool. The predicted free surface velocity in Future SFR is 0.72 m/s which is less than that of PFBR (1.2 m/s). This value could be reduced to 0.48 m/s by attaching a horizontal baffle of 0.5 m width to inner vessel at a depth of 1.3 m below free surface, which is acceptable from gas entrainment considerations.

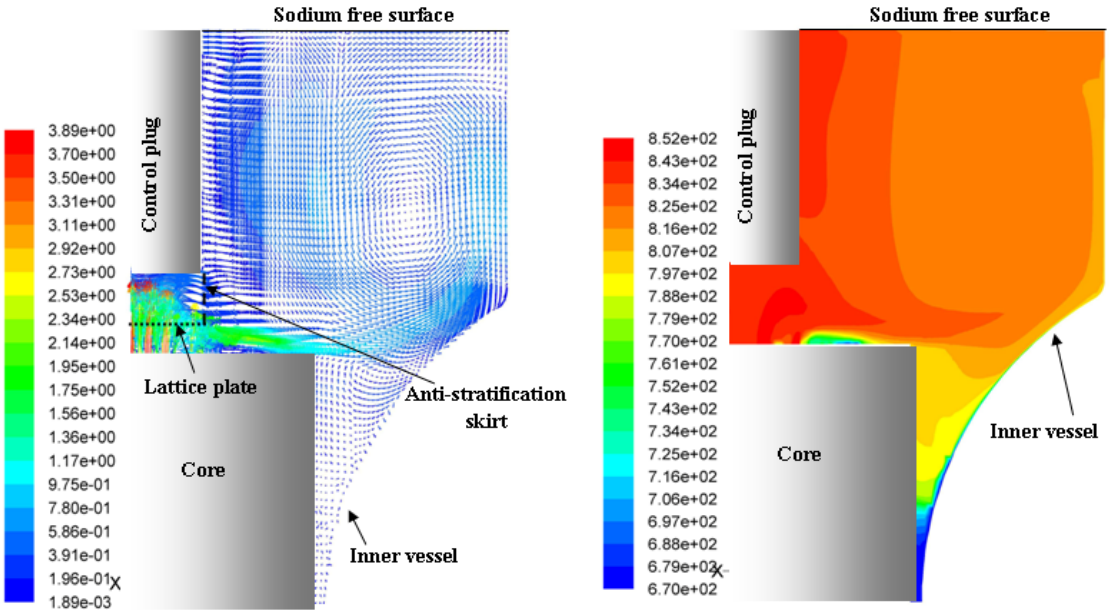

FIG. 2. Vector field (m/s) and temperature contours (K) in the hot pool at a symmetry plane between two IHX

The control plug of PFBR, which is cylindrical in shape, covers the fuel subassemblies and houses thermocouples for measuring the temperature of outlet sodium from all the fuel subassemblies and a few blanket subassemblies. Since the control plug in Future SFR is envisaged to be integrated with small rotatable plug, it is possible to increase the diameter of control plug at the bottom part. Thereby, it is possible to provide thermocouples in control plug for blanket subassemblies also. The provision for monitoring all the blanket subassemblies enhances the safety of reactor. To asses the influence of the shape of the control plug on the hot pool thermal hydraulics a set of 3-dimensional CFD studies were carried out. Three different control plug configurations, viz., cylindrical control plug, cylindrucal control plug with hemispherical bottom and conical control plug are considered. From the predicted temperature distributions (FIG. 3) it is seen that cylindrical and conical shapes of control plug with

anti-stratification skirt offer low axial temperature gradient in the hot pool when compared to cylindrical control plug with hemispherical bottom. The conical control plug also does not alter the major hot pool thermal hydraulic characteristics.

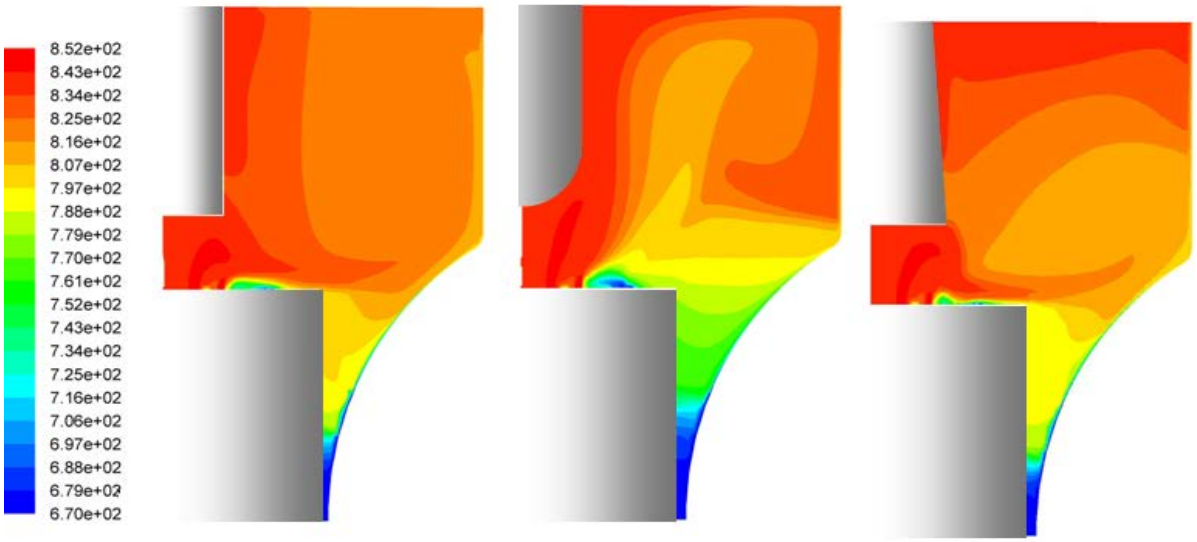

FIG. 3. Temperature contours (K) in the hot pool at 0^o plane for different configurations of control plug (from left: cylindrical, cylindrical with hemispherical bottom and conical)

4. Hydraulics of Primary Sodium Header

Liquid sodium from cold pool at 670 K is sucked by two primary sodium pumps operating in parallel, delivering 7000 kg/s at a pressure of 6.2 bars. Sodium from each of these pumps enters a spherical header, where it branches into multiple streams before entering the grid plate. Primary pipes connect the header to the grid plate which feeds fuel subassemblies. One of the important 'design basis events' to be investigated is 'rupture of one primary pipe'. Towards enhancing safety of the plant, it is planned to have four primary pipes per header in Future SFR, as depicted in FIG. 4. The four pipe design is expected to deliver more core flow under one pipe rupture condition with significant safety advantages. In addition to this, the four pipe arrangement leads to reduction in grid plate height and hence reduction in height of major primary system components with the associated benefit in terms of initial investment.

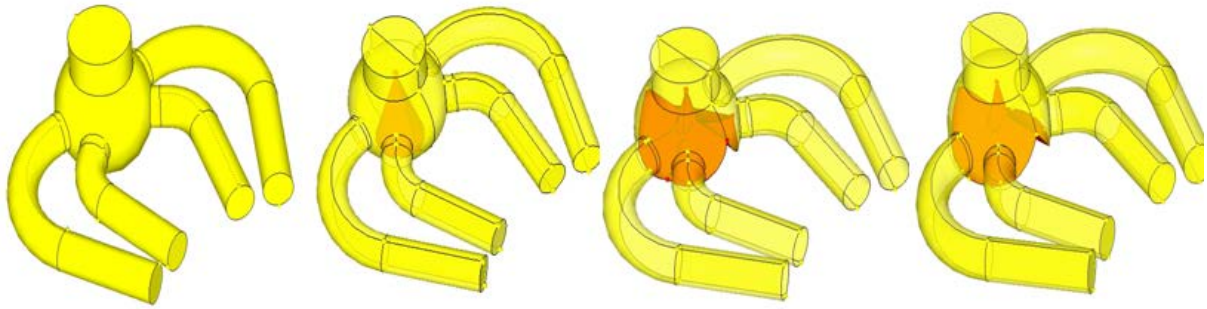

FIG. 4. Different configurations investigated to reduce pressure loss (from left: without internals, with central cone, with central cone and baffle-1, and with central cone and baffle-2)

It is essential to minimize the pressure loss in the "header-primary pipe" assembly to have significant saving in head to be developed by the sodium pump and hence the operating cost. Also, it is essential to quantify the pressure loss in the header towards proper specification of the pump. Further, it is required to identify proper flow distributing baffles inside the header to have a minimum pressure loss. Many innovative baffle options were studied and some of them are depicted in FIG. 4. In the reference header, large-scale recirculation and associated low pressure zone which are responsible for large pressure loss (FIG.5) were observed. By the introduction of central cone and baffle plate the

recirculation zone could be reduced significantly (FIG. 5). As a result of this, pressure loss in the 'header pipe' assembly reduced. The pressure loss coefficient defined by 'pressure loss/dynamic head at inlet' for various devices studied is presented in Table 1. It can be seen from the table that the pressure loss coefficient has reduced significantly with a central cone and baffle placed in the header. Further, the flow is evenly distributed among all primary pipes (0.5 % variation). In the reference header, however, the flow mal-distribution is 3%.

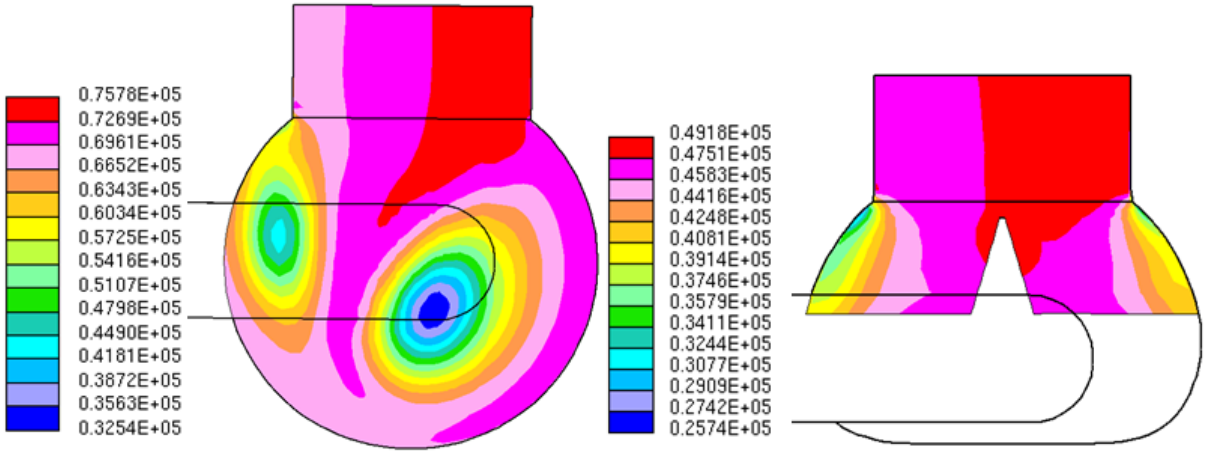

FIG. 5. Pressure distribution (Pa) in spherical header: reference header (left) and header with central cone and baffle-2 (Right)

Table 1 Pressure loss coefficient for header with various internal devices

Geometry	Pressure loss coefficient
Reference header (without any internal device)	2.78
Header with a central cone	2.09
Header with central cone and baffle-1	1.58
Header with central cone and baffle-2	1.38

5. Main Vessel Cooling System

From structural considerations, it is necessary to maintain the temperature of main vessel (MV) within 420°C under steady operation at all loads and to achieve this the vertical portion of MV is cooled by cold sodium. The source for this cold sodium is the subassembly foot leakage that gets collected in the plenum between the MV bottom and Core Support Structure (CSS). There are two thermal baffles in the MV cooling circuit, arranged in between inner vessel and MV coaxially to both the vessels. The larger diameter baffle which is adjacent to MV is known as outer thermal baffle and the baffle of smaller diameter, known as inner thermal baffle is attached to the outer thermal baffle. The outer annulus between the outer thermal baffle and MV is the 'feeding plenum'. There are a 24 numbers of coolant pipes arranged at discrete locations in the circumferential direction to feed cold sodium from CSS plenum to the feeding plenum. The radial gap between the outer thermal baffle and main vessel is 70mm and the maximum value of manufacturing tolerance allowed is ±15mm. The radial gap between the outer baffle and the MV, along the circumferential direction, varies from a narrow gap of 55mm to a broad gap of 85mm in every 30° sector. Since the dimensions of the components of Future SFR are different compared to that of PFBR and also economy is one of the objectives, it is necessary to optimize the cooling flow rate.

2-D axi-symmetric thermal hydraulic analyses are carried out to determine the heat flux distribution on thermal baffle and to decide the coolant flow rate. It is found that heat load on main vessel cooling system is 12 MW during normal operation and the coolant flow rate required is only 200 kg/s (which is 50% of the PFBR value). Further, a detailed 3-D thermal hydraulic analysis has been carried out to

understand flow and temperature non-uniformity in the cooling system and to ensure if the manufacturing tolerance of ±15mm is permissible. Subsequently, a safety analysis has been carried out to see the maximum temperature and temperature non-uniformity in the unlikely event of one cooling pipe rupture. Temperature distribution on the MV during full power condition with jet breaker plates above each pipe is depicted in FIG. 6. It is clear that jet breaker renders a fairly uniform temperature along the circumference, with a maximum temperature of 409°C. The same during 20% power condition and one cooling pipe rupture condition (FIG. 7) is 413°C and 416°C respectively. Also, the corresponding values of maximum circumferential temperature difference in main vessel are 5°C, 10°C and 15°C respectively. All these temperature values are within acceptable limits indicating the adequacy of reduced flow rate and acceptability of having 24 cooling pipes.

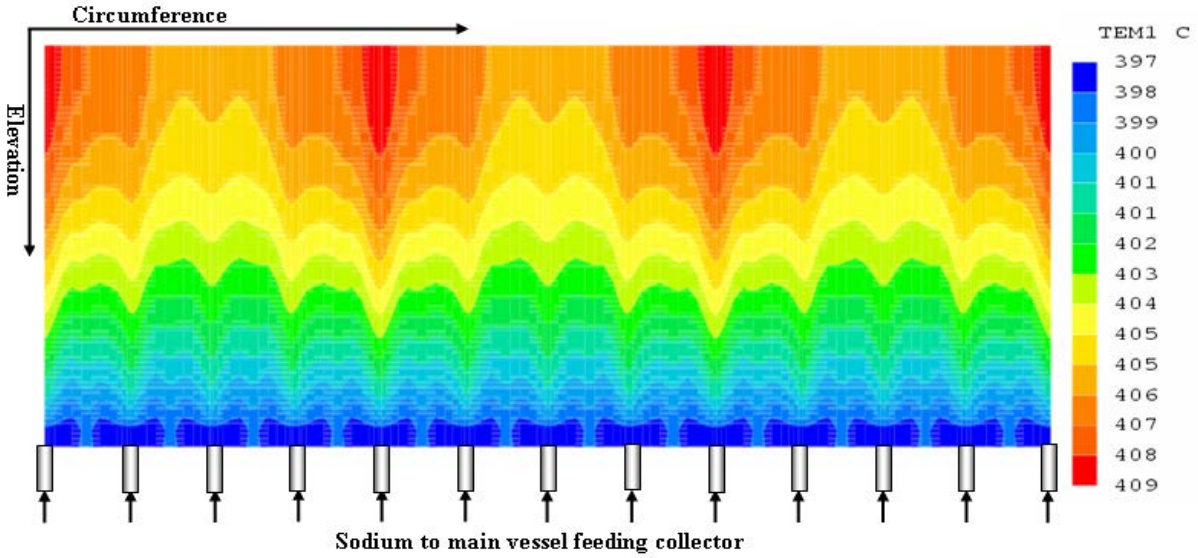

FIG. 6. Main vessel temperature (°C) distribution during normal condition at full power

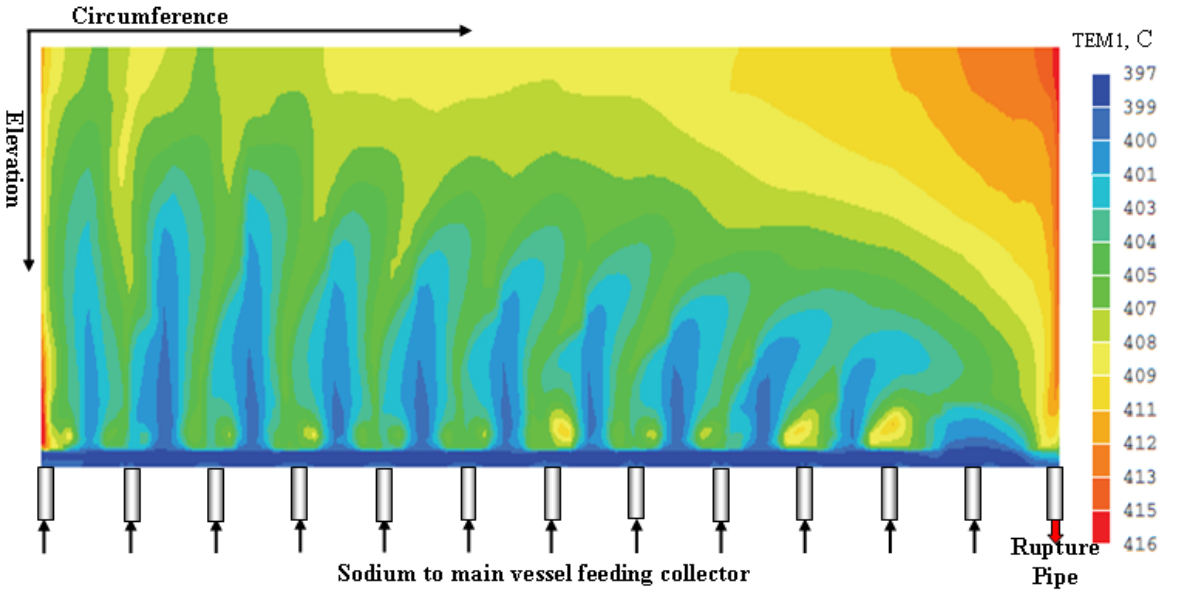

FIG. 7. Main vessel temperature (°C) distribution during one pipe rupture condition at full power

6. Safety Assesment of Pipe Rupture Event

Primary pipes are designed according to safety class I rules and to withstand design basis earthquake. High structural reliability is ensured by selecting highly ductile SS 316 LN material. Further, they are subjected to high quality manufacturing and relatively low operating temperature (less than 673 K) where in creep effects are insignificant during normal operation. Structural mechanics studies have

indicated low operating stress. These aspects render the Double Ended Guillotine Rupture (DEGR) of the pipe a very low probability event. However, due to the inability of Leak Before Break (LBB) justification because of difficulty in leak detection and as a measure of defense in depth, instantaneous and total DEGR in a single primary pipe has been considered as a Category 4 Design Basis Event (DBE) and analysed to establish that the event is detected in time and the reactor is shutdown safely. The transient following the event being rapid reduction in coolant flow through core and sharp rise in temperature, the consequences following the event are sensitive to various data used in the analysis viz., location of rupture, grid plate hydraulic resistance, incipient cavitation flow and amount of negative reactivity added during SCRAM etc. Thus, the evaluation of sensitivity of various parameters is very important for a complete understanding of the event.

Even though the safety of the PFBR (with a total of 4 pipes) is demonstrated through a conservative deterministic safety analysis approach [5], it is planned to increase safety margin in Future FBR against this event by increasing the total number of primary pipes from four to eight, as already mentioned. Also, the diameter of pipes is reduced from 600 mm (four pipe layout) to 420 mm maintaining sodium velocity same in both the configurations. Though the structural integrity of pipes improves with 8 pipes, it is judged that the event of DEGR of one primary pipe continues to be a category 4 event. Schematic of modelling of one pipe rupture for Future SFRs is show in FIG. 8.

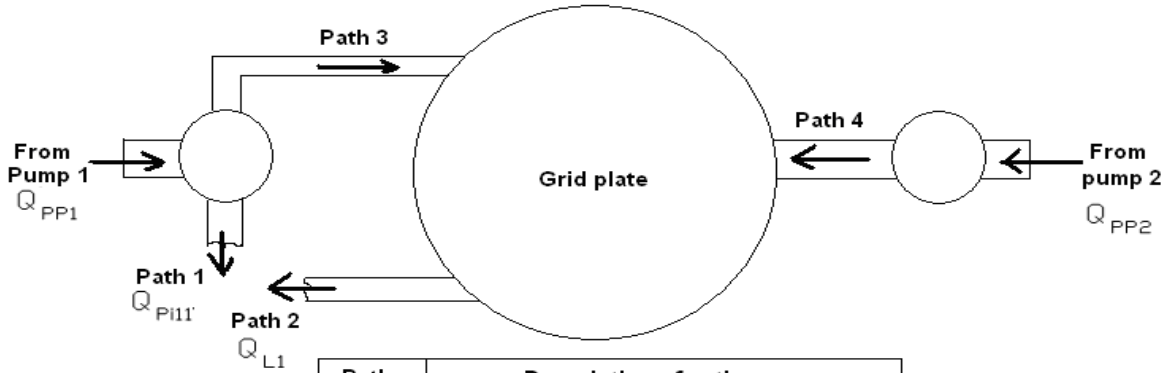

Paths	Description of path
Path 1	Pump 1 to ruptured end of single pipe
Path 2	Grid plate to ruptured end of single pipe
Path 3	Pump 1 to grid plate through three pipes
Path 4	Pump 2 to grid plate through four pipes

FIG. 8. Hydraulic modelling for one pipe rupture

The relevant Design Safety Limit (DSL) for category 4 event are: the clad hotspot temperature should be less than 1473 K and average sodium hotspot temperature should be less than 1213 K to prevent bulk sodium boiling. The thermal and hydraulic effects of DEGR are analysed using the one dimensional plant dynamics code DYANA-P [6]. Rupture of primary pipe causes the resistance against which the pumps operate to come down and hence the pump supplied flow increases to cavitation flow conditions (126 %). Primary sodium flow supplied by the pumps bypasses the core through the ruptured path back to the cold pool and the core flow decreases to a low value at a rapid rate. The reduction in the core flow in turn causes the sodium and clad temperatures to rise. Out of the 126 % of flow supplied by the pumps 69 % flows back to the cold pool bypassing the core and 57 % flows through the core. The maximum values of clad hotspot and average sodium hotspot temperatures reached are well below the Category 4 DSL (340 K and 194 K lower than the corresponding DSL) even without any safety action. The signals available for reactor SCRAM are power to flow ratio, and coolant temperature rise across central subassembly. Core temperature evolution with SCRAM by central subassembly sodium outlet temperature is shown in FIG. 9. Since, the maximum value of clad hotspot temperature reached (1112 K) is well below the boiling point of

sodium, there is no risk of bulk or local sodium boiling. By the selection of eight primary pipes, the risk of local subcooled sodium boiling is also avoided in the new design. It is clear that the clad and sodium temperature are much less in 8 pipe layout compared to the 4 pipe layout of PFBR

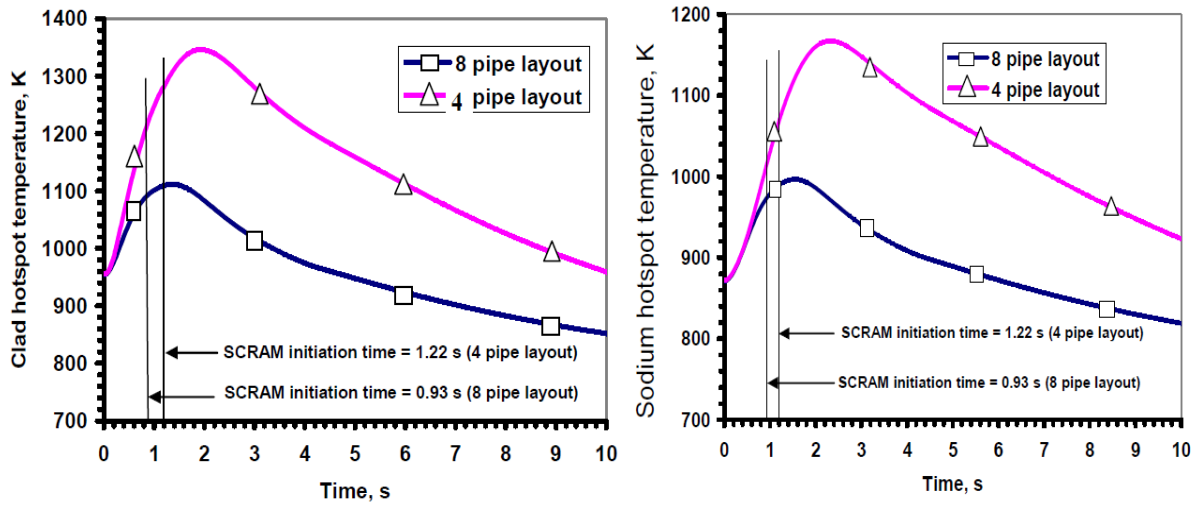

FIG. 9. Core temperature evolution during pipe rupture with SCRAM by second signal

7. Thermal Management of Top Shield and Reactor Vault

Due to the manufacturing difficulties of box type TS and the requirement of high load carrying capabilities, a dome shaped thick plate RS is conceived for future SFR. MV which holds the primary sodium and associated components is welded to the RS through a triple joint. The RV (FIG. 10) gets heated by the heat emanating from the outer surface of the Safety Vessel (SV) insulation as wells as by direct conduction through RS. This heat is removed from the RV by circulating demineralised water through the square pipes embedded in it. A dedicated water cooling system maintains concrete temperature below the allowable limit. This cooling system is designed by considering different loading conditions such as normal, SGDHR and 450^{o}C isothermal operations. The RV cooling system is designed for 100% redundancy by dividing embedded cooling pipes into 32 sectors and in each sector water from two loops is fed.

The RV is consists of inner 750 mm thick and outer 1000 mm thick concrete walls. The SV and MV are supported at the top of the inner and outer concrete walls respectively. Between these two walls, 50 mm thick Expanded Polystyrene (EPS or thermocol) insulation is sandwiched. For a better cooling management, the RV is divided into four regions viz. Upper Lateral Shield (ULS), Lower Lateral Shield, the Bottom Shield (BS) and Safety Vessel Support Embedment (SVSE). The analyses of LLS for the case of ‘one set of cooling coil unavailable’ under different loading conditions are carried out to validate the strength of cooling system. Studies indicate that maximum circumferential variation in concrete temperature persist only for a depth of about 175mm, i.e., 7 times the tube size. From this point to EPS layer the temperature of the concrete decreases gradually. About 6^{o}C and 8^{o}C drops for normal and SGDHR conditions respectively are experienced in the 50 mm thick EPS layer. The outer load bearing concrete is maintained at an average temperature of 42^{o}C. But the maximum temperature is 51.2^{o}C and 57.1^{o}C respectively for normal and SGDHR conditions (FIG. 11). These values are well below the corresponding limiting values. This ensures that reactor operation with one RV cooling loop is acceptable.

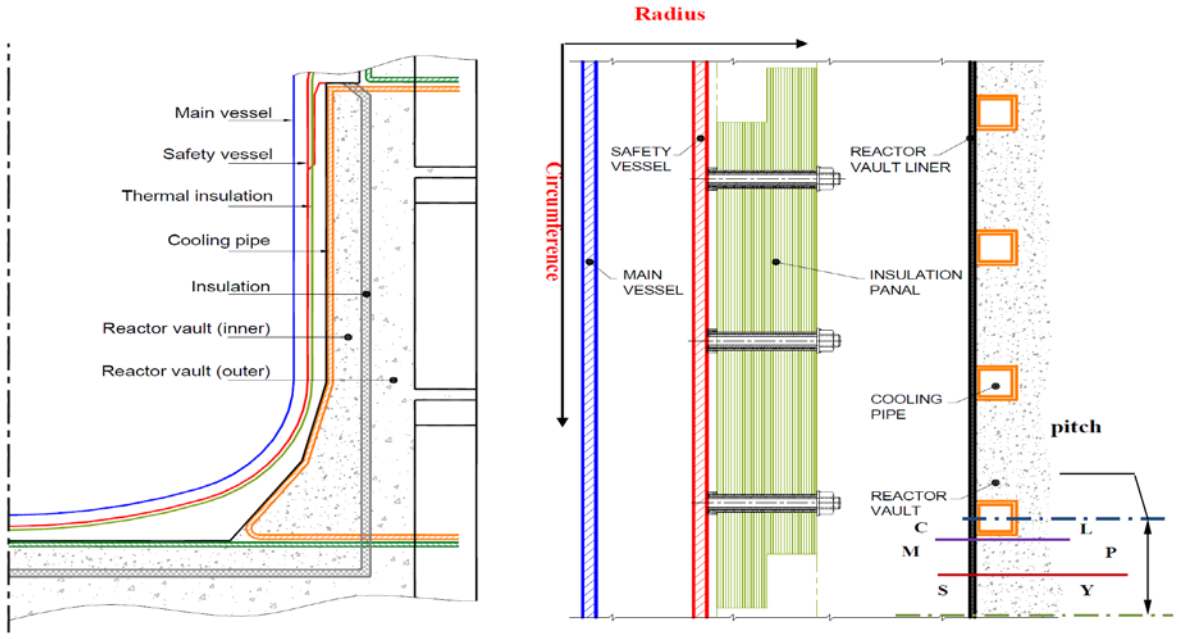

FIG. 10. Schematic sectional view of Reactor vault with square cooling pipe layout and planes along which temperatures of concrete is plotted

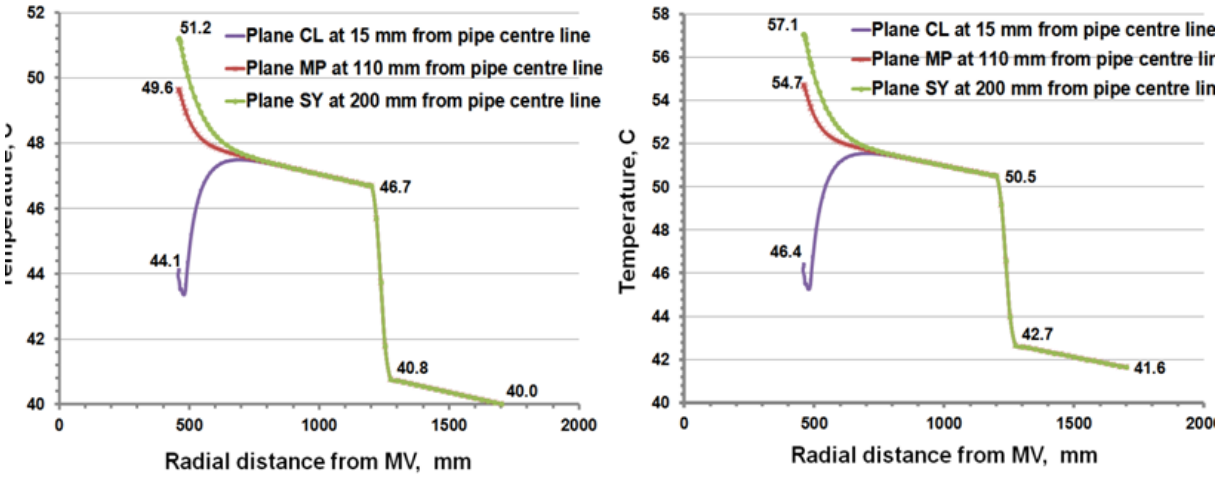

FIG. 11. Concrete temperatures at different circumferential planes (see, FIG. 10) during normal operating condition (left) and SGDHR condition (right)

Another set of integrated 3-dimensonal CFD studies are carried out towards finalization of the cooling arrangement for the ULS and reactor TS. The model considers natural convection of argon and nitrogen, surface radiation effects among the various walls and heat conduction in the structures and concrete wall. The predicted streamlines and temperature distribution in the RS-RV assembly is depicted in FIG. 12. A single cellular convection loop is formed in the bulk of argon gas with argon rising in the central part and descending near the main vessel. Weak multi-cellular convection loops are formed in nitrogen gas, between main vessel, safety vessel and reactor vault. The main mode of heat transfer was obseved to be by thermal radiation. The average heat flux value on the top shiled was observed to be 1295 W/m^2 which is about 13% more than that of PFBR. This marginal increase was found to be due to enhanced heat conduction through the MV, via., a thick triple joint. This heat load was found to be independent of the working condition of the RV cooling system. The heat flux on the ULS is determined to be 40 W/m^2 which is much less than that observed in PFBR (230 W/m^2). This is due to the presence of insulation between the RS and ULS. It is clear from the FIG. 12 that a small portion of concrete near SVSE and main vessel support embedment experience temperatures mildly

above 65°C. With reduced pitch for the RV cooling pipes and with a dedicated cooling segment for embedments, this temperature could be reduced to acceptable limits.

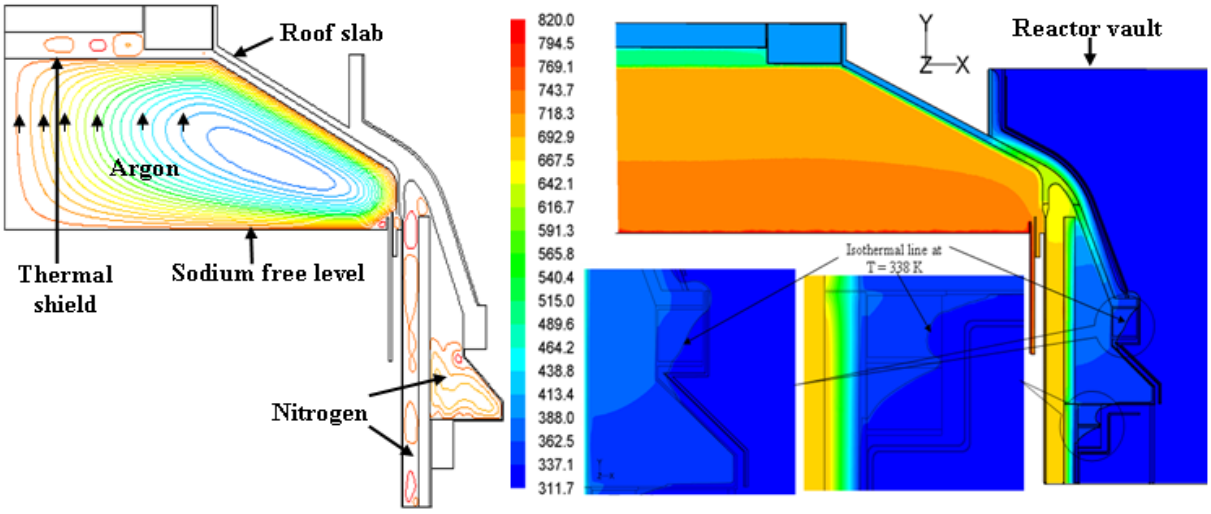

FIG. 12. Steam lines and temperature distribution (K) in the RV, RS and Cover gas space with both the loops of the RV cooling system working

8. Conclusions

Detailed multi-dimensional thermal hydraulic investigations have been carried out for the Future SFR, towards validating the adoption of various design modifications incorporated to improve economy and enhanced safety. It is seen that the proposed shape of inner vessel with single torus does not affect the hot pool mixing and gross temperature gradients in the pool. The adoption of conical control plug in order to facilitate the monitoring of more number of fuel and blanket SA found out to be beneficial in reducing the free velocity thereby helping to considerably mitigate gas entrainment phenomenon in Future SFRs. Sodium flow rate for main vessel cooling has been finalized to be 200 kg/s at full power which is ½ the value adopted for PFBR. Suitable baffle configuration inside the spherical header with four primary pipes has been identified which reduces the pressure loss by 50%. With four primary pipes per pump, the minimum core flow reached during one primary pipe rupture event is found to be 57 % which is nearly double the value in the case of two pipe design of PFBR. It is seen that design safety limits on fuel, clad and sodium temperatures are not crossed even without any safety action. An integrated CFD analysis of top shield and reactor vault reveals that the concrete temperature around main vessel and safety vessel support embedments can be maintained within limits by providing a dedicated cooling loop for the support embedment, as in the case of PFBR. The pitch and size of the vault cooling pipes and water flow rate have also been finalized.

REFERENCES

[1] Chetal, S.C., et al., The design of the Prototype Fast Breeder Reactor, Nucl. Eng. Des., Vol. 236, (2006), 852–860.

[2] Chellapandi, P., et. al., Design concepts for reactor assembly components of 500MWe future SFRs, Nucl. Eng. Des., Vol. 240, (2010), 2948-2956.

[3] Velusamy, K, et. al., Overview of Pool Hydraulic Design of Indian Prototype Fast Breeder Reactor, Sadhana, Vol. 35, (2010) 97-128.

[4] Venkatesulu, M., et al., Design Specification for Biological Shield Cooling System, PFBR/38000/DN/1001/R-B, (2001).

[5] Natesan, K., et al., Thermal hydraulic investigations of primary coolant pipe rupture in an LMFBR, Nucl. Eng. Des., Vol. 236, (2006), 1165-1178.

[6] Natesan, K., et al., Plant dynamics studies towards design of plant protection system for PFBR, Nucl. Eng. Des., Vol. 250, (2012), 339-350.

Preliminary Core Analysis for Regulatory Evaluation of SFR Nuclear Designs

Moo-Hoon BAE[*]*, Andong SHIN, Namduk SUH*

Korea Institute of Nuclear Safety, 62 Gwahak-ro, Yuseong-gu, Daejeon, Republic of Korea

[*]Corresponding author: mhbae@kins.re.kr

Abstract. In Korea, a conceptual design of SFR has been developed by Korea Atomic Energy Research Institute (KAERI). An application for the design approval of a prototype SFR is scheduled in 2017. In order to prepare the licensing of a prototype SFR, Korea Institute of Nuclear Safety (KINS) is developing the regulatory audit code system for SFR since 2012. The SFR nuclear evaluation system for regulatory verification has an object to verify core integral parameters, reactivity coefficients, and peaking power factor, etc. provided by the designers and generate reactivity coefficients and kinetic parameters for safety analyses. For these purpose, both stochastic (Monte Carlo) and deterministic tools can be used. In deterministic core analysis, the PARCS code is being considered for the whole-core steady-state and time-dependent, multi-group hexagonal diffusion calculations and additional code modules for cross-section generation and more accurate transport solution, etc. are planned to be developed from 2013 or be introduced. This paper presents the development strategy of SFR nuclear evaluation system for regulatory verification and the preliminary core analysis results of Korean SFR demonstration reactor with 600MWe (DEMO-600). The DEMO-600 core is preliminarily analyzed using PARCS, and global reactivity worths such as uniform expansion coefficients, rod worths are calculated by direct eigenvalue differences of the base and perturbed configurations. The results calculated by PARCS are compared with the DIF3D nodal solutions provided by KAERI.

1. Introduction

In Korea, a conceptual design of SFR has been developed by Korea Atomic Energy Research Institute (KAERI). Based on “Long-term R&D Plan for Future Reactor Systems” which was approved by the Korea Atomic Energy Commission in 2008, an application for the design approval of a prototype SFR is scheduled in 2017 and the design review will be implemented by 2020 as shown in Figure 1.

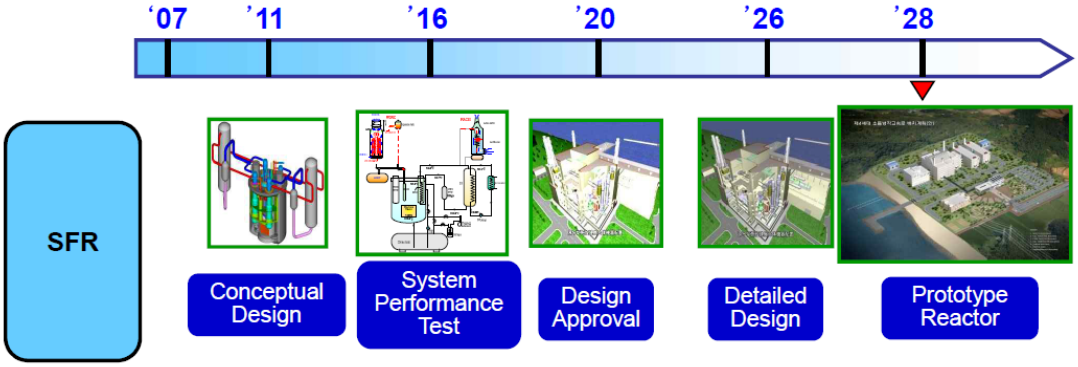

FIG. 1. Long-term R&D Plan for Korean SFR

In order to prepare the licensing of prototype SFR, Korea Institute of Nuclear Safety (KINS) is developing the reuglatory technologies for SFR since 2010. Fast reactors such as SFRs have

fundamental differences in nuclear characteristics compared to thermal reactors such as LWRs. As a result, there are significant differences in reactivity feedback mechanism to assure the inherent safety of reactors. Especially, positive coolant density coefficient and void worth are main concern in passive safety argument. However, the current computational code system for nuclear safety evaluation in Korea is specified to regulate nuclear facilities targeting on LWRs, and therefore the development of regulatory audit code system reflecting SFR nuclear features is required.

The SFR nuclear evaluation system for regulatory verification has an object to (1) verify core integral parameters, reactivity coefficients, and peaking power factor, etc. provided by the designers, (2) generate reactivity coefficients and kinetic parameters for safety analyses based on point-kinetics calculation, and (3) implement the space-dependent neutron dynamics analyses for neutronics coupled thermal-fluid calculation. For these purposes, both stochastic (Monte Carlo) and deterministic tools can be used. In deterministic core analysis, the PARCS code [1] is being considered as a tool for the whole-core steady-state and time-dependent, multi-group hexagonal diffusion calculations and additional code modules for cross-section generation and more accurate transport solution, etc. are planned to be developed from 2013 or be introduced.

This paper presents the development strategy of SFR nuclear evaluation system for regulatory verification and the preliminary core analysis of Korean SFR demonstration reactor with 600MWe. The preliminary core calculations are implemented using PARCS, and global reactivity worths such as uniform radial/axial expansion coefficient, primary/secondary rod worths are calculated by direct eigenvalue differences of the base and perturbed configurations. The results calculated by PARCS are compared with the DIF3D nodal solutions provided by KAERI.

2. Overview of Nuclear Characteristics and Design Codes for SFR

2.1. SFR Nuclear Characteristics

SFRs have distinct nuclear characteristics from LWRs, in which many assumptions employed in traditional LWR analysis methods are not applicable [2][3]. The significant differences are as follows: hard neutron spectrum in the keV and MeV, high neutron leakage by a large mean free path, low delayed neutron fraction dominated by Pu-239 as a key fission isotope, scattering resonances of intermediate atomic mass nuclides such as Na-23 and Fe-56, lack of 1/E spectrum for the calculation of heavy isotope resonance absorption, etc.

Especially, the long mean free path in fast reactors makes the reactivity effect sensitive to minor geometric changes, which causes dominant negative reactivity feedback by radial core expansion. Also, because the density decrease of sodium coolant causes the negative feedback, there is a possibility that the sodium voiding leads to severe accident with the rapid reactivity insertion. A typical set of feedback coefficients considered in fast reactors include [4]: the coolant density coefficient and void worth, the fuel and structural material Doppler coefficients, the fuel and structural material worth distributions, the axial expansion coefficient, the radial core expansion coefficient, and the control rod driveline expansion coefficient. It is noted that the temperature variation of Doppler coefficient ($=dk/dT$) is approximately $T^{-1} \sim T^{-3/2}$ for typical fast reactors (for thermal reactor, $T^{-1/2}$).

In general, all reactivity coefficients except for the coolant density coefficients and void worth give negative feedback effects. However, the role of specific reactivity coefficient depends on the transient. For example, the negative Doppler coefficient can play an adverse role in loss-of-flow accidents.

2.2. SFR Nuclear Design Codes

In general, both stochastic (Monte Carlo) and deterministic tools can be used for core performance analyses. The current deterministic code system applicable to SFRs are as follows: ANL code system (USA) [2], ERANOS (CEA, France) [5], FAST (PSI, Switzerland) [6], and K-CORE (KAERI, Korea)

[7], etc. These deterministic code systems which employ the multi-step calculation process similar to existing LWR's consist of separate tools for cross-section generation, whole-core diffusion/transport calculation, neutronics coupled system calculation, depletion calculation, perturbation analysis, and pin power reconstruction as shown in Figure 2.

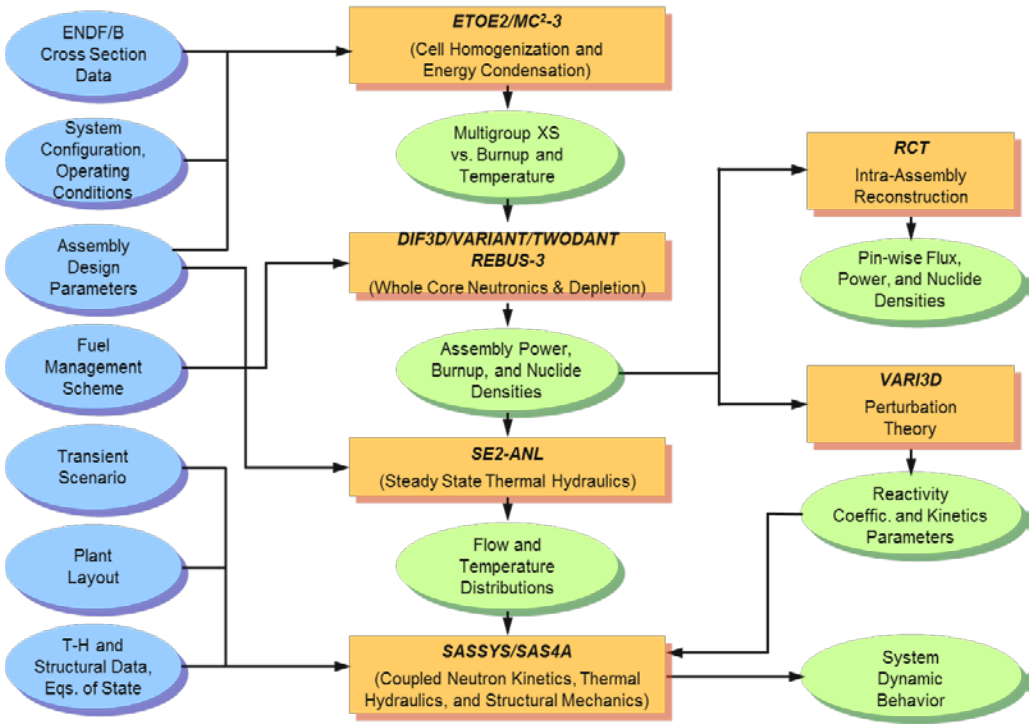

FIG. 2. ANL Code System

In CONRAD system (CEA, EU) [8] and SHARP project (ANL, USA) [9] which are recently being developed, the reduced multi-step approximations is being tried to utilize directly cross-section library data without cell or assembly homogenization in core calculation.

3. Development Perspective of SFR Regulatory Nuclear Code System

The objective of SFR nuclear evaluation system for regulatory verification is as follows:

- verification of core integral parameters, reactivity coefficients, and power peaking factor, etc. provided by the designers,
- generation of reactivity coefficients and kinetic parameters for safety analyses based on point-kinetics calculation, and
- implementation of the space-dependent neutron dynamics analyses for neutronics coupled thermal-fluid calculation

For these purpose, both stochastic (Monte Carlo) and deterministic tools can be used. The deterministic tools are more suitable for a large number of analyses, because of their computational efficiency. On the other hand, Monte Carlo methods are attractive because of its ability to accurately represent nuclear data details and to treat heterogeneity effects and complex geometries.

In regulatory verification calculations, because more accurate solutions are required regardless of computional efficiency, Monte Carlo methods seem more suitable than deterministic methods. However, Monte Carlo methods with the stochastic nature can become computationally impractical for several different classes of problems [2]. These include calculations of pin-wise power

distributions, small reactivity coefficients, some types of sensitivity/uncertainty propagation studies, time-dependent solutions, and some types of burn up calculations. As a result, the two basic computational methods should complement each other.

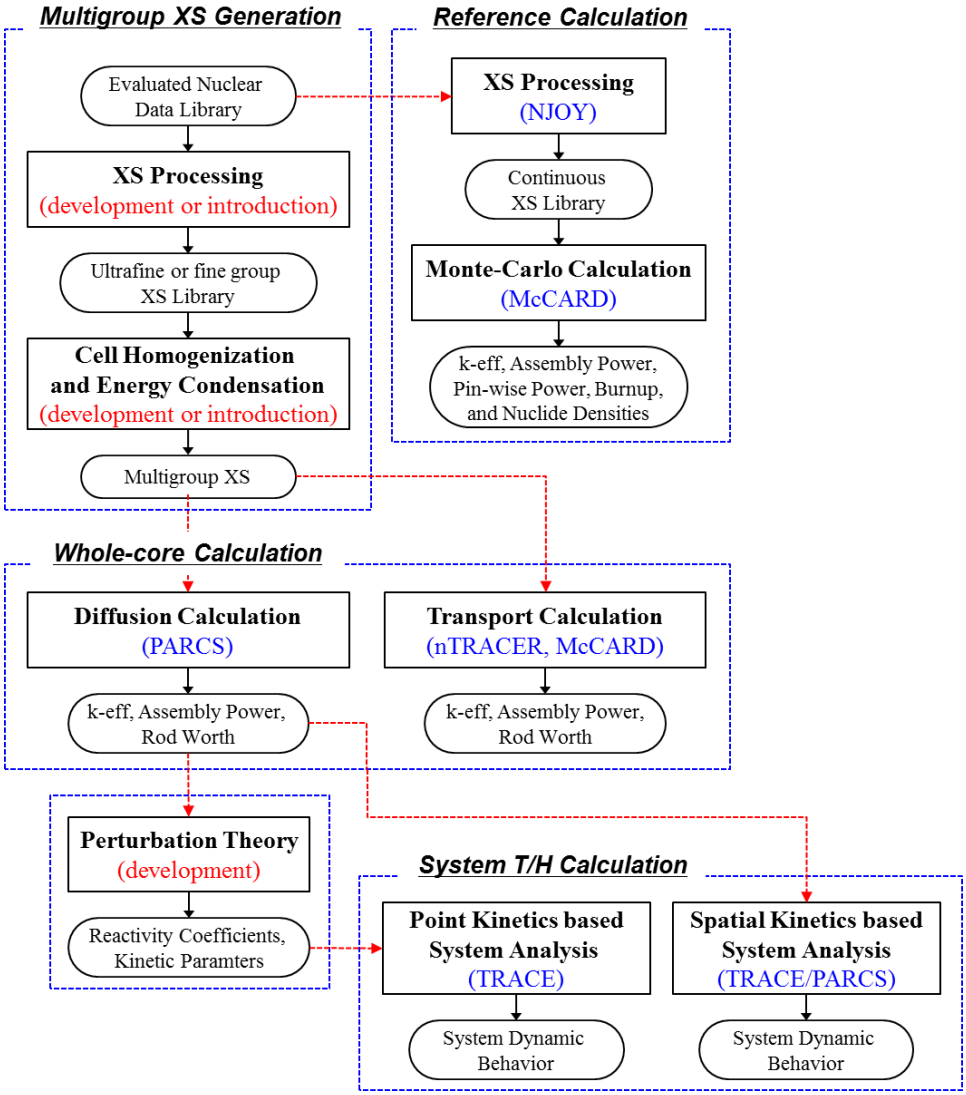

FIG. 3. Draft of SFR Regulatory Nuclear Code System

The draft of SFR nuclear evaluation code system is shown in Figure 3. In the deterministic regulatory code system, the code tools to process evaluated nuclear data into ultrafine or fine group cross section libraries and generate multigroup cross sections will be developed from 2013 or be imported. The main requirements for multigroup cross section generation tools can be summarized as: detailed slowing-down calculation capability, appropriate self-shielding of resolved/unresolved resonances, heterogeneity effects on resonance self-shielding, appropriate modeling of scattering source, etc.

For the whole-core diffusion calculation, the PARCS code [1] is being considered because PARCS which has been being used as regulatory code for LWRs in KINS has the verified capabilities such as whole-core steady-state and time-dependent, multi-group hexagonal diffusion calculation based on the TPEN method [10] and neutron kinetics coupled T/H caclulation using TRACE/PARCS [11].

For multigroup whole-core transport calculation, the nTRACER code [12] based on the MOC method and the McCARD code [13] based on the Monte Carlo method, which are advanced tools developed in Korea, are considered. Also, McCARD will be used as reference calculation code for the deterministic regulatory code system, because McCARD is capable of performing the whole-core neutronics

calculations, the reactor fuel burnup analysis, the few group diffusion theory constant generation, sensitivity and uncertainty analysis, and uncertainty propagation analysis.

4. Preliminary Analysis of SFR Demonstration Reactor Core

4.1. Description of DEMO-600 Core Design

In order to assess the calculation capability of PARCS in the view of reuglartory review, 600MWe SFR demonstration reactor (DEMO-600) [14] were analyzed. The DEMO-600 core has a homogeneous configuration in the radial direction which incorporates the annular rings of the inner and outer fuel assemblies. All the blankets are completely removed in the core to prevent the production of weapons-grade plutonium. The core is loaded with metal fules of U-Zr initially. As shown in Figure 4, the core consists of 817 hexagonal assemblies: 151 inner driver fuel assemblies, 174 outer driver fuel assemblies, 21 primary control rod assemblies, 3 secondary control rod assemblies, 72 reflector assemblies, 78 B_4C shield assemblies, 120 in-vessel storages (IVSs), and 198 radial shield assemblies. The core height is 367.517 cm with the acitve core height of 94.07 cm and the radial equivalent core diameter is 481.853 cm with the hexagonal pitch of 16.054 cm at cold condition.

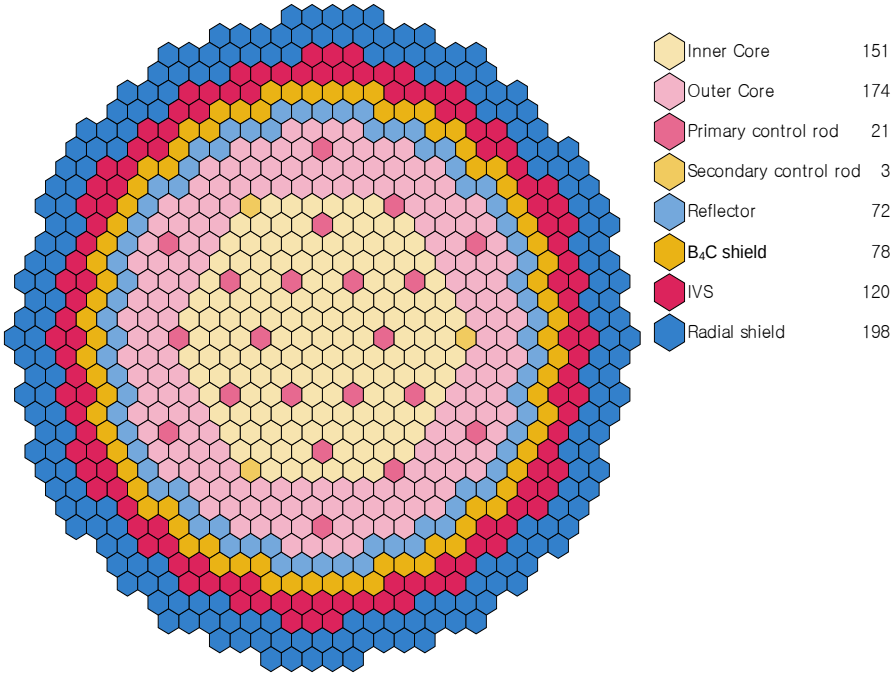

FIG. 4. Core Layout of SFR Demonstration Reator with 600 MWe

4.2. Core Calculation

The whole-core calculation procedure based on PARCS is shown in Figure 5. In this study, the isotope-wise microscopic 25-group cross section library of ISOTXS format and the material data on equilibrium cycles were provided by KAERI with the K-CORE system [7]. Using ISOTXS library and material data, the interface code TRINX generates assembly-wise group macroscopic cross sections for PARCS.

The PARCS model of DEMO-600 core was made with 60^o reflective symmetry, 37 planes with a thichness of about 10cm. In order to assess the calculation capability of PARCS, global reactivity worths such as primary/secondary rod worths, uniform axial/radial expansion coefficients were calculated using direct eigenvalue differences of the base and perturbed configurations. For reference

diffusion solutions, the triangle-based finite difference calculations performed with 24 and 54 triangles per hexagon and extrapolations using two sets of results for asymptotic convergence in spatial method, and 1 and 2 axial meshes per node (~10cm) were used for axially extrapolated solutions.

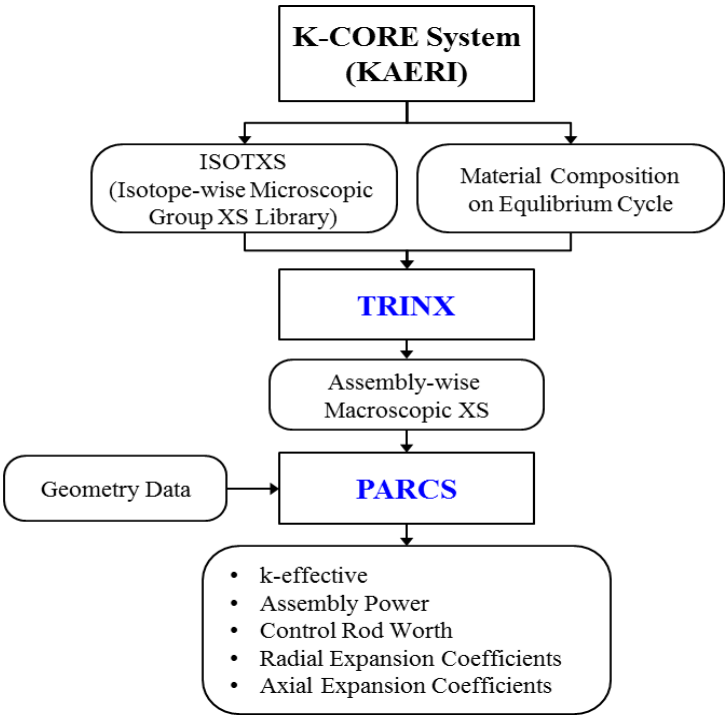

FIG. 5. Whole-core Diffusion Calculation based on PARCS

4.3. Results

In this stduy, the calculation results of PARCS were compared with DIF3D [15] nodal solutions provided by KAERI. The DIF3D code has been employed for whole-core diffusion calculation in the K-CORE system which is the deterministic SFR nucler design code system established in KAERI. In PARCS, the TPEN method [10] for hexagonal diffusion nodal calculation had been employed.

Table 1. Comparison of Various Parameters between PARCS and DIF3D

Cycle	Parameter		Method		
			FDM (Ref.)	PARCS	DIF3D nodal
BOEC	k-effective		1.01694	1.01696 (2)*	1.01923 (221)**
	Control Rod Worth [pcm]	Primary	11103	11203 (100)	10758 (-345)
		Secondary	1259	1309 (50)	1342 (81)
	Uniform Expan. Coef. [pcm/%]	Radial	-552	-550 (2)	-516 (36)
		Axial	-97	-93 (4)	-92 (5)
EOEC	k-effective		0.99964	0.99970 (6)	1.00188 (224)
	Control Rod Worth [pcm]	Primary	11432	11539 (106)	11047 (-385)
		Secondary	1275	1326 (51)	1343 (68)
	Uniform	Radial	-565	-563 (1)	-535 (30)

	Expan. Coef. [pcm/%]	Axial	-98	-98 (-1)	-96 (1)

* (Reactivity calculated by PARCS) – (Reactivity calculated by Reference Solution) [pcm or pcm/%]

** (Reactivity calculated by DIF3D) – (Reactivity calculated by Reference Solution) [pcm or pcm/%]

Table 1 shows the comparison results. As shown in the table, PARCS has higher accuracy than the DIF3D nodal solution particulary for the eigenvalue. The results for the highly rodded cases indicates that the accuracy of PARCS is far superior than the corresponding DIF3D nodal method which involves error of ~400 pcm. On the other hand, although the DIF3D nodal solutions have lower accuracy, the results of DIF3D show more conservative trend such as low primary rod worth and low axial/radial expansion coefficients, except somewhat high secondary rod worth. In consequence, it was verified that PARCS was considerably suitable code for independent verification in case of whole-core diffusion calculations.

5. Conclusions

In this study, the development strategy of SFR nuclear evaluation system for regulatory verification was introduced, and the preliminary core analysis of DEMO-600 was implemeted using PARCS. The nuclear evaluation system for regulatory verification will be established using advanced tools independent of design tools or newly developed tools. Also, in the system, the two basic computational methods such as stochastic (Monte Carlo) and deterministic ones should complement each other. In deterministic code system, PARCS is considered for whole-core diffusion calculations because PARCS has the verified capabilities such as whole-core steady-state and time-dependent, multi-group hexagonal diffusion calculation and neutron kinetics coupled T/H caclulation using TRACE/PARCS.

In order to assess the calculation capability of PARCS in the view of regulatory review, the DEMO-600 core were analyzed. The calculation results of PARCS were compared with DIF3D nodal solutions provided by KAERI. As a result, it was confirmed that PARCS was considerably suitable for regulatory verification calculation. Additional code modules for cross-section generation and more accurate transport solution, etc. are planned to be developed from 2013 or be introduced, and the evaluation of various uncertainties in calculation results will be implemented.

REFERENCES

[1] Joo, H. G., Barber, D., Jiang., G., and Downar, T. 1998. PARCS: A Multi-Dimensional Two-Group Reactor Kinetics Code Based on Nonlinear Analytic Nodal Method, PU/NE-98-26, Purdue University, Sept. 1998.

[2] Alan E. Waltar et al., “Fast Spectrum Reactors”, Springer, 2011

[3] W.S. Yang, “Fast Reactor Physics and Computational Methods”, Nucl. Eng. & Tech., Vol. 1, (2012).

[4] H. H. Hummel and D. Okrent, “Reactivity Coefficients in Large Fast Reactors”, American Nuclear Society, La Grange Park, Illinois (2010)

[5] G. RIMPAULT et al., “The ERANOS code and data system for fast reactor neutronic analysis”, Proc. of PHYSOR 2002, Seoul, Korea, 2002

[6] K. Mikityuk, et al., "FAST: An advanced code system for fast reactor transient analysis", Annals of Nuclear Energy, 32, 15, 1613-1631, 2005

[7] Dohee Hahn, et. al., “Advanced SFR Design Concepts and R&D Activities”, Nucl. Eng. & Tech., Vol.41, No.4, May. 2009

[8] De Saint Jean C. et al., “Status of CONRAD, a nuclear reaction analysis tool”, International Conference on Nuclear Data for Science and Technology 2007 – ND 2007, Nice, France,

2007

[9] W.S. Yang, et al., “Neutronics modeling and simulation SHARP for fast reactor analysis”, Nucl. Eng. & Tech., Vol.42, No.5, Oct. 2010

[10] J. Y. Cho, H. G. Joo, B. O. Cho, and S. Q. Zee, Hexagonal CMFD Formulation Employing Triangle-based Polynomial Expansion Nodal Kernel, M&C 2001, USA, Sept. 2001.

[11] T. Kozlowski, T. Downar, et al. Analysis of the OECD/NEA PWR Main Steam Line Break Benchmark with TRAC-M/PARCS, Nuclear Technology, September, 2004.

[12] Y. S. Jung, “nTRACER v1.0 Methodology Manual,” SNURPL-CM-001(10), Seoul National University Reactor Physics Laboratory, March 2010 (2010).

[13] Hyung Jin Shin, et al., “McCARD: Monte Carlo Code for Advanced Reactor Design and Analysis”, Nuclear Engineering and Technology, Vol.44, No.2, 2012.

[14] KAERI, “Conceptual Design Report of SFR Demonstration Reactor of 600MWe Capacity”, KAERI/TR-4598/2012, 2012.

[15] R. D. Lawrence, The DIF3D Nodal Neutronics Option for Two- and Three-Dimensional Diffusion Theory Calculations in Hexagonal Geometry, ANL-83-1, Argonne National Laboratory, Argonne, IL (1983).

Review Paper

Comparative Analysis of Effectiveness of Various Emergency Core Cooling System Design Options for Sodium Fast Reactors of High Rower

Iu.E. Shvetsov[a], Iu.M. Ashurko[a], S.L. Osipov[b], V.S. Gorbunov[b]

[a] State Scientific Center of the Russian Federation, Institute for Physics and Power Engineering, Obninsk, Russia

[b] OKBM

Abstract. Effectiveness of various design options for emergency core cooling systems has been compared as applied to a pool type sodium fast reactor of high power. Thermal hydraulic parameters of the reactor under cooling conditions are analyzed with the use of the Russian thermal hydraulic code GRIF which allows 3D velocity and temperature fields to be calculated in the reactor, with account of thermal hydraulic processes in the core inter-wrapper space. To realize the cooling system margin in case of additional parallel failures, the parameters were calculated for the cooling mode accompanied with additional conditions of malfunction of part of emergency heat exchangers (DHX) for unknown reasons. Based one the calculation analysis the conclusion is made about a relative effectiveness of the emergency cooling system design options considered.

1. Introduction

The problem of residual heat removal from the nuclear reactor core still remains very important, with its topicality enhancing with the increase in reactor power. Quite a number of potential engineering solutions are known, that are aimed at solving this problem. Usually these engineering solutions are an attempt to find a compromise between the system reliability and effectiveness, on the one hand, and the system implementation cost, on the other.

In compliance with the current tendencies to improve NPPs safety, the task is assigned for Russian fast reactors to meet the emergency cooling safety requirement that is more stringent than that stipulated in the Russian NPP Safety Standards, OPB 88/97. In particular, for the advanced designs the severe reactor core damage probability is required not to exceed the value of 10^{-6} per reactor year.

On the other hand, the current tendencies in nuclear power are aimed at justification of reduced safety costs, with achieving, in the ideal case, their positive economic effect.

In paper [1] consideration was already given to the issues related to improvement of the decay heat removal system (DHRS) effectiveness as applied to a sodium fast reactor of high power. However, the main stress was made on the analysis of the effect of heat - and mass - transfer processes in the core inter-wrapper space (IWS) on this performance. In the given paper different concepts of reactor heat removal system design are considered. On the one hand, they demonstrate different performance characteristics, and on the other hand, they differ in term of assumed levels of their implementation costs. For instance, the possibility for the cooling system to combine the functions of normal operation system and emergency safety system (the decay heat removal system) is considered as a potential way to reduce the costs. This option allows the following possibilities to compensate the safety costs:

— a possibility to use a standard commercial design of the third circuit;

- a possibility to eliminate the third circuit operation in the reactor cooling mode (the possibility to speed up the beginning of preventive maintenance work in the third circuit);
- a possibility not to ensure natural circulation in the secondary circuit design.

2. Design features of the reactor under consideration

A hypothetic version of a pool-type sodium fast reactor of a relatively high power, 4200 MW, was chosen for the analysis. The primary reactor circuit consists of three independent heat transfer loops, with each of them including a pump with a check valve and two intermediate heat exchangers (IHX). The decay heat removal system includes 6 emergency heat exchangers (DHX) immersed in the reactor upper plenum.

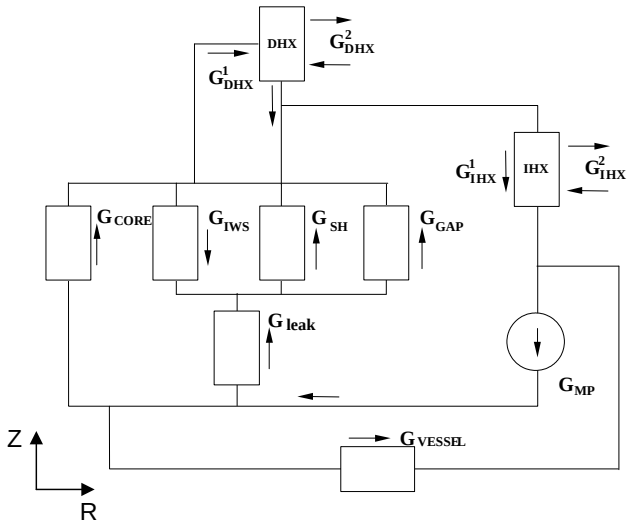

FIG.1. Hydraulic diagram of the reactor - Option 1. (Flow rates are given for rated power conditions)

The conventional hydraulic diagram of the reactor given in Fig.1, 2 corresponds to the DHRS design option with immersed DHXs. The arrows indicate the coolant flow direction under the normal reactor operation. The coolant supplied by primary pump G_{MP} to the core diagrid is divided into three main flows. The most part G_{CORE} goes to the core fuel assemblies (FSA), and two relatively small portions go to the reactor vessel cooling path - G_{VESSEL} and through the fuel assembly sealing to the core inter-wrapper space - G_{leak}. Then the main coolant flow goes inside fuel assemblies, and the leak flow is discharged to the upper plenum of the reactor in parallel through three channels: through the inter-wrapper space - G_{IWS}, though the assemblies of lateral shielding and in-vessel storage - G_{SH} and through the slot in the core periphery - G_{GAP}. Circulation in the DHX primary circuit - G^1_{DHX} goes through the upper plenum. From the upper plenum the coolant goes through the IHX to the pump suction (G^1_{IHX}).

3. Preliminary qualitative analysis of various emergency core cooling system designs

At the stage of preliminary analysis consideration was given to five options of core cooling system design:

(1) Option 1 – cooling is provided via the immersed emergency heat exchangers, with natural circulation in the primary circuit of the reactor and intermediate circuit of the emergency cooling system (Fig 2);
(2) Option 2 – in contrast to option 1, the emergency heat exchangers exit is connected with reactor core diagrid by means of a special pipeline (Fig.3);

(3) Option 3 – the emergency cooling system functions are performed by the secondary circuit; cooling is provided through intermediate heat exchangers due to natural circulation in the primary reactor circuit and intermediate and air DHRS circuits Fig.4);
(4) Option 4 – cooling is provided by means of specially arranged air blowing around the secondary circuit pipelines;
(5) Option 5 – cooling is provided by means of a specially designed path for air blowing around the steam generator (SG) shell.

The first option of the cooling system design has the advantage of being independent (the DHRS is independent of the other reactor systems), thus enhancing its reliability. At the same time, this design does not require any obligatory measures to provide natural circulation in the secondary circuit. And if it is so, it means that there is a possibility to decrease the dimensions of the secondary circuit, and finally, to reduce the cost. On the other hand, increased independence implies the availability of additional equipment and thus, a certain increase in the cost.

The above-mentioned statements are true in regard of option 2 as well. However, in this context it should be added that in this option, on the one hand, the DHX effectiveness should be improved due to a higher circulation path through which cooling is provided. But on the other hand, this system design with a specially arranged DHX path requires additional elements (valves) that could ensure its timely connection.

Option 3 also seems promising. Though, on the one hand, it is not as independent as the previous two options, on the other hand, it has quite a number of advantages from the economical point of view due to the fact that the secondary circuit components already existing can be used as the DHRS elements. For example, the IHX performs the DHX functions, and auxiliary gas and sodium systems can be used for the DHRS intermediate circuit. Similar to the previous two options, it is possible not to use natural circulation in the secondary circuit with the aim to reduce the cost.

Options 4 and 5 primarily meet the requirement to minimize the cost. In these cases the additional equipment will be the pipeline casing of the secondary circuit or SG and dampers with drives. However, there are serious drawbacks of these options as well. The principal ones are the following:

- First of all, it is quite obvious that with the existing tendency to economically reasonable reduction of sodium volume and increase in the equipment unit capacity, the secondary circuit or steam generator pipelines surface may turn out to be not enough to cool down a high power reactor with the use of ambient air natural circulation. Thus, it will be necessary to use an additional active element, i.e. an air compressor.
- Second, natural circulation development should be envisaged in the secondary circuit, thus, resulting in the necessity to have the SG building of excess height.
- Besides, the use of SG as a safety system element will result in the fact that the SG control system becomes more complicated and expensive.

So, it follows from the qualitative analysis performed that options 1, 2 and 3 are recommended to be chosen as the most promising candidates for the further and deeper analysis.

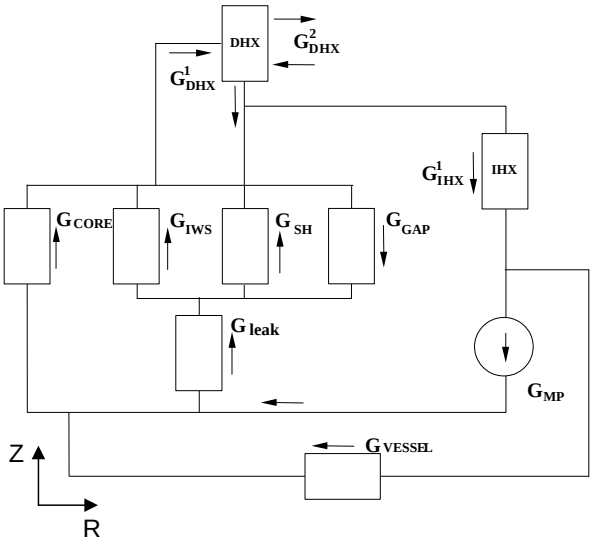

FIG. 2. Hydraulic diagram of the reactor - Option 1. (Flow rates are given for decay heat removal conditions)

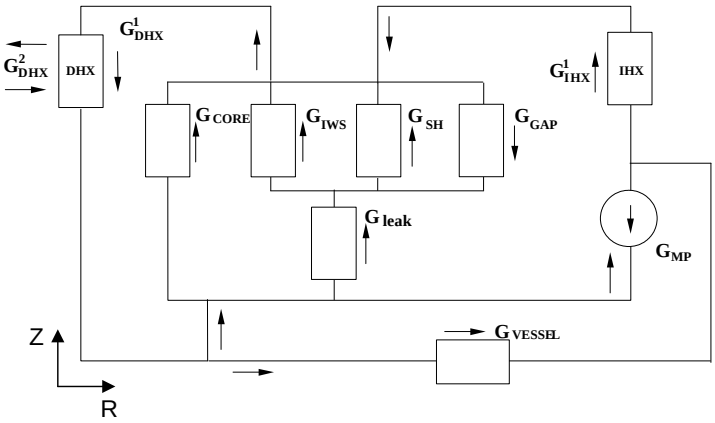

FIG. 3. Hydraulic diagram of the reactor - Option 2. (Flow rates are given for decay heat removal conditions)

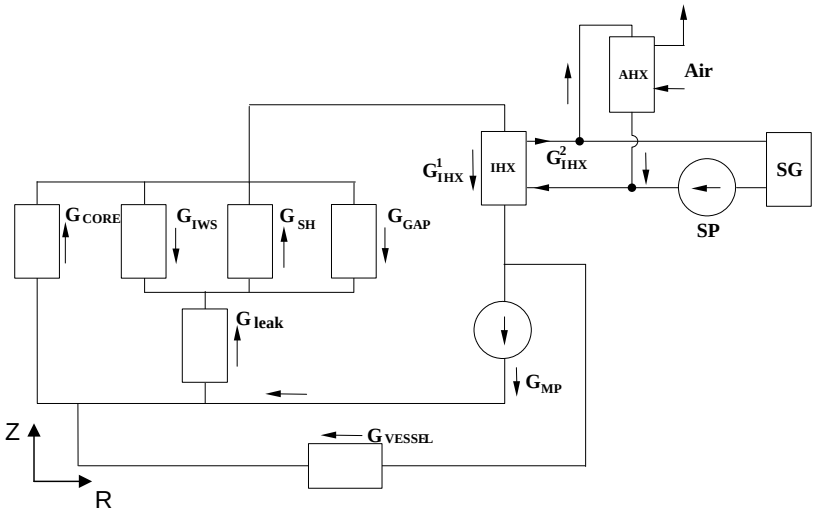

FIG. 4. Hydraulic diagram of the reactor - Option 3. (Flow rates are given for decay heat removal conditions)

4. Comparative analysis of various emergency core cooling system design options

Comparison of cooling system design options was made on the basis of the results of reactor parameters calculation for the steady-state conditions, in which the reactor power was equal to 1% of the rated power and the core heat was only removed with the help of coolant natural circulation. The main comparison criterion was the maximum fuel element cladding temperature. The calculations were made with the Russian thermal hydraulic code GRIF [2], [3].

4.1. Brief description of the GRIF code

GRIF is a one-phase comprehensive thermal hydraulic code designed to calculate dynamics of thermal hydraulic parameters in a liquid-metal nuclear reactor, both in steady-state and transient conditions. The specific feature of this code consists in the possibility to use the model of various geometrical dimensions for different reactor elements (components) and the possibility to model thermal hydraulic processes not only in the main reactor path, but also in the inter-wrapper space.

The code contains the following principal modules:

- a 3D thermal hydraulic model to calculate the fields of sodium velocity, pressure and temperature in the reactor primary circuit, based on the “porous body” model;
- a 3D model to calculate the fields of sodium velocity, pressure and temperature in the core inter-wrapper space;
- a set of 1D, 2D and 3D modules to calculate temperature fields in “impermeable” elements (fuel elements, FSA wrappers, etc.);
- a thermal hydraulic model of intermediate and emergency heat exchangers;
- a primary circuit pump model;
- a 1D model of the secondary circuit;
- a 1D model of the decay heat removal system of the reactor;
- a neutron point-kinetics model.

The thermal hydraulic module forms the basis of the code and is used to calculate 3D fields of primary coolant velocity, pressure and temperature in cylindrical r-φ-z geometry. The set of heat-and-mass-transfer equations includes the mass, impulse and energy balance equations written under the porous body model. Liquid is assumed incompressible, stratification effects are considered in the Bussinesk approximation.

A similar set of equations is solved for inter-wrapper sodium. The solutions of both sets of equations are joined up in the external outline of the sub-region that models the core, as two sodium flows, the main one that goes through the assemblies, and the other flow that goes through the IWS, are merged only on the boundary line. Heat is transferred between the flows through the FSA wrapper walls and is considered in the entire core volume.

4.2. Comparison of various options in terms of cooling effectiveness

The values of the preset parameters for three options selected above are given in Table 1, and the results of calculation of the principal primary circuit parameters are given in Table 2.

Table 1.IHX and DHX inlet coolant parameters for the secondary and intermediate circuits, respectively.

	Parameter	Option 1	Option 2	Option 3
IHX	Flow rate*, kg/s	0.328	0.33	76
	Inlet temperature, °C	450	450	300
DHX	Flow rate, kg/s	76	76	0
	Inlet temperature, °C	300	300	-

*All the flow rate data in this and the following tables are given for the 1/6 part of the reactor.

Table 2.Reactor coolant flow rate and temperature distributions at various DHRS design options.

	Parameter	Option 1	Option 2	Option 3
IHX	Flow rate† G^1_{IHX}, kg/s	-32.06	11.18	-70.13
	Inlet temperature, °C	390	391	370
	Outlet temperature, °C	388	390	300
DHX	Flow rate G^1_{DHX} , kg/s	-84.3	-84.6	-1.09
	Inlet temperature, °C	380	380	370
	Outlet temperature, °C	329	330	369
CORE	G_{MP}, kg/s	-30.7	10.6	-69.4
	G_{VESSEL}, kg/s	-1.4	0.6	-0.74
	G_{CORE}, kg/s	32.05	72.5	69.2
	G_{leak}, kg/s	0.013	0.78	1.0
	G_{IWS}, kg/s	21.95	0.89	0.98
	G_{SH}, kg/s	0.48	0.07	-0.002
	G_{GAP}, kg/s	-22.0	-0.18	-0.007
Core Tmax, °C		489	406	379
(Tmax - Tmin), °C		160	76	78

† The flow rate value sign in table 2 is determined by the coolant velocity vector direction in regard to R & Z coordinate axes.

On the whole, for option 1 of the cooling system design the flow pattern (Fig. 2) is close to the one observed in the nominal conditions (Fig. 1), with the exception of two points, namely

- the direction of flow in the vessel cooling path has changed into the opposite one and now the coolant from the IHX is supplied to the reactor core diagrid through two parallel lines: through the primary pump and through the vessel cooling path,
- The IWS flow pattern has changed as well. For example, in the nominal conditions the leak flow through FSA sealing turned to the path of the least hydraulic resistance and was discharged to the upper plenum of the reactor through the slot formed by the neutron reflector and external shell. On the contrary, in the cooling mode the coolant moves downwards through this slot and the core FSA heat is removed due to the circulation that goes through the "DHX – upper plenum- slot – IWS – upper plenum – DHX" path.

It should be pointed out that in option 1 the coolant flow rate through the DHX is almost 3 times higher than the flow rate through the IWS. As a result of that and due to such a high circulation factor the sodium temperature in the upper plenum (390 °C) is almost 100°C lower than Tmax in the core.

In option 2 the core is cooled by means of the circulation through a specially designed path - "DHX – special pipeline – core diagrid – core – upper plenum – DHX" (Fig. 3). In this case the contribution of the IWS sodium circulation is insignificant. It should be stressed that in this design option the primary coolant moves in the opposite direction, namely from the core diagrid through the primary pump and in parallel through the vessel cooling path it goes to the "cold" reactor plenum, and from there through the IHX to the upper plenum. It should be noted that inspite the additional pressure drop complying with the specified configuration of the Option 2 (additional valve and pipe line) primary DHX flow rate for Option 2 is not decreased and equal to the that for Option 1. This is because the total pressure drop along the whole circulation path for Option 1 is higher due to relatively large hydraulic friction in IWS. For Option 2 flow through IWS does not play significant role.

In design option 3 it is postulated as the boundary conditions that the coolant, with the same flow rate and temperature as in option 1, is supplied to the IHX inlet through the secondary circuit (Fig. 4). The flow pattern in this case is actually the same as in the principal cooling system design. However, the coolant flow rate in the IHX path is significantly higher and due to a large heat-transfer surface the IHX outlet temperature goes down, which is true for the reactor temperature on the whole. The fact that the core heating decreases results in significant reduction of the coolant flow rate through the IWS, and the circulation via the "CORE – IHX - MP – CORE" path plays a determining role in heat removal.

Based on the comparison of the results presented the following conclusions could be made:

(1) Option 3 provides the most efficient reactor cooling, when the intermediate emergency cooling system loop in connected to the secondary circuit and ensures sodium circulation through the IHX. In this case the maximum fuel elements cladding temperature is minimum and equal to 379°C;
(2) Design option 2 has approximately the same effectiveness in terms of cooling, when the DHX is connected with the core diagrid. In this case the maximum fuel element cladding temperature does not exceed 406°C much;
(3) When the conventional design option of the cooling system is implemented (with the use of immersed DHXs) the core heat removal is provided at a relatively higher temperature level of 490°C and at a much higher temperature value of sodium heating in the core.

4.3. DHRS effectiveness in case of additional failures

In the course of safety analysis it is impossible to rule out a possibility of malfunction of one or a few cooling system channels. In order to determine the cooling system margin in case of additional

malfunctions, calculations were made for options 1 and 2 with the additional condition that four out of six DHXs failed for unknown reasons. Options 1a and 2a are shown in Table 3.

Table 3.Coolant flow rate and temperature distributions in the reactor under the cooling conditions with additional malfunctions.

	Parameter	Option 1a	Option 2a	Option 3a-1	Option 3a-2
IHX	Flow rate G^1_{IHX}, kg/s	-37.3	4.76	-5.1	-4.6
	Inlet temperature, °C	537	521	370	370
	Outlet temperature, °C	531	468	336	327
DHX	Flow rate G^1_{DHX} , kg/s	-44.85	-81.05	-0.32	-0.31
	Inlet temperature, °C	537	521	373	369
	Outlet temperature, °C	423	457	360	356
CORE	G_{MP}, kg/s	-33.8	5.34	0	0
	G_{VESSEL}, kg/s	-1.5	-0.56	-5.1	-4.6
	G_{CORE}, kg/s	37.34	75.56	5.23	4.83
	G_{leak}, kg/s	-0.006	0.74	-0.22	-0.26
	G_{IWS}, kg/s	24.87	0.73	23.6	23.0
	G_{SH}, kg/s	1.53	0.19	-0.22	-0.258
	G_{GAP}, kg/s	-26.41	-0.18	-23.6	-23.0
Tmax in the core, °C		623	532	512	510
(Tmax - Tmin), °C		200	75	175	182

The indicated data show that even with such a serious additional failure as malfunction of four out of six IHXs, the system ensures core heat removal, with maintaining the acceptable temperature level. The most effective cooling is observed in the design option in which the DHX exit is connected with the core diagrid. In this case even with four out of six DHXs failed the maximum fuel element temperature in the core does not exceed 532°C.

For the DHRS design option, when the system operation becomes one of the secondary circuit functions, the most dangerous seems the accident that results in the flow rate stopped in the primary circuit by the cut-off valves. At the same time it is still possible to remove heat by means of sodium circulation through the IHX inlet windows. In this case the IHX operation at the level of inlet windows is similar to the operation of immersed DHX. The results of option 3a-1 calculations testify to the fact that if the primary flow rate is completely stopped, the core heat removal can be ensured by sodium

circulation through the IHX inlet windows and inter-wrapper space with an acceptable temperature level of 512°C. In this context, the question arises if it is possible to improve cooling effectiveness at the expense of a certain increase in the size of IHX inlet windows. The results of option 3a-2 calculations allows us to confirm that even a significant increase in the IHX surface involved in the heat transfer processes with the upper plenum coolant and achieved by means of the increase in the inlet window by 3 times, does not make it possible to appreciably improve the core heat removal effectiveness. The reason consists in the fact that it is the coolant flow rate through the inter-wrapper space, which is determined by the relevant hydraulic resistance values and temperature gradients in the core region, rather than the value of heat transfer surface, that is a limiting factor under these conditions.

REFERENCES

[1] KUZNETSOV I.A., SHVETSOV Iu.E., “Calculation of thermal-hydraulic parameters of fast neutron with account of inter-fuel-assembly space influence”, Book of extended synopses. (International meeting FR09, 2009), p.483, IAEA, CN-176, Kyoto (2009).

[2] SHVETSOV Iu.E., VOLKOV A.V, “GRIF and HYDRON – 3D Codes for Analysis of Thermal and Hydraulics Parameters or Reactors with 1-Phase Incompressible coolant”, Report (10-th International Meeting of IAHR Working Group on Advanced Nuclear Reactors Thermal Hydraulics), Obninsk (2001).

[3] KUZNETSOV I.A., POPLAVSKY V.M., Fast Neutron Reactor NPP Safety,IzdAT,Moscow (2012).

Characteristics of Modular Fast Reactor SVBR-100 Using Thorium-Uranium (233) Fuel

G.I. Toshinsky[ab], O.G. Komlev[b], I.V. Tormyshev[b], N.N. Novikova[b], K.G. Mel'nikov[b]

[a] JSC "AKME-Engineering", Moscow, Russia

[b] State Scientific Center Institute for Physics and Power Engineering (SSC IPPE), Obninsk, Russia

Abstract. Natural reserves of thorium are three times as much as those of uranium. For that reason, thorium is a very promising raw material for manufacturing an artificial fissionable isotope of uranium-233 that is formed when neutrons are absorbed by thorium. Many countries are investigating characteristics of reactors using thorium-uranium (233) fuel. First, breeding ratio (BR) is of interest because only when BR = 1, the reactor can operate in a closed fuel cycle in a mode of fuel self-providing without makeup by other fissionable isotopes. The report presents the results of calculations of neutron-physical and thermal-hydraulic characteristics of SVBR-100 - lead-bismuth cooled small power modular fast reactor using thorium-uranium (233) fuel. Reactor SVBR-100 has specific properties of inherent self-protection and passive safety. The NPP modular power-units, which power equals to a value divisible by 100 MWe, can be constructed on the basis of reactor modules SVBR-100.

1. INTRODUCTION

Thorium resources in the earth's crust are several times as much as those of uranium. This potentially results in an essentially increased raw basis for nuclear power especially in case the closed nuclear fuel cycle is used. However, in nature there are no fissile thorium isotopes, and realization of the $^{232}Th-^{233}U$ fuel cycle needs use of uranium and/or plutonium fissile isotopes (at least, at the initial stages of that fuel cycle).

Works on investigation on the opportunities of using thorium in the nuclear fuel cycle are for the most part connected with existence of large thorium resources (India), or the desire to reduce consumption of natural uranium (Norway), or available nuclear power technologies, which can use the advantages of the thorium-uranium fuel cycle (Canada, Russia).

Technical grounds to use the thorium fuel cycle are conditioned mainly by the following [1]. Being compared with uranium-238, thorium-232 is the best "raw" isotope for reactors with thermal and fast neutron spectrum (see Table 1). Uranium-238 emits over two neutrons counting on a primary neutron capture for a wide number of reactors with thermal neutron spectrum. Thorium dioxide is more chemically and radiation resistant as compared with uranium dioxide and its thermo-physical properties such as heat conductivity, linear expansion coefficient, are better. When the $^{232}Th-^{233}U$ fuel cycle is used, a considerably less number of plutonium isotopes and long-lived minor actinides is built that makes easier the task of solving the problem of further handling the spent nuclear fuel. The inherent properties of the thorium fuel cycle facilitate the solution to the problem of nuclear materials non-proliferation as built up uranium-232 has daughter fission products with hard gamma rays (bismuth-212, thallium-208). Moreover, the thorium fuel cycle is preferable for weapon plutonium burning since it does not result in plutonium breeding as it is when U-Pu fuel cycle is used.

Particularities of fast reactor physics and design features of the SVBR type reactor facility (RF) allow use of a wide number of various nuclear fuels based on $U-Pu$, such as oxide uranium fuel, mixed oxide uranium-plutonium fuel, nitride uranium fuel, mixed nitride uranium-plutonium fuel, and others [2]. With a purpose to analyze an opportunity of operating the RF SVBR core in the uranium-thorium fuel cycle and evaluate the corresponding characteristics of uranium-233 breeding, the results of preliminary computation investigations in use of thorium in the nuclear fuel cycle of the SVBR type modular fast reactor are presented below.

Table 1. Neutronic and physical properties of isotopes: ^{232}Th, ^{233}U, ^{235}U, ^{238}U, ^{239}Pu.

Nuclide	SVBR mean spectrum values[1]			
	σ_c, b	σ_f, b	$\alpha=\sigma_c/\sigma_f$	ν, neutron/fission
^{232}Th	0.30	0.01	29.5	2.01
^{233}U	0.22	2.46	0.09	2.52
^{235}U	0.43	1.69	0.26	2.47
^{238}U	0.26	0.04	6.03	2.44
^{239}Pu	0.38	1.68	0.23	2.95

2. BASIC TECHNICAL CHARACTERISTICS AND DESIGN FEATURES OF RF SVBR-100

A fast reactor with integral (monoblock) arrangement of the primary circuit equipment is used in the RF SVBR-100 design. The design of RF SVBR-100 is based on many-year domestic experience of constructing transport nuclear power facilities (NPF) with chemically inert heavy liquid-metal coolant (HLMC) – eutectic lead-bismuth alloy. The basic technical characteristics of RF SVBR-100 are presented in Table 2.

Table 2. Basic technical characteristics of RF SVBR-100

Parameter	Value
RF thermal power, MW	280
RF electric power (gross load), MW	101.5
Fuel: type	UO_2
load of U-235, kg	~1470
average enrichment in U-235, %	~16.5
Time between refuelings, years	7-8
Reactor monoblock dimensions (diameter/height), m	4.53/7.55

The RF SVBR-100 core is formed of 61 standardizated fuel sub-assemblies (FSA).

Today uranium dioxide UO_2 is considered as a fuel composition. From a side surface the core is surrounded by an irregular shape reflector, its effective thickness is ~ 250 mm.

3. CHARACTERISTICS OF URANIUM-THORIUM FUEL CYCLE WITH DIFFERENT TYPES OF FUEL

Calculations of the core neutron-physical characteristics for the SVBR type RF in the uranium-thorium cycle during the lifetime are performed in 26-group diffusion approximation in two-dimensional cylindrical geometry with use of code complex “REACTOR” [3] with system of constants “BNAB-93” [4].

The scheme of the core design is presented in Figure 1. Core loading was determined reasoning from a required reactivity margin for burnup. When the load was determined, in the calculations it was accounted the necessity to flatten the power distribution in the core, which was achieved by increasing fuel enrichment over a fissile isotope from the core center to periphery. In order to account burnup non-uniformity, four profiling zones were partitioned into several smaller parts along the radius and height.

Assessment of the probability of uranium-233 breeding was performed for three different types of fuel: oxide $\left(^{233}U+^{232}Th\right)O_2$, nitride $\left(^{233}U+^{232}Th\right)N$ and metallic $^{233}U+^{232}Th$ ones. Effective density (with account of gaps for swelling) of oxide and nitride fuel composition was taken to be equal to

[1] σ_c - absorption cross-section, σ_f - fission cross-section, σ_c- radiative capture cross-section; ν- a number of secondary neutrons

corresponding values for pure uranium fuel, and effective density of metallic fuel was taken to be equal to 0,9 of metallic thorium density.

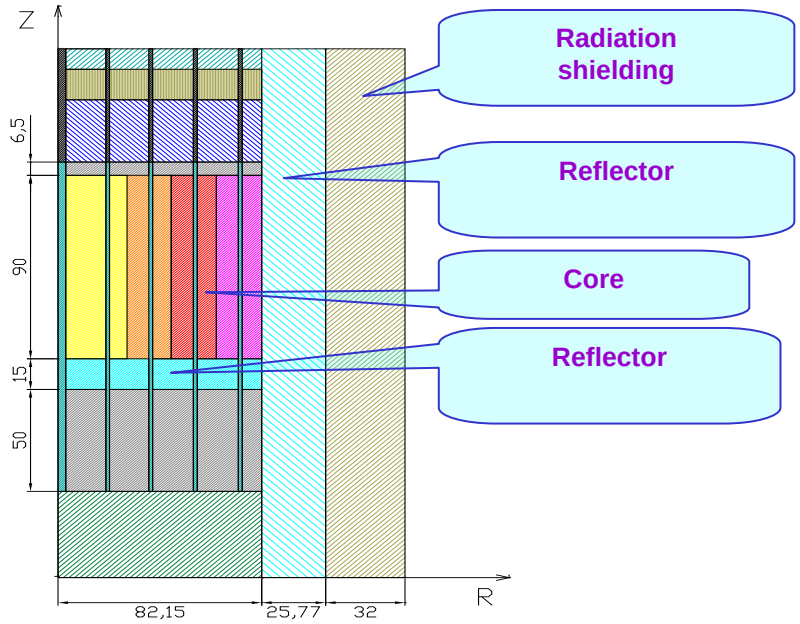

FIG. 1 The design scheme of facility SVBR-75/100

For the considered types of fuel the data on fuel load in the beginning of the lifetime are cited in Table 3.

To flatten the power distribution, four zone profiling by fuel enrichment over the fissile material: enrichment is increasing from the core center to periphery. Table 4 summarizes the values of enrichment over physical profiling zones in the core. These values provide the stated lifetime duration and acceptable values of non-uniformity coefficients $K_r^{\max}$ for energy release distribution over the lifetime (on the basis of experience of designing HLMC cooled fast reactors, permissible coefficient $K_r^{\max}$ is evaluated as ~ 1.25).

The total lifetime duration is divided in 5 burnup steps. For that initial composition the reactor operation at power 280 MW is assured during ~50000 full power hours.

During the entire lifetime the values of distribution along the core radius for non-uniformity coefficient of (heated) energy release distribution that is responsible for maximal temperature of fuel elements claddings for nitride fuel (U+Th)N is presented in Fig. 2.

Table 3. Parameters of the RF SVBR-75/100 cores for different types of uranium-thorium fuel

Parameter, dimensionality	Fuel type		
	Metal (U+Th)	Oxide $(U+Th)O_2$	Nitride (U+Th)N
Effective fuel density, g/cm^3	10.5	9.65	12.5
Average enrichment in uranium-233, %	11.52	13.21	11.46
Uranium-233 load G_3, kg	1281	1187	1431
Total load of uranium and thorium $G_{т.а.}$, kg	11122	8985	12488
Reactivity change over the lifetime, $\Delta\rho$, %	8.69	9.12	6.04
U-233 breeding ratio[1)]	0.85	0.85	0.9

[1)] Hereinafter a breeding ratio (BR) is a ratio of masses of basic fissile isotopes in the end of the lifetime to those in the beginning of the lifetime.

Table 4. Values of enrichment over physical profiling zones in the core

Profiling zone number	(U+Th)	$(U+Th)O_2$	(U+TH)N

	Enrichment in uranium-233, %		
1	9	10.4	9.3
2	9.6	11.0	9.7
3	10.8	12.4	10.97
4	13.6	15.6	13.2

Figure 2 shows that in the process of burnup during the lifetime a value of non-uniformity coefficient of (heated) energy release distribution is increasing near the core center and decreases at the core edges. During the lifetime a maximal value of non-uniformity coefficient of energy release distribution is evaluated by a value of 1.16, and over the entire lifetime that does not exceed $K_r^{\max}$ =1.25.

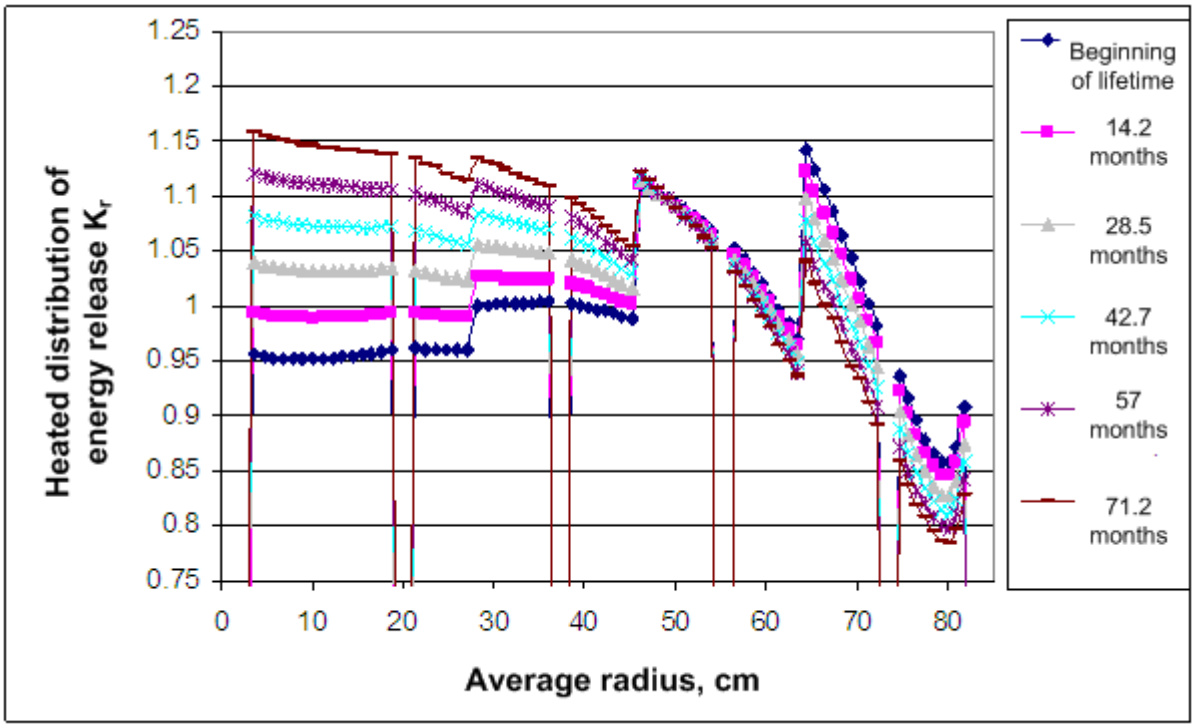

FIG. 2 Distribution along the core radius for non-uniformity coefficient of (heated) energy release distribution for nitride fuel (U+Th)N

In all cases during the lifetime approximately 620 kg of fission products is built in the core. At this point, maximal density of fission products in the fuel composition does not exceed 0.47 g/cm^3, and that corresponds to burnup depth of not more than 12 % of heavy atoms (h. a.) justified with reference to BN type reactors.

The diagram on neutron spectra in the core center for different kinds of the fuel composition is presented in Fig. 3.

4. SENSITIVITY OF URANIUM-233 BREEDING RATIO TO CORE DIMENSIONS AND EXISTENCE OF BREEDING BLANKETS

The data in Table 3 reveal that the uranium-233 breeding ratio that equals to 0.9 is achieved when fuel (U+Th)N with effective density of 12.5 g/cm^3. To analyze the opportunities of increasing the uranium-233 breeding ratio, we should consider the influence of special breeding zones and increase of core dimensions.

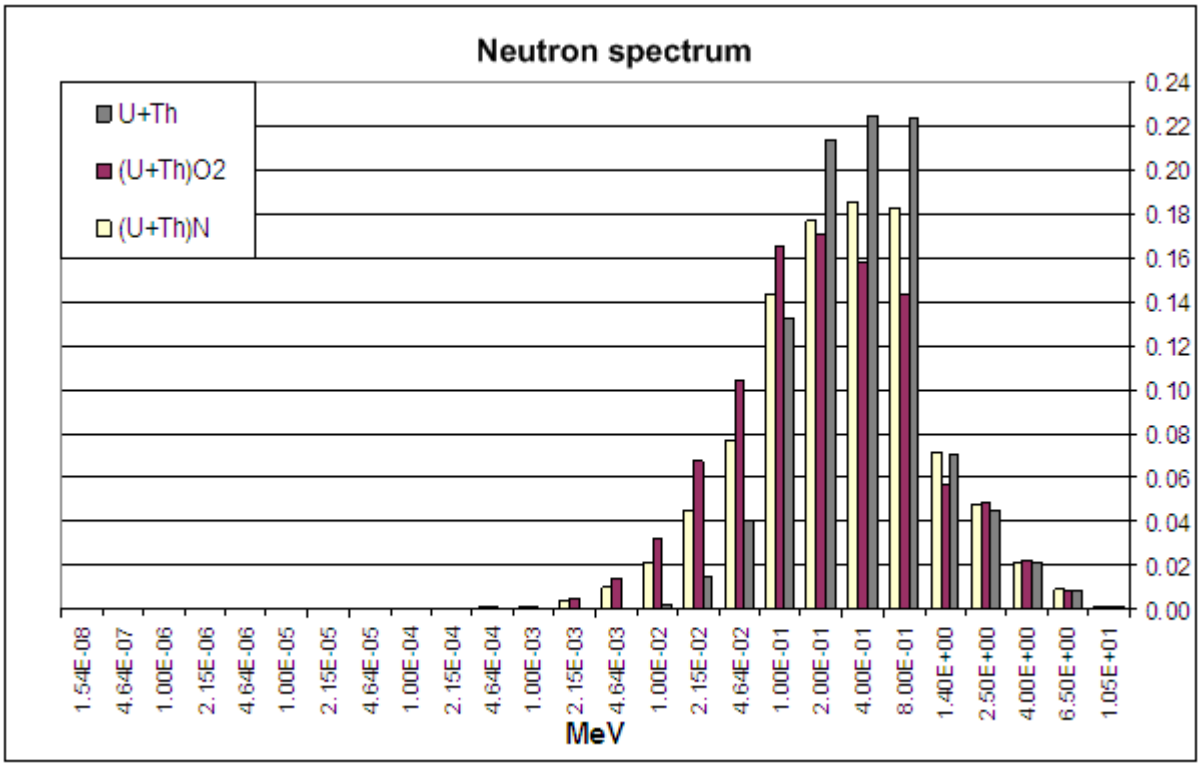

FIG. 3 Neutron spectra in the core for 3 kinds of fuel

Let us consider two variants of arrangement of the breeding zones: a) replacement of steel reflector in the fuel element by metallic Th-232 (at this point the quantity of loaded Th-232 will be increased by 2245 kg), b) to the previous breeding zone we should add a radial breeding zone made of standard in geometry fuel elements with metallic Th-232 instead of nuclear fuel. Width of breeding zone is15 cm without change of the RF overall dimensions (Th-232 load for that zone is 6863 kg).

It appears from the data in Table 5 that when the end breeding zone is added, breeding ratio of U-233 is increased by 2 % (increase of U-233 load by 20 kg results in increase of average enrichment in U-233 by ~ 0.2 %). In case the end and radial breeding zones are additionally inserted, breeding ratio of U-233 is increased by 7 % (increase of U-233 load by 75 kg results in increase of average enrichment in U-233 by ~ 0.6 %).

Table 5. Parameters of the RF SVBR-75/100 cores
for different breeding zones in the design of the core with (U+Th)N fuel

Parameter, dimensionality	Core design		
	(U+Th)N	core + end breeding zone	core + end and radial breeding zones
Average fuel enrichment in uranium-233, %	11.46	11.62	12.06
Uranium-233 load G_3, kg	1431	1451	1506
Total load of uranium and thorium $G_{т.а.}$, kg	12488	12488+2245= 14732	12488+2245+6863= 21596
Reactivity change over the lifetime, $\Delta\rho$, %	6.04	6.25	6.11
U-233 breeding ratio	0.9	0.92	0.97

During the lifetime 37 kg of U-233 is built up in the end breeding zone, and 92 kg is built up in the radial breeding zone.

In case of adding the end and radial breeding zones, a maximal value of non-uniformity coefficient of (heated) energy release distribution during the lifetime does not exceed K_r^{max}=1.25.

To assess the influence of core dimensions on uranium-233 breeding, two variants of increasing the core are considered: a) the core height is increased by 10 cm, b) the core height is increased by 20 cm, and in addition the core radius is increased (at this point, the core area is increased by 10 %).

It appears from the data in Table 6 that in case the core height is increased by 10 cm (total load of uranium and thorium is increased by 1244 kg, uranium-233 load is increased by 50 kg, average enrichment in uranium-233 is decreased by ~0.7 %), uranium-233 breeding ratio is increased by 4 %. In case the core height is increased by 20 cm and the core radius is increased (total load of uranium and thorium is increased by 4160 kg, uranium-233 load is increased by 291 kg, average enrichment in uranium-233 is decreased by ~1.8 %), uranium-233 breeding ratio is increased by 6 %.

Table 6. The content of the RF SVBR-75/100 core
for different dimensions of the design of the cores with (U+Th)N fuel

Parameter, dimensionality	Core design		
	(U+Th)N	Height is increased by 10 cm	Height is increased by 20 cm, area is increased by 10 %
Core dimensions $D_{eqv} \times H_{core}$, mm	1643 × 900	1643 × 1000	1716 × 1100
Average fuel enrichment in uranium-233, %	11.46	10.79	9.67
Uranium-233 load G_3, kg	1431	1481	1722
Total load of uranium and thorium $G_{т.а.}$, kg	12488	13732	16648
Reactivity change over the lifetime, $\Delta\rho$, %	6.04	4.81	3.19
U-233 breeding ratio	0.9	0.94	0.96

A maximal value of non-uniformity coefficient of (heated) energy release distribution during the lifetime does not exceed K_r^{max}=1.25.

5. CHARACTERISTICS OF URANIUM-THORIUM-PLUTONIUM FUEL CYCLE

To evaluate characteristics of uranium-233 build up in case of plutonium initial load, the calculations of the lifetime for the reactor with nitride fuel composition (Th+Pu)N were performed while plutonium was used as initial fissile isotope.

In calculations the isotopic content of Pu corresponds to the spent nuclear fuel of reactor WWER. The data on the isotopic content of plutonium mixture are summarized in Table 7 [5].

Table 7. Percentage of Pu isotopes in fuel

Isotope	Content, %
Pu-238	1.7
Pu-239	65.3
Pu-240	23.9
Pu-241	3.6
Pu-242	5.6

In Table 8 the data on fuel load in the beginning of the lifetime are presented for the (Th+Pu)N fuel comparing with similar parameters for the zone with (U+Th)N fuel.

Table 8. The content of RF SVBR-75/100 cores for (U+Th)N fuel and (Th+Pu)N fuel

Parameter, dimensionality	Fuel type	
	(U+Th)N	(Th+Pu)N
Average fuel enrichment in uranium-233 or Pu, %	11.46	14.6
Load of uranium-233 or Pu, kg	1431	1989
Total load of the core $G_{т.а.}$, кг	12488	12514
Reactivity change over the lifetime, $\Delta\rho$, %	-6.04	+2.01
Breeding ratio	0.9	0.98

A maximal value of non-uniformity coefficient of energy release distribution is achieved in the end of the lifetime and is evaluated by a value of 1,24, that does not exceed $K_r^{\max}$=1.25.

In Fig. 4 reactivity dependences on the lifetime moment for (U+Th)N fuel and (Pu+Th)N fuel are presented. It appears from Fig. 4 that for (Pu+Th)N fuel reactivity increases with a growth of the lifetime step as fissile isotope of U-233 is built up. As long as reactivity change in latter case won't exceed in magnitude reactivity change former case, this shouldn't be an issue, since reactivity worth of control rods should be sufficient to compensate it. In the end of the lifetime a quantity of U-233 is 364 kg.

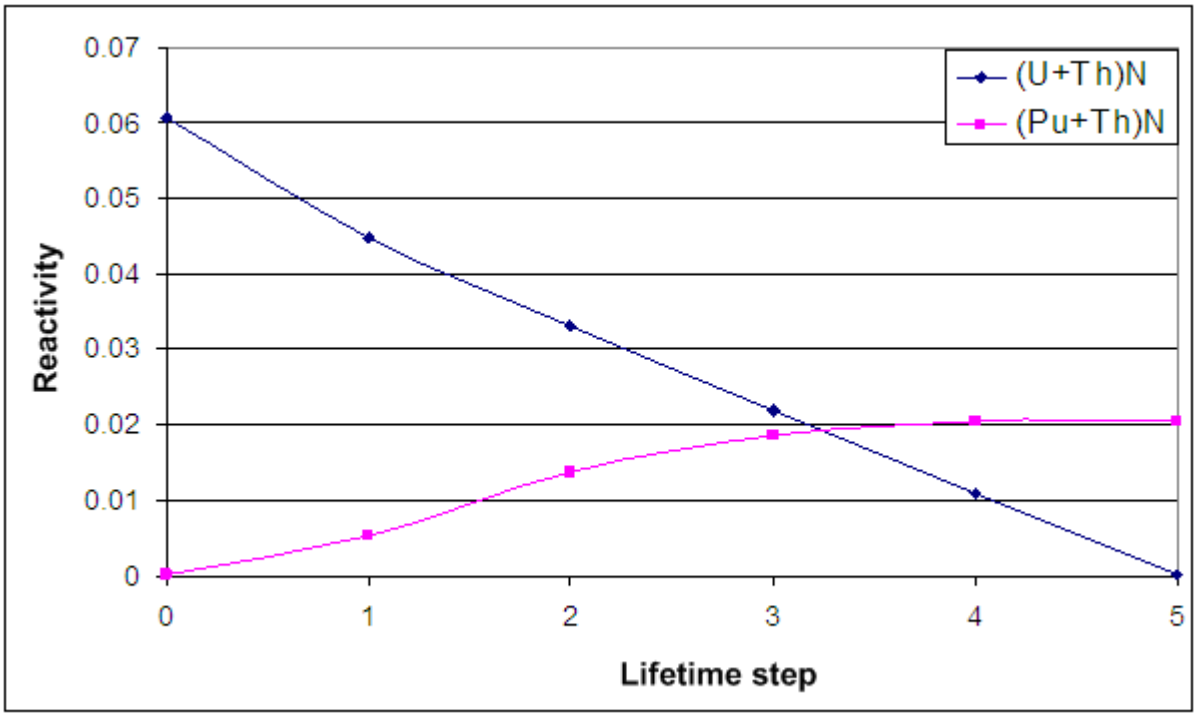

FIG. 4 Reactivity dependences on the lifetime moment

5. CONCLUSION

The performed computations for three different types of fuel, such as ceramic, oxide $\left(^{233}U+^{232}Th\right)O_2$, nitride $\left(^{233}U+^{232}Th\right)N$ and metallic $^{233}U+^{232}Th$, have revealed that maximum of uranium-233 breeding ratio, which equals to 0.9, is achieved when nitride type of fuel with effective density of 12.5 g/cm^3 and average fuel enrichment in uranium-233 that equals to ~11.5 % is used.

Sensitivity of uranium-233 breeding ratio to existence of breeding zones (max BR = 0.97) and increase of the core dimensions (max BR = 0.96) has been analyzed.

Assessment of the opportunity of uranium-233 isotope build up in RF SVBR while using plutonium as initial fissile isotope was carried out. Nitride fuel composition (Th+Pu)N with effective density of 12.5 g/cm^3 was analyzed. The computations have revealed that 364 kg of uranium-233 is being built up during the lifetime. At this point a breeding ratio of fissile materials over the lifetime equals to 0.98.

The obtained data have demonstrated that both for uranium-thorium fuel cycle and uranium-thorium-plutonium fuel cycle there is an opportunity to achieve a value of uranium-233 breeding ratio to be over one when using the breeding zones and increasing the core dimensions.

REFERENCES

[1] INTERNATIONAL ATOMIC ENERGY AGENCY, "Thorium Fuel Cycle – Potential Benefits And Challenges", IAEA, IAEA-TECDOC-1450, Vienna (2005).

[2] NOVIKOVA, N.N., KOMLEV, O.G., TOSHINSKY, G.I., "Neutronic and Physical Characteristics of Reactor SVBR-75/100 with Different Types of Fuel", Proc. of International Congress on Advances in Nuclear Power Plants (ICAPP 2006), Reno, NV, USA, June 4-8, 2006, American Nuclear Society (2006) (CD-ROM), Paper № 6355.

[3] VORONKOV, A.V., ARZHANOV, V.I., "REACTOR – Program System for Neutron-Physical Calculations", Proc. of International Topical Meeting on Advances in Mathematics, Computational and Reactor Physics, 1991, Pittsburg, USA (1991).

[4] MANTUROV, G.N., NIKOLAEV, M.N., TSIBULYA, A.M., "System of Group Constants BNAB-93. Part 1: Neutron and Photon Nuclear Constants", Issues of Nuclear Science and Technique, series Nuclear Constants, Issue 1 (1996).

[5] KOLOBASHKIN, V.M. "Radiation Characteristics Of Irradiated Nuclear Fuel. A Reference Guide", Moscow, Energoatomizdat (1983).

Invited Paper

Molten salt actinide recycler & transforming system and related fuel cycles

V.V. Ignatiev, O.S. Feynberg

NRC "Kurchatov Institute", Moscow, Russian Federation

Abstract. The achievement of a safe, reliable, low waste, flexible, self-sustainable and cheap nuclear power system is the priority task. A study is under progress to examine the feasibility of MOlten Salt Actinide Recycler & Transforming (MOSART) system without and with U-Th support fuelled with different compositions of transuranic elements trifluorides from spent LWR fuel. New design options with homogeneous core and fuel salt with high enough solubility for transuranic elements trifluorides are being examined because of new goals. Consideration is aiming to optimise core neutronic and thermal hydraulic performance, fuel salt / container material, fuel clean up and safety related parameters for MOSART system. Experimental data base created was used for further development of MOSART flowsheet as applied to consumption of transuranic elements trifluorides while extracting their energy. The flexibility of single fluid MOSART concept fuel cycle is underlined, e.g. possibility of its operation in self-sustainable mode using different loadings and feedings
Introduction

Within previous study main focus was placed on experimental and theoretical evaluation of single stream MOSART system operating in critical mode as pure burner of transuranic elements without thorium and uranium support [1]. As the starting loading and make up for MOSART the following compositions of TRU from used LWR fuel were investigated: (1) UOX spent fuel after one year of cooling with minor actinides (MA) to transuranic elements (TRU) ratio MA/TRU ≈ 0.1 and (2) MOX spent fuel after 1 year of cooling with MA/TRU ≈ 0.2. The optimum spectrum for MOSART is intermediate/fast spectrum of homogeneous core without graphite moderator (see Fig. 1). Promising configuration for 2.4GWt MOSART is the homogeneous cylindrical core (3.6 m high and 3.4 m in diameter) with 0.2 m graphite reflector filled with 100% of molten 15LiF-58NaF-27BeF_2 or 73LiF-27BeF_2 salt mixture [2,3]. Times and methods for fission product removal and actinides recycling in MOSART are given in Table 1. As can be seen in Fig. 2 it is feasible to design critical homogeneous core fuelled only by TRU trifluorides from UOX or MOX LWR used fuel while equilibrium concentration for trifluorides of actinides (1.1 mole% for Li,Na,Be/F and 0.4 mole% for Li,Be/F cores, respectively, with the rare earth removal cycle 1 EFPY (effective full power year) is truly below solubility limit (~2 mole%, see details in Table 2) at minimal fuel salt temperature in primary circuit 600-620^{o}C. The effective flux of such system is near 10^{15} n cm^{-2} s^{-1}.

The main attractive features of MOSART concept deals with the use of (1) simple configuration of the homogeneous core (no solid moderator or construction materials under high flux irradiation); (2) proliferation resistant multiple recycling of actinides (separation coefficients between TRU and lanthanide groups are high, but within the TRU group are very low); (3) the proven container materials (nickel-based alloys) and system components (pump, heat exchanger etc.) operating in the fuel circuit at temperatures below 750^{o}C, (4) inherent safety features of the system due to large negative temperature coefficients, (5) increased times for fission products removal.

At the same time, option of MOSART-burner does not settle completely the possibilities of the system. It seems that one of the basic advantages of MSR in whole and homogeneous configuration in particular is outstanding flexibility of the fuel cycle. The system without essential changes of the design is capable to operate in different modes: 1) as transmuter for a wide range of possible feedings (at higher than specified above ratios of minor actinides in TRU), 2) as TRU-^{233}U converter, 3) as self-sustainable system with Conversion Ratio CR=1 at transition to U-Th fuel cycle, 4) as breeder with CR > 1. Such kind of system can operate in the mode of transformer-reactor and can find its place in any scenario of nuclear power development from growth to closing.

Transforming system creation was not the original goal for prior MSR designs. Main technical questions arising from variations in fuel salt composition during system operation also include:

measurement of fuel salt key physical and chemical properties, corrosion & salt chemistry control, suitable fuel processing and waste form development. The objective of this activity is to find optimum core parameters while accounting for technology constrains determined by fuel salt and container materials properties. This paper describes the results of parametric study of the transforming system based on MOSART design mainly focused on single- and two-fluid homogeneous cores. As the calculation tool at all stages of the parametric work MCNP-4B+ORIGEN2.1 with the library on the base of ENDF 5,6 complex adapted for specificity of MSR designs with circulating fuel was used [1].

Table 1. Times and methods for fission product removal and actinides recycling in MOSART [1].

Element	Time	Method
Kr, Xe	50 s	Sparging with He
Zn, Ga, Ge, As, Se, Nb, Mo, Ru, Rh, Pd, Ag, Tc, Cd, In, Sn, Sb, Te	2-4 hrs	Partial plating on surfaces, removal to off-gas system, limited filtering
^{233}U, ^{234}U, ^{235}U, ^{236}U, ^{237}U, ^{238}U	10-15 days	Fluorination
Zr, ^{233}Pa	1-3 yrs	Reductive extraction; Distillation; Co-crystallization
Ni, Fe, Cr	1-3 yrs	
Pu, Am, Cm, Np	1-3 yrs	
Y, La, Ce, Pr, Nd, Pm, Gd, Tb, Dy, Ho, Er	1-3 yrs	
Sm, Eu	1-3 yrs	
Sr, Ba, Rb, Cs	5-10 yrs	
Li, Be, Th	30 yrs	Salt discard

Table 2. Solubility of PuF_3 in molten salt fluoride mixtures: log S, mole% = A + B/T,K [3].

LiF	NaF	KF	BeF_2	ThF_4	T, K	A	$-B \cdot 10^{-3}$	Method
46.5	11.5	42	0	0	823-973	5.59	3.949	isothermal saturation
73	0	0	27	0	825-1000	3.927	3.099	isothermal saturation
66	0	0	34	0	800-900	3.231	3.096	γ-spectrometry
15	58	0	27	0	825-925	3.639	2.750	γ-spectrometry
17	58	0	25	0	800-900	3.253	2.578	γ-spectrometry
78	0	0	0	22	873-973	2.58	1.73	γ-spectrometry
75	0	0	5	20	873-1023	2.06	1.34	γ-spectrometry
77	0	0	17	6	848-998	3.61	2.91	γ-spectrometry

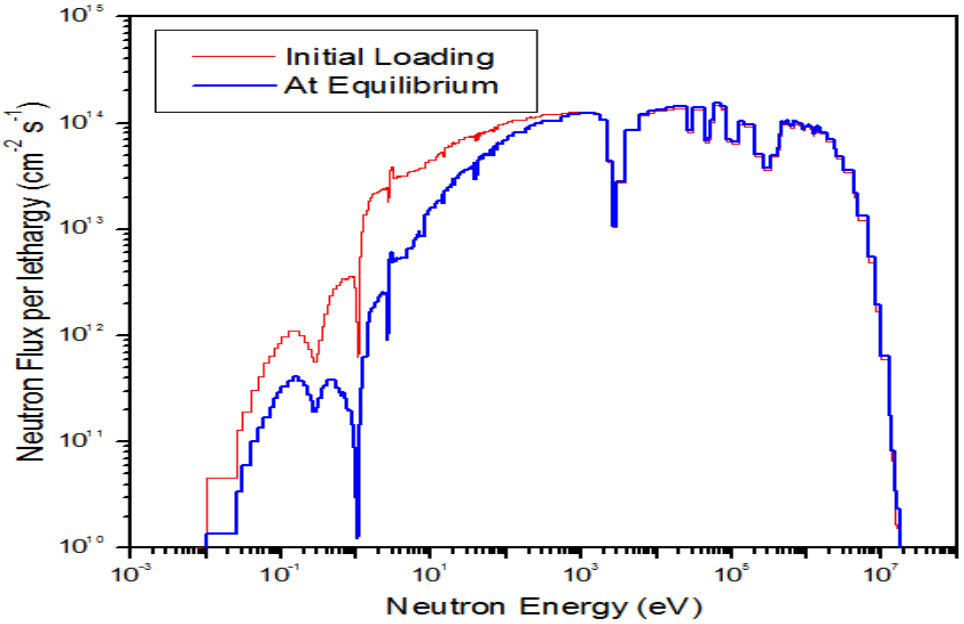

Fig. 1. Neutron specrtrum of single fluid 2.4GWt MOSART-TRU burner with Li,Na,Be/F core

1. Transmuter mode

As solvent of fuel salt in MOSART- TRU burner two melts are investigated: 73LiF-27BeF_2 and 15LiF-58NaF-27BeF_2 (mole %). The MOSART- TRU burner starting loading and feedings can be as the following: (UOX spent fuel after 1yr of cooling with minor actinides (MA) to TRU ratio MA/TRU ≈ 0.1 (^{238}Pu- 3.18%; ^{239}Pu-43.93%; ^{240}Pu-21.27%; ^{241}Pu-13.52%; ^{242}Pu-7.88%; ^{237}Np-6.42%; ^{241}Am-0.55%; ^{243}Am-2.33%) and (2) MOX spent fuel after 1 yar of cooling (^{238}Pu-2.77%; ^{239}Pu-48.36%; ^{240}Pu-19.97%; ^{241}Pu-8.30%; ^{242}Pu-6.25%; ^{237}Np-6.51%; ^{241}Am-5.56%; ^{243}Am-1.69%;)
with MA/TRU ratio ≈ 0.2.
The use of the melt without sodium essentially reduces parasitic absorption of neutrons (for a considered spectral range) and provides minimum concentration of transuranic elements in equilibrium loading (Fig. 2). It is necessary to notice that changing of lithium by sodium in the salt composition has some advantages, namely, reduces tritium production due to Li(n, α)T reaction and decreases composition cost.
The use of 73LiF-27BeF_2 melt (mole %) significantly increases MOSART-burner possible make up margins. The available gap up to solubility of actinides trifluorides in the solvent makes it possible to use as feeding any mixtures of transuranic elements with MA / TRU ratio up to 0.35 (Fig. 3) without changing of the core configuration and temperature parameters for the Li,Be/F MOSART design. It, naturally, leads to growth of heavy elements equilibrium loading up to 19 t (from 3.8 t for initial MOSART mode of operation), but allows to increase the rate of MA burning up to 300 kg/yr for the same as in initial mode of MOSART operation rate of burning for intire mass of TRUs burned.
It is possible to expand even more possibilities of MOSART burner mode of operation and to increase the rate of minor actinides burning, surrounding its core by thorium-containing blanket with molar composition 75LiF-5BeF_2-20ThF_4 or 78LiF_2-22ThF_4 (50-60 cm thickness). From blanket uranium (80-100 kg/yr) processed by the volatility process is recycled to fuel stream of two-fluid system, but the thorium-bearing salt is returned to the blanket. For this mode of operation the limit MA/TRU ratio within solubility for 73LiF-27BeF_2 solvent (mole %) will be near 0.5 (Fig. 3). Such composition of feeding leads to the further growth of total loading of the reactor (up to 23 t) and to the complication of the design due to the use of two-fluid configuration.

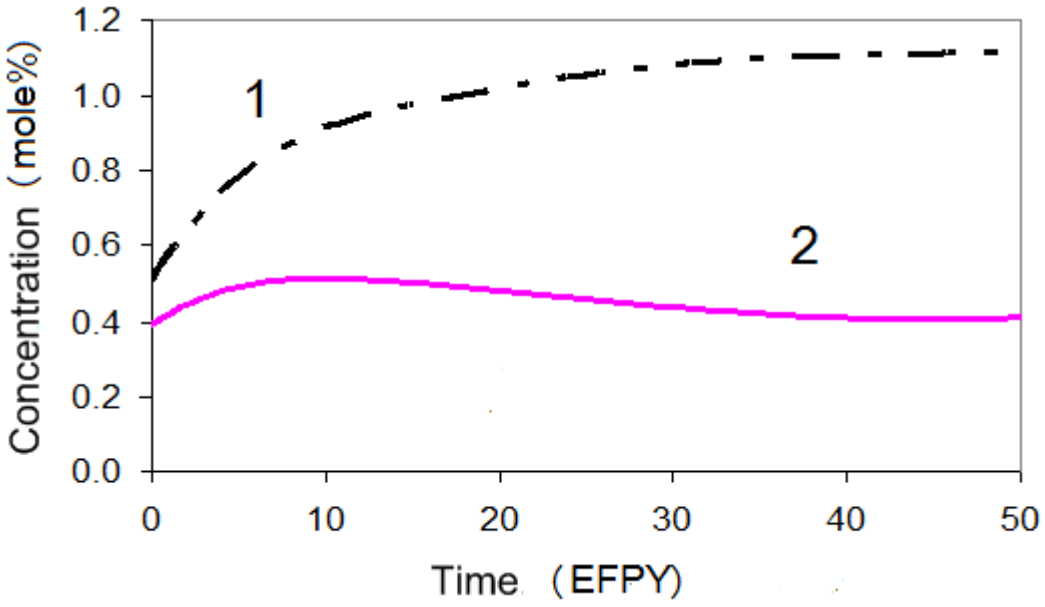

Fig. 2. Transition to equilibrium of single fluid 2.4.GWt MOSART with Li,Na,Be/F (1) and Li,Be/F (2) cores

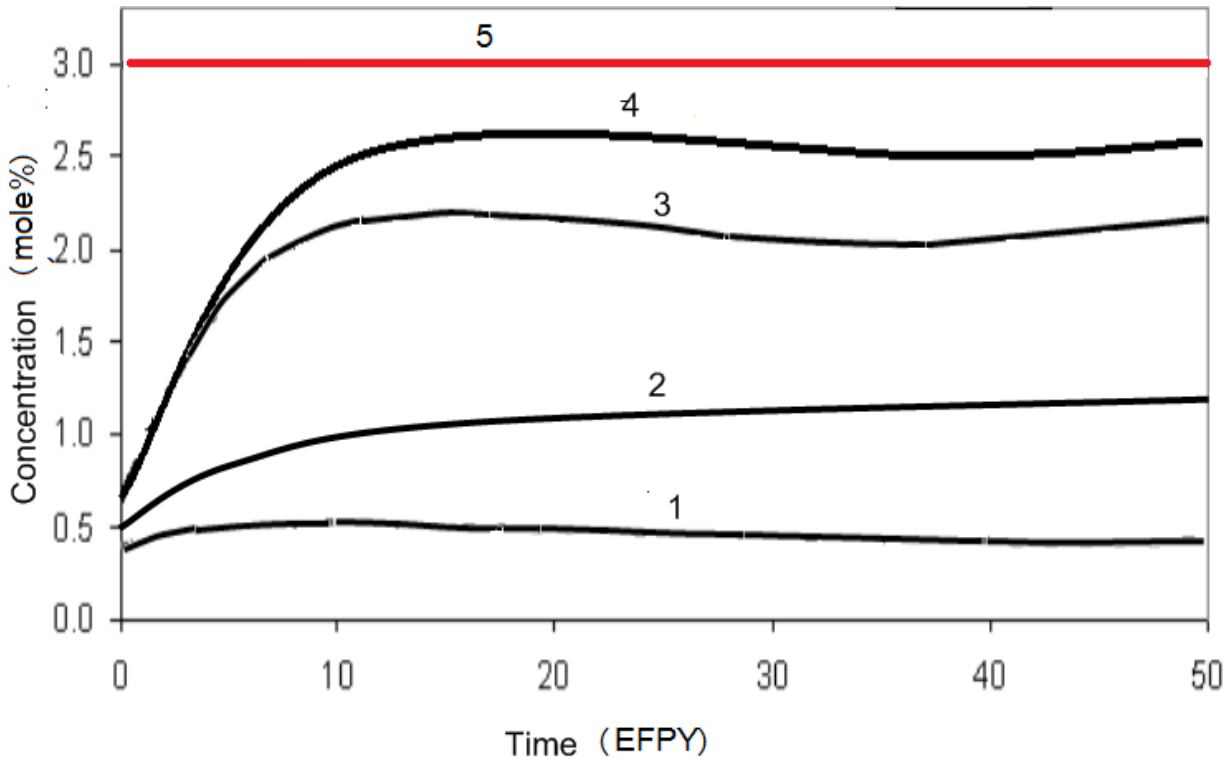

Fig. 3. Molar concentrations of TRU vs. time for Li,Be(Na)/F salt solvents and different feedings (MA/TRU ratios) for single fluid system (1 - MA / (Pu+MA) = 0,1 in LiF-BeF_2; 2 - MA / (Pu+MA) = 0,1 in NaF-LiF-BeF_2; 3 - MA / (Pu+MA) = 0,35 in LiF-BeF_2) and two fluid system with ^{233}U recycling from blanket to fuel stream (4 - MA / (Pu+MA) = 0,45 in LiF-BeF_2); actinides trifluorides solubility in eutectic at 923 K (5).

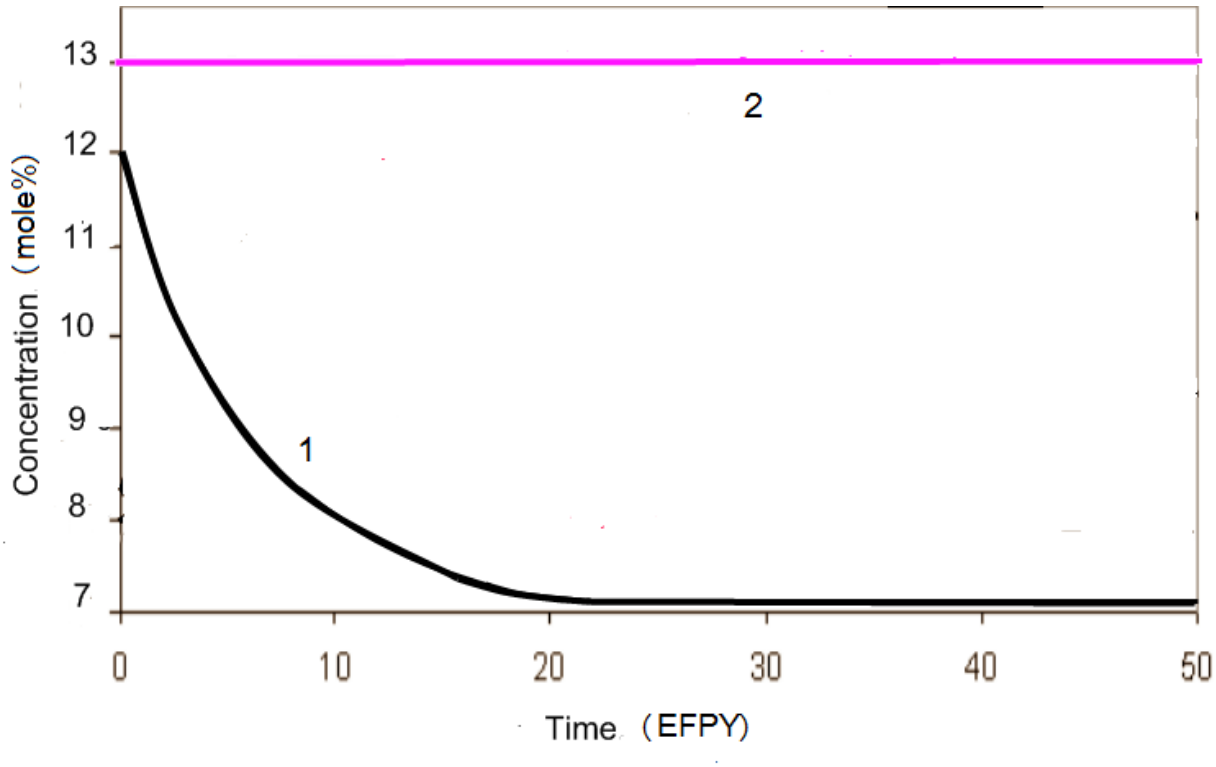

Fig. 4. Molar concentrations of TRU vs. time for Li,Na,K/F MOSART started with fuel composition MA/TRU=0.6 and then fed by MA only (1); actinides trifluorides solubility in the eutectic at 873 K (2).

For transition to fuels based on MA's only, solvent with higher solubility is required, e.g. 11.5LiF-46.5NaF-42KF eutectic (see Table 2). Such Li,Na,K/F MOSART design after starting with MA/TRU=0.61 fuel composition (Fig. 4) can be fed by MA only, but it is necessary to note that the system of this kind will have very high equilibrium loading of fissile nuclides (36 t) and number of unresolved problems connected with the choosing of (1) reliable metallic material and (2) effective methods of fuel processing. As the conclusion: in the MOSART it is possible to burn spent LWR fuel with MA/TRU ratio from 0.1 up to 1 within solubility limit for different salt solvents.

2. Converter mode

As it was mentioned above two-fluid MOSART design is capable to work in a converter mode and connsume approximately 700 kg of spent LWR fuel in 100 kg of ^{233}U per year. Total CR of the converter system and transmuting efficiency of the burner can be essentially increased at forcing of specific power of the core, i.e. at reducing of the core dimensions. Restricting factors here will be not only solubility of TRU trifluorides in the chosen salt solvent, but also possibilities of heat removal from the core and the lifetime of structural materials (a dividing wall between the core and the blanket, reflector, distribution plate, etc.). Traditional choice for the systems with molten salts are the alloys with high content of nickel as the metallic materials for the primary and secondary circuit elements and graphite (if necessary) as the material for inner core details and reflector. Early materials studies led to the development of a Ni-Mo alloy Hastelloy N, for use with fluoride salts. The good corrosion compatibility of Ni-Mo alloys of Hastelloy N type with fluorides was certified experimentally for temperatures 700°C and discussed elsewhere [4]. The weakest point of Ni-Mo alloys is high temperature (T>500°C) radiation-induced embrittlement under helium bubbles production as a result of neutron reactions on Fe, Cr, Ni and B (for Hastelloy type alloys reactions on Fe and Cr are negligible). Specifying a critical level of helium that would cause embrittlement is not presently possible. But analyzing of the existing experimental data [5] gives the upper estimation 60-80 appm for this process.

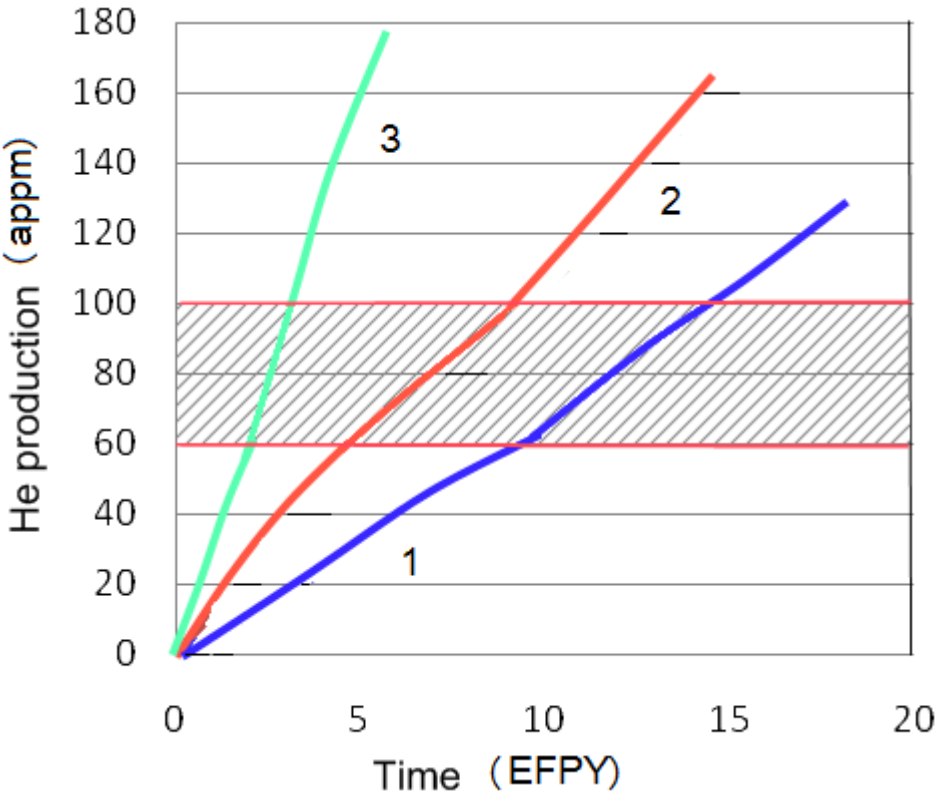

Fig. 5. He production on $^{58}Ni(n,\alpha)$ in Ni-Mo alloy (B content ≤0.001%) on the inner surface of the axial reflector over the center of the cylindrical core vs. time and specific power of the core: 1 - 70 W/cm^3 , 2 - 140 W/cm^3 and 3 - 330 W/cm^3

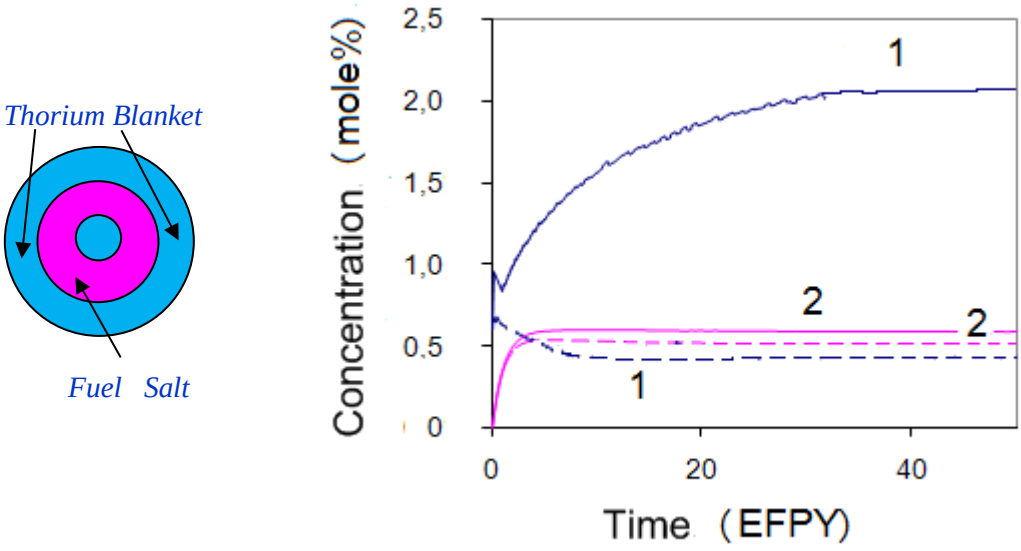

Fig. 6. Annular configuration of two-fluid converter system with Th-containing blanket (left) and concentrations of actinides and lanthanides trifluorides in fuel salt vs. time for annular core configuration in converter mode of operation (right): solid line - ^{233}U transfer to stock, dashed line - ^{233}U recycling from blanket to fuel stream, 1 - actinides trifluorides, 2 - rare earths trifluorides in the salt (multiplied by 10).

The following main reactions with He production take place for $^{58}Ni + n \rightarrow {}^{55}Fe + {}^{4}He$, (threshold for $E \geq 1Mev$), $^{60}Ni + n \rightarrow {}^{57}Fe + {}^{4}He$, $^{10}B + n \rightarrow {}^{7}Li + {}^{4}He$. In thermal or near thermal neutron spectrum two-stages reaction must be taken into account too: $^{58}Ni + n \rightarrow {}^{59}Ni + \gamma$, $^{59}Ni + n \rightarrow {}^{56}Fe + {}^{4}He$. The spectrum of neutrons on the inner surfaces of the designs under consideration is mainly intermediate that's why as it was shown by the calculations done the helium production will be determined by two main reactions: on ^{10}B and threshold reaction on ^{58}Ni. The ^{10}B concentration in the alloy may be decreased from 0.01mass. % for reference Hastelloy N to 0.001 mass.% in some of its modifications [4].

Fig. 5 results the calculations of helium time accumulation on ^{58}Ni (n, α) threshold reaction on the inside surface of axial reflector (over the center of the core) of a simple cylindrical core vs. specific power of the core. For the Li,Be/F MOSART core operating in transmuter mode with specific power 70 MW/m^3 possible operational time of the top reflector made of Ni-based alloy with the decreased concentration of boron (e.g., HN80MTY alloy [3]) is estimated as 10-15 yrs. When core specific power increased up to 330 MW/m^3 this top reflector will need to be replaced every 1.5 - 2 yrs. The core with 120-140 MW/m^3 specific power will provide the lifetime of the wall below 5 yrs.

For the 2.4GWt Li,Be/F MOSART core (radius / height - 1.4 / 2.8 m) with $11m^3$ volume of the fuel salt outside the core in the primary circuit (comparing with 18.3 m^3 for MSBR design of similar power, [4]) the rate of ^{233}U production in thorium blanket will be 160 kg per year.

In converter mode of operation the optimal result from the point of view of minimal concentration of TRU trifluorides in the fuel salt and maximum uranium production in the molten $75LiF\text{-}5BeF_2\text{-}20ThF_4$ salt blanket may be obtained for annular Li,Be/F core with height 3.2 m / outer radius 1.6 m supplied by inner 0.7 m radius blanket and outer 0.6 m thickness molten $75LiF\text{-}5BeF_2\text{-}20ThF_4$ salt blanket (see Fig. 6). The uranium removal time from the blanket is 15 days. For the soluble fission products removal time of about 1 EFPY this system has at equilibrium concentrations of TRU and lanthanides trifluorides in fuel salt of about 2 and 0.05 mole %, respectively and will need changing core - inner blanket dividing wall (detail of the design with maximum He accumulation) once in 6 yrs. With ^{233}U production rate ~300 kg/yr the system with thermal power of 2.5 GWt can quite efficiently produce uranium initial loading for other Th-U breeder system; e.g. 5 t required for 3GWt MSFR design [6] during 16-18 yrs.

3. Self-sustainable mode

Interesting possibilities may be demonstrated by the use of MOSART with the reduced dimensions as self-sustainable system with CR=1. For transition to this mode of operation a strategy of gradual increase of thorium maintenance in fuel salt is required.

Single fluid 2.4GWt Li,Be/F MOSART core (radius -1.4 m, height - 2.8 m) containing as initial loading 2 mole % of ThF_4 and 1.2 mole % of $TRUF_3$ with the rare earth removal time 1 EFPY after 12 yrs can operate without any $TRUF_3$ make up basing only on Th support as a self-sustainable system (Fig. 7). The maximum concentration of $TRUF_3$ during this transition does not exceed 1.7 mole %. At equilibrium molar fraction of ThF_4 in the fuel salt is near 6 % and it is enough to provide the system with CR=1 up to 50 yrs of the reactor operation. The reactivity temperature coefficient of the homogeneous core is not only essentially negative, but also practically has no inertion. In the case of self-sustainable MOSART its value on equilibrium is - 6.7 pcm/K.

The use of the thorium blanket in this scheme of operation permits to reduce the transition to self-sustainable mode of operation down to 3 - 4 yrs, but of course makes the system more complicated from technical point of view.

Any moment of self-sustainable mode of operation can be used for transition to breeder mode with CR> 1 due to increasing of thorium concentration in the fuel salt. So self-sustainable mode demonstrates the abilities of the MOSART system as transforming system and can be used for starting U-Th fuel cycle on the base of first loading from LWR spent fuel.

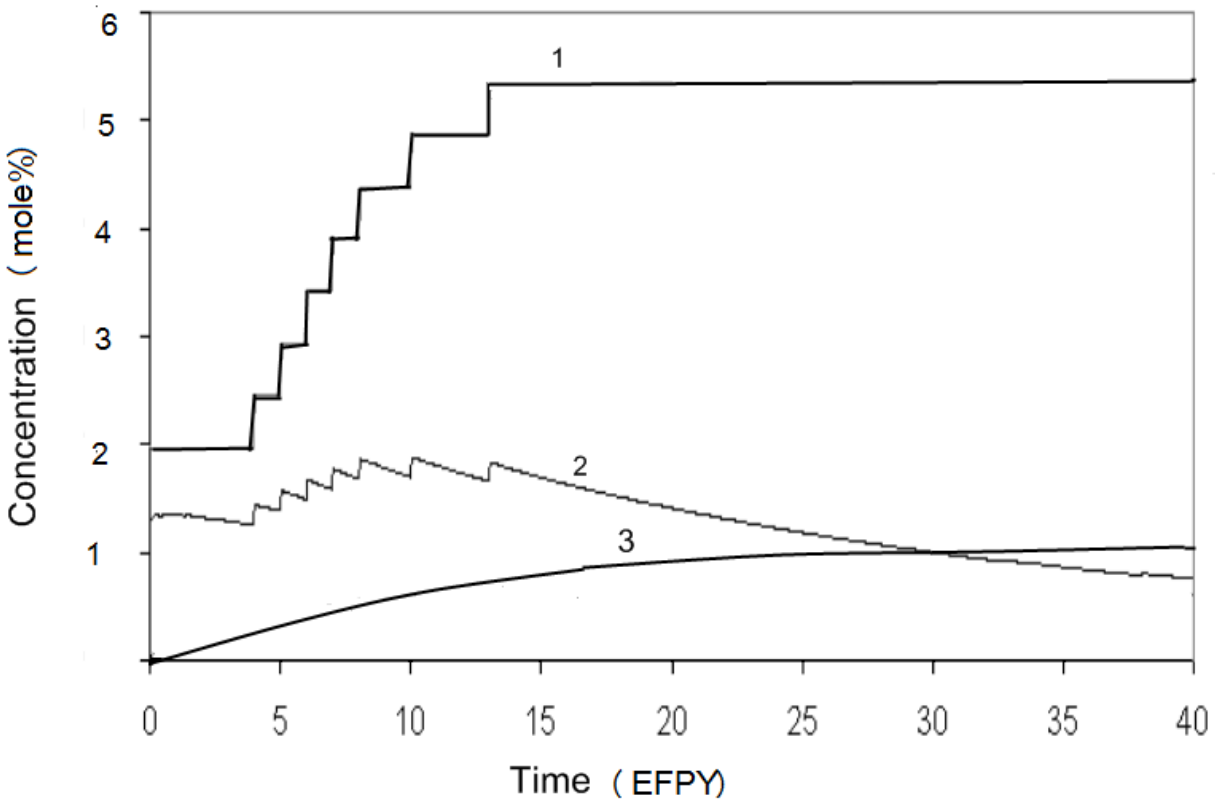

Fig. 7. Transition to equilibrium of ThF_4 (1), $TRUF_3$ (2), UF_4 (3) in single fluid 2.4GWt MOSART with Li,Be,Th/F core (CR=1 with gradual increase of ThF_4 concentration in the fuel salt)

4. Conclusions

In this study main attention has been paid to MOSART system with Th support fuelled with different compositions of transuranic elements from used LWR fuel with design objective to provide the fissile concentration and geometry of the fuel salt to obtain heat release of about 2.4GWt. The consideration done demonstrates the potential of the MOSART system as the system with flexible configurations and fuel cycle scenarios which can operate within technical limits with different loadings and make up based on TRU from used LWR fuel as special actinide burner (for spent LWR fuel with MA/TRU ratio down to 0.45), as self-sustainable system (CR=1) or even as a breeder (CR>1). However we are aware that many not only techinical difficulties remain, especially before the most advanced embodiment, the MOlten Salt Actinide Recycler & Transforming system, becomes a reality.

ACKNOWLEDGEMENTS

This work was supported in 2012 by ISTC in the frawork of 3749 Task, by Rosatom within MARS project, and by Russian Foundation for Basic Research grant No. 11-08-92004.

REFERENCES

[1] INTERNATIONAL SCIENTIFIC AND TECHNICAL CENTRE, “ISTC#1606 project final report”, Moscow, Russia (2007)

[2] IGNATIEV, V., FEYNBERG, O., “Molten salt reactor for TRU transmutation without and with Th-U support”, Trans. ANS 104 (2011) 722

[3] IGNATIEV, V., et. al., “Molten salt reactor: new possibilities, problems and solutions”, Atomic energy 112, 3 (2012) 157

[4] ENGEL, J., et. al., “Development status and potential program development of proliferation resistant molten salt reactors”, USAEC Report ORNL/TM-6415, Oak Ridge, USA (1979)

[5] KONOBEEV, YU., BIRZHEVOI, G., “Perspectives of high nickel alloys for the use in the nuclear power reactors with supercritical water coolant”, Atomic energy 96, 5, (2004) 365

[6] MERLE-LUCOTTE, E., et. al., “Launching the thorium cycle with molten salt fast reactor”, In: Proceedings of ICAPP 2011, Nice, France, May, (2011) 11190